Acknowledgments

Publication of this volume involved efforts of many. Some of the publisher's and printer's staffs are hidden by a "paper curtain" and remain anonymous; nevertheless, their efforts are fully appreciated even though they cannot be individually acknowledged. The work of others required personal communications with the Editor. Among these, I want to thank particularly R. S. Woolson for his encouragement over the many years of this project's development, Elodie Sabankaya for the design of the book's layout, Linda Riffle for editing the manuscript, and Louise Haberfeld for editing the galleys and the page proof. Finally, I want to thank Judy Sanders, who read the galleys and the page proof, helped prepare the index, and whose help and advice greatly lightened the arduous task of the Editor.

Contents

1 Fresh Concrete—Materials and Properties 1
P. K. MEHTA AND M. POLIVKA

2 Reinforcing Steel 42
J. F. McDERMOTT

3 Properties of Hardened Concrete 65
A. M. NEVILLE

4 Bond and Cracking in Reinforced Concrete 151
D. WATSTEIN AND B. BRESLER

5 Strength and Deformation of Reinforced Concrete Elements 194
O. M. GONZÁLEZ, F. ROBLES, R. DÍAZ DE COSSÍO

6 Strength and Deformation of Prestressed Concrete Elements 302
T. Y. LIN AND P. ZIA

7 Safety and Structural Design 407
E. ROSENBLUETH

Appendix 517

Index 521

List of Authors

BORIS BRESLER	Department of Civil Engineering University of California, Berkeley Berkeley, California
OSCAR M. GONZÁLEZ CUEVAS	Universidad Nacional Autónoma de México México, D.F.
ROGER DÍAZ DE COSSÍO	Universidad Nacional Autónoma de México México, D.F.
T. Y. LIN	Department of Civil Engineering University of California, Berkeley Berkeley, California
JOHN FRANCIS McDERMOTT	Research Laboratory U.S. Steel Corporation Monroeville, Pennsylvania
P. KUMAR MEHTA	Department of Civil Engineering University of California, Berkeley Berkeley, California
ADAM MATTHEW NEVILLE	Department of Civil Engineering The University of Leeds Leeds, England
MILOS POLIVKA	Department of Civil Engineering University of California, Berkeley Berkeley, California
FRANCISCO ROBLES	Universidad Nacional Autónoma de México México, D.F.
EMILIO ROSENBLUETH	Universidad Nacional Autónoma de México México, D.F.
DAVID WATSTEIN (deceased)	Center of Building Technology National Bureau of Standards Washington, D.C.
PAUL ZIA	Department of Civil Engineering North Carolina State University Raleigh, North Carolina

REINFORCED CONCRETE ENGINEERING

VOLUME 1
Materials, Structural Elements, Safety

Edited by BORIS BRESLER

Professor of Civil Engineering
University of California, Berkeley

A Wiley-Interscience Publication

JOHN WILEY & SONS

New York London Sydney Toronto

Copyright © 1974, by John Wiley & Sons, Inc.

All rights reserved. Published simultaneously in Canada.

No part of this book may be reproduced by any means, nor transmitted, nor translated into a machine language without the written permission of the publisher.

Library of Congress Cataloging in Publication Data:

Bresler, Boris.
Reinforced concrete engineering.

"A Wiley-Interscience publication."
Includes bibliographical references.
CONTENTS: v. 1. Materials, structural elements, safety.
1. Reinforced concrete construction. I. Title.
TA683.2.B69 624'.1834 73-19862
ISBN 0-471-10279-2

Printed in the United States of America

10 9 8 7 6 5 4 3 2 1

Preface

The first uses of iron and steel as concrete reinforcement, as well as many subsequent innovations in concrete construction, were introduced by practical men, not theorists. Many of these innovations were successful due to the sound judgment and courage of outstanding engineers who successfully built a variety of reinforced concrete structures.

While many innovations of practical men with vision must be honored for their success, many other early innovations failed. Usually, such failures resulted from a lack of knowledge or understanding of the essential nature of the structural behavior of reinforced concrete. Because of such failures, many engineers have hesitated to adopt new concepts until they were adequately validated not only by isolated experience, but also by experimentation and analysis leading to a fuller, clearer knowledge and understanding of the behavior of a given structural system.

The need for an integration of fundamental and practical knowledge of reinforced concrete was recognized by some of the earliest writers on the subject. Early gains from practical as well as experimental and analytical studies are reflected in such books as *Experimental Researches on Reinforced Concrete*, by Armand Considere, published by McGraw Publishing Co. in 1903, and in *Reinforced Concrete* by A. W. Buel and C. S. Hill, Second Edition, published by The Engineering News Publishing Co. in 1906. In their book *A Treatise on Concrete Plain and Reinforced*, Second Edition, published by John Wiley and Sons in 1909, F. W. Taylor and S. E. Thompson dealt extensively with materials, construction and design, including the latest information on the behavior of reinforced concrete beams, columns, slabs, arches, piers, dams, and retaining walls, as well as chapters on cement, aggregate, the proportioning of concrete, fire and rust protection, and the effects of sea water on concrete and mortar.

Later, this basic treatise was revised and became a classical reference work first printed in 1925 under the title *Concrete Plain and Reinforced* by Taylor, Thompson, and Smulski. The last edition was issued in two volumes in 1931 and covered the theory and design of concrete and reinforced concrete structures, including a full treatment of statically indeterminate

stuctures (continuous beams, frames, and arches) from both a theoretical and practical standpoint. Examination of these and other early publications clearly reveals that the widespread success of reinforced concrete structures was achieved by combining the innovative and creative ideas of practitioners with the development of theory which took into account the special nature of monolithic construction and the composite action of steel and concrete.

With the rapid technological progress in new structural forms (multistoried frames, larger spans in buildings and highway bridges, multi-level elevated roadways in the cities, nuclear reactor containment structures, and fixed, floating, and submerged ocean structures) and with the emergence of new materials (special concretes and high-strength steel reinforcing bars) and of new construction techniques (precasting and prestressing), the structural engineer faces a new generation of problems. These problems may be classified under two main categories:

(1) *The fundamental behavior of reinforced concrete.* The evaluation of the response of reinforced concrete elements to loading and environment and the proportioning and detailing of these elements for strength and serviceability require a thorough understanding of the structural characteristics of concrete. Particularly important among these are the effects of age, environment, and state of stress on concrete properties, the bond between the concrete and steel reinforcement, the initiation and propagation of cracking, the deformation and strength of reinforced concrete under various conditions of loading, temperature, humidity, and load history, and the durability, corrosion, and fire resistance of structural concrete elements.

(2) *The analysis of structural behavior.* The determination of the magnitude of the effects of loading and environment in reinforced concrete elements and of the nature of the overall behavior of the structural system requires the capability of evaluating the stresses and deformations in complex frames, plates, and shells, the dynamic response of structures, the "collapse loads" of elements and systems, and the instability of slender components. Analytical solutions of some of these problems have recently become feasible with the use of large, high speed digital computers.

In recent years, much new knowledge has been acquired about the behavior of reinforced concrete structures. Conventional codes and specifications do not adequately reflect this new knowledge and, therefore, cannot cope with the many new problems which can only be solved by more precise analysis and greater understanding of fundamental behavior. It is the objective of *Reinforced Concrete Engineering*, in the form of a three volume series, to provide a summary of this new knowledge in an authoritative work dealing with both theoretical and practical aspects of reinforced concrete structural design. The volumes are intended as references for the designer as well as for the advanced student of structural concrete.

In undertaking the task of preparing such an authoritative work, it became clear at the outset that it could not be the product of any one author. With the realization that such an undertaking required special expertise on diverse subject areas, contributions were invited from recognized authorities both in the United States and abroad. As the work progressed, it also became apparent that the information prepared by the authors could not be contained in one volume. It was therefore decided that the subject matter could logically be subdivided into three areas: (1) Materials, Structural Elements, and Safety, (2) Frames, Slabs, and Shells-Analysis and Design, and (3) Design, Performance, and Special Problems. Publication of the work has accordingly been divided into three volumes.

The selection of the general contents and the arrangement of the material in three volumes has been dictated by the need to provide a broad coverage of the current state of the art and science of reinforced concrete engineering, as well as by the limitations of producing books of reasonable size and unity of subject matter. An attempt has been made to develop some consistency in style and notation and to eliminate duplication of subject matter. However, the individual authors have retained primary responsibility for content, style, and point of view of the particular chapter which they contributed.

The authors and the editor are indebted to numerous sources for permission to reproduce photographs, tables, and diagrams. Wherever feasible, credit to the original source has been given in the text. The editor gratefully acknowledges the authors' cooperation during the lengthy period of assembling and completing this manuscript. Whatever merit the reader may find in this work is due entirely to the authors' efforts.

Boris Bresler
Berkeley, California

1

Fresh Concrete—Materials and Properties

P. K. MEHTA
MILOS POLIVKA

1.1 INTRODUCTION

In its simplest form, plain concrete is made up of a cementitious material, water, and aggregate. Aggregate usually comprises 60 to 75% of the total volume of structural concrete. Generally, 1 to 2% air is entrapped in concrete, but for certain purposes up to about 8% air entrainment in the form of very minute bubbles can be incorporated with the addition of special admixtures. Water reducing admixtures as well as admixtures capable of either accelerating or retarding the setting and hardening characteristics of cement also find frequent application as a part of concrete mix design.

Properties of fresh concrete, such as consistency, workability, and setting time, as well as properties of hardened concrete, such as compressive strength, tensile strength, shrinkage, creep, and durability can be controlled by careful selection of the characteristics and the proportions of the primary constituents of concrete, namely, the cementitious material, the water, and the aggregate. Modern concrete technology,[1] therefore, emphasizes a comprehensive knowledge of characteristics of the concrete-making materials.

1.2 CEMENTS

Any material which binds together the aggregate particles into a monolithic mass is called a cement. In general, cements used for commercial concrete

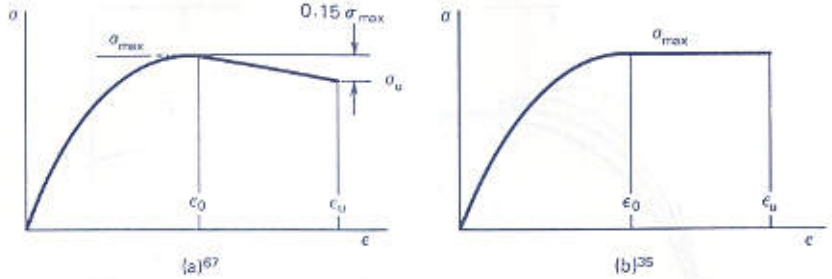

FIGURE 3.23. Typical idealizations of stress–strain curves.[67,35]

which corresponds to twice the secant modulus taken at the σ_{max} stress. On the basis of experimental data, Hognestad proposed that modulus of elasticity, in psi, be approximated by:

$$E = 1.8 \times 10^6 + 460\sigma_{max} \tag{3.9}$$

For prismatic members Hognestad also suggested that σ_{max} should be taken as $0.85f'_c$, where f'_c is compressive strength of standard cylinders.

Another commonly used expression is that proposed by the European Concrete Committee,[35] which consists of a parabola and a horizontal line, Fig. 3.23(b). An expression which appears to be generally satisfactory both in the ascending and the descending part of the curve is that developed by Desayi and Krishnan.[69]

$$\sigma = \frac{E\varepsilon}{1 + (\varepsilon/\varepsilon_0)^2} \tag{3.10}$$

Initial tangent modulus E is assumed to be twice the secant modulus at maximum stress σ_{max}, i.e.,

$$E = \frac{2\sigma_{max}}{\varepsilon_0} \tag{3.11}$$

Another expression to the stress–strain curve which shows good fit and is easy to apply is one developed by Saenz.[70] This is of the form

$$\sigma = \frac{\varepsilon}{A + B\varepsilon + C\varepsilon^2 + D\varepsilon^3} \tag{3.12}$$

where

$$A = \frac{1}{E}, \qquad B = \frac{R_E + R - 2}{R_E\sigma_{max}}, \qquad C = \frac{1 - 2R}{R_E\sigma_{max}\varepsilon_0},$$

$$D = \frac{R}{R_E\sigma_{max}\varepsilon_0^2}, \qquad R = \frac{R_E(R_\sigma - 1)}{(R_\varepsilon - 1)^2} - \frac{1}{R_\varepsilon},$$

$$R_E = \frac{E}{E_m}, \qquad R_\sigma = \frac{\sigma_{max}}{\sigma_u}, \qquad R_\varepsilon = \frac{\varepsilon_{max}}{\varepsilon_0}, \qquad E_m = \frac{\sigma_{max}}{\varepsilon_0},$$

and

σ_u = stress at failure.

Saenz's expression thus involves the modular ratio R_E, the stress ratio R_σ, and the strain ratio R_ε. It should be remembered, however, that in his, as well as in other expressions, ε_{max} is not an intrinsic property of concrete but depends on the rate of loading. The strain at failure should be clearly distinguished from the strain at the maximum applied load. The latter is nearly independent of the strength of the concrete, i.e., all concretes reach their maximum strength at the same strain, approximately 0.002, providing they are loaded at the same rate.[71]

This applies to concretes made with normal-weight aggregate; when lightweight aggregate is used, the strain at the maximum stress may be somewhat larger—up to 0.003. The general shape of the stress–strain relation of lightweight aggregate concrete has become of increased interest in recent years because this material is now being used in the construction not only of beams and slabs but also of columns.[72]

With the majority of lightweight aggregates, the slope of the ascending part of the stress–strain curve is considerably smaller than in concretes of the same strength and aggregate content made with normal-weight aggregate. This is considered further in the succeeding section. As far as the descending part of the stress–strain curve is concerned, the behavior of lightweight aggregate concrete depends primarily on the strength of the aggregate particles as compared with the strength of the surrounding mortar. If the aggregate is the weaker of the two, failure of the concrete takes place by rupture of the aggregate particles; such failure is sudden and may even be explosive. The stress–strain curve is of the shape shown in Fig. 3.24(a).

If, however, the coarse aggregate particles are not weaker than the mortar, the descending part of the stress–strain curve can be fully developed; failure is gradual and is reached by a widening of inclined cracks and spalling of the compression specimen. In such a case, the general form of the stress–strain curve is similar to that for concrete made with normal-weight aggregate but there are differences between lightweight aggregates of different types. Figure 3.24(b) shows behavior for sintered fly ash and for expanded clay aggregates in 3000 psi concretes. It may be added that the effect of the rate of loading on the ascending part of the stress–strain curve of lightweight aggregate concrete is smaller than with normal-weight aggregate.

While Fig. 3.24(b) shows that there are differences in the stress–strain curves of concretes of the same strength but made with different aggregates, these differences are not highly significant for ultimate strength design purposes. This is especially so in beams; in columns, the ductility and the load

commercially available masonry cements varies from 1000 to 2000 psi. ASTM C91 specifies a minimum compressive strength of mortar cubes of 500 psi at 7 days and 900 psi at 28 days.

Oil-Well Cements. These find applications in the sealing of porous beds in oil wells, and in the cementing of steel casings to the walls of the wells. Portland cement slurries required for such purposes must remain pumpable at the high temperature and high pressure conditions prevalent in oil wells. Slow-setting, coarsely ground cements, having relatively low $C_3S:C_2S$ ratio, and low A:F ratio, are suitable for use in oil wells. Set retardation can also be achieved in Type I or Type II portland cement by intergrinding a suitable set-retarding admixture. The American Petroleum Institute has issued a standard (API Standard 10A) which recognizes six classes of oil well cements, each class being applicable for use at certain range of well depths.

Plastic Cements. These, like masonry cements, are generally used for making mortar, plaster, and stucco. However, they have relatively higher rates of strength development than masonry cements. Plastic cements are produced by adding a suitable plasticizing agent—up to 12% of total volume—to Type I or Type II portland-cement clinker during the cement grinding operation.

Portland–Pozzolan Cements. These are principally used for mass concrete construction of large hydraulic structures such as dams, marine wharfs, and bridge piers. They are manufactured either by intergrinding portland-cement clinker with a suitable pozzolanic material or by blending a finely ground pozzolan with portland cement. ASTM Standard C595 specifies that the pozzolan content of the cement can range from 15 to 40% by weight of the portland–pozzolan cement.

A *pozzolan* is an amorphous or cryptocrystalline, reactive, siliceous material which by itself possesses no cementitious properties. Natural pozzolans consist of opaline shales, volcanic ashes, zeolites, etc., whereas processed pozzolans include calcined clays and shales, fly ash, etc. When present in an aqueous environment containing $Ca(OH)_2$, pozzolans are capable of combining slowly with lime to form calcium silicate hydrates possessing cementing properties. Since hydrated portland cements contain about 25% $Ca(OH_2)$, the presence of a pozzolan together with portland cement helps to convert a poorly cementitious $Ca(OH)_2$ into superior cementing material at later ages.

The major advantage of portland–pozzolan cements lies in their slower rate of heat liberation. The harmful effects of tensile strains caused by temperature changes in a mass concrete structure may thus be minimized if an excessive temperature rise is prevented by using this type of cement. In spite of their lower compressive strength at early ages, the ultimate compressive strength of a portland–pozzolan cement may equal or even exceed the compressive strength of the portland cement.

Concretes made with portland–pozzolan cement also show better resistance to sulfated and weak acidic waters. ASTM Standard C595 specifies four types of portland–pozzolan cements, including two types containing air-entraining additives. Frequently a pozzolan is added as a separate admixture to a portland cement concrete. Pozzolans used for this purpose are covered by ASTM C618, and discussed later in this chapter under *mineral admixtures*.

Portland–Blast-Furnace-Slag Cements. These possess superior resistance to sulfate attack and are, therefore, very suitable for concrete constructions which are in contact with sea water or with soils and water containing sulfates. Like portland–pozzolan cements, they are of moderate-heat type when compared to Type I portland cement. Type IS cement (ASTM C595) is made by intergrinding Type I portland-cement clinker and granulated blast-furnace slag, the proportion of the latter may range from 25 to 65% by weight of cement. When Type IS cement is ground finer than Type I portland cement, it may have about the same rate of strength development as Type I portland cement. A corresponding cement containing air-entraining agent is designated in ASTM C595 as Type IS-A.

Blast-Furnace Slag. A waste product in the manufacture of pig iron, blast-furnace slag contains high proportions of lime silica, and alumina. When quenched with a jet of cold water, it granulates to a reactive product because quick cooling prevents crystallization to stable phases. Hydration of granulated blast-furnace slag to products possessing cementitious value is accelerated in the presence of portland cement.

Water-Proofed Cements. These are portland cements which are specially processed to improve their storage life under prolonged storage conditions in a humid environment. Sometimes manufacturers claim that these cements produce more impermeable concrete than ordinary portland cement. However, this claim is not fully established. The cements are produced by intergrinding portland cement with a small amount of oleic acid or stearic acid or their calcium or aluminum salts.

White Cement and Colored Cements. These are primarily used for architectural purposes such as decorative concrete, precast curtain walls, and tile grout. White cement is also used as a base material for cement paint, and colored cements. White cement is a portland cement made with raw materials containing negligible amounts of iron and manganese oxide. The selection of raw materials, fuel, processing equipment, and processing conditions are so controlled that the color of the final product is white instead of grey.

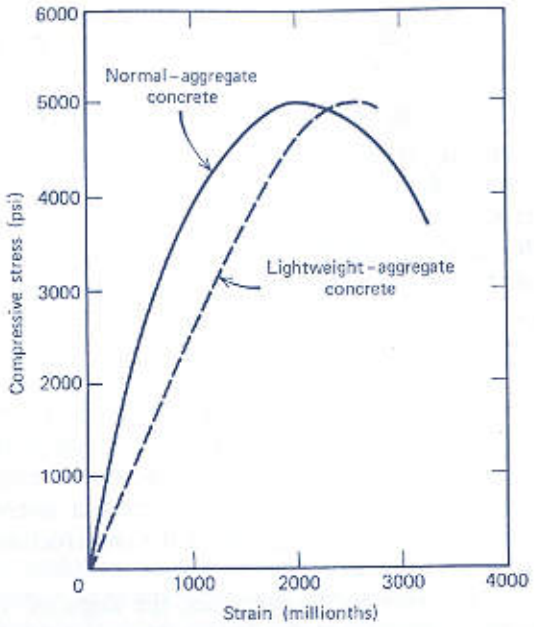

FIGURE 3.24(a). Stress–strain curve for lightweight aggregate concrete when the aggregate particles are weaker than the cement paste.[72]

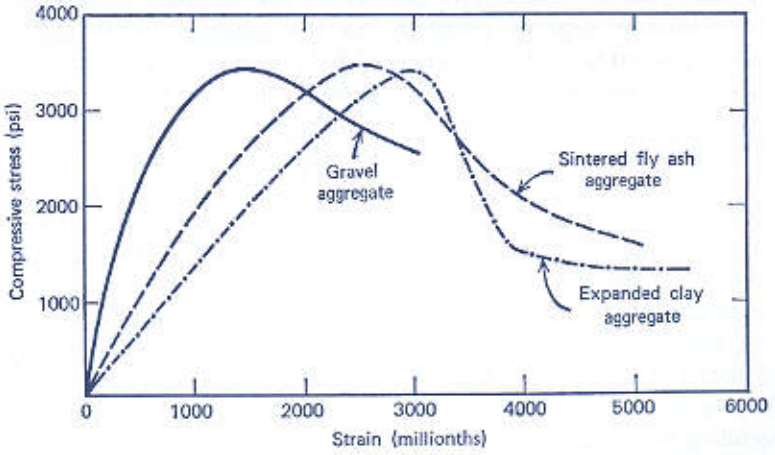

FIGURE 3.24(b). Typical stress–strain curves for concretes of the same strength but made with different aggregates.

capacity may be adversely affected if the ultimate strain is lower than 0.0035 and significantly so if it is lower than 0·0025. On the whole, however, the strength and rotational capacity of columns made with sufficiently strong lightweight aggregate concrete exhibit the same characteristics as when normal-weight aggregate is used.[72]

3.9.2 Modulus of Elasticity

From the foregoing it will be apparent that the modulus of elasticity of concrete does not have a unique value but a value determined in a specified manner is needed in design. The modulus normally used in practice is the secant modulus. ASTM C469-65 (1970) prescribes its determination at a stress–strength ratio of 0.4, but in special cases the upper stress limit may be taken as 0.15, 0.33, or 0.50 of the ultimate strength.[73] For the results of various tests to be comparable it is clearly essential that the stress–strength ratio used be the same.

In design calculations, advantage is frequently taken of the relation which exists between the modulus of elasticity, unit weight, and the strength of concrete. The expression recommended by the ACI Building Code 318-1971 is

$$E = w^{1.5}33\sqrt{f'_c} \tag{3.13}$$

where E is the secant modulus of elasticity in psi, f'_c is the compressive cylinder strength in psi, and w is the unit weight of concrete in lb/ft³. For concrete with unit weight of 150 lb/ft³, the expression reduces to $E = 57{,}000\sqrt{f'_c}$, and with unit weight of 105 lb/ft³, $E = 34{,}000\sqrt{f'_c}$.

Since the modulus of elasticity of concrete is affected by the content of aggregate, the ACI expression is valid only within the usual range of structural mixes but not, for instance, for the very lean mixes used in mass concrete. Furthermore, the modulus of elasticity of concrete is influenced also by the shape and surface characteristics of coarse aggregate as these are relevant to the development of bond microcracking (see Section 3.2.1).

As the modulus of elasticity of aggregate E_a is generally different from that of the paste E_p, the modulus of elasticity of concrete E can be predicted using an appropriate model of the composite material. Four principal types of composites have been suggested. Hansen[74] considered two models: equal strain (combined hard material) and equal stress (combined soft material), Fig. 3.25(a) and (b). The expressions for the modulus of elasticity are:

$$\text{Equal strain:}\quad E = E_a V_a + E_p V_p \tag{3.14}$$

$$\text{Equal stress:}\quad \frac{1}{E} = \left(\frac{V_a}{E_a} + \frac{V_p}{E_p}\right) \tag{3.15}$$

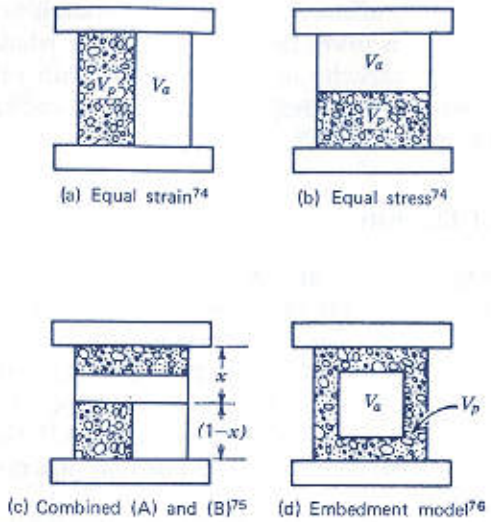

(a) Equal strain[74] (b) Equal stress[74]

(c) Combined (A) and (B)[75] (d) Embedment model[76]

FIGURE 3.25. Models for two-phase composite materials.[74,75,76]

where V_a and V_p are volume concentrations in the concrete of aggregate and paste respectively.

Hirsch[75] proposed a model of the composite material consisting of a portion where equal stress behavior applies, and a portion where equal strain governs the behavior, Fig. 3.25(c). If X is the fraction of total volume for which the equal stress model is applicable, then

$$E = X\left[\frac{V_a}{E_a} + \frac{V_p}{E_p}\right] + (1 - X)[E_a V_a + E_p V_p] \qquad (3.16)$$

Counto[76] proposed a more complex model in which the aggregate is embedded in a paste matrix, Fig. 3.25(d). For this model:

$$\frac{1}{E} = \left(\frac{1 - \sqrt{V_a}}{E_p}\right) + \frac{\sqrt{V_a}}{E_a\sqrt{V_a} + E_p(1 - \sqrt{V_a})} \qquad (3.17)$$

where V_p and V_a are volume concentrations in the concrete of paste and aggregate respectively.

The cement paste, too, can be considered as a combined soft material consisting of hard grains of unhydrated cement embedded in a continuous soft component of cement gel and pores. But the gel and pores phase is a combined hard material, with the pores having a modulus of elasticity of zero. Because modulus of elasticity of cement gel cannot be determined by experiment, we have to rely on models based on combinations of paste and aggregate. The modulus of elasticity of cement paste, E_p, lies between 1 and 4

million psi,[75] and is lower the higher the water–cement ratio. For instance, at a water–cement ratio of 0.55, the modulus is only half as large as at 0.3.

The modulus of elasticity of concrete depends on the age of the specimen; when concrete is exposed to weather, the increase in modulus with age is greater than the increase in strength.

In general, lightweight-aggregate concrete has a modulus of elasticity between 40 and 80% of concrete made with normal-weight aggregate when the two concretes have the same strength. An interesting point, however, is that, since the modulus of many lightweight aggregates differs little from that of cement paste, the aggregate content has only little effect on the modulus of lightweight-aggregate concretes.

An increase in temperature between 40 and 150°F slightly decreases the modulus of elasticity of concrete; at low temperatures, there is a substantial increase, e.g. at −20°F the modulus can be 50% higher than at room temperature.

3.9.3 Strain Capacity

In design calculations concerned with deformations and rotations near the ultimate, it is important to know the maximum strains that can be developed in concrete. The strain corresponding to maximum stress appears to vary within a limited range, 0.002 to 0.0025, for concretes of different strengths, Fig. 3.26. On the other hand, the strain at, or very near, the failing

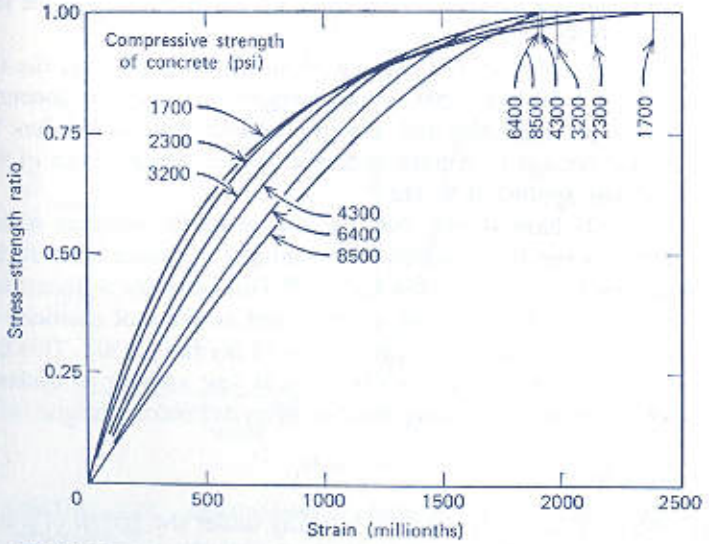

FIGURE 3.26. Relation between stress–strength ratio and strain for concretes of different strengths.[77]

load is usually higher the lower the strength of concrete. The following values may be taken as typical:

Compressive Strength, psi	Maximum Strain at Failure, 10^{-6}
1000	4000
2000	3700
4000	3500
6000	3200
10000	2500

The strain is somewhat lower for high contents of aggregate.[80]

As far as the tensile strain in flexure is concerned, the influence of strength on ultimate strain seems to be in the reverse direction to that in compression, viz. the ultimate strain is higher the higher the strength.[78] Strength is not the only factor influencing the ultimate tensile strain: generally, the larger the aggregate used and the more rounded it is, (i.e., the lower the bond) the lower the tensile strain at the maximum stress reached. However, if the descending part of the stress–strain curve is allowed to develop, very large strains can be achieved with large and rounded aggregates.[78] Aggregate content also influences the maximum tensile strain developed in that the strain is higher the lower the aggregate content.[79]

The above values refer to static loading. With dynamic loading, the trend of tensile strains is similar, at least as far as aggregate content is concerned. Concrete with gravel aggregate and a water–cement ratio of 0.5 has been found to have an average final peak dynamic surface tensile strain of 93×10^{-6} when load was applied at 90 Hz.[79]

Compression tests have shown that the elastic strain increases with the number of cycles in specimens which fail in fatigue but there is no such increase in specimens that do not fail in fatigue.[68] This behavior is illustrated in Fig. 3.27, which shows the decrease in the secant modulus of elasticity with the number of cycles expressed as a proportion of the fatigue life. This figure is of interest in that the modulus of elasticity at any number of cycles can be used in estimating the remaining number of cycles before fatigue failure.

3.9.4 Poisson's Ratio

Like other materials, concrete deforms laterally under the action of a longitudinal (axial) stress. If the lateral strain is ε_l and the axial strain ε_a, the volumetric strain ε_v is given by $\varepsilon_v = \varepsilon_a - 2\varepsilon_l$. Figure 3.28 shows that with an

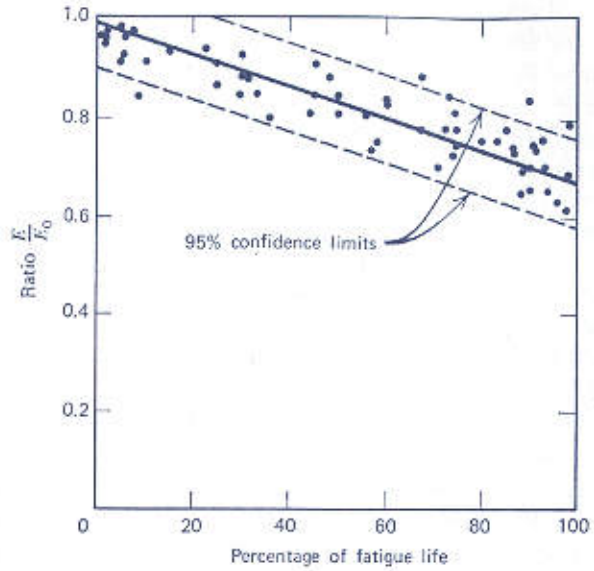

FIGURE 3.27. Relation between the ratio of the tangent modulus of elasticity after a number of cycles of loading to the initial modulus of elasticity and the percentage of fatigue life.[68]

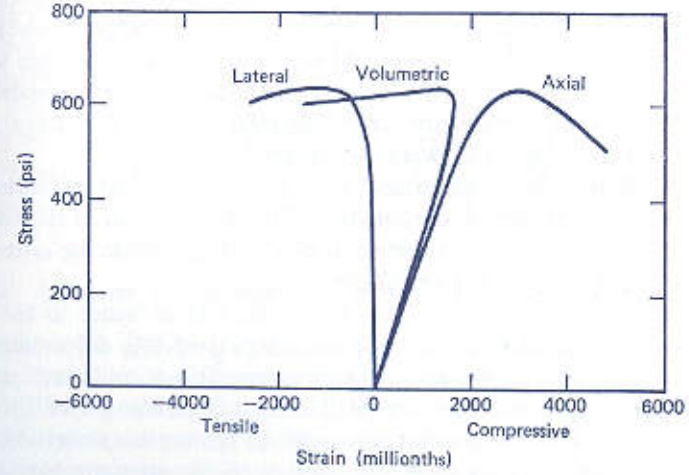

FIGURE 3.28. Development of strain in concrete: axial, lateral, and volumetric.[50]

increase in the axial stress, the volumetric strain (contraction) first increases, indicating that densification of concrete takes place. However, at some stress, the rate of change in volume changes sign and eventually an increase in volume takes place. This means that extensive cracking has developed and the concrete is, strictly speaking, no longer a continuous body. The stress under which this occurs is higher the higher the strength of concrete.

The value of the ratio of ε_l to ε_u in the early stages, i.e., of the Poisson's ratio, is generally between 0.15 and 0.20, sensibly regardless of the type of aggregate used. Poisson's ratio is lower the higher the aggregate content when normal-weight aggregate is used.[81] Neat cement paste can have a Poisson's ratio as high as 0.25.[82] Under biaxial stress, Poisson's ratio has been measured to be 0.20 in compression–compression, 0.18 in tension–tension, and between 0.18 and 0.20 for compression–tension.[39]

Poisson's ratio for creep strains, which may be called creep Poisson's ratio, is approximately the same as Poisson's ratio when the sustained load is uniaxial. However, under sustained multiaxial compression, creep Poisson's ratio is smaller, ranging between 0.09 and 0.17; the value is smaller the larger are the lateral stresses relative to the axial stress.[83] This means that the volume of concrete decreases with progress of creep.

3.10 SHRINKAGE OF CONCRETE

Concrete is distinguished from many of the other structural materials by having definite nonelastic deformations under nearly all practical conditions of service. In the present section, we deal with those volume changes which occur independently of externally imposed stresses and of temperature changes. These volume changes are commonly referred to as shrinkage, even though negative shrinkage, i.e. swelling, can also occur.

Broadly speaking, shrinkage arises from two causes: loss of water on drying and volume changes on carbonation. The deformation in the former case will, for brevity, be simply referred to as shrinkage, while the latter will be explicitly called carbonation shrinkage.

Let us consider the behavior of concrete when loss of water to the ambient medium (unsaturated air) takes place. A part of this deformation is reversible under alternating wet and dry storage conditions, and is referred to as moisture movement, the term irreversible shrinkage being used for that part of the deformation which is not recovered on subsequent rewetting. The process of moisture diffusion from the interior of the concrete toward its surface is exceedingly slow and complex. The surface dries more rapidly than the interior and therefore "free" shrinkage of concrete tends to develop primarily in the outer periphery of the section. The nonuniform distribution of this free shrinkage and the requirement for plane strain induce tensile

stresses in the outer fibers and compressive stresses in the inner fibers. The uniform "apparent" shrinkage is the combined result of the "free" shrinkage and the instantaneous and creep deformations caused by the induced stresses. Thus free unrestrained shrinkage is possible only in thin sections of concrete where uniform drying is achieved very quickly. However, the term free shrinkage is used sometimes to designate shrinkage in plain concrete specimens unrestrained by external containment (forms) or internal reinforcement.

Although shrinkage and loss of water are in a cause-and-effect situation, their relation is not simple. When drying of concrete begins, the water lost first is the free water held in the capillaries; this causes practically no shrinkage. As drying continues, adsorbed water is removed and the change in the volume of unrestrained cement paste at that stage is equal approximately to the loss of a water layer one molecule thick from the surface of all gel particles. Since the "thickness" of a water molecule is about 1 % of the gel particle size, a linear change in dimensions of cement paste on complete drying would be expected to be of the order of 1 %;[84] values up to 0.4 % have actually been observed, but the overall change in the volume of drying concrete is less than the volume of water removed.

The loss of water occurs from the cement paste only, but for engineering purposes we measure the overall shrinkage of the concrete. This is much smaller than the free shrinkage of neat paste owing to the restraining effect of the aggregate and inner nondrying portion. For design purposes, shrinkage is regarded as an ordinary linear strain, which is added to the elastic and creep strains in the determination of deformations, curvature, and deflection.

From the above discussion it is apparent that shrinkage is greatly influenced by the magnitude of the surface area of cement paste being desorbed. It is not surprising therefore that high-pressure-steam-cured cement paste, which is microcrystalline and has a low specific surface, shrinks only 1/10 to 1/5, and sometimes even only 1/17, as much as a similar paste cured normally.

3.10.1 Influence of Aggregate on Drying Shrinkage

Typical values of drying shrinkage of mortar and concrete specimens, 5 in. square in cross-section, stored at a temperature of 70°F and a relative humidity of 50 % for 6 months are given in Table 3.2, but these values are no more than a guide because shrinkage is influenced by many factors.

An important factor is the aggregate through its restraining effect on the free shrinkage of neat cement paste. The shrinkage of concrete, s_c, has been found to follow the relation[86]

$$s_c = s_p(1 - g)^n \tag{3.18}$$

TABLE 3.2. Typical Values of Shrinkage of Mortar and Concrete Specimens, 5 in. Square in Cross-Section, Stored at a Relative Humidity of 50% and 70°F.[85]

Aggregate–Cement Ratio	Shrinkage after 6 Months (10^{-6}) for Water–Cement Ratio of			
	0.4	0.5	0.6	0.7
3	800	1200	—	—
4	550	850	1050	—
5	400	600	750	850
6	300	400	550	650
7	200	300	400	500

where s_p is shrinkage of neat paste, g is the volume concentration of aggregate in the concrete (aggregate content by volume), and n is an empirical constant, which has been found to vary between 1.2 and 1.7.[87] Strictly speaking, the unhydrated portion of cement grains should be included in the aggregate content. A typical relationship between s_c/s_p and aggregate content is shown in Fig. 3.29.

We can see that the volumetric content of aggregate is of considerable

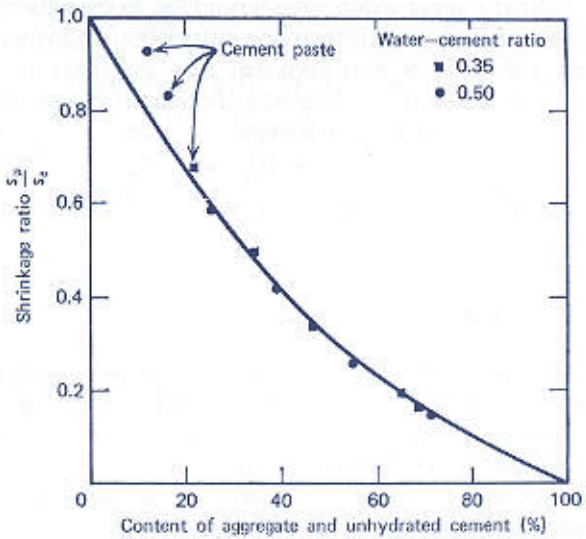

FIGURE 3.29. Influence of the volumetric content of aggregate and unhydrated cement on the ratio of the shrinkage of neat cement paste to the shrinkage of concrete.[88]

influence on the magnitude of shrinkage actually developed by concrete. The maximum aggregate size and its grading are not primary factors and affect shrinkage only in so far as they may control the leanness of the mix, i.e., the aggregate content. For instance, changing the maximum aggregate size from 1/4 in. to 6 in. means that the aggregate content can rise from 60 to 80% of the total volume of concrete; as a result, as shown in Fig. 3.29, shrinkage decreases to 40% of the value with the smaller aggregate.

The extent of restraint offered by the aggregate depends on its elastic properties. There thus exists a relation between shrinkage and the modulus of elasticity of the aggregate used.[97] Although there is no general quantitative relation, typical influence of aggregate type on shrinkage is shown in Fig. 3.30.

The range of shrinkage for the usual lightweight-aggregate and normal-weight-aggregate concretes is shown in Fig. 3.31. If the lightweight aggregate has a large content of fines (smaller than No. 200 sieve), the void content may be high, and consequently shrinkage larger than in Fig. 3.31 is possible.

Very few aggregates in common use are themselves subject to shrinkage. Those that are usually have also a high absorption so that an absorption test can be used to check the possibility of an aggregate being of the shrinking type. If the absorption is high, shrinkage tests on concrete made with the suspect aggregate should be performed.

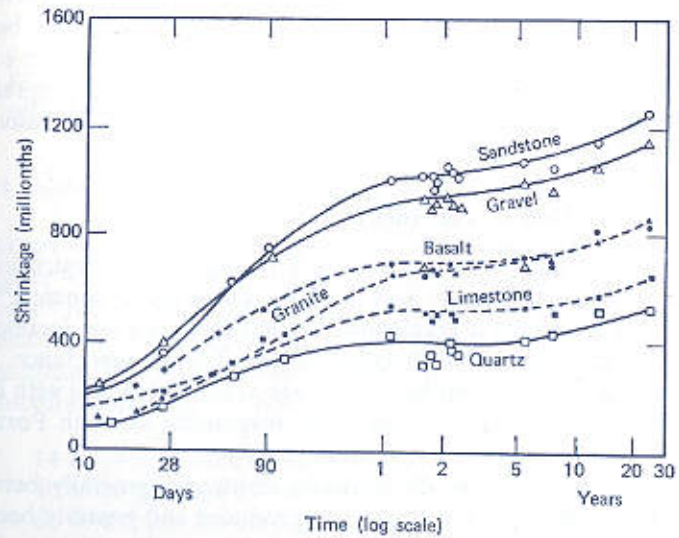

FIGURE 3.30. Shrinkage of concretes of fixed mix proportions but made with different aggregates, and stored in air at 70°F and a relative humidity of 50%.[89] (Time reckoned since end of wet curing at the age of 28 days.) (Reprinted by permission of the American Society for Testing and Materials, Copyright ASTM.)

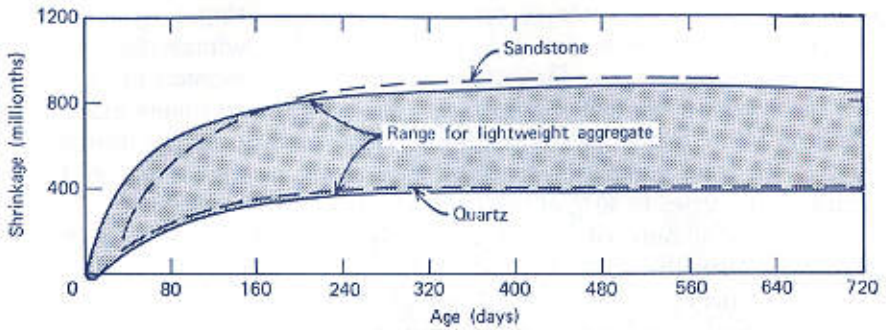

FIGURE 3.31. Ranges of shrinkage of typical lightweight and normal-weight aggregate concretes.[89,90] (Reprinted by permission of the American Society for Testing and Materials, Copyright ASTM.)

The presence of clay in aggregate lowers its restraining effect on shrinkage, and since clay itself is subject to shrinkage, clay coatings on aggregate can increase shrinkage by up to 70%.[84]

3.10.2 Influence of Water Content

Water content of concrete is sometimes considered as a primary factor in shrinkage. While some indication of the magnitude of shrinkage can be obtained from the water content of the mix (see Fig. 3.32), the main role of the water content is in reducing the volume content of the restraining aggregate. Thus the relation between water content and shrinkage is not a fundamental one.

3.10.3 Influence of Cement and Admixtures

The influence of the fineness of cement on shrinkage is still controversial. High fineness does not necessarily lead to higher shrinkage of concrete[92] but it is possible that shrinkage is accelerated so that there is some increase in cracking. Chemical composition of cement is not of large importance, provided the cement is properly retarded. Shrinkage of concrete made with high-alumina (aluminous) cement is of the same magnitude as when Portland cement is used, but takes place much more rapidly.[85]

The addition of calcium chloride increases shrinkage, generally between 10 and 50%, probably because a finer gel is produced and possibly because of greater carbonation of the more mature specimens with calcium chloride.[93] The influence on shrinkage of other admixtures cannot be generalized but those admixtures which allow a reduction in water content usually do not adversely affect shrinkage. Air entrainment also does not appear to influence shrinkage.[90]

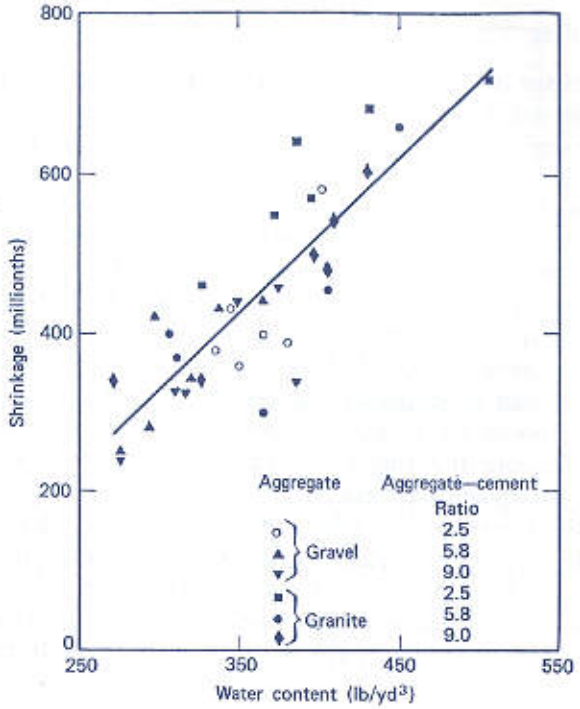

FIGURE 3.32. Relation between the water content of fresh concrete and drying shrinkage.[91]

3.10.4 Influence of Curing and Storage

Shrinkage occurs whatever the age at which drying begins and continues thereafter for a long time: some movement has been observed even after 28 years[89] but it is possible that a part of the long-term shrinkage is due to carbonation. In any case, the rate of shrinkage at long ages is so low as not to be significant. Not all concretes shrink at the same rate but for the usual range of structural concretes exposed to a relative humidity of 50 and 70%:

14 to 34% of the 20-year shrinkage occurs in 2 weeks;
40 to 80% of the 20-year shrinkage occurs in 3 months; and
66 to 85% of the 20-year shrinkage occurs in 1 year.

The magnitude of shrinkage depends on the relative humidity of storage (Fig. 3.33) but is unaffected by the rate of drying, providing this is not extreme as fracture may then occur. However, rapid drying does not allow a relief of stresses by creep so that cracking may result (see Section 3.12).

3.10.5 Size Effect

While free shrinkage is an inherent property of a given mix under given conditions, the observed shrinkage is governed by the extent of drying that can take place. The size of the concrete member undergoing drying is therefore a significant factor.

The influence of size on shrinkage illustrates the fact that at any instant different parts of a concrete member have dried to a different extent, and of course moisture loss from the concrete takes place only at the surface. Shrinkage is thus nonuniform and a restraint of the parts nearer the surface by the wetter core is inevitable. (This restraint is additional to the restraint by aggregate and by reinforcement.) As a result, any but a small concrete specimen is subjected to differential shrinkage. The differential strain is compensated by strains due to internal stresses, tensile near the surface and compressive in the core. If drying is from surfaces unsymmetric with respect to member axes, warping can result.

The differential extent of drying is reduced with time as drying extends inwards but the progress of drying is extremely slow. Desiccation was observed to reach the depth of 3 in. in 1 month but only 2 ft after 10 years.[87] Ross[91] found the difference between shrinkage strains in a mortar slab at the surface and at a depth of 6 in. to be 470 × 10^{-6} after 200 days. If the modulus

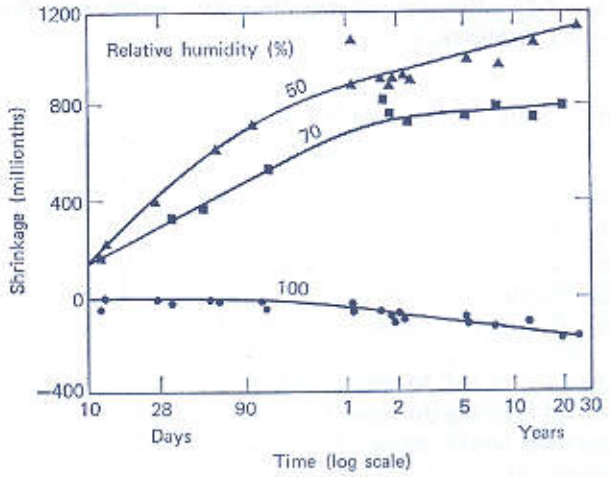

FIGURE 3.33. Relation between shrinkage and time for 4-in. concrete specimens stored at different relative humidities.[89] (Time reckoned since end of wet curing at the age of 28 days. Type I cement, 1:5.67 mix, water–cement ratio = 0.59.)

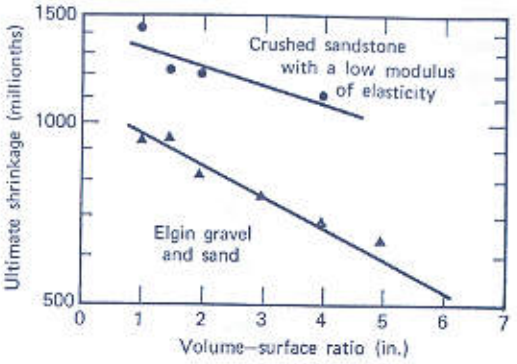

FIGURE 3.34. Relation between ultimate shrinkage and volume–surface ratio.[98]

of elasticity of mortar is 3 × 10^6 psi the differential shrinkage would induce a stress of 1400 psi; since the stress arises gradually it is relieved by creep, but even so surface cracking may result. Mathematical analyses to determine stresses and deformations in concrete prisms due to nonuniform shrinkage and based on diffusion theory have been carried out.[95,96] However, these use approximations of shrinkage diffusivity which are not clearly defined for all types of concrete.

Size effect can be taken into account indirectly by the ratio of the drying surface to the volume of the concrete enclosed within. The shape of the specimen has also some effect on the actual shrinkage but this factor is of secondary importance. Figure 3.34 illustrates the influence of the volume–surface ratio on shrinkage. It is useful to note that there is a linear relation between this ratio and the logarithm of time required for half the shrinkage to take place. This is valid for concretes made with different aggregates: in other words, the rate at which the final value of shrinkage is approached is unaffected by the type of aggregate.[98]

3.10.6 Swelling and Moisture Movement

Figure 3.33 also shows the magnitude of swelling when concrete is stored from the time of casting and over prolonged periods in water: this swelling is about six times smaller than shrinkage in air at a relative humidity of 70% or eight times smaller than shrinkage at 50%. Swelling takes place more rapidly than shrinkage and is usually completed in 6 to 12 months.

Swelling is accompanied by an increase in weight and is due to the adsorption of water by the cement gel. The adsorbed molecules force the gel particles further apart and this creates a swelling pressure. Also, the ingress of water

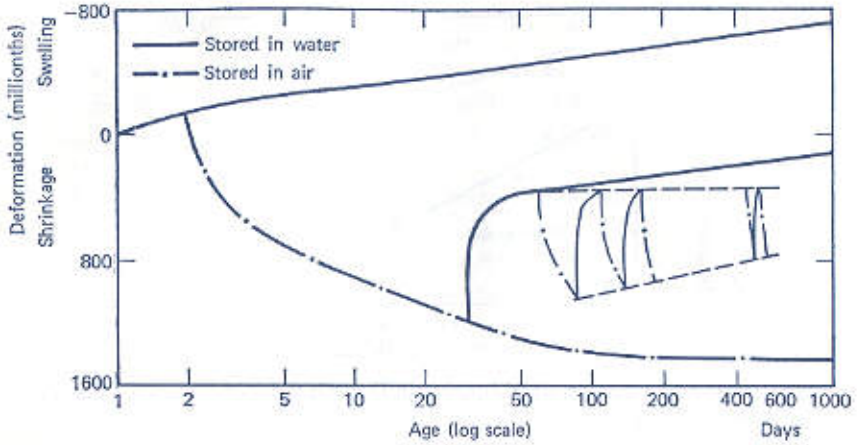

FIGURE 3.35. Moisture movement of a 1:1 cement–pulverized basalt mix stored alternately in water and in air at 50% relative humidity; cycle period 28 days.[50]

decreases the surface tension of the gel and thus causes an additional small expansion.[84]

If concrete which has been allowed to dry in air with a given relative humidity is subsequently placed in water (or at a higher humidity) it will swell. Not all initial drying shrinkage is, however, recovered, even after prolonged storage in water. For the usual range of concretes, the irreversible part of shrinkage, which is an indication of instability of the cement paste, represents between 0.3 and 0.6 of the drying shrinkage,[87] the lower value being more common.[91] Subsequent cycles of drying and wetting result in reversible deformation, known as moisture movement. Figure 3.35 shows this movement for cement paste subjected to alternating storage in water and in air at a relative humidity of 50%.

The magnitude of the moisture movement varies with the range of humidity and composition of concrete being smaller the larger the aggregate content. Lightweight concrete has a higher moisture movement than concrete made with normal weight aggregate.

3.10.7 Carbonation Shrinkage

In addition to shrinkage upon drying, concrete undergoes shrinkage due to carbonation,[89] and most of the experimental data on drying shrinkage include the effects of carbonation. Drying shrinkage and carbonation shrinkage are, however, quite distinct in nature.

CO_2 present in the atmosphere reacts, in the presence of moisture, with hydrated cement minerals (the agent being really the carbonic acid). $Ca(OH)_2$ carbonates to $CaCO_3$, but other cement compounds are also affected, hydrated silica, alumina, and ferric oxide being produced.[85]

Carbonation shrinkage is probably caused by the dissolving of crystals of $Ca(OH)_2$ while under a compressive stress (imposed by the drying shrinkage) and depositing of $CaCO_3$ in spaces free from stress; the compressibility of the cement paste is thus temporarily increased.

The rate of carbonation depends on the moisture content of the concrete and on the relative humidity of the ambient medium. The size of the specimen is a factor too, since the moisture released by the reaction of CO_2 with $Ca(OH)_2$ must diffuse out in order to preserve hygral equilibrium between the inside of the specimen and the atmosphere. If diffusion is too slow the vapour pressure within the concrete rises to saturation and the diffusion of CO_2 into paste is practically stopped.

Figure 3.36 shows the drying shrinkage of mortar specimens dried in CO_2-free air at different relative humidities, and also the shrinkage after subsequent carbonation. Carbonation increases the shrinkage at intermediate humidities but not at 100% or 25%. In the latter case, there is insufficient

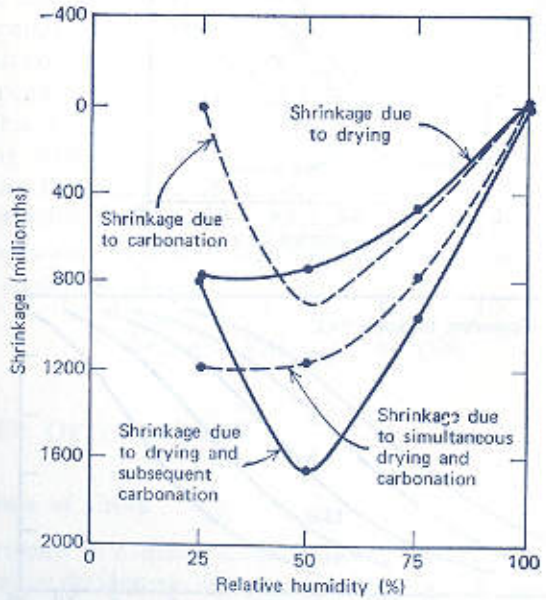

FIGURE 3.36. Influence of the sequence of drying and carbonation on shrinkage of mortar at different relative humidities.[98] (1:4 mix, Type I cement, water–cement ratio of 0.54, moist cured for 7 days.) (Reprinted by permission of the American Society for Testing and Materials, Copyright ASTM.)

water in the pores within the cement paste for CO_2 to form carbonic acid. On the other hand, when the pores are full of water the diffusion of CO_2 into the paste is very slow; it is also possible that the diffusion of calcium ions from the paste leads to precipitation of $CaCO_3$ with a consequent clogging of surface pores.[99]

3.10.8 Prediction of Shrinkage

A method for estimating shrinkage deformation has been proposed by the European Concrete Committee.[35] The effective shrinkage strain ε_{sh} of an unreinforced concrete prism is defined as

$$\varepsilon_{sh} = k_b k_c k_t \varepsilon_h \tag{3.19}$$

where

1. k_b depends on the composition of concrete; the values of this coefficient are given in Fig. 3.37(a).

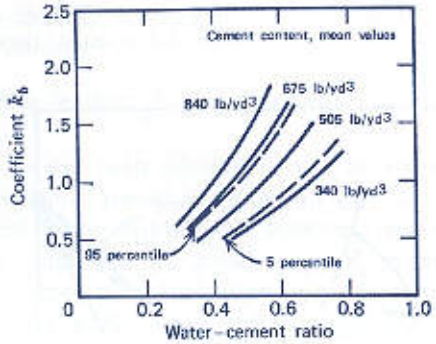

FIGURE 3.37. The European Concrete Committee shrinkage and creep prediction curves.[35]

TABLE 3.3. The European Concrete Committee Shrinkage Coefficients k_c and ε_h.

(a) Values of k_c						
Effective thickness, in.	2.3	4.5	8	12	15	20
k_c	1.20	1.00	0.80	0.65	0.57	0.50

(b) Values of ε_h							
Relative humidity of air, %	40	50	60	70	80	90	100
ε_h, millionths	420	380	330	275	210	115	0

2. k_c depends on the effective thickness of the member defined as the area A of the section divided by one-half of the perimeter in contact with the atmosphere; the values of this coefficient are given in Table 3.3.
3. k_t depends on the duration of drying and the effective thickness; the values of this coefficient are given in Fig. 3.37(b).
4. ε_h depends on the relative humidity. The values of this coefficient are given in Table 3.3 for concrete drying at temperatures below about 90°F. When drying takes place at higher temperatures, values of ε_h should be increased, but the influence of elevated temperature on shrinkage has not yet been established quantitatively. Where environmental conditions are constant, the increment of shrinkage deformation $\Delta\varepsilon_{sh}$ in an interval of time $\Delta t = (t_2 - t_1)$ can be taken as

$$\Delta\varepsilon_{sh} = k_b k_c [k_t(t_2) - k_t(t_1)]\varepsilon_h \tag{3.20}$$

3.11 CREEP OF CONCRETE

3.11.1 Nature of Creep

Creep occurs only in concrete subjected to stress, external or internal, and can be defined as the increase in strain under a sustained stress. It is important to note that creep is generally larger than the elastic deformation so that creep represents an important part of the deformation of concrete. As a result of creep, displacements and stresses change but, with the exception of prestressed concrete and slender columns,[100] the strength of structures is not adversely affected by creep.

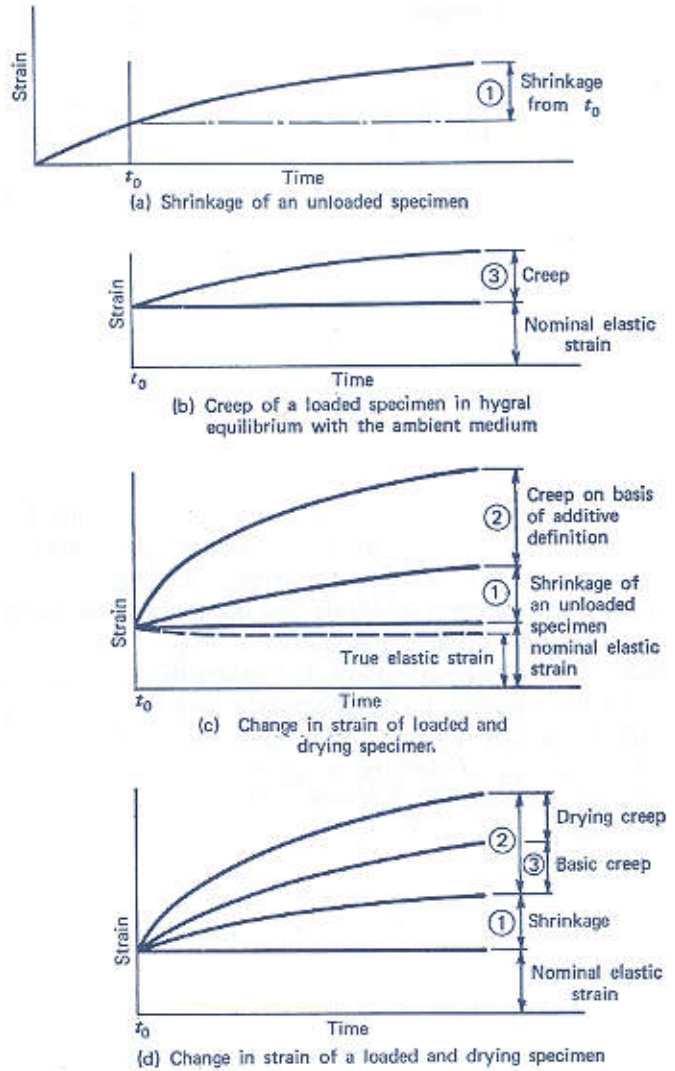

FIGURE 3.38. Definitions of creep terms.

Figure 3.38 defines the various components of deformation of concrete. The definition of creep of Fig. 3.38(b) applies when no shrinkage or swelling takes place. If a specimen is drying while under load it is usually assumed that creep and shrinkage are additive, Fig. 3.38(c). The overall increase in strain of a stressed and drying member is assumed to consist of shrinkage (equal in magnitude to that of a similar unstressed member)

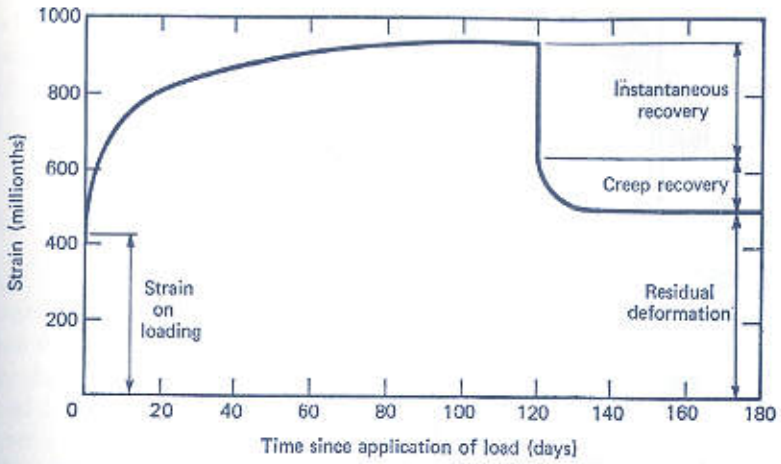

FIGURE 3.39. Creep and creep recovery of a 1:3 mortar specimen, stored in air at a relative humidity of 95%, subjected to a stress of 2150 psi and then unloaded.

and of a change in strain due to stress (creep). This approach has the merit of simplicity but not of accuracy. Creep and shrinkage are not independent phenomena to which the principle of superposition can be applied, and in fact the effect of shrinkage on creep is to increase the magnitude of creep. In the case of many actual structures, however, creep and shrinkage occur simultaneously and the treatment of the two together is from the practical standpoint often convenient. The additive approach will be followed here but it should be recognized that under drying conditions an additional creep, known as drying creep, occurs; the creep under conditions of no moisture movement to or from the ambient medium is referred to as true[101] or basic[102] creep [see Fig. 3.38(d)].

If a sustained load is removed, the strain decreases immediately by an amount equal to the elastic strain at the given age, generally lower than the elastic strain on loading. This instantaneous recovery is followed by a gradual decrease in strain, called creep recovery (Fig. 3.39). The shape of the creep recovery curve is similar to that of the creep curve, but the recovery approaches its maximum value much more rapidly.[103] The reversal of creep is not complete, and creep is thus not a completely reversible phenomenon.

Creep can also manifest itself in another way: if a stressed concrete specimen is subjected to a constant strain, there is a progressive decrease in stress with time. This is known as relaxation and is shown in Fig. 3.40.

Influence of creep on reinforced and prestresssed structures is treated in Reference 104.

Colored cements for making colored concrete can be made by intergrinding 5–10% of a suitable pigment with white cement. Listed below are the common mineral oxide pigments that are used to produce colored cements:

cobalt oxide	blue
red iron oxide	red
brown iron oxide	brown
black iron oxide	black
synthetic yellow iron oxide	buff
chromium oxide	green

1.6 CALCIUM ALUMINATE CEMENTS

Calcium aluminate cements are hydraulic cements, consisting mainly of aluminates of calcium, such as CA, CA_2, and $C_{12}A_7$. Due to their relatively high alumina content, they are also known as *aluminous cements* or *high-alumina cements*, and are usually available under different trade names, viz., Ciment Fondu (France and U.K.), Secar (U.K.), Lumnite and Alcoa CA-25 (U.S.A.), etc.

Calcium aluminate cements possess certain distinct advantages over portland cement. Concretes made with these cements are much superior to portland-cement concretes with regard to refractoriness, sulfate resistance, resistance to weak acids, and high rate of strength development. With normal concrete aggregates and 0.5 water–cement ratio about 8000 psi compressive strength can be reached in 24 h (about 80% of ultimate strength). Even higher strengths are attainable by using special aggregates and superior quality aluminate cements. The property of high early-strength development can be important for precast and prestressed concrete members, and also for emergency construction jobs requiring structures to be available for immediate use or reuse.

Regarding refractoriness, concretes made with aluminate cement and crushed firebrick aggregates are stable up to about 2400°F. With special aggregates, exposure up to 3000°F can be sustained. Since refractory lining made of cement concrete can be cast monolithically, it is more convenient to install than refractory brickwork.

CA is the major reactive aluminate phase in aluminate cements. Since commercially available limestone and bauxite are the generally used raw materials, siliceous and ferrous impurities in the final product can account for the presence of C_2AS, C_2S, and $C_xA_yF_z$ phases. A large proportion of these phases, if present, adversely affect the high early strength and the refractoriness characteristics of aluminate cement.

A major *disadvantage* has limited the structural application of aluminate cements almost exclusively to refractory concretes. It has been found that

aluminate-cement concretes suffer a gradual loss of strength, which is accelerated by heat and humidity. Over a period of several years the compressive strengths of these concretes, under warm–wet conditions, have been reduced in several instances from about 8,000–10,000 psi to less than 2,000 psi.

The cementitious properties of aluminate cement are due to the formation of hexagonal hydrates, such as CAH_{10} and C_2AH_8. The retrogression in binding strength is accompanied by conversion of the hexagonal hydrates to the more stable cubic hydrate, C_3AH_6. Due to the high heat of hydration of the anhydrous calcium aluminates, and due to the acceleration of the conversion reaction of the hexagonal hydrates to the cubic hydrates under warm–wet conditions, it is advisable to take special care in the casting and curing of aluminate-cement concretes. Special precautions include using a low water–cement ratio, prolonged periods of curing with cold water, and limited height of casting (up to 18 in.).

1.7 AGGREGATES

Aggregates make up about 70% of the total volume of concrete and, therefore, significantly influence the cost economy and the properties of fresh as well as hardened concrete. The physical properties of concrete that can be affected by aggregate characteristics include unit weight, workability, modulus of elasticity, strength, shrinkage, creep, thermal behavior, and durability.

All aggregate particles which pass through a No. 4 (0.187 in.) sieve are referred to as *fine aggregate*, while those retained on this sieve are classified as *coarse aggregate*. Natural siliceous sands are the major source of fine aggregate, although manufactured sands produced from rocks by crushing are frequently used when natural sands are not available. Natural river gravel, crushed granite, basalt, sandstone and other rocks, as well as manufactured light-weight aggregates are amongst the commonly used coarse aggregates.

When aggregates come from natural sources, it is possible to predict some of their *characteristics* from an elementary knowledge of geochemistry. It has been estimated that the upper 10 miles of Earth's crust consists of 95% igneous rock, and 5% sedimentary rocks (4% of shale, 0.75% sandstone and 0.25% limestone). On the other hand, the area of exposure of the sediments is 75% of the total land area, whereas the igneous rocks crop out in only 25% of the total land area. Although the thickness of sediments ranges from 0 to about 8 miles, over the continental areas they average only about 7500 ft.

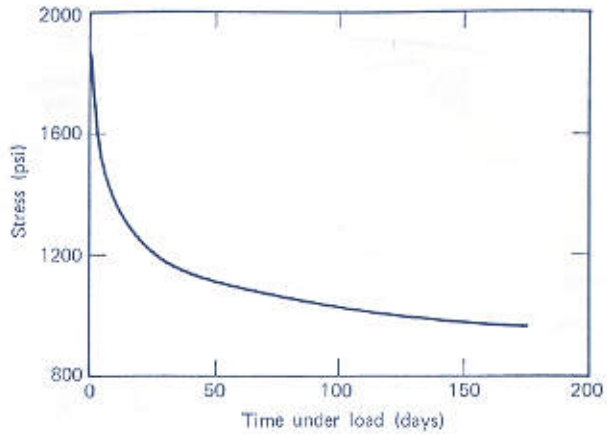

FIGURE 3.40. Relaxation of stress under a constant compressive strain of 400 × 10^{-6}.

3.11.2 Influence of Stress Intensity

Within the range of working stresses, creep is proportional to the applied stress, and it is therefore convenient for practical purposes to express creep as strain per unit stress or "specific" creep. At higher stress–strength ratios, probably 0.4 to 0.6, creep increases at an increasing rate; the departure from proportionality between creep and stress is associated with microcracking (see Section 3.2.1). Since the onset of cracking depends on the degree of

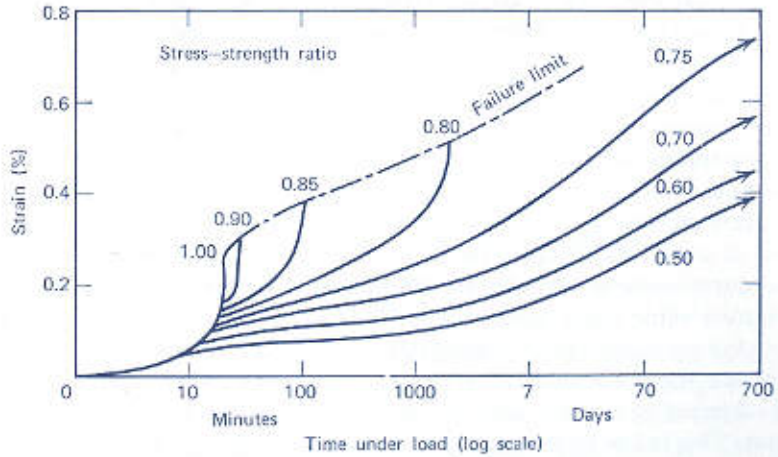

FIGURE 3.41. The strain–time relation for different stress–strength ratios.[64]

heterogeneity of the concrete, the limit of proportionality is higher in mortars (about 0.85) than in concrete. Above a stress-strength ratio of 0.8 to 0.9, creep produces failure in time. The development of strain in such a case is shown in Fig. 3.41.

3.11.3 Influence of Age at Loading

Age of concrete at loading is a factor in creep in so far as age influences the degree of hydration and the development of strength. Under conditions such that the degree of hydration remains substantially constant, the age at loading ceases to influence creep. For instance, the influence of the age at which the load is applied is much smaller in the case of dry-cured concrete. Also, at later ages the rate of creep becomes independent of the age at loading. The effect of age at loading on instantaneous and creep deformation can be shown by means of a surface, where compliance (defined as the total deformation—instantaneous and creep—produced by unit stress) is plotted as function of age at loading and time of observation, Fig. 3.42.

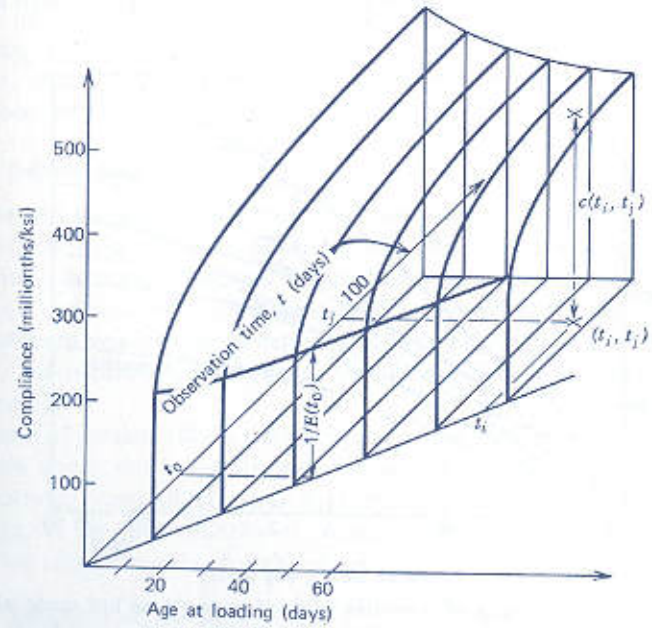

FIGURE 3.42. Influence of age at loading on instantaneous and creep deformations.

3.11.4 Influence of Aggregate

One of the important factors is the aggregate content, arising from the restraining effect of aggregate on the "free" creep of cement paste. The mode of action is similar to the restraining effect of aggregate on shrinkage. It should be noted that in the majority of the usual structural mixes, the variation in the aggregate content and therefore in creep is small.

As in the case of shrinkage, the modulus of elasticity of aggregate influences the degree of restraint to the free movement of the cement paste. Some tests have shown that the porosity of aggregate influences creep but, since aggregates with a higher porosity generally have a lower modulus of elasticity, it is not readily possible to separate the influence of these two factors.

The maximum size of aggregate, its grading and shape influence the aggregate content, and consequently influence creep. Because of the great variation in aggregate within any mineralogical or petrological type, it is not possible to make a general statement about the magnitude of creep of concrete made with aggregates of different types, and it is likely that the real factor is the modulus of elasticity of aggregate, already mentioned. As an illustration, however, the data of Fig. 3.43, obtained after 20 years' storage at a relative humidity of 50% are of interest; we may note that concrete made with sandstone aggregate exhibited creep more than twice as large as when limestone aggregate was used.

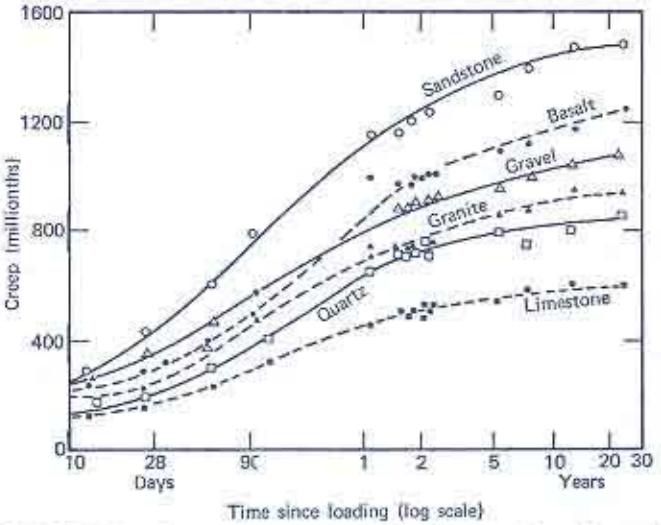

FIGURE 3.43. Creep of concretes of fixed proportions but made with different aggregates, loaded at the age of 28 days, and stored in air at 70°F and a relative humidity of 50%.[89] (Reprinted by permission of the American Society for Testing and Materials, Copyright ASTM.)

The usual normal-weight aggregates do not creep themselves but there exist a few rare exceptions.[104]

Lightweight aggregate deserves a special mention because of the rather common belief that its use leads to substantially higher creep than normal-weight aggregate. There appears to be no fundamental difference between normal and lightweight aggregates as far as the creep properties are concerned,[101] and the higher creep of concretes made with lightweight aggregates reflects only the lower modulus of elasticity of the aggregate. There is no inherent difference in the behavior of coated and uncoated aggregates or between those obtained by different manufacturing processes, but this of course does not mean that all the aggregates lead to the same creep.

Thus, the creep of structural quality lightweight-aggregate concrete is about the same as that of concrete made with ordinary aggregate at approximately the same aggregate content. There is one further interesting feature of the deformation of lightweight aggregate concrete. Because of the lower modulus of elasticity of this aggregate, the elastic deformation of lightweight aggregate concrete is larger than for concrete made with normal-weight aggregate (both concretes being of the same strength). If shrinkage is not large and creep of the two concretes is approximately the same, the ratio of time-dependent deformation to elastic deformation may be smaller in the case of lightweight aggregate than normal-weight aggregate. Thus, lightweight aggregate concrete compares favorably with normal-weight aggregate concrete, although of course the total deflection in the former case may be larger (but may be offset by the lower self-weight).

3.11.5 Influence of Cement

The type and composition of cement are not a factor in creep if the different rate of strength development of the various cements is taken into account by comparing concretes made with different cements at the same stress-strength ratio (i.e., the ratio of applied stress to the strength at the time of loading). This statement applies only to cements of Type I through V and to aluminous cement; some other cements, e.g., Portland blastfurnace cement, exhibit higher creep.[106]

Fineness of cement affects the strength development at early ages and thus influences creep, but is not an independent factor. The amount of gypsum in the cement may affect creep in a manner similar to the influence on shrinkage. In the vast majority of commercial cements, the gypsum content is near the optimum value for shrinkage and probably also for creep.

3.11.6 Influence of Strength

The influence of the strength of concrete on creep has already been mentioned, and we can state as a convenient practical approximation that, for a constant

TABLE 3.4. Creep of Concretes of Different Strengths

Compressive Strength at Time of Application of Load, psi	Ultimate Specific Creep 10^{-6} per psi	Ultimate Creep at a Stress–Strength Ratio of 0.3, 10^{-6}
2000	1.40	933
4000	0.80	1067
6000	0.55	1100
8000	0.40	1067

cement paste content and the same applied stress, creep is inversely proportional to the strength of concrete. This is illustrated in Table 3.4. Creep, therefore, increases with an increase in the water–cement ratio of the mix, as shown in Fig. 3.44. In general terms, viewing creep as a function of water–cement ratio and aggregate–cement ratio gives a correct general picture of the influence of mix proportions on creep.

All the above statements are predicated on full consolidation of concrete. If compaction is inadequate, the effect on creep is similar to the effect of capillary voids (whose presence is reflected by the influence of the water–cement ratio on creep). Thus strength of concrete (regardless of the nature of the factors influencing it) can be used as an overall parameter of creep.

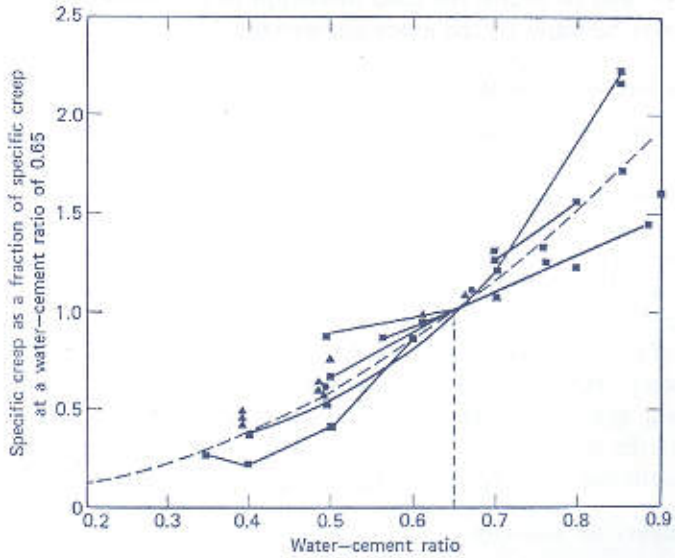

FIGURE 3.44. Specific creep as a function of water–cement ratio.[105] (Other factors adjusted.)

3.11.7 Influence of Size

As in the case of shrinkage, the size of the member is a factor in creep. Creep decreases with an increase in the size of the specimen, but when the specimen thickness exceeds about 3 ft no further effect is apparent. The influence of size is greatest during the initial period after the application of load; beyond several weeks the rate of creep is the same regardless of the size of the specimen.[98]

Because of the similarity to the size effect in shrinkage it might be thought that in creep, too, the nonuniform distribution of shrinkage within the body and the associated internal stresses are responsible for the influence of specimen size on deformation. Thus in a small specimen, the inner part of the concrete is subjected to high compressive stresses while drying takes place, and a greater creep is therefore recorded. The converse is true in a larger specimen and, even if with time the drying effect reaches the core, the concrete there will have changed substantially from the state which existed when load was first applied. A greater degree of hydration will have taken place and a higher strength will have been developed in the core so that the creep response to the creep-while-drying condition will be small. The size effect applies not to the true or basic creep, but to the increase in creep due to drying and therefore disappears when drying stops.

3.11.8 Influence of Ambient Humidity

Relative humidity is an important factor, as shown in Fig. 3.45. Strictly speaking, it is not the humidity itself that matters but the process of drying while the concrete is undergoing creep. Thus creep is not affected by the relative humidity of storage if the concrete has reached hygral equilibrium prior to loading. Likewise, at later ages the rate of creep is sensibly independent of the relative humidity (see Fig. 3.45) as by that time shrinkage is very small. The explanation of the phenomena involved is not merely in terms of an additional loss of water from the concrete; the mechanism through which relative humidity affects creep is rather complex, one of the key factors being that the equilibrium vapor pressure of the adsorbed water depends on its state of stress.[102]

3.11.9 Influence of Temperature

Information on this factor has been obtained mainly in connection with the design of prestressed concrete pressure vessels for nuclear reactors.[107,108,109] The general pattern of behavior now established with a reasonable reliability[110] is as shown in Fig. 3.46.

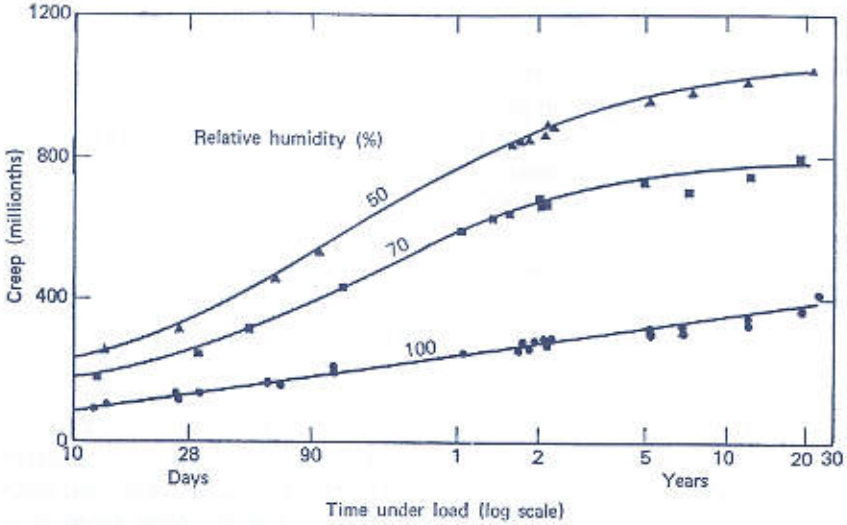

FIGURE 3.45. Creep of concrete fog-cured for 28 days, then loaded to 800 psi and stored at different relative humidities.[89] (4-in. diameter specimens, Type I cement, 1:5.67 mix, water–cement ratio = 0.59.) (Reprinted by permission of the American Society for Testing and Materials, Copyright ASTM.)

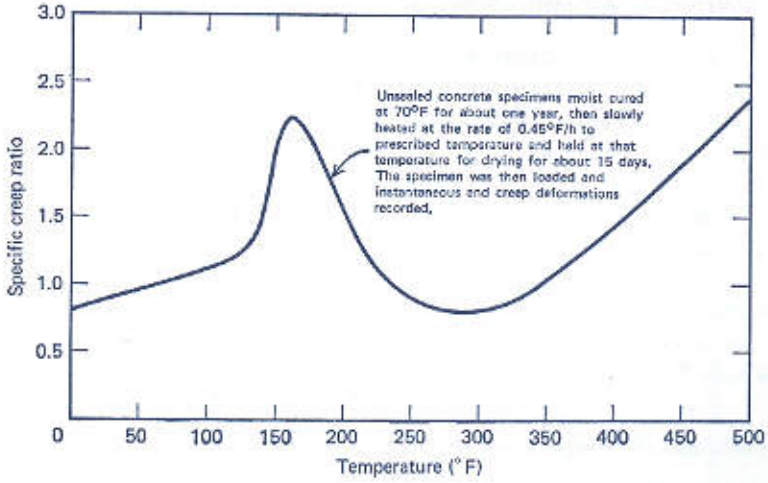

FIGURE 3.46. Specific creep at different temperatures as a ratio of specific creep at 70°F after 1 year under load.

3.11.10 Creep Under Different States of Stress

The preceding section referred to uniaxial compression but creep occurs also in other loading situations, and data on these are of value in design.

Creep takes place in tension in the same manner as in compression, the magnitude of the former, under a given stress, being higher. The difference may be as high as 100% at a relative humidity of 50% but is only 20 to 30% under mass-curing conditions. Drying enhances creep in tension as well as in compression.

Creep occurs under torsional loading, and is affected by stress, water–cement ratio, and ambient relative humidity in qualitatively the same manner as creep in compression. The creep-time curve is also of the same shape. The ratio of creep to elastic deformation in torsion was found to be the same as for compressive loading.[111]

Under uniaxial compression, creep occurs not only in the axial direction but also in the normal directions. This is referred to as lateral creep. The resulting creep Poisson's ratio was mentioned in Section 3.9.4. From the fact that there is lateral creep induced by an axial stress, it follows that, under multiaxial stress, in any direction there is creep due to the stress applied in that direction and also creep due to the Poisson's ratio effect of creep strains in the two normal directions. There is evidence[83] that the superposition of creep strains due to each stress separately is not valid, so that creep under multiaxial stress cannot be simply predicted from uniaxial creep measurements. Specifically, creep under multiaxial compression is less than under a uniaxial compression of the same magnitude in the given direction (Fig. 3.47). But even under hydrostatic compression there is considerable creep.

3.11.11 Prediction of Creep

The creep-time curves are all of similar shape, starting with a high creep rate and then having a continuously decreasing rate. For instance, for the usual range of structural concretes, loaded at ages of 28 and 90 days and stored at a relative humidity of 50 to 100%:

18 to 35% (average 26%) of the 20-year creep occurs in 2 weeks;
40 to 70% (average 55%) of the 20-year creep occurs in 3 months; and
64 to 83% (average 76%) of the 20-year creep occurs in 1 year.[89]

It is not certain whether the rate of creep ever becomes zero. The longest period for which creep data are available is 28 years, and at that time a small but measurable rate of creep was observed.[89]

Because of the similarity of all creep-time curves, the relation can be expressed in a general form and the values of creep for long periods under load

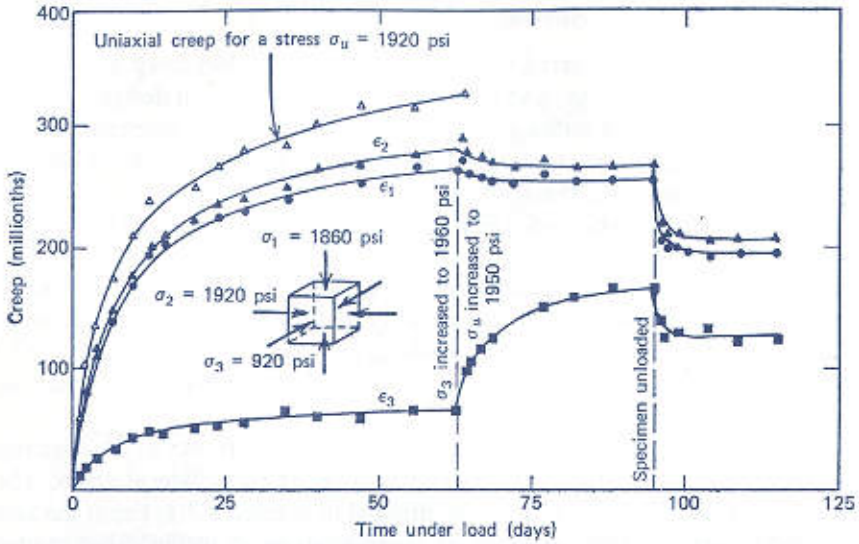

FIGURE 3.47. Typical creep–time curves for concrete under triaxial compression.[83]

can be predicted from tests over a limited period. A number of equations have been suggested.

In the hyperbolic expression, specific creep (creep strain per psi), c, and time under load, t, are related by

$$c = \frac{t}{a + bt} \tag{3.21}$$

where a and b are constants.

A plot of t/c against t is a straight line, and the constants can be easily evaluated (Fig. 3.48). The ultimate creep is $c_\infty = 1/b$ and the ease with which this value can be obtained is an advantage of the hyperbolic expression. It is interesting to observe that when $t = a/b$, $c = 1/2b$, i.e., one-half of the ultimate creep is realized at time $t = a/b$.

It should be noted that in drawing the straight line in Fig. 3.49 a greater weight is given to the points for larger values of t because this gives a better prediction of creep values for long periods under load and of the ultimate creep.

The logarithmic expression gives specific creep as

$$c = F(\tau) \log (t + 1) \tag{3.22}$$

where τ is the age at which the load is applied, $F(\tau)$ is a function representing the rate of creep with time, and t is duration of loading in days.

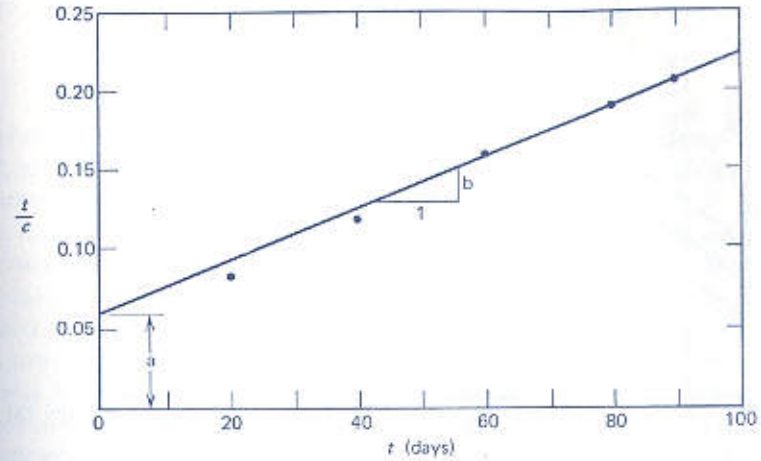

FIGURE 3.48. Creep constants according to Ross' expression $c = t/(a + bt)$.

In this expression creep is a linear function of the logarithm of the time under load (or, strictly speaking, $t + 1$), but values for short periods under load depart from the straight line, Fig. 3.49. This should be borne in mind when short-term values are of significance, as for instance when residual stresses and deflections are required.

Another form of specific creep expression is an exponential one which in

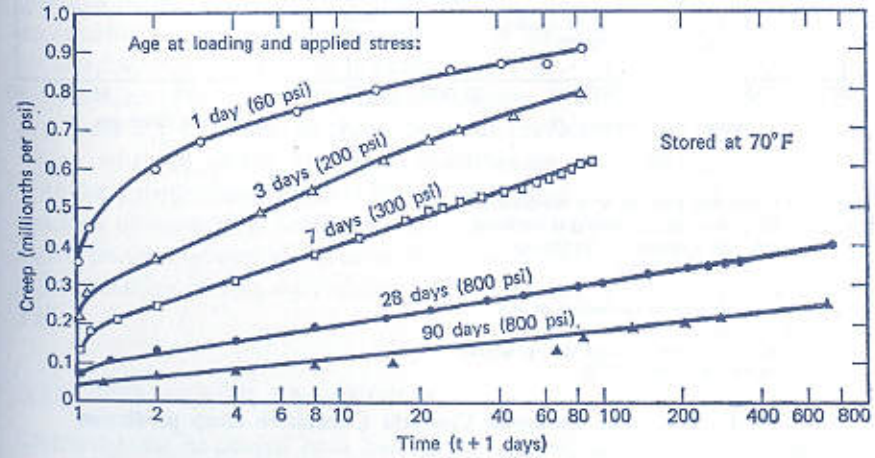

FIGURE 3.49. Specific creep plotted to a logarithmic time scale (6 × 18 in. cylinders stored at 70°F).

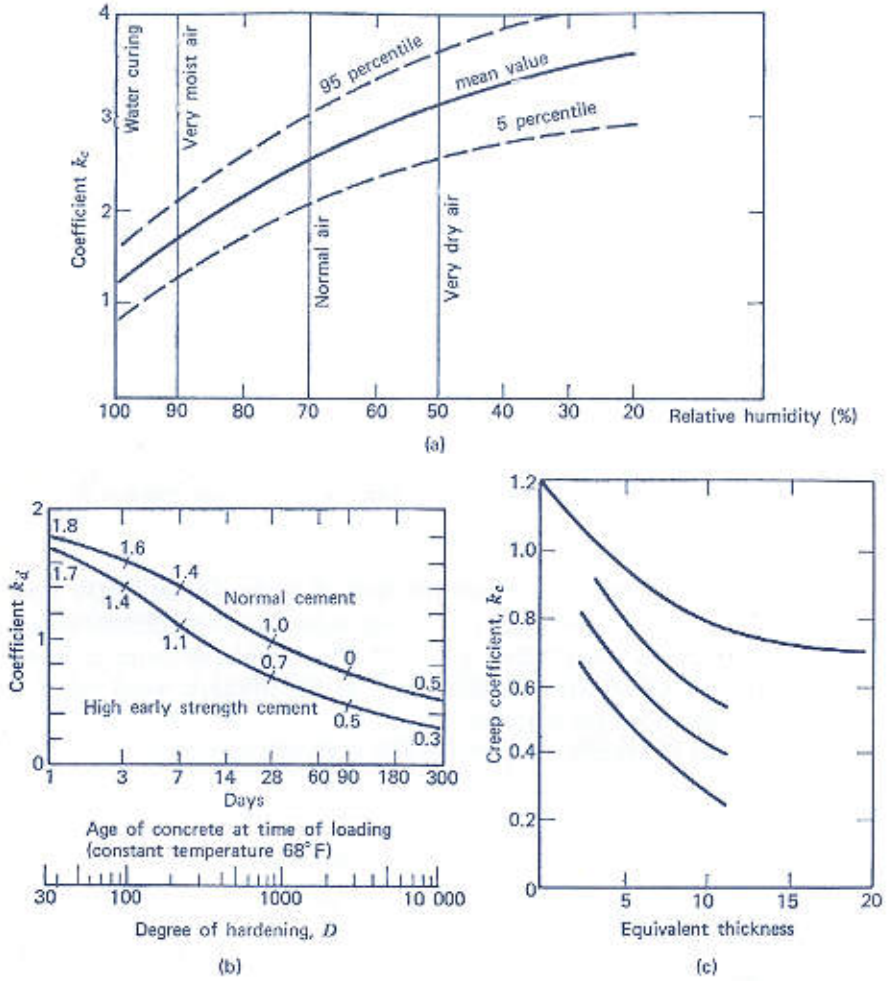

Note: If the concrete hardens at a temperature other than 68°F the age at loading is replaced by the corresponding degree of hardening:

$$D = \Sigma \Delta t (T - 14)\ 0.555$$

in which:
D represents the degree of hardening at the moment of loading.
Δt represents the number of days during which hardening has taken place at T°F.

FIGURE 3.50. The European Concrete Committee creep prediction curves.[35]

its general form can be stated as follows:

$$c = f(\tau) \sum_{1}^{n} \alpha_i (1 - e^{-\beta_i t}) \tag{3.23}$$

where τ and t are age at loading and duration of loading, respectively, α_i, β_i are coefficients determined for best fit of the data, and $f(\tau)$ is a polynomial function taking the age at loading into account.

Both the hyperbolic and logarithmic creep expressions require tests on the actual concrete, and a minimum period of 60 days under load is required to establish satisfactorily the constants involved. However, recently an accelerated one-week creep test was developed.[112] If a general prediction from the knowledge of the mix and the conditions involved but without any creep tests is required, the approach of the European Concrete Committee[35] is probably the best one. Here, a creep coefficient ϕ is used, whereby creep is expressed as a multiple of the instantaneous strain on loading, $\varepsilon_{\text{inst}} = \sigma/E$. Then specific creep (strain per psi) is

$$c = \frac{\phi}{E} \tag{3.24}$$

The estimated creep coefficient ϕ applies only to the usual range of mixes at stress–strength ratios not exceeding 0.35 and is calculated as:

$$\phi = k_b k_c k_d k_e k_t \tag{3.25}$$

where k_b depends on composition of the mix (water–cement ratio and cement content), k_c depends on environmental conditions (relative humidity), k_d depends on age at loading or the degree of hardening at the time, k_e depends on effective thickness of member, defined as the area A of the section divided by one half of the perimeter in contact with the atmosphere, and k_t depends on duration of loading and effective thickness. Values of k_b and k_t for typical concretes are the same as those used for predicting shrinkage (Fig. 3.37). Values of k_c, k_d, and k_e for typical concretes are shown in Fig. 3.50.

If the curing temperature is higher than normal (68°F), so that a greater fraction of strength is achieved at a given chronological age, a fictitious age based on the maturity of the concrete should be used. A formal procedure for determination of this equivalent or fictitious age is discussed in Reference 113.

3.12 SHRINKAGE CRACKING[50]

Cracking can be caused by a number of actions, such as applied stress, unsoundness of cement, alkali–aggregate reaction, sulphate attack, corrosion of reinforcement, freezing and thawing, and restrained or nonuniform

shrinkage or thermal volume change, but here we are concerned solely with shrinkage-induced cracking. Of course, it is only restrained shrinkage that causes cracking but, as already mentioned, in practice shrinkage is always restrained either externally or internally.

Strictly speaking, we are concerned with the cracking tendency as the presence or absence of cracking depends not only on the potential contraction but also on the extensibility of concrete, its strength and its degree of restraint to the deformation that may lead to cracking. Restraint in the form of reinforcing bars or a gradient of stress increases extensibility in that it allows concrete to develop strain well beyond that corresponding to maximum stress.

The development of cracking when stress is relieved by creep is shown in Fig. 3.51. Cracking can be avoided only if the stress induced by the free shrinkage strain, reduced by creep, is at all times smaller than the tensile strength of the concrete. Thus, time has a two-fold effect: the strength increases, thereby reducing the danger of cracking, but on the other hand the shrinkage and the modulus of elasticity also increase so that the induced stress becomes greater. Furthermore, the creep relief decreases with age so that the cracking tendency becomes greater.

It may be relevant to mention here that prolonged moist curing delays the advent of shrinkage, but the effect of curing on the magnitude of shrinkage is small though rather complex. As far as neat cement paste is concerned, the greater the quantity of hydrated cement the smaller is the volume of unhydrated cement grains which restrain the shrinkage: thus prolonged curing leads to greater shrinkage[84] but the paste becomes stronger with age and is able to attain a larger fraction of its shrinkage tendency without cracking. If, however, cracking takes place, for instance, around aggregate particles, the overall shrinkage, measured on a concrete specimen, apparently decreases. Well-cured concrete shrinks more rapidly and therefore the relief of shrinkage stresses by creep is smaller; also, the concrete, being stronger,

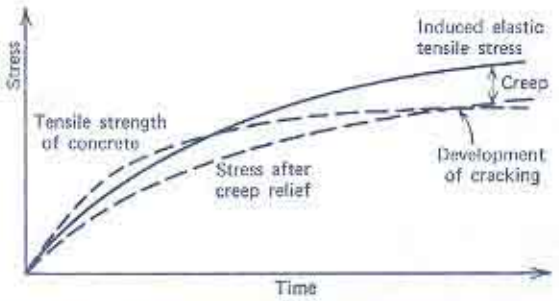

FIGURE 3.51. Crack development when tensile stress is relieved by creep.[50]

has an inherent low creep capacity. These factors may outweigh the higher tensile strength of well-cured concrete and may lead to cracking. In view of this it is not surprising that contradictory results on the effects of curing on shrinkage have been reported, but in general the length of the curing period is not an important factor in shrinkage.

One of the most important factors in cracking is the water content of the mix because its increase tends to increase shrinkage and at the same time to reduce the strength of the concrete. An increase in the cement content also increases shrinkage, and therefore the cracking tendency, but the effect on strength is positive. This applies to drying shrinkage. Carbonation, although it produces shrinkage, reduces subsequent moisture movement, and therefore is advantageous from the standpoint of cracking tendency. The presence of clay in aggregate leads both to higher shrinkage and greater cracking.

The use of admixtures may influence the cracking tendency through an interplay of effects on hardening, shrinkage and creep. Specifically, retarders may allow more shrinkage to be accommodated in the form of plastic shrinkage and also probably increase the extensibility of concrete, and therefore reduce cracking. On the other hand, if concrete has attained rigidity too rapidly it cannot accommodate the would-be plastic shrinkage and, having low strength, cracks.

The temperature at the time of placing determines the dimensions of concrete at the moment when it ceases to deform plastically (i.e., without loss of continuity). A subsequent drop in temperature will produce potential contraction. Thus placing in hot weather means a high cracking tendency. Steep thermal or moisture gradients produce severe internal restraints and thus represent a high cracking tendency. Likewise, restraint by the base of a member or by other members may lead to cracking.

These are some of the factors to be considered. Actual cracking and failure depend on the combination of factors and indeed it is rarely that a single adverse factor is responsible for cracking of concrete.

The importance of cracking and the minimum width at which a crack is considered significant depend on the conditions of exposure of the concrete. On the basis of a number of investigations, Kesler et al.[114] suggest the following permissible crack widths:

Interior members	0.014 in.
Exterior members under normal exposure conditions	0.010 in.
Exterior members exposed to particularly aggressive environment	0.006 in.

Since under given physical conditions the total crack width per unit length of concrete is fixed and we want the cracks to be as fine as possible, it is desirable to have more cracks. For this reason, the restraint to cracking should be uniform along the length of the member.

We should note that, from energy considerations (see Section 3.2), it is easier to extend an existing crack than to form a new one. This explains why under an applied load, each subsequent crack occurs under a higher load than the preceding one. The total number of cracks developed is determined by the size of the concrete member, and the distance between cracks depends on the maximum size of aggregate present.[115]

3.13 THERMAL PROPERTIES[50]

Thermal properties of concrete affect its performance over long periods under varying conditions and are also of vital importance in planning mass concrete construction. For this reason, data on thermal properties of concrete may be required in design. For instance, a building may require a specific degree of insulation; a slab may have to be free from cracking and warping when subjected to a change in temperature; the stresses induced in statically indeterminate structures by a change in temperature must be calculated; and in mass concrete construction the potential rise and distribution of temperature owing to hydration of cement have to be estimated so that a suitable cooling system may be designed.

The basic quantities involved are: thermal conductivity, thermal diffusivity, specific heat, and the coefficient of thermal expansion. The first three are largely interrelated.

3.13.1 Thermal Conductivity

This measures the ability of the material to conduct heat and is defined as the ratio of the flux of heat to temperature gradient. Thermal conductivity is measured in British thermal units per hour per square foot of area of body when the temperature difference is 1°F per ft of thickness of the body.

The conductivity of ordinary structural concrete depends on its composition, and, when the concrete is saturated, the conductivity ranges generally between about 0.8 and 2.1 Btu ft/ft²h°F. The relation between conductivity and density is shown in Fig. 3.52. However, some concretes depart from the curve shown, especially if they contain a significant amount of air, because the conductivity of air is low. Thus air entrainment reduces the conductivity.

The mineralogical character of the aggregate greatly affects the conductivity of the concrete made with it. In general terms, basalt, trachyte, and barytes have a low conductivity, dolomite and limestone are in the middle range, and quartz exhibits the highest conductivity, which depends also on the direction of heat flow relative to the orientation of the crystals. Some typical values of conductivity of concrete are given in Table 3.5.

The cement paste has a lower thermal conductivity than normal weight

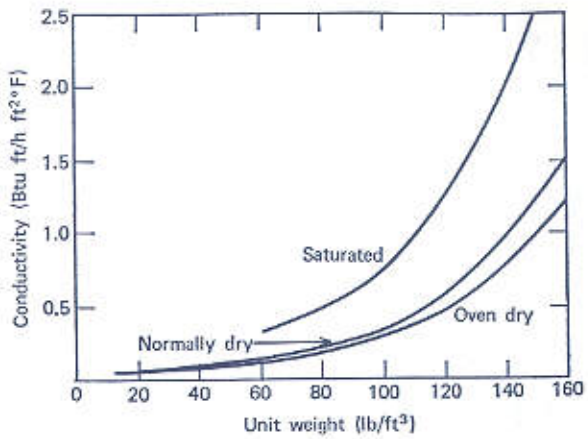

FIGURE 3.52. Relation between thermal conductivity of concrete and its unit weight.[116]

aggregate (but not than the majority of lightweight aggregates) so that the leaner the mix the higher its conductivity.

Since the conductivity of air is lower than that of water, the degree of saturation of concrete strongly affects its conductivity: for a given mix, the conductivity increases linearly with the moisture content of the concrete;[118] some typical data are shown in Fig. 3.53. On the other hand, the conductivity of water is less than half that of the cement paste, so that the lower the water content of the mix at the time of placing of the concrete the higher the conductivity of the hardened concrete. Because of the influence of the moisture content, the conditions of exposure to weather affect the conductivity of the concrete in a given structure; some typical values are given in Table 3.6.

Conductivity is little affected by temperature, the general effect of an increase in temperature being to decrease slightly the conductivity of ordinary concrete, but the reverse is the case with lightweight concrete.[122]

TABLE 3.5. Typical Values of Thermal Conductivity of Concrete.[117]

Type of Aggregate	Unit Weight of Concrete lb/ft³	Conductivity Btu ft/ft²h°F
Barytes	227	0.8
Igneous	159	0.83
Dolomite	160	2.13
Lightweight concrete (oven-dried)	30–110	0.08–0.35

Reprinted by permission of the American Society for Testing and Materials, Copyright ASTM.

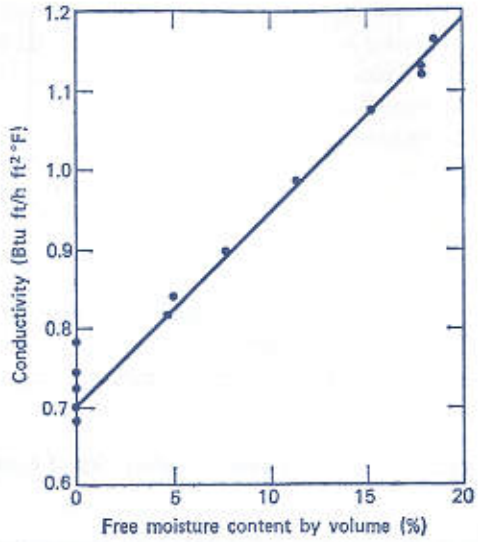

FIGURE 3.53. Relation between thermal conductivity of concrete made with dolerite aggregate and moisture content by volume.[119]

Thermal conductivity is usually calculated from the diffusivity, the latter being easier to measure, but a direct determination of conductivity is of course possible. In the latter case, the choice of the method is governed by whether or not the concrete is dry as steady-state methods cause migration of moisture under test.[50]

3.13.2 Thermal Diffusivity and Specific Heat[11]

Diffusivity represents the rate at which temperature changes within a mass can take place, and is thus an index of the facility with which concrete can undergo temperature changes. Diffusivity, δ is related to the conductivity K by the equation

$$\delta = \frac{K}{cw} \tag{3.26}$$

where c is the specific heat, and w is the unit weight of concrete.

From this expression it can be seen that conductivity and diffusivity vary in step. The range of typical values of diffusivity of ordinary concrete is between 0.02 and 0.06 ft²/h, depending on the type of aggregate used. The following rock types are listed in order of increasing diffusivity: basalt, rhyolite, granite, limestone, dolerite, and quartzite.[121]

The measurement of diffusivity consists essentially of determining the relation between time and the temperature differential between the interior

TABLE 3.6. Values of Conductivity (Btu ft/ft²h°F) Recommended by Loudon and Stacy.[120]

Unit Weight lb/ft³	For Concrete Protected from Weather					For Concrete Exposed to Weather				
	Aerated Concrete	Lightweight Concrete with Foamed Slag	Lightweight Concrete with Expanded Clay or Sintered Fly Ash	Normal Weight Aggregate Concrete		Aerated Concrete	Lightweight Concrete with Foamed Slag	Lightweight Concrete with Expanded Clay or Sintered Fly Ash	Normal Weight Aggregate Concrete	
20	0.053	0.050	0.075			0.071	0.058	0.084		
30	0.084	0.067	0.100			0.096	0.075	0.108		
40	0.117	0.092	0.133			0.129	0.100	0.150		
50	0.150	0.117	0.175			0.158	0.133	0.192		
60	0.182	0.150	0.217			0.208	0.167	0.250		
70	0.225	0.182	0.267			0.250	0.208	0.300		
80	0.275	0.225	0.325			0.308	0.250	0.367		
90		0.267	0.392							
100		0.317	0.459	0.408					0.467	
110		0.375	0.550	0.484					0.550	
120				0.610					0.690	
130				0.760					0.860	
140				0.980					1.100	
150				1.310					1.480	

and the surface of a concrete specimen initially at a constant temperature when a change in temperature is introduced at the surface. Details of procedure and calculation are given in U.S Army Corps of Engineers Standard CRD-C36-48.[122] Because of the influence of moisture in the concrete on its thermal properties, diffusivity should be measured on specimens with a moisture content which will exist in the actual structure.

Specific heat, which represents the heat capacity of concrete is little affected by the mineralogical character of the aggregate, but is considerably increased by an increase in the moisture content of the concrete. Specific heat depends also on the actual range of temperature. The common range of values for ordinary concrete is between 0.20 and 0.28 Btu/lb°F. The specific heat of concrete is determined by elementary methods of physics.

3.13.3 Coefficient of Thermal Expansion

Like most engineering materials, concrete has a positive coefficient of thermal expansion, but its value depends both on the composition of the mix and on its hygral state at the time of the temperature change.

The influence of the mix proportions arises from the fact that the two main constituents of the concrete, cement paste and aggregate, have dissimilar thermal coefficients, and the coefficient for concrete is a resultant of the two values. The coefficient of thermal expansion of cement paste varies between about 6×10^{-6} and 11×10^{-6} per °F,[121] and is higher than the coefficient of aggregates, which varies for the more common rocks between 0.5×10^{-6} and 8.9×10^{-6} per °F, with the majority of aggregates lying between 3×10^{-6} and 7×10^{-6} per °F. In general terms, the coefficient of concrete is a function of the quantity of aggregate in the mix, Table 3.7, and of the coefficient of the aggregate by itself,[124] and Table 3.8 gives the values of the coefficient of thermal expansion of 1:6 concretes made with different aggregates. The significance of the difference between the coefficients of the aggregate

TABLE 3.7. Influence of Aggregate Content on the Coefficient of Thermal Expansion.[123]

Mix Proportions by Weight	Linear Coefficient of Thermal Expansion at the Age of 2 Years 10^{-6} per °F
Neat cement	10.3
1:1	7.5
1:3	6.2
1:6	5.6

TABLE 3.8. Coefficient of Thermal Expansion of 1:6 Concretes Made with Different Aggregates.[125]

Type of Aggregate	Linear Coefficient of Thermal Expansion 10^{-6} per °F		
	Air-Cured Concrete	Water-Cured Concrete	Air-Cured and Wetted Concrete
Gravel	7.3	6.8	6.5
Granite	5.3	4.8	4.3
Quartzite	7.1	6.8	6.5
Dolerite	5.3	4.7	4.4
Sandstone	6.5	5.6	4.8
Limestone	4.1	3.4	3.3
Portland stone	4.1	3.4	3.6
Blastfurnace slag	5.9	5.1	4.9
Foamed slag	6.7	5.1	4.7

and the cement paste lies in the fact that if they differ too much from one another, a large change in temperature may introduce differential movement and a break in the bond between the aggregate and the surrounding paste. However, possibly because the differential movement is affected also by other forces, such as those due to shrinkage, a large difference between the coefficients is not necessarily detrimental when the temperature does not vary outside the range of about ±50°F from the mean. Nevertheless, when the two coefficients differ by more than 3×10^{-6} per °F, the durability of concrete subjected to freezing and thawing may be affected.[11]

The influence of the moisture condition on the coefficient of thermal expansion of concrete applies to the paste component and is due to the fact that the thermal coefficient is made up of two movements: the true kinetic thermal coefficient and swelling pressure. The latter arises from a decrease in the capillary tension of water held by the paste with an increase in temperature.[12] No swelling is possible, however, when the specimen is dry, i.e., when it contains no water. It follows that when the paste is dry the coefficient of thermal expansion is lower than when the paste is partially saturated. When the paste is self-desiccated the coefficient is higher because there is not enough water for free exchange of moisture to occur between capillary and gel pores after the temperature change.

When saturated paste is heated, the moisture diffusion from gel to capillary pores at constant gel water content is partially offset by contraction as gel loses water so that the apparent coefficient is smaller.[126] Conversely, on cooling the contraction due to moisture diffusion from capillary to gel pores

Sedimentary rocks are formed from the products of weathering of Earth's surface by recombination and consolidation. Depending upon the heat and pressure conditions existing at the time of formation, their physical characteristics such as durability, porosity, and specific gravity vary widely as shown in Table 1.3.[5]

Igneous rocks constitute the major bulk of concrete aggregates. They are formed by the cooling of magma which consists essentially of molten silicate originating within the interior of the Earth. The rate at which igneous rocks are cooled at the time of their formation is an important factor in determining their character and properties. The two principal classes of igneous rocks are plutonic or intrusive, and volcanic or extrusive. The former comprises deep-seated, below-surface rocks which have solidified slowly within the interior of the Earth, while the latter have formed on the surface as a result of the rapid cooling of the molten lava issuing from volcanoes. Due to their slow crystallization rate the plutonic rocks have fully crystalline, granular texture, and uniform grain size. When crushed, they yield hard, almost equidimensional particles possessing superior chemical and physical stability. On the other hand, volcanic rocks generally reflect glassy texture and are susceptible to weathering, hydrothermal alternations, and alkali–aggregate reactions in portland-cement concrete.

Structural damage to concrete due to *alkali–aggregate reactions* has been reported in several concrete dams and highway pavements in various parts of the United States.[5] Chalcedony, tridymite, cristobalite, and opal constitute some of the siliceous minerals found in volcanic igneous rocks possessing high chemical reactivity. Rhyolites, andesites, and cherts (see Table 1.3) are among the rock types belonging to this class. Alkali hydroxides, usually derived from portland cement, can react with the reactive silicates to form alkalic silica gels which subsequently absorb water from their surroundings through osmosis.[5] This leads to internal stresses in hardened concrete until its tensile strength is reached and it cracks.

One method to control alkali–aggregate reaction is to limit the alkali content of portland cement to 0.6%, or less (expressed as the Na_2O equivalent of the total alkalis) whenever reactive aggregates are to be used for making concrete. Another method consists of adding to concrete a finely ground pozzolanic material. If the pozzolan is of adequate quality, the deleterious effects of alkali–aggregate reactions may be prevented by reducing the alkali concentration through alkali–pozzolan reaction.

At the other end of the spectrum are aggregates consisting predominantly of quartz and feldspar which have a smooth texture and possess little surface reactivity. Since a certain depth of cement–aggregate interaction layer is essential for good bonding so that concrete may respond as a more or less monolithic mass to stresses caused by load or thermal strains, the aggregates

TABLE 1.3. Characteristics of Common Aggregate Types.[5]

Rock Types	Specific Gravity (dry)	Absorption and Porosity	Potential Alkali Attack	Durability	Typical Shape
Igneous					
Granite	2.52–2.99	Very low	Insignificant	Good	Equidimensional
Rhyolite	2.30–2.70	Low to moderate	Deleterious	Good	Equidimensional
Andesite	2.22–2.79	Low to moderate	Deleterious	Good	Equidimensional
Basalt	2.21–3.11	Low to moderate	Insignificant	Good	Equidimensional
Sedimentary					
Sandstone	1.60–2.68	Low to high	Insignificant	Good to poor	Equidimensional to platey
Limestone	1.74–2.76	Low to high	Insignificant	Good to poor	Equidimensional to platey
Shale	1.54–3.17	Moderate to high	Insignificant	Satisfactory to poor	Platey
Chert	1.81–2.65	Low to moderate	Deleterious	Good to poor	Equidimensional

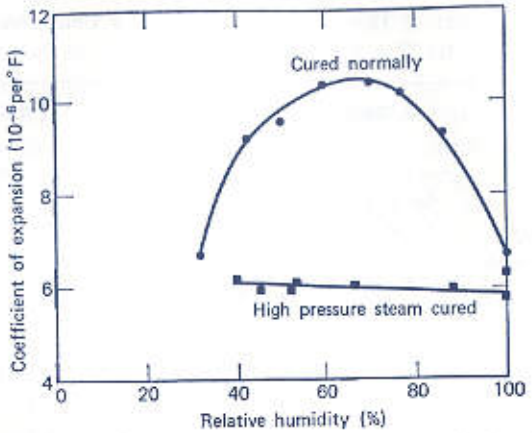

FIGURE 3.54. Relation between ambient relative humidity and the linear coefficient of thermal expansion of neat cement paste cured normally and high-pressure steam cured.[121]

at a constant gel water content is partially offset by the expansion which occurs when the gel absorbs water.[126] Some actual values are shown in Fig. 3.54, and it can be seen that for young pastes cured normally the coefficient is a maximum at a relative humidity of about 70%. The relative humidity at which the coefficient is a maximum decreases with age, down to about 50% for very old pastes. Likewise, the coefficient itself decreases with age due to a reduction in the potential swelling pressure owing to an increase in the amount of crystalline material in the hardened paste. No such variation in the coefficient of thermal expansion is found in high-pressure steam cured pastes since they contain no gel (Fig. 3.54).

Figure 3.54 refers to neat cement pastes but the effects are apparent also in concrete; here, however, the variation in the coefficient is smaller as only the paste component is affected by the ambient humidity and aging. Table 3.8 gives values of the coefficient for 1:6 concretes: cured in air at 64% relative humidity, saturated (water cured), and wetted after air-curing.

Only the values determined on saturated or desiccated specimens can be considered to represent the "true" coefficient of thermal expansion, but it is the values at intermediate humidities that are applicable to many concretes under practical conditions. When the increase in temperature from winter to summer is associated with some drying, shrinkage enters the picture and the net expansion is lower than when no loss of water from the concrete takes place.

The chemical composition and fineness of cement affect the thermal expansion only in so far as they influence the properties of gel at early ages. The presence of air voids is not a factor.

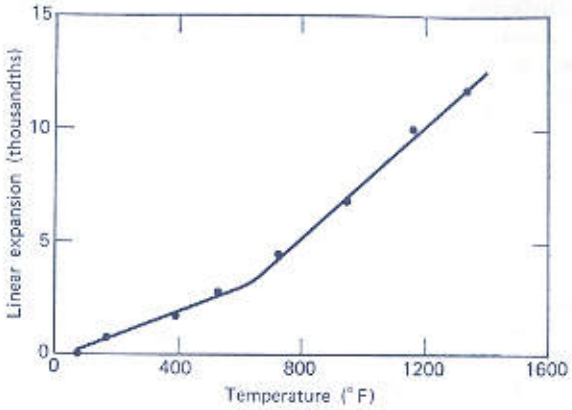

FIGURE 3.55. Linear expansion of concrete on heating.[127] (Calcareous aggregate; water–cement ratio = 0.4.)

The data considered so far apply only to the normal range of temperatures, say, below 150°F. Considerably higher temperatures can, however, be encountered in the vicinity of jet exhausts on airfields and in industrial applications. Figure 3.55 shows that above about 600°F the coefficient of thermal expansion of concrete increases, probably owing to dehydration of the cement paste; values of the coefficient of thermal expansion are listed in Table 3.9.

Laboratory tests have shown that concretes with a higher coefficient of thermal expansion are less resistant to temperature changes than concretes with a lower coefficient.[124] However, the data are not sufficient for the coefficient of thermal expansion to be considered as a quantitative measure of durability of concrete subjected to frequent or rapid changes in temperature.

Nevertheless, rapid changes in temperature, generally faster than encountered under normal conditions, may lead to deterioration of concrete.

3.13.4 Effect of Temperature on Strength

The effect of temperature on the strength of concrete is small and somewhat irregular below 480°F but above about 570°F a definite loss of strength takes place. At low temperatures the strength of concrete is higher than at room temperature. For instance, at from −75 to −250°F the strength of moist concrete is two to three times higher than at room temperature, but dry concrete is only 20% stronger.[128] The loss in strength at higher temperatures is greater in saturated than in dry concrete, and it is probably the moisture content at the time of compressive testing that is responsible for the difference.[129] The strength of mass-cured concrete beyond the age of 14 days seems

TABLE 3.9. Coefficient of Thermal Expansion of Concrete at High Temperatures.[127]

Curing Condition	Water-Cement Ratio	Cement Content lb/yd³	Aggregate	Linear Coefficient of Thermal Expansion, 10^{-6} per °F, at the Age of			
				28 days		90 days	
				Below 500°F	Above 800°F	Below 500°F	Above 800°F
Moist	0.4	735	Calcareous gravel	4.2	11.3	3.6	6.2
	0.6	520		7.1	11.4	4.7	12.5
	0.8	415		6.1	11.7	9.3	18.2
Air 50% Relative Humidity	0.4	735	Calcareous gravel	4.3	10.5	6.8	11.5
	0.6	520		4.3	11.7	4.9	11.2
	0.8	415		5.3	11.5	6.5	12.0
Moist	0.68	600	Expanded shale	3.4	4.2	—	—
Air	0.68	600		2.6	5.4	2.8	4.9

to be unaffected by temperature within the range 70 to 205°F.[107] This behavior is probably due to an absence of a change in moisture content and an absence of shrinkage.

REFERENCES

1. Hsu, T. T. C., F. O. Slate, G. M. Sturman, and G. Winter, "Microcracking of Plain Concrete and the Shape of the Stress-Strain Curve," *J. Am. Concrete Inst., Proc.* Vol. 60, pp. 209–224, February 1963.
2. Griffith, A. A., "The Phenomena of Rupture and Flow in Solids," *Philosophical Transactions (Royal Society)*, Ser. A, Vol. 221, pp. 163–198, 1920.
3. Lott, J., and C. E. Kesler, "Crack Propagation in Plain Concrete," *Symposium on Structure of Portland Cement Paste and Concrete*, SR 90, Highway Research Board, pp. 204–218, 1966.
4. Neville, A. M., "Some Aspects of the Strength of Concrete," *Civil Engineering* (London), Vol. 54, pp. 1153–1156, October 1959; pp. 1308–1311, November, 1959; pp. 1435–1439, December, 1959.
5. Glucklich, J., "Fracture of Plain Concrete," *J. Eng. Mech. Div., Proc. Am. Soc. Civil Engrs.*, Vol. 89, No. EM6, pp. 127–138, December 1963.
6. Jones, R., and M. F. Kaplan, "The Effect of Coarse Aggregate on the Mode of Failure of Concrete in Compression and Flexure," *Mag. Concrete Res.*, Vol. 9, No. 26, pp. 89–94, August 1957.

7. Berg, O. Y., "Strength and Plasticity of Concrete," *Doklady Akademii Nauk, S.S.S.R.*, Vol. 70, No. 4, pp. 617–620, 1950.
8. Kaplan, M. F., "Strains and Stresses of Concrete at Initiation of Cracking and Near Failure," *J. Am. Concrete Inst., Proc.* Vol. 60, pp. 853–880, July 1963.
9. Gilkey, H. J., "Water-Cement Ratio Versus Strength—Another Look," *J. Am. Concrete Inst., Proc.* Vol. 57, pp. 1287–1312, April 1961.
10. "Discussion of paper by H. J. Gilkey: Water-Cement Ratio Versus Strength—Another Look," *J. Am. Concrete Inst., Proc.* Vol. 58, pp. 1851–1878, December 1961, Pt. 2.
11. Neville, A. M., *Properties of Concrete*, Sir Isaac Pitman and Sons Ltd., London; Wiley-Interscience, New York, 2nd Ed., 1973, 686 pp.
12. Powers, T. C., and T. L. Brownyard, "Studies of the Physical Properties of Hardened Portland Cement Paste" (nine parts), *J. Am. Concrete Inst., Proc.* Vol. 43, October 1946 to April 1947.
13. Neville, A. M., "A Study of Deterioration of Structural Concrete Made with High-alumina Cement," *Inst. Civil Engrs., Proc.* Vol. 25, pp. 287–324, July 1963.
14. Neville, A. M., "The Effect of Warm Storage Conditions on the Strength of Concrete Made with High-alumina Cement," *Inst. Civil Engrs., Proc.* Vol. 10, pp. 185–192, June 1958.
15. *Code of Practice for the Structural Use of Concrete*, CP110, British Standards Institution, 1972, 440 pp.
16. Cordon, W. A., and H. A. Gillespie, "Variables in Concrete Aggregates and Portland Cement Paste which Influence the Strength of Concrete," *J. Am. Concrete Inst., Proc.* Vol. 60, pp. 1029–1052, August 1963.
17. Bloem, D. L., "Effect of Maximum Size of Aggregate on Strength of Concrete," *National Sand and Gravel Assoc. Circular* No. 74, Washington D.C., February 1959.
18. Neville, A. M., "The Influence of the Direction of Loading on the Strength of Concrete Test Cubes," *ASTM Bull.*, pp. 63–65, July 1959.
19. Neville, A. M., "The Failure of Concrete Compression Test Specimens," *Civil Engineering* (London), pp. 773–774, July 1957.
20. Murdock, J. W., and C. E. Kesler, "Effect of Length to Diameter Ratio of Specimen on the Apparent Compressive Strength of Concrete," *ASTM Bull.*, pp. 68–73, April 1957.
21. Gonnerman, H. F., "Effect of Size and Shape of Test Specimen on Compressive Strength of Concrete," *Proc. ASTM*, Vol. 25, Pt. 2, pp. 237–250, 1925.
22. Newman, K., "Concrete Control Tests as a Measure of the Properties of Concrete," *Symposium on Concrete Quality*, Cement and Concrete Association, London 1965.
23. Sherman, M., "Factors Affecting Measurement of Compressive Strength of Insulating Concretes," *Proc. ASTM*, Vol. 57, pp. 1096–1121, 1957.
24. Blanks, R. F., and C. C. McNamara, "Mass Concrete Tests in Large Cylinders," *J. Am. Concrete Inst., Proc.* Vol. 31, pp. 280–303, January/February 1935.
25. "Effect of Maximum Size of Aggregate Upon Compressive Strength of Concrete," *U.S. Department of the Interior, Bureau of Reclamation, Laboratory Report* No. C-1052, 11 pp., 3 June 1963.
26. Tucker, J., "Statistical Theory of the Effect of Dimensions and of Method of Loading upon the Modulus of Rupture of Beams," *Proc. ASTM*, Vol. 41, pp. 1072–1088, 1941.
27. Neville, A. M., "A General Relation for Strengths of Concrete Specimens of Different Shapes and Sizes," *J. Am. Concrete Inst., Proc.* Vol. 63, No. 10, pp. 1095–1109, October 1966.

28. McHenry, D., and J. J. Shideler, "Review of Data on Effect of Speed in Mechanical Testing of Concrete," *ASTM Spec. Tech. Publ.*, No. 185, pp. 72–82, 1956.
29. Price, W. H., "Factors Influencing Concrete Strength," *J. Am. Concrete Inst., Proc.* Vol. 47, pp. 417–432, February 1951.
30. Evans, R. H., "Effect of Rate of Loading on Some Mechanical Properties of Concrete," *Mechanical Properties of Non-Metallic Brittle Materials*, pp. 175–190, Butterworths Scientific Publications, London, 1958.
31. McNeely, D. J., and S. D. Lash, "Tensile Strength of Concrete," *J. Am. Concrete Inst., Proc.* Vol. 60, pp. 751–761, June 1963.
32. Iyengar, K. T. S., K. Chandrashekhar, and K. T. Krishnaswamy, "On the Determination of True Tensile Strength of Concrete," *RILEM Bull.*, No. 21, pp. 39–45, December 1963.
33. Narrow, I., and E. Ullberg, "Correlation Between Tensile Splitting Strength and Flexural Strength of Concrete," *J. Am. Concrete Inst., Proc.* Vol. 60, pp. 27–38, January 1963.
34. Malhotra, V. M., N. G. Zoldners, and H. M. Woodrooffe, "Ring Test for Determining the Tensile Strength of Concrete," *Matls. Research and Standards*, Vol. 6, No. 1, pp. 2–12, January 1966.
35. Comité Européen du Béton, *International Recommendations for the Design and Construction of Concrete Structures*, English edition, Cement and Concrete Association, London, 1970.
36. Shacklock, B. W. and P. W. Keene, "Comparison of the Compressive and Flexural Strengths of Concrete with and without Entrained Air," *Civil Engineering* (London), pp. 77–80, January 1959.
37. Bresler, B., and K. S. Pister, "Failure of Plain Concrete under Combined Stresses," *Trans. Am. Soc. Civil Engrs.*, Vol. 122, pp. 1049–1059, 1957.
38. Bresler, B., and K. S. Pister, "Strength of Concrete under Combined Stresses," *J. Am. Concrete Inst., Proc.* Vol. 55, pp. 321–345, September 1958.
39. Kupfer, H., H. K. Hilsdorf, and H. Rüsch, "Behavior of Concrete under Biaxial Stresses," *J. Am. Concrete Inst., Proc.* Vol. 66, pp. 656–666, August 1969.
40. Nelissen, L. J. M., "Biaxial Testing of Normal Concrete," *Heron*, Vol. 18, pp. 1–90, 1972.
41. King, J. W. H., "An Accelerated Test for the Seven-and Twenty-Eight-Day Compressive Strengths of Concrete," *J. Appl. Chem.* (London), Vol. 10, pp. 256–262, 1960.
42. Smith, P., and B. Chojnacki, "Accelerated Strength Testing of Concrete Cylinders," *Proc. ASTM*, Vol. 63, pp. 1079–1101, 1963.
43. Petersons, N., "Should Standard Cube Test Specimens be Replaced by Test Specimens Taken from Structures," *Materials and Structures*, Vol. 1, No. 5, pp. 425–435, September/October 1968.
44. Willetts, C. H., "Investigation of the Schmidt Concrete Test Hammer," *Miscellaneous Paper* No. 6–267, U.S. Army Engineer Waterways Experiment Station, Vicksburg, Miss., 9 pp., June 1958.
45. Whitehurst, E. A., "Evaluation of Concrete Properties from Sonic Tests," *ACI Monograph* No. 2, 94 pp., 1966.
46. Jones, R., and E. N. Gatfield, "Testing Concrete by an Ultrasonic Pulse Technique," *D.S.I.R. Road Research Tech. Paper* No. 34, London, H.M.S.O., 48 pp., 1955.
47. Kaplan, M. F., "The Relation Between Ultrasonic Pulse Velocity and the Compressive Strength of Concretes Having the Same Workability but Different Mix Proportions," *Mag. Concrete Res.*, Vol. 12, No. 34, pp. 3–8, March 1960.

48. Jones, R., and P. J. F. Wright, "Some Problems Involved in Destructive and Non-Destructive Testing of Concrete," *Proceedings of a Symposium on Mix Design and Quality Control of Concrete*, pp. 441–450, Cement and Concrete Association, London, 1954.
49. Jones, R., The Development of Microcracks in Concrete," *RILEM Bull.*, No. 9, pp. 110–114, December 1960.
50. Neville, A. M., "Hardened Concrete: Physical and Mechanical Aspects," *ACI Monograph* (Detroit), 1971, 260 pp.
51. Green, H., "Impact Strength of Concrete," *Inst. Civil Engrs., Proc.* Vol. 28, pp. 383–396, July 1964.
52. Welch, G. B., and B. Haisman, "Fracture Toughness Measurements of Concrete," University of New South Wales, Kensington, Australia, *Report* No. R42, 17 pp., January 1969.
53. Watstein, D., "Properties of Concrete at High Rates of Loading," *Symposium on Impact Testing, ASTM Spec. Tech. Publ.*, No. 176, pp. 156–169, 1955.
54. Nordby, G. M., "Fatigue of Concrete—A Review of Research," *J. Am. Concrete Inst., Proc.* Vol. 55, pp. 191–220, August 1952.
55. Neville, A. M., "Current Problems Regarding Concrete Under Sustained Loading," *International Assoc. for Bridge and Structural Engineering*, Vol. 26, pp. 337–343, 1960.
56. Neville, A. M., "Concrete—a Non-Elastic Material in the Laboratory and in Structures," *Stanton Walker Lecture No. 6*, National Sand and Gravel Assoc. and National Ready Mixed Concrete Assoc., 1968, 24 pp.
57. Ople, F. S., Jr., and C. L. Hulsbos, "Probable Fatigue Life of Plain Concrete with Stress Gradient," *J. Am. Concrete Inst., Proc.* Vol. 63, pp. 59–81, January 1966.
58. Linger, D. A., and H. A. Gillespie, "A Study of the Mechanism of Concrete Fatigue and Fracture," *HRB Res. News* No. 22, pp. 40–51, February 1966.
59. Assimacopoulos, B. M., R. F. Warner, and C. E. Ekberg, Jr., "High Speed Fatigue Tests on Small Specimens of Plain Concrete," *J. Prestressed Concrete Inst.*, Vol. 4, pp. 53–70, September 1959.
60. Murdock, J. W., "The Mechanism of Fatigue Failure in Concrete," Thesis submitted to the Univ. of Illinois for the degree of Ph.D., 1960, 131 pp.
61. Bate, S. C. C., "The Strength of Concrete Members Under Dynamic Loading," *Proceedings of a Symposium on the Strength of Concrete Structures*, pp. 487–524, Cement and Concrete Association, London, 1958.
62. Hsu, T. T. C., "Inelastic Behaviour of Concrete under Short-time Loading," *Colloquium on Nature of Inelasticity of Concrete and its Structural Effects*, Cornell University, Ithaca, New York, November 1965, 6 pp.
63. Neville, A. M., "Some Problems in Inelasticity of Concrete and its Behaviour under Sustained Loading," *Structural Concrete*, Vol. 3, No. 4, pp. 261–268, July/August 1966.
64. Rüsch, H., "Researches Toward a General Flexural Theory for Structural Concrete," *J. Am. Concrete Inst., Proc.* Vol. 32, pp. 1–28, July 1960.
65. Bresler, B., "Discussion of paper by L. H. N. Lee: Inelastic Behavior of Reinforced Concrete Members," *Trans. Am. Soc. Civil Engineers*, Vol. 120, pp. 203–205, 1955.
66. Hognestad, E., N. W. Hanson, and D. McHenry, "Concrete Stress Distribution in Ultimate Strength Design," *J. Am. Concrete Inst., Proc.* Vol. 52, pp. 455–479, December 1955.
67. Hognestad, E., "A Study of Combined Bending and Axial Load in Reinforced Concrete Members," Univ. of Illinois Engineering Experiment Station, *Bulletin Series* No. 399, *Bulletin* No. 1, 28 pp., 1951.

68. Bennett, E. W., and N. K. Raju, "Cumulative Fatigue Damage of Plain Concrete in Compression," *Proceedings of an International Conference on Structure, Solid Mechanics and Engineering Design*, Pt. 2, Wiley-Interscience, New York, pp. 1089–1102, 1969.
69. Desayi, P., and S. Krishnan, "Equation for the Stress–Strain Curve of Concrete," *J. Am. Concrete Inst., Proc.* Vol. 61, pp. 345–350, March 1964.
70. Saenz, L. P., "Discussion of Reference 69," *J. Am. Concrete Inst., Proc.* Vol. 61, pp. 1229–1235, September 1964.
71. Liebenberg, A. C., "A Stress–Strain Function for Concrete Subjected to Short-term Loading," *Mag. Concrete Res.*, Vol. 14, No. 41, pp. 85–90, July 1962.
72. Bresler, B., "Lightweight Aggregate Reinforced Concrete Columns," Symposium on Lightweight Aggregate Concretes, *Am. Concrete Inst.* SP-29, pp. 81–132, 1971.
73. Philleo, R. E., "Comparison of Results of Three Methods for Determining Young's Modulus of Elasticity of Concrete," *J. Am. Concrete Inst., Proc.* Vol. 51, pp. 461–469, January 1955.
74. Hansen, T. C., "Creep and Stress Relaxation of Concrete—A Theoretical and Experimental Investigation," *Proc.* No. 31, Swedish Cement and Concrete Research Institute, Stockholm, 1960, 112 pp.
75. Hirsch, T. J., "Modulus of Elasticity of Concrete Affected by Elastic Moduli of Cement Paste Matrix and Aggregate," *J. Am. Concrete Inst., Proc.* Vol. 59, pp. 427–451, March 1962.
76. Counto, U. J., "The Effect of the Elastic Modulus of the Aggregate on the Elastic Modulus, Creep, and Creep Recovery of Concrete," *Mag. Concrete Res.*, Vol. 16, No. 48, pp. 129–138, September 1964.
77. Rüsch, H., "Versuche zur Festigkeit der Biegedruckzone," *Deutscher Ausschuss für Stahlbeton*, No. 120, Berlin, 1955, 94 pp.
78. Welch, G. B., "Tensile Strains in Unreinforced Concrete Beams," *Mag. Concrete Res.*, Vol. 17, No. 54, pp. 9–18, March 1966.
79. Welch, G. B., "Factors Influencing the Tensile Strains and Flexure Failure of Plain Concrete," *Proceedings of an International Conference on the Structure of Concrete*, Cement and Concrete Association, London, pp. 525–533, 1968.
80. Kaplan, M. F., "Strains and Stresses of Concrete at Initiation of Cracking and Near Failure," *J. Am. Concrete Inst., Proc.* Vol. 60, pp. 853–880, July 1963.
81. Anson, M., and K. Newman, "The Effect of Mix Proportions and Methods of Testing on Poisson's Ratio for Mortars and Concretes," *Mag. Concrete Res.*, Vol. 18, No. 56, pp. 115–130, September 1966.
82. Anson, M., "An Investigation into a Hypothetical Deformation and Failure Mechanism for Concrete," *Mag. Concrete Res.*, Vol. 16, No. 47, pp. 73–82, June 1964.
83. Gopalakrishnan, K. S., A. M. Neville, and Amin Ghali, "Creep Poisson's Ratio of Concrete Under Multiaxial Compression," *J. Am. Concrete Inst., Proc.* Vol. 66, pp. 1008–1020, December 1969.
84. Powers, T. C., "Causes and Control of Volume Change," *J. Portland Cement Assoc. Res. Develop. Lab.*, Vol. 1, pp. 29–39, January 1959.
85. Lea, F. M., *The Chemistry of Cement and Concrete*, Edward Arnold (Publishers) Ltd., London, 1970, 727 pp.
86. Pickett, G., "Effect of Aggregate on Shrinkage of Concrete and Hypothesis Concerning Shrinkage," *J. Am. Concrete Inst., Proc.* Vol. 52, pp. 581–590, January 1956.
87. L'Hermite, R., "Volume Changes of Concrete," *Proceedings of the Fourth International Symposium on the Chemistry of Cement*, Washington, D.C., pp. 659–694, 1960.

88. Powers, T. C., "Aspects Fondamentaux du Retrait du Béton," *Rev. Matér. Construct. Trav. Publ.* No. 545, pp. 79–85, February 1961.
89. Troxell, G. E., J. M. Raphael, and R. E. Davis, "Long-time Creep and Shrinkage Tests of Plain and Reinforced Concrete," *Proc. ASTM*, Vol. 58, pp. 1101–1120, 1958.
90. Jones, T. R., Jr., T. J. Hirsch, and H. K. Stephenson, "Physical Properties of Structural Quality Lightweight Aggregate Concrete," *Report* No. E 52–59, Texas Transportation Institute, August 1959, 46 pp.
91. Shacklock, B. W., and P. W. Keene, "The Effect of Mix Proportions and Testing Conditions on Drying Shrinkage and Moisture Movement of Concrete," *Cement and Concrete Association Tech. Report* TRA/266, London, June 1957, 7 pp.
92. Neville, A. M., "Shrinkage and Creep in Concrete," *Structural Concrete*, Vol. 1, No. 2, pp. 49–85, March/April 1962.
93. Mather, K., "High Strength, High Density Concrete," *J. Am. Concrete Inst., Proc.* Vol. 62, No. 8, pp. 951–962, August 1965.
94. Ross, A. D., "Shape, Size, and Shrinkage," *Concrete Construct. Eng.*, London, pp. 193–199, August 1944.
95. Pickett, G., "Shrinkage Stresses in Concrete," *J. Am. Concrete Inst., Proc.* Vol. 42, pp. 165–204, January 1946; pp. 361–400, February 1946.
96. Bresler, B., D. Helmich, and L. V. Ramakrishna, "Non-Uniform Drying Shrinkage in Reinforced Concrete," Preliminary Publication, *Symposium on Design of Concrete Structures for Creep, Shrinkage, and Temperature Changes*, Int. Assoc. for Bridge and Structural Engineering, Madrid, pp. 171–179, 1970.
97. Reichard, T. W., "Creep and Drying Shrinkage of Lightweight and Normal-Weight Concretes," U.S. Department of Commerce, *Nat. Bur. of Standards Monograph* 74, March 1964, 30 pp.
98. Hansen, T. C., and A. H. Mattock, "The Influence of Size and Shape of Member on the Shrinkage and Creep of Concrete," *J. Am. Concrete Inst., Proc.* Vol. 63, pp. 267–290, February 1966.
99. Verbeck, G. J., "Carbonation of Hydrated Portland Cement," *ASTM Spec. Tech. Publ.* No. 205, pp. 17–36, 1958.
100. Dilger, W., and A. M. Neville, "Creep Buckling of Long Columns," *The Structural Engineer*, Vol. 49, No. 5, pp. 223–226, May 1971.
101. Neville, A. M., "Theories of Creep in Concrete," *J. Am. Concrete Inst., Proc.* Vol. 52, pp. 47–60, September 1955.
102. Ali, I., and C. E. Kesler, "Mechanisms of Creep in Concrete," *Symposium on Creep of Concrete, Am. Concrete Inst.* SP-9, pp. 35–57, 1964.
103. Neville, A. M., "Creep Recovery of Mortars Made with Different Cements," *J. Am. Concrete Inst., Proc.* Vol. 56, pp. 167–174, August 1959.
104. Neville, A. M., *Creep of Concrete: Plain, Reinforced, and Prestressed*, North-Holland Publishing Co., Amsterdam, 1970, 620 pp.
105. Wagner, O., "Das Kriechen Unbewehrten Betons, "*Deutscher Ausschuss für Stahlbeton*, No. 131, Berlin, 1958, 74 pp.
106. Neville, A. M., "Role of Cement in the Creep of Mortar," *J. Am. Concrete Inst., Proc.* Vol. 55, pp. 963–984, March 1959.
107. Nasser, K., and A. M. Neville, "Creep of Concrete at Elevated Temperatures," *J. Am. Concrete Inst., Proc.* Vol. 62, pp. 1567–1579, 1965.
108. Ross A. D., G. England, and R. Svan, "Prestressed Concrete Beams Under a Sustained Temperature Crossfall," *Mag. Concrete Res.*, Vol. 17, No. 52, pp. 117–126, September 1965.

109. Hannant, D., "Strain Behavior of Concrete Up to 95°C Under Compressive Stresses," *Proceedings of a Conference on Prestressed Concrete Pressure Vessels*, London, Group C, Paper 17, pp. 57–71, 1967.
110. Maréchal, J. C., "Le Fluage du Béton en Fonction de la Temperature," *Materials and Structures*, Vol. 2, No. 8, pp. 111–115, March/April 1969.
111. Lambotte, H., "Le Fluage du Béton en Torsion," *RILEM Bull.*, No. 17, pp. 3–12, December 1962.
112. Neville, A. M. and W. Z. Liszka, "An Accelerated Determination of Creep of Lightweight Aggregate Concrete," *Civil Engineering and Public Works Review* (London), Vol. 68, No. 803, pp. 515–519, June 1973.
113. Mukâddam, H. A. and Bresler, B., "Behavior of Concrete under Variable Temperature and Loading," *ACI International Seminar on Concrete Nuclear Reactors*, Berlin, *Am. Concrete Inst.* SP-34, Vol. 2, pp. 771–798, 1972.
114. Reis, E. E., J. D. Mozer, A. C. Bianchini, and C. E. Kesler, "Causes and Control of Cracking in Concrete Reinforced with High-Strength Steel Bars—A Review of Research," University of Illinois, Engineering Experiment Station *Bull.* 479, 1965, 61 pp.
115. Hansen, T. C., "Cracking and Fracture of Concrete and Cement Paste," *Symposium on Causes, Mechanism, and Control of Cracking in Concrete, Am. Concrete Inst. SP-20*, pp. 5–28, 1968.
116. Brewer, H. W., "General Relation of Heat Flow Factors to the Unit Weight of Concrete," *J. Portland Cement Assoc. Res. Develop. Lab.*, Vol. 9, No. 1, pp. 48–60, January 1967.
117. Mitchell, L. J., "Thermal Properties," *ASTM Spec. Tech. Publ.* No. 169, pp. 129–135, 1956.
118. Crammerer, J. S., "The Thermal Conductivity of Lightweight Concretes," *National Research Council, Tech. Transl.* 319, Ottawa, 1952, 12 pp.
119. Campbell-Allen, D., and C. P. Thorne, "The Thermal Conductivity of Concrete," *Mag. Concrete Res.*, Vol. 15, No. 43, pp. 39–48, March 1963.
120. Louden, A. G., and Stacy, E. F., "The Thermal and Acoustic Properties of Lightweight Concretes," *Structural Concrete*, Vol. 3, No. 2, pp. 58–76, March/April 1966.
121. Meyers, S. L., "How Temperature and Moisture Changes May Affect the Durability of Concrete," *Rock Products*, Chicago, pp. 153–157, August 1951.
122. *Handbook for Concrete and Cement*, U.S. Army Corps of Engineers, Vicksburg, Miss., 1949.
123. Meyers, S. L., "Thermal Coefficient of Expansion of Portland Cement—Long-time Tests," *Ind. Eng. Chem.* (Easton, Pa.), Vol. 32, No. 8, pp. 1107–1112, 1940.
124. Walker, S., D. L. Bloem, and W. G. Mullen, "Effects of Temperature Changes on Concrete as Influenced by Aggregates," *J. Am. Concrete Inst., Proc.* Vol. 48, pp. 661–679, April 1952.
125. Bonnell, D. G. R., and F. C. Harper, "The Thermal Expansion of Concrete," *D.S.I.R. National Building Studies, Tech. Paper* No. 7, H.M.S.O., London, 1951, 22 pp.
126. Helmuth, R. A., "Dimensional Changes of Hardened Portland Cement Pastes Caused by Temperature Changes," *Proc. Highway Res. Board*, Vol. 40, pp. 315–336, 1961.
127. Philleo, R., "Some Physical Properties of Concrete at High Temperatures," *J. Am. Concrete Inst., Proc.* Vol. 54, pp. 857–864, April 1958.
128. Monfore, G. E., and A. E. Lentz, "Physical Properties of Concrete at Very Low Temperatures," *J. Portland Cement Assoc. Res. Develop. Lab.*, Vol. 4, pp. 33–39, May 1962.
129. Hannant, D. J., "Effects of Heat on Concrete Strength," *Engineering* (London), Vol. 197, p. 302, 21 February 1964.

4

Bond and Cracking in Reinforced Concrete

D. WATSTEIN
and
B. BRESLER

4.1 INTRODUCTION

Early experimenters and designers of reinforced concrete recognized that slip of the reinforcement had to be prevented in order to minimize cracking, to develop flexural and shearing strengths, and to maintain the composite behavior of reinforced concrete. Wilkinson in England (1854) and Monier in France (1867) used wire ropes and wire netting as reinforcement with a view to developing the required anchorage. In the United States, it was one of the early pioneers of reinforced concrete, Thaddeus Hyatt, who realized that reinforced concrete can function as a composite material only if the reinforcement is bonded to the concrete along its entire length, and not merely anchored at the ends. He proposed in his patent of 1878 that the reinforcing bars be ". . . specially rolled for this purpose with bosses or raised portions formed upon the flat faces of the metal." This was the earliest formulation of the principle that bond between concrete and reinforcement is essential to maintain integrity in the composite material known as reinforced concrete. Different types of such bars, which became known as deformed bars, were developed in the United States. These were the Johnson (corrugated square), cup, lug, and Thatcher bars. Twisted bars with and without lugs also made their appearance on the market.

In the early part of this century a number of bond tests were reported. However, these tests were conducted using a variety of test specimens and test procedures. Also, in almost all the tests only the maximum bond values were reported. There was a need for a comprehensive series of tests based on a standard procedure. Such a series of tests was conducted by Duff Abrams[1] who employed both pullout and beam specimens and measured slip as well as bond strength. This investigation laid the foundation for the many subsequent studies which culminated in the adoption of ASTM A305. This Standard defined the minimum requirements for deformed reinforcing bars as we know them today.

As long as reinforced concrete structures were built with relatively low-strength steel bars and relatively low-strength concretes, bond strengths of deformed bars were adequate to assure reliable composite action of these structures. However, the recent development of high-strength reinforcing bars, the widespread use of high-strength concretes, and the introduction of new large-diameter bars caused designers of reinforced concrete to examine the subject of bond anew. Although the development of modern deformed bars which conform to ASTM A615, A616, and A617, makes bond stress less critical in design than it was in the days when mostly plain bars were used, use of high-strength deformed bars gave rise to new problems related to crack width limitations and failures by splitting rather than slipping.

4.2 BOND PROBLEM IN FLEXURAL MEMBERS

Bond stresses between concrete and reinforcement may be divided into two classes: (1) bond stresses which develop in an anchorage zone at the ends of bars which extend into a support, or at the ends of bars cut off within a span, and (2) flexural bond stresses which exist at the surface of the reinforcement and vary generally with the shear or change in bending moment. In the following discussion we will refer to these as anchorage bond and flexural bond stresses.

The well-known bond formula derived in standard textbooks, assuming concrete resists no tension,

$$u = \frac{V}{\sum ojd} \tag{4.1}$$

does not yield in general the true anchorage or flexural-bond values. Mylrea[2] was one of the first to state explicitly that Eq. (4.1) yields true values of bond stress only when the total tension force in the steel varies directly with the ordinate of the moment curve, and when all bars are straight and run the full length of the member; he pointed out that under these conditions the external shear curve will represent, to scale, the distribution of the internal bond

stresses. Strictly speaking, Mylrea also should have stipulated that in order to apply the bond formula, the beam must be free of cracks, since cracks greatly modify the distribution of bond stresses. If we keep in mind the fact that prior to cracking the steel reinforcement carries only a small part of the total tension, we can see that the bond formula in reality is only applicable to uncracked beams in which only the reinforcement carries tension, and that this tension varies along the length of the beam directly as the ordinate to the moment curve. These requirements for the applicability of the bond formula are as contradictory as they are unrealistic, since beams carrying loads heavy enough to develop design stresses in reinforcement are invariably cracked at various sections and it is well known that while the steel stresses at cracked sections approach the theoretical values computed by neglecting the tensile zone of the concrete, the stresses in uncracked portions of the beams are in general considerably less than the computed values.

It is apparent from the preceding discussion that at no stage of loading of the beam does the bond formula, Eq. (4.1), give a true picture of the distribution of bond stresses.

In order that a reinforced-concrete, flexural member of constant depth containing straight, full-length bars act as a true beam, the distance between the centroid of tensile reinforcement and the resultant of the compressive stress block must be a constant along its entire length. Then the total tension in the reinforcement will be represented to some scale by the bending-moment curve. Since we also assume that the reinforcement resists all the tension at every section, the difference between, the total tensile forces T_1 and T_2 at adjacent sections I and II must be developed in the steel (Fig. 4.1).

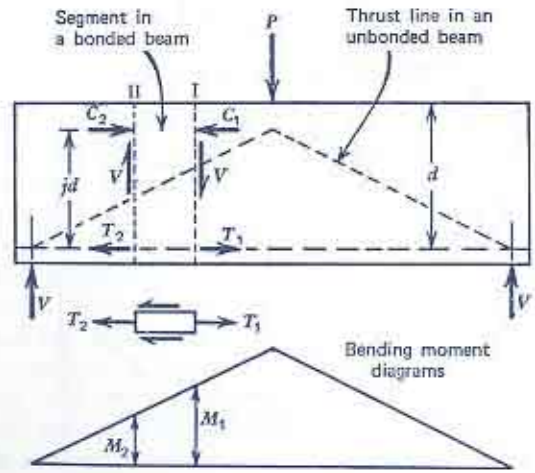

FIGURE 4.1. Idealized beam action.

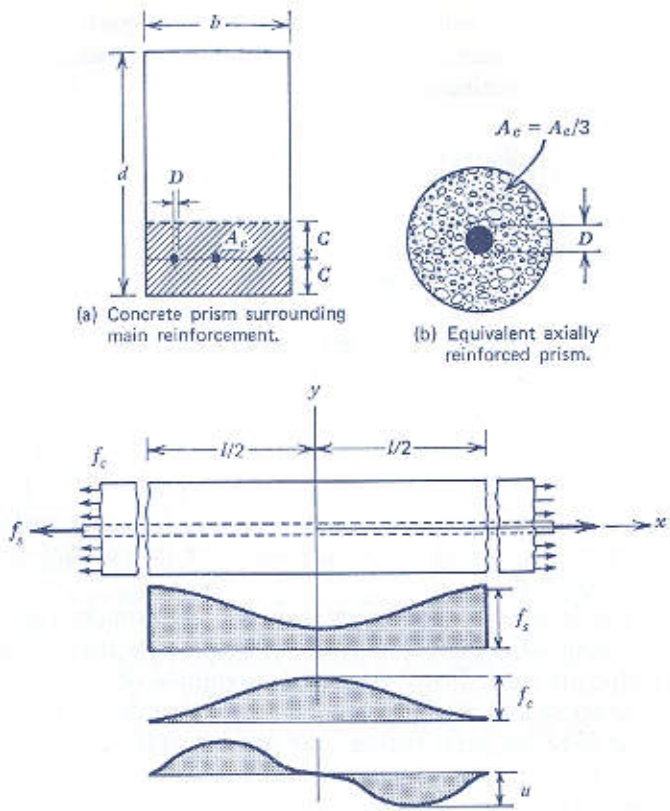

(a) Concrete prism surrounding main reinforcement.

(b) Equivalent axially reinforced prism.

(c) Stresses in a cracked axially reinforced concrete prism.

FIGURE 4.3. Idealized stresses in cracked beams and prisms.

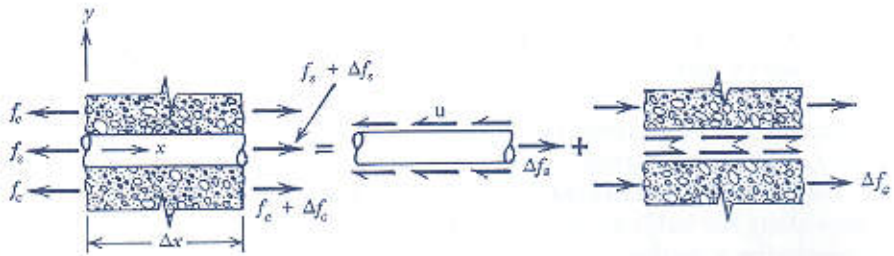

FIGURE 4.4. Stresses on isolated steel and concrete elements.

where D is the diameter of the round steel bar, and u is the bond stress uniformly distributed over the length Δx. When Δx becomes small, approaching an infinitely small length dx, the local bond stress u_x is:

$$u_x = \frac{df_s}{dx}\frac{A_s}{\pi D} = \frac{df_s}{dx}\frac{D}{4} \tag{4.3}$$

or

$$u_x = -\frac{df_c}{dx}\frac{A_c}{\pi D} = -\frac{df_c}{dx}\frac{D}{4\bar{\rho}} \tag{4.4}$$

where $\bar{\rho} = A_s/A_c$ is the reinforcement ratio based on concrete prism area A_c which is subjected to uniformly distributed stress f_c. Equation (4.3) can be used to calculate the bond stress u_x at the interface, if the gradient (df_s/dx) of the steel stress is known.

Assuming that the origin O of reference axes corresponds to a point of no relative displacement between steel and concrete, then at a point x the relative displacement g between steel and concrete is:

$$g = \int_0^x \varepsilon_s\,dx - \int_0^x \varepsilon_c\,dx \tag{4.5}$$

where ε_s and ε_c are strains in steel and concrete respectively. Differentiating Eq. (4.5) and assuming elastic behavior of steel and concrete:

$$\frac{dg}{dx} = \varepsilon_s - \varepsilon_c = \frac{f_s}{E_s} - \frac{f_c}{E_c} = \frac{1}{E_s}(f_s - nf_c) \tag{4.6}$$

where E_s, E_c are elastic moduli of steel and concrete, respectively, and n is the modular ratio E_s/E_c. Differentiating Eq. (4.6)

$$\frac{d^2g}{dx^2} = \frac{1}{E_s}\left(\frac{df_s}{dx} - n\frac{df_c}{dx}\right) \tag{4.7}$$

and substituting from Eqs. (4.3) and (4.4)

$$\frac{d^2g}{dx^2} = \frac{1}{E_s}\frac{4}{D}u_x(1 + n\bar{\rho}) \tag{4.8}$$

The following assumptions have been made in deriving Eq. (4.8): (1) steel and concrete behave elastically, i.e., strain is uniquely defined as $\varepsilon = f/E$; (2) slip g and stresses f_s and f_c are continuous functions of x, i.e., no cracks or discontinuities exist in the section of the length under examination; and (3) the stresses in concrete are uniformly distributed over the cross-sectional area A_c, thus neglecting shearing distortions in the concrete. Equation (4.8) has been derived without considering any bond characteristic of the steel–concrete interface which may be defined by the bond stress–slip relationship. If such a relationship is defined in terms of slip only, then a function $u = F(g)$ defines a bond slip law.

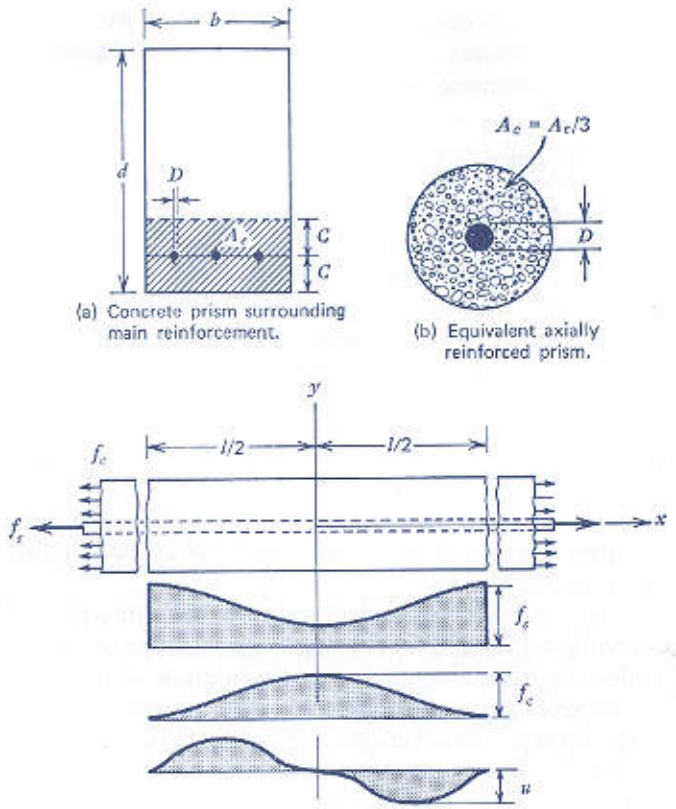

FIGURE 4.3. Idealized stresses in cracked beams and prisms.

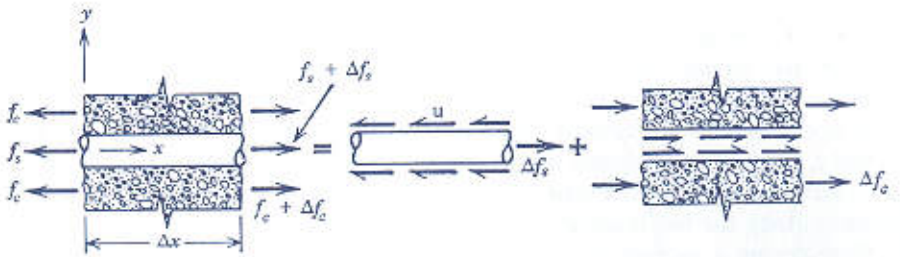

FIGURE 4.4. Stresses on isolated steel and concrete elements.

where D is the diameter of the round steel bar, and u is the bond stress uniformly distributed over the length Δx. When Δx becomes small, approaching an infinitely small length dx, the local bond stress u_x is:

$$u_x = \frac{df_s}{dx}\frac{A_s}{\pi D} = \frac{df_s}{dx}\frac{D}{4} \tag{4.3}$$

or

$$u_x = -\frac{df_c}{dx}\frac{A_c}{\pi D} = -\frac{df_c}{dx}\frac{D}{4\bar{\rho}} \tag{4.4}$$

where $\bar{\rho} = A_s/A_c$ is the reinforcement ratio based on concrete prism area A_c which is subjected to uniformly distributed stress f_c. Equation (4.3) can be used to calculate the bond stress u_x at the interface, if the gradient (df_s/dx) of the steel stress is known.

Assuming that the origin O of reference axes corresponds to a point of no relative displacement between steel and concrete, then at a point x the relative displacement g between steel and concrete is:

$$g = \int_0^x \varepsilon_s\, dx - \int_0^x \varepsilon_c\, dx \tag{4.5}$$

where ε_s and ε_c are strains in steel and concrete respectively. Differentiating Eq. (4.5) and assuming elastic behavior of steel and concrete:

$$\frac{dg}{dx} = \varepsilon_s - \varepsilon_c = \frac{f_s}{E_s} - \frac{f_c}{E_c} = \frac{1}{E_s}(f_s - nf_c) \tag{4.6}$$

where E_s, E_c are elastic moduli of steel and concrete, respectively, and n is the modular ratio E_s/E_c. Differentiating Eq. (4.6)

$$\frac{d^2g}{dx^2} = \frac{1}{E_s}\left(\frac{df_s}{dx} - n\frac{df_c}{dx}\right) \tag{4.7}$$

and substituting from Eqs. (4.3) and (4.4)

$$\frac{d^2g}{dx^2} = \frac{1}{E_s}\frac{4}{D}u_x(1 + n\bar{\rho}) \tag{4.8}$$

The following assumptions have been made in deriving Eq. (4.8): (1) steel and concrete behave elastically, i.e., strain is uniquely defined as $\varepsilon = f/E$; (2) slip g and stresses f_s and f_c are continuous functions of x, i.e., no cracks or discontinuities exist in the section of the length under examination; and (3) the stresses in concrete are uniformly distributed over the cross-sectional area A_c, thus neglecting shearing distortions in the concrete. Equation (4.8) has been derived without considering any bond characteristic of the steel–concrete interface which may be defined by the bond stress–slip relationship. If such a relationship is defined in terms of slip only, then a function $u = F(g)$ defines a bond slip law.

In assuming such a simple relationship between bond stress and slip the following assumptions are made: (1) the influence of stresses on the bar surface due to shrinkage, local surface roughness, or other effects, which may influence resistance to slip, is neglected; and (2) effects of stress history and other time effects on resistance to slip are also neglected.

Substituting $u = F(g)$ into Eq. (4.8), a differential equation is obtained as follows:

$$\frac{d^2g}{dx^2} = \frac{4(1 + n\bar{p})}{DE_s} F(g) \tag{4.9}$$

Solution of this differential equation with a given set of boundary conditions defines the amount of slip g along the reinforcement, and thus would also define the distribution or the bond stress u_x.

Early studies of bond and slip did not pursue this approach, however. It is probable that they were discouraged by the difficulties of determining $F(g)$ experimentally, which requires separate measurements of strains ε_s and ε_c at the concrete–steel interface. While ε_s can be measured with adequate precision, the difficulty of measuring ε_c at the interface has not as yet been satisfactorily overcome, and therefore the nature of $F(g)$ can be examined only in terms of some speculative assumptions. Nevertheless, such examination may be helpful in establishing some of the variables which have considerable influence on the nature of $F(g)$. Recent studies[5] have shown, however, that existence of a simple functional relationship between u and g is most unlikely, particularly where the effects of stress history are important.

Because the distribution of bond stresses along the reinforcing steel could be determined experimentally in a relatively simple manner, early studies focused attention on the solution of this aspect of the problem. Rewriting Eq. (4.3) in terms of strain ε_s:

$$u_x = \frac{D}{4} E_s \frac{d\varepsilon_s}{dx} \tag{4.10}$$

and measuring ε_s along the bar permits calculation of u_x by differentiating ε_s with respect to x and using Eq. (4.10).

Based on such experimental studies a number of approximations for u_x were proposed. Some of the simple expressions are indicated below:

$$u_x = \text{constant} = \bar{u} \tag{4.11a}$$

$$u_x = 2u_m \frac{x}{l} \tag{4.11b}$$

$$u_x = 4u_m \left[\frac{x}{l} - \left(\frac{x}{l}\right)^2\right] \tag{4.11c}$$

$$u_x = u_m \sin\left(\frac{2\pi x}{l}\right) \tag{4.11d}$$

where $\bar{u}$ is the average bond stress, u_m is the maximum bond stress at the free end of the crack, l is the distance between two adjacent cracks, and $0 \leq x \leq l/2$.

These equations prescribing the distribution of bond stresses between adjacent cracks permit calculation of crack spacing and crack widths for certain limit conditions. Maximum tensile stress in concrete f_{cm} will occur at $x = 0$. As the stress in concrete is zero at the crack, $x = l/2$, the following equilibrium condition must be satisfied:

$$f_{cm}A_c = \pi D \int_0^{l/2} u_x \, dx \qquad \text{or} \qquad f_{cm} = \frac{\pi D}{A_c} \int_0^{l/2} u_x \, dx \tag{4.12}$$

In the simplest case when $u_x = \text{constant} = \bar{u}$

$$f_{cm} = \frac{\pi D}{A_c} \bar{u} \frac{l}{2} \qquad \text{or} \qquad l = 2\frac{f_{cm}}{\bar{u}} \frac{A_c}{\pi D} \tag{4.13}$$

If f_{cm} reaches tensile strength of concrete f_t' and corresponding mean bond stress $\bar{u}$ reaches its maximum value u_m, then crack spacing l is

$$l = 2\frac{f_t'}{u_m} \frac{A_c}{\pi D} \tag{4.14}$$

The length l is just sufficient to form a new crack at midlength. Normal variations in f_t' and u_m could lead to variations in l. For example, a decrease in f_t' and an increase in u_m of about 30% could lead to a crack spacing $l/2$, or conversely an increase in f_t' and a decrease in u_m of 30% would limit the maximum crack spacing to $2l$. Thus, considerable scatter in experimental data could be expected with minimum spacing l_m of a crack $2l \geq l_m \geq l/2$.

This approach to determining crack spacing l is based on a limit equilibrium analysis. The assumptions are that u_x is constant and equal to $\bar{u} = u_m$ and that values of f_t' and u_m are defined empirically; the rest of the analysis requires only that equilibrium condition is satisfied. In view of the difficulties associated with the definition of a "bond–slip" law and the general scatter in the values of minimum spacing l_m predicted by limit equilibrium analysis, it seems that empirical values of l_m based on statistical studies might be more useful from a practical point of view.

The crack width w is a result of slip between steel and concrete. If there is no relative displacement between steel and concrete at $x = 0$, then the crack width reflects the excess of elongation in the steel over that in concrete in length l:

$$w = \int_0^l \varepsilon_s \, dx - \int_0^l \varepsilon_c \, dx \tag{4.15}$$

Neglecting the concrete elongation the crack width may be approximated by the average strain in the steel multiplied by the crack spacing, i.e., $w = (f_s/E_s)l$.

4.4 NATURE OF BOND STRENGTH

Before analyzing the nature of bond failure in beams containing deformed bars, it is well to consider the mechanism of bond failure in beams with plain bars. In the early days of reinforced concrete it was commonly assumed that bond between plain bars and concrete was basically due to adhesion between the cement paste and the steel surface. However, it was soon recognized that even at low steel stresses cracks formed in concrete causing sufficient slip to destroy the adhesion immediately next to a crack. After the failure of adhesion only the frictional resistance remained and the bond stress could be thought of as the overall average of the bond on the section where adhesive bond was still intact, with the lower bond stress where only frictional resistance was present, and possibly the zero bond stress in portions of steel not yet stressed.

The nature of bond failure of plain bars is described by K. V. Mikhailov[6] who studied the relative values of adhesion and frictional bond with hot rolled and smooth cold rolled bars using pullout and beam specimens. This study led to the following conclusions:

1. The adhesive forces between the steel and concrete are not large and amount only to 70–100 psi. The author concluded that adhesion itself is of no significance in the development of the resistance of reinforcement to slip.
2. Comparison of bond strengths of smooth cold-rolled and untreated hot-rolled bars indicated that adhesion and frictional resistance resulting from shrinkage account for 25 to 30% of the bond strength.
3. The bond value of plain bars depends basically on the degree of roughness of the surface and the change in the lateral dimension of the bars along their embedded length; these factors account for about 70 to 75% of the total resistance to slip.

With the advent of modern deformed bars the mechanism of bond failure changed radically. Frictional resistance and adhesion are still present but the primary reliance for the bond strength is on the bearing of lugs and the strength of concrete between lugs. There is also a fundamental change in the manner of failure. With deformed bars embedded either in a pullout or a beam specimen the failure is almost invariably associated with longitudinal splitting along the surface nearest the reinforcing bar, and the splitting usually develops before the stress-free end of the bar begins to slip. With plain hot-rolled

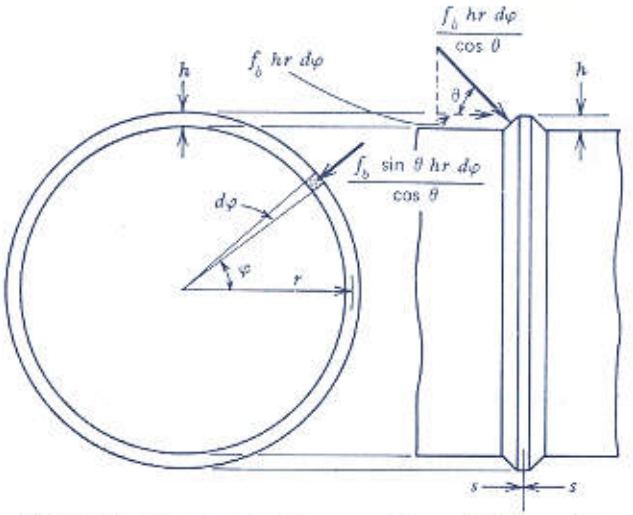

FIGURE 4.5. Bearing forces on lugs of deformed bars.

bars splitting also occurs, but only after substantial slips at both loaded and free ends of the pullout specimen. For a smooth cold-rolled bar failure occurs by slip of the bar as a whole which may be pulled completely out of the concrete leaving a smooth bore in the specimen.

Although in pullout test specimens the concrete is in compression while in beams the concrete surrounding the bars is in tension, fundamentally in both cases bond failure is produced by splitting of the concrete from the wedging action of the lugs against the concrete. The splitting force produced by the lugs of a deformed bar can be estimated by considering the forces set up by their wedging action.

In Fig. 4.5, the bearing stress f_b is shown normal to the surface of the lug height h. The bearing force is $f_b(h/\cos\theta)r\,d\varphi$, its radial component is $f_b h \tan\theta r\,d\varphi$ and the horizontal component of the radial force is $f_b h \tan\theta \cos\varphi\, r\, d\varphi$.

Since the splitting force is concentrated at the face of the lugs spaced a distance s apart, the splitting force per unit of length of bar is given by T:

$$T = \frac{2}{s}\int_0^{\pi/2} f_b h \tan\theta \cos\varphi r\, d\varphi$$
$$= \frac{2}{s}(f_b h \tan\theta r)(\sin\varphi)\Big|_0^{\pi/2}$$
$$= \frac{D}{s} f_b h \tan\theta \qquad (4.16)$$

comprising essentially of coarse-grained quartz may prove *incompatible* in a concrete mix.

The shape and the surface texture of a crushed rock reflect the environmental conditions during rock formation and the internal crystalline structure of the minerals composing the rock. Crushed quartzite, granite, gabbro, and basalt frequently yield smooth, equidimensional particles which require less cement paste to produce the desired workability of concrete. Rough-textured and angular aggregate particles, however, produce a relatively harsh concrete mix. On the other hand, the roughness in the surface texture of aggregate favorably affects the bonding quality. Surface roughess and pores assist the physical adherence of cement paste to the aggregate. It is obvious that the attrition action on river gravels makes them smooth and well-rounded, thereby imparting all the merits and demerits that are characteristic of smooth-textured aggregate.

Regarding *size of aggregate*, the maximum size permissible for a job should be used, because it is generally more economical (less surface area and less voids require less cement paste), and also the drying shrinkage of concrete will be reduced. The factors limiting the maximum size of aggregate include the thickness of the concrete section, the spacing of the reinforcement, and the equipment to be used for mixing and placing the fresh concrete. *Grading of aggregate* refers to the size distribution of the aggregate particles. If all the aggregate particles are of one size, or if there is a large excess of a particular size in the total aggregate, the void space becomes large and more cement paste is required to fill this void space. On economic grounds an ideal gradation of a concrete aggregate is one which will result in a minimum void content, but this may not yield the best possible workability; hence, trial mixes are frequently necessary to establish desirable grading limits.

Typical grading limits are specified in ASTM C33. In Fig. 1.2 these limits are illustrated for concrete aggregates graded up to 1 1/2 in. maximum size. Usually aggregates that have no large deficiency or excess of any one size, and give a smooth grading curve, show satisfactory results. Although several different gradings may be used to produce suitable concrete, once a grading has been selected it should be maintained within closely controlled limits in order to obtain uniform consistency, workability and the desired properties in hardened concrete.

Fineness modulus of aggregate is often used as an index of coarseness. The fineness modulus is defined as the sum of the percentages in the sieve analysis of the aggregate divided by 100, when the sieve analysis is expressed as the cumulative percentages retained on sieves No. 4, 8, 16, 30, 50, and 100. In Table 1.4 are shown calculations and fineness moduli for typical coarse, medium and fine sands.

Since uniform quality control is of great importance on large jobs some

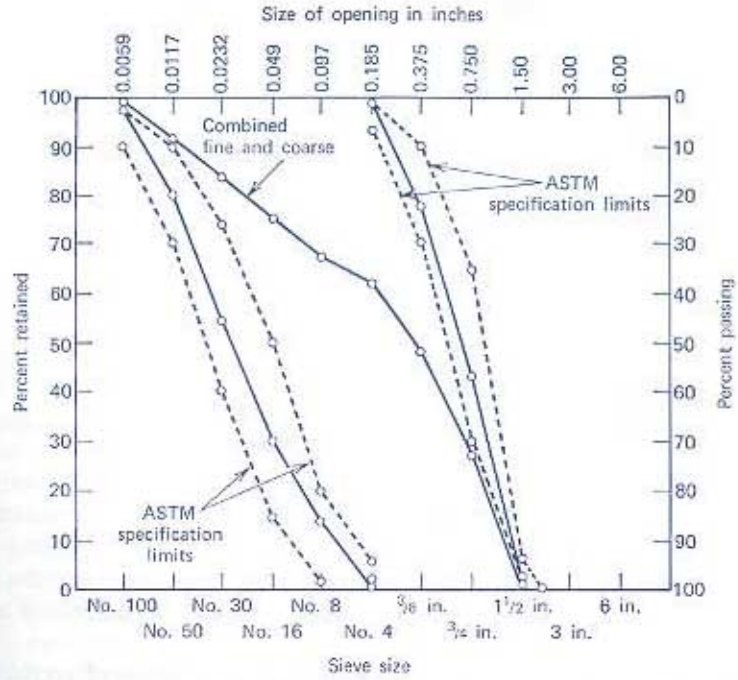

FIGURE 1.2. Typical size distribution for aggregate graded up to 1 1/2-in. max. size.[6] (Reprinted by permission of the American Society for Testing and Materials, Copyright ASTM.)

agencies, such as the Corps of Engineers, require that fineness moduli of at least four of any five consecutive test samples of the fine aggregate, as delivered to the mixer, shall not vary by more than 0.15 from the average fineness modulus of all samples taken during the first month's operation. ASTM C33 requires that the fineness modulus not vary by more than 0.20 from the value assumed in selecting the proportions for the concrete mix.

The workability, bleeding, and finishing of concrete is much affected by the amount of fines in the sand (minus 50 mesh material). In general, very fine sands prove to be uneconomical, and very coarse sands will produce harsh mixes.

Since porosity, shape, and texture of aggregate particles and their size distribution affect the characteristics of fresh concrete, it is obvious that no predictions in concrete proportioning can be made through a consideration of the fineness modulus alone. Making trial mixes with job materials is, therefore, desirable to predetermine the consistency, workability, and finishing characteristics of the concrete.

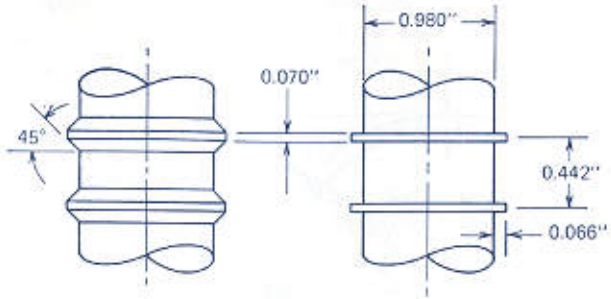

FIGURE 4.6. Experimental deformed bars.

There is evidence[7] from tests of special experimental bars shown in Fig. 4.6 that as slip between concrete and steel develops, failure in bearing takes place on an inclined plane at each bar deformation, and it appears that the plane producing failure at the least stress is inclined at 45° to the bar surface. This conclusion is based on the observation that experimental bars with both square and 45° lugs yielded essentially the same stress–slip characteristics in pullout tests.

Keeping in mind the fact that the longitudinal splitting develops along the nearest surface as shown in Fig. 4.7 the splitting force given by Eq. (4.16) may be assumed to be resisted only by the thinnest cover of concrete over the bar. Thus, the splitting stress across the concrete cover of thickness t is given by:

$$\frac{T}{t} = \frac{Dh}{st} f_b \tan\theta = f_t \tag{4.17}$$

The angle θ may be assumed to be 45° and in American practice both h and s are linear functions of the diameter D.[8] Equation (4.17) can thus be

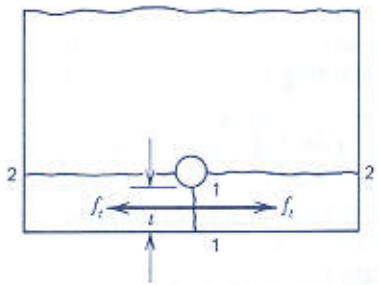

FIGURE 4.7. Splitting action of bar slipping in a beam.

reduced to the following form:

$$f_b \frac{h}{s} = f_t \frac{t}{D} \tag{4.18}$$

The summation of the longitudinal components of the bearing forces around the perimeter of a given lug represents the total bond force in a length of bar equal to s, the lug spacing, or

$$\int_0^{2\pi} f_b h r \, d\varphi = u_m \pi D s \tag{4.19}$$

and

$$\pi D h f_b = u_m \pi D s \tag{4.20}$$

Substituting from Eq. (4.18) into Eqs. (4.19) and (4.20)

$$u_m = f_b \frac{h}{s} = f_t \frac{t}{D} \tag{4.21}$$

Equation (4.21) states that the bond strength varies directly as the tensile splitting strength and it varies inversely as the bar diameter D, a fact which has been established by a number of investigators. It also states that for a given bar diameter, the bond strength increases with the thickness t of the clear cover over the bar. This observation has been clearly confirmed by Ferguson and Thompson[9] who reported a linear relationship between the bond strength and the clear cover over the bar for bar sizes ranging from No. 7 to No. 11. There is some indication that the increment in bond strength per inch increase in thickness of cover is less for the larger bars and additional work is needed to establish the effect of bar diameter on the influence of concrete cover.

In addition to the bar diameter D and the cover thickness t, the bond strength is also decisively affected by the length of the bar under consideration. It appears that it matters little whether we are considering bond in pullout specimens or in beams, and whether the bond in question is that at the end of a bar in a simply supported beam, at the end of a bar cutoff within the span, or the portion of a bar between the point of inflection and the end of that bar. The relationship between the bond strengths and the length of embedment is well illustrated in Fig. 4.8 (taken from Reference 9). It is noteworthy that the data for both No. 3 and No. 7 bars fall into a single family of points through which a single curve was drawn. A similar relationship was observed by Mathey and Watstein,[10] except that the bond strengths were plotted against the ratios of length of embedment to the bar diameter, and the data fell into two distinct curves for No. 4 and 8 bars.

Additional insight into the nature of bond strength can be obtained from recent studies on internal cracking associated with the development of bond

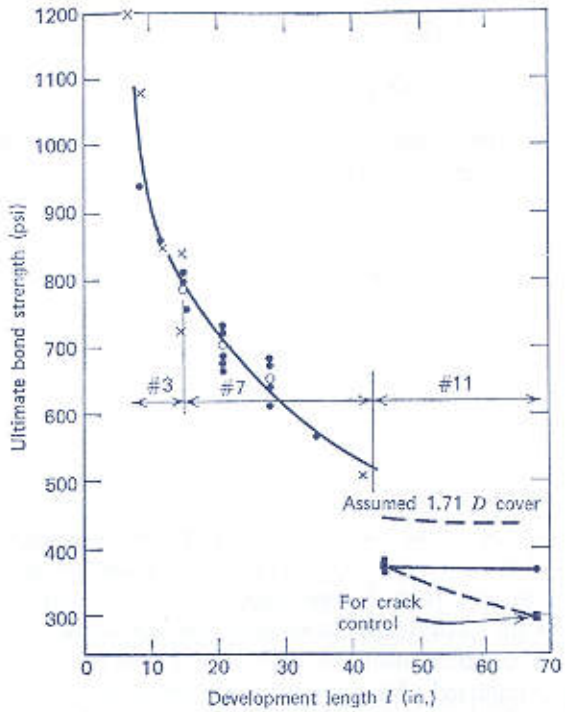

FIGURE 4.8. Ultimate bond strength for $b = 18$ in., $f_c = 3300$ psi, 1.5-in. cover.[9]

stresses in concrete tension prisms. The analytical and experimental data presented by Broms and Lutz[11] established existence of radial cracks originating at the steel–concrete interface and terminating within the prism, i.e., not extending to the concrete surface and therefore not visible to the outside observer. Further studies by Bresler and Bertero[12] indicated that at low load levels principal tensile stresses at the steel–concrete interface are inclined at an angle with the longitudinal axis varying from about 60° at the crack face and decreasing to 0° at the midway section between two adjacent cracks, as shown in Fig. 4.9(a). Goto's[13] experimental studies confirmed that inclined cracks approximately normal to the direction of principal stresses, developed within the concrete prism, as shown in Fig. 4.9(b).

Based on these studies the mechanism of bond development with increasing loads can be described as follows. At low stress levels in the steel reinforcement high principal stresses occur only at the interface, in the zones adjacent to the full transverse cracks, where local inclined cracking occurs. This local cracking relieves the high tension near the ends and shifts the zone of maximum principal stress inward from the transverse crack face. With increasing

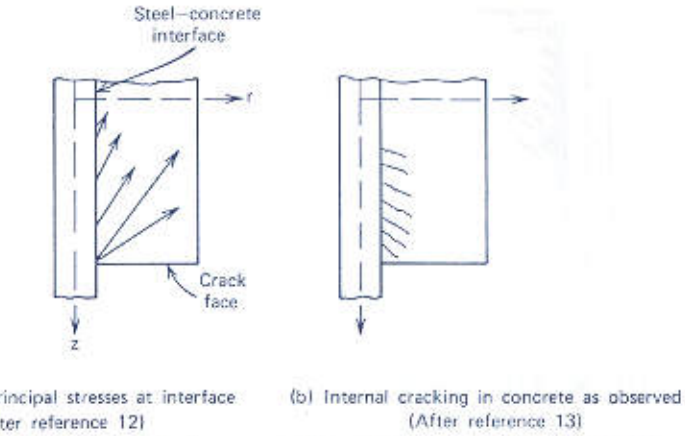

FIGURE 4.9. Internal stresses and cracking in axially reinforced concrete prism subjected to tension.

load these maximum stresses reach the tensile strength of the concrete generating additional internal cracking. With further increase in load the process of internal cracking and consequently of shifting the peak stresses continues. At yield stress level the internal cracks propagate through most of the prism, so that concrete adjacent to the steel reinforcement forms a "boundary layer" of teeth-like segments which resist the pullout forces by wedging action, as shown in Fig. 4.10. The effective "shear modulus" of the cracked concrete is reduced by the cracking, so that the concrete adjacent to steel reinforcement can be idealized as a homogenized soft boundary layer. Using such a model, principal stresses at the steel–concrete interface and deformations at the crack face were evaluated[12] and are shown in Fig. 4.11.

The extent of cracking and of resulting "softening" of the boundary layer cannot as yet be defined quantitatively in a realistic manner. The cracking is

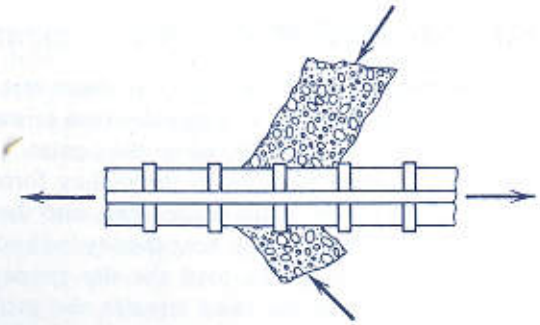

FIGURE 4.10. Wedging action in resisting pullout.

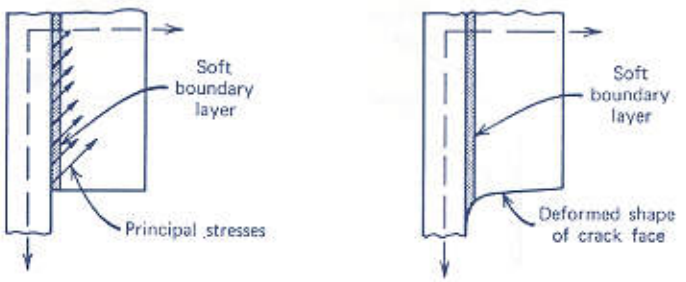

FIGURE 4.11. Internal stresses and deformations in concrete prism.[12]

highly sensitive to previous load history, to geometric details—such as the shape of the deformed surface of the steel bar and the effective thickness of cover—and to environmental history—such as temperature, humidity, and chemically aggressive atmosphere, which can significantly influence local stress conditions and internal cracking.

One corollary of this complex bond mechanism is that the relationship between bond stress and slip is highly variable along the length of the bar between two adjacent cracks, and therefore this relationship is not likely to be adequately defined by a single-valued function such as Eq. (4.9).

From the preceding analysis and supporting experimental evidence, it appears that the customary method of design for bond does not correspond to the actual bond and anchorage values which a bar can develop. It is now generally recognized that a more realistic approach to the bond problem is to regard it as a problem of computing the anchorage or development length of a bar necessary to transmit the stress in the steel to the surrounding concrete. Application of this approach is discussed in Section 4.8.4.

4.5 FLEXURAL AND ANCHORAGE BOND STRENGTHS

Bond strength is determined either from pullout or beam test specimen data. In a pullout test the bar is embedded in a cylinder or a prism and then subjected to tension at one end (Fig. 4.12), while the concrete bearing on the supporting platten provides the reaction to the pulling force. At relatively low stresses the bar begins to slip at the loaded end, and the corresponding bond stresses are concentrated in a zone near the loaded end while most of the bar is unstressed. With increasing load the slip propagates from the loaded end to the unloaded end, the bond stresses also propagating along the length of the bar.[14] Over a short length of the bar the bond stresses are

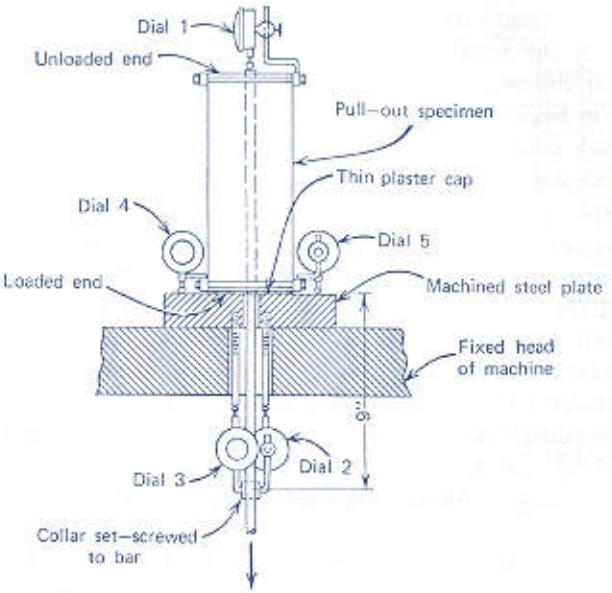

FIGURE 4.12. Pull-out test specimen. (Dial gage 1 measures slip at unloaded end. Dial gages 2 and 3 measure relative displacement of steel bar at unloaded end. Calculated strain in steel bar between point of attachment of dial gages 2 and 3 and loaded end as well as local crushing measured by dial gages 4 and 5 are deducted from displacement readings to obtain lip at loaded end.)

high, decreasing over the remaining portion. The nominal bond stress in a pullout specimen is obtained by dividing the total load by the embedded bar surface. The shorter the specimen, the more nearly uniform is the distribution of bond stresses at loads approaching ultimate and the more closely the nominal bond stress approaches the bond strength under given test conditions.

Pullout tests are satisfactory for measuring the relative bond values of bars with different deformations. The test results generally give bond-strength values considerably greater than that developed in flexural bond, because the concrete in compression restrains the tendency to fail by splitting, while flexural bond failures involve splitting in the tensile zone of the concrete beam.

Experience has shown that bond values derived from pullout tests cannot in general be applied to design of reinforced concrete beams and that beam tests are necessary to develop design criteria. The differences between bond values obtained from pullouts and from beams are due primarily to the different crack patterns which develop in the two types of specimens. Although

longitudinal cracks develop along the reinforcing bars in both beams and pullouts as the stresses increase and slip becomes appreciable, the crack patterns in the two types of specimens are quite different. As the steel stresses increase in beam specimens, transverse cracks develop and each new transverse crack tends to initiate a new longitudinal crack. Transverse cracks are entirely absent in pullout specimens and the cracking is confined to longitudinal splitting. Mains[3] observed in his study of distribution of tensile and bond stresses along reinforcing bars that the tensile-stress distribution curves for the beams and pullouts were quite similar when plotted to the same scale and with the free end of the beam bar coincident with the free end of the pullout bar. The similarity of the curves, however, was limited to the portion of the beam between the support and the nearest transverse crack.

The Bond Committee of the American Concrete Institute developed a test procedure[15] providing a uniform basis for comparison of flexural bond values of different reinforcing bars. This standard did not include any minimum performance criteria since its primary purpose was to establish relative bond values for different bars.

Although the test procedure and the test beams described in ACI Standard 208–58[15] served the Committee's purpose well, the Standard was rather restrictive since it limited bars to one size, concrete to one strength, and the embedment length to a maximum of 16 in. In order to study the effect of the various parameters on the bond values of deformed bars in simply supported beams subjected to concentrated loads, a beam specimen and a test procedure were developed[10] which represent a considerable departure from the ACI Standard 208–58. This procedure described in the report of ACI Bond Committee[16] was intended to provide greater flexibility in the design of the recommended test specimen and test procedure, and to permit the use of bars of different diameters, more than one strength of concrete, and longer lengths of embedment needed to develop stresses equal to the high yield strengths of modern deformed bars. This bond test specimen shown in Fig. 4.13 was also intended to provide a research tool yielding data that could be readily translated into design criteria.

The test beam was designed to permit the measurement of the average value of bond stress and the slip at both the loaded and free ends of the portion of the bar between the supports and load points. The beam was provided with T-shaped ends in order to shift the reactions to points where they would not contribute to the restraint of longitudinal splitting. A strip of metal embedded in the concrete directly opposite each load point assured formation of a crack at that plane, and slip measurements were made at each load point plane.

Another type of beam specimen designed for investigating bond in the area of bar cut-offs and points of inflection was recently used in a bond study

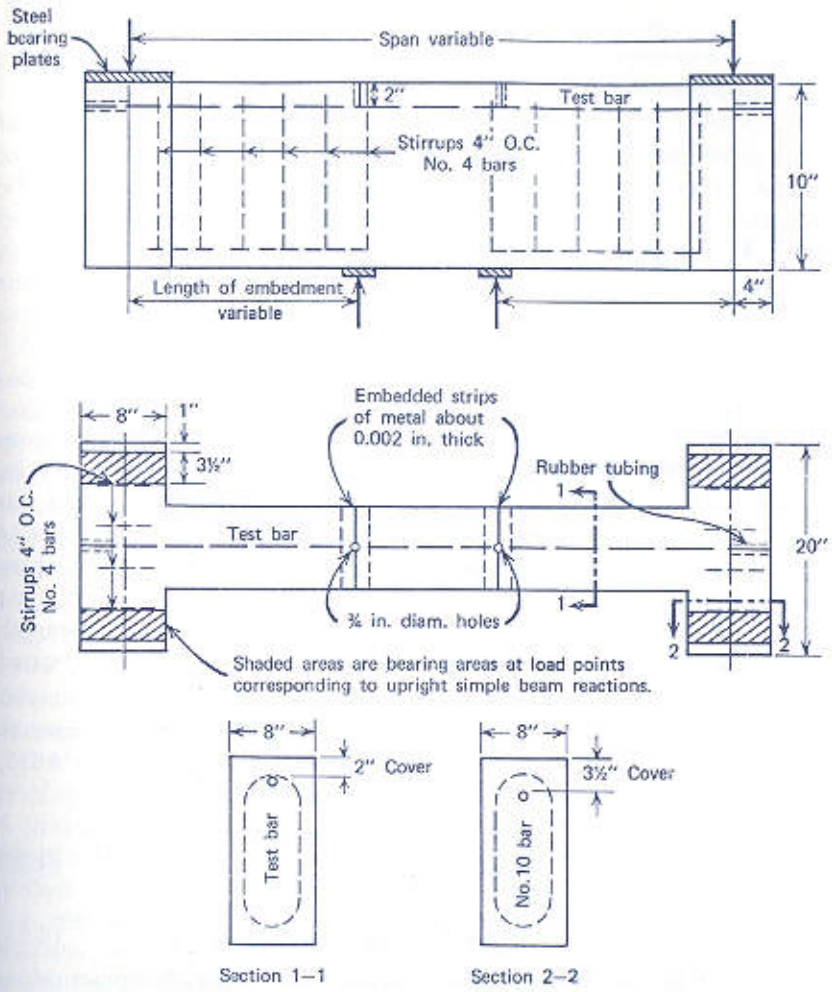

FIGURE 4.13. Elevation, plan, and cross section of beam specimen.[16]

which included bar sizes from No 3 to No. 11[9]; two additional bar sizes, No. 14S and No. 18S, were included in a subsequent study.[17]

The test beam shown in Fig. 4.14 was designed to place the development length of the test bar, designated as L, in a negative moment region between the point of inflection and the point where the other bars were cut off. This arrangement permitted the calculation of the maximum steel stress and the average bond stress in a given development length of the bar. The dimensions of the beam specimen were varied in order to study the effect of the bar cover and beam width.

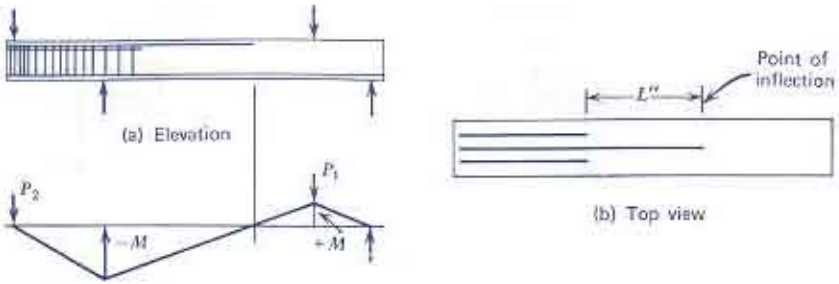

FIGURE 4.14. Bond test beams.[9,17]

The two bond investigations described in References 9 and 10 were concerned with different critical sections of beams, and in this sense they may be considered as supplementing each other. The beam shown in Fig. 4.13 was designed to investigate the bond at the support, while the beam in Fig. 4.14 was concerned with the bond at the point of inflection and the section where tension bars terminate within a span. In spite of the differences in the test specimens, both investigations have conclusively shown that the bond strength is a function of the bar diameter and that the average bond strength varied approximately in proportion to $\sqrt{f'_c}$ when other factors were constant. Empirical relationships for limits for flexural and anchorage bond stresses in tension bars with sizes and deformations conforming to ASTM A615, A616, and A617 were derived as follows:

$$u = \frac{K\sqrt{f'_c}}{D} \qquad \text{for bar sizes No. 11 or smaller} \qquad (4.22)$$

$$u = K'\sqrt{f'_c} \qquad \text{for bar sizes greater than No. 11} \qquad (4.23)$$

The values of u in Eqs. (4.22) and (4.23) are limited to certain maximum values irrespective of the bar size and strength of concrete.

4.6 INFLUENCE OF BOND IN CONTROL OF CRACKING

The economical and efficient use of high yield strength reinforcement is limited by the necessity of avoiding flexural cracks of excessive width. These cracks may be objectionable from the standpoint of appearance, or because they may be the point of entry of sufficient air and water to cause corrosion of the reinforcement. Considerable research was carried out in recent years with modern improved types of deformed reinforcing bars in studies of the mechanism of cracking and the effect of various parameters such as the ratio

of reinforcement, the diameter of bars, and the dimensions of cross-sections of flexural members on the width and spacing of cracks.

The investigations by Watstein and Parsons[18] and Watstein and Seese,[19] have demonstrated with tensile tests of longitudinally reinforced cylindrical concrete specimens that a direct relationship exists between the bond strength of reinforcing bars and both the width and spacing of tensile cracks. A tension specimen devised to measure the bonding efficiency of a reinforcing bar[19] yielded values which correlated well with the spacing and width of cracks observed in the parallel independent set of long tensile concrete specimens with longitudinal reinforcement.

Clark[20] in an extensive series of tests investigated crack widths in beams and slabs. The formula derived by Clark expressed the average width of flexural cracks in terms of the computed tensile stress in the reinforcement, the ratio of the diameter of bar to the percentage of longitudinal reinforcement and to the quantity $(h - d)/d$ which represents the ratio of the thickness of concrete cover to the effective depth of the slab or beam. Clark reported that his equation was in qualitative agreement with the findings of other investigators who found that the width of cracks may be reduced by using a large number of small bars, and that the widths of cracks were approximately proportional to the increase of stress in steel beyond that causing cracking. Clark's formula for the average width of cracks in beams was developed for deformed bars meeting the requirements of ASTM A305, and the empirical constants in that formula reflect the bond characteristics of those bars.

Chi and Kirstein[21] made use of Clark's data in addition to their own to develop a simplified formula for the average width of crack in a beam or slab. A parameter which was not previously taken into account by Clark, but introduced by Chi and Kerstein in this formula, was the distance from the surface of the reinforcing bar to the nearest surface of the beam.

A comprehensive review of the studies on flexural cracking in reinforced concrete element[11,22–29] suggests that the crack width w under service load conditions can be expressed in general terms by the following equation:

$$w = \left(\frac{k_1 R t_i k_f f_s}{E_s}\right) = K R t_i f_s \qquad (4.24)$$

where f_s is the tensile stress in the steel reinforcement; k_f is the stress reduction coefficient which depends on surface bond characteristics and bond effectiveness of steel reinforcement, on tensile strength, modulus, and creep properties of concrete, as well as on stresses due to temperature and humidity conditions; k_1 is a numerical coefficient depending on loading and boundary conditions of the structural element; t_i is a geometric index having dimensions of length and sometimes expressed as effective thickness of concrete surrounding each bar (this is related to the shape and size of the member, area and

arrangement of tensile steel reinforcement, spacing of reinforcing steel bars across the width of the structural element, concrete cover measured from the surface to the center of the nearest bar, and bar diameter); E_s is the modulus of elasticity of reinforcing steel; K is $(k_i k_f)/E_s$, a coefficient; and R is the ratio of the distance between the neutral axis and the level where the crack is located to the distance between the neutral axis and the centroid of the reinforcing steel.

Precise definition of the coefficients k_i, k_f, and of the geometric index t_i is difficult and a large number of empirical equations for crack widths has been proposed.

The common primary variable in all of these expressions is the tensile stress or strain in steel reinforcement and the second major variable in determining crack width w is the effective thickness t of concrete surrounding the bar.

Several empirical equations proposed for evaluating crack width in reinforced concrete beams are given in Table 4.1. For one and two-way slabs modifications of the basic equation 4.24 has been proposed by Nawy.

Various limitations on crack widths have been proposed by different investigators and code writing authorities.[11,22,27,28] Clearly, excessive cracking

TABLE 4.1. Maximum Crack Width Equations.[a]

Source	Estimated Crack Width in 10^{-3} in.	
	w_1—at the Level of Reinforcement	w_2—at the Tension Face of the Beam
Broms	$w_1 = 0.133 t_s f_s$	$w_2 = 0.133 R t_c f_s$
Kaar–Mattock	$w_1 = 0.067 \sqrt{A} f_s$ or $w_1 = 0.115 \sqrt[4]{A} f_s$	$w_2 = w_1 R$
Gergely–Lutz	$w_1 = 0.076 K f_s$, $K = (\sqrt[3]{t_s A})/(1 + 2t_s/3h_1)$	$w_2 = 0.076 R \sqrt[3]{t_b A} f_s$
	$w_1 = 0.091 K'(f_s - 5)$, $K' = (\sqrt[3]{t_s A})/(1 + t_s/h_1)$	$w_2 = 0.091 R \sqrt[3]{t_b A}(f_s - 5)$

[a] A is the average effective concrete prism area for one reinforcing bar, h_1 is the distance from the neutral axis to the centroid of the reinforcing steel, h_2 is the distance from the neutral axis to the tension face of the beam, R is the ratio (h_2/h_1), t_b is the bottom cover measured from the center of the lowest bar, t_c is the distance from any point on the beam surface to the centroid of the nearest reinforcing bar, t_s is the side cover measured from the center of the outer bar, and f_s is the steel stress, in ksi, calculated by the linear theory for cracked reinforced concrete beams.

is undesirable because it reduces stiffness, enhances the possibility of deterioration and corrosion, and causes undesirable appearance. Typical values of allowable crack widths have been summarized by Nawy* and are shown in Table 4.2.

Using appropriate values of K, R, t_i and a limiting crack width w, the corresponding limiting values of stress f_s can be calculated from Eq. 4.24. For example, adopting Gergely–Lutz equation for beams (Table 4.1), when $K = 0.076$, $t_i = \sqrt[3]{t_b A}$, and choosing $R = 1.2$ and $w_2 = 0.008$ in. for an 18 in. wide beam with $t_b = 2.5$ in. (net cover of 1.5 in.) and n = number of reinforcing bars, the limiting values of f_s are obtained as follows:

$$f_s = \frac{w}{KRt_i} = \frac{8}{0.076 \times 1.2 \times t_i} = \frac{87.7}{t_i}$$

$$A = \frac{b \times 2 \times d_c}{n} = \frac{18 \times 2 \times 2.5}{n} = \frac{90}{n}$$

$$t_i = \sqrt[3]{t_b A} = \sqrt[3]{\frac{2.5 \times 90}{n}} = \sqrt[3]{\frac{225}{n}}$$

n	2	3	4
t_i, in.	4.82	4.22	3.83
f_s, ksi	18.2	20.8	22.9

It is clear that for a given beam width, a larger number of bars ($n = 4$) permits a larger working stress f_s and therefore a smaller total area A_s for a given bending moment M and crack width limit.

4.7 INFLUENCE OF BOND ON STIFFNESS OF REINFORCED CONCRETE

The bond characteristics of reinforcing bars also affect the flexural rigidity of beams and slabs, because the magnitude of bond stresses in the uncracked portions of the beam determines the extent of the contribution of the concrete between cracks to deformation and consequently to the stiffness of the beam. The contribution of the concrete between vertical cracks to flexural stiffness was considered in a number of papers presented at the 1957 RILEM Symposium on Bond and Crack Formation in Reinforced Concrete.[22] The papers

* E. G. Nawy, "Crack Control in Reinforced Concrete Structures," ACI Journal, Proceedings Vol. 65, No. 10, pp. 825–836, October 1968.

TABLE 4.2. Typical Allowable Crack Widths.[29]

Investigator	Exposure Conditions	Maximum Allowable Crack Width, in.[d]	
Brice[a]	Severe	0.004	
	Aggressive	0.008	
	Normal	0.012	
Rusch[a]	Aggressive (salt water)	0.008	
	Normal	0.012	
Efsen[a]	Severe to aggressive	0.002–0.006	
	Normal (outside)	0.006–0.010	
	Normal (inside)	0.010–0.014	
ACI 318-63	Exterior	0.010	
	Interior	0.015	
CEB[b]	Interior or exterior aggressive and watertight	0.004	
	Aggressive	0.008	
	Normal	0.012	
U.S. Bureau of Public Roads (maximum allowance w at steel level under working load)[c]		Dead load causes compression. Live load causes tension.	Dead load causes tension. Live load causes tension.
	Air or protective membrane	0.012	0.010
	Salt, air, water and soil	0.010	0.008
	Deicing chemicals, humidity	0.008	0.006
	Seawater and seawater spray, alternate wetting and drying	0.008	0.006

[a] Reference 22.
[b] Reference 27.
[c] Reference 28.
[d] Note: 0.001 in. = 0.025 mm.

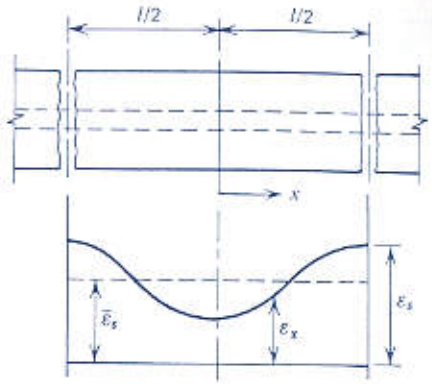

FIGURE 4.15. Strain distribution in cracked prism.

which presented discussions of the various parameters affecting the distribution of the flexural rigidity were by Soretz,[30] Baker, Ashdown, and Wildt,[31] and Murashev.[32] Watstein and Mathey[33] discussed the effect of bond on the apparent modulus of elasticity of the reinforcing bars embedded in concrete; this property was determined with axially reinforced concrete tensile specimens simulating portions of beams between adjoining tensile cracks.

In a cracked reinforced concrete prism subjected to tension (Fig. 4.15) the maximum tensile strain in steel reinforcement occurs at the crack and is

$$\varepsilon_s = \frac{f_s}{E_s} \tag{4.25}$$

The average strain in the reinforced concrete prism is less than ε_s as a result of the participation of the concrete in resisting the tension between adjacent cracks. This average strain is

$$\bar{\varepsilon}_s = \frac{2}{l}\int_0^{0.5l} \varepsilon_x \, dx \tag{4.26}$$

This strain can be expressed in terms of maximum stress f_s in the steel by using an effective modulus of the reinforcement, as

$$\bar{\varepsilon}_s = \frac{f_s}{\bar{E}_s} = \psi\varepsilon_s = \psi\frac{f_s}{E_s} \tag{4.27}$$

where $\psi = \bar{\varepsilon}_s/\varepsilon_s$ and consequently $\bar{E}_s = E_s/\psi$. Thus, ψ is the ratio of the average strain (or stress) in the reinforcement between cracks to the strain (or stress) in the reinforcement at the cracks, and is also the ratio of the actual modulus to the effective modulus. The reciprocal of ψ indicates the relative contribution of concrete in tension to the overall stiffness of the reinforced concrete element. When the extent of cracking is small, value of $1/\psi$ approaches 1.4; when cracking is extensive and contribution of concrete in tension is negligible, $1/\psi$ approaches 1.0.

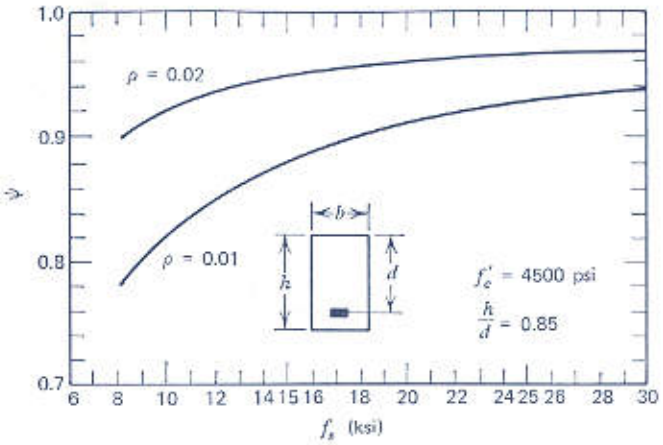

FIGURE 4.16. Relative contribution of concrete in tension to stiffness.

For rectangular concrete beams reinforced only in tension Winter and Yu[34] following work of Murashev[32] and others, derived the following expression for ψ:

$$\psi = 1 - 0.5\frac{M_{ct}}{M} = 1 - \frac{0.1(f'_c)^{2/3}bh(h - kd)}{f_s A_s jd} \tag{4.28}$$

where M_{ct} is the portion of the bending moment M due to participation of concrete in tension between the cracks and M is the total bending moment. For two typical cases values of ψ are plotted as a function of f_s in Fig. 4.16. It can be seen that as f_s and ρ increase, the values of ψ approach 1.0, i.e., the contribution of concrete becomes less significant. Experimental studies[12] have shown that for elements with high percentage of reinforcement the value of ψ at any particular stress level is sensitive to the stress history of the reinforced concrete element, and particularly to the magnitude of the previous maximum stress. The greater the magnitude of this stress the less is the relative contribution of concrete to the stiffness. Values of ψ have been increased from 0.77 at initial loading at steel stress of 20 ksi, to 0.95 after a few cycles of repeated loading up to a stress of 40 ksi. Therefore, special anchorage provisions may be required when the working stress level is increased for high-strength steel bars, as repeated applications of this high stress are likely to reduce bond effectiveness at lower stress levels. When the structure may be subjected to repeated loads, particularly repeated cycles of high intensity loading, such as an earthquake, the value of ψ is usually taken as 1.0 for all subsequent loading conditions.

4.8 MISCELLANEOUS BOND AND ANCHORAGE PROBLEMS

4.8.1 Bond of Top Bars

The bond development in deep forms, wherein the settlement of concrete affects the intimacy of contact between the concrete and the steel bar, was first discussed in a paper by R. E. Davis, E. H. Brown, and J. W. Kelly.[35] P. M. Ferguson,[36] in his review of bond, pointed out that for a vertical bar the consolidation is better at the top of the lugs than beneath the lugs, and consequently the slip and the ultimate bond resistance are more favorable when the bar is pulled against the direction of casting of concrete than in the opposite direction. Similarly, for a horizontal bar, the consolidation of the concrete is better above the bar than below it. It is recognized that any bleeding of the concrete mix contributes to the accumulation of water and air beneath the lugs with consequent loss of bond strength. The greater the depth of concrete beneath the bar and the greater the slump of concrete, the greater is the loss of bond strength.

The loss of bond strength in "top bars" due to the settlement of concrete is often taken as 30 to 40%. "Top bars" by definition are those which have at least 12 in. of concrete below them. The magnitude of this loss was determined by A. P. Clark[37] in tests of pullouts which contained horizontally cast "top" and "bottom" bars. However, in Clark's tests the bars were held rigidly in the mold at both ends. There is evidence that for modern low-slump concretes the reduction in bond values for the top bars is not as large as indicated by earlier investigations. Ferguson[36] reported that in recent tests with concrete depths of 12 to 18 in. below the bars, the loss of bond strength has been less—of the order of 10 to 20% and he indicated that further experimental study is needed, particularly for very deep beams.

He also reported that in pullout tests of long, high-strength steel bars one significant difference in the behavior of top and bottom bars was observed. Bottom-cast bars did not slip at their unloaded end until almost at their ultimate load, while top-cast bars slipped at their free end at low loads. Apparently the presence of air and water pockets under the top bars permitted them to slip along their entire length prior to the appearance of any serious splitting cracks. This slip lowered their ultimate splitting resistance by 15 to 20% compared with the bottom-cast bars.

4.8.2 Bond in Compressive Reinforcement

In compressive reinforcement, as in the case of a lapped splice in a column, the end bearing of each bar strengthens the splice, whereas in a tensile splice

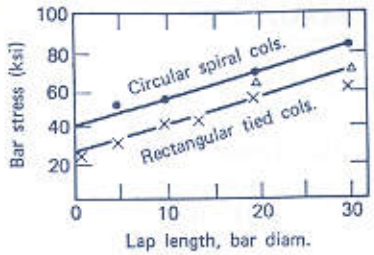

FIGURE 4.17. Compression splice strengths in columns.[38]

a tensile crack forms at the end of each bar, producing two planes of weakness at which longitudinal splitting cracks are generally initiated.

The tests of concentrically loaded columns with lapped splices[38] indicated that strength of the splice increased with lap length and was greater for spiral than for tied columns (Fig. 4.17). The average compressive bond strength in compression computed from the slopes of the lines given for circular spirally reinforced and rectangular tied columns is about 350 psi for No. 8 bars. It is of interest to note that for laps of zero length the end bearing stress was about 27 ksi for tied columns, and 40 ksi for spirally reinforced columns. Thus, it is the increased capacity in end bearing which accounts chiefly for the greater strength of compression splices in spirally reinforced columns than in rectangular tied columns.

4.8.3 Bond in Lightweight-Aggregate Concrete

The unpublished data developed at the University of Missouri and cited by P. M. Ferguson[36] indicates that the mode of failure of deformed bars in pullout specimens of lightweight-aggregate concrete is somewhat different from that in normal-weight concrete specimens. The tests show that roughly one-third of the bars pull out without causing the concrete specimens to split; this is particularly true of the top-cast bars. This mode of failure indicates that in lightweight concrete the lugs crush and shear the concrete, while in normal-weight concrete specimens the failure is invariably by splitting action involving a tensile failure in concrete.

The data on bond strengths in lightweight-aggregate concrete indicate lower bond strengths than for normal-weight concrete. The reduction of bond strength ranges from 13%, when based on certain slip comparisons, to 36%, when the average ultimate bond values are considered. For this reason ACI Building Code (318–71) recommends a 33% increase in basic development length of deformed bars in lightweight-aggregate concrete.

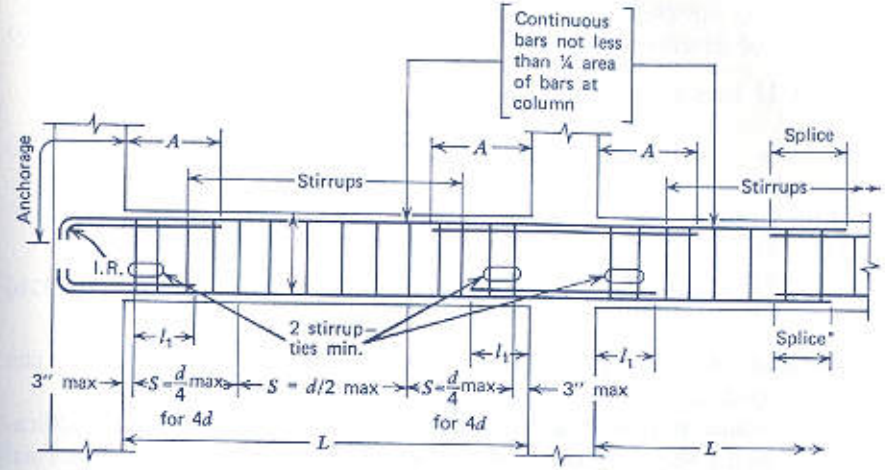

FIGURE 4.18. Arrangement of longitudinal steel reinforcement. Dimensions A and l_1 to be determined by anchorage requirements.

4.8.4 Anchorage Requirements and Effects of Bar Cutoff

Figure 4.18 shows a typical arrangement of longitudinal steel reinforcement in a girder of a building frame. As the bending moments vary along the girder the amount of reinforcement may be varied by terminating bars where they are no longer needed for bending moment resistance. In establishing the point of safe bar cutoff it is necessary to consider two factors: (1) the distance from the cutoff point to the point of peak stress, and (2) the location of peak stress point and the magnitude of the peak stress.

The distance from the point of actual cutoff to the point of peak stress f_s must be sufficient to develop stress f_s in the bar without exceeding the limit value of bond. This distance l_d, called the "development length," for a given bar of diameter D which can develop a limit value of average bond stress $\bar{u}$, must satisfy the following equilibrium condition:

$$f_s \frac{\pi D^2}{4} \leq \bar{u} \pi D l_d \tag{4.29}$$

from which

$$l_d \geq 0.25 f_s \frac{D}{\bar{u}} \tag{4.30}$$

It is reasonable to require that f_s at a point of peak stress be taken as f_y, and that $\bar{u}$ be taken as the bond capacity u which for No. 11 bars and smaller

is defined by Eq. (4.22) and for large bars (14S and 18S) by Eq. (4.23). Then, the ratio of development length l_d to bar diameter D is defined as follows:

for No. 11 bars and smaller:

$$\frac{l_d}{D} = 0.25 f_y \frac{D}{K\sqrt{f'_c}} \tag{4.31a}$$

and for large bars (14S and 18S):

$$\frac{l_d}{D} = 0.25 f_y \frac{1}{K'\sqrt{f'_c}} \tag{4.31b}$$

where K and K' are coefficients which depend on the bond capacity which can be developed in the particular structural element.

For practical purposes values of K and K' are defined in design specifications in such a way as to take into account the type of concrete used (normal weight or lightweight aggregate), yield strength and general ductility of steel reinforcement, position of reinforcement ("top" or "bottom"), thickness of concrete cover, presence of stirrups or other transverse reinforcement, etc. Such factors may vary with type of structure, uncertainties in design assumptions, and quality control of materials and construction. Values of K usually range from 4 to 10, and for K' from 3 to 7. Basic development length values of l_d specified by the ACI Building Code (318–71) for standard size deformed bars in tension are listed in Table 4.3 for different yield strengths.

In a beam reinforced with several steel bars, one or more of these can be terminated at a distance l_d beyond the point of peak stress, provided the remaining (continued) bars are not overstressed and the resisting moment which can be developed by the remaining bars is at least equal to or greater than that produced by the critical loading condition.

Generally the location of the point of peak stress corresponds to either the point of maximum bending moment or the point where some bars have been terminated, increasing the intensity of stress in the remaining bars. In some cases the crack pattern may also affect the position of the peak-stress point.

The basic moment diagrams obtained from frame analysis may not accurately reflect the distribution of stresses in steel reinforcement. The shift of the peak-stress points may be associated with: (1) differences between the idealized loadings used in calculations and the real loads, (2) differences between the idealized homogeneous, isotropic, linear characteristics of the frame assumed in analysis and the actual reinforced, cracked, concrete frame, and (3) effects of shrinkage and temperature changes, as well as possible foundation movements, usually neglected in the calculations of moments. Therefore, peak stresses may occur at some distance from the theoretically determined critical sections. For example, in the presence of diagonally

TABLE 4.3. Basic Development Length l_d, inches, for Deformed Bars in Tension (from Building Code Requirements for Reinforced Concrete—ACI 318–71).

f_y, ksi	40			60			75		
f'_c, ksi	3	4	5	3	4	5	3	4	5
Bar Size No.									
3	(6)+	(6)+	(6)+	(9)+	(9)+	(9)+	14	14	14
4	(8)+	(8)+	(8)+	12	12	12	18	18	18
5	(10)+	(10)+	(10)+	15	15	15	23	23	23
6	13	12	12	19	18	18	29	27	27
7	18	15	14	26	23	21	40	34	32
8	23	20	18	34	30	27	52	45	40
9	29	25	23	44	38	34	65	57	51
10	36	31	28	54	47	42	81	70	63
11	43	38	34	65	56	50	98	84	76
14	62	54	48	93	81	72	140	121	108
18	80	70	62	121	104	93	181	157	140

+ Calculated values in parentheses are below minimum required 12 in.

1. For top reinforcement in tension the basic length l_d shall be increased 40%.
2. Standard end hooks may be used to replace part of the required embedment.
3. For bars spaced laterally at least 6 in. on center and at least 3 in. from the side face the basic length l_d may be reduced 20%.
4. For bars in lightweight-aggregate concrete longer basic length l_d is required depending on tensile splitting strength (see section 12.5.(c) of ACI 318–71).
5. Basic length l_d may be reduced when flexural reinforcement area A_s exceeds the required amount by the ratio (A_s required)/(A_s provided).
6. For bars enclosed within a suitable spiral embedment length may be reduced 25%.
7. For bundled bars the basic length l_d for each bar is that given in the table, except that for a 3-bar bundle it must be increased 20%, and for a 4-bar bundle it must be increased 33%.

inclined (shear) cracks, the load in the reinforcement T at a section x is based on a moment $M = V(x + d)$ at a section shifted a distance d from section x (Fig. 4.19). For this reason, it is often recommended to shift the bending moment curve a distance d, or $12D$ if greater than d, to right or left (whichever is more critical) in establishing a design envelope for the location of peak stresses in the reinforcement. This shift must be made in addition to the provision of development l_d from peak-stress point to cutoff.

P. M. Ferguson and S. I. Husain[39] reported tests on a large number of simply supported beams reinforced with No. 8 and No. 11 bars. Most of these beams had bars cut off at the point where they were no longer theoretically required to resist the bending moment, or at $12D$ to $15D$ beyond this point. The control specimens either contained full-length bars or had bars bent up. Although the beam specimens with bars cut off were designed to

TABLE 1.4. Sieve Analysis and Fineness Modulus of Typical Sands.

Sieve Size	Cumulative Percent of Sample Retained on the Sieve		
	Fine Sand	Medium Sand	Coarse Sand
No. 4	0	0	5
No. 8	5	16	25
No. 16	15	28	42
No. 30	35	50	65
No. 50	53	71	83
No. 100	82	90	95
Fineness modulus	1.90	2.55	3.15

Grading requirements may be adjusted when using air entrainment in a concrete mix. ASTM C33 recognizes the effect of entrained air on the workability of concrete and permits a smaller percentage of fines, (passing No. 50 and No. 100 sieves), usually resulting in a lower water content of the mix. Gap-graded or jump-graded aggregate may also produce a concrete of satisfactory workability when air entrainment is used.

Absorption and surface moisture of aggregate should be known so that the true water content of concrete can be determined. This is important because the strength and several other characteristics of both fresh and hardened concrete depend upon the actual water–cement ratio of a concrete mix. Usually, the sand received at a job site is wet, and coarse aggregate is dry. If mix design calculations are not corrected on the basis of the saturated surface-dry condition* serious differences may arise between the desired properties and the actual properties of concrete.

Deleterious substances in aggregates may affect setting, hardening and durability characteristics of concrete. ASTM C33 gives limits for permissible amounts of deleterious substances in aggregates. Organic impurities such as sugar or molasses may seriously delay the setting of cement; humus and peat may also cause similar problems. The presence of coal, lignite, or wood usually cause staining and popouts, and may affect the durability of concrete. Silt and clay, when present, affect the water requirement. Aggregate particles coated with clay possess poor bonding characteristics with cement paste. If clay or shale is present in coarse aggregate in lumps, these may break up during mixing and thus affect the workability of fresh concrete, and the durability of hardened concrete.

* At "saturated surface-dry" condition, the aggregate surface neither absorbs water from nor contributes water to the concrete mix.

The *strength of an aggregate* generally does not have a major influence on the strength of concrete, since usually the aggregates are very strong. Cement paste–aggregate bond strength is of more importance with regard to both the compressive strength and the tensile strength of concrete.

The strength and the modulus of elasticity of an aggregate may, however, be used as an index of general quality for certain purposes, such as the abrasion resistance of the concrete (important in pavements or heavy-duty floors). Special tests are available for determining abrasion-resisting qualities of an aggregate (ASTM C131—using the Los Angeles testing machine), but due to the uncertain correlation between the abrasion resistance of the aggregate and of concrete, direct tests on wear resistance of concrete are often preferred. The *elastic property* or deformability of an aggregate has a significant influence on the shrinkage and creep characteristics of concrete. Aggregates of low density and high absorption (some gravels and sandstones) will generally produce concretes of high shrinkage and high creep characteristics. *Resistance to freezing and thawing* of aggregate becomes important for structures exposed to freezing and thawing conditions. When aggregates are saturated with water and insufficient pore-space exists, the expansion accompanied by freezing of water may crack the aggregate particles. Resistance to freezing and thawing depends on the porosity, permeability, and tensile strength of aggregate particles. At any freezing rate there may be a critical aggregate size above which the particle will fail if it is saturated with water. The critical particle size is relatively higher for coarse-grained materials and for those materials which contain voids too large to hold moisture by capillary action.

The *thermal properties* of an aggregate which may affect the performance of concrete are the coefficient of thermal expansion, the specific heat, and the conductivity. The last two become important when dealing with insulating concrete and mass concrete, and it is only the coefficient of thermal expansion which needs consideration in concrete structures. It is possible that if an aggregate is incompatible with cement paste (if the coefficients of thermal expansion of the two differ considerably), large changes in temperature may introduce differential strains leading to breaking of bonds between the aggregates and the paste. This problem can be quite serious with some aggregates such as quartz, especially at high temperatures. For instance, at 1063°F the change in crystalline form of quartz is suddenly accompanied by 0.85% expansion. Therefore, the fire-resistance of concrete made with quartz aggregate will be poor. For hydrated portland-cement paste the linear coefficient of thermal expansion varies between 6×10^{-6} and 9×10^{-6} per °F, depending upon the degree of saturation. For most of the aggregates the coefficient usually lies between 4 and 7×10^{-6} per °F and is of no serious consequence, but some quartzites may have too high a value and certain

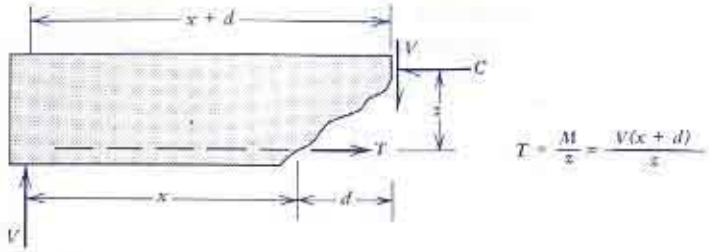

FIGURE 4.19. Tension in reinforcing steel in beam with a diagonal crack.

develop the same strength as the control beams only 2 out of 33 specimens developed full strength, the others failing prematurely either in bond or in shear. The deficiencies in the strength ranged from 15 to 25% and one specimen failed at 40% below design strength. When the bars in the beams were fully continuous or bent up no strength deficiencies were noted. The addition of extra stirrups improved the performance of some of the weaker beams, but the stirrups were not fully effective.

The authors recommended that the allowable shear values for beams be reduced to 20 to 30% where bars are cut off without providing special web reinforcement. For slabs 12 in. or less in thickness the authors recommended a shear reduction of 10%. Also the authors recommended that for beams additional web reinforcement be provided in the region of the bar cut off. B. Bresler and A. C. Scordelis[40] reported tests on simply supported beams with additional web reinforcement in the region of the bar cut off, which essentially compensated for the adverse effect and raised the shear capacity to that of control beams with continuous longitudinal reinforcement.

4.8.5 Splices of Tension Reinforcement

Splicing tension-reinforcing bars can be accomplished in three basically different ways: (1) they can be welded, (2) they can be mechanically connected (by Cadweld and other means), and (3) they can be lapped over a specified length. Each of these arrangements can be designed to transfer tension adequately through the splice region, and each scheme has particular advantages and disadvantages. A welded splice is the most advantageous from the point of view of stress transfer, but may give rise to metallurgical problems reducing the safe load-carrying capacity of the splice and it also may be too costly under given field conditions. All welding must conform to AWS Recommended Practices for Welding Reinforcing Steel, and for a full welded splice must develop a tensile capacity at least 125% of the specified yield strength of the bar.

Properly installed mechanical connectors offer the next best splice from the point of view of simplicity of stress transfer, but they may develop local slip within the connectors, and may give rise to cracking in the region of the splice, decreasing the stiffness of the reinforced concrete member (increase in deflections) and sometimes may decrease the load-carrying capacity of the member. For full positive connections a capacity of 125% of specified yield strength is required. The cost of such splices may also be a consideration in the selection of the splicing scheme. An investigation of mechanical splices has been reported by Sozen and Gamble[41] which provides some basis for predicting crack widths and local slip within the connectors. However, neither the welded splice nor the mechanical splice depend on bond between concrete and reinforcing steel.

The advantage of lapped splice is the relative simplicity of accomplishing it in the field. The disadvantages are the complex nature of stress transfer leading to local cracking at or near the sections where bars terminate and some possible loss of stiffness and load-carrying capacity, particularly when lap lengths or stirrups in the splice zone are not adequate. Lap splices rely on bond for stress transfer, and therefore the length of the lap is the distance required for stress development and can be defined similarly to development length:

$$l_s = 0.25 f_s \frac{D}{u_s} \tag{4.32}$$

where f_s is the stress in steel reinforcement at the splice and u_s is the effective average bond capacity. Because of the similar forms of equations defining l_s and l_d, Eqs. (4.31) and (4.32), it is possible to define l_s in terms of l_d.

Test data on tensile lapped splices are rather meager[12,13] but they indicate that splices in 3000 psi concrete without spiral or equivalent transverse reinforcement fail at lower values of bond stress than unspliced bars. Therefore, lap length "requirement" is generally greater than the development length required for unspliced bars, particularly for large values of f_s. For this reason it is usually recommended that lapped splices be avoided at points of maximum tensile stress and that splices of bars be staggered, so that only half or less of the bars are spliced within the lap length, in which case the splice length may be based on a bond stress of only about 75% of the normal value.

If the proportion of steel reinforcement spliced at a given section is greater than one-half but less than three-quarters, the splice length should be based on a bond stress about 60% of the normal value, and if more than three-quarters of reinforcement is spliced the lap length should be based on 50% of the normal value.

Advantage can be taken of the splice location away from section of maximum stress and determining the length of lap on the basis of f_s less than f_y. Value of f_s/f_y at the splice may be taken as the ratio $1.1\, M_{zu}/M_{uD}$,

where M_{su} is the design (ultimate load) moment at the section, and M_{uD} is the moment capacity based on yield strength of the reinforcement at the section.

When it is not possible to locate all the splices at sections of relatively low tensile stress, the splice at a section of high stress requires increased safety, obtained by increasing the lap length. This is obtained by taking $f_s = f_y$ and by using reduced values of effective bond. For example, if no more than half of the steel is spliced at a maximum-stress section the bond strength is taken as 60%, and if more than half the steel is spliced the value of u_s is reduced to 50% of normal bond strength.

One of the most adverse conditions for a tension splice is a tension tie member, in which all sections are subjected to the same tension. In such cases it is customary to provide special spiral cages around lapped splices, as well as using only 50% of normal bond strength in calculating the lap length. Laboratory investigations show that stirrups or spiral reinforcement in the region of the lapped splice significantly increase the capacity to transfer stress. However, data are not adequate to provide a basis for a reliable quantitative prediction of the effect of transverse reinforcement on splice strength.

Studies at the University of Texas[43] in which test beams of different widths were employed indicated that strengths of adjoining splices decrease as they are more closely spaced. For example with No. 7 bars lapped 24 diameters the splice developed 39,500 psi for a 6-diameter spacing of splices, while for a 3.1-diameter spacing the splice only developed 30,700 psi. This observation led to a recommendation that contact splices spaced less than 12-bar diameters apart, or closer than 6-bar diameters from an outside edge, must either be enclosed in a suitable spiral or must have a 20% increase in lap length.

As the bar diameter increases lap splicing becomes increasingly less effective, as the average bond strength decreases and the ratio of surface to cross-sectional area also decreases. The required lap lengths, as well as the space required to accommodate lapped pairs of large bars with adequate concrete cover, become excessive. For this reason it is usual to use mechanical or welded splices for large bars.

Another restriction must be placed on transverse spacing of individual bars in noncontact lap splices. If this spacing becomes too great, without any other longitudinal reinforcement in the interval, potential failure may occur on a zigzag pattern. It is recommended to limit the bar spacing to a maximum of one-fifth of the lap length, or 6 in., whichever is smaller. Based on considerations similar to the above, ACI Building Code Requirements (318-71) proposed four categories of tension splices. For lap splices in flexural members with or without axial compression classes A, B, and C are defined as follows.

Class A. Required length of splice lap $l_s = l_d$. Maximum tensile stress not to exceed $0.5f_y$. Splices staggered so that steel area spliced within one lap length is not greater than 75%.

Class B. Required length of splice lap $l_s = 1.3l_d$.

1. Maximum tensile stress f_s not to exceed $0.5f_y$. Splices are so arranged that more than 75% of steel area may be spliced within one lap length.
2. Maximum tensile stress f_s may exceed $0.5f_y$; lap length shall be provided for full f_y. Splices staggered so that steel area spliced within one lap length is not greater than 50%.

Class C. Required length of splice lap $l_s = 1.7l_d$. Maximum tensile stress f_s may exceed $0.5f_y$; lap length shall be provided for full f_y. Splices are so arranged that more than 50% of steel area may be spliced within one lap length.

Welded or full positive mechanical connections are recommended for splices in tension tie members. If lap splices have to be used, a class D splice is required. The required length of splice is $2.0l_d$ and a spiral not less than 1/4 in. in diameter and not more than 4 in. pitch must enclose the splice. No reduction in l_d is allowed due to the use of a spiral, and for bars sizes larger than No. 4, 180° standard hooks shall be used at the ends of the bars.

From a bond and anchorage point of view splicing of steel bars in compression is somewhat less critical than that in tension. End bearing plays a greater role, but lateral buckling of bars under extreme loading conditions also may pose a problem. Therefore special lateral reinforcements (ties or spirals) are usually called for.

4.8.6 Anchorage of Hooked Bars

In order to increase the anchorage capacity of reinforcing steel, it is sometimes bent into a hook at its end. The shape of the hook is controlled partly by the ductility of the reinforcing steel, as excessively sharp radius of bend results in severe coldwork and possible embrittlement of the steel. The shape of the hook also influences its anchorage capacity. In U.S. practice a "standard" (ACI) hook is defined as one conforming to the requirements shown in Fig. 2.11. In European practice smaller bend radii of ($R = 2.5D$) and shorter straight extensions ($2D$) have been used. "Standard" hooks conforming to ACI requirements are considered capable of developing a tensile stress f_h in bar reinforcement, defined as follows:

$$f_h = 9\sqrt{f'_c}\frac{f_y}{1000} \leq \xi\sqrt{f'_c} \tag{4.33}$$

where ξ varies with bar size, yield strength, and bond effectiveness. Values of f_h specified by the ACI Building Code (318-71) for standard hooks in deformed

TABLE 4.4. Tensile Stress f_h(ksi) Developed by Standard Hooks.

f_y, ksi	40			$f_y \geq 60$					
Bars	All			Top			Other		
f'_c, ksi	3	4	5	3	4	5	3	4	5
Bar Size Number									
3	19.7	22.7	25.4	29.6	34.2	38.2	29.6	34.2	38.2
4	19.7	22.7	25.4	29.6	34.2	38.2	29.6	34.2	38.2
5	19.7	22.7	25.4	29.6	34.2	38.2	29.6	34.2	38.2
6	19.7	22.7	25.4	24.7	28.5	31.9	29.6	34.2	38.2
7	19.7	22.7	25.4	19.7	22.7	25.4	29.6	34.2	38.2
8	19.7	22.7	25.4	19.7	22.7	25.4	29.6	34.2	38.2
9	19.7	22.7	25.4	19.7	22.7	25.4	29.6	34.2	38.2
10	19.7	22.7	25.4	19.7	22.7	25.4	26.3	30.4	33.9
11	19.7	22.7	25.4	19.7	22.7	25.4	23.0	26.6	29.7
14	18.1	20.9	23.4	18.1	20.9	23.4	18.1	20.9	23.4
18	12.5	14.4	16.1	12.5	14.4	16.1	12.5	14.4	16.1

bars in tension for different yield strengths and bar sizes are listed in Table 4.4. The value of f_h may be increased by 30% where enclosure is provided for the concrete in a plane perpendicular to that of the hook.

An equivalent anchorage development length l_h corresponding to a standard hook can be obtained by replacing f_y by values of f_h in Eqs. (4.31a) and (4.31b). Using values of l_d in Table 4.3 the values of l_h can be obtained simply as follows:

$$l_h = f_h l_d / f_y \tag{4.34}$$

In evaluating available anchorage of a hooked bar l_h may be added to the length of the straight portion of the bar to meet the total required development length. Given a bar in tension fully stressed to yield strength f_y the appropriate anchorage can be provided either by a straight embedment l_d, or by a hooked bar with straight embedment s' ahead of the hook, so that $s' = (l_d - l_h)$, or by a short straight embedment s'', with a standard hook and an added straight extension x at the end of the hook, such that $x = (l_d - l_h - s'')$. When the steel bar is subjected to cyclic stress reversals, particularly in yield stress range, deterioration of bond may significantly reduce the effectiveness of the straight embedment ahead of the hook. Special confinement by reinforcing steel hoops may be required to develop adequate anchorage.

4.8.7 Bond in Brackets and Short Cantilevers

The bond problem in brackets, corbels, ends of bent caps, and other extremely short cantilevers is quite different from that in conventional flexural members. In a study of bent caps with overhanging ends P. M. Ferguson[44] found that although the maximum steel stress at the face of the support can be calculated with adequate precision, as for any cracked beam the development length between that point and the free end of the bracket is the critical feature in the design. This is due to the fact that the steel stress is still quite large near the point of application of load, and the reinforcing bar must be anchored beyond this point in order to develop this stress in bond. Ferguson's tests have shown that with an anchorage of 15 in. for No. 11 bars or 12 in. for No. 8 bars, there was no difficulty developing a stress of 75 ksi.

In those situations where the length beyond the load point is not available, the designer can avail himself of the recommendations in the Report of ACI–ASCE Committee 512, J. R. Janney, Chairman.[45] This report, which deals with suggested design of joints and connections in precast structural concrete, details the welded anchorage necessary in short brackets and corbels where anchorage cannot be developed by a straight bar. In this situation the top bar should be run straight as far as possible and must be anchored by a welded crossbar of the same diameter as the main reinforcing bar.

The Report of ACI–ASCE Committee 512 is based largely on the experimental work of L. B. Kriz and C. H. Raths[46] carried out at the PCA laboratories. The authors conclude that the shear strength in a corbel is a function of the ratio of the shear span to the effective depth, the reinforcement ratio, and the ratio of the horizontal and vertical components of the applied loads. Tensile reinforcement and horizontal stirrups were found to be equally effective in increasing the strength of a corbel subject to vertical loads only. Loads carried by a column do not affect the strength of the corbel, nor does the amount or arrangement of the principal column reinforcement.

4.8.8 Bond of Structural Steel to Concrete

Although numerous investigators have studied the factor affecting the bond between concrete and deformed reinforcing bars, there is a scarcity of data on the bond between rolled structural steel sections and concrete. This type of bond is important in the design of composite structural members in order to assume "composite" action of such a structural unit.

J. O. Bryson and R. G. Mathey[47] studied the effect of the surface condition of steel beams embedded in concrete on their bond strength. The results indicated that the bond strengths of freshly sandblasted beams and those that were sandblasted and allowed to rust were about 460 psi, while the strengths

of similar beams with normal rust and mill scale surface average about 320 psi.

The tests made by Bryson and Mathey involved steel beams completely embedded in concrete, and the bond in this type of construction is quite reliable. The situation is quite different when concrete slabs in buildings or bridges are supported on steel I-beams. Here the resulting structure is considered to be composed of a series of composite T-beams. Although the concrete is usually bonded to the I-beam through adhesion, this type of bond is considered unreliable and it may not provide composite action throughout the life of the structure. In the design of composite T-beams it is necessary to provide positive anchorage of the slab to the steel I-beams by means of mechanical shear connectors fastened to the top flange of the I-beams. Various types of shear connectors have been proposed and have been found to be satisfactory in experimental investigations.[48,49]

A comprehensive investigation by I. M. Viest[50] involving the study of welded steel shear connectors has demonstrated that a steel stud is suitable for use as a shear connector in composite concrete and steel construction.

It was observed by Viest[50] that only negligible inelastic deformation developed in the tests of stud connectors until the critical load was reached. The author concluded that the critical loads represent the useful load capacities of stud connectors. Based on the data obtained from push-out tests of stud connectors ranging in diameters from 0.5 in. to 1.25 in. Viest developed the following expressions for the critical loads:

$$\text{for } d < 1 \text{ in.:} \qquad Q_{cr} = 330\, d^2\sqrt{f'_c} \tag{4.35a}$$

$$\text{for } d \geq 1 \text{ in.:} \qquad Q_{cr} = 315\, d\sqrt{f'_c} \tag{4.35b}$$

where Q_{cr} is the critical load on a stud, in lb, d is the stud diameter, in in., and f'_c is the compressive strength of concrete, in psi.

Comparison of test results on flexible shear connectors obtained in push-outs and in composite beams[51] showed that the shear connectors in beams provided a somewhat larger capacity than that predicted from push-out tests. For this reason some design specifications[52] permit more liberal working values for various types and sizes of shear connectors than those in use prior to 1961.

4.8.9 Anchorage in Mass Concrete

Many types of anchoring devices are used to secure heavy fixtures, conduits, machinery, etc., to mass concrete. Although these devices vary in design, tests have indicated that the same principles apply in a general way to many types of anchoring devices.

R. F. Adams[53] describes pull-out tests of bolt anchors known as multiple expansion type, or more commonly, as machine bolt anchors. The investigation included such variable factors as strength of concrete, size of the hole, degrees of cleanliness and surface texture of the drilled hole, and the depth of the anchor bolt. The diameter of the bolts ranged from 1/2 to 7/8 in., and the strengths of concrete from 1600 to 5100 psi.

While the bond failure of deformed reinforcing bars in flexural members is associated with formation of nearly vertical tensile cracks and longitudinal splitting cracks along the surface nearest the bar, anchors set in a shallow hole in concrete will probably fail by "spalling" the concrete, or pulling a conically shaped piece out of the concrete. As the depth of the hole increases a point is reached where the spall-type failure no longer occurs, but the anchor fails by slipping. When the failure occurs by slipping, increasing the depth of embedment will not in general increase the load that the anchor will carry. This can be achieved either by increasing the strength of concrete or by increasing the number of anchor units on the bolt.

D. Watstein also carried out a limited number of tests in which a shearing load was applied to the bolt. These tests show that to secure the maximum resistance from a bolt anchor carrying a shear load the annular space between the bolt and the inner surface of the drilled hole must be filled with a tubular section of appropriate size, or some other means must be used to provide lateral support to the bolt and to prevent it from bending when a shearing load is applied.

Adams' tests show that workmanship is of utmost importance to secure the maximum capacity from anchor bolts used in securing fixtures or machinery to concrete. The anchors must be adequately set in a well-cleaned hole cut with a drill which leaves the inner surface of the hole in a rough condition; it is also important to keep the clearance between the hole and the anchors to a minimum. The hole must be of sufficient depth to prevent spall-type failure, and it must not be near a corner or an edge of the concrete. It is suggested that the depth of the anchor should be about four times the diameter of the bolt and the clear distance from the nearest edge should be two to three times the depth of the hole.

R. F. Conard[54] reported tests of anchor bolts grouted in drilled holes in concrete blocks having compressive strength of 3000 psi. The bolts were 1/2 and 3/4 in. in diameter, the holes were drilled using bits twice the nominal bolt diameter and were 3 in. long. Tests were conducted for tension (pull-out) capacity and for shear capacity. Different types of grout were used, including 1:3 Portland cement–sand grout, nonshrink grout, and polymer emulsion cement–sand grout.

It can be seen from Table 4.5 that for tension (pullout) loads the grout must be nonshrink type to develop adequate bond at the grout–concrete

TABLE 4.5. Maximum Load for Grouted 3/4-in. Diameter Bolts.

Type of Grout	Pull-out Load, lb.	Shear Load, lb.
1. Normal grout	825	12,550
2. Nonshrink	4250	12,200
3. Polymer based grout	2550	14,250

interface. For shear loads the bond is not a critical factor and all grouts performed reasonably well.

REFERENCES

1. Abrams, D. A., "Tests of Bond Between Concrete and Steel," *Bulletin No. 71*, University of Illinois Engineering Experiment Station, 1913.
2. Mylrea, T. D., "Bond and Anchorage," *ACI Journal*, Proceedings Vol. 44, pp. 521–552, March 1948.
3. Mains, R. M., "Measurement of the Distribution of Tensile and Bond Stresses Along Reinforcing Bars," *ACI Journal*, Proceedings Vol. 48, pp. 225–252, November 1951.
4. Bianchini, A. C., Kesler, C. E. and Lott, J. L., "Cracking of Reinforced Concete Under External Load," *Causes, Mechanism and Control of Cracking in Concrete*, ACI Publication SP-20, 1968.
5. Bresler, B., Bertero, V. and Bradford, J., "Studies on Bond-Slip Relationship Under Repeated Loading," unpublished, private communication, 1969.
6. Mikhailov, K. V., *Sizepleniye Armatury s Betonom* ("Bond of Reinforcement to Concrete"—in Russian), Moscow, 1952.
7. Cattaneo, L. E., National Bureau of Standards, private communication on Comparative Bond Strengths of Experimental Deformed Bars, June 1965.
8. *Specification for Minimum Requirements for the Deformation of Deformed Steel Bars for Concrete Reinforcement*, (A305), ASTM Standards, Part 4, 1965.
9. Ferguson, P. M. and Neils Thompson, J., "Development Length of High Strength Reinforcing Bars in Bond," *ACI Journal*, Proceedings Vol. 59, No. 7, pp. 887–917, July 1962.
10. Mathey, R. G., and Watstein, D., "Investigation of Bond in Beam and Pullout Specimens with High Yield-Strength Deformed Bars," *ACI Journal*, Proceedings Vol. 57, pp. 1071–1090, March 1961.
11. Broms, B. and Lutz, LeRoy A., "Effect of Arrangement of Reinforcement on Crack Width and Spacing in Reinforced Concrete Members," *ACI Journal*, Proceedings Vol. 62, No. 11, pp. 1395–1409, November 1965.
12. Bresler, B., and Bertero, V., "Behavior of Reinforced Concrete Under Repeated Load," *Journal of the Structural Division of ASCE*, Vol. 94 ST 6, pp. 1567–1590, June 1968.
13. Goto, Y., Ueda, S., and Maki, Y., "Investigation on Tension Cracks in Reinforced Concrete Members," (in Japanese) *Japan Society of Civil Engineers, The Second Symposium on Deformed Bars*, Concrete Library No. 14, Tokyo, Japan, December 1965.

14. Gilkey, H. J., Chamberlin, S. J., and Beal, R. W., "Bond Between Concrete and Steel and the Spacing of Reinforcement," *Iowa State College Bulletin*, Eng. Rep. No. 26, 1955–56.
15. "Report of ACI Committee 208, Proposed Test Procedure to Determine Relative Bond Value of Reinforcing Bars," *ACI Journal*, Proceedings Vol. 41, pp. 273–292, February 1945.
16. "Report of ACI Committee 408, A Guide for Determination of Bond Strength in Beam Specimens," *ACI Journal*, Proceedings Vol. 61, p. 129, February 1964.
17. Ferguson, P. M., and Thompson, J. N., "Development Length for Large High Strength Deformed Bars," *ACI Journal*, Proceedings Vol. 62, No. 1, pp. 71–91, January 1965.
18. Watstein, D., and Parsons, D. E., "Width and Spacing of Tensile Cracks in Axially Reinforced Concrete Cylinders, RP 1545," *Journal of Research, National Bureau of Standards*, Vol. 31, July 1943.
19. Watstein, D., and Seese, N. A. Jr., "Effect of Type of Bar on Width of Cracks in Reinforced Concrete Subjected to Tension," *ACI Journal*, Proceedings Vol. 41, pp. 293–304, February 1945.
20. Clark, A. P., "Cracking in Reinforced Concrete Flexural Members," *ACI Journal*, Proceedings Vol. 52, pp. 851–862, April 1956.
21. Chi, M., and Kirstein, A. F., "Flexural Cracks in Reinforced Concrete Beams, *ACI Journal*, Proceedings Vol. 54, pp. 865–878, April 1957.
22. *Symposium on Bond and Crack Formation in Reinforced Concrete*, RILEM, Stockholm, Sweden, 1957.
23. Kaar, P. H., and Mattock, A. H., "High Strength Bars as Concrete Reinforcement: Part 4—Control of Cracking," *Journal PCA Research and Development Laboratories*, Vol. 5, No. 1, p. 15, January 1963.
24. "Control of Cracking in Concrete Structures," Report of ACI Committee 224," *ACI Journal*, Proceedings V. 69, No. 12, pp. 717–752, December 1972.
25. Ferry-Borges, J., "Cracking and Deformability of Reinforced Concrete Beams," Publications, International Association for Bridge and Structural Engineering, Zurich, V. 26, pp. 75–95, 1966.
26. Gergely, P., and Lutz, LeRoy A., "Maximum Crack Width in Reinforced Concrete Flexural Members, Causes, Mechanism, and Control of Cracking in Concrete," *ACI Publication* SP-20, p. 87, 1968.
27. *Recommendations for an International Code of Practice for Reinforced Concrete*, Comite Européen du Beton, Paris 1964.
28. *Strength and Serviceability Criteria, Reinforced Concrete Bridges, Ultimate Design*, U.S. Dept. of Transportation, Bureau of Public Roads, October 1969.
29. "Cracking, Deflection, and Ultimate Load of Concrete Slab Systems," ACI Publication SP-30, pp. 55–75, 1971.
30. Soretz, S., "Factors Affecting the Stiffness of Reinforced Concrete Beams," *RILEM Symposium on Bond and Crack Formation*, Stockholm, 1957.
31. Baker, A. L. L., Ashdown, A. J., and Wildt, R. H., "The Deformation of Cracked Rectangular Reinforced Concrete Beams," *RILEM Symposium on Bond and Crack Formation*, Stockholm, 1957.
32. Murashev, V. I., "Calculation of Crack Width in, and Flexural Rigidity of Reinforced Concrete Members in Flexure," *RILEM Symposium on Bond and Crack Formation*, Stockholm, 1957.
33. Watstein, D., and Mathey, R. G., "Evaluation of Width of Cracks in Concrete at the Surface of Reinforcing Steel by Means of Tensile Bond Specimens," *RILEM Symposium on Bond and Crack Formation*, Stockholm, 1957.

34. Yu, W., and Winter, G., "Instantaneous and Long Time Deflections of Reinforced Concrete Beams Under Working Loads," *ACI Journal*, Proceedings Vol. 57, No. 7, July 1960.
35. Davis, R. E., Brown, E. H., and Kelly, J. W., "Some Factors Influencing the Bond Between Concrete and Reinforcing Steel," *Proceedings ASTM* Vol. 38.11, pp 394–409, 1938.
36. Ferguson, P. M., "Bond Stress—The State of the Art," *ACI Journal*, Proceedings Vol. 63, No. 11, pp. 1161–88, November 1966.
37. Clark, A. P., "Comparative Bond Efficiency of Deformed Concrete Reinforcing Bars," *Journal of Research of the National Bureau of Standards*, Vol. 37, RP 1755, pp. 399–407, December 1946.
38. Pfister, J. F., and Mattock, A. H., "High Strength Bars as Concrete: Reinforcement, Part 5, Lapped Splices in Concentrically Loaded Columns," *Journal PCA Research and Development Laboratories*, Vol. 5, No. 2, May 1963.
39. Ferguson, P. M., and Husain, S. I., "Strength Effect of Cutting off Tension Bars in Concrete Beams," *Research Report* 80-IF, Center for Highway Research, The University of Texas, Austin, June 1967.
40. Bresler, B., and Scordelis, A. C., "Shear Strength of Reinforced Concrete Beams—Series III," *Structures and Materials Research Report* No. 65–10, Dept. of Civil Engineering, University of California, Berkeley, June 1966.
41. Sozen, M., and Gamble, W. L., "Strength and Cracking Characteristics of Beams with 14S and 18S Bars Spliced with Mechanical Splices," *ACI Journal*, Proceedings Vol. 66, No. 12, pp. 949–956, December 1969.
42. Segner, E. P. Jr., "Flexural Test Results from Splices In Tensile Reinforcing Bars," *ACI Journal*, Proceedings Vol. 63, No. 11, pp. 1279–1281, November 1966.
43. Ferguson, P. M., and Breen, J. E., "Lapped Splices for High Strength Reinforcing Bars," *ACI Journal*, Proceedings Vol. 62, No. 9, pp. 1063–1077, September 1965.
44. Ferguson, P. M., "Design Criteria for Overhanging Ends of Bent Caps—Bond and Shear," Center for Highway Research, The University of Texas, Austin, August 1964.
45. Janney, J. R., Report of ACI–ASCE Committee 512, Suggested Design of Joints and Connections in Precast Structural Concrete, *ACI Journal*, Proceedings Vol. 61, No. 8, pp. 921–937, August 1964.
46. Kriz, L. B., and Raths, C. H., "Connections in Precast Concrete Structures—Strength of Corbels," *PCA Research and Development Laboratories, Bulletin* D85, pp. 16–61, February 1965.
47. Bryson, J. O., and Mathey, R. G., "Surface Condition Effect on Bond Strength of Steel Beams Embedded in Concrete," *ACI Journal*, Proceedings Vol. 59, No. 3, pp. 397–405, March 1962.
48. Ros, M., "Les Constructions Acier-Beton, Systeme Alpha," *L'Ossature Metallique* (Brussels), Vol. 3, No. 4, April 1934.
49. Viest, I. M., Siess, C. P., Appleton, J. H., and Newmark, N. M., "Studies of Slab and Beam Highway Bridges, Part IV: Full Scale Tests of Channel Shear Connectors and Composite T-Beams," *Bulletin* No. 405, University of Illinois Engineering Experiment Station, December 1952.
50. Viest, I. M., "Investigation of Stud Shear Connectors for Composite Concrete and Steel T-Beams," *ACI Journal*, Proceedings Vol. 52, No. 8, pp. 875–891, April 1956.
51. Slutter, R. G., and Driscoll, G. C., "Flexural Strength of Steel Concrete Composite Beams," *ASCE Journal of the Structural Division*, Vol. 91, No. ST2, pp. 71–99, April 1965.

52. *Specification for the Design, Fabrication and Erection of Structural Steel for Buildings*, American Institute of Steel Construction, February 1969.
53. Adams, R. F., "Some Factors Which Influence the Strength of Bolt Anchors in Concrete," *ACI Journal*, Proceedings Vol. 52, No. 2, pp. 131–138, October 1955.
54. Conard, R. F., "Tests of Grouted Anchor Bolts in Tension and Shear," *ACI Journal*, Proceedings Vol. 66, No. 9, September 1969.

5

Strength and Deformation of Reinforced Concrete Elements

OSCAR GONZÁLEZ CUEVAS,
FRANCISCO ROBLES,
ROGER DÍAZ de COSSIO

5.1 INTRODUCTION

This chapter deals with the *strength* of reinforced concrete members under the action of short-time flexure and axial loading, shear, and torsion, and with the *deformation* of members under short- and long-time service loads and at final collapse. In most cases, ordinary reinforced concrete members are subjected to the combined action of flexure, axial load, shear, and, in some cases, torsion. In this chapter, the actions are considered separately because this separation simplifies the study of reinforced concrete members and is reasonable for ordinary members. However, attention is given to important interactions, such as flexure and axial load, influence of flexure on shear strength, and to the combined action of torsion, flexure and shear.

The word "action" is used in this chapter to denote a generalized force (its effect) or a disturbance caused by some change in the environment; "strength" is used to denote the maximum value of the applied action that can be resisted by a member; and the term "final collapse" is used to denote the final stage, after maximum load is attained.

5.2 FLEXURE AND AXIAL LOADS

5.2.1 General Remarks

A reinforced concrete element may reach its strength under innumerable combinations of bending moment and axial load. These may vary from a maximum axial load, P_0, which can be either tensile or compressive and is associated with zero bending moment, to a maximum moment, M_0, associated with a zero axial load. It can be assumed that axial loads and flexure act independently of each other on a given cross section of a member. Figure 5.1 shows a schematic representation of a member under a bending moment, M, and an axial load, P, and Fig. 5.2, a statically equivalent system in which $M = Pe$. It is important to note that for some structures P and M vary in the same proportion when the external load varies; in other words, e remains constant. For other structures, however, the variation in external load may be such that P and M do not change in the same proportion.

The locus of the combinations of axial load, P, and moment, M, at which a member attains its strength is usually represented by an *interaction diagram* or *P–M diagram*. A typical diagram is shown schematically in Fig. 5.3, for a rectangular cross section. If exactly the same element were tested under different ratios of axial load and moment, and the maximum values for P and M attained in each case were recorded and represented in a P–M graph, the interaction diagram would be similar to the one shown in Fig. 5.3. Because the eccentricity $e = M/P$ may be obtained from any two values of M and P, an interaction diagram can also be defined as the locus of the maximum values of axial load which can be applied to a short element, when the eccentricity of the load varies from zero (zero bending moment) to infinity (zero axial load).

Line OA in Fig. 5.3 represents a case in which the external load varies in such a way that the values of axial load and moment increase in the same

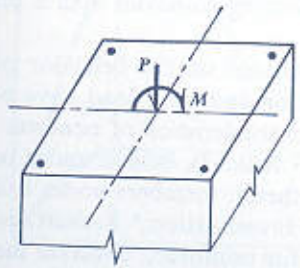

FIGURE 5.1. Member under axial load and flexure.

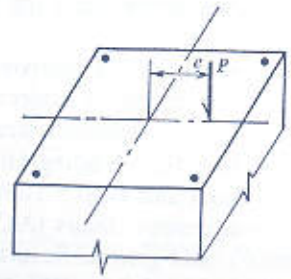

FIGURE 5.2. Eccentrically loaded member.

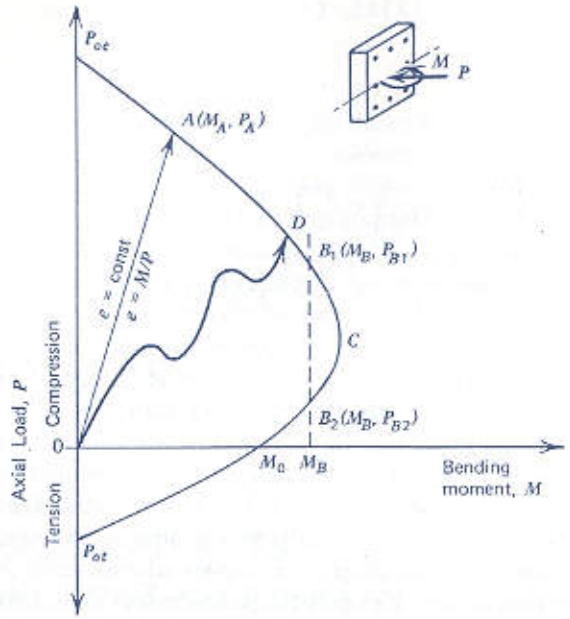

FIGURE 5.3. Interaction P-M diagram.

proportion. The slope of this line is the eccentricity $e = M/P$. The strength of the member for this case would be M_A, P_A. For a bending moment such as M_B there exist, in general, two values of axial load with which the strength of the element may be attained as indicated by points B_1 and B_2. Line OD represents an arbitrary loading history where axial load and bending moment do not increase in the same ratio.

The interaction diagram shown in Fig. 5.3 corresponds to an element with a given cross section, reinforcement, concrete, and plane of bending. For the case shown in the figure the plane of bending coincides with a plane of symmetry.

The experimental and analytical investigations on the behavior of reinforced concrete members subjected to bending and axial load have covered the following main aspects: stress–strain characteristics of concrete under short- and long-time loading (Brandtzaeg,[1] Rüsch[2]), beams under bending (Mörsch,[3] Bach and Graf,[4] Talbot,[5] and others), members under axial and eccentric compressive loads (ACI Column Investigation,[6] Richart, *et al.*[7,8], Hognestad[9]), and general flexural theories for reinforced concrete members under short-time loads (Whitney[10]; Mattock, Kriz, and Hognestad[11]; Granholm[12]; Rüsch[2]). Studies of the problem of bending and axial tension are meager. According to the above information, it has been possible to establish

a generalized set of assumptions from which to obtain interaction diagrams such as that shown in Fig. 5.3. Reliability analyses of concrete members have shown that the probability of underestimating the strength of beams and columns, computed by the simplified method described later, is sufficiently small for engineering design purposes.[13]

In the following sections, the general aspects of the behavior under load will be described first for members under axial compression, bending, and bending and compression. Next, a basic procedure to obtain values of P and M from known or assumed stress–strain characteristics will be explained. Based on this, and on the information from the behavior under load, the more generally made simplifying assumptions for strength computations will be justified.

5.2.2 Behavior and Modes of Failure of Members under Axial Compression

Load–deformation curves are shown in Fig. 5.4 for three types of concrete members under axial compression. The curves shown are typical of those obtained from tests of short members under increasing load.

Curve A of Fig. 5.4 corresponds to a plain concrete specimen with a slenderness ratio (length/minimum cross-section dimension) larger than 2, but

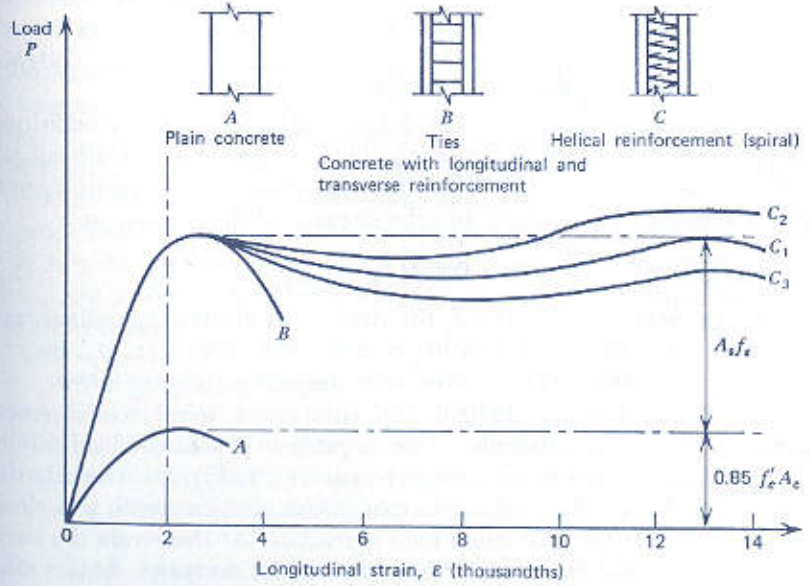

FIGURE 5.4. Load–deformation diagrams of members under axial compression.

smaller than about 8. As in the case with control cylinders, the maximum axial load is reached at a longitudinal strain of about 0.002. During the ACI Column Investigation it was found that the strength of a relatively short (slenderness of 8 or less) plain concrete prism could be estimated by multiplying the maximum stress in a control cylinder (f'_c) by 0.85 and by the area of the prism, that is, $P_0 = 0.85f'_cA_c$. The factor 0.85 is only a rough average of the results of tests of vertically cast prisms. This factor ranges from 0.69 to 0.93. Several reasons have been advanced to explain this: (1) bleeding due to which, in a longer vertically cast and cured prism, the upper portions will have a larger water–cement ratio and consequently lower compressive strength; (2) eccentricity of loading and lateral deflection which decrease the strength, no matter how short the specimen; and (3) decreasing strength with increasing size of the specimen due to the greater probability of having a weak zone. None of these explanations is fully satisfactory. Few comparisons have been made between vertically and horizontally cast specimens. For design purposes it is sufficient to consider a factor of about 0.85 for vertically cast members.

If longitudinal reinforcement is added to a short member and if transverse reinforcement in the form of closed ties is used, the typical load–deformation curve will be similar to curve *B* of Fig. 5.4. Strength is attained again at strains of about 0.002, after which final collapse occurs very rapidly at strains from around 0.003 to 0.005. At a strain close to the maximum load, significant longitudinal or inclined cracking appears, depending on the end restraints, and the concrete cover begins to spall off. At final collapse, longitudinal reinforcing bars buckle out between ties.

Comparing curves *B* and *A* of Fig. 5.4, it can be seen that the additional capacity may be attributed to the longitudinal reinforcement, which usually yields at strains of about 0.002. Thus, the contribution of the reinforcement may be evaluated as $P_s = A_sf_y$, and the strength of the member as

$$P_0 = 0.85f'_cA_c + A_sf_y \tag{5.1}$$

where A_s represents the area and f_y the yield stress of the longitudinal reinforcement; A_c represents the area of concrete. The gross area, A_g, may be used instead of A_c without much error when the steel percentage is low.

If the member has longitudinal and continuous spiral reinforcement throughout its length, sufficiently close in pitch to insure confinement, its behavior under load may be represented by curves *C* of Fig. 5.4. The behavior of a member with spirals is similar to that of one with ties until, at a strain of about 0.002, the first maximum load is reached. At this strain the cover begins to spall off and therefore the total load carried decreases. At this stage the lateral deformation of the concrete is significant and the spiral reinforcement is then subjected to a strain which produces a confining action upon the concrete core. This confining action again increases the load capacity, and a second maximum is reached. Depending on the type of spiral reinforcement, its pitch, and thus on the amount of confining action, the second maximum may correspond to a load larger (curve C_2), equal (curve C_1) or smaller (curve C_3) than the first maximum. All this occurs at relatively large strains, as can be seen in Fig. 5.4.

From the above it can be concluded that the strength of a member under axial compression may be obtained from the contribution of four factors: concrete in the core, longitudinal steel, concrete cover, and spiral reinforcement. The contribution of the two latter factors cannot exist simultaneously, since the spiral reinforcement acts only when the cover spalls off.

The contribution of the concrete (core and cover) as mentioned previously, may be evaluated as the product of the area by 85% of the cylinder stress, f'_c. The contribution of the longitudinal steel may be evaluated as the product of the steel area, A_s, times the yield stress, f_y, or, in general, the stress f_s, corresponding to a strain of about 0.002 in the steel stress–strain curve. In order to evaluate the contribution of the spiral, it is convenient to review some concepts of the behavior of concrete under triaxial compression.

Brandtzaeg, *et al.*[1] found, from tests of control cylinders subjected to a lateral pressure, f_2, that the maximum average vertical stress, f_1, required to attain the strength of the specimen may be evaluated approximately according to the expression

$$f_1 = f'_c + 4.1f_2 \tag{5.2}$$

Brandtzaeg also found from tests that the confining effect of lateral pressure is comparable to that of spiral reinforcement. For a given concrete area of core, A_n, the contribution of the lateral pressure to the vertical load capacity would be $4.1\,f_2A_n$. (Recent tests show that for some lightweight-aggregate concretes the increase in vertical load capacity due to spiral reinforcement is much less than that observed for normal weight concrete.)

If h is the core diameter, out to out of the spiral reinforcement, A_b, the area, and s, the pitch of the spiral, the volumetric steel percentage may be obtained from

$$\rho_s = \frac{\pi hA_b}{\pi h^2 s/4} = \frac{4A_b}{hs} \tag{5.3}$$

The lateral confining pressure may be expressed approximately in terms of the tension in the spiral reinforcement. From the equilibrium of forces in the free-body diagram shown in Fig. 5.5,

$$2A_bf_s = f_2hs$$

where f_s is the stress in the spiral reinforcement and f_2, the lateral confining pressure acting on the diametral plane. Using the definition of ρ_s given by

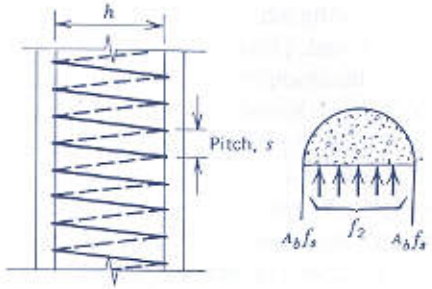

FIGURE 5.5. Free-body diagram of a section with spiral reinforcement.

Eq. (5.3),

$$f_2 = \frac{\rho_s f_s}{2} \tag{5.4}$$

Furthermore, according to Eq. (5.2), the contribution to the vertical capacity will be 4.1 times the lateral pressure times the area of the core, from which this contribution can be expressed by

$$2.05\rho_s f_s A_n$$

The validity of the coefficient 2.05 was verified approximately during the ACI Column Investigation[6]; it ranged from 1.7 to 2.9. In this chapter it will be taken as 2.0.

In its report, the majority committee of the ACI Column Investigation recommended making the contribution of the transverse reinforcement at least equal to the contribution of the concrete cover. Thus

$$0.85f'_c(A_c - A_n) = 2\rho_s f_s A_n$$

and therefore

$$\rho_s = 0.425\left(\frac{A_c}{A_n} - 1\right)\frac{f'_c}{f_s} \tag{5.5}$$

According to this criterion, Eq. (5.1) gives the strength of reinforced members with any type of transverse reinforcement. (In the 1971 ACI Code,[14] Eq. (5.5) appears with the coefficient rounded off to 0.45, and $f_s = f_y$.)

In practice there are no members subjected to axial compression, but the knowledge of the strength under this condition provides an upper theoretical bound to the values of normal force which a member can resist.

5.2.3 Behavior and Modes of Failure of Members under Pure Bending

The behavior of a simply supported beam with an ordinary amount of tensile steel, under gradually increasing load is characterized by a typical load-deflection diagram as shown in Fig. 5.6. Behavior is essentially linear until

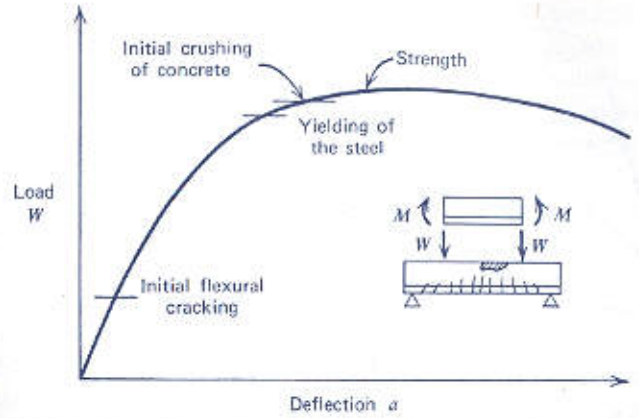

FIGURE 5.6. Schematic load–deflection curve of an element with ordinary amount of tensile steel.

the appearance of the first flexural cracks in the constant moment region. After cracking, which gradually produces loss of stiffness, the load–deflection curve decreases in slope. At a certain load level the steel at midspan begins to yield, and at this stage the load–deflection curves experience an abrupt change of slope. From then on, small increases in load produce considerable deflections in the member. During this process the compression zone of the member becomes smaller until it is incapable of carrying the internal compression force. Crushing of the concrete begins after yielding of the steel, the load decreases, and final collapse follows at a load smaller than the strength. The maximum load reached in this stage is the strength of the member.

A member which exhibits the behavior just described, with the tensile steel yielding before crushing of the concrete and final collapse, is said to be *under-reinforced*. On the other hand, when the percentage of tensile steel is sufficient, crushing of the concrete and final collapse may occur before the tensile steel has yielded. In this case the member is said to be *over-reinforced*. When the steel yields at the same time that the strength is attained, the member is said to be *balanced*. Both balanced and over-reinforced members are much less ductile and undergo much less deflection than under-reinforced members.

The effect of variations in the amount and distribution of steel on the load–deflection characteristics of a given reinforced concrete beam is presented qualitatively in Fig. 5.7. In this figure the solid lines represent curves for beams with tensile steel only, varying from 0%, for the limiting case of plain concrete, to a very high percentage (about 6 or 7). The curves show that failure is brittle for very small percentages, roughly less than about 0.5% (curves

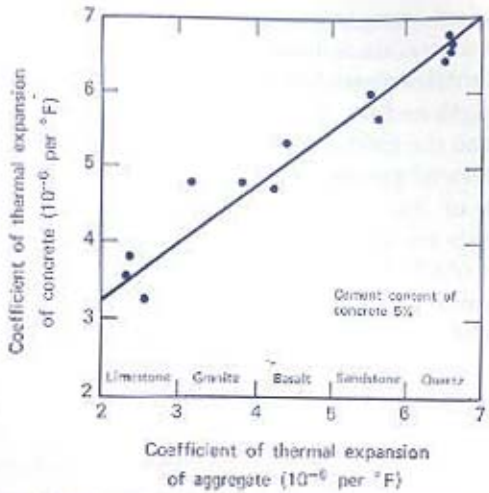

FIGURE 1.3. Effect of aggregate on thermal expansion of concrete.[7] (Reprinted by permission of the American Society for Testing and Materials, Copyright ASTM.)

granites and limestones may have too low values to be compatible with cement paste. Figure 1.3 illustrates the correlation between the thermal expansion of various aggregate types and the corresponding values for concrete.

The *unit weight* of an aggregate is not only useful in concrete-mix-design calculations but also in determining whether or not an aggregate is suitable for making special concretes such as insulating concrete, structural lightweight concrete, and heavyweight concrete. Typical bulk densities, in pounds per cubic foot of aggregate, for use in various types of concretes are: insulating concrete 10–50; structural lightweight concrete 40–70; normal-weight concrete 75–110; and heavyweight concrete 110 and greater. The most commonly used aggregates, i.e., sand, gravel, and crushed rocks produce normal-weight concrete (140–160 pcf); expanded shale, clay, slate, or fly ash aggregates are used to make structural lightweight concrete (85–115 pcf); perlite, and vermiculite produce insulating concretes (15–50 pcf); and barite, magnetite, hematite, limonite, ilmenite, and ferrophosphorous are generally used in heavyweight concretes (200–300 pcf).

ASTM Specification C330 deals with *lightweight aggregates* for structural concrete. The two general types of cellular and granular inorganic materials used as lightweight aggregate include the aggregates prepared by expanding, calcining, or sintering products such as shale, clay or slate, blast furnace slag, diatomaceous earth, fly ash; and the aggregates prepared by processing natural materials of volcanic origin such as pumice, scoria, or tuff. The

TABLE 1.5. Aggregates Used in Shielding Concrete.[10] (Reprinted by permission of the American Society for Testing and Materials, Copyright ASTM.)

Natural Mineral		Manufactured	
Local sand and gravel		Crushed aggregates	
Calcareous, Siliceous	(2.5 to 2.7)[a]	Heavy slags	(~5.0)
		Ferrophosphorus	(5.8 to 6.3)
Basaltic	(2.7 to 3.1)	Ferrosilicon	(6.5 to 7.0)
Hydrous ore		Metallic iron products	
Bauxite	(1.8 to 2.3) [15 to 25 %]	Sheared bars, Steel punching	(7.7 to 7.8)
Serpentine	(2.4 to 2.6) [10 to 13 %]	Iron shot	(7.5 to 7.6)
		Boron additives	
Goethite, Limonite	(3.4 to 3.8) [8 to 12 %]	Boron frit	(2.4 to 2.6)
		Ferroboron	(5.0)
Heavy ore		Borated diatomaceous	
Barite	(4.0 to 4.4)	earth	(~1.0)
Magnetitite, Ilmenite, Hematite	(4.2 to 4.8)	Boron carbide	(2.5 to 2.6)
Boron additives			
Calcium borates			
Borocalcite, Colemanite	(2.3 to 2.4)		
Gerstley borate	(2.0)		

[a] Specific gravity is shown in parentheses. Water of hydration is indicated in brackets.

application of natural materials is limited due to their quality variations and unavailability in many geographical areas. A summary paper by Lewis[8] and the ACI Committee 213 Report[9] provide good discussions on lightweight aggregates and concretes.

ASTM Specification C637 deals with special and *heavyweight aggregates* for use in radiation-shielding concretes in which composition (viz. hydrous minerals), or high specific gravity, or both, are of prime consideration. In Table 1.5 are listed aggregates commonly used in shielding concrete.

1.8 MIXING WATER

Generally, if the water is good enough for drinking, it is considered good enough for concrete making. However, taste, odor, or source of supply alone should not be taken as sufficient reasons for rejecting any water. Bog and marsh waters, mine waters, several industrial-waste waters, and sea water were used for concrete mixing in special cases.[11]

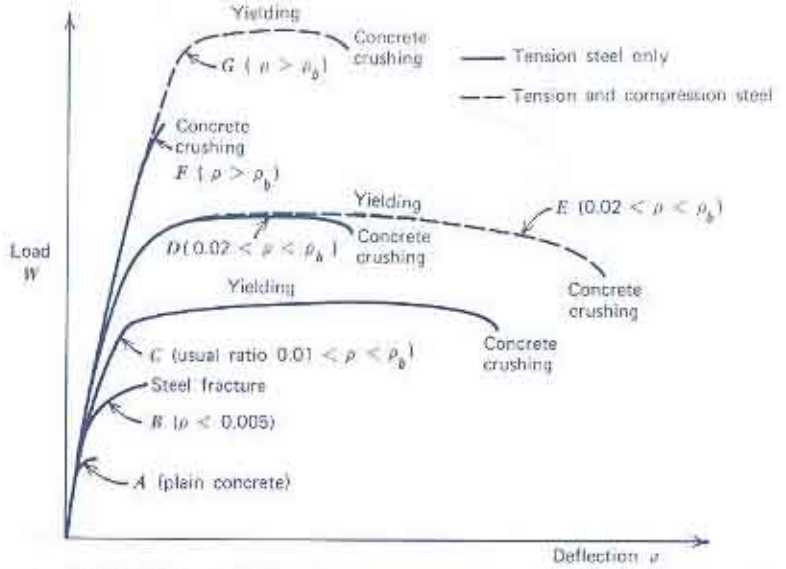

FIGURE 5.7. Load–deflection curves for beams of a given section with varying reinforcements.

A and B), and for percentages higher than that required for a balanced condition. For the intermediate range, ductility decreases with increasing steel percentage, so that in the design of a given section a trade-off must be considered between strength requirements on one side and ductility and weight requirements on the other. For example, beam C has less steel, and therefore less strength than beam D, but more ductility. Curve F illustrates the lack of ductility of an over-reinforced beam. To avoid nonductile behavior codes limit both the minimum and the maximum amount of steel. Thus, for minimum reinforcement, the amount of steel must be such that the strength of the reinforced section is greater than that of the plain concrete section computed from its modulus of rupture. The minimum value of $\rho = 200/f_y$ recommended by the ACI Code[14] is based on this reasoning. A similar though more refined recommendation is given in Reference 15. Maximum steel is usually fixed as a percentage of that corresponding to a balanced condition. The amounts specified by different codes vary from 50 to 100% of ρ_b.

The effect of adding compression steel is illustrated by the two broken line curves of Fig. 5.7. In both cases the addition of compression steel with adequate lateral ties improves ductility. Strength is significantly increased only in over-reinforced sections, in which adding steel to the compression zone permits the full development of the tension steel (curve G). In practice doubly reinforced sections of this type are seldom used because of their

excessive cost, though there are situations in which restrictions in dimensions make them necessary. In sections with normal amounts of tension steel which contain compression steel, because of detailing requirements, it is usual to neglect this steel in strength computations, because it does not significantly increase strength, as indicated by curves D and E. It is important to note that in order to obtain the additional ductility from the compression steel, it is necessary to avoid premature failures due to the buckling out of this steel. This is done by providing adequate cover and transverse reinforcement, usually in the form of closed ties. Requirements for such reinforcement are given in the codes. An attempt to formulate a rational method for establishing such requirements is described in Reference 16.

In the above considerations, only the influence of the amount of steel was discussed. The load–deflection properties are also a function of the strength characteristics of the materials, f'_c and f_y. An increase in f_y or ρ increases the capacity of tensile reinforcement and an increase in f'_c increases the capacity of the compression zone. The behavior of the member depends strongly on the ratio between the tension and compression capacities, which can be measured directly by the *reinforcement index*, $\omega = \rho f_y/f'_c$, for members in which the compression zone is rectangular. (For other types of cross sections, ω is only an approximate measure.) For members with both tension and compression steel, the reinforcement index is $\omega = (\rho - \rho')f_y/f'_c$, where ρ' is the compression steel ratio. Table 5.1 summarizes the above discussion and complements Fig. 5.7.

Another important aspect of the behavior of elements under bending is the strain distribution across the depth. Measurements of deformations in the laboratory[6] indicate that for members with a good bond between concrete and steel,[17] and for gage lengths larger than the average crack spacing, the distribution of strain in a cross section is practically linear throughout the depth. (For members with poor bond this is true only in the compression zone.)

5.2.4 Behavior and Modes of Failure of Members under Bending and Axial Compression

A typical specimen used in the study of the behavior of members under bending and compression is shown in Fig. 5.8, together with a typical cracking pattern. Generally P is applied at a constant eccentricity, so that cross sections are subjected to increasing values of P and M at a constant ratio.

Failure can be either in compression or in tension. In a compression failure, the concrete in the most compressed zone crushes before the steel on the tension side yields. This mode of failure occurs for high axial loads and corresponds to a point on the interaction diagram of Fig. 5.3 between points C

TABLE 5.1. Characteristics of Members with Different Reinforcement Indexes.

Steel Ratio		Reinforcement					
Tension $\rho = A_s/bd$	Compression $\rho' = A'_s/bd$	Index $\omega = (\rho - \rho')f_y/f'_c$	Type of Member	Mode of Failure	Ductility or Brittleness	Typical Curve (Fig. 5.7)
zero	zero	zero	plain concrete	concrete in tension	brittle	A
very low $\rho < 0.005$	zero	very low	under-reinforced	sudden fracture of tension steel	brittle	B
low (normal range) $0.01 < \rho < 0.03$	zero	low–normal	under-reinforced	crushing after yielding	very ductile	C
high, $0.02 < \rho < 0.05$	zero	high–normal	under-reinforced	crushing after yielding	ductile	D
high (normal range)	similar to the tension steel	low–normal	under-reinforced	crushing after yielding	very ductile	E
very high	zero	very high	over-reinforced	crushing	brittle	F
very high	similar to the tension steel	normal	under-reinforced	crushing after yielding	ductile	G

FIGURE 5.8. Specimen under bending and axial load.

and P_{oc}. A tension failure takes place when the steel yields in tension before crushing of the concrete occurs. This mode of failure occurs for low axial loads and is represented in the interaction diagram by points between points C and M_0. Point C (Fig. 5.3) marks the theoretical boundary between compression and tension failures and is usually called balanced point. In some cases it is not easy to identify point C, so that the transition between brittle compression failures and ductile tension failures is not well defined.

The effect of spiral steel on strength is hardly noticeable in members under eccentric loads, but the increase in ductility is still considerable.

5.2.5 Fundamental Relationships Between Stresses, Normal Forces and Moments

Fundamental relationships between the external forces acting on a member and the internal forces which are generated can be established if the geometrical properties of the cross sections of the member and the stress–strain characteristics of concrete and steel are known. These relationships are derived on the basis of conditions of equilibrium and compatibility.

In general, when nonlinear stress–strain characteristics are considered and both axial load and bending moment act on the section, it is not possible to derive simple algebraic expressions directly relating location of neutral axis and maximum stresses in steel and concrete with external loads P and M. However, iterative numerical procedures have been developed[18–20] which are

based on the possibility of obtaining the values of P and M corresponding to an arbitrary distribution of strains across the depth of the section.

The derivation of these fundamental relationships is based on the following hypotheses:

1. *Strain distribution is linear across the depth of the section.* This implies that there is no slip between concrete and steel, which is essentially accurate for concrete members reinforced with deformed bars since there is a good bond between steel and concrete. For such members linear strain distribution has been confirmed for bending and axial loads as well as for pure bending (Section 5.2.3).

2. *Concrete does not resist tensile stresses.* Although small tensile stresses can be resisted by concrete, neglecting these has little influence on calculated flexural strength.

3. *Stress–strain relationships for steel and concrete are known.* Usually the stress–strain relationship for steel reinforcement may be idealized by an elasto–plastic curve with a strain hardening branch. While under load reversal in the inelastic range the steel may depart from such ideal behavior, it is usually assumed that stress–strain relationships for steel reinforcement in tension and compression are identical and single-valued.

Stress–strain curves for concrete in compression depend on many variables (Section 3.9). However, for practical applications it is sufficient to use a simple idealization of the curve, such as that shown in Fig. 5.10, as the strength computed using different shapes of stress–strain curves are approximately the same, provided concrete ultimate strain exceeds 0.003.[19] When time-effects (creep, shrinkage, variable temperature) can be neglected, the stress–strain relationship for concrete in compression can be represented by a single-valued nonlinear curve.

The following relationships can be established for a section such as the one shown in Fig. 5.9, subjected to axial load P and bending moment M acting in a plane of symmetry. An arbitrary linear strain distribution is defined by specifying strain, ε_c, at the extreme fiber and the depth c of the compression zone. Then the strain-gradient or "curvature" ϕ is

$$\phi = \frac{\varepsilon_c}{c} \tag{5.7}$$

The strains ε_i at any level i and distance y_i from the neutral axis can be obtained as

$$\varepsilon_i = \phi y_i \tag{5.8}$$

The distributions of stresses in concrete, f_c, and in steel, f_s, are obtained from the known strains and the stress–strain functions for concrete:

$$f_{ci} = f_c(\varepsilon_i) \tag{5.9a}$$

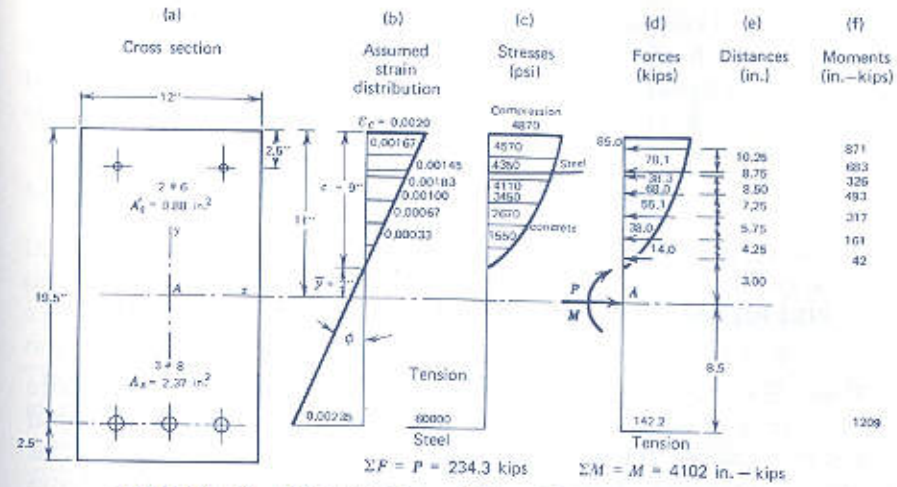

FIGURE 5.9. Determination of internal stresses and moments.

and for steel:

$$f_{si} = f_s(\varepsilon_i) \tag{5.9b}$$

The internal stress resultants, forces and moments are obtained by summing over the corresponding small areas, ΔA_c, (concrete) and, ΔA_s, (steel):

$$F_c = \sum f_{ci}\,\Delta A_{ci} \qquad M_c = \sum f_{ci}(y_i + \bar{y})\,\Delta A_{ci} \tag{5.10a}$$

and

$$F_s = \sum f_{si}\,\Delta A_{si} \qquad M_s = \sum f_{si}(y_i + \bar{y})\,\Delta A_{si} \tag{5.10b}$$

where $\bar{y}$ is the distance from the x axis about which moments are taken, to the neutral axis, from which the distances y_i are measured.

Equilibrium conditions require that

$$P = F_s + F_c \qquad M = M_c + M_s \tag{5.11}$$

This procedure is illustrated in Fig. 5.9. The strain distribution is defined by assuming $\varepsilon_c = 0.002$ and $c = 9$ in., and the stress–strain relationships are obtained from the curves in Figs. 5.10 and 5.11. The internal actions P and M corresponding to the prescribed strain distributions are calculated by summing the internal stresses over the areas and enforcing equilibrium.

The above procedure to determine load P and M is quite simple when the geometry of the cross section, material properties, and the strain gradient are given. This is not the case in the usual design process, wherein the values of P and M are given and the proportions of the sections are to be determined. Various design aids can be used for this purpose and will be discussed in Section 5.2.8. The method outlined above is the basis for producing such design aids.

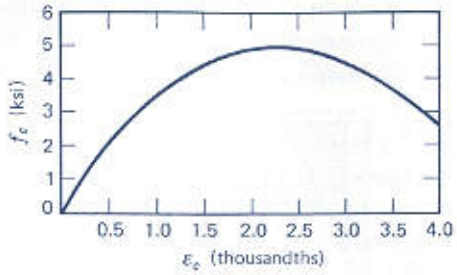

FIGURE 5.10. Stress–strain curve for concrete assumed in example.

Some design considerations, particularly under service loads, require determination of stresses in steel and concrete corresponding to prescribed values of P and M. The method outlined above is too cumbersome for this purpose as it requires a large number of iterations and the maximum stresses obtained by it are sensitive to the idealized shape of the stress–strain curves used in the analysis.

A simpler, commonly used method, which is adequate for some purposes is the traditional elastic approach which considers that the stress–strain functions of the concrete and steel are linear.[21,22] The method consists in converting the concrete section into what is called a transformed section by substituting the steel by a concrete area having an equivalent effect. The transformed area of the steel is obtained by multiplying by the ratio between the elastic moduli of the steel and the concrete ($n = E_s/E_c$). The member can

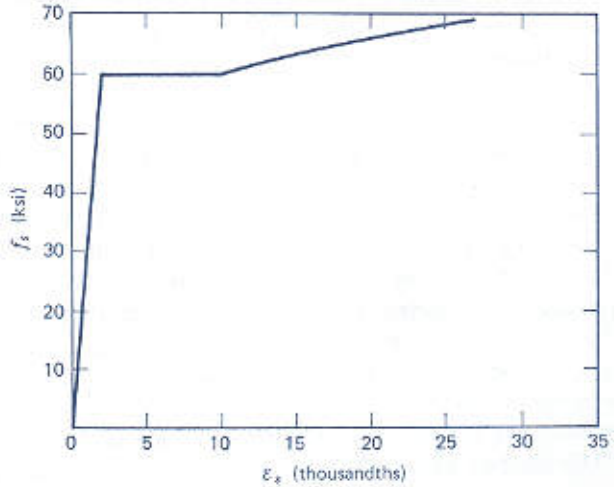

FIGURE 5.11. Stress–strain curve for steel assumed in example.

thus be analyzed as an ordinary homogeneous member of an elastic material. The method has obvious limitations, which have often been discussed in the literature, the principal one being the difficulty of establishing a correct value of n.

5.2.6 Determination of Maximum Values of P and M

In the preceding section, a method for obtaining the internal forces corresponding to an arbitrary distribution of strains was described. In this section, a general method for obtaining the maximum values of P and M at a constant ratio $e = M/P$ that can be developed by a given section will be presented. These maximum values or strengths define a point of the interaction diagram of the section.

Consider an element under a normal force P applied at an eccentricity e with respect to the geometric center of the cross section. The corresponding bending moment will be $M = Pe$. When P increases, the concrete strain in compression increases. For a given, known or assumed stress–strain curve, there is a one-to-one relation between load and concrete strain at a given fiber, and therefore there is a certain value of concrete strain, ε_o, for which the value of P is maximum at the given eccentricity. If the stress-strain curve has a descending branch, the value of P may decrease with increasing strain.

In order to find the strength at a given eccentricity, it will be necessary to determine values of P and M such that the ratio M/P coincides with that previously given, for increasingly larger concrete strains, until the whole stress–strain curve is covered, or until a maximum value is reached. This can be done by applying several times the procedure described in the preceding section. For a given eccentricity, the procedure may be summarized as follows:

1. *Selection of a linear strain distribution.* For a given value of concrete strain, ε_c, a strain distribution is fixed by selecting a neutral axis depth or a steel strain.
2. *Determination of internal forces.* From the known or assumed stress–strain curves and the strain distribution considered in (1), the internal forces are obtained by integration of the corresponding stresses.
3. *Determination of eccentricity.* The forces determined in (2) are expressed by their resultants, P and M. The eccentricity is then computed as M/P.
4. *Verification.* If the eccentricity determined in (3) coincides with that previously given, the problem is solved for the value of ε_c considered. If not, the strain distribution should be changed either by changing the neutral axis depth or the steel strain, and steps (1)–(3) should be repeated as many times as necessary until a satisfactory approximation is obtained.

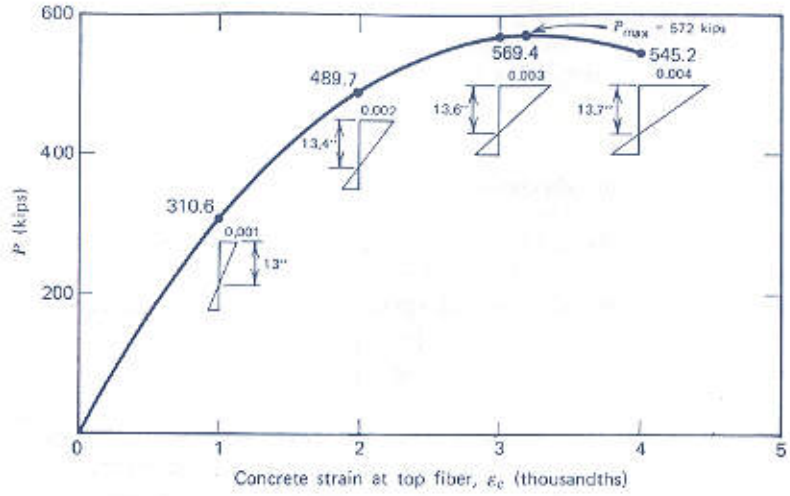

FIGURE 5.12. P–ε_c curve.

By repeating for different values of ε_c the procedure outlined in steps (1)–(4) above, $P - \varepsilon_c$ or $M - \varepsilon_c$ curves may be obtained, from which the maximum value can be read directly.

Figure 5.12 shows the $P - \varepsilon_c$ curve obtained following the above method for the cross section of Fig. 5.9 and for an eccentricity of 8 in. It can be seen that the maximum value, $P_{max} = 572$ kips, is reached at a strain ε_c of 0.00325.

The procedure just described is completely general and can be applied to elements with any cross section or distribution of steel bars. When the stress–strain curves can be approximated by known mathematical functions, an analytical function can be found in which the internal actions, P and M, are functions of the strains. It is then possible to find the values of strain which correspond to the maximum values of P or M by equating their first derivatives to zero. The complexity of the analytical problem will depend on the types of function assumed for the stress-strain curve and on the shape of the cross section and the distribution of the reinforcement.

5.2.7 Determination of Interaction Diagrams

Interaction diagrams can be obtained by applying the procedure illustrated in the preceding section, as many times as necessary, for different eccentricities. The interaction diagram for the cross section of Fig. 5.9(a) is shown in Fig. 5.13. As can be seen, its shape is similar to that of the one in Fig. 5.3. The diagram shown in the figure represents the case of normal compressive forces with eccentricities varying towards the side with less steel. In the same

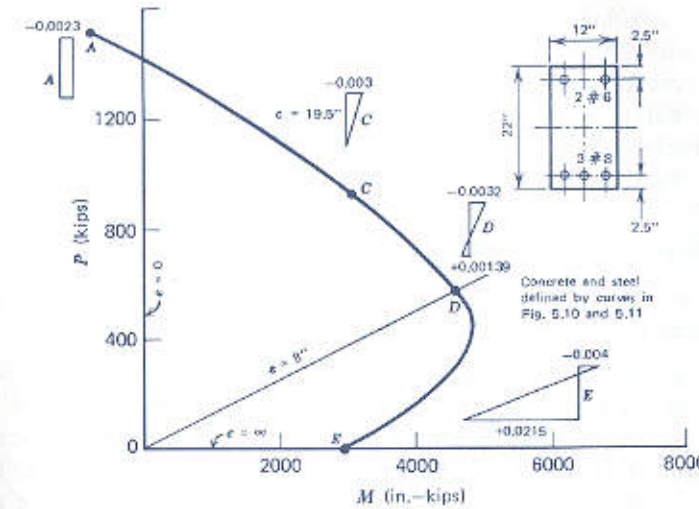

FIGURE 5.13. Construction of an interaction diagram.

manner a diagram for eccentricities varying towards the other side could be obtained, which would be shown in the third and fourth quadrants.

5.2.8 Design Aids

Design aids fall into three categories: computer programs, tables and charts, and calculations based on simplifying assumptions. *Computer programs* are becoming increasingly useful in the design process. One advantage of using computers is that a large number of alternative design studies can be made and the optimum solution can be chosen. Another advantage is that one need not simplify the basic assumptions merely to reduce the "arithmetic" involved in the process. The main disadvantage is that computer facilities and "design-oriented" programs are not always available.

Tables and Charts have been used traditionally to shortcut tedious calculations. For reinforced concrete members subjected to bending with or without axial load several design aids have been prepared. For pure bending of singly and doubly reinforced slabs and beams, References 23, 24 and 138 provide tables and diagrams. For bending combined with axial load, nondimensional interaction diagrams are provided in References 25 and 26. Tables which give the number and diameter of bars necessary for a given cross section to support a given combination of bending and axial load are provided in References 27, 28 and 138. In using tables and diagrams it is essential that the designer be fully aware of the assumptions made in developing the design aids, which often conform to local or regional specifications, and may become outdated.

Simplifying assumptions can be made which deal with specified strains or stresses defining "strength," characteristic stress–strain curves, or with equivalent "stress-blocks" so that it is not necessary to assume any particular shape of the curve. Most codes specify such simplifying assumptions and sometimes develop simple algebraic expressions which greatly simplify design calculations. These simplifications are discussed further in the next section.

5.2.9 Simplified Strength Computations

The two following hypotheses, additional to those mentioned in Section 5.2.8, have been proposed in order to simplify strength computations.

1. *Strength is attained at a fixed value of ε_c at the top fiber of the member.* Values of P do not vary much for values of ε_c between 0.003 and 0.004, as can be seen, for example, in Fig. 5.12. Thus it can be assumed that maximum values of P and M are always attained at the same value of ε_c, whatever the stress–strain functions and the mechanical and geometrical properties of the member. The value of ε_c at which strength is attained is denoted by ε_{cu}. It is usual to adopt values of ε_{cu} between 0.003 and 0.004. This hypothesis greatly simplifies strength computations, since it is not necessary to calculate P and M corresponding to different strains ε_c until maximum values are obtained.

2. *The stress distribution in the compression zone of concrete is defined by three factors β_1, β_2, β_3 as shown in Fig. 5.14(c).* This hypothesis, proposed by Stüssi in 1932, makes it possible to compute strengths without

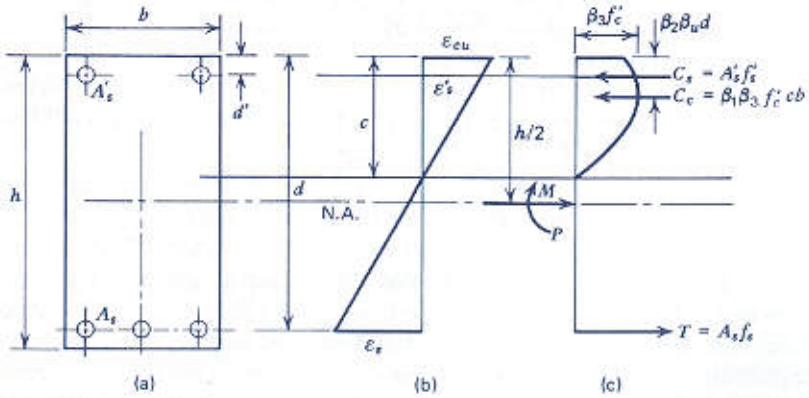

Summation of forces, $P = C_c + C_s - T$

Moments with respect to N.A., $M = C_s(h/2-d') + C_c(h/2-\beta_2 c) + T(d-h/2)$

FIGURE 5.14. Hypotheses for the simplified procedure.

supposing any particular stress–strain function for concrete. The parameters β_1, β_2, and β_3 define the magnitude and position of the resultant concrete compressive force C_c in Fig. 5.14(c). The parameter β_3 relates the maximum stress in compression due to flexure to the strength of control cylinders; β_1 relates the average and the maximum stresses in the compression zone; β_2 relates the position of the resultant C_c to the depth of the neutral axis. Some values of these parameters are presented below when particular assumptions of building codes are discussed. The parameters β_1 and β_3 appear usually as a product, $\beta_1\beta_3$. Thus it is sufficient to consider the value of the product, without considering the individual values of β_1 and β_3.

Once suitable values of ε_{cu} and β_1, β_2, and β_3 have been selected, the interaction diagram for a given cross section may be determined in accordance with the following steps:

1. *Selection of a value of the depth of the neutral axis, c.* This value, together with ε_{cu}, defines a strain distribution diagram.

2. *Computation of the compression and tension forces in the cross section.* The tension and compression forces in the steel can be computed from corresponding strains and using the actual stress–strain function or an idealization, for example, an elasto–plastic diagram without strain hardening. The compression force in concrete can be computed from the assumed value of c and the accepted value of parameter $\beta_1\beta_2$ [Fig. 5.14(c)].

3. *Computation of P and M from the sum of forces and the sum of moments with respect to the geometrical axis of the section.* These values define a point in the interaction diagram. If the process is repeated, enough points may be obtained to define the whole diagram.

ACI Assumptions. The ACI Code recommends the set of assumptions summarized in Fig. 5.15. The parameter β_1 has the same meaning as previously described. Its value depends on the nominal cylinder stress f'_c as

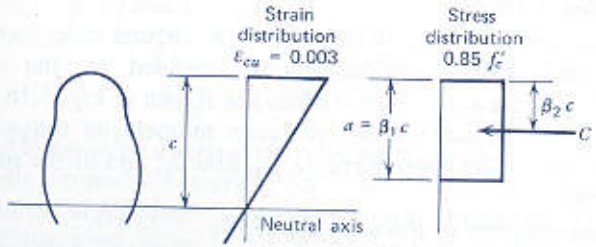

$$\beta_1 = (1.05 - \frac{f'_c}{20{,}000}) \leq 0.85$$

(f'_c in psi)

FIGURE 5.15. ACI hypotheses for flexure.

shown; it is constant and equal to 0.85 for $f'_c \leq 3000$ psi, and decreases by 0.05 for each 100 psi increase in f'_c in excess of 4000 psi. This variation takes into account the change in shape of the stress–strain curve for high values of concrete cylinder stress.

It can be seen from Fig. 5.15 that for cross sections of uniform width $\beta_3 = 0.85$ and $\beta_2 = \beta_1/2$. For other cross sections β_2 also depends on the shape. These values were determined by means of comparisons with test results.[29]

The ACI Code[14] also permits any other reasonable assumption for the compressive stress distribution that has been verified by comprehensive tests.

CEB Assumptions. Like ACI, the European Concrete Committee (CEB)[30] accepts any reasonable shape for the concrete stress distribution in compression. The CEB specifically recommends three alternative distributions: rectangular, parabolical to the neutral axis, and a combination of both. For the maximum concrete strain, the CEB recommends a value of 0.0035.

5.2.10 Bending and Axial Tension

The general procedure to determine strength is applicable also to the case where the axial force is tensile. However, as previously mentioned, the body of research supporting its applicability is meager, principally because this case is not so common in practice. Unless future research shows otherwise, the general simplifying assumptions are applicable to the case of axial tension. A possible theoretical approach is discussed in Reference 20.

5.2.11 Pure Bending

Pure bending is so common in practice that it merits a more detailed treatment. A general approach will be described using the simplifying assumptions given in Section 5.2.9.

To illustrate this approach, an element of rectangular cross section will be used, reinforced with tensile steel only, defined by the steel ratio $\rho = A_s/bd$. The forces and other variables are shown in Fig. 5.16. The problem is then to find the value of the maximum moment, or flexural strength, M_s, as a function of the parameters β_1, β_2, and β_3, and of the properties of the cross section.

From the equilibrium of forces in Fig. 5.16,

$$\rho bdf_s = \beta_u\beta_1\beta_3 f'_c bd$$

from which

$$\beta_u = \frac{1}{\beta_1\beta_3}\frac{\rho f_s}{f'_c} \tag{5.12}$$

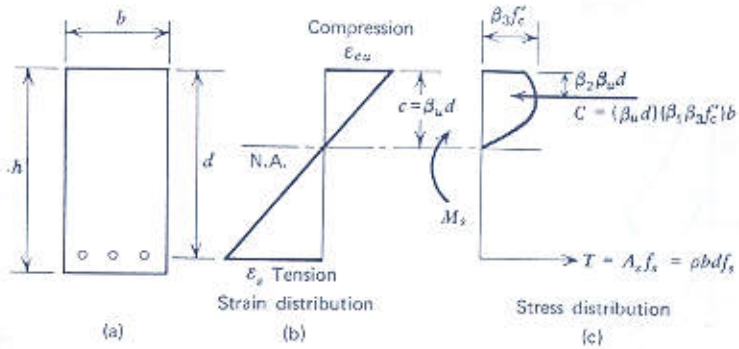

FIGURE 5.16. Hypotheses for bending.

From the equilibrium of moments with respect to the tension steel

$$M_s = Cd(1 - \beta_2\beta_u)$$

$$M_s = \beta_u\beta_1\beta_3 f'_c bd^2(1 - \beta_2\beta_u)$$

Substituting β_u from Eq. (5.12)

$$M_s = bd^2 f'_c \frac{\rho f_s}{f'_c}\left(1 - \frac{\beta_2}{\beta_1\beta_3}\frac{\rho f_s}{f'_c}\right) \tag{5.13}$$

Equation (5.13) shows that if reasonable values are assumed for $\beta_2/\beta_1\beta_3$ and if the value of the steel stress is known, the strength M_s can be computed.

The stress, f_s, can be obtained from the compatibility condition, combined with the stress–strain curve for the steel. From Fig. 5.16

$$\beta_u = \frac{\varepsilon_{cu}}{\varepsilon_{cu} + \varepsilon_s} \tag{5.14}$$

Combining Eqs. (5.12) and (5.14),

$$\frac{\varepsilon_{cu}}{\varepsilon_{cu} + \varepsilon_s} = \frac{1}{\beta_1\beta_3}\frac{\rho f_s}{f'_c} \tag{5.15}$$

Equation (5.15) provides a relationship between f_s and ε_s. Another relationship is given by the steel stress–strain curve. By making a reasonable assumption for the values of $\beta_1\beta_3$ and ε_{cu}, for a given value of concrete cylinder stress, f'_c, and a given steel ratio, ρ, it is possible to find pairs of values (ε_s, f_s) which satisfy Eq. (5.15) and also belong to the stress–strain curve for the steel. This has been done graphically in Fig. 5.17 for $f'_c = 3000$ psi, $\beta_1\beta_3 = 0.72$, and $\varepsilon_{cu} = 0.003$. These values correspond to the ACI assumptions.

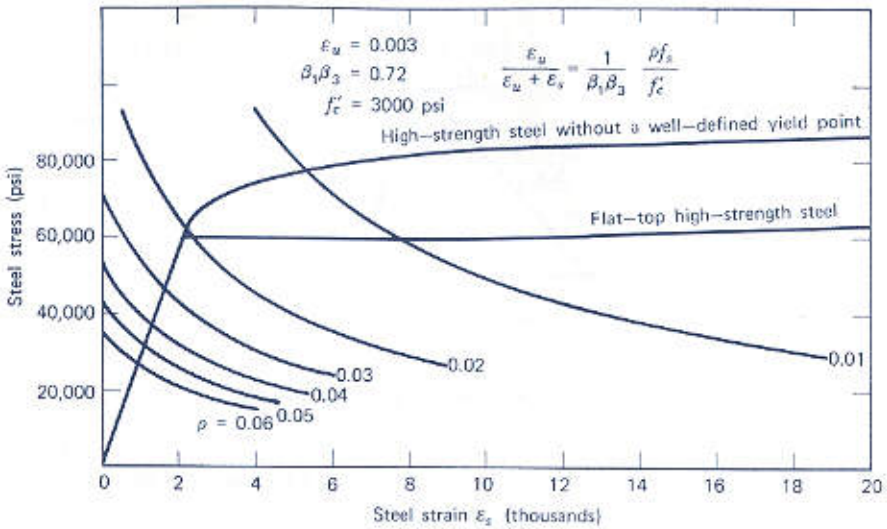

FIGURE 5.17. Graphical procedure for obtaining values of ε_s.

The graphical solution was obtained for steel ratios from 0.01 to 0.06. The intersection of the desired stress–strain curve with the curve corresponding to a given steel percentage defines the value of f_s at maximum moment. With this value, the moment M_s can be obtained directly from Eq. (5.13) using a reasonable value for β_2 (about 0.4) and the same value of $\beta_1\beta_3$ used before.

This type of solution is general and may take into account the strain hardening characteristics and the ductility of the steel.[19] When the steel stress at failure is below f_y the section is over-reinforced. It can be seen from Fig. 5.17 that this occurs only with large steel percentages and steels with high f_y values. For low steel percentages the strain at maximum moment is considerably larger than the yield strain.

A "balanced" condition for beams under pure flexure is obtained when initial yielding in steel ($\varepsilon_s = \varepsilon_y = f_y/E_s$) occurs simultaneously with compressive failure in concrete ($\varepsilon_c = \varepsilon_{cu}$). This corresponds to reinforcement ratio, ρ_b, which for beams without compression reinforcement can be determined from Eq. (5.15), as

$$\rho_b = \left(\beta_1\beta_3\frac{f'_c}{f_y}\right)\left(\frac{\varepsilon_{cu}}{\varepsilon_{cu} + \varepsilon_y}\right)$$

Using $\varepsilon_{cu} = 0.003$, $E_s = 29 \times 10^6$ psi, and $\beta_3 = 0.85$ (corresponding to the ACI recommendations),

$$\rho_b = \frac{0.85\beta_1 f'_c}{f_y}\frac{87{,}000}{87{,}000 + f_y}$$

For rectangular beams with compression reinforcement, the balanced ratio can be computed with the following equation:

$$\rho_b = \bar{\rho}_b + \rho' f'_s/f_y$$

where $\bar{\rho}_b$ is the balanced ratio for a rectangular beam without compression reinforcement, computed with the preceding equation; ρ' is the compression reinforcement ratio; and f'_s is the stress in the compression reinforcement which can be obtained using equation[139]

$$f'_s = 87{,}000\left[1 - \frac{d'}{d}(1 + f_y/87{,}000)\right]$$

For T-beams without compression steel, the following equation can be used to compute the balanced ratio:

$$\rho_b = \frac{b_w}{b}(\bar{\rho}_b + \rho_f)$$

where b_w is the web width, b is the flange width, $\bar{\rho}_b$ is the balanced ratio for a rectangular beam of width b_w, and ρ_f is computed from

$$\rho_f = \frac{0.85 f'_c(b - b_w)h_f}{b_w d f_y}$$

h_f being the flange thickness.

According to the 1971 ACI Building Code, the tension reinforcement ratio must not exceed 75% of the balanced ratio if ductile behavior is to be ensured.

5.2.12 Axial Load and Biaxial Bending

The general design problem for this case consists in finding the maximum value of the load P acting at eccentricities e_x and e_y from the planes of symmetry (Fig. 5.18). This condition is statically equivalent to considering the element under the action of the load, P, acting on the centroid of the overall cross section accompanied by two moments, $M_x = Pe_x$ and $M_y = Pe_y$, acting in the two planes of symmetry.

For an element of known cross section, eccentricities, and reinforcement distribution, it is possible to apply the basic procedure of Section 5.2.6 or the simplifying assumptions of Section 5.2.9. One typical computation using the ACI assumptions is shown in Fig. 5.18 for an assumed position of the neutral axis. The load is obtained by summation of internal forces, and moments are then taken with respect to the x and y axes for the assumed position of the neutral axis. If the eccentricities $e_x = M_x/P$ and $e_y = M_y/P$

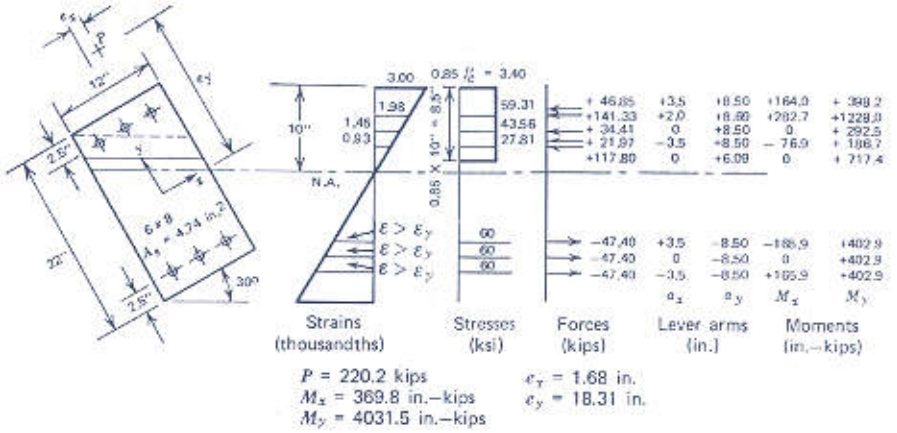

FIGURE 5.18. Example of biaxial bending.

are sufficiently close to the given eccentricities, the problem is solved. If not, another trial is necessary with another position of the neutral axis.

Strength can be satisfactorily predicted by the process just described. However this method is very laborious and therefore impractical for everyday use. The convergence towards the correct solution is slow because the values of e_x and e_y are very sensitive to small changes in the position of the neutral axis. Some graphical design aids based on this approach are available for special cases, such as those included in References 25 and 26.

Simpler approaches have been proposed for routine design. Among these, the one proposed by Bresler[31] reduces the case of biaxial bending and axial load to several applications of simple bending and axial load by using the following interaction equation:

$$\frac{1}{P_u} = \frac{1}{P_x} + \frac{1}{P_y} - \frac{1}{P_0} \tag{5.16}$$

where P_u is the maximum axial load (strength) at eccentricities e_x and e_y, P_x and P_y are the maximum axial loads under compression with uniaxial eccentricities, e_x and e_y respectively, and P_0 is the maximum axial load when $e_x = e_y = 0$.

For symmetrical elements, with normal force acting on any point in the cross section the locus of the maximum values of axial load is an interaction surface such as the one shown in Fig. 5.19. The interaction diagrams obtained previously for uniaxial loading are the intersection of this surface with the $P - M_x$ and $P - M_y$ planes. Equation (5.16) predicts the available test results with a maximum discrepancy of 25%. It is valid for values of P_0/P_u

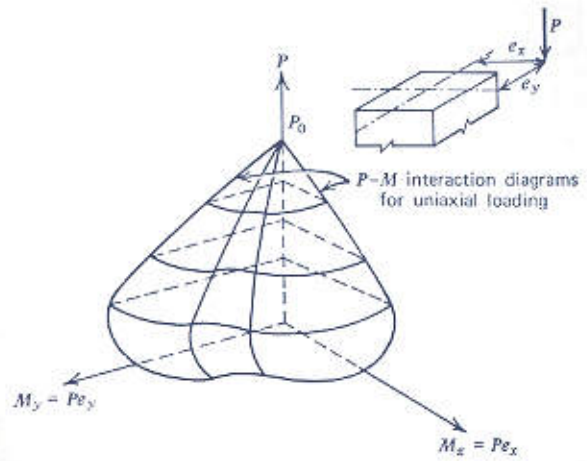

FIGURE 5.19. Interaction surface for biaxial bending.

larger than about 0.15, and is not applicable for axial tension loads. Aas-Jakobsen[32] has proposed another simplified procedure in which for any two eccentricities e_x and e_y, an equivalent eccentricity is taken equal to $\sqrt{e_x^3 + e_y^2}$ from which the load, P_u, is computed as if it were acting about one axis only.

For sections under biaxial flexure the following approximate relationship may be used[15]:

$$\frac{M_x}{M_{ux}} + \frac{M_y}{M_{uy}} \leq 1 \tag{5.17}$$

where M_x and M_y are external moments and M_{ux} and M_{uy} are the flexural strengths in the corresponding planes. This expression may also be used for axially loaded members in which P_0/P_u is less than about 0.15.

5.3 SHEAR

5.3.1 General Remarks

External shear acting on a member produces inclined tensile stresses. In concrete members, these inclined stresses produce inclined cracking due to the low tensile strength of the concrete (Fig. 5.20), so that failures take place at loads that may be much lower than those causing flexural failure. To increase the resistance of concrete members to external shear, it is customary to use transverse reinforcement in the form of vertical or inclined stirrups or ties, or inclined bars (Fig. 5.21).

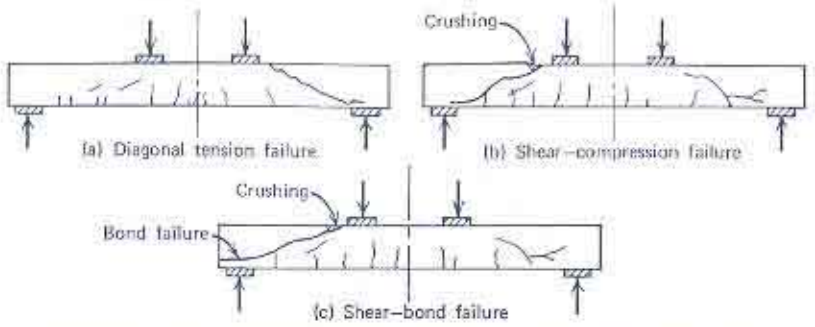

FIGURE 5.20. Principal failure modes in shear of beams without transverse reinforcement.

The magnitude and direction of the inclined tensile stresses as determined by the theory of elasticity are not directly applicable to reinforced concrete members, since the distribution of stresses changes considerably once the tensile strength of the concrete is exceeded and cracking takes place. It is not possible to predict the locations where cracks will appear because the stress field cannot be precisely defined and because there are local variations in the strength of concrete. In spite of the considerable amount of experimental and theoretical research on the behavior of reinforced concrete in shear, it has not yet been possible to establish a general theory for all types of concrete structures. Therefore, present methods of design are largely based on experimental studies of specific problems.[33,34]

5.3.2 Behavior and Modes of Failure of Beams[33–37]

In practice, some kind of transverse reinforcement is usually provided in structural elements. The ACI Code permits omission of such reinforcement only in the case of elements in which shear stresses are very low, such as

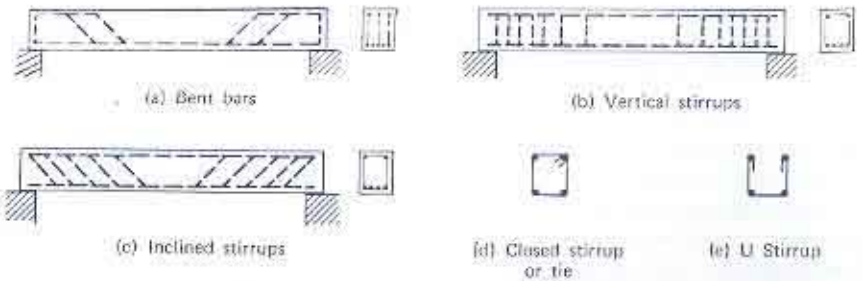

FIGURE 5.21. Types of transverse reinforcement.

slabs, floor joists, and wide shallow beams. Otherwise a specified minimum web reinforcement must be used to prevent sudden failure as a consequence of diagonal cracking. However, it is helpful to discuss the behavior of members without transverse reinforcement because it is closely related to the behavior of members with transverse reinforcement.

Consider a rectangular member *without transverse reinforcement*, subjected to an increasing transverse load. Before the appearance of the first cracks in the tension zone due to flexure, the behavior of the member is essentially elastic. As the load increases, inclined cracks may develop at approximately mid-depth when the tensile principal stresses become greater than the tensile strength of the concrete. These cracks may either appear suddenly in regions where there is no flexural cracking, or, as is often the case, they may have their origin in a flexural crack which bends into the beam in an inclined direction. If an axial compression or tension is also acting, the inclined cracking loads are respectively higher or lower than those corresponding to members without axial loads. Once cracking takes place, the behavior of the member differs considerably from that of members failing in flexure. Inclined cracking can appear suddenly, without warning, and propagate rapidly until the member collapses, as shown in Fig. 5.20(a). Such failures are called diagonal tension failures. On the other hand, inclined cracking may develop gradually, final collapse taking place due to crushing as the available compression zone is progressively reduced. This kind of failure is called a shear–compression failure [Fig. 5.20(b)]. The essential difference between these two types of failures is that, while in a diagonal tension failure inclined cracking is sudden and causes immediate collapse, in a shear–compression failure the member is able to withstand a load greater than that producing inclined cracking. Some authors distinguish still another type of failure, which is usually called a shear–bond failure. This type of failure is sometimes referred to as a shear–tension failure.[36] It is characterized by extensive longitudinal cracking along the tension steel, coinciding with some crushing of the compression zone at the end of the inclined crack, as shown in Fig. 5.20(c). The described modes of failure are undesirable, as they take place abruptly at relatively small deformations, resulting in brittle behavior.

In beams *with transverse reinforcement* it has been observed that transverse reinforcement, whatever the type, does not contribute significantly to the resistance to inclined tension stresses until the first inclined cracks appear approximately at mid-depth of the member. In other words, transverse reinforcement has little influence on the load at which inclined cracking first occurs. But once cracks have appeared, the transverse reinforcement begins to deform gradually as the load increases, until it yields. If the member has only a small amount of transverse reinforcement, failure may take place through one or several of the transverse reinforcement bars. If the amount of

transverse reinforcement is sufficient, the inclined cracking will be of little significance and failure will be due to flexure.

Providing suitable transverse reinforcement in beams that could fail in shear can greatly increase the shear capacity and usually can assure flexural failure under given loading conditions. Indeed, one of the principal objectives in providing web reinforcement is to eliminate shear as a mode of failure. This approach to the design of web reinforcement does not eliminate the shear problem but only changes its form, as the question is then focused on how much web reinforcement is required to prevent shear failure. A rational answer to this question awaits the general theoretical solution of the problem. In the meantime, transverse reinforcement is usually designed for the "excess shear," generally defined as the difference between the design shear load and the acceptable inclined cracking load limit in a beam without transverse reinforcement. Thus, definition of this inclined cracking load is important, not only because of its fundamental significance as an essential stage in the mechanism of potential shear failure, but also as a crucial design parameter for a beam in which shear failure may be prevented.

5.3.3 Inclined Cracking Load

The load causing the first complete inclined crack is called the "inclined cracking load." An inclined crack is usually considered complete when it extends across most of the depth of a member and is beginning to progress along the tension steel. However, the criteria used by different researchers to define inclined cracking are based on visual observation, and consequently the value of this load may vary considerably as it depends on subjective judgement.

In the early studies of reinforced concrete, engineers attempted to solve the problem of shear by using concepts developed for other materials. Many of these early theories are discussed by Hognestad.[38] In 1903, Mörsch[39] examined a series of beam tests and suggested diagonal tension as the cause of inclined cracking, and established the classical expression for the limit cracking shear,

$$V_c = v_c bjd \tag{5.18}$$

in which v_c is defined empirically from test results as a function of f'_c.

This equation is based on the usual assumptions of linear behavior in a cracked reinforced concrete beam, except that shear (and consequently diagonal tension) can exist in the tension zone in the concrete, but that flexural tension stresses can not exist in the same zone. The value of j is calculated in the conventional manner (or it may be closely approximated by $j = 7/8$ for rectangular beams), and then the shearing strength, v_c, corresponding to shear load, V_c, at failure can be calculated from test results using Eq. (5.18).

Values of v_c calculated in this manner exhibit considerable scatter, with a typical range from $0.4f'_c$ to $0.10f'_c$.

In studying the behavior and strength of reinforced concrete beams failing in shear, it is important to distinguish between the loads which cause inclined cracking and those which cause ultimate shear failure. Because inclined cracking is an essential prerequisite to shear failure, it is important to determine the inclined cracking load before it is known whether shear failure or some other type of failure would occur. For the purpose of establishing a design criterion, the cracking load is frequently considered to be equal to the strength of beams without transverse reinforcement.

The manner in which inclined cracks develop and grow and the types of failure that subsequently develop are strongly affected by the relative magnitudes of the shearing stress v and the flexural stress f_x (Fig. 5.22). In a cracked reinforced concrete beam, the stresses may be approximated by

$$v = \zeta_1\left(\frac{V}{bd}\right) \qquad f_x = \zeta_2\left(\frac{M}{bd^2}\right) \tag{5.19}$$

in which ζ_1 and ζ_2 are coefficients which depend on several variables including the geometry of the beam, the type of loading, the amount and arrangement of steel reinforcement, the type of steel, and the bond between concrete and steel.

The *critical cracking load* may be related to the maximum principal stress in an element subjected to shear and flexural tension. Using this approach Viest,[33] in collaboration with others, developed a semirational expression for inclined cracking shear load in reinforced concrete beams,

$$V_c = bd\left[1.9\sqrt{f'_c} + 2500\frac{\rho Vd}{M}\right] \le 3.5f'_c(bd) \tag{5.20}$$

In the case of circular sections the gross area may be substituted for the product bd, and the external diameter for the effective depth, d. ACI Code (1971) recommends that for circular sections the effective depth d in Eq. 5.20 need not be taken less than the distance from the extreme compression fiber

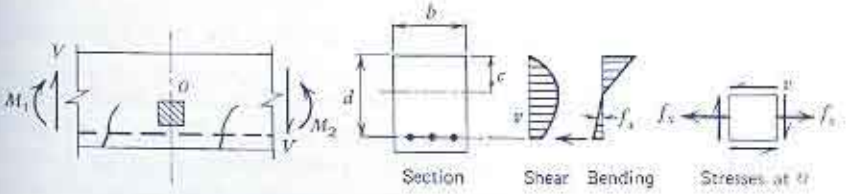

FIGURE 5.22. Stresses in a cracked beam.

TABLE 1.6. Typical Analyses of City Water Supplies (PPM).[12] (Reprinted by permission of the American Society for Testing and Materials, Copyright ASTM.)

	1	2	3	4	5
Silica (SiO_2)	2.4	12.0	10.0	9.4	22.0
Iron (Fe)	0.1	0.0	0.1	0.2	0.1
Calcium (Ca)	5.8	36.0	92.0	96.0	3.0
Magnesium (Mg)	1.4	8.1	34.0	27.0	2.4
Sodium (Na)	1.7	6.5	8.2	183.0	215.0
Potassium (K)	0.7	1.2	1.4	18.0	9.8
Bicarbonate (HCO_3)	14.0	119.0	339.0	334.0	549.0
Sulfate (SO_4)	9.7	22.0	84.0	121.0	11.0
Chloride (Cl)	2.0	13.0	9.6	280.0	22.0
Nitrate (NO_3)	0.5	0.1	13.0	0.2	0.5
Total Dissolved Solids	31.0	165.0	434.0	983.0	564.0

Impurities in the mixing water, when excessive, may adversely affect the setting time, concrete strength, and volume stability, and may also lead to the corrosion of the reinforcement. Generally, water containing less than 2000 ppm (parts per million) of total dissolved solids is satisfactory for concrete. Most municipal water contains less solids than this, as is seen from Table 1.6, wherein typical analyses of public water supplies constituting about 45% of the cities of the United States are given. Any water comparable in chemical analysis to these waters will probably be suitable for mixing concrete. Water of an unknown quality may be used provided it can be shown that it does not have an adverse influence on the setting time, strength development, and durability of concrete. The U.S. Army Corps of Engineers' specifications require that the 7- and 28-day compressive strengths of mortar cubes made with water from a new source should be at least 90% of the reference specimens made with distilled water.

No special tests for determining the quality of mixing water are generally required, but the tolerable concentrations of impurities shown in Table 1.7 may be used as a guideline. Certain cases requiring special attention are now discussed.

Seawater containing up to 35,000 ppm of dissolved salts is generally suitable for unreinforced concrete. Although the initial rate of strength development may not be affected, or may even be slightly enhanced, it has been reported[14] that the use of seawater as mix water in concrete may cause a moderate reduction in ultimate strength. It has also been reported that these concretes have shown efflorescence. In reinforced concrete, the possible corrosive effect of seawater on the reinforcement must be considered.

Water containing algae when used for mixing concrete has the effect of entraining considerable amounts of air in concrete, with an accompanying

TABLE 1.7. Tolerable Concentrations of Impurities in Mixing Water.[13]

Impurity	Maximum Tolerable Concentration
1. Sodium and potassium carbonates and bicarbonates	1,000 ppm
2. Sodium chloride	20,000 ppm
3. Sodium sulfate	10,000 ppm
4. Calcium and magnesium bicarbonates	400 ppm of bicarbonate ion
5. Calcium chloride	2% by weight of cement in plain concrete
6. Iron salts	40,000 ppm
7. Sodium iodate, phosphate arsenate, and borate	500 ppm
8. Sodium sulfide	even 100 ppm warrants testing
9. Hydrochloric and sulfuric acids	10,000 ppm
10. Sodium hydroxide	0.5% by weight of cement if set not affected
11. Salt and suspended particles	2,000 ppm

decrease in strength. In a particular instance,[14] an increase in algae content from 0.09% to 0.23% reduced 10.6% air entrainment with a 50% reduction in compressive strength.

Water containing sugar may not have an adverse affect on concrete strength if the sugar content is less than 500 ppm. A sugar content equivalent to 0.03 to 0.15% by weight of cement usually has a retarding influence on the setting characteristics of concrete, but a little larger concentration of sugar (about 0.2% by weight of cement) may actually make the concrete quick-setting.[4] The exact amount of sugar that will cause these different effects in a concrete varies with the composition of cement, the cement content of concrete, and the temperature of the environment.

Water containing mineral oil may have to be used occasionally for mixing concrete. In small amounts, there may not be any adverse effects, but if the mineral-oil concentration is greater than 2% by weight of cement, this may reduce the concrete strength by more than 20%.

The data given above should serve as broad guidelines only. It is always desirable to determine the limiting values of deleterious impurities by experimentation with actual materials, mix design, and environmental conditions.

1.9 ADMIXTURES

Admixtures are defined as materials other than water, aggregates, and portland cement that are used as ingredients for concrete and are added to the

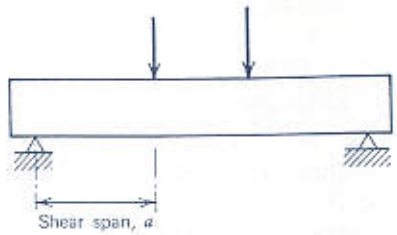

FIGURE 5.23. Definition of shear span.

to the centroid of the longitudinal reinforcement in the opposite half of the member.

The ratio (M/Vd) is often expressed in terms of the ratio of *shear span* $a = (M/V)$ to depth d. For simply supported beams with concentrated loads the *shear span* a is approximated by the distance from the support to the concentrated load where $M = Va$ (Fig. 5.23). For beams with uniformly distributed loads and for continuous beams the *shear span* can be taken as (M/V) except that the value of a should not be taken less than the effective depth, d.

Bresler and Scordelis[40] have suggested that for beams of ordinary proportions a simple and sufficiently close approximation to the cracking load can be obtained using Eq. (5.21):

$$V_c = 2bd\sqrt{f'_c} \tag{5.21}$$

The CEB has proposed a similar expression.

From the above discussion it is seen that the main variables affecting the cracking shear load are the following:

1. *Tensile strength of the concrete.* Cracking loads increase with increasing tensile strength of the concrete and decrease when tensile strength is low. Equation (5.20) defining the cracking load is based on the assumption that splitting cylinder tensile strength, f_{ct} of a given concrete is not less than $6.7\sqrt{f'_c}$. For lightweight-aggregate concrete the tensile strength may fall below this value,[67] and therefore special provisions must be made for evaluating the cracking load. The ACI Building Code recommends that $(f_{ct}/6.7)$ be substituted for $\sqrt{f'_c}$ in Eqs. (5.20) and (5.21) provided that this value is not greater than $\sqrt{f'_c}$.

2. *Ratio of longitudinal steel.* Tests have shown that the inclined cracking load increases with the ratio of longitudinal steel, ρ. This may be partly explained by the fact that flexural cracking, which contributes to the development of inclined cracks, decreases with increasing ratios of longitudinal steel. The longitudinal steel also influences the inclined cracking load through

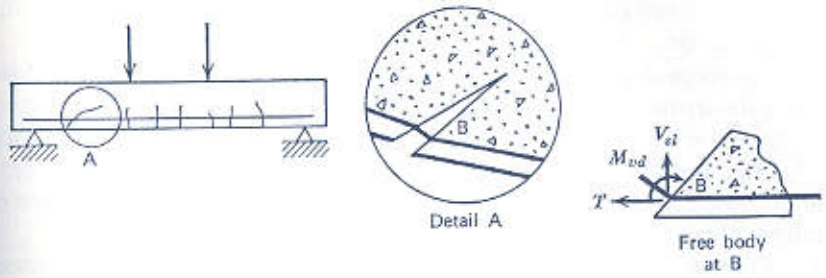

FIGURE 5.24. Dowel effect.

the dowel effect: when cracking takes place within the shear zone of a reinforced concrete beam the longitudinal steel undergoes relative displacement between the two sides of a crack, as shown in Fig. 5.24. As a result of this displacement a shear component V_{si} usually called the dowel force, is generated in the longitudinal steel and provides part of the resistance to the applied shear. Some experimental results show that the magnitude of V_{si} is approximately 5 to 15% of the inclined cracking load.

3. *Shear–span/depth ratio* (a/d). The inclined cracking load decreases as the $(a/d) = (M/Vd)$ ratio increases, since flexural cracking tends to increase with this ratio. The a/d ratio also influences the type of failure. If the value of a/d is less than 2.5 or 3, failure is of the shear–compression type; if greater, failure may be caused by diagonal tension. The exact critical value at which the transition between the two types of failure occurs depends on a number of variables, and it has not been possible to establish an analytic method for determining it. For values of (a/d) greater than about 6 or 7 flexural failure usually controls the capacity.

4. *Cutoff of longitudinal bars.* It has been found that if a certain number of longitudinal tension bars are cut off, in a part of the member where there is shear, the inclined cracking load is less than when the bars are continuous. Significant stress concentrations are originated at cutoff points, which cause flexural cracking. This in turn increases the shearing stresses in this part of the beam and brings about the premature development of inclined cracking as an extension of the flexural cracks.[41] The reduction in shear capacity resulting from cutting off longitudinal bars in the tension zone must be accounted for. The ACI Code recommends the following alternative provisions:

(a) the shear at the cutoff point should not exceed 2/3 the capacity normally permitted, including the shear strength of web reinforcement; or

(b) for bars not exceeding No. 11 in size, the continuing longitudinal reinforcement should provide double the area required for flexure at the

cutoff point and the shear should not exceed 3/4 of the capacity normally permitted; or

(c) stirrups in excess of that required for shear and torsion are provided along the terminated bar a distance (each way) from the cutoff point equal to 3/4 the effective depth of the member. The excess stirrups shall provide $(A_v/bs)f_y$ not less than 60 psi. The resulting spacing, s, shall not exceed $d/8\beta_b$, where β_b is the ratio of the area of bars cut off to the total area of longitudinal bars at the section.

5. *Effect of member size.* There is some evidence that strength in shear is inversely proportional to the size of a member.[42] In a series of tests of beams with equal reinforcement ratios, a/d ratios and concrete strengths, but with varying depth, it was found that resistance to diagonal tension was reduced by more than 50% when increasing the depth from 6 to 48 in. However, for most beams in typical structures the size effect may be disregarded, as other uncertainties in the calculated value of shear capacity are considerably greater than the size effect.

6. *Axial load.* The expressions for the flexure–shear cracking load described above apply to reinforced concrete beams subjected only to shear and flexure. As noted previously, cracking load and shear capacity are greatly reduced by tension, and, conversely, they are increased by compression. Approximate expressions for cracking shear load in the presence of axial force have been developed.[33] Two alternative approaches have been proposed.

One is based on the assumption that the extent of cracking is related to the moment of the tension force in longitudinal steel reinforcement taken with respect to the compression stress resultant (Fig. 5.25). In the absence of axial force N, this moment is $T \cdot z = M$, which is the same as the moment at the section caused by the external forces. In the presence of axial force, N, assuming compression to be positive, the moment $T \cdot z$ is (Fig. 5.25)

$$T \cdot z = M - N(0.5h - d + z) = M_m$$

The effect of axial force, N, on the cracking load, according to this point of view can be taken into account by using in Eq. (5.20) this modified moment, M_m, in lieu of the external moment, M.

The second approach to the problem is based on the consideration of the change in the effective area over which shear stresses act. In the presence of an axial force, N, assuming compression is positive, the change in effective shear area may be approximated by $N/2000$. Then, the cracking load, V_c, is approximately

$$V_c = 2\sqrt{f'_c}\left[1 + 0.005\frac{N}{A_g}\right]bd \qquad (5.22)$$

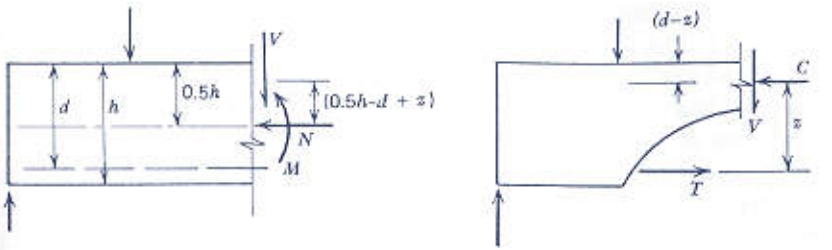

FIGURE 5.25. Effect of axial load—modified moment.

However, in any case, V_c should not exceed the value

$$V_c \leq 3.5\sqrt{f'_c}\left(\sqrt{1 + 0.002\frac{N}{A_g}}\right)bd \qquad (5.23)$$

Both methods are entirely empirical in nature and further information regarding shear capacity of members simultaneously subjected to flexure, axial load, and shear is required for development of a more rational design procedure.

5.3.4 Shear Strength

Shear strength, V, in reinforced concrete beams *without web reinforcement* has three components (Fig. 5.26):

$$V = (V_{cc} + V_{ci}) + V_{st} \qquad (5.24)$$

where V_{cc} is the shear component of the stress resultant in the uncracked concrete (compression) zone, V_{ci} is the shear component of the friction and aggregate interlock in the cracked concrete region, and V_{st} is the shear component (dowel force) of the stress resultant in the longitudinal steel reinforcement.

The dowel force V_{st} was usually neglected in the early studies of shear resistance.[38] Also no distinction was made between V_{cc} and V_{ci}, so that the

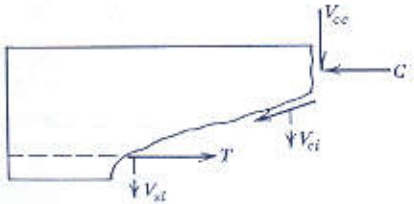

FIGURE 5.26. Components of shear strength—without web reinforcement.

contribution of concrete to shear strength was expressed by a single term $V_c = (V_{ce} + V_{cl})$. Thus the shear capacity of a beam without web reinforcement (assuming $V_{sl} = 0$) was taken as the critical inclined cracking load V_c defined by Eqs. (5.20) or (5.21).

The shear strength of a reinforced concrete beam *with transverse reinforcement* can be defined in terms of the shear carried by concrete, longitudinal steel, and transverse steel reinforcement. The presence of transverse reinforcement modifies the nature and extent of inclined cracking and therefore influences the amount of shear carried by the concrete (V_c) and the longitudinal steel (V_{sl}). However, as there is no general theory which would permit precise evaluation of these quantities, the shear capacity of a beam with transverse reinforcement is usually obtained by adding the contribution of the web reinforcement to the capacity (inclined cracking load) of a similar beam without web reinforcement.[40] Neglecting dowel action,

$$V = V_c + V_s = V_c + \sum_n f_{usi} A_{vi} \sin \alpha_i \tag{5.25}$$

where V_c is defined by Eq. (5.20) [or approximately by Eq. (5.21)], V_s may be expressed as a function of the number of reinforcing bars or stirrups, n, crossing the diagonal crack (Fig. 5.27), f_{usi} is the actual tensile stress in the ith bar or stirrup having cross-sectional area A_{vi} and inclined to the horizontal at an angle α_i. Thus, if the stress f_{usi} in the stirrups is variable and expressed by $\beta_i f_y$, where β_i is a variable coefficient depending on the location of the ith stirrup with respect to the crack apex, and if the cross-sectional area A_{vi} of the stirrups is a constant equal to A_v, then

$$V_s = f_y A_v \sum_n \beta_i \tag{5.26}$$

The number of stirrups n crossing the crack is equal to the horizontal projection of the crack λd divided by stirrup spacing s (Fig. 5.27), i.e., $n = \lambda d/s$.

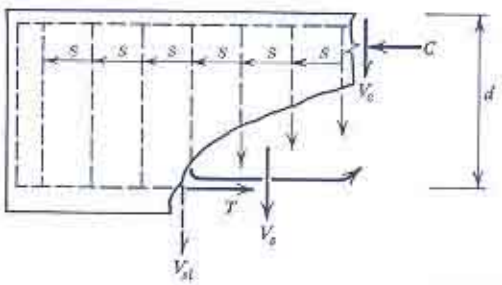

FIGURE 5.27. Components of shear strength—with web reinforcement.

The usual approximation for V_s is to assume that $\lambda = 1$ and all values of β_i are equal to unity as well. Then

$$V_s = f_y A_v \frac{d}{s} \tag{5.27}$$

and taking V_c as defined by Eq. (5.21), the total shear capacity V is

$$V = V_c + V_s = 2\sqrt{f'_c}\, bd + f_y A_v \frac{d}{s} = (2\sqrt{f'_c} + \rho_{vs} f_y) bd \tag{5.28}$$

where $\rho_{vs} = A_v/bs$ is the web reinforcement ratio.

Web reinforcement should be spaced along the axis of the member in such a way that any potential inclined crack that may appear is crossed by one or more transverse bars, depending on the intensity of shear stress $v = V/bd$.

The above discussion of the behavior of beams refers to simply supported rectangular beams subjected to concentrated loads. However, results of tests have shown that the conclusions derived from tests of beams with concentrated loads and the equations for design presented later are also applicable to beams with uniform loads if the shear span is defined as $a = M/V$.

There is much less information available on the behavior and strength of members with nonrectangular section than on those with rectangular section. Some tests have been carried out on members with a circular cross section with the longitudinal steel distributed around the perimeter.[48] The behavior of these members was similar to that of rectangular members, with the exception that the inclined cracks tended to develop in a more gradual manner because of the presence of steel around the entire perimeter. In testing members with an I section an additional type of failure may be identified which consists in crushing due to compressive stresses in a direction approximately parallel to the direction of the inclined cracks. This type of failure takes place only when the web is relatively thin in comparison with the width of the compression zone. Otherwise the behavior of I beams is similar to that of rectangular members.

Tests of continuous beams[44–46] have shown that the behavior and modes of failure of these beams are similar to those observed in simple beams, so that the same design-procedures may be used. However, the meaning of the term M/Vd is not well defined once the inclined cracks have developed. In view of this, Ferguson[21] has proposed that only Eq. 5.21 be used for continuous beams.

Shear strength is reduced by alternating loads producing flexural deformations beyond yielding of the reinforcement.[47] This reduction is attributed to cracking in the effective compression zone in previous load cycles, deterioration of the interlocking resistance of the aggregates and deterioration of bond in stirrups and flexural reinforcement. The Structural Engineers Association of California[49] has proposed neglecting the shear resistance of the concrete in

practice are composed of calcareous materials. Calcined gypsum products, such as plaster of paris, $CaSO_4 \cdot \frac{1}{2}H_2O$, and hydrated lime, $Ca(OH)_2$, form the major *nonhydraulic cements*. Upon aeration, hydrated lime cements develop weak bonding characteristics through the formation of $CaCO_3$, while plaster of paris cements harden through the formation of intertwined crystals of $CaSO_4 \cdot 2H_2O$. The carbonates and the sulfates of the nonhydraulic cements, being slowly soluble in water, impose limitations on their application. On the other hand, cements composed essentially of reactive calcium silicates or calcium aluminates yield relatively insoluble hydration products, and are therefore termed *hydraulic cements*. Hydraulic cements find wide application in concrete construction and are discussed below in detail.

1.3 CALCIUM SILICATE CEMENTS

Cements of this class are represented by portland cement and its modifications. *Portland cement* is defined in ASTM C150 as a hydraulic cement produced by pulverizing clinker consisting essentially of hydraulic calcium silicates, usually containing one or more of the forms of calcium sulfate as an interground addition.* The use of processing additives such as grinding aids is permitted at the option of the cement manufacturer provided they meet the requirements of ASTM C465.

The usual *cement manufacturing process* consists of pulverizing together calcareous and argillaceous or other silica-, alumina-, and iron-bearing materials†; heat treating the raw-mix to clinkering temperature (2600–2800°F); and grinding the resultant clinkers with 4–6% gypsum in tube mills that are cooled externally or internally with water. If adequate cooling during cement grinding is not provided, the gypsum might decompose to form hemihydrate which is usually responsible for the *false set* or premature stiffening phenomenon in such cements.

1.3.1 Composition of Portland Cement

Abbreviations used by cement chemists for denoting various oxides are as follows: $C = CaO$; $S = SiO_2$; $A = Al_2O_3$; $F = Fe_2O_3$; $\bar{S} = SO_3$; $H = H_2O$. The principal calcareous compounds formed during heat treatment of a portland-cement raw-mix are C_3S, C_2S, C_3A, and C_4AF.

* Materials definitions, specifications, and testing procedures meeting with the requirements of *American Society for Testing and Materials* are under continuous revision. The readers are advised to refer to the latest editions of the relevant ASTM publications to determine any changes in the requirements from those given in this text.

† Examples of calcareous raw materials are limestone and chalk; of argillaceous materials are shales, clays and laterite; of siliceous materials are quartzite and sand; of aluminous material are bauxites; and of iron-oxide bearing materials are iron ore and pyrites.

Since the techniques and the instrumentation for precise quantitative determination of compounds in portland cement are complex, the ASTM requirements of compound composition of cement are based on mathematical calculations from the oxide analysis of cement. The following mathematical *equations developed by Bogue*[2] are used to compute the compound composition:

$$C_3S = 4.07C - 7.60S - 6.72A - 1.43F - 2.85\bar{S}$$
$$C_2S = 2.87S - 0.754\,C_3S$$
$$C_3A = 2.65A - 1.69F$$
$$C_4AF = 3.04F$$

where all the oxides and compounds in the above equations are on weight percentage basis.

The two calcium silicates, C_3S and C_2S, constituting about 75% of the compounds in portland cement, are the principal components responsible for its cementitious characteristic. The presence of aluminate, ferrite, and other impurities such as magnesia, titania, alkalis, sulfates, etc., provides the necessary fluxing action which helps formation of C_3S at much lower temperatures in the cement kiln than theoretically predicted.

The compounds in portland-cement clinker do not possess exactly the same chemical composition as denoted by the chemical notations. They invariably contain in the crystal structure small amounts of other oxides which significantly modify their hydration characteristics. The impure C_3S in commercial portland cements, called *alite phase*, contains small quantities of alumina and magnesia, while the impure C_2S, generally occurring as beta-modification, called *belite phase*, may contain alkaline impurities (K_2O) in addition to magnesia and alumina.[3]

The constituent phases of portland cement are thermodynamically unstable, hence they tend to react with water to form stable hydration products. Since the nature of the hydration products and the rates of reactivity with water are not the same for different phases, an intimate knowledge of hydration characteristics of the individual phases provides the basis for designing several types of portland cements.

The aluminate phase, C_3A, is the most reactive phase in portland cements. Upon addition of water to cement, C_3A tends to hydrate immediately with the evolution of a relatively large amount of heat. Subsequently, there is formation of calcium aluminate hydrate crystals which cause hardening of the cement paste. This phenomenon, called *quick set*, is undesirable because it interferes with placement and finishing of concrete. The *primary function of gypsum*, which is interground with portland-cement clinker, is to retard the reactivity of C_3A by virtue of the fact that gypsum is readily soluble in water. When sulfate is present in the solution, the solubility of C_3A is significantly depressed.

members subjected to load reversals, particularly when the axial compression load P is less than $0.12f'_c A_g$.

5.3.5 Shear Failure Mechanisms*

In the search for a general understanding of the shear failure mechanisms and for simple realistic models which would provide a basis for determining the failure loads or strengths, two broad types of analysis have been followed: (1) arch, truss, and frame analogies, and (2) limit analysis mechanisms. Because concrete beams without web reinforcement frequently fail in shear at the inclined cracking load, a number of authors have presented strength analyses which are actually attempts to predict the inclined cracking load.[49,50]

Tooth Mechanism of Inclined Cracking. For a/d ratios greater than about 3 to 4, inclined cracks develop in the shear span as an extension of a flexural crack which progressively bends over until the inclined crack is formed (Fig. 5.28). A number of authors have idealized this mechanism as the breaking off of a concrete "tooth" between two flexural cracks. Kani[51] and Moe[52] have proposed inclined cracking theories based on this type of behavior.

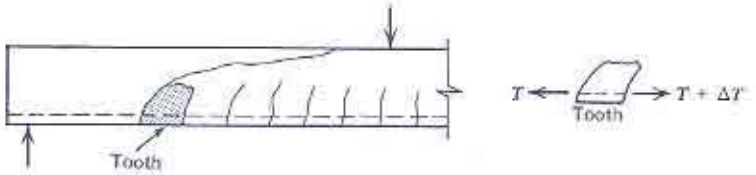

FIGURE 5.28. Tooth mechanism of inclined cracking and diagonal tension failure.

Both Kani and Moe considered an isolated tooth acted on by a force ΔT, which represented the difference in steel tension forces at the two sides of the tooth. This tooth was assumed to fail when the tensile stress at the root of the tooth equalled the tensile strength of the concrete. In computing the tensile force on each tooth, the steel force was assumed to vary linearly from a maximum at the load point to zero at the supports. Moe considered the longest, and thus the weakest, "tooth" and assumed a certain amount of shear transfer across the crack resulting from aggregate interlock and doweling. Kani considered the average tooth rather than the longest and weakest one and neglected any shear transfer across the crack caused either by aggregate interlock or doweling.

More recently, Walters and MacGregor[19] have attempted to predict the inclined cracking load using an iterative analysis, which included the effects of tooth stresses in a computation of the principal tensile stresses in

* The material in Section 5.3.5 has been reproduced almost literally from Reference 37 with the permission of the authors.

elements at the head of flexural cracks in a reinforced concrete beam. This analysis was based on nonlinear stress–strain curves for concrete in tension and compression. The deflections of each of the teeth were determined, and the tooth stresses included allowances for the effects of aggregate interlock and dowel action between the teeth. This analysis provided a fairly good prediction of the crack pattern and cracking load, although in each case the analysis indicated failure just before the major inclined crack, which caused failure in the real beam, was predicted.

Lorentsen's Analysis. Lorentsen[50] has presented an analysis which defined three components of shear strength: (1) the shear carried by dowel action of longitudinal reinforcement, (2) the shear in the concrete compression zone carried by a "tooth" or "lamella," and (3) the shear carried by the vertical component of the inclined thrust in the arch rib. Prior to inclined cracking, shear is assumed to be carried partly by tied arch and partly by beam action. The shear failure is considered to be initiated as a result of bond failure between reinforcement and concrete in the transition zone between the cracked and uncracked parts of the beam. Local bond failure causes the outermost "tooth" to break off, forming the inclined crack and reducing the shear component carried by the tooth. It is interesting to note that Lorentsen's studies suggested that the shear is essentially independent of crack spacing, which was contrary to the assumption made by Kani and Moe.

The value of the vertical component of the compression force was much harder to determine because the load is carried partly by beam and partly by tied arch action. Because Lorentsen's expression for V_c is based on limited experimental data, it cannot be considered as generally valid in its present form.

Arch Analogies. Arch, truss, and frame models, representing behavior of reinforced concrete beams subjected to flexure and shear, were recognized in the earliest investigations. Observation of crack patterns in different beams suggested such analogies, the aims of which were to reduce the complexity and indeterminancy of the actual cracked beams.

Partly because the geometry of the arch rib elements is not precisely defined, and partly because stress analysis of a system of statically indeterminate arches is relatively complicated, this analogy has been used largely as a model to describe beam behavior, rather than as a precise analytical tool.

For example, in a beam cracked as shown in Fig. 5.29 an element between adjacent cracks can be isolated and considered as a "tied-arch free body." Here, neglecting dowel action in the longitudinal reinforcement, the transverse shear is carried by stress components along the arbitrary arch boundaries in the uncracked parts of the beam.

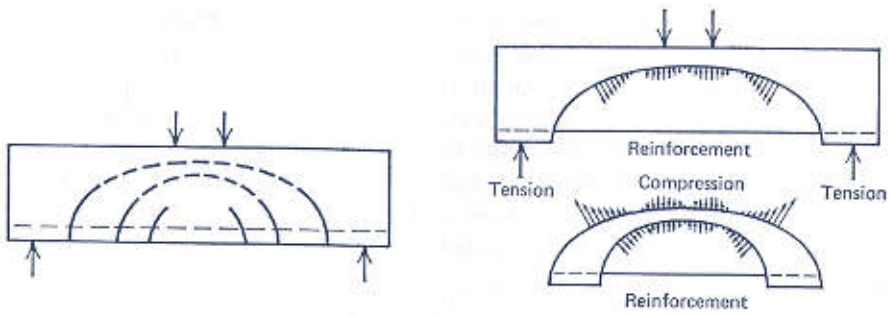

FIGURE 5.29. Arch analogy of reinforced concrete beam (without transverse reinforcement).[51]

The arch ribs are capable of supporting transverse load only as long as they act essentially in compression, not in bending. Without transverse reinforcement, only short deep beams can develop tied-arch action. As the length of the span increases, bending develops in the rib and failure occurs. With transverse reinforcement (Fig. 5.30), it is possible to develop arch action in longer spans, and substantial shear loads can be transmitted essentially by compression forces in the arch ribs. A recent elaboration by Kani[53] of the arch analogies clearly describes this conceptual model representation of the real beam.

Truss Analogies. For beams with transverse reinforcement, a more familiar and generally more useful model for the designer is based on an analogous truss. In this model the beam is replaced by a pin-connected, statically determinate truss in which the concrete compression zone is represented by the compression chord, the tensile steel reinforcement is represented by the tension chord, the transverse reinforcement corresponds to the tension web members, and the concrete between inclined cracks corresponds to compression web members [Fig. 5.31(a)]. All the external loads are assumed to be acting only at the nodes. Thus the analysis of this analogous truss is greatly simplified.

In a classical truss model[54] the chords are assumed to be parallel to each other. As neither chord can transmit any transverse load, all shear must be

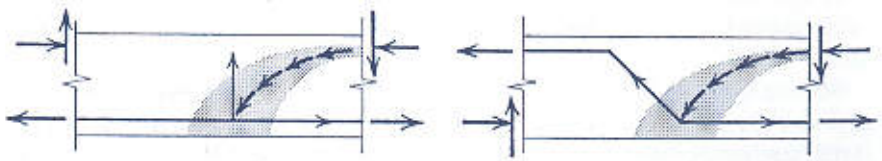

FIGURE 5.30. Arch analogy of reinforced concrete beam (with transverse reinforcement).[51]

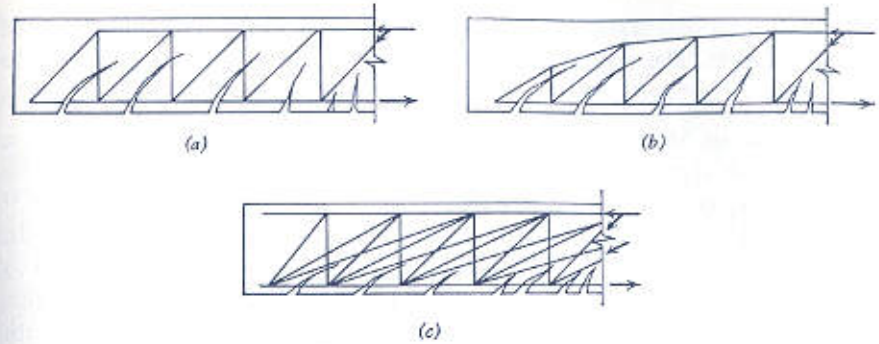

FIGURE 5.31. Truss analogy.

carried by tension in the transverse reinforcement. To account for the experimentally observed shear capacity of the concrete in a beam with or without web reinforcement, the compression chord of the truss may be assumed curved [Fig. 5.31(b)]. This modified truss approaches the arch analogy described in the preceding section.

Partly to account for the shear capacity of the concrete, and partly to account for the complex stress field in the real reinforced concrete beam, the statically indeterminate truss system shown in Fig. 5.31(c) has been proposed by Baker and Ahmad.[55]

Frame Analogy. Rüsch[56] has proposed a frame analogy consisting of curvilinear concrete elements, which more nearly approximate the geometry of the concrete segments in a cracked beam, and linear steel elements, which represent longitudinal and transverse reinforcement (Fig. 5.32). The steel reinforcement, wherever it crosses a crack, is capable of resisting both axial and transverse forces, but not bending. The nodal points are considered rigid joints, and the stiffness of the frame elements is varied along their length to approximate the stiffness of the beam segments.

It is evident that none of the above analogies provides a sufficiently accurate and, at the same time, sufficiently simple solution. Even the most complex

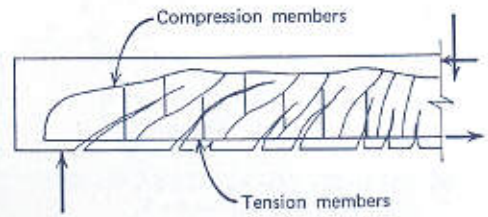

FIGURE 5.32. Frame analogy.[56]

of the models deviates considerably from the three-dimensional behavior of the real beam. The simplest model, the classical truss analogy, is simple to use but does not give results which are in general agreement with test results.

Limit Analysis Mechanisms. A simple rigid–plastic mechanism, based on a limit analysis approach, has been proposed as a model for reinforced concrete beams subjected to combined flexure and shear by Gvozdev and Borishansky.[57] In a monograph, based on extensive experimental studies, they proposed an equilibrium solution of such a model (Fig. 5.33). This solution was limited to cases wherein either the yield strength or the bond anchorage capacity of both longitudinal and transverse steel reinforcement was exceeded, and failure followed a relative rotation of the two segments. In this model only one degree of freedom (relative rotation) was considered, and dowel-forces in transverse and longitudinal reinforcement were neglected. For assumed inclinations of the cracks and for given empirical values of shear capacity of the concrete in the compression zone (the "plastic hinge") different values for "limit" or "collapse" load can be determined.

Zwoyer and Siess[58] and Sozen, *et al.*[59] have considered a shear failure to be a special case of a flexural failure in which the steel strains were less than those corresponding to the plane section hypothesis. In Sozen's studies the strains were assumed to be linearly distributed until inclined cracking occurred. After inclined cracks had developed, the additional steel strains were generally computed to be less than 30% of the corresponding flexural steel strains. Failure was assumed to occur when a limiting compressive strain was reached

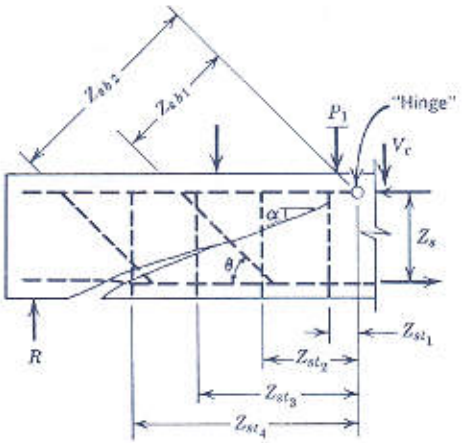

$$M_r \leqq f_s \cdot A_s \cdot Z_s + \Sigma f_{sb} \cdot A_{sb} \cdot Z_{sb} + \Sigma f_{st} \cdot A_{st} \cdot Z_{st}$$
$$V_r \leqq \Sigma f_{st} \cdot A_{st} + \Sigma f_{sb} \cdot A_{sb} \cdot \sin\theta + V_c$$

FIGURE 5.33. Plastic mechanism.[57]

at the top of the beam. Similar analyses have also been derived by Moody, *et al.*[60] None of these analyses included the effect of shearing stresses on the strength of the compression block.

Bresler and Pister,[61] Walther,[62] Paez,[63] and Guralnick[64] have used failure criteria for concrete subjected to combined shear and compression and an assumed collapse mechanism to define the shear capacity V_c of concrete in the compression zone. In addition to using failure criteria, Walther proposed a compatibility equation with approximations for evaluating deformations in the compression zone in concrete and in the tension zone, which included the effect of local slip between reinforcing steel and concrete. The principal limitations of Walther's model lie in the approximations suggested for evaluating deformations in the compression and tension zones, and in neglecting dowel action of the reinforcing steel.

A more sophisticated rigid–elasto–plastic model has been proposed by Moore.[65] The model consists of three rigid bodies joined by a hinge, as shown in Fig. 5.34. The rigid bodies are further connected by an elasto–plastic spring representing the compression zone, by elasto–plastic links representing the longitudinal and transverse steel reinforcement, and by elastic "threads" representing the concrete in tension. This model has two degrees of freedom representing the rotations between each pair of adjacent rigid elements, and the solution is obtained using the minimum energy principle together with a yield or failure criterion for the connecting elements. As failure in one element does not necessarily cause failure of the entire system, the energy expressions must be evaluated with due regard to the consecutive failures in the weaker links of the system.

None of the shear failure theories or analogies which are currently used is sufficiently general to consider all the possible failure modes. As a result, it is difficult to generalize about the nature of shear failures.

Finite Element Approach. Bresler and MacGregor[87] have suggested the application of the finite element method to determine the stress and strain fields and the propagation of inclined cracks in reinforced concrete beams. The analysis must be carried out using successive load increments and taking

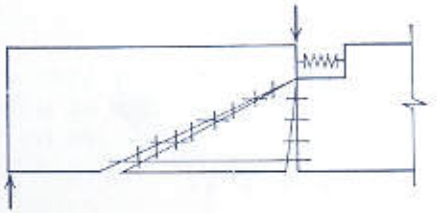

FIGURE 5.34. Rigid-elasto-plastic mechanism.[65]

into account the state of cracking in each increment. Failure occurs when a stable crack pattern can no longer be achieved. When this approach is used, the extent of cracking and the deflections of a beam under working conditions (serviceability) as well as its load capacity and mode of failure (strength) can be predicted.

The successful application of this approach requires a knowledge of the deformability and fracture characteristics of concrete and steel and the formulation of the appropriate constitutive equations for composite action, for example, an adequate bond–slip law. Although the present empirical knowledge of concrete and steel considered independently is sufficient for this purpose, composite action of concrete and steel has not yet been sufficiently studied, and breakdown in the composite action of concrete and steel cannot be adequately predicted. On the other hand, the determination of stress and strain fields compatible with crack patterns requires a detailed study of the dowel effect, especially concerning the development and propagation of secondary cracks at the level of the reinforcement, which always precede the failure of the beam. These secondary cracks are of paramount importance in the development of inclined cracks. More analytical and experimental research in these aspects may lead eventually to a rational solution of the problem of shear in reinforced concrete beams.[66]

5.3.6 Flat Slabs and Footings

5.3.6.1 Behavior and Modes of Failure

Numerous tests[143] have been carried out to investigate the transmission through shear of load from a flat plate to a column or from a column to a footing. Usually the specimens are supported along the perimeter, and the concentrated load is applied on a square surface (Fig. 5.35). A few tests have been made in which the entire surface is supported on a series of springs simulating the effect of the soil reaction in footings.[68] These types of specimens do not provide for the continuity existing in actual structures.[143] Figure 5.36 represents a typical load-deflection curve at the center of

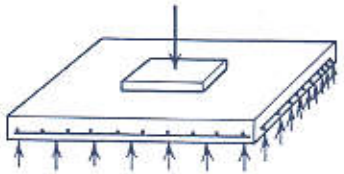

FIGURE 5.35. Test specimen simulating a footing or a portion of a flat plate.

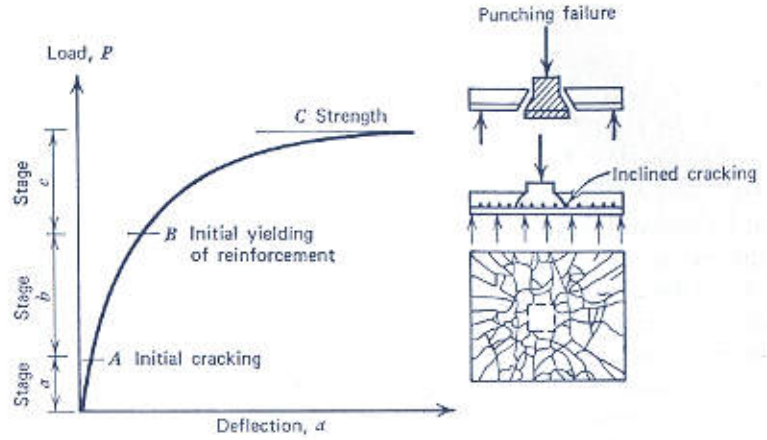

FIGURE 5.36. Load-deflection curve of the test specimen shown in Fig. 5.35.

a slab specimen such as the one shown in Fig. 5.35. If the slab is sufficiently ductile, the following three stages may be identified:

1. From the origin to A, the behavior is approximately linear, until the first cracks appear on the tension face of the slab.
2. Between A and B, cracking develops throughout the slab. At point B, yielding of the longitudinal reinforcement begins.
3. Strength (point C) is attained at the end of this stage, and final collapse takes place by punching of the column through the slab, the failure surface being in the shape of a pyramid or truncated cone.

Depending on the ratio between the span and the depth of the slab, the ratio between the area of the slab and the area on which the load is applied, and the amount of flexural steel, punching failure can occur either before or after yielding of the longitudinal steel. If the steel does not yield, only stages OA and AB develop.

The nominal shear stress (acting load divided by the product of the effective depth and the width of the critical section) corresponding to the strength of a slab of this type is usually greater than that for beams. This is mainly due to the effect of the width of the element, to the fact that the concrete surrounding the loaded area is subjected to normal stresses in two directions, which provide a lateral confining effect, to the location of the inclined crack and to greater dowel forces.

5.3.6.2 Computation of Strength

The method of computing the shear strength of footings, flat plates, and flat

slabs given in the 1971 ACI Code is mainly based on the recommendations of ACI–ASCE Committee 326 and on Moe's[68] and Elstner's[69] studies. The method is based on the assumption that the critical section in shear is located around the periphery of the loaded area, at a distance of half the effective depth of the slab. The reasoning behind this recommendation is presented in Reference 33. The maximum nominal shear stress in the critical section must not be greater than $4\sqrt{f'_c}$ (psi). This value is considerably greater than the value permitted in beams, due to the confining effect mentioned above. The ratio of flexural reinforcement has a certain influence on the shear strength, but it is neglected in the ACI recommendation. Moe[68] and Nylander, Kinnunen, and Andersson[70] have proposed methods of taking this contribution into account. The ACI method is conservative in most cases[143] where the loaded areas are approximately square or rectangular in shape, but the strength decreases with increased rectangularity of the loaded area. Also, it has not been demonstrated that enough ductility[143] is developed by this method.

The strength of slabs and footings may be governed by their behavior as wide beams with a potential diagonal crack extending in a plane across the entire width. Therefore, in design both types of behavior should be considered.

5.3.6.3 Influence of Holes

Tests carried out by various investigators[71] have shown that the reduction in shear strength due to the presence of holes in the neighborhood of a column may be taken into account by subtracting from the perimeter of the critical section the distance intercepted by the two tangents to the borders of the hole drawn from the center of the loaded area. This reduction must be considered only when the distance from the hole to the support is less than ten times the effective depth. Small horizontal ducts in the mid-plane of the slab do not reduce the strength, provided they are located at least two slab thicknesses away from either the column face or the end of shear reinforcement.[144]

5.3.6.4 Shear Reinforcement in Slabs and Footings

Several types of reinforcement have been proposed to increase the strength in punching shear of slabs and footings. One of the first approaches consisted in placing spearhead reinforcement or bent bars in the area of potential cracking. Performance of these types of reinforcement is not entirely satisfactory mainly because anchorage is inadequate.

Another type of shear reinforcement developed recently as a result of experimental research done at the PCA laboratories[72] is shown in Fig. 5.37.

It consists of channel or I shapes of structural steel welded at right angles and continuous to the column section. The main effect of such shearheads is to push out the critical section, increasing its perimeter. This is illustrated by Fig. 5.38. The following procedure may be used for the design of shearheads of this type. The arms of the shearhead are detailed so that their flexural capacity is enough to insure that the shear capacity of the slab is reached before the flexural capacity of the shearhead is exceeded. The nominal shear stress along a fictitious critical section determined as shown in Fig. 5.38(c) and (d) should be less than $4\sqrt{f'_c}$. The designer is permitted to reduce the negative

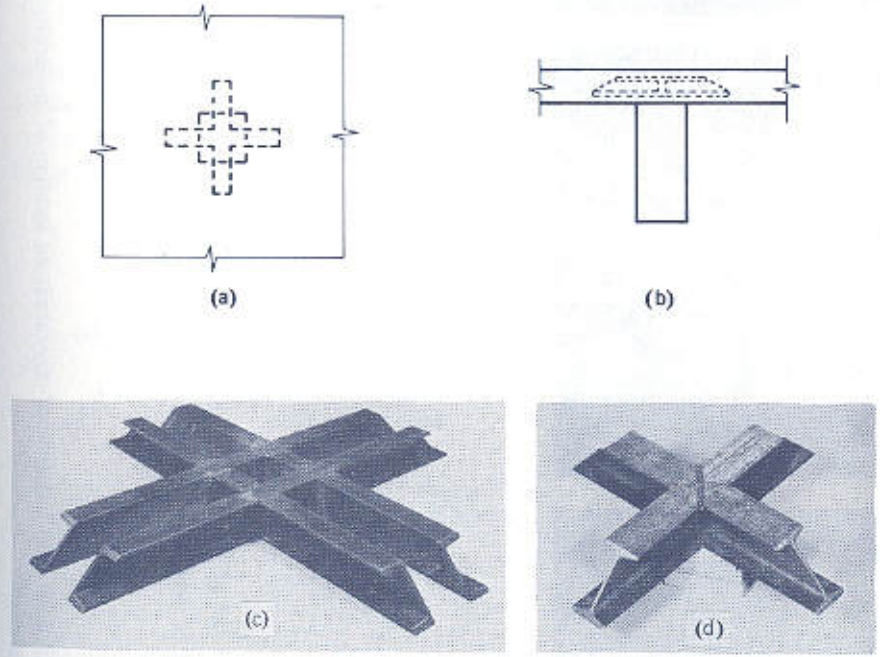

FIGURE 5.37. Shear reinforcement in slabs.

slab reinforcement in proportion to the contribution of the shearhead to flexural strength. The development of this type of reinforcement is given in Reference 72 in which a design example is also included.

A third alternative, which seems more promising from a technical and a practical point of view, consists of integral beams with stirrups, as shown in Fig. 5.39. The stirrups must be anchored following the rules for anchorage of

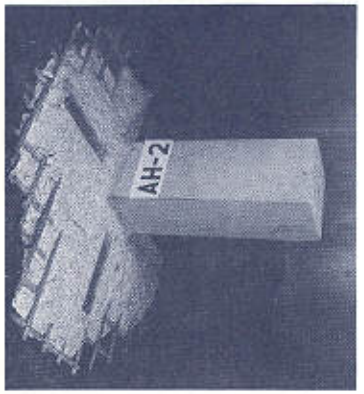

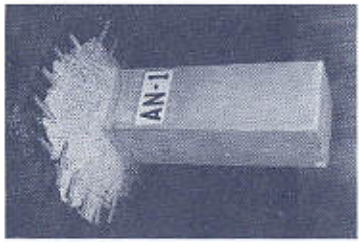

(a)

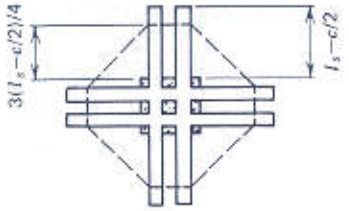

(d) Large shearhead

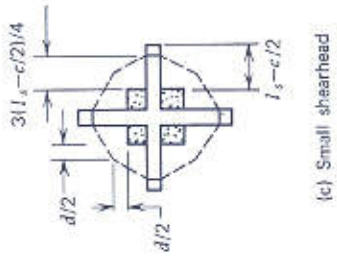

(c) Small shearhead

(b) No shearhead

FIGURE 5.38. (a) Influence of shearheads on location of the critical section. (b, c, d) Location of the critical section.

web reinforcement in beams. The design of this type of punching shear reinforcement is similar to that of shear reinforcement in beams, with concrete shear contribution taken as $2\sqrt{f'_c}$. The specimen shown in Fig. 5.39 was tested at the PCA Laboratories under unbalanced loads without evidence of impending anchorage failure in the shear reinforcement.[73]

5.3.6.5 Transfer of Moments from Slabs to Columns

Very frequently slabs must transfer moment in addition to shear in exterior columns of flat plates and slabs, interior columns in such floor systems when the adjacent spans are different in length or loading, and columns that transfer axial load and moment to a footing. Such a situation is illustrated in Fig. 5.40. The moment to be transferred is resisted partially by flexure along sides AB and CD of the critical section and partly by torsion along sides AC and BD. The torsional moments give rise to shear stresses [Fig. 5.40(c)] which increase those corresponding to the axial loads [Fig. 5.40(b)]. The resulting distribution of shearing stresses is shown in Fig. 5.40(d). The maximum shearing stresses should not exceed the allowable stress $4\sqrt{f'_c}$. Stresses, v_1, can be calculated by adding the stresses produced by the axial load, and those

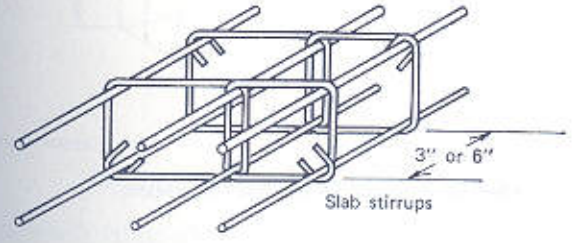

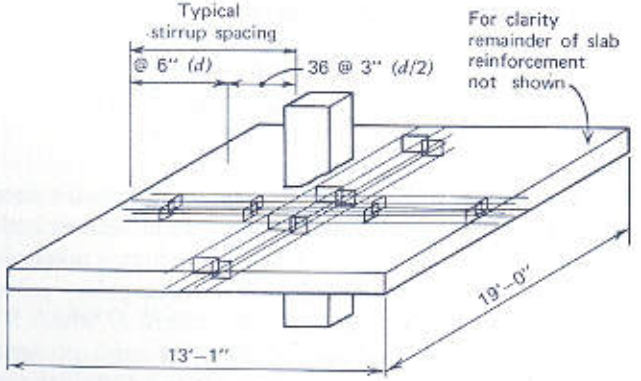

FIGURE 5.39. Integral beams for shear reinforcement in slabs.

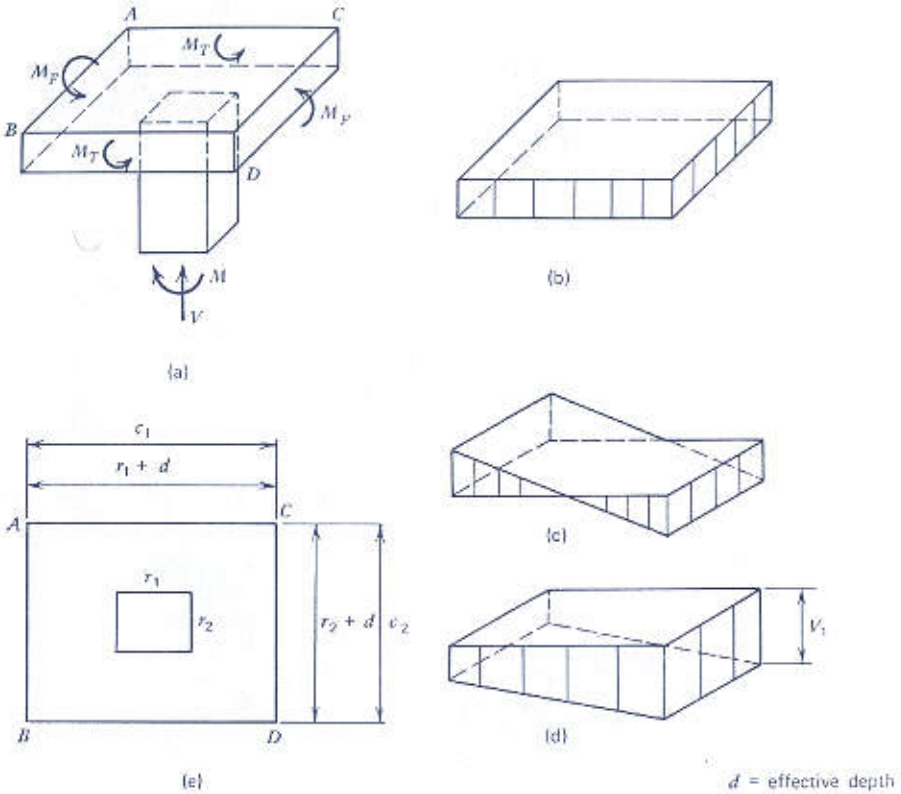

FIGURE 5.40. Transfer of moment from slab to column.

produced by the torsional moment:

$$v_1 = \frac{V}{b_0 d} + \frac{\alpha M}{J} y_1 \qquad (5.29)$$

The first term of the second member represents the shearing stresses due to the axial load. The perimeter of the critical section is the same as that considered in Section 5.3.6.2 for axial loads, which is taken as $4(r + d)$, for square columns, and $2(r_1 + r_2 + 2d)$ for rectangular columns [Fig. 5.40(e)]. α is the fraction of the unbalanced moment M which is transferred through shear. Though the proportions of the unbalanced moment transferred through shear and through flexure on sides AB and CD of the critical perimeter, respectively, have not been measured experimentally, it has been found that

$$J = \frac{d(r_1 + d)^3}{6} + \frac{(r_1 + d)d^3}{6} + \frac{d(r_2 + d)(r_1 + d)^2}{2}$$

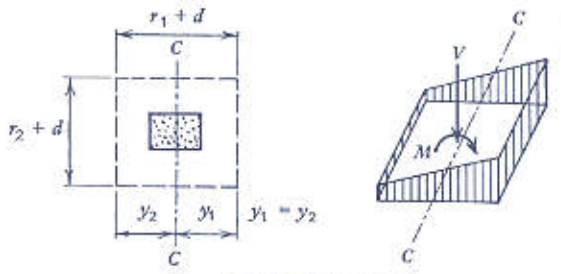

(a) Interior column

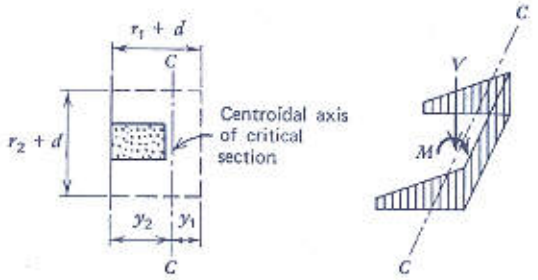

$$J = \frac{(r_1 + d)d^3}{6} + \frac{d(r_1 + d)^3}{6} + \frac{d(r_1 + d)}{2}\left[\frac{1}{2}(r_1 + d) - y_1\right]^2 + (r_2 + d)dy_1$$

(b) Edge column

FIGURE 5.41. Values of J for computing transfer of moment.

strength values obtained from Eq. (5.29) tally reasonably well with measured values if α is taken as 0.4. The parameter, J, is a modified polar moment of inertia corresponding to the critical section. Figure 5.41 gives values of J for interior and exterior columns. The slab should be designed so that the remaining 60% of the unbalanced moment can be resisted through flexure in a width of slab equal to that of the critical section; in other words, on sides AB and CD (Fig. 5.40). In the case of border columns only one side is available for resisting the remaining unbalanced moment, as the other side is a free border. Other approaches to the problem of transfer of moments are discussed in Ref. 143.

5.3.7 Shear in Beam–Column Joints

Important shear forces develop in beam–column joints of structures in seismic areas. In order to insure adequate strength and ductility of such joints, shear reinforcement is required. The shear force acting in the joint

batch immediately before or during mixing. Broadly speaking, concrete admixtures can be divided into three classes: chemical admixtures for water-reduction, workability, and set-control; air-entraining admixtures for workability, reduced bleeding, and durability; and mineral admixtures for control of heat of hydration and alkali–aggregate reactions. Chemical admixtures other than air-entraining agents are included in ASTM Specification C494, whereas air-entraining admixtures are described separately in ASTM C260.

According to ASTM C494 the chemical admixtures are classified as follows:

Type A	Water-reducing admixtures
Type B	Retarding admixtures
Type C	Accelerating admixtures
Type D	Water-reducing and retarding admixtures
Type E	Water-reducing and accelerating admixtures

The basic ingredients of the commercially available water-reducing admixtures can be divided into three groups: (1) calcium, sodium, or ammonium salts of lignosulfonic acid, and other derivatives of lignosulfonic acids and their salts; (2) hydroxylated carboxylic acids, their salts, and modifications; and (3) hydroxylated polymers.

The water-reducing admixtures frequently function as set-retarders when used in sufficient quantity. Where retardation of the setting time is desired, or is not objectionable, the water reducers can be used without modification. However, if a normal setting time or an accelerated set is wanted in addition to water reduction, the composition of the admixture must be modified by suitable accelerators such as $CaCl_2$ or triethanolamine, etc. In the United States the major producers of admixtures are the W. R. Grace and Co., Master Builders, Protex Industries, Inc., and Sika Chemical Corporation.

Water-reducing admixtures can be used to achieve *any one* of the purposes listed below:

1. By permitting water-reduction at a given slump and cement content, they make possible related benefits arising from reduced water–cement ratio (viz. higher strength).
2. By permitting water-reduction and corresponding cement-reduction for a given water–cement ratio, they help in reducing heat generation as well as the cost of the concrete mix.
3. By permitting improvement in consistency at a fixed cement-content and water-content, they provide additional workability which, otherwise, may not have been possible without resorting to expensive means such as aggregate regrading.

Dosages of water-reducing and set-retarding admixtures required to produce specific effects are usually recommended by the admixture manufacturers, but in the case of large jobs it is desirable to conduct laboratory tests for optimum dosages, which may vary with the physical–chemical characteristics of cement and the conditions under which concrete is used.

Retarding admixtures may be required for the elimination of cold joints in mass concrete construction, the hot-weather concreting of large piers and foundations, the cementing of oil-well casings, and the transporting of concrete over long distances.

Accelerating admixtures find their primary use in cold-weather concreting, where it may be desirable to normalize the rate of hardening and thus permit earlier removal of forms, and earlier loading of concrete. The accelerating admixture which has gained widespread use is calcium chloride. Triethanolamine may be preferred as a set-accelerator where a danger of corrosion of the reinforcement by calcium chloride exists, but it is a sensitive admixture requiring precise control.

If calcium chloride is used as an accelerator, its amount should not exceed 2% by weight of cement, otherwise too rapid a rate of concrete stiffening may result, in addition to the possible corrosion of ordinary steel reinforcement. In order to achieve a uniform distribution of calcium chloride, it is desirable to add it in a solution form as part of the mixing water.

It is generally not a recommended practice to use any chloride salts in concretes vulnerable to disruption by alkali–aggregate reactions or sulfate-bearing waters. Because of the danger of accelerated corrosion of the reinforcement, admixtures containing chlorides should not be used when concrete is prestressed. ASTM D98 and D345 cover specifications and testing methods for calcium chloride admixtures.

An *air-entraining admixture* is defined in ASTM C260 as a material that is used as an ingredient of concrete, added to the batch immediately before or during its mixing, for the purpose of entraining air. The intentionally entrained air bubbles are extremely small in diameter, well distributed throughout the concrete, and are not interconnected. Entrained air can improve the workability, water-tightness, freeze–thaw resistance, sulfate resistance, and resistance of concrete to deicer salts.

Generally, small quantities of air-entraining admixtures, of the order of 0.05% of active ingredient by weight of cement, are required to entrain the desired amount of air in concrete. The admixtures should comply with the requirements of ASTM C260. The materials capable of functioning as air-entraining agents are grouped into the following classification[15]: (1) salts of wood resins, (2) synthetic detergents, (3) salts of sulfonated lignin, (4) salts of petroleum acids, (5) salts of proteinaceous materials, (6) fatty and resinous acids and their salts, (7) organic salts of sulfonated hydrocarbons.

Several factors may affect the amount of air-entrainment in concrete.[16] The air-entrainment potential of an admixture tends to decrease with an increase in fineness of cement or in cement content of a concrete batch.

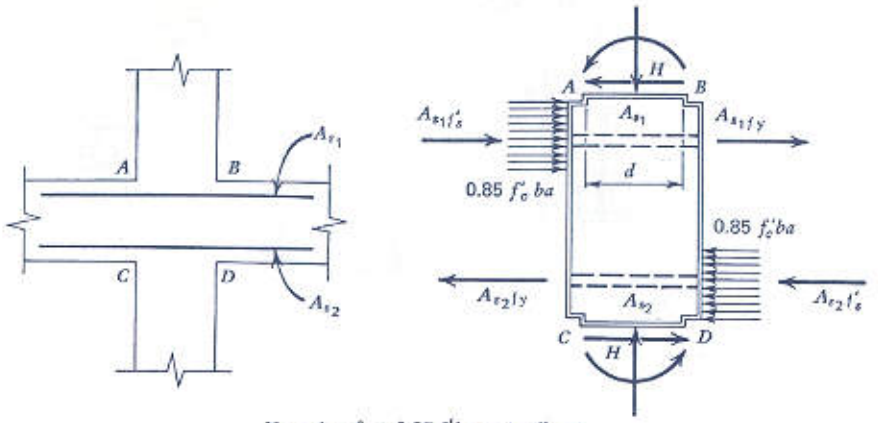

$$V_u = A_{s_1} f_y + 0.85 f'_c ba + A_{s_1} f'_s - H$$

$$V_u = A_{s_1} f_y + A_{s_2} f_y - H$$

FIGURE 5.42. Shear in beam–column joints.

may be computed as shown in Fig. 5.42. The necessary amount of reinforcement can be determined by applying the same rules as for beams. This reinforcement is provided by horizontal stirrups distributed along the depth of the beams. Half the computed steel area can be used if the joint is confined by beams framing into the four sides of the joint. Full sized specimens designed according to the above procedure have shown satisfactory behavior when tested under repetitive loading.[14,74]

5.3.8 Shear Friction

It was mentioned previously that the stresses causing so-called shear failures in reinforced concrete are not actually shear stresses but rather principal tensile stresses due to the combined action of normal flexural stresses and shear stresses. Nevertheless, there are some cases in which pure shear stresses may be critical. Although the strength of concrete in direct shear is quite high, there may be sections across which it is necessary to transfer shear and in which the capacity to do so is doubtful or nonexistent because of the presence of cracks or because of the nonmonolithic nature of a connection. In such cases, the only way of developing shear is through the friction that arises when one element tends to slip with regard to the other one.

The way in which shear capacity may be developed through friction is illustrated in Fig. 5.43(a), which shows the test specimen usually employed to investigate the resistance to slippage between two concrete elements. As indicated in the figure, the contact surface between the two elements is irregular. On slippage a relative displacement between the two elements takes

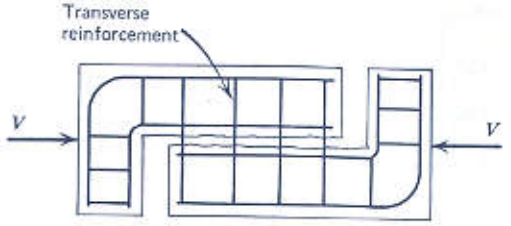

(a) Test specimen

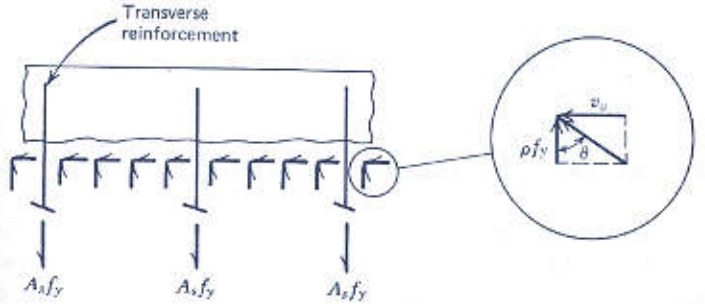

(b) Shear friction concept

FIGURE 5.43. Shear strength based on "shear friction" concept. (a) test specimen, (b) shear friction concept.

place in a direction perpendicular to the contact surface, as shown in Fig. 5.43(b). This displacement gives rise to tensile forces in the transverse reinforcement which produce reacting compressive forces on the contact surface. Through the presence of these compressive forces, friction forces are generated which can be estimated by means of equation

$$V = \mu N \tag{5.30}$$

in which V is the friction force, μ is the coefficient of friction, and N is the normal force. The friction force, V, is equal to the shear developed between the two elements. The normal force, N, is equal to the tension developed in the transverse reinforcement. Considering that the reinforcement yields, $N = A_s f_y$. Therefore, substituting this value of N and dividing both members of Eq. (5.30) by the area of the contact surface, the following equation is obtained:

$$v = \mu \rho f_y \tag{5.31}$$

Values of the coefficient of friction have been determined experimentally, by Anderson,[75] Birkeland and Birkeland,[76] Mast,[77] and Hofbeck, Ibrahim

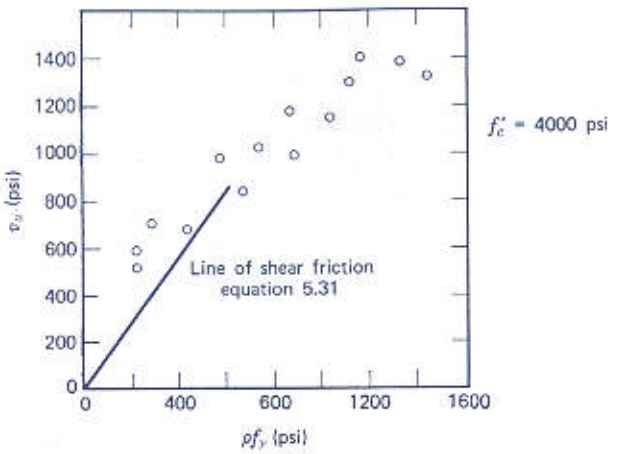

FIGURE 5.43. (c) comparison of test data with calculated values.[78]

and Mattock.[78] It has been found that for monolithic concrete a conservative figure is 1.4. The ACI Code also gives values of the coefficient of friction for concrete placed against rough, hardened concrete (1.0) and for concrete placed against as-rolled structural steel (0.7). According to the Code, values of ρf_y must not be greater than $0.2 f'_c$ nor 800 psi.

A comparison between the frictional shear stresses obtained by means of Eq. (5.31) with experimental values is given in Fig. 5.43(c). The experimental data of this figure correspond to specimens in which cracking has taken place along the contact surface before the loads were applied. For monolithic specimens and in specimens with special roughening of the contact surfaces, shearing stresses are somewhat larger. For such specimens, it has been suggested that an approach based on the use of a failure envelope for combined stresses, similar to the one developed by Zia,[79] would give more realistic results. The application of the shear friction principle depends on the correct selection of an assumed crack. Some examples are illustrated in Fig. 5.44. Detailed discussions of similar examples are included in Reference 77. The shear friction concept has found application mainly in the design of connections and other details in precast structures.

As an example of the application of the shear-friction concept, consider a very short corbel (Fig. 5.45). The reinforcement, which is perpendicular to the column, is equivalent to the transverse reinforcement shown in Fig. 5.43. Therefore, the required ratio of such reinforcement may be obtained from Eq. (5.31) as follows:

$$\rho = \frac{v}{\mu f_y} \tag{5.32}$$

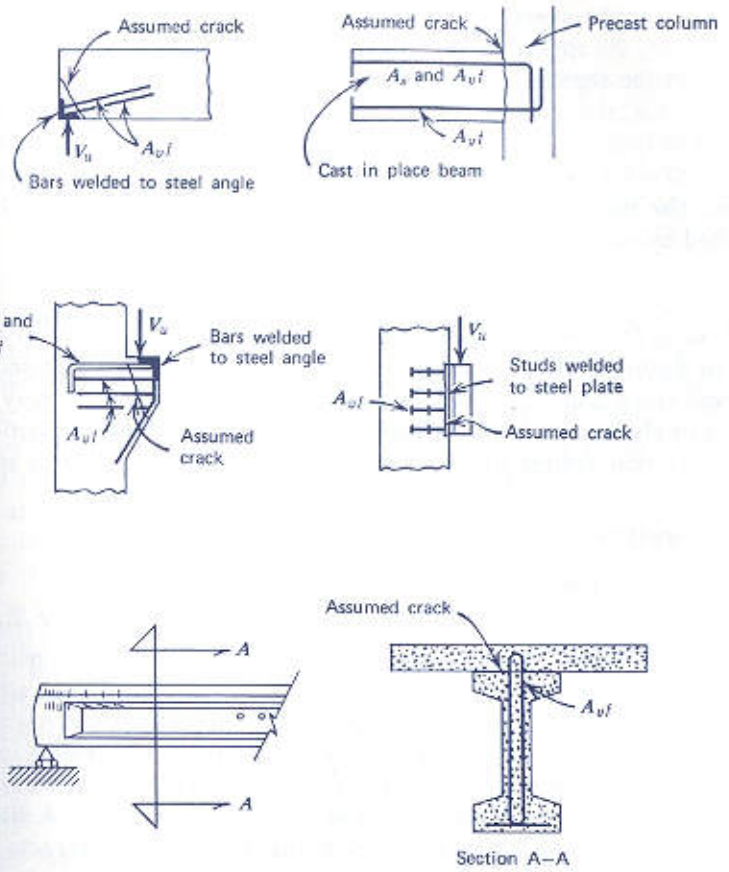

FIGURE 5.44. Examples of application of shear-friction theory.

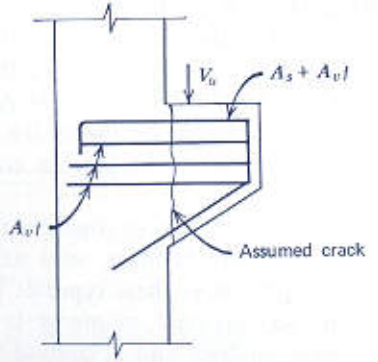

FIGURE 5.45. Shear-friction in corbels.

in which v is the average shearing stress along the contact surface, or, in other words, the applied V_u divided by the area of the contact surface, which is equal to the depth of the corbel multiplied by its width

$$v = \frac{V_u}{bh} \tag{5.33}$$

Once the ratio, ρ, has been computed, the required steel area, A_{vf}, is obtained by multiplying the ratio, ρ, by the contact surface bh,

$$A_{vf} = \rho bh \tag{5.34}$$

The shear friction steel must be added to the steel required for other actions, such as flexure or direct tension, and it must be well distributed across the assumed crack and adequately anchored. In some situations it may be advisable to place secondary reinforcement transverse to the shear friction steel as a protection against stress concentrations and local spalling or splitting.

5.4 TORSION

5.4.1 General Remarks

Torsion was long considered a secondary problem in the design of reinforced concrete structures. However, recently, greater attention has been paid to this aspect of design as a result of the increasing frequency with which structural failures have been attributed to torsion.[80,81] Furthermore, there is a growing tendency among architects to use structural systems and shapes in which torsion is a major type of loading. Such is the case of any transversely loaded curved member, such as helical stairs or curved bridge girders. A discussion of other cases in which torsion is significant is found in References 82, 83, and 84.

Extensive research has been carried out during the last decade, which has greatly improved understanding of the behavior of structural elements subjected to torsion. However, as in the case of shear, the body of knowledge that has been accumulated is mostly empirical. On the basis of the experimental information obtained, the 1971 version of the ACI Code includes, for the first time, specific recommendations for the design of reinforced concrete members under the action of torsion, and torsion combined with bending and shear.

In this section, the behavior of reinforced concrete members under torsion and torsion combined with shear, bending, and axial load is described; methods for predicting strength under these types of loading are presented. The computation of external torsional moments is not considered; this problem is one of structural analysis and is beyond the scope of this section.[84]

5.4.2 Pure Torsion

Pure torsion is seldom found in actual members. It is usually combined with bending and shear and sometimes with axial loads. However, since in order to estimate the strength of an element it is usually necessary first to estimate its strength under pure torsion, this type of loading is discussed in the following sections.

5.4.2.1 Behavior and Modes of Failure

Plain Concrete. Failure in torsion in a plain concrete beam occurs suddenly in a manner similar to a failure in bending. To detect the failure mechanism, Hsu[85] filmed a test with a high-speed camera. When projecting the film in slow motion, he found the failure process begins when an inclined tension crack develops in one of the wider faces (Fig. 5.46). This crack grows rapidly and extends into the two narrower faces. Failure occurs finally by crushing in compression in the opposite wider face. The process described is similar to the one occurring in a plain concrete beam under bending. In this case the tension crack starts at the lower face and extends along the lateral faces; failure is due to crushing in compression in the upper face. Therefore, a failure in torsion occurs by bending in a plane inclined about 45° to the longitudinal axis of the beam. Figure 5.47 shows the failure surface of a specimen tested by Hsu.[85] In this specimen the cracks in the narrower faces are practically perpendicular to the edges of the beam; this is not always the

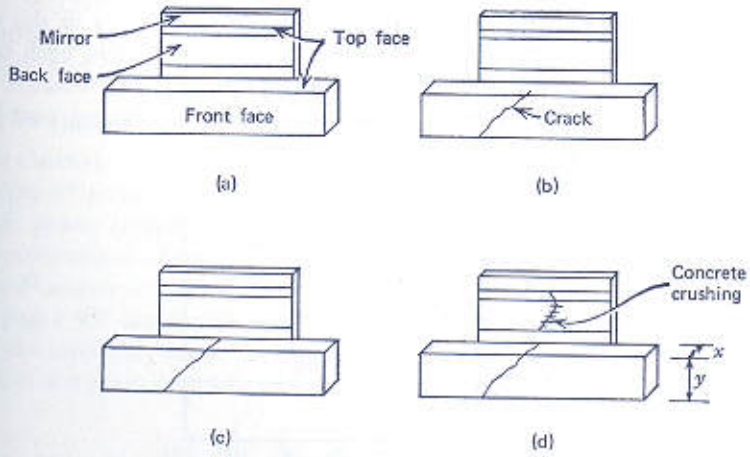

FIGURE 5.46. Torsion failure process of plain concrete beam (10 × 15-in. cross section) taken by movie camera with speed of 1200 frames/sec.[88]

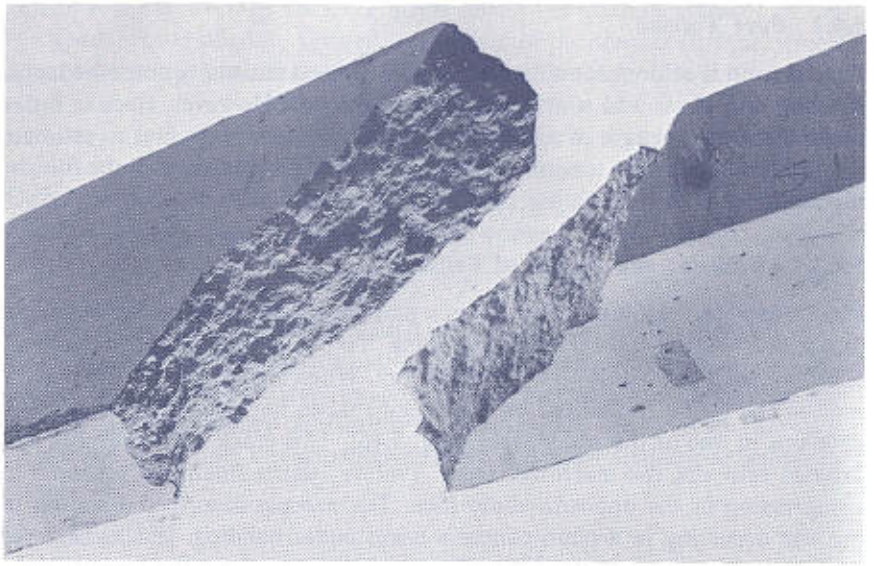

FIGURE 5.47. Failure surface of a plain concrete beam tested in pure torsion.[88]

case, so that the failure surface is not strictly a plane; though for practical purposes it can be taken as such.

Reinforced Concrete. A beam under pure torsion reinforced only in the longitudinal or in the transverse direction behaves practically in the same manner as a plain concrete beam. The behavior changes when both transverse and longitudinal reinforcement are present in adequate amounts. Two stages may be identified: from initial loading until first cracking, and from first cracking to failure.[85]

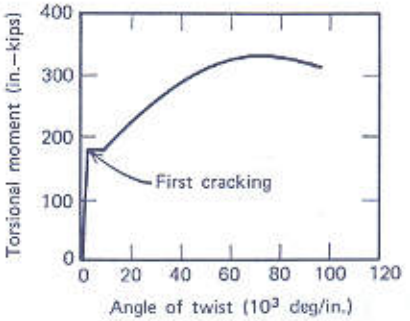

FIGURE 5.48. Torque–twist curve of a reinforced beam.[85]

Before cracking, the beam behaves as a plain concrete beam (Fig. 5.48). Steel strains at this stage are very small. The cracking torque, T_{cr}, is equal or slightly larger than the strength of a plain section, T_{up}.

When the cracking torque is reached, the twist, θ, increases rapidly under constant torque, as shown in the curve of Fig. 5.48. Steel strains also increase rapidly. This behavior is different from that of an element under pure bending, in which steel stresses increase gradually and there are no sudden changes in deflection after the concrete cracks. In an element under pure torsion, the internal equilibrium changes suddenly after cracking. The external moment which was resisted first by the concrete alone is resisted by the concrete together with the steel. Since the external moment remains constant, a part of the moment is transferred to the steel, and the portion of the moment resisted by the concrete decreases. Therefore the concrete contribution, T_c, is smaller than the strength of an equivalent plain concrete section.

After transfer the load again increases, but the stiffness is smaller than before cracking, as shown by the slope of the curve in Fig. 5.48. Both stiffness and strength depend on the amounts of transverse and longitudinal reinforcement used. After the strength of the member is attained, the torque–twist curve shows a descending branch, which develops very rapidly.[85]

When the strength, T_u, is reached, the concrete in one of the wider faces is crushed, and there may be yielding, depending on the ratios of transverse and longitudinal reinforcement. According to this, three types of members can be defined: (1) under-reinforced, when the strength is reached after both transverse and longitudinal reinforcement have yielded; (2) over-reinforced, when concrete crushes before yielding of the steel; and (3) partially over-reinforced, when either the transverse or the longitudinal reinforcement yields before collapse.

5.4.2.2 Computation of Strength

Plain Concrete. Several theories[86,87] have been presented for computing the strength of plain concrete members under torsion. They are based on the elastic theory (membrane analogy), the plastic theory (sand heap analogy), or combinations of both.

Hsu[88] assumed that failure in torsion occurs by skew bending about a plane, forming a 45° angle with the longitudinal axis of the element. (Hsu shows that the minimum torsional resistance corresponds to a plane at this angle.) Since it is a plain concrete section, Navier's formula can be applied:

$$M = f_r S \tag{5.35}$$

where M is the projection of the torque T_{up} on the skew plane; f_r is the concrete modulus of rupture; and S is the section modulus. Therefore,

$$M = T_{up} \cos 45° = T_{up}/\sqrt{2} \tag{5.36}$$

and

$$S = \frac{yx^2}{3\sqrt{2}} \tag{5.37}$$

Substituting Eqs. (5.36) and (5.37) in Eq. (5.35)

$$T_{up} = \frac{yx^2}{3} f_r \tag{5.38}$$

where x and y are, respectively, the shorter and the longer dimensions of the plain concrete rectangular section.

In the plane where cracking starts, there exist, besides normal tensile stresses, normal compressive stresses due to the projection of the torque on the plane perpendicular to the failure surface. Therefore the modulus of rupture is smaller than for a section under simple bending, since the tensile strength of concrete, according to Mohr's theory, will be reduced by this perpendicular compression. On this basis and by comparison with test results, Eq. (5.38) was modified to

$$T_{up} = \frac{yx^2}{3}(0.85 f_r) \tag{5.39}$$

Since reliable values of f_r are not normally available for design purposes, it is convenient to express Eq. (5.39) in terms of the concrete compressive strength, f'_c. The value of the modulus of rupture may be approximated as

$$f_r = 7.5\sqrt{f'_c} \quad \text{(in psi)} \tag{5.40}$$

Substituting in Eq. (5.39)

$$T_{up} = 2.12 yx^2 \sqrt{f'_c} \tag{5.41}$$

or approximately,

$$T_{up} = 2yx^2 \sqrt{f'_c} \tag{5.42}$$

A comparison between measured and computed values of ultimate torques, obtained by using Eq. (5.42), is shown in Fig. 5.49. The agreement is reasonable, but it can be improved if some refinements are introduced, which take into account a better relationship between modulus of rupture and compressive strength.[88]

For I, T, or L sections the torsional strength may be approximated as the sum of the strengths of the component rectangles. In beams monolithic with slabs, the effective width of the flange is taken as three times its effective depth. For circular cross sections the basic expression, with a reduced modulus of rupture, is

$$T_{up} = \frac{\pi h^3}{16}(0.85 f_r) \tag{5.43}$$

in which h is the diameter of the section.

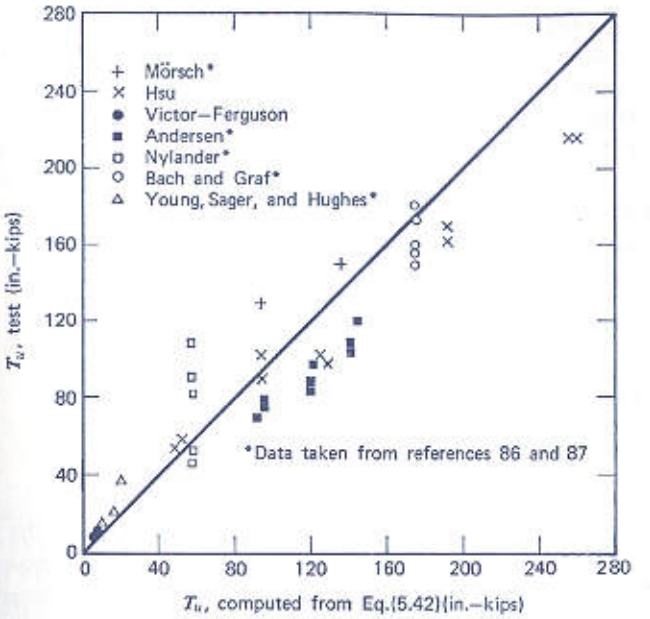

FIGURE 5.49. Comparison of experimental and theoretical ultimate torsional moments.

Reinforced Concrete. As mentioned before, a member under torsion which is reinforced only in one direction behaves practically as a plain concrete member. Therefore, only elements with both longitudinal and transverse reinforcement will be considered. This latter reinforcement must be in the form of closed ties to be efficient. Spiral reinforcement can also be used.

As in the case of shear, the strength in torsion of a reinforced concrete member can be expressed as the sum of two terms, representing the contributions of the concrete, T_c, and the steel, T_s.

$$T_u = T_c + T_s \tag{5.44}$$

Several ways have been proposed for evaluating the two contributions. Some codes have assumed that the concrete contribution, T_c, is equal to the equivalent torque for a plain concrete element, or $T_c = T_{up}$, while others have assumed this contribution to be zero after cracking, or $T_c = 0$. The actual value of T_c probably lies between these two extremes.

Most procedures assume that the steel contribution can be evaluated by an expression of the following form

$$T_s = \frac{\alpha_t A_{sv} f_{sv}}{s} x_1 y_1 \tag{5.45}$$

where α_t is an experimentally determined constant, A_{sv} is the area of one stirrup leg, f_{sv} is the stirrup stress, x_1 is the short center-to-center stirrup dimension, y_1 is the long center-to-center stirrup dimension, and s is the stirrup spacing.

Equation (5.45) can be justified in the following manner. Consider that all cracks have an inclination of 45° in each face of the rectangular section. The number of stirrups crossing a 45° crack in the y_1-direction will be y_1/s in each face. Taking torsional moments with respect to the longitudinal axis, the contribution of the stirrups in the y_1-direction is

$$T_{s1} = A_{sv}\kappa_1 f_{sv} \frac{y_1}{s} x_1 \tag{5.46}$$

Similarly, for the x_1 direction,

$$T_{s2} = A_{sv}\kappa_2 f_{sv} \frac{x_1}{s} y_1 \tag{5.47}$$

The coefficients κ_1 and κ_2 are introduced to take into account the fact that steel stresses are not uniform along the stirrup, as has been observed experimentally.[88] The total contribution of the transverse reinforcement is obtained by adding Eqs. (5.46) and (5.47):

$$T_s = T_{s1} + T_{s2} = \frac{A_{sv}f_{sv}}{s} x_1 y_1(\kappa_1 + \kappa_2) \tag{5.48}$$

Equation (5.48) becomes identical with Eq. (5.45) if $(\kappa_1 + \kappa_2) = \alpha_t$.

The values of T_c and α_t have been obtained experimentally from tests of beams in which the principal variable is the term $(A_{sv}f_{sv}x_1y_1/s)$. If the results are presented graphically as shown in Fig. 5.50, the ordinate to the origin of the straight line representing the test results is the value of T_c and the slope of the line is the value of α_t. The concrete contribution obtained in this manner is an extrapolated value. It cannot be measured directly. For the value of α_t to be independent of the steel ratio, it is necessary for the experimental points to define a straight line reasonably well. This occurs with under-reinforced and some partially over-reinforced beams, which are the most common types of members in practice.

From tests of 53 rectangular beams, some of them hollow, in which the main variables were the amount and type of reinforcement, size, and concrete strength, Hsu[88] found the following values for T_c and α_t:

$$T_c = \frac{2.4}{\sqrt{x}} x^2 y \sqrt{f'_c} \tag{5.49}$$

$$\alpha_t = 0.66 + 0.33 \frac{y_1}{x_1} \tag{5.50}$$

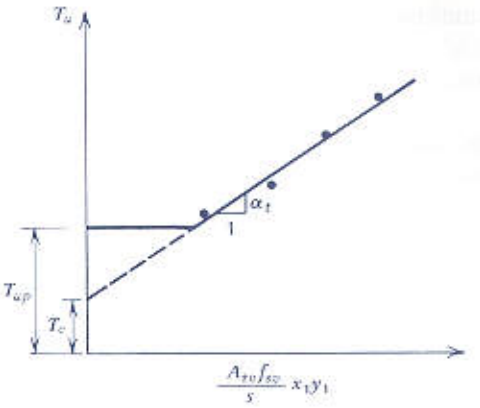

FIGURE 5.50. Experimental determination of T_c and α_t.

The value of T_c obtained in this manner is smaller than the strength of an equivalent plain section. For elements of ordinary dimensions, it is of the order of 40% of T_{up}. According to Hsu, the strength of hollow beams is practically the same as the strength of similar solid beams. Therefore the contribution of concrete does not depend on the concrete in the core, but rather on the peripheral layer.

The value of α_t is not constant, as had been assumed by some authors, but depends chiefly on the ratio of stirrup leg lengths, x_1/y_1. Other variables such as the volumetric ratio of longitudinal and transverse reinforcement, η, and the scale effect, were found to affect the value of α_t, but their influence was minor and therefore they are not considered explicitly in Eq. (5.50).

The strength of a reinforced member may therefore be obtained by substituting Eqs. (5.45), (5.49), and (5.50) in Eq. (5.44):

$$T_u = \frac{2.4}{\sqrt{x}} x^2 y \sqrt{f'_c} + \left(0.66 + 0.33 \frac{y_1}{x_1}\right) \frac{A_{sv}f_{sv}}{s} x_1 y_1 \tag{5.51}$$

In order to use Eq. (5.51), it is necessary to know the stirrup stress, f_{sv}. For under-reinforced beams the stirrups yield before collapse, and $f_{sv} = f_{yv}$. To insure that a beam is under-reinforced, the total steel ratio, ρ_t (longitudinal plus transverse reinforcement), should be limited, as should be the relation between the ratios of the transverse and the longitudinal steel. Hsu[88] has proposed the following limitations:

$$\rho_t \leq 2400 \sqrt{\frac{f'_c}{f_{yv}}} \tag{5.52}$$

$$0.7 < \eta < 1.5 \tag{5.53}$$

The value of the ratio η may be calculated by means of Eq. (5.54):

$$\eta = \frac{A_s s}{2A_{sv}(x_1 + y_1)} \tag{5.54}$$

in which A_s is the total area of the longitudinal steel. This steel should be distributed around the perimeter of the transverse section.

If the conditions expressed in Eqs. (5.52) and (5.53) are complied with, the torsional strength of a reinforced concrete member can be determined by making f_{sv} equal to f_{yv} in Eq. (5.51). This results in the following expression:

$$T_u = \frac{2.4}{\sqrt{x}} x^2 y \sqrt{f'_c} + \left(0.66 + 0.33 \frac{y_1}{x_1}\right) \frac{A_{sv} f_{yv}}{s} x_1 y_1 \tag{5.55}$$

5.4.3 Torsion Combined with Flexure

Various theories for predicting the strength of members subjected to the combined action of torsion and flexure have been developed. Tests have also been carried out in support of these theories and in order to obtain torsion–flexure interaction diagrams based on experimental data. A diagram of this type is the geometrical locus of flexural and torsional moments causing the failure of a member. In this section only reinforced concrete members shall be considered.

Theories for combined torsion and flexure can be divided into two groups. The theories of the first group are based on the hypothesis that the member can be idealized, at failure, as a mechanism for which equilibrium equations can be established. The first theory of this group was developed by Lessig[87] and is based on the failure mechanism illustrated in Fig. 5.51, which can be visualized as a member subjected to flexure on a plane inclined with respect to its longitudinal axis. By taking moments with respect to the neutral axis of all the external and internal forces shown in Fig. 5.51, expressions for the torsional moment T and the flexural moment M can be obtained. Lessig's

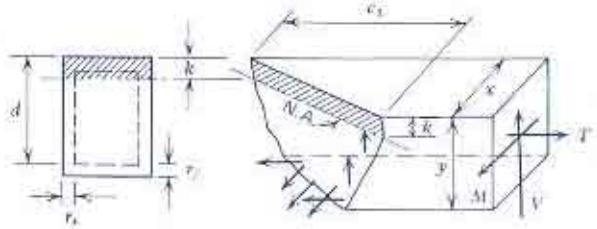

FIGURE 5.51. Failure surface for Lessig's theory for torsion and bending.

theory was later modified by Yudin,[87] who pointed out that the moments of the external and the internal forces should be taken simultaneously with respect to both the longitudinal and the transverse axes passing through the centroid of the compression zone.

According to more recent theories, the type of failure mechanism is dependent on the ratio between flexural and torsional moments, the mechanism proposed by Lessig being valid only for high values of this ratio. The various theories of this group differ in the characteristics of the failure mechanism and in the axes, with respect to which the moments of the external and internal forces are taken. A complete presentation of these theories is outside the scope of this chapter. For a more complete treatment, References 89–92 may be consulted.

Theories of the second group establish an analogy between a reinforced concrete member and another structural member that is easier to analyze. Lampert[93-145] has described a space truss analogy in which the reinforced concrete member is substituted by a tridimensional truss, the longitudinal reinforcement being the longitudinal chords of the truss, the stirrups being the transverse members of the truss, and the concrete between helical cracks being the inclined compression members of the truss (Fig. 5.52). Based on this analogy, and on experimental results, Lampert has proved that the slope of helical cracks depends on the ratio between torsional and flexural moments and that this slope is such that both longitudinal and transverse reinforcement yield at failure. The reinforcement can be minimized for design purposes, by choosing a longitudinal to transverse reinforcement ratio such that the slope of helical cracks is 45°. In its present state of development Lampert's theory considers the torsion–flexure interaction only, but work is going on to extend it to the torsion–flexure–shear interaction.

As previously mentioned, the interaction between torsion and flexure may be studied by means of diagrams based on experimental data. In the following sections, interaction diagrams obtained from experimental results are described and discussed. Members with and without transverse reinforcement are considered separately.

5.4.3.1 Members without Transverse Reinforcement

Figure 5.53 shows a nondimensional interaction diagram corresponding to T-beams tested by Victor and Ferguson[94] under different combinations of flexure and torsion. The value of T_u was obtained by determining the average of specimens tested under pure torsion, and the value of M_u was calculated by means of the equation given by the ACI Code for simple flexure. This test series did not include elements in pure flexure, since the corresponding strength can be estimated analytically with adequate precision.

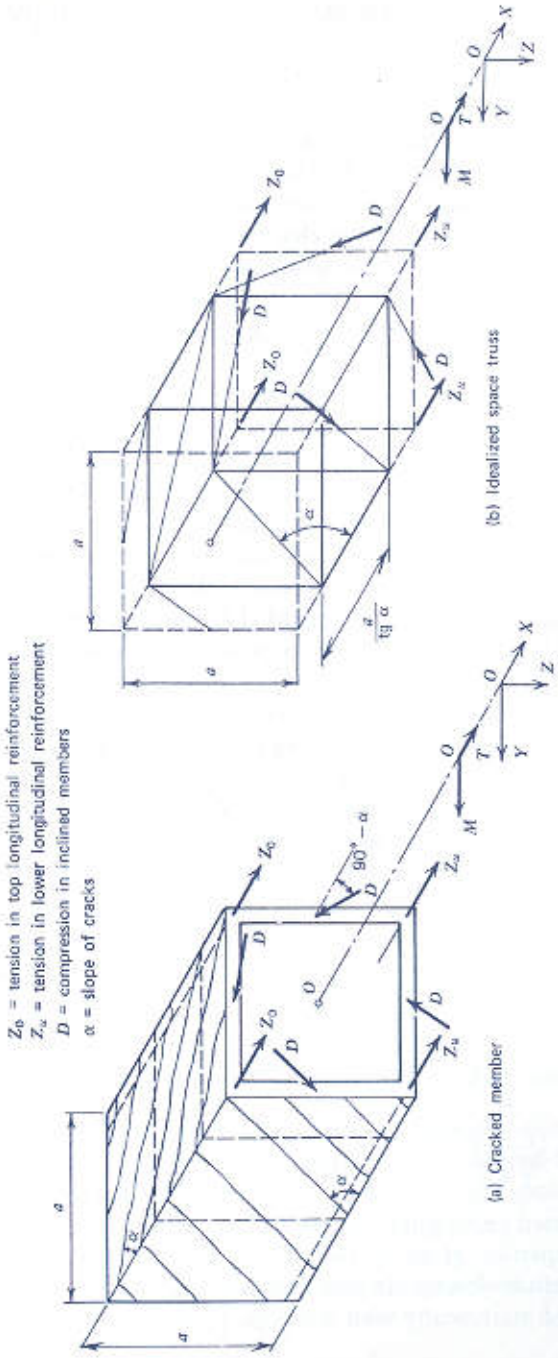

FIGURE 5.52. Space truss analogy for members subjected to torsion combined with flexure.[93]

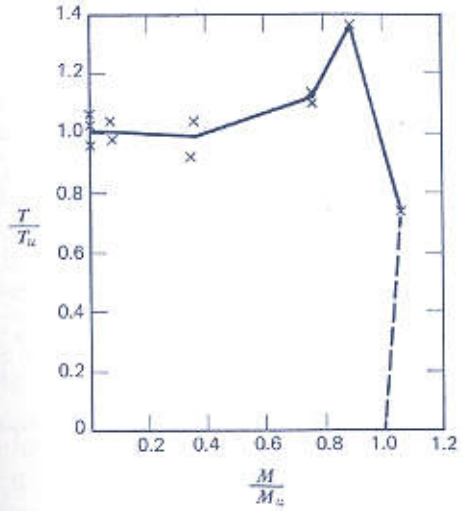

FIGURE 5.53. Torsion–flexure interaction diagram for members without transverse reinforcement.[91]

In this series of tests, the presence of a flexural moment did not reduce the torsional strength of the members, and vice versa; in other words, there was little interaction between flexure and torsion. Moreover, for values of the flexural moment approaching M_u, the torsional strength increased.

Other tests of members under the combined action of flexure and torsion have been carried out, but their range was not sufficiently large to obtain diagrams such as the one reproduced in Fig. 5.53. However, such diagrams may be constructed by representing the measured flexural and torsional moments on a nondimensional diagram, such as that of Fig. 5.54, in which the values of T_u and M_u have been computed respectively by means of Eq. (5.43) and the ACI equation for pure flexure. This diagram shows that for some sections the torsional strength does decrease when a flexural moment acts at the same time as a torsional moment. The greatest reductions correspond to square sections with very small steel percentages. Lim and Mirza[95] have pointed out that this reduction does not exist when the total percentage of longitudinal reinforcement is greater than 1%.

The tentative conclusion that may be derived from Figs. 5.53 and 5.54 is that for practical purposes there is no interaction between flexure and torsion except for members with low steel ratios and perhaps for members with small depths. This conclusion should be accepted only tentatively until more definite information is available as to the types of elements in which there is interaction and as to how this interaction can be quantified. Hsu[96] has suggested the interaction diagram shown in Fig. 5.54.

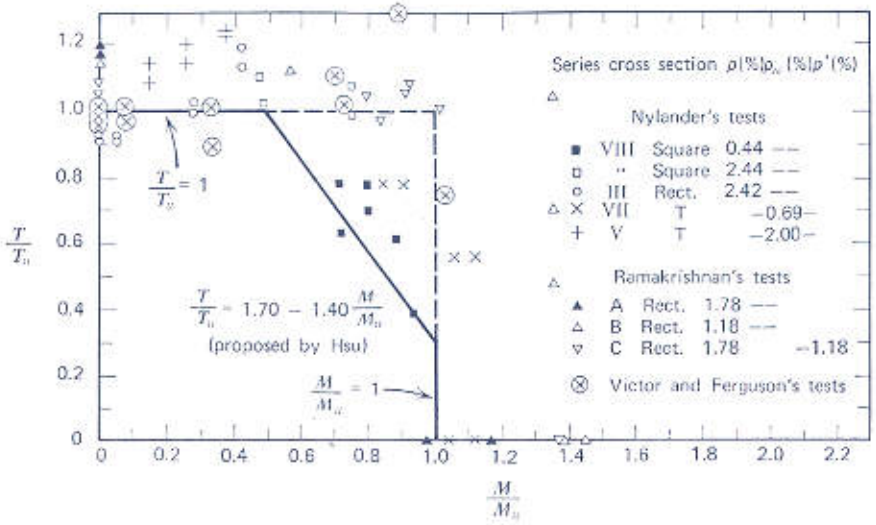

FIGURE 5.54. Comparison of torsion–flexure tests by different researchers in members without web reinforcement.[96]

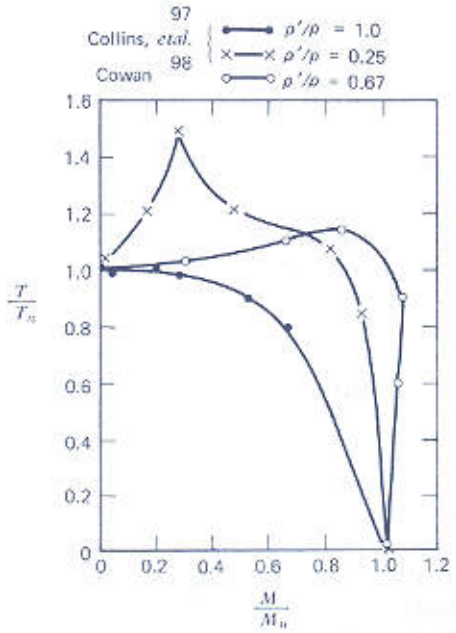

FIGURE 5.55. Torsion–flexure interaction diagrams for beams with web reinforcement.

5.4.3.2 Members with Transverse Reinforcement

The shape of the torsion–flexure–interaction diagrams for this type of member is significantly influenced by the relation between the ratios of the compression and the tension reinforcement, ρ'/ρ, as illustrated in Fig. 5.55. When the percentage of tension reinforcement is greater than that of the compression reinforcement ($\rho'/\rho < 1$), the torsional strength under combined loading is greater than the strength in pure torsion, as indicated by Collins' tests,[97] with $\rho'/\rho = 0.25$, and Cowan's tests[98] with $\rho'/\rho = 0.67$ (Fig. 5.55). However, when the tension steel ratio is equal to the compression steel ratio ($\rho'/\rho = 1$), the presence of flexure reduces the torsional strength and vice versa, as in Collins' test for $\rho'/\rho = 1$. This effect seems to indicate that if compression steel is added to a member while the tension steel is kept constant, its capacity under combined loading is reduced. This does not happen in practice because increasing the compression reinforcement increases the strength of the member in pure torsion, as illustrated in the diagrams of Fig. 5.56, which were constructed with information from Reference 99. The beams of Series 1 differ from those of Series 2 only in having more compression steel. Although the shape of the interaction diagram is different in both series, the strength of the beams of Series 2 is never less than that of the beams in Series 1.

The effects of the distribution and the amount of longitudinal steel discussed above have been explained physically by Mattock[100] as follows. If the distribution and amount of longitudinal steel are such that the steel yields in pure torsion, any additional flexural moment will reduce the torsional strength, since the tension steel must also resist flexure. However, if the longitudinal steel does not yield in pure torsion (over-reinforced members), the torsional strength increases when an external flexural moment is acting. The increase may be attributed to the fact that the compressive stresses in the concrete enhance its torsional strength.

It may be tentatively concluded that, in an element with transverse reinforcement, torsional strength is not significantly reduced by the presence of flexure, as long as there is sufficient longitudinal steel arranged so that most of it is located in the tension zone of the member.

5.4.4 Torsion Combined with Shear

Shear cannot act on a member without the simultaneous existence of flexure. In view of this, when the interaction of shear and torsion is studied, it is always necessary to consider the simultaneous action of a flexural moment. For the sake of simplicity, the term torsion–shear interaction shall be used, in the understanding that one is actually referring to a torsion–flexure–shear interaction.

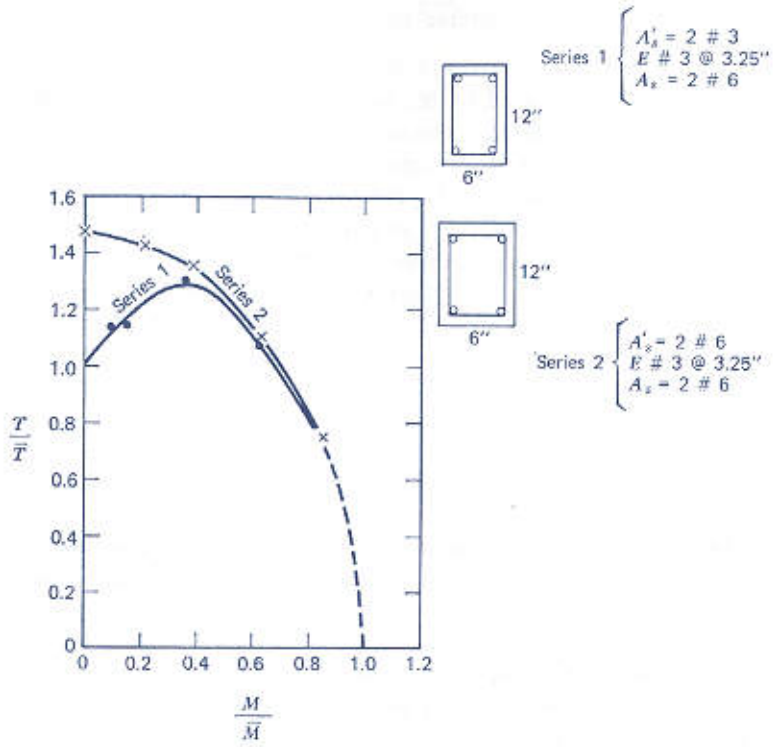

FIGURE 5.56. Effect of increasing the compression steel.[99]

Both shear and torsion produce shear stresses in a member. On one side, the stresses are added, while on the other, they are subtracted. Since there is little information on stress distributions originated by shear or torsion acting alone, it is very difficult to determine the actual distribution of stresses due to the combined action of torsion and shear. Consequently, the problem of constructing torsion–shear-interaction diagrams has usually been approached experimentally. The theoretical approaches that have been attempted[86] shall not be presented in this chapter. In the remaining part of this section, the shape of the interaction diagrams of members with and without transverse reinforcement will be discussed.

5.4.4.1 Members without Transverse Reinforcement

A number of tests of this type of member have been carried out in order to determine interaction diagrams. The results of three series of tests of L-beams

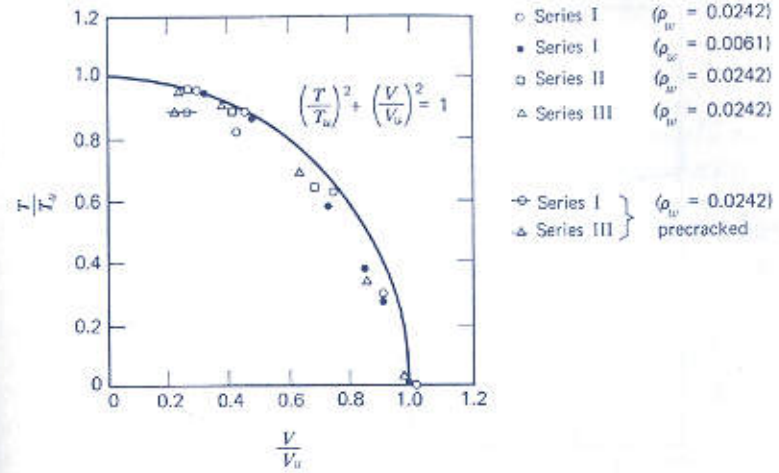

FIGURE 5.57. Torsion–shear interaction diagram for members without web reinforcement.[101]

with varying percentages of reinforcement and compression flange lengths are shown in Fig. 5.57.[101] The values of V_u were obtained by testing beams without torsion, failing in shear. The shear strengths were consistently larger than the values estimated in accordance with the ACI Code. The values of T_u were obtained by extrapolating the measured torsional moments, since no members in pure torsion were tested. The experimental values give an approximately circular diagram. Other series of tests have given similar results.[100]

Although the experimental results give a quite well-defined circular diagram, a difficulty arises when an attempt is made to generalize such a diagram to members for which the value of V_u is not known. The ACI formula usually employed for computing shear strength does not give the actual failure strength but the load corresponding to visual diagonal cracking, which is frequently lower. This means that computed cracking loads are compared with measured failure loads so that the dispersion of the experimental results is considerably increased. Unfortunately a reliable method for computing the shear corresponding to the actual failure of reinforced concrete members is yet to be developed.

Figure 5.58 shows the results obtained in six independent series of tests,[102] including the series of Fig. 5.57, in a nondimensional interaction diagram in which V_u was determined by means of the equation proposed in the ACI Code, while T_u was estimated by means of the sand heap analogy and a stress of $5\sqrt{f'_c}$. The considerable dispersion which is evident is partly due to the

Similarly, an increase in the proportion of fines in sand also tends to decrease air entrainment. In the temperature range 40–100°F, entrained air varies inversely with the temperature at which the concrete is mixed. Generally, increase in slump and in the water content of concrete results in more air-entrainment. Mixing conditions such as the type of mixer and the mixing time also affect the amount of entrained air. The air content of concrete increases with increased time of mixing to about 2 min in stationary mixers and up to about 15 min in transit mixers, beyond which it may remain constant for a considerable period before diminishing. Regarding the effect of vibration, which is frequently applied to get consolidation of concrete, if the intensity and time of vibration is properly controlled, the amount and the critically important spacing of small entrained air bubbles is little affected. Air-entraining admixtures are among the most commonly used admixtures in concrete practice.

Mineral admixtures include any essentially insoluble materials other than cement and aggregate, which are used as an ingredient of concrete and are added to the batch immediately before or during mixing. Mineral admixtures for concrete include natural cement (ASTM C10), hydrated lime, granulated blast-furnace slag, stone dust, raw natural pozzolans (opaline cherts, volcanic ashes, pumicites, diatomaceous earth) and heat-treated pozzolans (fly ash, calcined shale, or clay) which are covered by ASTM C618. Since better workability and reduction in bleeding can be more uniformly and more economically achieved by air entrainment, the mineral admixtures used presently are, generally, limited to those having pozzolanic properties. In the United States, the amount of pozzolan generally used in concrete ranges between 15% and 30% of the total cementitious material.

The possible advantages from the use of pozzolanic admixtures in concrete are improved workability, increased water tightness, lower heat of hydration, and reduced alkali–aggregate disruptive expansion. A disadvantage of using pozzolan in some cases may be an undesirably low rate of initial strength development.

Several organizations such as ASTM, the U.S. Army Corps of Engineers, and the Bureau of Reclamation have established comprehensive physical–chemical requirements for pozzolanic admixtures. The main features of their chemical specifications include a minimum of 70–75% argillaceous oxides ($SiO_2 + Al_2O_3 + Fe_2O_3$) and no more than 5.0% MgO.

Natural pozzolans have a tendency to increase the water requirement of concrete, while the artificial pozzolan, such as fly ash, may lower the water requirement slightly. Since a higher water requirement may affect the durability of concrete by increasing the drying shrinkage and the cracking tendency, the pozzolan specifications limit the percent increase in both water requirement and drying shrinkage.

Regarding the disruptive alkali–aggregate reactions in concretes containing reactive siliceous aggregates, the addition of some pozzolans is found to reduce the expansion caused by these reactions. Since not all pozzolanic materials are effective in this respect, and since the dosages necessary to prevent disruption may vary from one pozzolan to another, the minimum amount of a pozzolan required should be determined by actual tests. ACI Committee 212[18] warns that in amounts less than 15% by weight of total cementitious materials some pozzolans may increase rather than decrease expansion due to alkali–aggregate reactions.

1.10 PROPERTIES OF FRESH CONCRETE

Properties of fresh concrete are an important part of the overall concrete quality. The concrete materials and mix proportions must be selected not only to attain the required strength but to produce a fresh concrete which can be easily transported, placed, consolidated, and finished. The properties of fresh concrete are also important because they will affect the quality and appearance of the finished structure as well as its cost.

As soon as water is added to the other concrete ingredients, freshly mixed concrete undergoes several changes and becomes rigid within a few hours. The concrete remains plastic for only a short period of time. The properties of fresh concrete here discussed refer to the concrete while it is plastic. The time of setting, or rate of stiffening, of the concrete is also of interest and must be taken in account in difficult or large concrete placement operations. The influence of temperature of concrete on its fresh properties needs also to be considered. In controlling the quality and uniformity of freshly mixed concretes, tests for consistency, air content, and unit weight are usually made in the field.

The subject matter of properties of fresh concrete is sometimes referred to as the rheology of fresh concrete. *Rheology of fresh concrete* may be defined as the study of responses of a fresh concrete mass to applied forces. The understanding of the rheology of fresh concrete is at least as important as the knowledge of the physical and mechanical characteristics of hardened concrete.

The important properties of fresh concrete include *workability*, *consistency*, *segregation*, and *bleeding*. These properties are *physical* phenomena and they are related; a change in one will influence the others. The *setting*, or rate of stiffening, is a *physico-chemical* phenomenon.

1.10.1 Structure of Fresh Concrete

The structure of fresh concrete can be described as a continuum of cement paste (cement plus water) in which aggregate particles are embedded. These

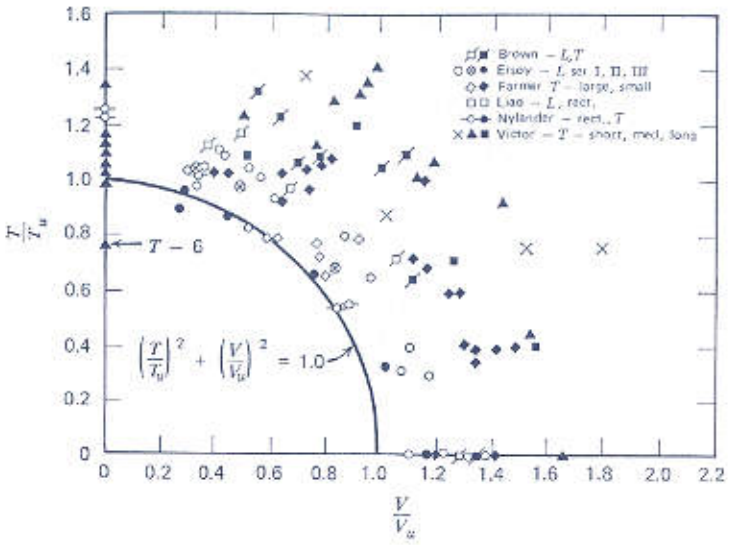

FIGURE 5.58. Comparison of torsion–shear tests by different researchers.[102]

fact that the measured shear strength, without torsion, is always greater than the computed shear strength.

The dispersion apparent in Fig. 5.58 is also influenced by other factors which modify the strength under combined loading, such as the type of section, the type of load, and the magnitude of the flexural moment. With regard to the first of these, it has been shown that the strength of a T section is greater than that of an L section with the same flange width.[103] With respect to the type of loading, it has been seen that the strength of members under a uniformly distributed loading is greater than that of members with a concentrated load producing the same internal actions.[102] With regard to the magnitude of the flexural moment, it was mentioned in Section 5.4.3.1 that for certain types of elements torsional strength is reduced when the flexural moment is large. Since the tests included in Fig. 5.58 correspond to different types of sections, different types of loading and different load levels, a considerable dispersion is to be expected. Various coefficients have been proposed to take these variables into account,[102] but more experimental evidence is required before their acceptance is justified.

Regarding torsion–shear interaction of members without transverse reinforcement, it can be concluded that the circular interaction diagram proposed by a number of writers constitutes a lower bound of the available experimental results. The strength is very often greater than that indicated by such diagrams. Another conclusion to be derived from a study of Fig. 5.58

is that for values of the torsional moment smaller than 40% of T_u, there is no reduction in shear strength.

5.4.4.2 Members with Transverse Reinforcement

It was stated in Section 5.4.2.2 that the strength in pure torsion of a member with transverse reinforcement is equal to the sum of the contribution of the concrete and the contribution of the steel reinforcement. The contribution of the concrete is about 40% of the strength of a similar member without transverse reinforcement, as indicated in the above-mentioned section. On the other hand, the strength of a member, when no torsion is acting, is equal to the sum of the strength of the member without transverse reinforcement and the contribution of such reinforcement. Therefore, the contribution of the concrete varies from a value corresponding to the strength of a member without transverse reinforcement, for shear without torsion, to a smaller value for the case of torsion without shear. The law for the variation in the value of the contribution of the concrete cannot be determined experimentally because what is measured in tests of members simultaneously subjected to shear and torsion is the total strength, that is, the sum of the contributions of the concrete and the steel reinforcement, not the magnitude of the independent contributions.

An interaction diagram obtained experimentally by Klus[104] is shown in Fig. 5.59. The values of T_u and V_u were obtained by testing specimens in pure torsion and in shear without torsion. It can be seen that the interaction is greater than for members without transverse reinforcement; in other words, the presence of shear has a greater influence on the rate at which the torsional

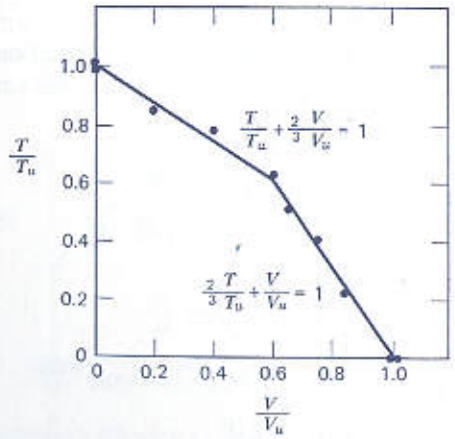

FIGURE 5.59. Torsion–shear interaction diagram for members with transverse reinforcement.[104]

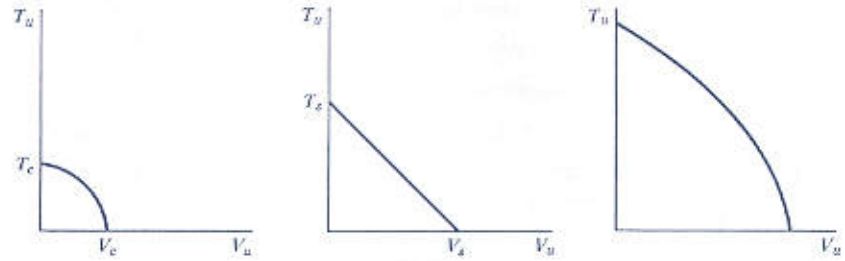

(a) Interaction of concrete contribution (b) Interaction of web reinforcement contribution (c) Total interaction

FIGURE 5.60. Torsion–shear interaction diagrams of the contributions of the concrete and the transverse reinforcement.

strength decreases. This may be explained as follows. The interaction for a member with transverse reinforcement is the sum of the interactions of the contributions of the concrete and the steel (Fig. 5.60). The interaction of the contribution of the concrete is not known, as mentioned before, but it can be considered similar to the interaction in members without transverse reinforcement [Fig. 5.60(a)]. The interaction of the contribution of the steel reinforcement is more significant than of concrete. If the two interactions are added, a diagram such as that of Fig. 5.60(c) is obtained. Therefore, the torsion–shear–interaction effect will be more significant with increasing steel percentage.

5.4.5 Flexure–Shear–Torsion Interaction Surfaces

By combining a torsion–flexure–interaction diagram with torsion–shear diagrams for different levels of flexural moment, an interaction surface is obtained, such as the one shown in Fig. 5.61. A point on this surface represents

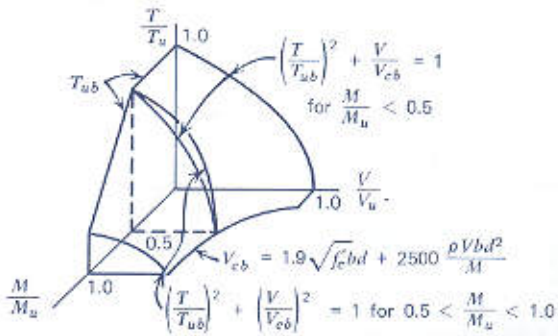

FIGURE 5.61. Interaction surface.[96]

the combination of flexural moment, shear, and torsional moment that causes failure of the member.

Due to the uncertainties in the determination of the torsion–flexure and torsion–shear–interaction diagrams, it has not been possible to obtain interaction surfaces acceptable to all researchers. The surface shown in Fig. 5.61 as an example, was developed by Hsu.[96] Different interaction surfaces have been proposed by other researchers.

5.4.6 Torsion Combined with Axial Load

This combination of actions may appear in columns and prestressed members. To investigate the behavior under this type of loading, tests have been carried out both on specimens in which the axial load was applied by a universal testing machine and on specimens in which it was set up by prestressing tendons, the results obtained being similar in both cases. Some of the experimental results are summarized in the following sections.

5.4.6.1 Members without Transverse Reinforcement

The nondimensional diagram of Fig. 5.62 shows the results of several series of tests. In this diagram the ordinates are values of the torsional moment measured under the combined action of axial load and torsion divided by the torsional strength in pure torsion. The abscissas are values of the average applied compressive stress on the section, divided by the compressive strength of the concrete, f'_c. The average stress, f, is obtained by dividing the axial load, P, by the gross area of the cross section. The ratio f/f'_c is equivalent to the ratio P/P_u for members without longitudinal reinforcement. Figure 5.62 shows that axial loading increases the torsional strength of a member for

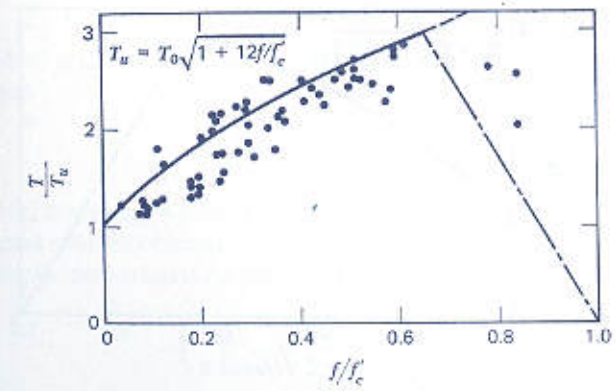

FIGURE 5.62. Torsion combined with axial compression for members without transverse reinforcement.[105]

values of f/f'_c up to about 0.7. For higher values, the few tests made in this range seem to indicate that the torsional strength has a tendency to decrease. Bishara and Peir[105] have proposed the following equation for calculating the strength of members simultaneously subjected to torsion and axial loading:

$$T = T_{up}\sqrt{1 + 12\frac{f}{f'_c}} \tag{5.56}$$

A similar approach has been proposed by Hsu.[106]

This equation is considered valid for values of f/f'_c of up to 0.7. For higher values, strength may be estimated by connecting with a straight line the value of T corresponding to $f/f'_c = 0.7$ with the point corresponding to pure axial loading; the results of the few available tests all lie above this line.

5.4.6.2 Members with Transverse Reinforcement

Very few tests of members of this type have been made. Figure 5.63 shows the results of a series of tests carried out by Bishara and Peir.[105] The interaction between torsion and axial loading is similar to that of members without transverse reinforcement; their strength under combined loading may be estimated by means of Eq. (5.56) if T_{up} is taken as the strength under pure torsion of a member with transverse reinforcement, T_u. Therefore,

$$T = T_u\sqrt{1 + 12\frac{f}{f'_c}} \tag{5.57}$$

The value of T_u can be computed by means of Eq. (5.55), proposed in Section 5.4.2.2 for members with transverse reinforcement under pure torsion.

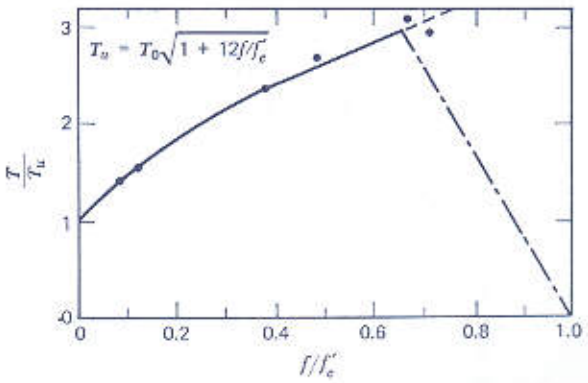

FIGURE 5.63. Torsion combined with axial compression for members with transverse reinforcement.[105]

Equation (5.57) is considered applicable for values of f/f'_c of up to 0.65. For higher values of this ratio, the same method described for members without transverse reinforcement may be used.

5.4.7 Design for Torsion

Since torsion usually acts simultaneously with flexure and shear, it is necessary to consider in design the interaction of all three actions. As indicated in Section 5.4.5, there is as yet no universally accepted rigorous method for taking such interaction into account. However, several design methods have been proposed recently which consider it in an approximate though conservative way.[100,107–109,110] Reference 107 gives a summary of the design methods which were in use before the results of the more recent investigations were available. In this section, a design method based on these later results is suggested, and the provisions of the 1971 ACI Code are briefly reviewed.

Suggested Design Procedure. To design the reinforcement required in a section subjected to a combination of actions T_u, V_u, and M_u the procedure described below may be followed:

1. The shear web reinforcement, A_v, is determined in the same way as for beams without torsion.
2. The contribution of the concrete to pure torsion is estimated by means of Eq. (5.49).

$$T_c = \frac{2.4x^2y\sqrt{f'_c}}{\sqrt{x}}$$

3. The torsion to be resisted by the transverse reinforcement, T_s, is computed from

$$T_s = T_u - T_c$$

[cf. Eq. (5.44)] and the amount of transverse reinforcement for torsion is obtained from

$$\frac{A_{sv}}{s} = \frac{T_s}{\alpha_t f_{yv} x_1 y_1}$$

[cf. Eq. (5.45)] where $\alpha_t = 0.66 + 0.33\, y_1/x_1$ but is not greater than 1.5.

4. The total amount of transverse reinforcement is computed by adding the shear and the torsion transverse reinforcements:

$$\left(\frac{A_v}{s}\right)_{\text{total}} = \frac{1}{2}\frac{A_v}{s} + \frac{A_{sv}}{s}$$

This total amount corresponds to the area of one stirrup leg. Generally, the shear transverse reinforcement, A_v, as computed from the usual equations, is

the area of all the stirrup legs. Thus, in the above equation A_v/s has been multiplied by 1/2, since transverse reinforcement for torsion usually consists of two leg stirrups.

5. The longitudinal torsion reinforcement is obtained from the following equation, which is derived from Eq. (5.54) by making $\eta = 1$:

$$A_s = \frac{2A_{sv}}{s}(x_1 + y_1)$$

6. The total longitudinal reinforcement is determined by adding the longitudinal reinforcements for torsion and flexure. The reinforcement designed in this way must comply with the following two requirements.

(a) The beam must be under-reinforced. This can be checked by applying Eq. (5.52).

(b) The strength of the section must be greater than that of the same section without transverse reinforcement. This can be done as explained below.

Since the torsional reinforcement must be added to the flexural reinforcement, the tension steel ratio of members designed by this procedure will always be greater than the compression steel ratio. Therefore, it is not necessary to consider torsion–flexure interaction as the torsional strength is not diminished by flexure, in members in which $\rho > \rho'$ (Section 5.4.3). This design criterion was proposed by Mattock.[100]

It was mentioned in Section 5.4.4.2 that the torsion–shear–interaction diagram for a member with transverse reinforcement can be considered as the combination of the interactions of the contributions of the concrete and of the steel. In the proposed design method, the interactions shown in Fig. 5.64 were assumed. Figure 5.64(a) means that in the concrete contribution, interaction is neglected; that is, that torsion does not reduce the concrete contribution to shear and vice versa. Figure 5.64(b) means that separate amounts of transverse reinforcement are required for torsion and shear.

It is difficult to determine the concrete contribution interaction, and, therefore, some kind of assumption must be made. This assumption should be a simple one as the error that may be committed when evaluating this interaction is not significant when referred to the total interaction, for members with ordinary amounts of transverse reinforcement.

As indicated previously, it is necessary to check that the strength of the beam is greater than the strength of a similar beam without transverse reinforcement. This is accomplished if the interaction diagram of the reinforced beam envelops the interaction diagram of the beam without transverse reinforcement, as shown in Fig. 5.64(c). The latter can be assumed to be circular, if represented in a nondimensional diagram, or elliptical, if represented in a dimensional diagram.

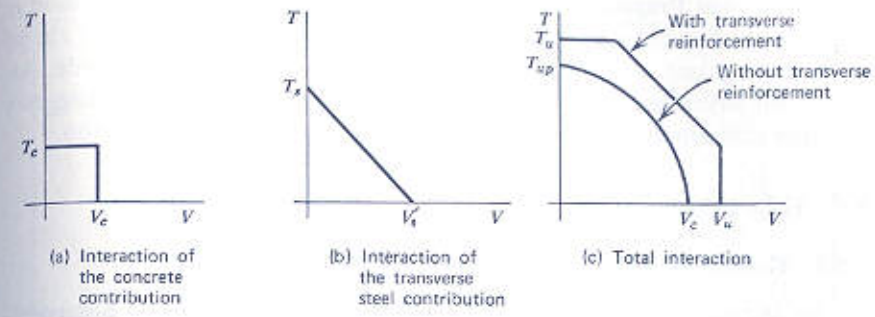

FIGURE 5.64. Torsion–shear interaction assumed in the design procedure.

Strengths computed with the suggested design method have been compared with the measured strengths of beams tested under combined torsion, shear and flexure by Osburn, Mayoglou, and Mattock,[110] Klus[104] and McMullen.[99] The average value of the ratio between the experimental and the computed values of T is 1.17 and the coefficient of variation is 14%. Some of McMullen's tests which did not comply with the limitations of under-reinforced beams were not included in the comparisons.

ACI Design Procedure. In this procedure a circular interaction diagram is assumed for the concrete contribution and a straight line, such as the one shown in Fig. 5.64(b), for the transverse reinforcement contribution. The procedure is similar to the one proposed before, but the amount of torsional moment and of shear force resisted by the concrete contribution is computed from the following equations:

$$T_{ca} = \frac{2.4\sqrt{f'_c}}{\sqrt{1 + (1.2v_u/v_{tu})^2}} \sum \frac{x^2 y}{3}$$

$$V_{ca} = \frac{2\sqrt{f'_c}}{\sqrt{1 + (v_{tu}/1.2v_u)^2}} bd$$

where

$$v_{tu} = \frac{3T_u}{\sum x^2 y}$$

$$v_u = \frac{V_u}{bd}$$

Requirements on maximum stresses and on limitations of reinforcement are included in the Code.

Design Method Proposed by Walsh, Collins, and Archer.[108] This method is also derived from the concept of interaction diagrams, although the shape of these diagrams is not the same as that considered in the ACI Code. An important advantage of the method is its simplicity. Reference 108 suggests a design procedure and presents an example illustrating its application.

5.5 SPECIAL CASES

5.5.1 General Remarks

In this section, some members with special problems are briefly discussed. The discussion is limited to a general presentation of the problems. Useful references are recommended.

5.5.2 Deep Beams

Deep beams are beams with span–depth ratios of about 3 or less. The classical theory of flexure cannot be applied to deep beams, even if the material is considered linear and elastic, because the stress distribution differs significantly from a linear one. Several authors have determined theoretical stress distributions in elastic deep beams, some of which are presented in Reference 111.

Results of tests of deep beams by various researchers have been summarized by Leonhardt,[111] including those corresponding to the Stuttgart deep-beam tests carried out by Leonhardt himself and Walther.[112] According to the experimental evidence, before cracking takes place, the stress distribution in a concrete deep beam is similar to that obtained from an elastic analysis. Once cracking has appeared, the stress distribution changes completely. If the flexural steel is sized following elastic assumptions, the actual stresses in the steel are much lower than the theoretical stresses since the lever arm increases considerably because of cracking. To take this into account, Leonhardt recommends a simplified procedure for determining the flexural steel area. This procedure consists in dividing the maximum required external moment by a lever arm, which depends on the span–depth ratio, the type of loading and on whether the beam is simply supported or continuous.[20,111]

The behavior after cracking roughly approximates that of a tied arch, as shown schematically in Fig. 5.65. (This figure also shows typical cracking patterns for two different types of loading.) Consequently, the stress in the flexural steel is practically constant along this span. Therefore end anchorage is an important consideration, and cutoffs and bends must be avoided.

The support reactions of deep beams are usually quite high. Frequent failures in the bearing areas have been observed in laboratory tests. Therefore, care should be taken in the design of the bearing details. It is sometimes

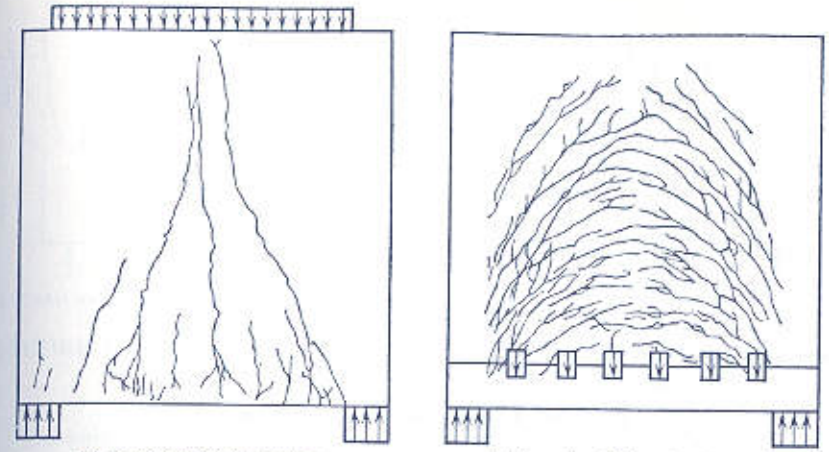

FIGURE 5.65. Typical crack patterns in deep beams.[111]

advisable to widen the part of the beams over the bearing area. Special reinforcement should be provided. Detailed recommendations are given by Leonhardt.[111,112]

The effect of shear in deep beams has been studied by Paiva and Siess,[113] who found that shear reinforcement does not contribute significantly to strength. However, stirrups are helpful in the control of cracking. Both vertical and horizontal reinforcement are used.

The ACI 1971 Code recommendations for deep beams are based mainly on the work of Paiva and Siess.[113] Design for shear is covered in detail. Requirements for the vertical and transverse shear reinforcement are given. On the basis of the Paiva and Siess findings, the ACI Code permits a greater concrete contribution, V_c, than for long beams. With regard to flexure, the Code merely indicates that lateral buckling and the nonlinear distribution of stresses should be taken into account.

5.5.3 Corbels

Corbels (sometimes also called brackets) are structural elements with shear–span/depth (a/d) ratios of less than 1. Their behavior has been investigated experimentally by testing specimens such as the one shown in Fig. 5.66. Two main types of failures have been observed,[114] which are described in the following paragraphs:

1. *Diagonal splitting failure.* In this type of failure, an initial flexural cracking is followed by an inclined crack extending from the top face of the

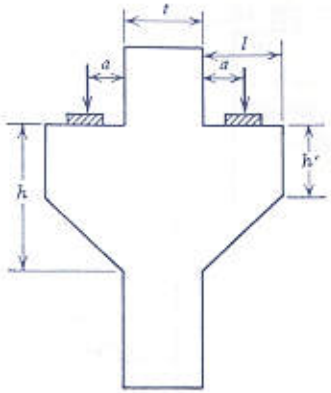

FIGURE 5.66. Corbel test specimen.

corbel, at the border of the loaded area, to the intersection of the sloping face of the corbel and the column. Failure takes place in the concrete compression zone and is similar to the shear–compression failure of long members. Two specimens which failed in this way are shown in Figs. 5.67(a) and 5.67(b).

2. *Direct shear failures.* This type of failure is characterized by the development of small inclined cracks along the face between the column and the corbel. The cracks weaken this region until a direct shear failure takes place, as shown in Figs. 5.68(a) and 5.68(b).

In addition to these two types of failure and the flexural type of failure, which is similar to that of long members, there are two other ways in which corbels may fail: by spalling of the concrete on the end of the member [Fig. 5.69(a)] or by crushing of the concrete under the bearing plate [Fig. 5.69(b)]. Such failures may be avoided by correct detailing of the reinforcement and the geometrical shape of the corbel.[114,115]

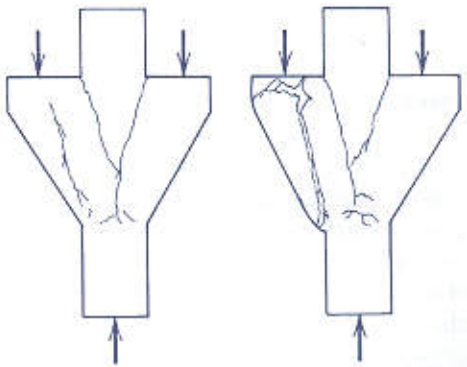

FIGURE 5.67. Diagonal splitting failures.[114]

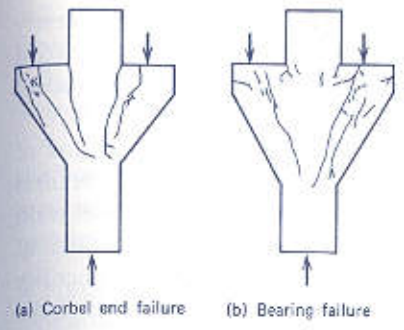

FIGURE 5.68. Direct shear failure.[114]

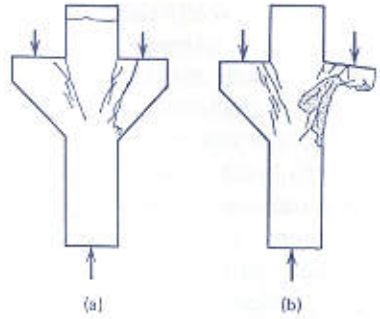

FIGURE 5.69. Secondary modes of failure.[113]

Corbels are often used as supports for precast beams, which are subject to volumetric changes caused by temperature variations, shrinkage, and creep. The corresponding longitudinal changes originate additional horizontal forces acting on the corbels. Horizontal forces may also be generated by seismic or wind loads. There is experimental evidence that horizontal forces have considerable influence on the behavior of corbels and can significantly reduce their strength. This effect may be explained by the fact that the horizontal forces increase the flexural cracking, which precedes a splitting failure and reduces the available shear strength in the case of direct shear failures.

In this type of member, vertical stirrups are inefficient, since the angle of the inclined cracks is much larger than 45°. Therefore, in corbels under vertical load it is common to use horizontal stirrups only. The effect of horizontal forces should be considered in design, as these tend to reduce the effectiveness of such horizontal reinforcement.

The formulas currently used in the design of corbels are based on experimental results. The 1971 ACI Code includes recommendations which are based mainly on References 114 and 115. Design examples are presented in References 20 and 114. When the a/d ratio is less than 0.5, the shear strength of corbels may be obtained by means of the shear-friction method (Section 5.3.8).

Franz and Niedenhoff[116] have made a thorough experimental and theoretical investigation of the behavior of corbels, including the influence of the shape of the corbel, the type of reinforcement and the point of application and type of load. These authors suggest simplified design methods. The state of the art is summarized in References 111 and 146.

5.5.4 Shear Walls

Shear walls are used to provide strength and stiffness in tall buildings subjected to horizontal forces. There are two important differences between deep

beams and shear walls. First, deep beams are usually loaded transversely through the extreme fibers in compression, while shear walls are loaded through slab diaphragms. Second, deep beams are not subjected to axial loads, as shear walls are.

The flexural strength of tall shear walls can be evaluated by means of conventional interaction diagrams.[117] Sometimes the required flexural reinforcement is uniformly distributed over the whole depth of the wall. Cárdenas, *et al.*[118] have developed equations for predicting the flexural strength when this kind of reinforcement is used. However, when ductility is an important design consideration it is better to concentrate much of the flexural reinforcement near the ends of the wall.[117]

The 1971 ACI Code includes design equations for shear which are based on Ref. 118. According to these equations the shear strength of a wall is the sum of a concrete contribution and a web reinforcement contribution. However, according to Paulay[117] where yielding of the flexural reinforcement can occur the concrete contribution must be neglected and horizontal stirrup reinforcement should be provided for the total shear.

In shear walls with heights comparable to their depth, Paulay[117] recommends limiting the nominal shear stresses to $6\sqrt{f'_c}$ and resisting the whole shear force with web reinforcement, since the flexural failure mechanism is associated with large cracks.

Some damage has been observed at construction joints of shear walls subjected to severe earthquakes. A minimum amount of reinforcement can be provided in the web to avoid these damages using the shear friction concept.

The coupling beams in coupled shear walls are often subjected to large deformations. It has been proved that compression reinforcement is not effective in increasing the ductility of these short beams and that better behavior is obtained by using diagonal reinforcement.[117]

Design recommendations for shear walls are also given by Blume, Corning, and Newmark,[119] in the SEAOC Code[18] and in the Uniform Building Code.[120]

5.5.5 Beams with Openings

It is becoming increasingly common to provide large openings in beams in order to permit the placement of utility ducts and pipes. Nasser, Acavalos, and Daniel[121] have carried out a research program to investigate the effect of openings on the behavior of beams and to find simplified design methods for taking this effect into account. The results of their tests indicate that the following hypotheses are reasonable.

1. The behavior of a beam with large openings is comparable to that of a Vierendeel panel.

2. The members at the top and bottom of an opening may be assumed to have contraflexure points approximately at the midspans.
3. These members resist the external shear in proportion to their cross sectional areas when they have adequate transverse reinforcement.
4. The diagonal force concentration at the corners due to the shear in the horizontal member may be taken as twice the simple shear force. Nasser *et al.* recommend that these diagonal shear force concentrations be resisted by diagonal corner reinforcement.

If proper reinforcement is used, the strength of a beam with openings is not significantly reduced. However, openings reduce the stiffness, so that deflections become an important criterion in design.

5.6 DEFORMATIONS OF REINFORCED CONCRETE MEMBERS

5.6.1 General Remarks

Development of high-strength concrete and steel reinforcement has led to a growing tendency towards the use of slender structural members, so that deformation often becomes a major design consideration. Excessive deflections of a member under service loads can produce damage in other structural members or, more frequently, in nonstructural elements, such as partition walls, or may lead to problems such as ponding. Values of allowable deflections depend, from this viewpoint, on several factors, such as type of nonstructural element, type of connection between the structural member and the structural or nonstructural elements, and type of construction method. Also the human response to deflection is sometimes significant. Excessive deflections of structures are objectionable because they may give rise to a feeling of insecurity or because they are undesirable aesthetically. Deformations are also important in connection with the evaluation of stiffness of structural members, which may influence their capacity to resist compression loads. Under certain conditions of catastrophic loading, e.g., earthquakes or explosions, deformations are important as a measure of the energy absorbing capacity of the structure.

Two aspects are to be considered when dealing with deformations. On the one hand, it is necessary to be able to estimate deformations under given loading and environmental conditions; on the other, criteria for establishing acceptable limits for deformations must be developed.

The problem of fixing acceptable limits to deflections from these two points of view has as yet received little attention, though a few empirical rules limiting the deflection/span ratios or the absolute value of deflection are available, such as those presented by ACI Committee 435.[122,132]

The computation of deflection has been the subject of a considerable

amount of research and several methods for computing deflections have been proposed.[123,124] Selection of an appropriate method is complicated by the scatter in the laboratory test data on deflections for apparently "similar" beams. This scatter is partly due to uncertainties in positioning of reinforcement, dimensions, concrete and steel properties, and partly due to variations in shrinkage, curing conditions, concrete tensile strengths, and other such factors neglected in defining the characteristics of "similar" beams.

The problem of estimating deflections of members in actual structures is even more difficult than that of estimating deflections of laboratory tested members. Among the causes that complicate the problem, the following are the most important:

1. The behavior of concrete is time-dependent and therefore in any rigorous approach the loading history of the member investigated must be taken into account; in practice this is not usually possible, as loading conditions are uncertain both in magnitude and in time and duration of application. The variations of humidity and temperature with time, which influence long-time deflections, are also difficult to predict.
2. It is not easy to evaluate the effect of the interaction of the member under consideration with other structural members and nonstructural elements.
3. There are considerable uncertainties in the values of the moment of inertia that should be used in deflection computations because of the random nature of the distribution of cracks along the members. Furthermore, it is usually impractical to take into account the actual variations of moment of inertia due to the changes in steel distribution from one section to another.

In the following sections, methods for computing deflections in beams due to bending both under short- and long-time service loading as well as at collapse are presented. Some comments on the effects of shrinkage, creep, and temperature, are included, and longitudinal shortening and lengthening of structural members are discussed briefly.

5.6.2 Deflections under Short-Time Service Loading

5.6.2.1 General Treatment and Principal Variables

The level of cracking and the distribution of strains and stresses at various cross sections of a beam subjected to flexure are schematically shown in Fig. 5.70. The condition shown is typical at the service load level.[122]

In the regions where the external moment is less than the cracking moment, M_{cr}, the member is not cracked, the concrete in the tension zone effectively contributes to resist the external moment, and strains are quite small (Section A–A).

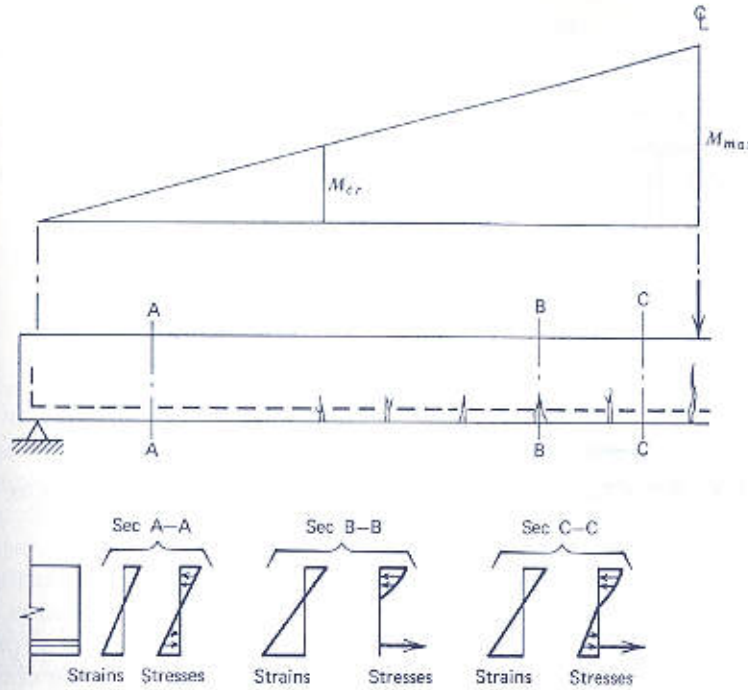

FIGURE 5.70. Cracking strains and stress distribution in a beam under service load.

In those regions where the external moment is greater than the cracking moment, two cases may be distinguished. The first case (Section B–B) corresponds to cross sections in which tension has caused cracking. In such cases, the concrete of the tension zone does not contribute significantly to the resistance to external moment. The second case (Section C–C) corresponds to sections between the tensile cracks. At such sections the concrete of the tension zone provides part of the resistance to moment, and the strains and stresses are less than those at a section coinciding with a crack.

If the strain distribution at a given section is known, it is possible to compute the curvature at this section by dividing the strain in a selected fiber, ε_c, by the distance to the neutral axis, y, provided that a linear distribution of strains across the depth of the member is accepted. Figure 5.71 shows the approximate distribution of curvature along the length of the beam, corresponding to the strain distributions given in Fig. 5.70. This distribution is somewhat irregular, since larger curvatures appear in the sections coinciding with cracks. Once the magnitude and the distribution of curvature along the beams are known, deflections can be computed by means of the area-moment or conjugate beam theorems.

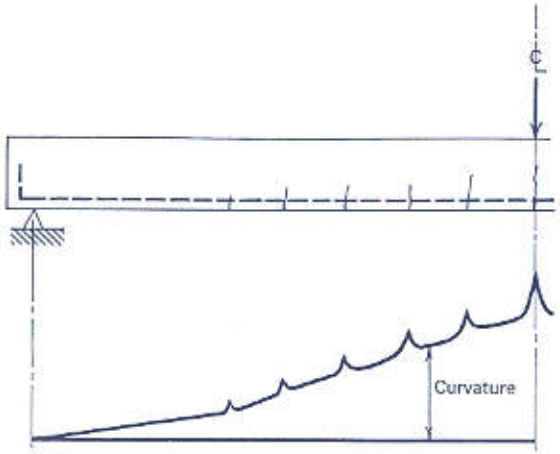

FIGURE 5.71. Distribution of curvatures in the beam of Fig. 5.70.

Obtaining deflections from the curvature diagrams is not practical in the case of reinforced concrete members, because of the labor involved in computing the curvature of different sections and because it is difficult to predict the distribution of curvature due to the random manner in which cracking takes place. In view of this, various simplified procedures have been developed, some of which are briefly described in Section 5.6.2.2. These simplified procedures attempt to take into account the following variables, which are those that seem to influence deflections most significantly:

1. *Tensile strength of the concrete.* Deflections tend to be smaller with increasing concrete tensile strength, as this means less cracking and thus a greater contribution to the flexural strength of the concrete in tension.
2. *Modulus of elasticity of the concrete.* Deflections also tend to decrease with increasing modulus, since strains, and consequently curvatures, are smaller.
3. *Longitudinal steel ratio.* Deflections increase with decreasing steel ratio.
4. *Cracking.* Deflections increase with cracking because the "peaks" in the curvature diagram are larger and more numerous (Fig. 5.71). The main variables influencing cracking are reviewed in another chapter of this text.

In Section 5.6.2.2 some simplified methods for calculating deflections of beams under short-time loading are given. Methods for long-time loading are discussed in Section 5.6.2.3.

5.6.2.2 Methods for Computing Deflections of Beams under Short-Time Loading

According to the more commonly used methods, deflections of reinforced concrete beams may be computed as for beams of a homogeneous and elastic material, so that the following well-known equations are applicable:

$$\frac{d^2y}{dx^2} = \frac{M}{EI} \tag{5.58}$$

$$y = \iint \frac{M}{EI} = \kappa_1 \frac{Wl^3}{EI} \tag{5.59}$$

in which κ_1 is a coefficient depending on the type of loading and restraints, and W is the total load on the span l.

The difference among the various methods consists mainly in the way in which the values of the modulus of elasticity, E, and of the moment of inertia, I, are chosen. Both quantities are difficult to define in a reinforced concrete member. The following discussion refers to the way in which these values are calculated in the various simplified methods.

Effective Beam Stiffness. Calculating curvature, ϕ, on the basis of cracked sections and linear behavior leads to the following equations:

$$\frac{M}{EI} = \phi = \frac{\varepsilon_s}{d-c} \qquad \varepsilon_s = \frac{f_s}{E_s} \qquad M = f_s A_s z$$

and therefore:

$$EI = \frac{M}{\phi} = E_s A_s (d-c) z \tag{5.60}$$

where c is the depth of the neutral axis and z is the arm of the internal couple of the beam.

This expression is based on neglecting the participation of concrete in tension between cracks. Actual deflections observed in tests under loads of short duration are often smaller than the calculated values based on a fully cracked section throughout the member. This is partly due to the participation of concrete in resisting tension stresses between the cracks and partly due to the variation of effective cross sections with varying bending moments along the span.

The participation of concrete in tension between cracks would reduce the elongation of the reinforcement and can be accounted for by defining an effective modulus E_s' of reinforcement and consequently an effective EI_{eff}. If tension in concrete is neglected, then the stress f_s in steel reinforcement at a cracked section caused by a constant bending moment M would produce in

the reinforcement an elongation δ between the cracks:

$$\delta = \int_l \frac{f_s}{E_s}\,dx = \frac{f_s}{E_s}\,l = \varepsilon_s l \tag{5.61}$$

If the contribution of the concrete in tension is considered, then the stress f_s in the steel reinforcement is a variable and the elongation δ' is less than δ and may be defined using a reduction factor ψ:

$$\delta' = \int_l \frac{f_s}{E_s}\,dx = \psi\delta = \psi\varepsilon_s l = \psi\,\frac{f_s}{E_s}\,l \tag{5.62}$$

where $\psi\varepsilon_s$ is the reduced average strain in the steel reinforcement. If the average curvature ϕ' is now defined as $\psi\varepsilon_s/(d-c)$, then the effective stiffness EI_{ett} can be expressed as M/ϕ'

$$EI_{ett} = E_s' A_s (d-c)z = \frac{E_s}{\psi} A_s (d-c)z = \frac{E_s d^2}{\psi}\left(1-\frac{c}{d}\right)\left(\frac{z}{d}\right) \tag{5.63}$$

The values of $c/d = k$ and $z/d = j$ in Eq. (5.63) must be calculated using effective modulus E_s'. Values of ψ, proposed by some investigators, have been indicated in Chapter 4, Section 4.7, pp. 175–176.

For practical purposes the value of EI has often been calculated using a moment of inertia I based on a gross uncracked concrete section ignoring the effect of steel. This approach gives reasonable values for relatively deep beams lightly cracked, but for many beams it often underestimates actual deflections.

Methods Proposed by Yu and Winter.[123] These writers have proposed two methods. In the first method, E is taken as the modulus of elasticity of concrete, E_c, and I, as the moment of inertia of the cracked transformed section. In simply supported beams the moment of inertia corresponding to the midspan section is used; in continuous beams the average of the moments of inertia corresponding to the regions of positive and negative moments is taken. This method does not take into account that the behavior of a reinforced concrete beam is fundamentally different before and after cracking of the concrete in the tension zone. The contribution of the concrete in tension between cracks is neglected.

The second method is a refined version of the first method, which does consider the contribution of the concrete acting in tension between cracks. To take this contribution into account, the deflections computed by the first method, that is, using the moment of inertia of the transformed cracked section, are multiplied by the following corrective factor:

$$1 - b_w \frac{M_1}{M_{\max}} \tag{5.64}$$

where b_w is the width of the web in the tension zone, $M_{\max}$ is the maximum external moment under service loads, h is the total depth, and

$$M_1 = 0.1(f_c')^{2/3} h(h-c)$$

The Yu and Winter methods have been checked against the results of 90 tests. The measured deflections do not differ from the computed values by more than 20% in most of the cases. The comparison indicates that the second method gives better results than the first, but the difference with regard to the first method is not significant.

ACI 1971 Code Method. This method is based on proposals by Branson,[124] according to which the influence of cracking can be taken into account by using an average effective moment of inertia, I_{eff}, along the length of the beam. The value of I_{eff} recommended by the Code is as follows:

$$I_{\text{eff}} = \left(\frac{M_{cr}}{M_{\max}}\right)^3 I_g + \left[1 - \left(\frac{M_{cr}}{M_{\max}}\right)^3\right] I_{cr} \tag{5.65}$$

where M_{cr} is the cracking moment of the homogeneous concrete section calculated using a modulus of rupture of $7.5\sqrt{f_c'}$, $M_{\max}$ is the external maximum moment, but not less than M_{cr}, I_g is the moment of inertia of the complete section without considering the reinforcement, and I_{cr} is the moment of inertia of the transformed cracked section. The value of I_{eff} computed with Eq. (5.65) should not be taken larger than I_g.

For continuous beams the Code specifies that the average of the effective moments of inertia of the regions of positive and negative moments should be used. For lightweight-aggregate concrete the modulus of rupture should be reduced appropriately.

Variations on the above methods[125,126] have been developed in Europe and form the basis for CEB[30] and other[127] codes.

5.6.3 Deflections under Long-Time Service Loads

5.6.3.1 Behavior and Main Variables

If a beam remains under sustained loading during a long period of time, new cracks develop, the width of the existing cracks increases, and the deflection may duplicate or even triplicate. Such behavior is due to shrinkage and creep, the mechanisms of which are covered in detail in Chapter 3.

Effect of Shrinkage. This effect is illustrated in Fig. 5.72 for a simply supported beam with tension reinforcement only. The top fibers shorten freely, while shortening of the bottom fibers is restricted by the presence of the steel reinforcement. The curvature and consequently the deflection caused

particles are separated from each other by the paste. A freshly mixed *cement paste* is a body having a structure which exhibits properties not possessed by a perfect fluid, namely, *plasticity* and *viscoelasticity*. These two properties largely determine the rheological behavior of fresh concrete. The *aggregates* also have significant influence on the properties of fresh concrete primarily through their shape, texture, grading, and maximum size. The concrete mix proportions, including the water-cement ratio and the aggregate content, or richness of mix, are important factors influencing properties of fresh concrete. Many of these properties and factors are discussed in detail by T. C. Powers.[19]

1.10.2 Workability and Consistency

Workability and consistency of fresh concrete[1,20] are two closely related properties. *Workability* is that property of freshly mixed concrete which determines the ease and homogeneity with which it can be mixed, transported, placed, compacted, and finished. It is a property which depends on the specific conditions of placement; a concrete that is workable under some conditions may not be workable under some other conditions. For example, a concrete mix suitable for massive construction, e.g., of a bridge pier, would not have the required workability for placement in a heavily reinforced column. Thus, a concrete mix should have the needed workability for its intended use. Also, it should not segregate nor bleed excessively. None of the test methods proposed or in use today simultaneously measure all of the properties involved in workability. In practice, the workability of a mix is judged by several properties including consistency, ease of conveying and placing, and lack of segregation or of excessive bleeding. An experienced concrete technician can readily judge when fresh concrete has adequate workability for use in a given situation. In the laboratory, one of the tests sometimes used for evaluation of the workability of a concrete mix is the Remolding Test,[20] which measures the relative effort required to change the shape of a mass of concrete from one definite shape to another. However, it does not give a measure of the tendency to segregate and bleed or ease of finishing.

Some of the important factors that affect the workability of concrete are (1) relative quantities of paste and aggregates, (2) plasticity of the paste itself, (3) maximum size and grading of aggregates, and (4) shape and surface characteristics of aggregate particles.

Consistency or fluidity of concrete is an important component of workability and refers in a way to the wetness of the concrete. However, it must not be assumed that the wetter the mix the more workable it is. If a mix is too wet, segregation may occur with resulting honeycomb, excessive bleeding, and sand streaking on the formed surfaces. On the other hand if a mix is too dry it may be difficult to place and compact, and segregation may occur because of lack of cohesiveness and plasticity of the paste.

Consistency of concrete is generally measured by the *slump test* (ASTM C143). This test is performed by measuring the slump (subsidence), in inches, of concrete after removal of the truncated cone mold in which the freshly mixed concrete was placed. Details of the test procedure and the dimensions of the cone and tamping rod are given in ASTM C143. The greater the slump, the wetter or more fluid is the concrete mix. The consistency or degree of wetness corresponding to a slump of 0 to 1 in. could be classified as dry, of 1 to 2 in. as stiff, of 2 to 5 in. as medium, and of 5 to 7 in. as wet. For structural concrete a slump of 3 to 4 in. is ample for placement in forms. What is sometimes regarded as a need for wetter concrete may be better satisfied by more thorough vibration. The use of adequate vibration rather than of a wetter mix will not only insure a more thorough compaction but also the quality of concrete will be superior by not increasing the water content to obtain a greater slump. Excessive vibration in local zones may cause undesirable segregation, and care must be taken to prevent this. Heavy structural members and slabs can be satisfactorily placed using a 2-in.-slump concrete if properly vibrated.

Another method frequently used in the field and laboratory to measure the consistency of concrete is the *ball penetration test* (ASTM C360). It is performed by measuring the penetration, in inches, of a 6-in.-diameter steel cylinder with a hemispherically shaped bottom, weighing 30 lb. The ball penetration test can be performed on the concrete in a hopper, buggy, wheelbarrow, or other suitable container. The principal advantage of this method is its simplicity and the rapidity with which the consistency of the concrete can be determined. Details of the test procedure and the ball-penetration apparatus are given in ASTM C360. There is a direct relationship between slump and ball penetration for a given mix but it varies according to the mix. The ratio of slump to the penetration of the ball is between 1.5 and 2.

In addition to the two standard methods of measuring consistency here described, there are several other methods which are principally used as research tools. They include the Vebe consistometer and the Thaulow concrete tester. These two methods are useful in measuring the consistency of a very stiff concrete such as used for precast concrete products. The Compacting Factor test is a standard method used in Great Britain. The various methods of measuring consistency are described by C. A. Vollick.[20]

1.10.3 Segregation and Bleeding

Since concrete is not a homogeneous material but a mixture of ingredients differing in particle size and specific gravity, it is subject to *segregation*. This undesirable property is a separation or differential settlement of the

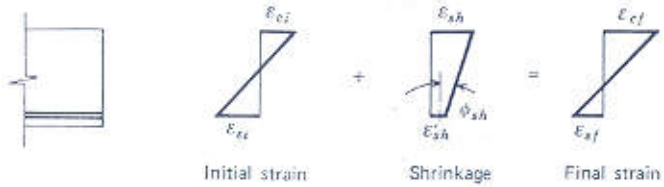

FIGURE 5.72. Effect of shrinkage in a beam with tension reinforcement only.

by shrinkage in such members are of the same sign as those produced by the transverse loads.

In members with both tension and compression reinforcement, the top fibers cannot shorten freely, and the curvatures and deflections are less than for beams with tension reinforcement only. If the section is symmetrical in shape, and the tension and compression reinforcements are equal, shortening of the top and bottom fibers of the member is the same; therefore, shrinkage does not produce curvatures and deflections other than those originating in the natural variations in the properties of concrete and in the placing of reinforcing bars.

The principal variables influencing deflections due to shrinkage, in addition to the ratio between the tension and compression reinforcement, are the same as those influencing shrinkage of plain concrete. Consequently, the greater the shrinkage unit strain, ε_{sh} (Fig. 5.72), the greater the deflections of the member. It should be mentioned that shrinkage deflections occur even when the member is unloaded.

Effect of Creep. The effect of creep on the change in curvature is illustrated in Fig. 5.73. Lines *A* represent the distributions of strains and stresses immediately after loading, while lines *B* represent the distributions which result when the loads have been applied for a certain time. Strains in the concrete

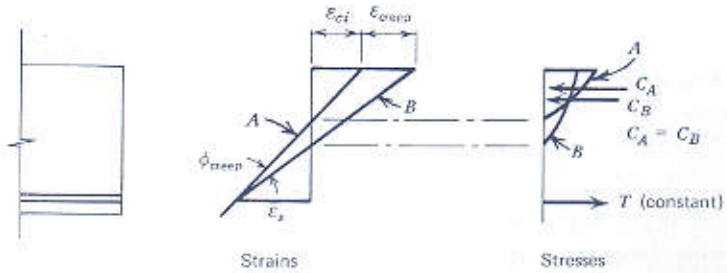

FIGURE 5.73. Effect of creep in a beam with tension reinforcement.

increase with time, while stresses decrease as a result of the downward movement of the neutral axis of the section. However, it has been shown experimentally that strains at the level of the reinforcement remain practically constant.[128]

The increase in strains in simple concrete caused by creep is discussed in Chapter 3. In a reinforced concrete element this increase in strain takes place under a variable state of stress because of the changing position of the neutral axis. It can be computed from the increase in strain under constant load by the rate of creep method or the superposition method.[129]

In a member with compression reinforcement, in addition to the reduction of stresses in the concrete resulting from the changing position of the neutral axis, there is another decrease in stress caused by the transfer of stresses from the concrete to the reinforcement. Consequently, the reduction of the stresses in the concrete is greater than in members with tension reinforcement only. On the other hand, strains due to creep increase with the applied stresses (Chapter 3). Therefore, in a member with compression reinforcement, the strains caused by creep are less than in a member with tension reinforcement only because in such members the decrease in long-time stresses is greater.

The main variables influencing the deformations caused by creep are the ratio of compression reinforcement, the magnitude of the applied stresses, and all the variables which affect the deformations due to creep in plain concrete. These variables are discussed in Chapter 3.

In contrast with behavior under shrinkage, a member must be loaded for creep to produce variations in strain.

5.6.3.2 Methods for Computing Deflections of Members under Long-Time Loading

So many variables influence the deformations caused by shrinkage and creep that it is not possible to consider all of them in a simple, and at the same time rigorous, method. As a result, the methods that have been proposed take into account only the most significant variables and, furthermore, do so in a simplified manner.

The effects of shrinkage and creep are usually considered simultaneously, though some methods evaluate them independently.[122] In the first three methods described below, which correspond to those presented for short-time loading, those effects are considered simultaneously, while in the fourth one, they are taken independently.

Yu and Winter's Methods.[123] These authors propose two methods. In one, the influence of time is taken into account by use of a reduced modulus of elasticity, E'_{ct}. The recommended values are given in Table 5.2. The moment of inertia is computed from the cracked transformed section and the modular ratio $n' = E_s/E'_{ct}$.

TABLE 5.2. Table for Computing the Modified Modulus of Elasticity[a] (Yu and Winter's Method).

f'_c, psi		2000			2500			3000			3750			5000		
Loaded age, days		7	14	28	7	14	28	7	14	28	7	14	28	7	14	28
Duration of Loading	30 days	0.55	0.66	0.79	0.58	0.71	0.86	0.60	0.75	0.91	0.63	0.79	0.97	0.66	0.83	1.04
	90 days	0 41	0.51	0.63	0.43	0.54	0.67	0.45	0.56	0.70	0.46	0.58	0.73	0.47	0.61	0.77
	1 year	0.28	0.36	0.44	0.29	0.37	0.47	0.30	0.38	0.48	0.30	0.39	0.50	0.31	0.40	0.51
	3 years	0.23	0.29	0.37	0.24	0.30	0.38	0.24	0.31	0.39	0.24	0.31	0.40	0.25	0.32	0.42
	5 years or more	0.22	0.28	0.35	0.22	0.29	0.37	0.23	0.29	0.38	0.23	0.30	0.39	0.24	0.31	0.40

[a] The modified modulus is equal to the instantaneous modulus multiplied by the factors of this table.

TABLE 5.3. Table for Computing Long-Time Deflections[a] (Yu and Winter's Method).

Duration of Loading, t	F			Duration of Loading, t	F		
	A_s only	$A'_s = A_s/2$	$A'_s = A_s$		A_s only	$A'_s = A_s/2$	$A'_s = A_s$
1 month	1.58	1.42	1.27	2 years	2.65	2.15	1.80
3 months	1.95	1.77	1.55	2 1/2 years	2.72	2.16	1.81
6 months	2.17	1.95	1.69	3 years	2.78	2.18	1.81
9 months	2.31	2.03	1.73	4 years	2.87	2.20	1.82
1 year	2.42	2.08	1.78	5 years	2.95	2.21	1.82
1 1/2 years	2.54	2.12	1.80				

[a] Long-time deflections are obtained by multiplying the instantaneous deflections by the factors of this table.

The second method is based on multiplying the value of the short-time deflections by a factor which is dependent on the ratio of the compression reinforcement and the duration of the applied load. This factor was obtained by statistical methods from the analysis of 68 tests. The recommended factors are given in Table 5.3.

ACI 1971 Code Method. This method is based on the second method proposed by Yu and Winter. The additional long-time deflections are obtained by multiplying the short-time deflections by the factor $[2 - 1.2(A'_s/A_s)]$. This factor was derived from the values proposed by Yu and Winter for a five-year duration of load. Further increases in deflections are considered negligible.

Corley and Sozen's Method.[130] These authors suggest that shrinkage deflections be computed from the corresponding curvatures, ϕ_{sh}, (Fig. 5.72), as given by the following expression:

$$\phi_{sh} = \frac{0.035}{d}(\rho - \rho') \tag{5.66}$$

Equation (5.66) was developed for concrete which exhibits a free shrinkage strain of the order of 500×10^{-6}. It can be modified for other concretes, although, according to Corley and Sozen, the modification is not worth considering, because of the large variations in observed shrinkage strains of ostensibly identical concretes and because shrinkage deflections are relatively small compared to the total deflection.

The creep deflections are computed from the creep curvatures (Fig. 5.73), which can be obtained from the following expression:

$$\phi_{creep} = \frac{\varepsilon_{creep}}{d} \tag{5.67}$$

Values of ε_{creep} depend mainly on the ratio between the compression and the tension reinforcement, ρ'/ρ, and on the shape of the cross section. Corley and Sozen propose the following values:

for rectangular sections,

$$\varepsilon_{creep} = \varepsilon_{ci}\left(3 - \frac{\rho'}{\rho}\right) \tag{5.68}$$

for flanged sections with $c > 2t/3$,

$$\varepsilon_{creep} = 2\varepsilon_{ci}\left(3 - \frac{\rho'}{\rho}\right) \tag{5.69}$$

where ε_{ci} is the instantaneous compression concrete strain and t is the thickness of the compression flange.

5.6.4 Deflections at Collapse

5.6.4.1 Moment–Curvature Diagrams

The behavior and the load–deflection curve of a member subjected to flexure until collapse was described in Section 5.2.3 and Fig. 5.6. The deflection for any given value of the applied loading may be computed by the general method of integrating the curvatures along the length of the member. In order to apply this method, it is first necessary to know the curvature at the cross sections of the member for different values of the flexural moment. This relationship is defined by a moment–curvature diagram, which can be obtained as follows.

A strain, ε_c, is selected for the top fiber, and the depth of the neutral axis, c, required for equilibrium of the cross section, is determined by means of the procedure described in Section 5.2.5. The values of ε_c and c define the distribution of strains in the cross section. From this distribution of strains, the tension and compression forces, together with the internal moment, M, are computed (Section 5.2.5). The curvature, ϕ, is computed by dividing the strain, ε_c, by the depth of the neutral axis, c. Thus, a value of M and a value of ϕ are determined, which define a point of the moment-curvature diagram. By repeating this procedure for other values of ε_c, other points of the diagram can be obtained.

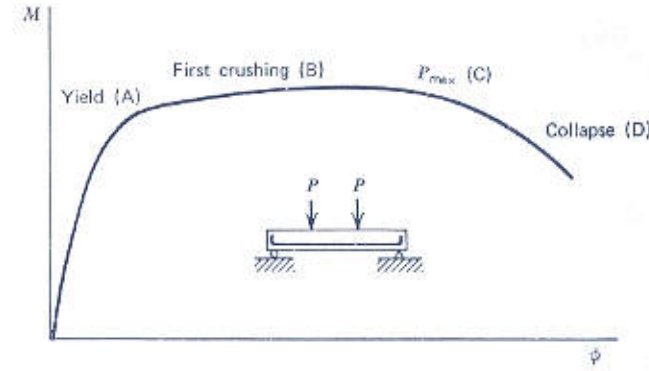

FIGURE 5.74. Moment—curvature diagram of a beam tested to collapse.

The shape of a moment–curvature diagram is similar to that of a load–deflection diagram (Fig. 5.74). To define the general shape of an $M - \phi$ diagram, it is sufficient to determine the points corresponding to the first yielding of the steel, to the initial crushing of the concrete, to the maximum load and, finally, a point on the descending portion of the curve. These points are represented in Fig. 5.74 by letters A, B, C, and D. The distributions of strains and stresses for each of these points are shown in Fig. 5.75.

For the point corresponding to first yielding of the steel, the steel strain is known ($\varepsilon_s = \varepsilon_y$), and c is determined from equilibrium. The distribution of stresses in the concrete is practically linear because the strains are small [Fig. 5.75(a)].

For the point corresponding to initial crushing of the concrete, the strain, ε_c, of the top fiber of the cross section, usually taken as approximately 0.003, is known. The distribution of stresses is determined from the stress–strain curve of the concrete. The strain in the steel is larger than that corresponding to first yielding; the corresponding stress must be determined from the stress–strain curve. The effect of strain-hardening must be considered, as otherwise the error may be significant [Fig. 5.75(b)].

The point corresponding to the maximum load is not well defined in the load–deflection and moment–curvature diagrams; within a considerably wide range of curvatures the load remains practically constant. Nor is the beginning of the descending branch of the curve clearly established. It is possible to determine a number of points corresponding to this part of the curve by considering various values of ε_c and determining c from equilibrium requirements [Fig. 5.75(c)], but for this it is necessary to have stress–strain curves for the concrete showing the descending branch. There is some evidence indicating that values of ε_c much higher than 0.003 may be attained

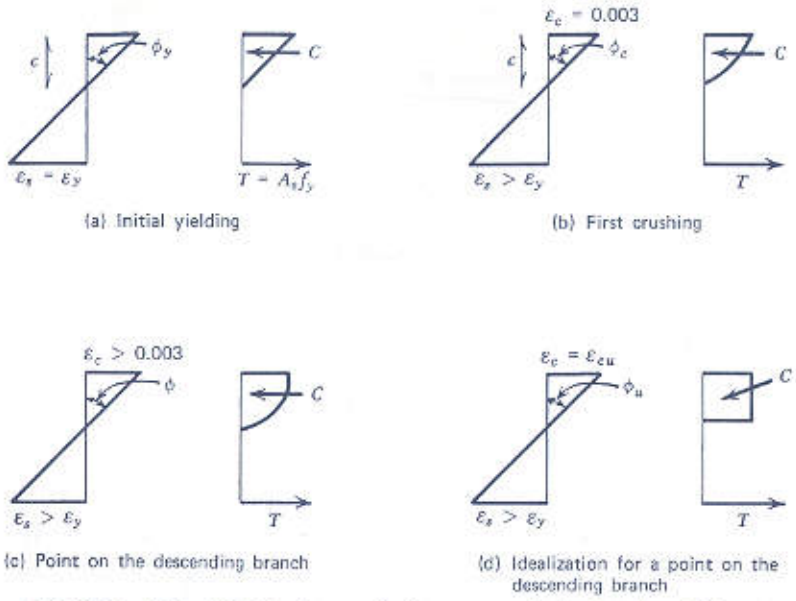

FIGURE 5.75. Distributions of stresses and strains for different points of the $M - \phi$ diagram.

and that the shape of the curve varies with the amount of transverse reinforcement, since such reinforcement increases the ductility of the concrete. In Section 5.2.9 it was mentioned that the shape of the stress–strain curve of the concrete has little influence on the flexural strength of members. However, this factor is of great significance in the values of the deformations at maximum load and at collapse. It is usual to resort to simplified hypotheses according to which the actual $f_c - \varepsilon_c$ curve is substituted by an idealized diagram; the member is considered to attain its strength or its collapse load when the concrete reaches the strain corresponding to failure, ε_{cu} [Fig. 5.75(d)]. In Section 5.6.4.3 values suggested for ε_{cu} are presented.

The inelastic deflections computed by integrating the curvature diagrams are less than the corresponding measured values obtained from tests. The reason for this is that in the region of maximum moment of a member, the maximum curvature extends along a certain length. Thus, in a beam with a concentrated load (Fig. 5.76), the maximum curvature exists not only in the cross-section of maximum moment, but also along a certain distance on each side of this section. In the methods that have been proposed, it is considered that the maximum curvature is maintained along a certain length g (Fig. 5.76), which is called *length of plastic hinging* or *contamination length*. The product of the curvature, ϕ_u, and the length g, is called the *inelastic rotation* and accounts for an important proportion of the total rotation of a member.

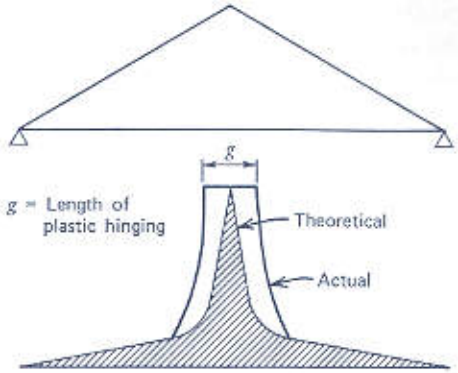

FIGURE 5.76 Theoretical and actual distributions of curvatures in beam with a concentrated load.

5.6.4.2 Main Variables

The main variables influencing deflections at collapse are evident from the preceding description and may be summarized as follows:

1. The ratios of longitudinal reinforcement, which influences the extent of the range of nonlinear behavior.
2. The amount of transverse reinforcement. The strain at failure of the concrete, ε_{cu}, increases with increasing transverse reinforcement.
3. The strength of the concrete, f'_c, and the stress–strain curve of the steel, which affect the distributions of strains and stresses.
4. The variables on which g depends. There is as yet little information available on these variables.

5.6.4.3 Methods for Computing Deflections of Beams at Collapse

All the methods are based on the determination of simplified moment-curvature diagrams and the computation of deflections from these diagrams by applying the principles of the theory of strength of materials. The maximum curvature is considered to extend a distance $g/2$ beyond each end of the region or section of maximum moment.

The moment–curvature diagram is usually idealized as two straight lines: one from the origin to the point of yielding and one from the point of yielding to the point of maximum load. However, if it is desired to take into account the influence of the descending branch of the curve, the significance of which was mentioned previously and is discussed in Reference 141, it is necessary to include the point corresponding to collapse.

The point of yielding is determined from the distribution of strains and stresses of Fig. 5.75(a). The points of maximum loading or of collapse can be determined from the distributions shown in Fig. 5.75(d).

The differences between the various methods that have been proposed lie in the values of ε_{cu} [Fig. 5.75(d)] used in computing ϕ_u and in the values of g considered to take into account the extent of the region in which the maximum curvature is maintained. The following discussion of the various methods is limited to the presentation of the values of ϕ_u and g considered in them. In some cases, instead of the independent values of these parameters, their product, $\phi_u g$, or inelastic rotation, is given. All the values that have been suggested to date are based on experimental information.

Baker and Amarakone's Method.[131] According to this method, the strain of the concrete at failure should be calculated with the following equation, which is based on the results of a test program sponsored by CEB:

$$\varepsilon_{cu} = 0.0015\left[1 + 150\rho'' + (0.7 - 10\rho'')\frac{d}{c}\right] \leq 0.010 \tag{5.70}$$

where ρ'' is the ratio of the confining transverse reinforcement.

The inelastic rotation for the section of maximum loading is computed with the equation

$$\theta_p = 0.8(\varepsilon_{cu} - \varepsilon_1)\kappa_1\kappa_3\frac{i}{d} \tag{5.71}$$

In this equation ε_1 is the strain in the top fiber of the concrete when the steel strain is ε_y [Fig. 5.75(a)]; κ_1 is equal to 0.7 for hot-rolled steel and to 0.9 for cold-worked steel; κ_3 is 0.6 when the strength of the concrete is 6000 psi and 0.9 when it is equal to 2000 psi, with intermediate values for intermediate strengths; i is the distance from the point of maximum moment to the point of inflection; and d is the effective depth of the section.

Corley's Method.[132] For determining the failure strain of concrete, the following equation is proposed:

$$\varepsilon_{cu} = 0.003 + 0.02\frac{b}{i} + \left(\frac{\rho''' f_{yv}}{20{,}000}\right)^2 \tag{5.72}$$

In this equation ρ''' is the ratio of confining reinforcement (volume of one closed stirrup plus the volume of compression steel between two stirrups, divided by the volume of the confined concrete); f_{yv} is the yield stress of the stirrup steel; b is the width of the section; and i is the distance from the point of maximum moment to the point of inflection.

With the value of ε_{cu} obtained in this way and the rectangular stress block recommended by the ACI Code, the curvature at failure, ϕ_u is computed

[Fig. 5.76(d)]. Once ϕ_u has been obtained, the inelastic rotation, θ_p, corresponding to the maximum load can be computed from equation

$$\theta_p = \phi_u d\left[1 + \frac{0.4}{\sqrt{d}}\frac{i}{d}\right] \tag{5.73}$$

González Cuevas and Díaz de Cossío's Method.[133] The failure strain of the concrete is obtained from the following equation:

$$\varepsilon_{cu} = 0.008 + 0.006f \tag{5.74}$$

where f is the confining stress as given by

$$f = \frac{2A_{sv}f_{yv}d''}{sc(2d'' - c)} \tag{5.75}$$

In Eq. (5.75) A_{sv} is the area of the stirrup, d'' is the distance between the tension and compression reinforcement, s is the stirrup spacing; the remaining parameters were defined previously.

The curvature ϕ_u is computed from this value of ε_{cu} and a rectangular stress block [Fig. 5.75(d)]. The length of plastic hinging, g, is taken as 20 in., so that the inelastic rotation is

$$\theta_p = 20\,\phi_u \tag{5.76}$$

Since in this method the failure strain depends on the confining stress, f, which in turn depends on the depth of the neutral axis, it is necessary to proceed by trial and error until a distribution of strain is found such that the section is in equilibrium and Eq. (5.74) is satisfied. Reference 133 presents graphs giving the value of θ_p for different sections, tension reinforcement ratios, and confining reinforcement ratios.

The deflections obtained by this method correspond to a point of the load deflection diagram located on the descending branch, such that the load is 85% of the maximum load. Consequently, the deflections computed by this method are larger than those obtained with the other methods. According to Reference 133, this point is easy to reproduce in tests and makes it possible to use the descending branch of the load-deflection and moment-rotation diagrams.

Other Methods. Gaston,[134] Burns,[135] and Yamashiro[136] have proposed other methods which are of interest.

5.6.4.4 Moment–Rotation Diagrams

The moment–curvature diagrams can also be used to obtain moment–rotation diagrams. The procedure is practically the same one that was described for the computation of deflections, the only difference being that the

curvature diagram is integrated only once, in accordance with the theory of strength of materials.

5.6.5 Column Shortening

The previous sections have dealt with deformations caused by flexural loads. Axial loads also produce deformations, for example, column shortening or lengthening. Since columns are subjected in most cases to compression loads, only column shortening is considered here.

Column shortening, especially when time effects are considered, is important in multistory buildings because differential shortening of columns produces bending moments in the beams or slabs connected to the columns and causes transfer of load to the column that shortens less.

Time-dependent column shortening is caused by creep and shrinkage of concrete. Thus, it can be computed by multiplying the creep and shrinkage strains by the length of the member. However, the following factors must be taken into account:

1. The load is applied to the columns in several stages, depending on the construction time and on the number of stories. The age of the concrete corresponding to each stage must be considered, since the rate of creep strain is a function of the age of concrete at loading.
2. Reinforced concrete columns in multistory buildings are appreciably larger and of different shape than the specimens usually tested in the laboratory to determine creep and shrinkage strains. This fact must be taken into account, since the strains depend on the volume-to-surface ratio of the specimen.
3. Relative humidity in the structure can be different from the relative humidity in the laboratory. This fact changes the shrinkage strains.
4. Longitudinal reinforcement restricts creep and shrinkage strains. Thus, time-dependent shortening of a reinforced concrete column is smaller than the corresponding shortening of a plain concrete specimen.

Design aids to take the above mentioned factors into account can be found in Reference 137.

REFERENCES

1. Richart, F. E., Brandtzaeg, A., and Brown, R. L., "A Study of the Failure of Concrete under Combined Compressive Stresses," *University of Illinois Engineering Experiment Station, Bull.* 185, 1928.
2. Rüsch, H., "Researches Toward a General Flexural Theory of Structural Concrete," *ACI Journal*, July 1960.
3. Mörsch, E., *Concrete–Steel Construction* (Translation of the 3rd German Edition, Engineering News Publishing Co., New York, 1909.

4. Bach, C. and Graf, O., *Versuche mit bewehrten und unbewehrten Betonkörpern, die durch zentrischen und exzentrischen Druck belastet wurden," Julius Springer Verlag*, Berlin, 1914.
5. Talbot, A. N., "Tests of Reinforced Concrete Beams," *University of Illinois Engineering Experiment Station, Bull.* 1, 1904.
6. Slater, W. A., Lyse, I., Richart, F. E., Stachle, G. C., and Kreidler, C. L., "ACI Column Investigation," *ACI Journal*, Apr. 1930; Feb. 1931; March 1931; Nov, 1931; Jan. 1932; Feb. 1933; June 1933.
7. Richart, F. E. and Brown, R. L., "An Investigation of Reinforced Concrete Columns," *University of Illinois Engineering Experiment Station, Bull.* 267, 1934.
8. Richart, F. E., Draffin, J. O., Olson, T. A., and Heitman, R. H., "The Effect of Eccentric Loading, Protective Shells, Slenderness Ratios and other Variables in Reinforced Concrete Columns," *University of Illinois Engineering Experiment Station, Bull.* 368, 1948.
9. Hognestad, E., "A Study of Combined Bending and Axial Load in Reinforced Concrete Members," *University of Illinois Engineering Experiment Station, Bull.* 399, 1951.
10. Whitney, C. S., "Plastic Theory of Reinforced Concrete Design," *Trans. ASCE*, Vol. 107, 1942.
11. Mattock, A. H., Kriz, L. B., Hognestad, E., "Rectangular Concrete Stress Distribution in Ultimate Strength Design," *ACI Journal*, February 1961.
12. Granholm, H., *A General Flexural Theory of Reinforced Concrete*, John Wiley & Sons, Inc., 1965.
13. Sexsmith, R. G., "Reliability Analysis of Concrete Members," *ACI Journal*, May 1969.
14. "Building Code Requirements for Reinforced Concrete" (ACI 318–71), Amer. Concrete Institute Standard, 1971.
15. *Strength and Serviceability Criteria of Reinforced Concrete Bridge Members, Ultimate Design*, U.S. Dept. of Commerce, Bureau of Public Roads, 1966.
16. Bresler, B. and Gilbert, P. H., "Tie Requirements for Reinforced Concrete Columns," *ACI Journal*, November 1961.
17. Warwaruk, J., Sozen, M. A., and Siess, C. P., "Strength and Behavior in Flexure of Prestressed Concrete Beams," *University of Illinois, Engineering Experimental Station Bull.* 464, 1962.
18. Jensen, V. P., "The Plasticity Ratio of Concrete and Its Effect on the Use of Ultimate Strength of Beams," *ACI Journal*, Vol. 14, No. 6, pp. 565–582, June 1943.
19. Bresler, B., "Lightweight Aggregate Reinforced Concrete Columns," *ACI Symposium on Lightweight Aggregate Concrete*, SP–29, 1971.
20. González Cuevas, O., Robles, F., Casillas, J., Díaz de Cossío, R., *Aspectos Fundamentales del Concreto Reforzado*, Editorial Limusa-Wiley, Mexico, 1974.
21. Ferguson, P. M., *Reinforced Concrete Fundamentals*, 3rd Ed., John Wiley & Sons, Inc., 1972.
22. Winter, G. and Nilson, A. H., *Design of Concrete Structures*, 8th Ed., McGraw-Hill, Inc., 1972.
23. ACI Committee 340, "Ultimate Strength Design Handbook, Vol. 1," *ACI Special Publication* No. 17, 1973.
24. Robles, F., *Manual de Diseño de Obras Civiles, Sección H. Concreto reforzado*, Comisión Federal de Electricidad, México, 1969.
25. ACI Committee 340, "Ultimate Strength Design Handbook, Vol. 2: Columns," *ACI Special Publication* No. 17A, 1970.

26. Meli, R., *Gráficas para el Dimensionamiento Plástico de Columnas de Concreto Reforzado*, Instituto de Ingeniería, Universidad Nacional Autónoma de México, México, 1969.
27. Reese, R. C., *Columns by Ultimate Strength Design*, Concrete Reinforcing Steel Institute, Chicago, 1967.
28. González, O., *Manual de Diseño de Concreto Reforzado*, Instituto Mexicano del Cemento y del Concreto, Mexico, 1970.
29. Mattock, A. H., Kriz, L. B., and Hognestad, E., "Rectangular Concrete Stress Distribution in Ultimate Strength Design," *ACI Journal*, February 1961.
30. Comité Européen du Béton-Fédération Internationale de la Précontrainte, "International Recommendations for the Design and Construction of Concrete Structures, Principles and Recommendations," Cement and Concrete Association, London, June 1970.
31. Bresler B., "Design Criteria for Reinforced Columns under Biaxial Bending," *ACI Journal*, November 1960.
32. Aas-Jakobsen, A., "Biaxial Eccentricities in Ultimate Load Design," *ACI Journal*, March 1964.
33. ACI–ASCE Committee 326 "Shear and Diagonal Tension," *ACI Journal*, January, February, March 1962.
34. ACI–ASCE Committee 426 "The Shear Strength of Reinforced Concrete Members," *Journal of the Structural Division, ASCE*, June 1973.
35. Díaz de Cossío, R. and Siess, C. P., "Behavior and Strength in Shear of Beams and Frames without Web Reinforcement," *ACI Journal*, February 1960.
36. Leonhardt, F. and Walther, R., *The Stuttgart Shear Tests, 1961*, Translation No. 111, Cement and Concrete Association, London, 1964.
37. Bresler, B. and MacGregor, J. G., "Review of Concrete Beams Failing in Shear," *Journal of the Structural Division, ASCE*, February 1967.
38. Hognestad, E., "What Do We Know about Diagonal Tension and Web Reinforcement in Concrete," *Circular Series No. 64, University of Illinois Engineering Experimental Station*, 1952.
39. Mörsch, E. "Versuche über Schubspannungen in Betoncisentrager." *Beton und Eisen*, Vol. 2, No. 4, Berlin, October 1903.
40. Bresler, B. and Scordelis, A. C., "Shear Strength of Reinforced Concrete Beams," *ACI Journal*, January 1963.
41. Baron, M. J., "Shear Strength of Reinforced Concrete Beams at Points of Bar Cutoff," *ACI Journal*, January 1966.
42. Kani, G. N. J., "How Safe Are Our Large Reinforced Concrete Beams?" *ACI Journal*, March 1967.
43. Faradji, M. J. and Diaz de Cossío, R., "Tensión Diagonal en Miembros de Concreto de Sección Circular," *Revista Ingeniería*, Mexico, April 1965.
44. Rodriguez, J. J., Bianchini, A. C., Viest, I. M., and Kesler, C. E., "Shear Strength of Two-Span Continuous Reinforced Concrete Beams," *ACI Journal*, April, 1959.
45. Bryant, R. H., Bianchini, A. C., Rodriguez, J. J., and Kesler, C. E., "Shear Strength of Two Continuous Reinforced Concrete Beams with Multiple Point Loading," *ACI Journal*, September 1962.
46. Leonhardt, F., Walther, R., and Dilger, W., "Schubversuche an Durchlaufträgern," *Deutscher Ausschuss für Stahlbeton*, Heft 1963, Wilhelm Ernst und Sohn, Berlin, 1964.
47. Popov, E. P., Bertero, V. V., and Krawinkler, H., "Cyclic Behavior of Three Reinforced Concrete Flexural Members with High Shear," Report No. EERC 72-5, Earthquake Engineering Research Center, College of Engineering, University of California, Berkeley, October 1972.

48. Structural Engineers Association of California (SEAOC), "Recommended Lateral Force Requirements and Commentary," 1967.
49. Walters, J. R. V. and MacGregor, J. G., "An Analytical Study of Inclined Cracking in Reinforced Concrete Beams," Dept. of Civil Engr., Univ. of Alberta, Edmonton, Alberta, Canada, July 1966.
50. Lorentsen, M., "Theory for the Combined Action of Bending Moment and Shear in Reinforced and Prestressed Concrete Beams," *ACI Journal*, April 1965.
51. Kani, G. N. J., "The Riddle of Shear Failure and Its Solution," *ACI Journal*, April 1964.
52. Moe, J., Discussion of ACI-ASCE Committee 326, "Shear and Diagonal Tension," *ACI Journal*, January, February, March 1962.
53. Kani, G. N. J., "A Rational Theory for the Function of Web Reinforcement," *ACI Journal*, March 1969.
54. Ritter, W., "Die Bauweise Hennebique," *Schweizerische Bauzeitung*, Vol. 33, No. 7, Zurich, February 1899.
55. Baker, A. L. L. and Ahmad, S., "A Statically Indeterminate Truss Model for Reinforced Concrete Beam Failing by Shear," *Bulletin d'Information* No. 37, Comité Européen du Béton, Paris, October 1962.
56. Rüsch, H., "Über die Grenzen der Anwendbarkeit der Fachverkanalogie bei der Berechnung der Schubfestigkeit von Stahlbetonbalken," Ehrenbuch Prof. Ing. F. Campus, Amici et Alumni, Belgium, 1964.
57. Borishansky, M. S., and Gvozdev, A. A., "Raschet Otognutykh Sterzknei I Khomutov v Izgibaemykh Zhelezobetonnykh Elementakh po Stedii Razrushenia," Stroiizdat, Moscow, 1946.
58. Zwoyer, E. M. and Siess, C. P., "Ultimate Strength in Shear of Simply Supported Prestressed Concrete Beams without Web Reinforcement," *ACI Journal*, October 1954.
59. Sozen, M. A. and Hawkins, N. M., Discussion of "Shear and Diagonal Tension," Report of ACI–ASCE Committee 326, *ACI Journal*, September 1962.
60. Moody, K. G., Viest, I. M., Elstner, R. C., and Hognestad, E., "Shear Strength of Reinforced Concrete Beams, Part 4: Analytical Studies," *ACI Journal*, March 1955.
61. Bresler, B. and Pister, K. S., "Strength of Concrete Under Combined Stresses," *ACI Journal*, September 1958.
62. Walther, R., "The Ultimate Strength of Prestressed and Conventionally Reinforced Concrete Under the Combined Action of Moment and Shear," Ph.D. Thesis, Lehigh University, 1957.
63. Paez, A., "Esfuerzos Cortantes de Vigas Agrietadas," *Proceedings, Fédération Internationale de la Précontrainte*, Berlin, 1958.
64. Guralnick, S. A., "Strength of Reinforced Concrete Beams," *Transactions, ASCE*, Vol. 125, pp. 603, 643, 1960.
65. Moore, W. P., Jr., "An Analytical Study of the Effect of Web Reinforcement on the Strength of Reinforced Concrete Beams Subjected to Combined Flexure and Shear," *Civil Engineering Studies, Structural Research Series* No. 282, University of Illinois, May 1964.
66. Ngo, D. and Scordelis, A. C., "Finite Element Analysis of Reinforced Concrete Beams," *ACI Journal*, March 1967.
67. Viest, I. M., Discussion of "Shear Strength of Lightweight Reinforced Concrete Beams," by J. A. Hanson, *ACI Journal*, March 1959.

68. Moe, J., "Shearing Strength of Reinforced Concrete Slabs and Footings under Concentrated Loads," *Development Department Bulletin D 47, Portland Cement Association*, April 1961.
69. Elstner, R. C. and Hognestad, E., "Shearing Strength of Reinforced Concrete Slabs," *ACI Journal*, July 1956.
70. Kinnunen, S. and Nylander, H., "Punching of Concrete Slabs Without Shear Reinforcement," Transactions No. 158, Royal Institute of Technology, Stockholm, 1960.
71. Roll, F. *et al.*, "Shear Resistance of Perforated Reinforced Concrete Slabs," *Cracking, Deflection, and Ultimate Load of Concrete Slab Systems*, ACI Publication SP–30, 1971.
72. Corley, W. G. and Hawkins, N. M., "Shearhead Reinforcement for Slabs," *ACI Journal*, October 1968.
73. Carpenter, J. E., Kaar, P. H., Hanson, N. W., "Discussion of Proposed Revision of ACI 318–63 Building Code Requirements," *ACI Journal*, September 1970.
74. Hanson, N. M. and Conner, H. W., "Seismic Resistance of Reinforced Concrete Beams–Column Joints," *Proceedings ASCE*, Vol. 92, No. ST5, October 1967.
75. Anderson, A. R., "Composite Designs in Precast and Cast-in-Place Concrete," *Progressive Architecture*, September 1960.
76. Birkeland, P. W. and Birkeland, H. W., "Connections in Precast Concrete Construction," *ACI Journal*, March 1966.
77. Mast, R. F., "Auxiliary Reinforcement in Precast Concrete Connections," *Journal of the Structural Division, ASCE*, June 1968.
78. Hofbeck, J. F., Ibrahim, I. O., and Mattock, A. H., "Shear Transfer in Reinforced Concrete," *ACI Journal*, February 1969.
79. Zia, P., "Torsional Strength of Prestressed Concrete Members," *ACI Journal*, April 1961.
80. Esteva, L., Nieto, J. A., "El Temblor de Lima, Perú, Octubre 17, 1966," *Revista Ingeniería*, Vol. XXXVII, January 1967.
81. Díaz de Cossío, R. and González Cuevas, O., "Torsión Sísmica en Columnas de Concreto Reforzado," *Ingeniería Sísmica*, No. 3, May 1970.
82. Tamberg, K. G., "Aspects of Torsion in Concrete Structure Design," *Torsion of Structural Concrete*, ACI Publication SP-18, 1968.
83. Cowan, H. J., *Reinforced and Prestressed Concrete in Torsion*, St. Martin's Press, 1964.
84. Analysis of Structural Systems for Torsion, ACI Publication SP–35, 1973.
85. Hsu, T. T. C., "Torsion of Structural Concrete-Behavior of Reinforced Concrete Rectangular Members," *Torsion of Structural Concrete*, ACI Publication SP-18, 1968.
86. Zia, P., "Torsion Theories for Concrete Members," *Torsion of Structural Concrete*, ACI Publication SP-18 1968.
87. Gvozdev, A. A., Lessig, N. N., and Rulle, L. K., "Research on Reinforced Concrete Beams Under Combined Bending and Torsion in the Soviet Union," *Torsion of Structural Concrete*, ACI Publication SP–18, 1968.
88. Hsu, T. T. C., "Torsion of Structural Concrete-Plain Concrete Rectangular Sections," *Torsion of Structural Concrete*, ACI Publication SP-18, 1968.
89. McMullen, A. E. and Warwaruk, J., "Strength of Reinforced Concrete Beams with Web Reinforcement in Combined Bending, Torsion, and Shear," Preprint 777, ASCE Annual Meeting, 1969.
90. Gesund, A. and Boston, L. A., "Ultimate Strength in Combined Bending and Torsion of Concrete Beams Containing Only Longitudinal Reinforcement," *ACI Journal*, November 1964.

91. Gesund, H., Shuette, F. J., Buchanan, G. A., and Gray, G. A., "Ultimate Strength in Combined Bending and Torsion of Concrete Beams Containing Both Longitudinal and Transverse Reinforcement," *ACI Journal*, December 1964.
92. *"Torsion of Structural Concrete,"* ACI Special Publication SP–18, 1968.
93. Lampert, P., "Torsion and Bending in Reinforced and Prestressed Concrete Members," Proceedings, Institution of Civil Engineers, December 1971.
94. Victor, D. J. and Ferguson, P. M., "Reinforced Concrete T-Beams Without Stirrups Under Combined Moment and Torsion," *ACI Journal*, January 1968.
95. Lim, S. N. and Mirza, M. S., Discussion of Ref. 94, *ACI Journal*, July 1968.
96. Hsu, T. T. C., "Torsion of Structural Concrete-Interaction Surface for Combined Torsion, Shear and Bending in Beams Without Stirrups," *ACI Journal*, January 1968.
97. Collins, M. P., Walsh, P. F., Archer, F. E., and Hall, A. S., "Ultimate Strength of Reinforced Concrete Beams Subjected to Combined Torsion and Bending," *Torsion of Structural Concrete*, ACI Publication SP-18, 1968.
98. Cowan, A. J. and Armstrong, S., "Experiments on the Strength of Reinforced and Prestressed Concrete Beams and of Concrete Encased Steel Joists in Combined Bending and Torsion," *Magazine of Concrete Research*, Vol. 6, No. 19, March 1955.
99. McMullen, A. E. and Warwaruk, J., "The Torsional Strength of Rectangular Reinforced Concrete Beams Subjected to Combined Loading," *Department of Civil Engineering, University of Alberta, Canada*, July 1967.
100. Mattock, A. H., "How to Design for Torsion," *Torsion of Structural Concrete*, ACI Publication SP-18, 1968.
101. Ersoy, V., and Ferguson, P. M., "Concrete Beams Subjected to Combined Torsion and Shear-Experimental Trends," *Torsion of Structural Concrete*, ACI Publication SP-18, 1968.
102. Victor, D. J. and Ferguson, P. M., "Beams Under Distributed Load Creating Moment, Shear and Torsion," *ACI Journal*, April 1968.
103. Farmer, L. E. and Ferguson, P. M., "T-Beams Under Combined Bending, Shear and Torsion," *ACI Journal*, November 1967.
104. Klus, J. P., "Ultimate Strength of Reinforced Concrete Beams in Combined Torsion and Shear," *ACI Journal*, March 1968.
105. Bishara, A. and Peir, J. C., "Reinforced Concrete Rectangular Columns in Torsion," *Journal of the Structural Division, ASCE*, December 1968.
106. Hsu, T. T. C., "Torsion of Structural Concrete-Uniformly Prestressed Rectangular Members Without Web Reinforcement," *Journal of the Prestressed Concrete Institute*, April 1968.
107. Fisher, G. P. and Zia, P., "Review of Code Requirements for Torsion Design," *ACI Journal*, January 1964.
108. Walsh, P. F., Collins, M. P., and Archer, F. E., "Design of Concrete Beams for Torsion." *Constructional Review*, February 1968.
109. Hsu, T. T. C. and Kemp, L. E., "Background and Practical Application of Tentative Design Criteria for Torsion," *ACI Journal*, January 1969.
110. Osburn, D. A., Mayoglou, B., and Mattock, A. H., "Strength of Reinforced Concrete Beams with Web Reinforcement in Combined Torsion, Shear, and Bending," *ACI Journal*, January 1969.
111. Leonhardt, F., "Poutres-Cloisons," *Comité Européen du Béton, Bulletin d'Information* No. 65, February 1968.
112. Leonhardt, F. and Walther, R., "Wandartige Träger-Bericht über Versuche," *Deutscher Ausschuss für Stahlbeton, Heft 178, Wilhelm Ernst und Sohm*, 1965.

113. De Paiva, H. A. R. and Siess, C. P., "Strength and Behavior of Deep Beams in Shear," *Journal of the Structural Division, ASCE*, October 1965.
114. Kriz, L. B. and Raths, C. H., "Connections in Precast Concrete Structures-Strength of Corbels," *Journal of the Prestressed Concrete Institute*, February 1965.
115. Cohen, E., Crist, R. A., de Paiva, H. A. R., Mathey, R. G., O'Donnell, K. O., and Sbarounis, J. A., "Shear Design for Brackets and Deep Beams," presented at the 20th Fall Meeting, ACI, Des Moines, Iowa, November 1967.
116. Franz, G. and Niedenhoff, H., "Die Bewehrung von Konsolen und gedrungenen Balken," *Beton und Stahlbetonbau 58*, Heft 5, 1963.
117. Paulay, T., "Some Aspects of Shear Wall Design," Bulletin of New Zealand Society for Earthquake Engineering, Vol. 5, No. 3, September 1972.
118. Cárdenas, A. E., Hanson, J. M., Corley, W. G., and Hognestad, E., "Design Provisions for Shear Walls," J. ACI, March 1973.
119. Blume, J. A., Mewmark, N. M., and Corning, L. H., *Design of Multistory Reinforced Concrete Building for Earthquake Motions*, Portland Cement Association, 1961.
120. Uniform Building Code, International Conference of Buildings Officials, Pasadena, 1967, and 1970 editions.
121. Nasser, K. W., Acavalos, A., Daniel, H. R., "Behavior and Design of Large Openings in Reinforced Concrete Beams," *ACI Journal*, January 1967.
122. ACI Committee 435, Report, "Deflections of Reinforced Concrete Flexural Members," *ACI Journal*, June 1966.
123. Yu, W. and Winter, G., "Instantaneous and Long-Time Deflections of Reinforced Concrete Beams under Working Loads," *ACI Journal*, July 1960.
124. Branson, D. E., "Design Procedures for Computing Deflections," *ACI Journal*, September 1968.
125. Jaeger, K., "Die Biegefestigkeit von Stahlbetonbalken. Theorie und Versuch," *Oesterreichische Bauzeitschrift*, September 1956.
126. Beeby, A. W., "Short-Term Deformations of Reinforced Concrete Members," *Cement and Concrete Association*, TRA 408, London, March 1968.
127. Regulamento de Estructuras de Betao Armado." *Diário de Governo, I Serie*, No. 119, Lisbon, May 1967.
128. Washa, G. W., "Plastic Flow of Thin Reinforced Concrete Slabs," *ACI Journal*, November 1947.
129. Ross, A. D., "Creep of Concrete Under Variable Stress," *ACI Journal*, March 1958.
130. Corley, W. G. and Sozen, M. A., "Time-Dependent Deflections of Reinforced Concrete Beams," *ACI Journal*, March 1966.
131. Baker, A. L. L. and Amarakone, A. M. N., "Inelastic Hyperstatic Frames Analysis," *Proceedings of the International Symposium on Flexural Mechanics of Reinforced Concrete, ACI-ASCE* ACI Publication SP-12, 1964.
132. Subcommittee I, ACI Committee 435, Report, "Allowable Deflections," *ACI Journal*, June 1968.
133. González Cuevas, O. M. and Díaz de Cossío, R., *Vigas de Concreto Sujetas a Flexión de Corta Duración*, Publicación 163, Instituto de Ingeniería, Universidad Nacional Autónoma, de México, Mexico, March 1968.
134. Gaston, J. R., Siess, C. P., and Newmark, N. M., "An Investigation of the Load-Deformation Characteristics of Reinforced Concrete Beams up to the Point of Failure," *Civil Engineering Studies, Structural Research Series*, No. 40, University of Illinois, 1952.
135. Burns, N. H. and Siess, C. P., "Load-Deformation Characteristics of Beam Column Connections in Reinforced Concrete," *Civil Engineering Studies, Structural Research Series*, No. 234, University of Illinois, 1962.

136. Yamashiro, R. and Siess, C. P., "Moment-Rotation Characteristics of Reinforced Concrete Members Subjected to Bending, Shear and Axial Load," *Civil Engr. Studies Structural Research Series*, No. 260, University of Illinois, December 1962.
137. Fintel, M. Y. and Khan, F. R., "Effects of Column Creep and Shrinkage in Tall Structures-Prediction of Inelastic Column Shortening," *ACI Journal*, December 1969.
138. *CRSI Handbook*, Concrete Reinforcing Steel Institute, Chicago, 1972.
139. Commentary on Building Code Requirements for Reinforced Concrete (ACI 318–71), American Concrete Institute, Detroit, 1971.
140. Kuyt, B., "A Method for Ultimate Strength Design of Rectangular Reinforced Concrete Beams in Combined Torsion, Bending, and Shear," *Magazine of Concrete Research*, March 1972.
141. Rosenblueth, E., and Díaz de Cossío, R., "Instability Considerations in Limit Design of Concrete Frames," *Proceedings of the International Symposium on Flexural Mechanics of Reinforced Concrete*, ACI-ASCE, ACI Publication SP-12, 1964.
142. Corley, W. G., "Rotational Capacity of Reinforced Concrete Beams," *Journal of the Structural Division, ASCE*, October 1966.
143. ACI-ASCE Joint Committee 426, "The Shear Strength of Reinforced Concrete Members, Chapter 5—Shear Strength of Slabs," Draft Publication, August 1973.
144. Hanson, J. M., "Influence of Embedded Service Ducts on the Strength of Flat Plate Structures," *Portland Cement Association Research and Development Bulletin, RD 005.01 D*, 1970.
145. Lampert, P. and Collins, M. P., "Torsion, Bending and Confusion—An Attempt to Establish the Facts," *ACI Journal*, August 1972.
146. Somerville, G., "The Behaviour and Design of Reinforced Concrete Corbels," *Technical Report 42.472*, Cement and Concrete Association, August 1972.

6

Strength and Deformation of Prestressed Concrete Elements

T. Y. LIN
PAUL ZIA

6.1 INTRODUCTION

6.1.1 History

The modern development of prestressed concrete is credited to Eugene Freyssinet of France, who in 1928 started using high-strength steel wires for prestressing. In 1939, he developed conical wedges for anchoring the wires and designed double-acting jacks for tensioning the wires and thrusting the cones. Soon after, prestressed concrete was introduced and applied in Europe, particularly in France, Belgium, England, and Germany.

In the U.S.A., circular prestressing of storage tanks using the preload wire-winding machine began about 1935, but linear prestressing of concrete elements did not start until 1949 when the Walnut Lane Bridge in Philadelphia was constructed using the Magnel system. In 1972, there were about 350 plants in the U.S.A. producing prestressed elements, with an annual production volume of over 3,500,000 cu yd of concrete, of which about one-fourth were used for bridges and the remainder for buildings and other construction projects. The amount of concrete posttensioned at the job site in

the U.S.A. cannot be easily determined but is estimated to have been about 700,000 cu yd in 1972.

General acceptance of prestressed concrete in the U.S.A. is also indicated by the publication of the PCI Building Code Requirements in 1961, and the inclusion of prestressed concrete in the Uniform Building Code (1961), the ACI Building Code Requirements (1963), as well as the AASHO Standard Specifications for Highway Bridges (1961), and all revised editions.

6.1.2 Pre- and Posttensioning

There are basically two methods for prestressing concrete: pretensioning and posttensioning. In pretensioning, the tendons (steel wires or strands) are tensioned against some abutments or molds, prior to the placement of concrete. After the concrete has developed sufficient strength, the tendons are released from their temporary anchorages, thus transferring their stress to the concrete, generally by bond near the ends of the tendons. For the long-line process of pretensioning, the tendons are stretched between two abutments, several hundred feet apart, enabling the production of a number of elements in one operation. Pretensioning can also be accomplished by the individual mold process, wherein the tendons are first tensioned and anchored to the mold, then concrete is placed in it and cured, to be followed by demolding after the hardening of concrete.

In postensioning, the tendons (steel wires, strands, or bars) are tensioned against and anchored to the concrete after it has developed adequate strength. The tendons are separated from the surrounding concrete before tensioning and then bonded to it by subsequent grouting. They can also be permanently unbonded to the concrete, being greased and wrapped to achieve complete separation.

6.1.3 Basic Concepts

The behavior of prestressed concrete may be explained and analyzed by three different concepts: (1) the combined loading concept, (2) the internal couple concept, and (3) the load balancing concept. Each has certain advantages over the others. The use of the combined loading concept provides the designer a complete knowledge of stress variations under various loading conditions. On the other hand, the internal couple concept is especially useful in flexural design with either working stress or ultimate strength method. For camber or deflection control and for design of continuous beams and slabs, the concept of load balancing is a very powerful design tool.

Combined Loading Concept. Concrete is a brittle material, strong in compression but weak in tension. Prestressing imparts a precompression to a

coarse aggregate resulting in a nonuniform concrete mass. Segregation can occur during improper handling, placing, vibrating, and possibly finishing of a concrete mix. Excessive lateral movement, such as will occur when concrete is deposited at one location in a form and permitted to flow within the form, will cause the coarse aggregate and mortar to separate. Dropping concrete into deep, narrow, reinforced walls can cause segregation. To minimize segregation not only good construction practice must be employed, but for difficult placement conditions the mix employed should be properly designed. The tendency for a concrete mix to segregate increases greatly with an increase in slump, maximum size and amount of aggregate, and with reduction in cement content. There is no standard test for measuring this property A proper concrete mix selection and the use of good construction practice can prevent the occurrence of segregation. There is no excuse for honeycomb, caused by segregation, to occur in concrete structures.

Bleeding, sometimes called water gain, is closely related to segregation. During the settlement of the solid materials within the concrete mass water tends to rise towards the surface. Some of this water becomes trapped under horizontal reinforcing bars and larger pieces of aggregate. Water reaching the top surface dilutes the cement paste and may accumulate laitance or scum on the surface. *Laitance* is a layer of weak nondurable material containing diluted cement paste and fines from the aggregate brought to the surface by the bleeding water. Excessive bleeding may also cause sand streaking along formed surfaces. The amount of bleeding can be minimized by reducing the water content, increasing cement content, using sands with adequate amounts of fines, or adding some finely divided admixtures like a pozzolan. Air entrainment is also effective in reducing bleeding. The bleeding characteristics of a concrete mixture can be evaluated by performing a bleeding test (ASTM C232). This test consists essentially of determining the relative quantity of mixing water that appears on the surface of a concrete sample placed in a cylindrical container of about 1/2 ft^3 capacity. The water that has accumulated on the surface is withdrawn and measured at regular intervals until the cessation of bleeding, which normally occurs within about 2–4 h after mixing.

During bleeding the top surface of the concrete subsides. This behavior, known as *plastic shrinkage* or settlement of the concrete, is especially noticeable in building walls or columns. Some of this volume reduction may be also caused by leakage or by absorption of water by forms, absorption of water by aggregate, and the combination of water with cement. Like bleeding, this settlement occurs only within the first few hours after mixing.

1.10.4 Air Entrainment

An *air-entrained concrete* contains intentionally introduced air in the form of minute bubbles dispersed throughout the mix as a result of the use of air-entraining admixtures discussed earlier in this chapter. The two principal

reasons for using intentionally entrained air is to improve the resistance of hardened concrete to freezing and thawing exposures and to improve the workability of fresh concrete. When water in a hardened concrete freezes, it expands, developing pressures that can cause cracking and spalling. The entrained air voids act as reservoirs for excess water forced into them, thus relieving pressure and preventing damage to the concrete. The pressures developed depend largely upon the distance the water must travel to the nearest air void. Therefore, the air voids must be spaced closely enough (less than 0.008 in.) to keep the pressure below the tensile strength of the concrete. Also the size of the air void is important. It must be small enough (0.001 to 0.003 in. diameter) to ensure that it remains empty of water even when concrete becomes saturated and thus can act as a reservoir for the water expelled by ice formation in the capillaries during freezing. Workability of fresh concrete is improved by air entrainment because the presence of air bubbles greatly increases the plasticity and cohesiveness of the mix. Because of this improved workability, water and sand content can be reduced significantly in air-entrained mixes. Also, air entrainment reduces segregation and bleeding in freshly mixed concrete.

Air contents are expressed in terms of percent by volume of the concrete, although air is entrained only in the mortar fraction of the concrete. Laboratory tests and field experience have shown that about 9% air in the mortar fraction of the concrete will provide the needed durability. Since concretes made with small-size aggregates require more mortar, their air content (expressed as percentage of concrete volume) will be greater than that of concretes made with larger size aggregates requiring less mortar. The recommended air contents that should be specified for structural concrete to provide adequate durability are indicated in Table 1.8. When entrained air is not required for protection against frost action but is used to improve workability, the given air contents can be reduced by about one-third.

TABLE 1.8 Recommended Air Contents for Concretes Subject to Severe Exposure Conditions.[4]

Maximum-Size Coarse Aggregate, in.	Air Content, Percent by Volume[a,b]
1 1/2, 2, or 2 1/2	5 ± 1
3/4 or 1	6 ± 1
3/8 or 1/2	7 1/2 ± 1

[a] For structural lightweight concrete, add 2% to the values to allow for entrapped air in the aggregate particles; a range of ±1 1/2% is permissible.

[b] The air content of the mortar fraction of the concrete should be about 9%.

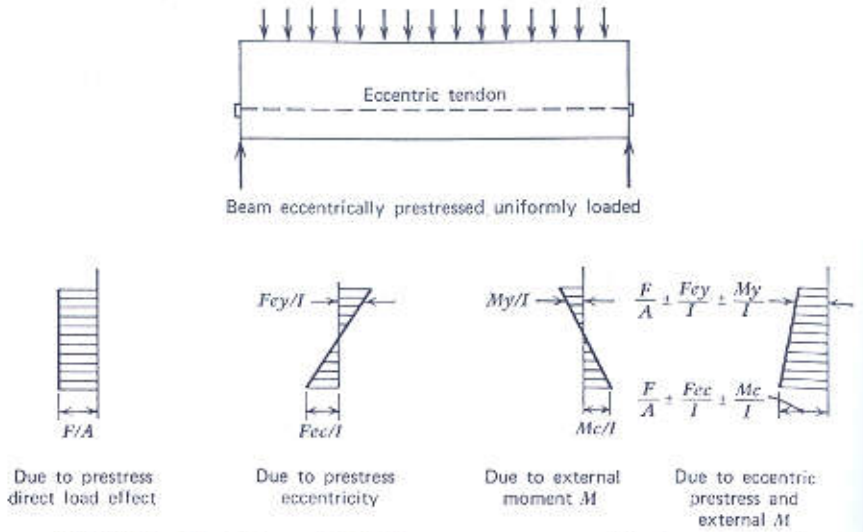

FIGURE 6.1. Stress distribution across an eccentrically prestressed concrete section.

concrete member in its tension zone so as to increase its cracking resistance. Such a concrete member is, therefore, subjected to a combination of internal prestress and external (design) loads.

Consider a simple rectangular beam eccentrically prestressed by a tendon and subjected to transverse external loads (Fig. 6.1). It can be visualized that the stress at any point in the beam at a distance y from the centroidal axis (c.g.c.) is due to a combination of the direct compression of prestress, F, the moment resulting from the eccentricity e of the prestress, and the moment M at the section in question produced by the external load, which includes the weight of the beam. Thus, the resulting stress is given by

$$f = \frac{F}{A} \pm \frac{Fey}{I} \pm \frac{My}{I} \tag{6.1}$$

where A is the area of the concrete section and I is the moment of inertia of the section. The stress diagrams shown in Fig. 6.1 illustrate the stress distributions due to each of the different loadings.

Internal Couple Concept. Prestressed concrete can be considered as an efficient combination of high-strength steel with concrete. Using this concept, one compares prestressed concrete to reinforced concrete, with steel taking the tension and concrete taking the compression so that the two materials form an internal couple resisting the external moment. The difference lies

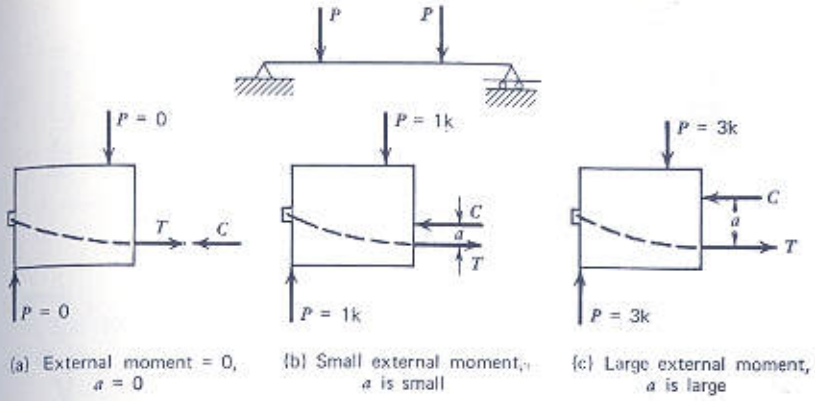

FIGURE 6.2. Variable a in a prestressed concrete beam.

in the use of high-strength steel for prestressed concrete. If such steel is simply cast in the concrete without being prestressed, concrete will have to crack seriously before the strength of the steel is sufficiently developed. By prestretching the steel and anchoring it against the concrete, we can achieve an efficient combination of the two materials.

The internal resisting couple, the C–T couple (Fig. 6.2) in a prestressed concrete beam differs from that in a reinforced concrete beam. Under working load conditions, the forces C and T in a prestressed concrete beam remain virtually constant and the lever arm a increases with increasing moment. On the other hand, the internal lever arm jd in a reinforced concrete beam is considered to be constant while the forces C and T increase with increasing moment.

If the moment at a section is M, and since the prestressing force F is also the tension T, it follows that

$$a = \frac{M}{T} = \frac{M}{F} \tag{6.2}$$

Having determined the lever arm a and knowing the center of the prestressing force F, the center of compression C is located. Depending upon the location of C, various stress distributions in the concrete section can be obtained. Referring to Fig. 6.3, it can be seen, for example, that when C is at the c.g.c., we have a uniform stress distribution. When C is at the top or bottom kern point (at k_t and k_b from c.g.c.), a triangular stress distribution is obtained.

Once C is located, the stress at any point on the section is given by

$$f = \frac{C}{A} \pm \frac{Ce_c y}{I} \tag{6.3}$$

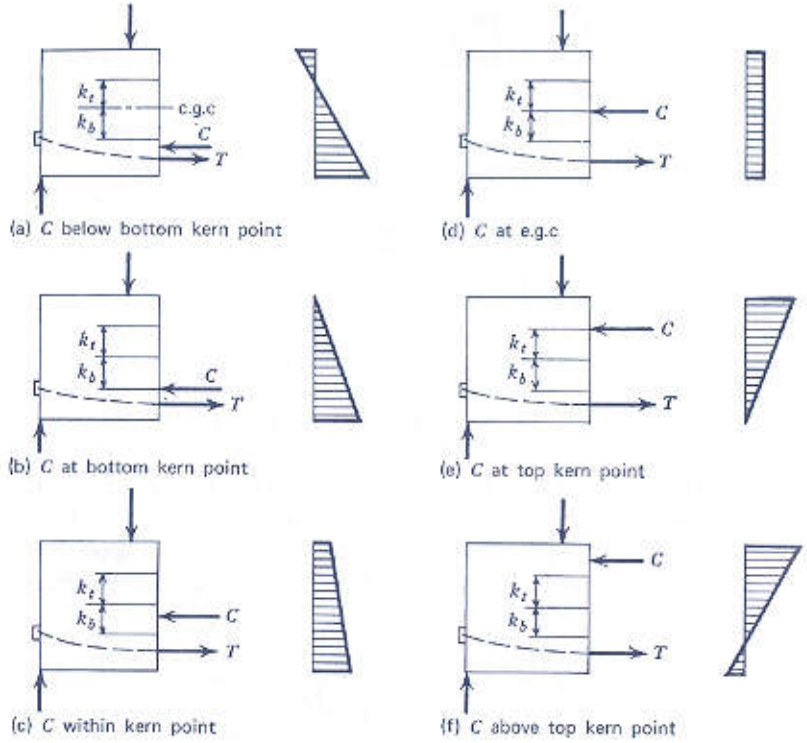

FIGURE 6.3. Stress distribution in concrete by the elastic theory.

where e_c is the eccentricity of C with respect to the c.g.c. while other terms are as previously defined.

This concept is applied to the ultimate load range in Sections 6.4 and 6.6.

Load Balancing Concept. By this concept, one visualizes the effect of prestressing force primarily as an attempt to balance a certain portion of the external loads on a member. In its simplest form, one can conceive a parabolic tendon in a simple beam prestressed so as to apply a uniform upward force on the concrete beam. If this beam carries a downward external load of equal intensity, then the net transverse load on this beam is zero, and we are left with a constant stress of $f = F/A$ across any section of the beam.

When the external load differs from the balancing load due to prestressing, only the moment M' produced by the unbalanced load needs to be considered in computing bending stresses f'. Thus,

$$f' = \frac{M'y}{I} \tag{6.4}$$

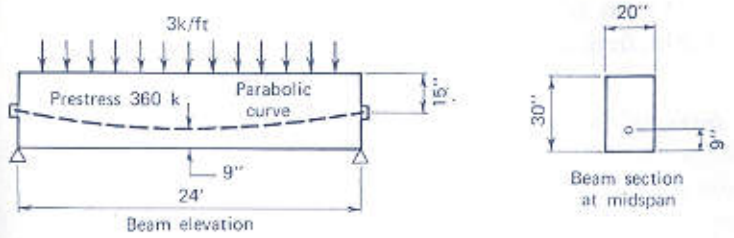

FIGURE 6.4. Example 6.1.

The prestress F required to balance a uniform load of intensity w lb per ft is given by,

$$F = \frac{wL^2}{8h} \tag{6.5}$$

where L is the span length in feet and h is the sag of a parabolic cable in feet.

EXAMPLE 6.1. A prestressed concrete rectangular beam 20 in. by 30 in., has a simple span of 24 ft and is loaded by a uniform load of 3 k/ft. which includes its own weight (Fig. 6.4). The parabolic prestressing tendon is located as shown and produces an effective prestress of 360 k. Compute the extreme fiber stresses in the concrete at the midspan section.

Solution: (a) By the combined load concept. The moment at the midspan section due to the external load is

$$M = 3 \times 24^2/8 = 216 \text{ k-ft.}$$

Now we have $F = 360$ k, $A = 20 \times 30 = 600$ in.^{2} (neglecting any hole due to the tendon), $e = 6$ in., $I = bd^3/12 = 20 \times 30^3/12 = 45{,}000$ in.^{4}, $y = 15$ in. for extreme fibers. Therefore, from Eq. (6.1),

$$f = \frac{F}{A} \pm \frac{Fey}{I} \pm \frac{My}{I}$$

$$= \frac{-360{,}000}{600} \pm \frac{360{,}000 \times 6 \times 15}{45{,}000} \pm \frac{216 \times 12{,}000 \times 15}{45{,}000}$$

$$= -600 \pm 720 \pm 864$$

$$= -600 + 720 - 864 = -744 \text{ psi} \qquad \text{for the top fiber}$$

$$= -600 - 720 + 864 = -456 \text{ psi} \qquad \text{for the bottom fiber}$$

(b) By the internal couple concept. The internal couple C–T must develop a resisting moment equal to the applied moment $M = 216$ k-ft. From Eq. (6.2), the lever arm is

$$a = 216/360 \times 12 = 7.2 \text{ in}$$

Since $T(=F)$ acts at 9 in. from the bottom fiber, C must be acting at $9 + 7.2 = 16.2$ in. from it. Hence the eccentricity of C with respect to the c.g.c. is

$$e_c = 16.2 - 15 = 1.2 \text{ in.}$$

Thus, from Eq. (6.3),

$$\begin{aligned} f &= \frac{C}{A} \pm \frac{Ca_c y}{I} \\ &= \frac{-360{,}000}{600} \pm \frac{360{,}000 \times 1.2 \times 15}{45{,}000} \\ &= -600 \mp 144 \\ &= -744 \text{ psi} \quad \text{for the top fiber} \\ &= -456 \text{ psi} \quad \text{for the bottom fiber} \end{aligned}$$

(c) By the load balancing concept. The length of the prestressing tendon is $L = 24$ ft. and the sag of the tendon is $h = 6$ in. $= 0.5$ ft. Hence, according to Eq. (6.5), the tendon produces an upward balancing load of

$$w = \frac{8Fh}{L^2} = \frac{8 \times 360 \times 0.5}{24^2} = 2.5 \text{ k/ft.}$$

The unbalanced load on the beam amounts to $3 - 2.5 = 0.5$ k/ft, and the moment at midspan is

$$M' = \frac{0.5 \times 24^2}{8} = 36 \text{ k ft.}$$

Thus, the bending stress in the extreme fibers produced by this unbalanced load of 0.5 k/ft is

$$f' = \pm \frac{M'y}{I} = \pm \frac{36 \times 12{,}000 \times 15}{45{,}000} = \pm 144 \text{ psi}$$

The beam is also subjected to an axial compression of F at both ends, causing a uniform stress of $F/A = 360{,}000/600 = 600$ psi. The resulting stresses in the extreme fibers due to combined effect of prestress and the external load of 3 k/ft are

$$\begin{aligned} f &= -600 \mp 144 \\ &= -744 \text{ psi} \quad \text{for the top fiber} \\ &= -456 \text{ psi} \quad \text{for the bottom fiber} \end{aligned}$$

It should be noted that the bending of the beam will be completely eliminated if the external load is totally balanced by the uplifting effect of prestress. For the case in question, the required prestress, according to Eq. (6.5), will be

$$F = \frac{3 \times 24^2}{8 \times 0.5} = 432 \text{ k}$$

Under this prestressing force, the beam will be without bending and it will be only under a uniform compressive stress of $432{,}000/600 = 720$ psi. (Note that the horizontal component of F should be used, if greater accuracy is desired. Furthermore, if the tendon is anchored at points other than the c.g.c. at beam ends, then the effect of the end moments must also be considered.)

6.2 METHODS AND SYSTEMS OF PRESTRESSING

6.2.1 Tensioning Methods

The methods of tensioning the tendons can be classified into four groups: (1) mechanical prestressing by means of jacks, (2) thermal prestressing by application of electric heat, (3) chemical prestressing by means of expansive cements, (4) others.

Mechanical stressing of the tendons is by far the most common method for both pretensioning and posttensioning. In posttensioning, hydraulic jacks are used to pull the tendon against the hardened concrete; while in pretensioning, to pull the tendon against some bulkheads or molds. The capacity of these jacks vary from about 3 tons up to 1000 tons. The Clifford–Gilbert system in England employs a small screwjack weighing about 20 lb pulling one wire at a time. The BBRV and Prescon systems employ jacks of various capacities to fit cables of different sizes. The Leonhardt system in Germany employs reinforced, concrete jacks tensioning hundreds of wires at one time. In all cases, both the jack gage pressure and the tendon elongation are measured to determine the amount of prestress.

Tendons can be lengthened by electric heating. Originated in the U.S.A. for the posttensioning process, it has not proved to be commercially applicable. A combination of electrical and mechanical stressing has been developed in the U.S.S.R. for pretensioning, known as the electrothermal method.

Chemical prestressing utilizes expansive cements that expand chemically after setting and during hardening. When these cements are used to make concrete with embedded steel, the steel is elongated by the expansion of the concrete. Thus the steel is prestressed in tension, which in turn produces compressive prestress in the concrete, resulting in chemically prestressed or self-stressed concrete. Modern development of expansive cement, known as Lossier cement, started in France in 1940. Its use for self-stressing has been

investigated intensively in the U.S.S.R. since 1953. At the University of California, Berkeley, the use of calcium sulfoaluminate admixtures for expansive cement was developed by A. Klein in 1956 and a number of field experimental structures have been built since 1963, most of which had an expansion of about 0.05 to 0.10%, intended to compensate the expected amount of shrinkage strain.

The Preflex method in Belgium consists of prebending a high strength steel beam and encasing its tensile flange in concrete. Releasing the bending places the concrete under compression, thus enabling it to take tension and also to greatly increase the stiffness of the beam.

Prestressing in the U.S.A. is usually accomplished in the plant by the long-line process first developed by E. Hoyer of Germany. In order to improve the behavior of prestressed beams, their tendons are often bent to given profiles. In the long-line process, this is achieved by deflecting the tendons up and down along the length of the bed, known as harping or draping. When individual molds are used for prestressing, complicated patterns of tendon arrangement can be accomplished, such as carried out in the U.S.S.R. by their continuous prestressing process whereby the tendons are mechanically fed under a controlled tension force and weaved around pegs fixed to the mold.

6.2.2 Posttensioning Systems

Throughout the world, there are hundreds of patents and systems for posttensioning. Patent royalties are indirectly included in the bid price for supplying the tendons and anchorages, which sometimes also include furnishing equipment and technical supervision for tensioning operations. A partial list of these systems are classified in Table 6.1. Addresses of some posttensioning systems in the U.S.A. are given in Table 6.2. Tables 6.3 through 6.8 give some data for a few prestressing systems commonly used in the U.S.A. Readers wishing further details should write to the respective system manufacturer.

6.3 LOSSES OF PRESTRESS

The prestressing force initially established in the tendon diminishes with time. This loss of prestress results from a number of factors and, for the most part, is due to the time-dependent properties of concrete and steel. The factors that contribute to the loss of prestress are: (1) elastic shortening of concrete, (2) creep and shrinkage of concrete, (3) relaxation in steel, (4) slippage and slackening of tendons during anchoring, and (5) friction between tendon and concrete during tensioning. Some of these factors are more important for pretensioned members while the others are more significant for posttensioned members.

TABLE 6.1. Linear Prestressing Systems.

Type	Classification	Description		Name of System	Country of Origin
Pretensioning	Methods of stressing	Against buttresses or stressing beds		Hoyer	Germany
		Against central steel tube		Shorer Chalos	U.S. France
		Continuous stressing against molds		Continuous wire winding	U.S.S.R.
		Electric current to heat steel		Electrothermal	U.S.S.R.
	Methods of anchoring	During prestressing	Wires	Various wedges	
			Strands	Strandvise	U.S.
		For transfer of prestress	Bond, for strands and small wires		Europe U.S.
			Corrugated clips, for big wires	Dorland	U.S.
Posttensioning	Methods of stressing	Steel against concrete		Most systems	
		Concrete against concrete		Leonhardt	Germany
				Billner	U.S.
		Expanding cement		Lossier	France
		Electrical prestressing		Billner	U.S.
		Bending steel beams		Preflex	Belgium

(continued)

TABLE 6.I. (*continued*)

Type	Classification	Description	Name of System	Country of Origin
Posttensioning (*continued*)	Methods of anchoring	Wires, by frictional grips	Freyssinet	France
			Magnel	Belgium
			Morandi	Italy
			Holzmann	Germany
			Preload	U.S.
		Wires, by bearing	B.B.R.V.	Switzerland
			General prestressing or Prescon	U.S.
			Texas P.I.	U.S.
		Wires, by loops and combination of methods	Billner	U.S.
			Monierbau	Germany
			Huttenwerk Rheinhausen	Germany
			Leoba	Germany
			Leonhardt	Germany
		Bars, by bearing and by grips	Lee-McCall	England
			Stressteel	U.S.
			Stress rods	U.S.
			Finsterwalder	Germany
			Dywidag	Germany
			Karig	Germany
			Polensky and Zollner	Germany
			Wets	Belgium
			Bakker	Holland
		Strands, by bearing	Roebling	U.S.
			Wayss and Freytag	Germany
		Strands, by friction grips	CCL	England
			Freyssinet	U.S.
			Anderson	U.S.
			Atlas	U.S.
			VSL	Switzerland

6.3.1 Elastic Shortening of Concrete

Consider a pretensioned member. As prestress is transferred to the concrete, it shortens and the tendons shorten with it, resulting in loss of prestress. If F_0 is the total prestress just after transfer, that is, after shortening has taken place, then the axial shortening of concrete produced by prestressing will be

$$\varepsilon = \frac{f_c}{E_c} = \frac{F_0}{A_c E_c}$$

Hence the loss of prestress in steel is

$$\Delta f_s = E_s \varepsilon = \frac{E_s F_0}{A_c E_c} = \frac{n F_0}{A_c} \tag{6.6}$$

where

$$n = \frac{E_s}{E_c}$$

The value of F_0, being the prestress after transfer, may not be known exactly. However, the value of the initial prestress F_i is usually known; hence another solution can be obtained. Using the transformed-section method, with $A_t = A_c + nA_s$, the axial shortening of concrete is

$$\varepsilon = \frac{F_i}{A_c E_c + A_s E_s}$$

Thus

$$\Delta f_s = E_s \varepsilon = \frac{E_s F_i}{A_c E_c + A_s E_s} = \frac{n F_i}{A_c + n A_s} = \frac{n F_i}{A_t} \tag{6.7}$$

For posttensioning, the problem is somewhat different. If there is only a single tendon in the member, the concrete shortens as that tendon is jacked against the concrete. Since the force in the tendon is measured after the elastic shortening of the concrete has taken place, no loss due to that shortening needs be accounted for.

If we have more than one tendon and the tendons are stressed in succession, then the prestress is gradually applied to the concrete. The shortening of concrete, in this case, increases as each tendon is jacked against it, and the loss of prestress due to elastic shortening differs in the various tendons. The tendon that is first tensioned would suffer the maximum amount of loss due to the shortening of concrete by the subsequent application of prestress from all the other tendons. The tendon that is tensioned last will not suffer any loss,

TABLE 6.2. Addresses of Some Posttensioning Systems in U.S.A.

Anderson system, Concrete Technology Corp., 1123 Port of Tacoma Road, Tacoma, Washington 98421

Atlas system, Atlas Service Corp., 14809 Calvert St., Van Nuys, California 91400.

BBRV system, Inland–Ryerson Construction Products Co., P.O. Box 5532, Chicago, Illinois 606080

Freyssinet system, Freyssinet Co., Inc., 181 Main Street, Tuckahoe, New York 10017

General Prestressing system, Western Concrete Structures, 19113 S. Hamilton Avenue, Gardena, California 90248.

Gifford–Udall system, Holly–Edwards Sales, Inc., P.O. Box 4818, Jacksonville, Florida 32201.

Magnel–Blaton system, Precompressed Concrete Engineering Company, Ltd., 5012 Western Avenue, Montreal, Quebec, Canada.

PI system, Prestressing Inc., 8546 Broadway, San Antonio, Texas 78200.

Preload system, The Preload Company, 837 Old Country Road Westbury, Long Island, New York 11100.

Prescon system, The Prescon Corporation, P.O. Box 2723, Corpus Christi, Texas 78403.

Roebling system, CF & I Steel Corporation, Roebling Division, P.O. Box 127, Roebling, New Jersey 08554.

Stressteel system, Stressteel Corporation, P.O. Box 190, Wilkes–Barre, Pennsylvania 18703.

VSL system, VSL Corporation, 236 N. Santa Cruz Avenue, P.O. Box 459, Los Gatos, California 95030.

since all shortening will have already taken place when the prestress in the last tendon is being measured. The precise computation of such losses is quite complicated. But for all practical purposes it is accurate enough to determine the loss for the first tendon and use half of that value for the average loss of all the tendons. If each tendon is tensioned to a value above the specified initial prestress by the magnitude of the expected loss, then no loss due to elastic shortening needs to be considered again.

6.3.2 Creep and Shrinkage of Concrete

If ε_{cr} and ε_{sh} are creep and shrinkage strains of concrete, respectively, then the loss of prestress is

$$\Delta f_s = E_s \varepsilon_{cr} + E_s \varepsilon_{sh} \tag{6.8}$$

Creep varies with many factors and is often estimated at one to five times the instantaneous elastic shortening. As a very rough approximation, a

TABLE 6.3. BBRV and Prescon Systems. (Almost any number of 1/4-in. wires up to 192 can be made into a cable. Some typical ones are listed below.)

	Number of (1/4-in.) Wires			
	1	14	28	40
Section area of wires, in.^{2}	0.04909	0.687	1.3744	1.963
Final force (60% of ultimate), lb	7,070	98,980	197,960	283,000
Initial force (70% of ultimate), lb	8,250	115,500	231,000	330,000
Overstressing force (80% of ultimate), lb	9,420	131,880	263,760	376,800
Ultimate strength, lb	11,780	164,920	329,840	471,200
Base plate, BBRV, in.		6 3/4" × 6 3/4"	9 1/4" × 9 1/4"	11" × 11"
Base plate, Prescon, in.		6" × 8 1/2"	7" × 12"	

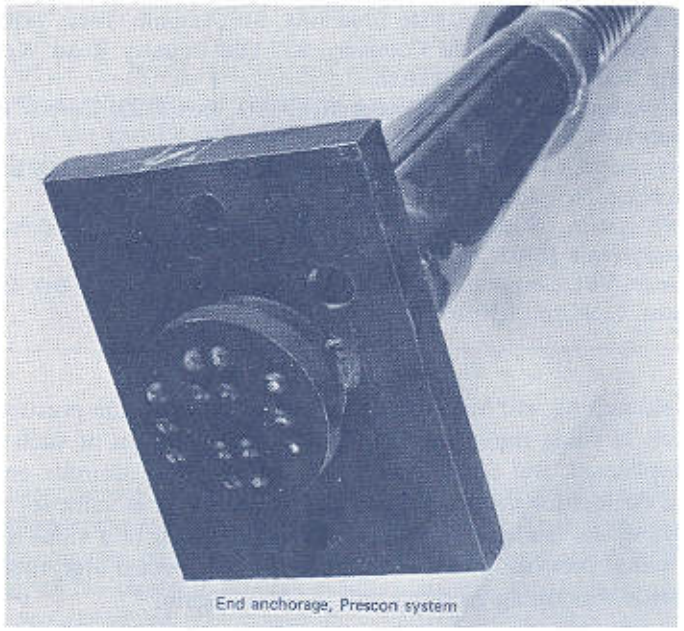

End anchorage, Prescon system

TABLE 6.4. Freyssinet System.

(a) Wires. (0.196-in. and 0.276-in. diameters)

Cable Size	Cable Characteristics		
	12/0.196	18/0.196	12/0.276
Nominal steel area, in.^{2}	0.362	0.543	0.718
Ultimate strength, lb	90,000	135,000	168,500
Max. tensioning load, lb (80% ultimate)	72,000	108,000	135,000
Max. design load, lb (60% ultimate)	54,000	81,000	101,100
Cable weight—sheath not included, lb/ft	1.23	1.85	2.45
Recommended hole diameter, in.	1 1/8	1 1/2	1 1/2
Anchorage diameter, in.	3 7/8	4 7/8	4 7/8
Anchorage length, in.	4	4 7/8	4 7/8

(b) Strands (1/2-in. 7-wire strands)

	Cable Characteristics
Nominal steel area (12 strands cable), in.^{2}	1.73
Ultimate cable strength (1.73 × 250,000 psi), lb	432,000
Maximum tensioning load (75% of ultimate), lb	324,000
Maximum design load (60% of ultimate), lb	259,000
Cable weight (sheath not included), lb/ft	5.93
Recommended hole diameter (I.D.), in.	2 5/8
Anchorage diameter, in.	8 1/4

shrinkage of concrete equal to 0.0003 in./in. is frequently used for estimating loss of prestress, although values can be much higher. Readers should refer to Chapter 3 for a more reliable estimation of shrinkage and creep.

In general, prestress is transferred to the concrete of pretensioned members at an earlier age when the concrete is less mature. Therefore, more creep and shrinkage take place in pretensioned members, resulting in a higher loss of prestress, than in posttensioned members.

6.3.3 Relaxation in Steel

Relaxation in steel is the loss of its stress when the steel is tensioned and maintained at a constant strain for a period of time. Relaxation varies with steel of different compositions and treatments, but its approximate characteristics

TABLE 6.5. Roebling System Galvanized Strands for Posttensioning.

Diameter, in.	Weight, lb per ft	Area, in.²	Minimum Guaranteed Ultimate Strength, lb	Recommended Design Load, lb	Anchorage Plate in.
0.600	0.737	0.215	46,000	26,000	4 × 4
0.835	1.412	0.409	86,000	49,000	6 × 6
1	2.00	0.577	122,000	69,000	8 × 8
1 1/8	2.61	0.571	156,000	90,000	—
1 1/4	3.22	0.931	192,000	112,000	9 × 9
1 3/8	3.89	1.12	232,000	134,000	—
1 1/2	4.70	1.36	276,000	163,000	10 3/4 × 10 3/4
1 9/16	5.11	1.48	300,000	177,000	—
1 5/8	5.52	1.60	324,000	192,000	—
1 11/16	5.98	1.73	352,000	208,000	12 × 12

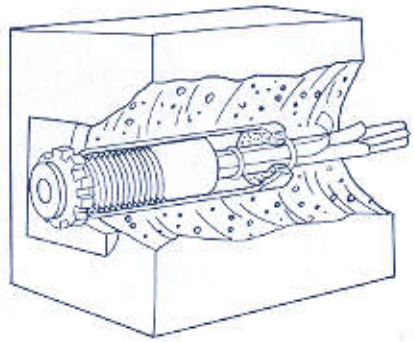

End anchorage—Roebling system

are known for most of the prestressing steels now in the market. Speaking in general, the percentage of relaxation increases with increasing stress; and when a steel is under low stress, the relaxation is negligible. Typical curves giving the relation between relaxation and initial stress level in two types of steel wires are shown in Fig. 6.5.

Relaxation in stress-relieved 7-wire strands has characteristics similar to those of stress-relieved wires. A study made by Magura, et al.,[1] shows that the relaxation in stress-relieved 7-wire strands can be expressed as

$$\Delta f_s = f_{si}\left[\frac{\log_{10} t}{10}\left(\frac{f_{si}}{f_y} - 0.55\right)\right] \tag{6.9}$$

TABLE 6.6. Stressteel Bars.

Bar Size ϕ"	Weight lb/lin ft	Area in.²	Ultimate Strength Guaranteed Minimum		Initial Tensioning Load—$0.7f'_s$[a]		Design Load—$0.6f'_s$		Anchorage Plate, in.
			Regular[b]	Special[c]	Regular	Special	Regular	Special	
			(All values in units of 1000 lb)						
3/4	1.50	0.442	64.1	70.7	44.9	49.5	38.5	42.4	4 × 4
7/8	2.04	0.601	87.1	96.2	61.0	67.3	52.3	57.7	4 1/2 × 5
1	2.67	0.785	113.8	125.6	79.7	87.9	68.3	75.4	5 × 5 1/2
1 1/8	3.38	0.994	144.1	159.0	100.9	111.3	86.5	95.4	6 × 6
1 1/4	4.17	1.227	177.9	196.3	124.5	137.4	106.7	117.8	6 × 7
1 3/8	5.05	1.485	215.3	237.6	150.7	166.3	129.2	142.6	7 × 7 1/2

[a] Losses due to creep and shrinkage of concrete and steel relaxation should be deducted from this value. Overtension to $0.8f'_s$ is permitted to account for friction loss and/or wedge seating loss.
[b] Regular is for minimum ultimate strength of 145,000 psi.
[c] Special is for minimum ultimate strength of 160,000 psi.

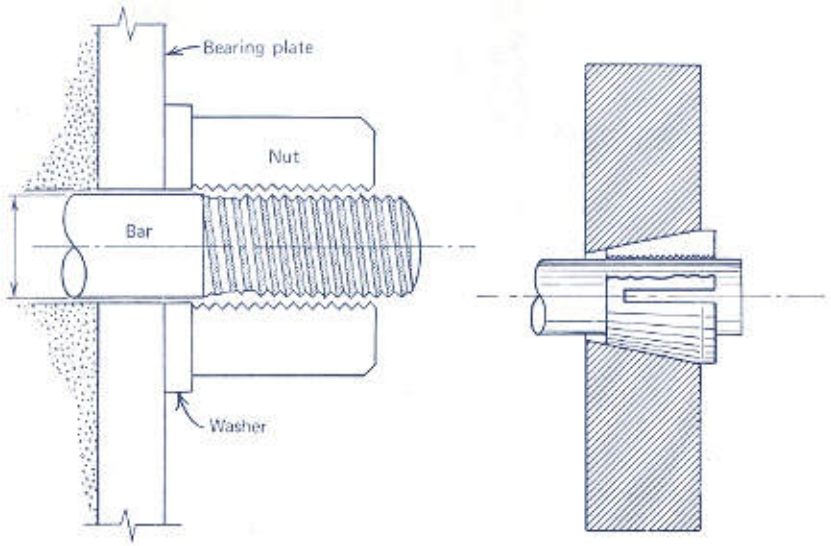

(a) Tapered thread and anchorage (b) Wedge anchorage

where f_{si} is the initial stress in the prestressing strand, in psi, f_y is the yield strength of the strand at one percent elongation, in psi, t is the time in hours. A similar expression for stabilized strands is

$$\Delta f_s = f_{si}\left[\frac{\log_{10} t}{45}\left(\frac{f_{si}}{f_y} - 0.55\right)\right] \tag{6.10}$$

Both formulae are applicable only for $f_{si} \geq 0.60 f_y$.

6.3.4 Slippage of Tendons during Anchoring

For most systems of posttensioning, when the jack is released and the prestress is transferred to the anchorage, the tendon tends to slip slightly. The amount of slippage depends on the type of wedge and the stress in the wires, an average value for friction anchorages being around 0.1 in. but may go up to 0.2 in. For direct bearing anchorages, the heads and nuts are subject to a slight deformation at the release of the jack of about 0.03 in. Again, a shim 1 ft long may deform 0.01 in. In the Roebling system, the deformation of the lead anchorage may be as much as 0.2 in. for the 1 11/16-in. strands. A general formula for computing the loss of prestress due to deformation δ_a at anchorage is

$$\Delta f_s = \frac{\delta_a E_s}{L} \tag{6.11}$$

where L is the length of tendon, also measured in inches.

TABLE 6.7. VSL Posttensioning System Using 1/2-in. 7-Wire Strands of 270K Grade.

Unit	No. of Strands	Steel Area ($in.^2$)	Weight (lb/ft)	Max. Temp. Force (kips)	Initial Force (kips)	Wording Force (kips)	Sheath Diameter (in.) Flexible Tubing	Sheath Diameter (in.) Rigid Tubing	Bearing Plate (in.)
E5-1	1	0.153	0.525	33.0	28.9	24.8	3/4	1	3 × 3
E5-3	2	0.306	0.050	66.1	57.8	49.6	1 1/4	1 1/2	5 1/2 × 5 1/2
	3	0.459	1.575	99.1	86.7	74.3	1 1/2	1 3/4	5 1/2 × 5 1/2
E5-4	4	0.612	2.100	132.2	115.6	99.1	1 5/8	1 3/4	6 1/4 × 6 1/4
E5-7	5	0.765	2.625	165.2	144.5	123.9	1 3/4	2	8 1/4 × 8 1/4
	6	0.918	3.150	198.2	173.5	148.7	1 7/8	2	8 1/4 × 8 1/4
	7	1.071	3.675	231.3	202.4	173.5	2	2 1/4	8 1/4 × 8 1/4
E5-12	8	1.224	4.200	264.3	231.3	198.2	2	2 1/4	10 3/4 × 10 3/4
	9	1.377	4.725	297.4	260.2	223.0	2 1/8	2 1/2	10 3/4 × 10 3/4
	10	1.530	5.250	330.4	289.1	247.8	2 1/4	2 1/2	10 3/4 × 10 3/4
	11	1.683	5.775	363.4	318.0	272.6	2 3/8	2 1/2	10 3/4 × 10 3/4
	12	1.836	6.300	396.5	346.9	297.4	2 1/2	2 3/4	10 3/4 × 10 3/4
E5-19	13	1.989	6.825	429.5	375.8	322.1	2 5/8	3	13 1/2 × 13 1/2
	14	2.142	7.350	462.6	404.7	346.9	2 5/8	3	13 1/2 × 13 1/2
	15	2.295	7.875	495.6	433.6	371.7	2 3/4	3 1/4	13 1/2 × 13 1/2
	16	2.448	8.400	528.6	462.6	396.5	2 7/8	3 1/4	13 1/2 × 13 1/2
	17	2.601	8.925	561.7	491.5	421.3	3	3 1/2	13 1/2 × 13 1/2
	18	2.754	9.450	594.7	520.4	446.0	3	3 1/2	13 1/2 × 13 1/2
	19	2.907	9.975		549.3	470.8	3 1/8	3 1/2	13 1/2 × 13 1/2
E5-22	19	2.907	9.975	627.8			3 1/8	3 1/2	14 3/4 × 14 3/4
	20	3.060	10.500	660.8	578.2	495.6	3 1/4	3 3/4	14 3/4 × 14 3/4
	21	3.213	11.025	693.8	607.1	520.4	3 1/4	3 3/4	14 3/3 × 14 3/4
	22	3.366	11.550	726.9	636.0	545.2	3 3/8	3 3/4	14 3/4 × 14 3/4
E5-31	23	3.519	12.075	759.9	664.9	569.9	3 1/2	4	17 1/2 × 17 1/2
	24	3.672	12.600	793.0	693.8	594.7	3 1/2	4	17 1/2 × 17 1/2
	25	3.825	13.125	826.0	722.7	619.5	3 5/8	4	17 1/2 × 17 1/2
	26	3.978	13.650	859.0	751.7	644.3	3 5/8	4	17 1/2 × 17 1/2
	27	4.131	14.175	892.1	780.6	669.6	3 3/4	4 1/4	17 1/2 × 17 1/2
	28	4.284	14.700	925.1	809.5	693.8	3 7/8	4 1/4	17 1/2 × 17 1/2
	29	4.437	15.225	958.2	838.4	718.6	3 7/8	4 1/4	17 1/2 × 17 1/2
	30	4.590	15.750	991.2	867.3	743.4	4	4 1/2	17 1/2 × 17 1/2
	31	4.743	16.275	1024.2	896.2	768.2	4	4 1/2	17 1/2 × 17 1/2
E5-55	55	8.415	28.875	1817.6	1590.4	1363.2	5 1/2	6	24 × 24

TABLE 6.8. Seven-Wire Uncoated Stress-Relieved Strands for Pretensioning.*

Nominal Diameter in.	Weight per 1000 ft, lb	Approximate Area in.²	Ultimate Strength, lb	Tensioning Load, lb
ASTM A-416 Grade				
1/4	122	0.0356	9,000	6,300
5/16	198	0.0578	14,500	10,150
3/8	274	0.0799	20,000	14,000
7/16	373	0.1089	27,000	18,900
1/2	494	0.1438	36,000	25,200
270K Grade				
3/8	292	0.085	23,000	16,100
7/16	400	0.117	31,000	21,700
1/2	525	0.152	41,300	28,910

* Addresses of some United States suppliers:
Colorado Fuel and Iron Corp., Continental Oil Building, Denver
Leschen Wire Rope Division, H. K. Porter Co., 2727 Hamilton Ave, St. Louis
John A. Roebling's Sons, 640 S. Broad St., Trenton, N. J.
Union Wire Rope Corp., 21st and Manchester Avenue, Kansas City, Mo.
American Steel & Wire Division, U.S. Steel Corp., Cleveland

Since this loss of prestress is caused by a fixed total amount of shortening, the percentage of loss is higher for short wires than for long ones. Hence it is quite difficult to tension short wires accurately, especially for systems of prestressing whose anchorage losses are relatively large. On the other hand, in the long-line process of pretensioning, this type of loss is insignificant and is not taken into consideration in design.

6.3.5 Friction

The stress in a tendon gradually decreases as the distance increases from the tensioning end, because there is friction between the tendon and its surrounding concrete or sheathing.

This frictional loss can be conveniently considered in two parts: the length effect and the curvature effect. The length effect is the amount of friction that would be encountered if the tendon is a straight one, that is, one that is not

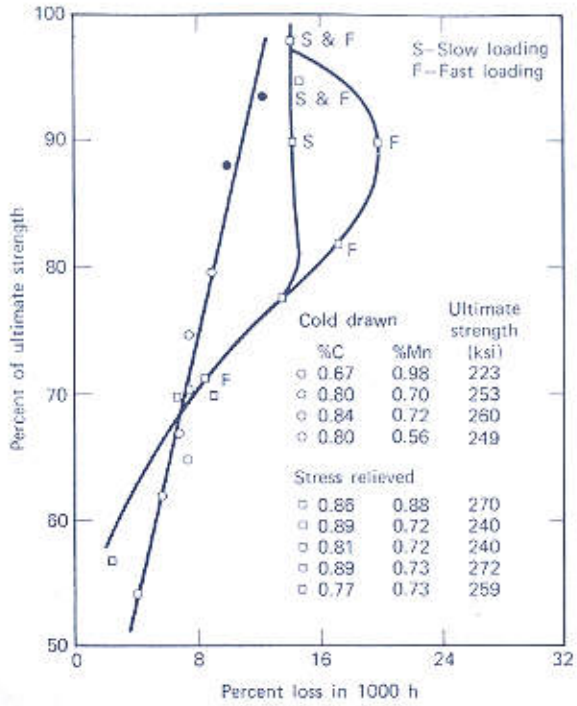

FIGURE 6.5. Relaxation of prestressing wires. (After W. O. Everling, "Prestressing Steel Under High Stress," Proceedings World Conference on Prestressed Concrete, San Francisco, 1957.)

purposely bent or curved. Since in practice the duct for the tendon cannot be perfectly straight, some friction will exist between the tendon and its surrounding material even though the tendon is meant to be straight. This is sometimes described as the wobbling effect of the duct and is dependent on the length and stress of the tendon, the coefficient of friction between the contact materials, and the workmanship and method used in aligning and obtaining the duct.

The loss of prestress due to a curvature effect results from the intended curvature of the tendons in addition to the unintended wobble of the duct. This loss is again dependent on the coefficient of friction between the contact materials and the pressure exerted by the tendon on the concrete. The coefficient of friction, in turn, depends on the smoothness and nature of the surfaces in contact, the amount and nature of lubricants, and sometimes the length of contact. The pressure between the tendon and concrete is dependent on the stress in the tendon and the total change in angle.

The most common method of measuring the air content of freshly mixed concrete is the *pressure method* (ASTM C231) which makes use of the fact that in fresh concrete only the air is compressible. In this method pressure is applied to a concrete sample placed into an air meter and the reduction in volume is observed on a gage calibrated in terms of percent air. The observed amount of air includes both the purposely entrained air as well as the entrapped air. The *entrapped air* are air voids which are unintentionally introduced during the mixing operation. Non-air-entrained concrete will contain about 1–2% entrapped air. The pressure method is not recommended for use on concretes made with lightweight and porous aggregates. The *volumetric method* (ASTM C173) is a suitable method for determining the air content of concretes containing such porous aggregates as well as ordinary aggregates.

The factors which affect the amount of air entrained include the aggregate proportions and gradation, mixing time, temperature, and slump. The volume of entrained air can readily be adjusted to meet job conditions by changing the amount of air-entraining admixture.

1.10.5 Unit Weight and Cement Content

The *unit weight* of concrete in pcf (pounds per cubic foot) is frequently determined as a job quality control measure in conjunction with tests for other properties of fresh concrete. The method of test for unit weight is given in ASTM C138. It is a simple test in which the weight of a given volume of concrete is determined and the unit weight computed.

The unit weight of structural concrete ranges from about 148 to 152 pcf depending upon the specific gravity and maximum size of aggregate. High specific gravity aggregates, such as some basalts and granites, will produce concretes of unit weights up to 156 pcf. The larger the maximum size of aggregate used the greater the unit weight. Air-entrained concrete will have a 3–5% lower unit weight depending on the amount of entrained air.

Structural lightweight concrete has a unit weight ranging from about 100 to 115 pcf. Concretes for radiation shielding containing heavy aggregates, such as barite, magnetite, or ilmenite, have a unit weight of about 215–240 pcf. With iron ore for sand and steel punchings for coarse aggregate, concretes weighing about 270 pcf have been produced.

The *cement content* of concrete, in pcy (pounds per cubic yard) can be computed from the unit weight and batch quantities of a concrete mix as follows:

$$\text{Cement Content (pcy)} = \frac{\text{Wt. of Cement}}{\text{Total Batch Wt.}} \times \text{Unit Wt.} \times 27$$

The cement content of concrete is sometimes referred to as the cement factor and expressed in units of scy (sacks per cubic yard), with the weight of one sack of portland cement being 94 lb.

1.10.6 Time of Setting

Another property of freshly mixed concrete that needs to be considered in construction practice is its stiffening characteristic. After completion of mixing, concrete gradually stiffens until it becomes rigid. It is essential that it remain plastic for a sufficient period of time to permit being transported, placed, consolidated, and finished. One of the standard methods used to determine the *time of setting*[21] of concrete is the penetration resistance test (ASTM C403). In this test a plunger is forced into a sample of mortar sieved from the concrete and the stress required for this plunger to penetrate to a depth of 1 in. is determined. Several size plungers are used in this test. An example of results obtained from this test are shown in Fig. 1.4 for concrete temperatures of 50 and 73°F. The time of *initial set*, taken at a penetration resistance of 500 psi, and the time of *final set*, taken at 4000 psi, are obtained from these curves. Laboratory and field experience has indicated that once the concrete has reached its initial set, sometimes called the *vibration limit*, it can no longer be properly vibrated. Thus, when concrete is placed in a wall or column in several layers, the age of the preceding layer must be less than the time of initial set to insure a monolithic mass of concrete.

Although concrete is usually compacted by vibration immediately after placing, *revibration* or delayed vibration of a previously compacted concrete may be intentionally performed to improve the bond between aggregate and the paste as well as between the concrete and reinforcing steel. This revibration should be performed about 1 to 2 h after placing. Any bleeding water that has collected on the underside surfaces of the coarse aggregate or of the reinforcing steel will be expelled during revibration, improving the bond significantly. Laboratory tests[22] have shown that the compressive strength of revibrated concrete is about 10–15% greater than that of the same concrete

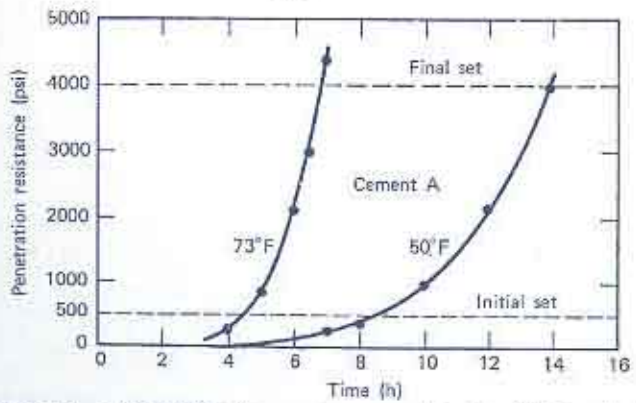

FIGURE 1.4. Effect of low temperature on setting time.[21] (Reprinted by permission of the American Society for Testing and Materials, Copyright ASTM.)

TABLE 6.9. Coefficients of Frictional Loss.

		Wobble Coefficient, K	Curvature Coefficient
Grouted Tendons in Metal Sheathing	Wire tendons	0.0010–0.0015	0.15–0.25
	High strength bars	0.0001–0.0006	0.08–0.30
	7-wire strand	0.0005–0.002	0.15–0.25
Unbonded tendons: Mastic-coated	Wire tendons	0.001–0.002	0.05–0.15
	7-wire strand	0.001–0.002	0.05–0.15
Unbonded tendons: Pre-greased	Wire tendons	0.0003–0.002	0.05–0.15
	7-wire strand	0.0003–0.002	0.05–0.15

If F_1 is the total stress at the jacking end, in lb, F_2 is the total stress at another point on the tendon, in lb, x is the length between the two points above, in ft, θ is the total angular change of the tendon between the two points above, in radians, μ is the coefficient of friction between tendon and surrounding material, and K is the wobble coefficient, per ft, we have,

$$F_2 = F_1 e^{-(\mu\theta + Kx)} \tag{6.12}$$

where e is the base for the natural logarithm.

When $\mu\theta + Kx$ is less than 0.3, the following approximate formula can be used,

$$F_2 = F_1(1 - \mu\theta - Kx) \tag{6.13}$$

For estimating the value of μ and K, Table 6.9 is taken from the Commentary on the 1971 ACI Code. It is to be noted that actual values may differ greatly from those given in the table and can only be obtained from experience. For example, the μ and K values depend a great deal on the care exercised in construction. Tendons wrapped in plastic tubes will have little friction, but if mortar leaks through openings in the tube, the cables may be tightly stuck.

There are several methods for overcoming the frictional loss in tendons. One method is to overtension them. Jacking from both ends is another means to reduce frictional loss. For unbonded tendons, lubricants can be used to advantage. For bonded tendons, water soluble oils can be used to reduce friction while tensioning, and the lubricant is flushed off with water afterwards before grouting.

6.3.6 Elongation of Tendons

The force in the tendon is generally measured by the gage pressure of the hydraulic jack but also verified by the elongation of the tendon at the jacking end. If a tendon has uniform stress F along its entire length L, the total elongation is given by

$$\delta_s = \frac{FL}{E_s A_s} \tag{6.14}$$

For a curved tendon with uniform curvature, considering frictional loss throughout its length L, then the total elongation is

$$\delta_s = \frac{F_2 L}{E_s A_s} \frac{e^{(\mu\theta + KL)} - 1}{\mu\theta + KL} \tag{6.15}$$

If only an approximate solution is desired, one can use

$$\delta_s = \frac{F_1 + F_2}{2} \frac{L}{E_s A_s} \tag{6.16}$$

6.3.4 Total Amount of Losses

The effective prestress in steel is obtained by deducting the losses from the initial prestress. It should be kept in mind that the total amount of loss of prestress varies with many factors. For a close estimate of prestress loss, it is necessary to consider the amount of various losses in successive time intervals such as before transfer of prestress, during transfer of prestress, first year after transfer of prestress and from first year to the end of service life of the structure. However, for the average case, the following are representative.

	Pretensioning, %	Posttensioning, %
Elastic shortening of concrete	3	1
Creep of concrete	6	5
Shrinkage of concrete	7	6
Relaxation in steel	2	3
Total loss not including frictional loss	18	15

6.4 ANALYSIS FOR FLEXURE

The flexural behavior of prestressed concrete beams under working loads is essentially elastic. Therefore, it can be analyzed by the usual elastic beam theory based on uncracked sections.

During bending of the beam, there is actually an increase of prestressing force. However, under working loads, this increase is nearly always neglected since it is only a small amount in the order of less than 5%. Likewise, the effects of transformed area of steel and the change in length of tendon due to its curvature are also neglected in analysis.

6.4.1 Stresses in Concrete

Stresses in concrete can be analyzed by any one of the three concepts presented in Section 6.1. Only the combined loading concept will now be considered, since it provides a complete knowledge of stress variations under different loading conditions. As mentioned before, the stress at any point y from the c.g.c. of a beam is given by

$$f = \frac{F}{A} \pm \frac{Fey}{I} \mp \frac{M_G y}{I} \mp \frac{M_L y}{I} \tag{6.17}$$

where M_G is the moment due to weight of girder, and M_L is the moment due to the live load. Similarly, in a more general case where the prestress F is eccentric with respect to both principal axes X and Y of the section with eccentricities e_x and e_y, the stress is then given by

$$f = \frac{F}{A} \pm \frac{Fe_y y}{I_x} \pm \frac{Fe_x x}{I_y} \mp \frac{M_x y}{I_x} \mp \frac{M_y x}{I_y} \tag{6.18}$$

where M_x and M_y are external moments with respect to the principal axes X and Y.

The above equations indicate that the stresses due to prestressing counteract those produced by external moments. Clearly, for beams containing straight tendons with a constant eccentricity, the critical section at transfer would be at points where the external moment is minimum such as at the support of a simple beam; and the stresses thereof should be investigated when F has its maximum value. After the prestress has been reduced by the losses and when the beam is carrying its full design load, the critical section would then be at the point of maximum external moment. For beams with curved and draped tendons where the tendon eccentricity is varying throughout, it is not uncommon to have critical sections located at points other than that of maximum moment. Therefore, concrete stresses should be investigated at several critical sections of a beam for a number of loading conditions, if the various points of maximum stress are to be determined.

6.4.2 Stresses in Steel

The variation of steel stress at midspan of a simple beam under increasing load is shown in Fig. 6.6. As the tendons are tensioned, the steel stress increases from A to B. This initial prestress in steel is measured during the jacking operations by the elongation of steel and by the gage pressure of the jack.

In most cases, because of eccentric prestressing, there is a tendency for prestressed beams to camber up and to carry their own weight immediately after transfer of prestress. If the beam is relatively light, it may begin to camber up even before the steel stress reaches the initial prestress f_0. Hence, the steel stress may change from A to B' and then to C', the exact path $B'C'$ being dependent upon how rapidly the beam cambers up and picks up its own weight. Because of the upward curvature, the tendons shorten slightly so that its stress as represented by C' is a bit less than f_0.

For a beam, which is heavy relative to its live load, the situation would be somewhat different. During transfer of prestress, the weight of the beam would keep it from cambering up and therefore no load will be carried by the beam until its falsework is removed, at which time the beam will deflect downward slightly, thus changing the steel stress from B to C.

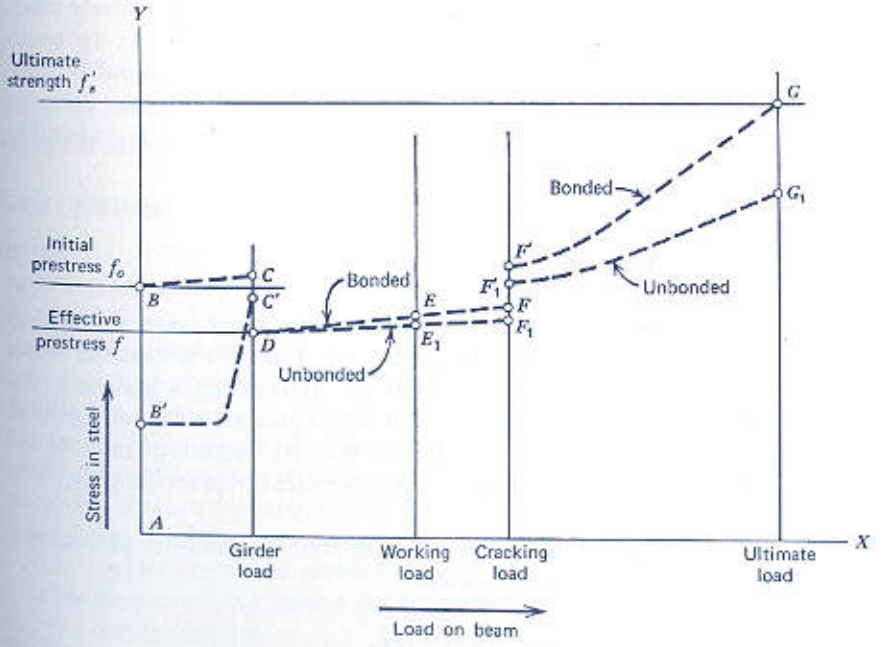

FIGURE 6.6. Variation of steel stress with load.

Immediately after transfer of prestress, the losses of prestress will take place, reducing the steel stress from C or C' to D. Actually, the losses will not take place all at once but will continue for some length of time. However, for convenience in discussion, it is assumed that all losses take place before the application of superimposed dead and live loads. The losses are computed or estimated to obtain the effective prestress f.

When superimposed dead and live loads are applied to the beam, only minor changes in stress will be induced in the steel as shown from D to E and then to F. These changes in steel stress are equal to the modular ratio n times the corresponding changes in concrete stresses adjacent to the steel, using transformed section.

As cracking takes place, the beam suddenly changes into a cracked section, and consequently behaves as a conventional reinforced concrete beam. The stress in the steel across the crack increases suddenly from F to F' This stress is further raised to point G, as the beam reaches its ultimate load.

If the tendons are not bonded to the concrete, they would be free to slip with respect to the concrete except for the resistance of the friction between them. This slippage would allow any strain in the unbonded tendon to distribute throughout its entire length. Consequently, as load increases, the stress in an unbonded tendon will increase more slowly than that in a bonded tendon, especially so in the range between cracking load and ultimate load, as shown by $DE_1F_1F_1'G_1$ in Fig. 6.6. It should be noted that as the beam reaches its ultimate load, the stress in the unbonded tendon could be substantially lower than its ultimate strength f_s'. This explains why the ultimate moment capacity of an unbonded beam is often less than that of a comparable bonded beam.

6.4.3 Cracking Moment

The external moment producing the first hairline cracks in a prestressed concrete beam is known as the cracking moment. The behavior of the beam changes significantly at the cracking moment. As cracking takes place, the beam increasingly loses its stiffness, resulting in greater deflections. It also becomes more vulnerable to corrosion and thus its durability could be reduced. The cracking moment, therefore, is a measure of the serviceability of a prestressed concrete beam.

Cracking occurs when the tensile stress in the extreme fiber of concrete reaches its modulus of rupture f_r. Thus,

$$-\frac{F}{A}-\frac{Fec}{I}+\frac{Mc}{I}=f_r \tag{6.19}$$

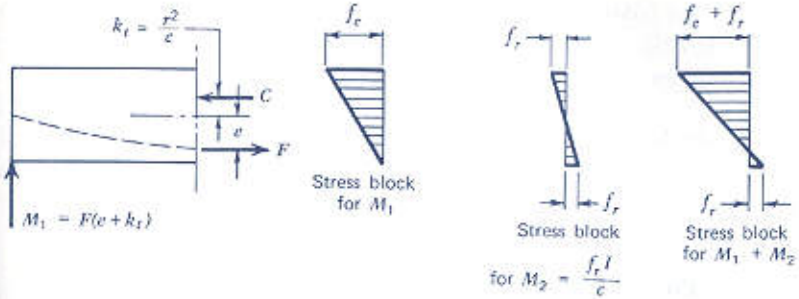

FIGURE 6.7. Cracking moment.

Transposing, we have the value of cracking moment,

$$M = Fe + \frac{FI}{Ac} + \frac{f_r I}{c}$$

This can also be written as,

$$M = F\left(e + \frac{r^2}{c}\right) + \frac{f_r I}{c} \tag{6.20}$$

$$= F(e + k_t) + \frac{f_r I}{c}$$

which is shown as $M = M_1 + M_2$ in Fig. 6.7. Unless the value of f_r is known from tests, it is commonly specified as $7.5\sqrt{f_c'}$ psi.

6.4.4 Ultimate Moment

In relation to the ultimate moment capacity, a prestressed concrete beam may be either under-reinforced or over-reinforced, just as in the case of a conventional reinforced concrete beam. However, since the tendon commonly used in prestressed concrete beams does not have a well-defined yield point and a flat yield plateau, it is impossible to obtain a truly "balanced section" whereby the concrete would reach its crushing strength at the same time when the tendons just begin to yield. If the steel strain at failure is well beyond the commonly specified yield strain (such as 1 % elongation), then the prestressed concrete beam is under-reinforced. On the other hand, if the steel strain is considerably less than the specified yield strain, the beam is over-reinforced.

For an under-reinforced bonded beam, the steel is almost always stressed to its ultimate strength f_s' under the action of the ultimate moment. Thus the ultimate tension force is

$$T' = A_s f_s'$$

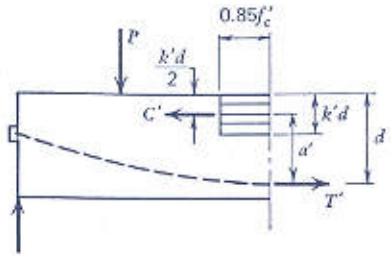

FIGURE 6.8. Stress distribution at ultimate moment.

Using a rectangular stress block with an average stress of $0.85f'_c$ and a depth of $k'd$ as shown in Fig. 6.8, we have for a rectangular section

$$C' = 0.85f'_c bk'd = T'$$

(Note that the ACI Code uses 0.85 $k'd$ for a rectangular block, and locates the N. A. more accurately. For simplicity, the full value of $k'd$ is used here.) It follows that

$$k' = \frac{A_s f'_s}{0.85f'_c bd} \tag{6.21}$$

The above formula is also applicable if the compression zone at failure has a uniform width b, even though the section is not rectangular. Now, the ultimate resisting moment is

$$M_u = T'a' = A_s f'_s\left(d - \frac{k'd}{2}\right) = A_s f'_s d\left(1 - \frac{k'}{2}\right) \tag{6.22}$$

Most building codes and bridge specifications give a slightly different and more conservative formula for the ultimate moment of a rectangular section, namely,

$$M_u = A_s f_{su} d\left(1 - 0.6\frac{\rho f_{su}}{f'_c}\right) \tag{6.23}$$

where ρ is the A_s/bd and f_{su} is the stress in the steel tendon at failure. For flanged sections in which the neutral axis falls outside the flange (usually where the flange thickness t is less than $1.4d\rho f_{su}/f'_c$),

$$M_u = A_{sr} f_{su} d\left(1 - \frac{k'}{2}\right) + 0.85f'_c(b - b')t\left(d - \frac{t}{2}\right) \tag{6.23a}$$

where b is the effective width of the flange, b' is the width of the web, and

$$A_{sr} = A_s - A_{sf}$$
$$A_{sf} = 0.85f'_c(b - b')t/f_{su}$$

It can be seen that the ultimate moment capacity of a flanged section is taken as the ultimate moment of the rectangular web section plus the ultimate moment of the outstanding flanges under a uniform compressive stress of $0.85f'_c$.

Unless the value of f_{su} is determined from detailed analysis, the following is often specified:

for bonded members:
$$f_{su} = f'_s\left(1 - 0.5\frac{\rho f'_s}{f'_c}\right) \tag{6.24}$$

for unbonded members:
$$f_{su} = f_{se} + 10{,}000 + \frac{f'_c}{100\rho} \tag{6.25}$$

but is not more than f_{sy} or $f_{se} + 60{,}000$.

where f_{se} is the effective stress in prestressing steel after losses, in psi, and f_{sy} is the specified yield strength of prestressing steel. The above equation for unbonded members is a modification of the results of a study made by Yamazaki, et al.[2]

In unbonded members, if the tendons do not come into contact with the concrete between the anchorages, a single crack usually forms at the section of maximum moment. At cracking, the beam behaves as a shallow tied arch, rather than as a flexural member. As the load increases, the crack increases rapidly both in width and in depth. At the same time, the deflection of the beam also increases rapidly. If the tendons do come into contact with the concrete between the anchorages, frictional forces will develop between the tendons and the concrete, causing additional cracks to form, and thus slightly improving the behavior of the beam. Nevertheless, the cracks are usually few in number and still open wider and more rapidly than those of a comparable bonded beam. Such undesirable behavior can be improved substantially by the addition of a moderate amount of bonded reinforcement. This type of reinforcement will help distribute cracks so that their widths and spacings are greatly reduced. In addition, the postcracking stiffness and the ultimate strength of the beam are also increased. Therefore, based upon the recommendations of ACI–ASCE Committee 423,[3] the ACI Code requires that a minimum amount of bonded reinforcement of

$$A_s = \frac{T_c}{0.5f_y} \tag{6.26}$$

or

$$A_s = 0.004A_t$$

whichever is larger, be used in all unbonded prestressed concrete beams and one way slabs in order to ensure improved serviceability under overloads.

In the above equations, A_t is the area between the flexural tension face and the center of gravity of the gross section, T_c is the tensile force in the concrete under dead load plus 1.2 times live load, and f_y shall not exceed 60,000 psi.

A rectangular section can be safely considered as being under-reinforced if pf_{su}/f'_c is not more than 0.30. When pf_{su}/f'_c exceeds 0.30, the section becomes over-reinforced and it is often specified that the ultimate moment of such sections shall not be taken as greater than

$$M_u = 0.25 f'_c b d^2 \tag{6.27}$$

By comparison with more accurate analysis, it can be shown that Eq. (6.27) is a very conservative estimate of the ultimate moment capacity of over-reinforced sections. However, since the failure of over-reinforced beams is usually sudden and destructive, it is prudent to specify a conservative value such as is given by Eq. (6.27).

To compute more accurately the ultimate moment capacity of an over-reinforced section, one must consider not only equilibrium but also strain compatibility as shown in Fig. 6.9. Whether the section is rectangular or of some other shape, the following trial and error procedure may be followed.

The maximum strain of concrete at the top fiber is assumed to be 0.003 at failure. Based on the assumption that plane section remains plane as shown in Fig. 6.9, and if the value of $k'd$ is assumed so as to locate the neutral axis, we can obtain the strain of steel at failure as

$$\varepsilon_{s2} = 0.003\left(\frac{d - k'd}{k'd}\right) = 0.003\left(\frac{1 - k'}{k'}\right)$$

This strain ε_{s2} is in addition to the steel strain due to prestress, ε_{s1}, at the time when concrete strain is zero at the top fiber. The total strain of the steel is

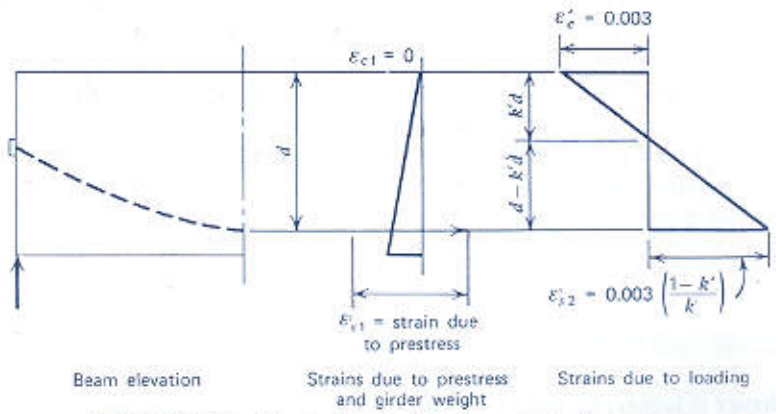

FIGURE 6.9. Strains in steel and concrete at rupture.

therefore

$$\varepsilon_s = \varepsilon_{s1} + \varepsilon_{s2}$$

From the stress–strain diagram of steel, the corresponding stress f_{su} can be obtained. If f_{su} is substituted for f'_s in Eq. (6.21) and can satisfy the equilibrium equation, then the ultimate moment can be obtained from Eq. (6.22). If Eq. (6.21) is not satisfied, then the value of $k'd$ should be modified so as to find a new location of the neutral axis and the above steps are repeated.

In most practical cases, prestressed concrete beams are under-reinforced. If the amount of prestressing steel used in a beam is extremely small, then there is a danger that the beam may fail suddenly as soon as the applied moment on the beam exceeds the cracking moment. To guard against such a sudden failure, most design specifications require that a beam must have a sufficient amount of prestressing steel (including nonprestressed bonded reinforcement, if any) to develop an ultimate moment capacity at least 1.2 times the cracking moment.

6.4.5 Moment–Curvature Relationship

Curvature is a measure of the deformation of a beam. A complete moment–curvature relationship is essential for the determination of moment–deflection or load–deflection diagram for the complete range of loading. In addition, the analysis of moment redistribution in continuous structures also requires the knowledge of moment–curvature relationship.

A typical moment–curvature curve is shown as the dotted line and an idealization of the curve as the solid line in Fig. 6.10. It can be seen that before cracking the moment–curvature relationship is linear. At cracking, the

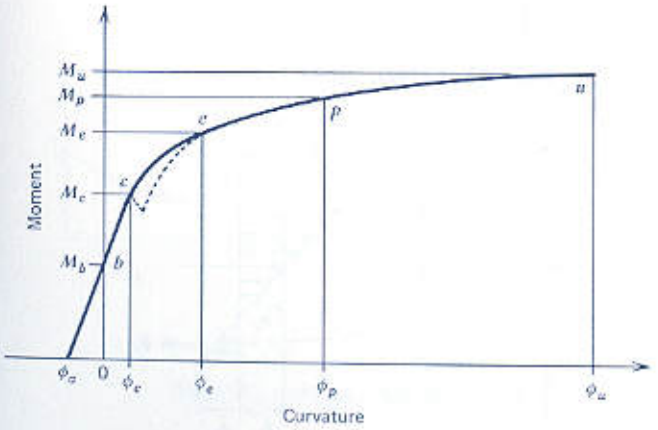

FIGURE 6.10. Moment—curvature relationship.

moment drops slightly before it begins to increase with curvature. This indicates that the beam loses its stability temporarily immediately after cracking and regains the stability with addition of load. Beyond this stage, the moment increases with decreasing rate as the curvature increases.

The moment–curvature curve can be conveniently obtained by establishing successively the points b, c, e, p, and u on the curve. The corresponding moment and curvature for these points can be determined by referring to the stress and strain diagrams shown in Fig. 6.11. Having established the points b and c, the extension of line bc will locate ϕ_0.

At point b, the beam is under balanced load condition and is therefore subjected to a uniform compressive stress [Fig. 6.11(a)]. Under this condition, the beam remains straight and has no curvature. Thus, we have $M_b = Fe$ and $\phi_b = 0$.

At point c, the beam reaches its cracking moment [Fig. 6.11(b)]. This moment produces a stress in the extreme fiber that exceeds the precompression f_a by an amount equal to the modulus of rupture f_r. Hence, we have

$$M_c = M_b + \frac{(f_a + f_r)I}{c_b}$$

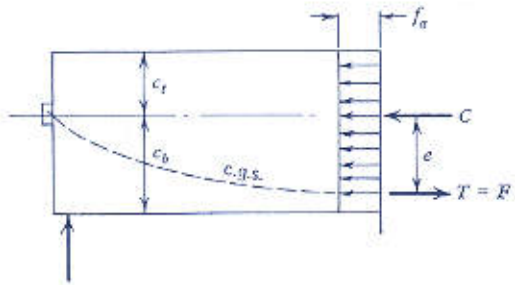

FIGURE 6.11(a). Balanced moment.

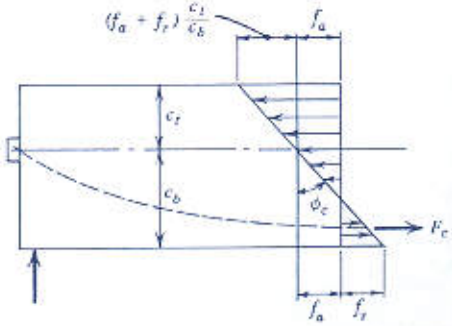

FIGURE 6.11(b). Cracking moment.

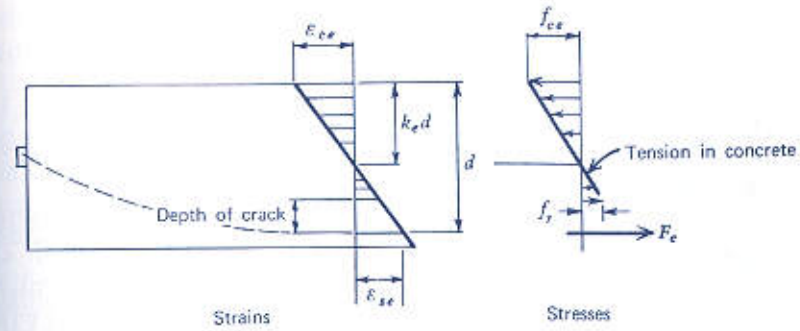

FIGURE 6.11(c). Postcracking; elastic range.

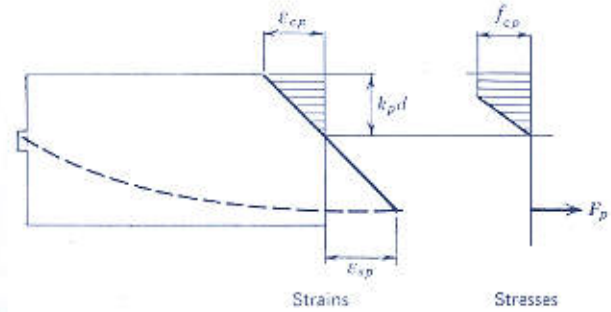

FIGURE 6.11(d). Postcracking; plastic range.

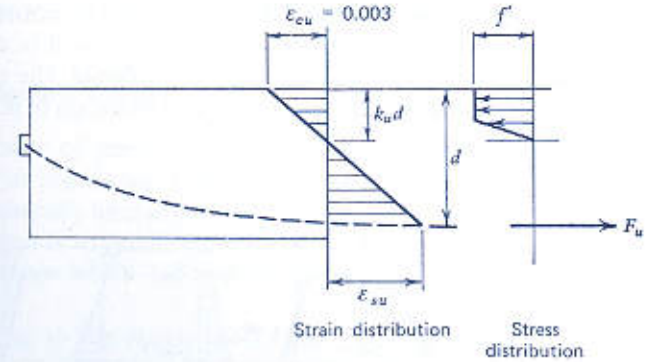

FIGURE 6.11(e). Ultimate moment.

and

$$\phi_c = \frac{(f_a + f_r)}{E_c c_b}$$

where $f_a = F/A_c$, E_c is the modulus of elasticity of concrete, and I is the moment of inertia of the beam cross section.

At point e, the beam is in the postcracking stage, but the concrete stress is still low enough to be considered in the elastic range [Fig. 6.11(c)]. The moment and curvature at this stage can be determined by a simple procedure: Assume $k_e d$ and determine ε_{ce} by satisfying $T = C$. (This can be done either by a trial and error procedure or by solving directly the equation of equilibrium.) Then compute M_e and $\phi_e = \varepsilon_{ce}/k_e d$.

At point p, the beam is also in the postcracking stage, but the concrete stress is usually high enough to be considered in the plastic range as indicated by the trapezoidal stress distribution in Fig. 6.11(d). A similar procedure as given above is used to obtain the moment and curvature: Assume $k_p d$ and determine ε_{cp} by satisfying statics $T = C$. Then compute M_p and $\phi_p = \varepsilon_{cp}/k_p d$.

At point u, the beam reaches its ultimate moment which can be determined by the methods presented before. The corresponding curvature is then $\phi_u = \varepsilon_{cu}/k_u d$ [Fig. 6.11(e)].

6.4.6 Composite Section

Figure 6.12 shows a composite section at the midspan of a simply supported beam, whose lower stem is precast and lifted into position with the top slab cast in place resting directly on the stem. If no temporary intermediate support is furnished, the weight of both the slab and the stem will be carried by the stem acting alone. After the slab concrete has hardened, the composite section will carry any live and dead loads that may be added on to it.

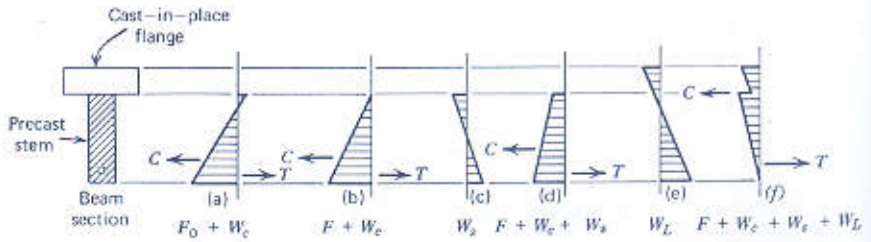

FIGURE 6.12. Stress distribution for a composite section.

In the same figure, stress distributions are shown for various stages of loading. These are discussed as follows:

1. Owing to the initial prestress F_0 and the weight of the stem W_G, there will be heavy compression in the lower fibers and possibly some small tension in the top fibers. The tensile force T in the steel and the compressive force C in the concrete form a resisting couple with a small lever arm between them.
2. After losses of prestress have taken place, the effective prestress F together with the weight of the stem will result in a slightly lower compression in the bottom fibers and some small tension or compression in the top fibers. The C–T couple will act with a slightly greater lever arm.
3. Owing to the addition of the slab, its weight W_s produces additional moment and stresses as shown. Stresses resulting from differential creep and shrinkage between the slab and the stem are neglected.
4. Adding (2) to (3), a smaller compression is found to exist at the bottom fibers and some compression at the top fibers. The lever arm for the C–T couple further increases.
5. Stresses resulting from live load W_L are shown, the moment being resisted by the composite section.
6. Adding (4) to (5), we have stress block as in (f). The couple T and C now acts with an appreciable lever arm.

The above shows the stress distribution under working load conditions. The cracking and ultimate moments can be determined using methods similar to those previously described for noncomposite sections.

6.5 SHEAR, BOND AND END BEARING

6.5.1 Principal Tension

The behavior of prestressed concrete beams under flexural shear can be examined in two stages, before and after cracking. Under working load, the beam is generally uncracked and its behavior is virtually elastic. The effect of flexural shear is to produce a state of combined stresses resulting in principal tensile stresses which indicate the points where potential cracks may develop.

According to the elastic theory, the maximum principal tensile stress is given by

$$S_t = \sqrt{v^2 + \left(\frac{f_c}{2}\right)^2} - \left(\frac{f_c}{2}\right)$$

where v is the shear stress, $V_c Q/Ib$, and f_c is the normal stress due to prestress and external moment, i.e.,

$$f_c = \frac{F}{A} \pm \frac{Fey}{I} \mp \frac{My}{I}.$$

The shear force V_u carried by concrete is equal to the total shear force V minus the shear V_s carried by the transverse component of the tendon force. Occasionally, the tendon inclination with respect to the beam axis is such that its transverse component might add to the shear on the concrete.

The distribution of the normal stress f_c is usually nonuniform and, consequently, the maximum principal tensile stress does not necessarily occur at the centroidal axis where the maximum vertical shear stress exists. At other points, where f_c is diminished, a higher principal tension may exist even though v is not a maximum. In a flanged section, investigation should be made not only at the centroid of the section but also at the junction of the tensile flange and the web.

The elastic analysis for the maximum principal tension is reliable only if the section remains uncracked. When the beam cracks under overload, this method of analysis is no longer valid. Even for the uncracked section, the inadequacy of using the method for design is quite apparent. Under increasing load, the shear stress v increases and the normal stress f_c usually decreases; thus S_t generally increases at a much faster rate than the load. Furthermore, the tensile strength of concrete is known to be dependent upon the state of stress. In view of these factors, it is somewhat difficult to fix a consistent limiting value for the allowable principal tension for purposes of design. Generally speaking, the maximum principal tension is often limited to roughly $2\sqrt{f'_c}$ for beams without web reinforcement and to $4\sqrt{f'_c}$ for beams with web reinforcement.

6.5.2 Ultimate Flexural Shear Strength of Beam Without Web Reinforcement

When the principal tension exceeds the tensile strength of concrete, cracks are initiated. There are two types of crack development in the region of flexural shear. The first type consists of the cracks that are vertical at initiation primarily due to flexural stress and become inclined as they develop. Under increasing load, one of these cracks propagates a large distance and becomes a major inclined crack, greatly reducing the depth of the compression zone of the beam and leading to crushing failure of concrete. This type of failure is called shear–compression failure and is likely to occur in prestressed concrete beams with thick unreinforced web and low levels of prestress.

The second type of crack development includes those originating in the web, independent from the flexural cracks. This type of web distress leads to a violent formation of a large size inclined crack, usually resulting in sudden failure of the beam in the following forms:

1. Separation of tension flange from web, destroying the bond
2. Crushing of web as a result of tied-arch action developed after the bond is destroyed
3. Secondary inclined cracking from near the support toward compression flange and separating it from the web.

Failure by web distress is likely to occur in beams with thin web and high prestress.

From the above discussion, it is clear that flexural shear failure of a prestressed concrete beam is always characterized by the formation of a major inclined crack in the region of combined moment and shear. Once the inclined crack is fully developed, the behavior of the beam is radically changed. Although the ultimate load of the beam is usually greater than the inclined cracking load, the latter is considered as the useful capacity of the beam since there could be a wide variation of beam behavior between the cracking and ultimate load.

The complex behavior of the beam with inclined cracks is not amenable to precise theoretical analysis. The current design method is basically an empirical approach based on extensive test results.[4]

It has been observed that if a beam fails in shear–compression, the critical inclined crack must have a horizontal projection longer than d, the effective depth of the beam. Thus, a flexural crack located at a distance d from a given section under consideration (in the direction of decreasing moment) may lead to a diagonal crack that could be critical. The formation of such a diagonal crack is usually triggered by another flexural crack located at $d/2$ from the given section (Fig. 6.13). The shear capacity of the beam at section A as governed by shear–compression failure is given by

$$V_{ci} = \frac{M_{cr}}{M/V - d/2} + V_d + 0.6b'd\sqrt{f'_c} + V_p \qquad (6.28)$$

where M is the maximum moment at section A due to superimposed dead and live loads, V is the shear at section A corresponding to M, M_{cr} is the moment due to superimposed dead and live loads to cause flexural crack of section at distance $d/2$ from section A, V_d is the shear due to the dead load of the beam at section A, V_p is the shear carried by the vertical component of force in curved or draped tendon, and b' is the width of the web of the beam. In the above formula, the term $0.6\,b'd\sqrt{f'_c}$ is empirically obtained which accounts

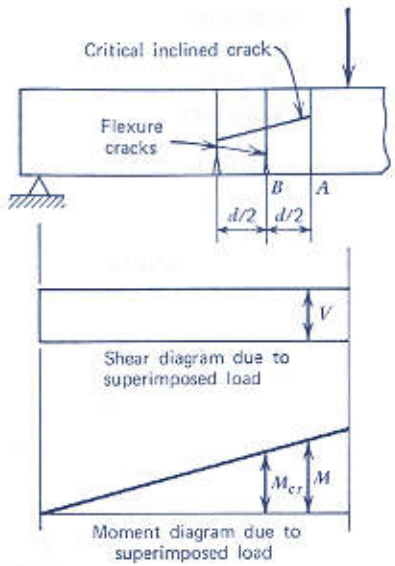

FIGURE 6.13. Inclined crack initiated by a flexure crack for shear–compression failure.

for the additional shear required for the inclined crack to develop after the flexural crack has initiated at the section B. The cracking moment M_{cr} may be calculated from the following expression:

$$M_{cr} = \frac{I}{c_b}(6\sqrt{f'_c} + f_p - f_d) \tag{6.29}$$

where I is the moment of inertia of beam section, c_b is the distance from c.g.c. to bottom fiber, f_p is the stress at bottom fiber due to effective prestress at section B where flexural crack occurs, f_d is the stress at bottom fiber due to dead load of beam at section B, and $6\sqrt{f'_c}$ is the modulus of rupture of concrete. Test results indicate that V_{ci} as expressed by Eq. (6.28) need not be taken less than $1.7\,b'd\sqrt{f'_c}$.

Based on the principal tension theory with a simplification, it has been shown[4] that the shear capacity of a beam as controlled by web-distress is given by

$$V_{cw} = (3.5\sqrt{f'_c} + 0.3f_{pc})b'd + V_p \tag{6.30}$$

where f_{pc} is the compressive stress in concrete at the centroid of the section due to effective prestress. Alternately, V_{cw} may be taken as the external shear producing a principal tensile stress of $4\sqrt{f'_c}$ at the centroid of the section.

In the 1971 ACI Code, Eq. (6.28) is simplified by evaluating the shear at the section under consideration rather than at $d/2$ distance thereof, and also by neglecting the term V_p since it is usually a small quantity where flexural shear cracks are likely to occur. These simplifications result in a slightly conservative expression for V_{ci} as

$$V_{ci} = \frac{VM_{cr}}{M} + V_d + 0.6b'd\sqrt{f'_c} \tag{6.28a}$$

6.5.3 Design of Web Reinforcement

As mentioned before, the useful capacity of a beam without web reinforcement that is vulnerable to shear is taken as the inclined cracking load. Such a beam generally fails abruptly and without developing its flexural capacity. The purpose of web reinforcement is therefore to strengthen the beam so that it will develop its flexural capacity as well as ductility.

Test data indicate that the shear (in excess of that corresponding to inclined cracking load) which can be carried by web reinforcement is in direct proportion to the amount of the reinforcement provided. Thus, the required web reinforcement in a beam is given by

$$A_v = \frac{(V_u - V_c)s}{f_y d} \tag{6.31}$$

where V_u is the shear at a section due to ultimate load corresponding to flexural failure, V_c is the shear corresponding to inclined cracking load, and is equal to V_{ci} or V_{cw}, whichever is smaller, s is the longitudinal spacing of web reinforcement, and f_y is the yield-point stress of web reinforcement less than 60,000 psi. To minimize crack size and spacing, and to ensure adequate serviceability under overload conditions, a minimum amount of web reinforcement is usually specified. According to the 1971 ACI Code, this amount is

$$A_v = 50b's/f_y \tag{6.32}$$

or, when the effective prestressing force is at least 40% of the tensile strength of the prestressing steel, an alternative is

$$A_v = \frac{A_s f'_s}{80 f_y}\frac{s}{d}\sqrt{\frac{d}{b'}} \tag{6.33}$$

where b' is the width of web, A_s is the area of prestressing steel, and f'_s is the ultimate strength of prestressing steel. Similarly, to avoid over-reinforcing a beam with web reinforcement, a maximum amount of shear that can be

carried by web reinforcement is also specified by the Code. This amount is

$$V_u - V_c = 8b'd\sqrt{f'_c} \tag{6.34}$$

It should be emphasized that the spacing of web reinforcement must be such that a potential inclined crack can be intercepted at least by one stirrup. The Code specifies that the maximum spacing of stirrups shall not exceed 0.75 times the depth of the section nor be more than 24 in., and when $(V_u - V_c)$ exceeds $4\,b'd\sqrt{f'_c}$ this spacing should be reduced by 50%.

6.5.4 Horizontal Shear Stress in Composite Section

In composite construction, the horizontal shearing stress v between precast and in-place portions is computed by the usual formula

$$v = \frac{VQ}{Ib}$$

where V is the total shear applied after the in-place portion has been cast, Q is the statical moment of the cross-sectional area of in-place portion taken about the centroidal axis of the composite section, I is the moment of inertia of the composite section, and b is the width of the contact area between the precast and the in-place portions. Allowable value of v varies from about 40 psi for a smooth surface without ties to 160 psi for a roughened surface with adequate ties.

Generally speaking, no ties are required for composite slabs or panels where large contact area is provided. For beams with a narrow strip of top flange to be made composite with in-place slabs, ties are almost always required.

Push-off tests conducted at the Portland Cement Association indicated that the ultimate shearing stress for composite action was about 500 psi for a rough bonded surface and 300 psi for a smooth bonded surface. Approximately 175 psi shear capacity may be added for each percent stirrup reinforcement crossing the joint.

6.5.5 Transfer Bond

In pretensioned beams, the transfer of prestressing force from steel to concrete is principally by bond at the ends of the beam. The stress in the tendon varies from zero at the exposed end to full effective prestress in a distance called transfer length as shown in Fig. 6.14. In a sense, this transfer zone at each end of the tendons performs the function of anchorage.

The transfer bond is largely dependent upon the friction between steel and concrete, and to some degree upon the mechanical shear effect created by the

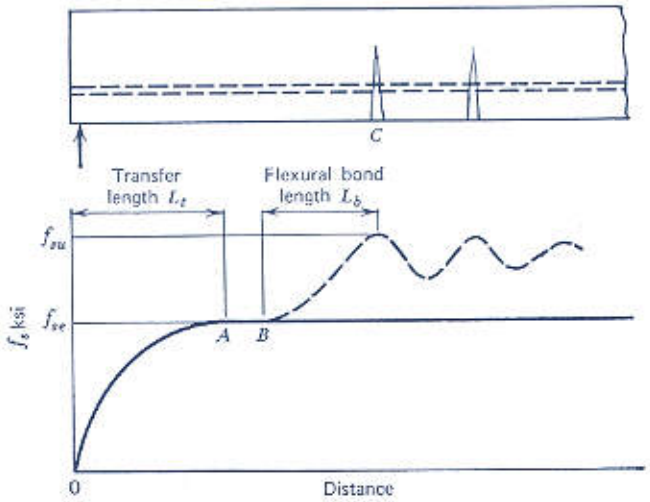

FIGURE 6.14. Variation of steel stress within transfer length and flexural bond length.

surface shape of the strands. Theoretically, the magnitude of the transfer bond stress and the transfer length can be analyzed by the elastic theory of a thick-wall cylinder. However, such an analysis can only be considered as an approximate qualitative guide since inelastic behavior of concrete with possible cracking invalidates the theory.

Test results indicate that the transfer length increases with the size of wire or strand and with the effective stress in the steel. Wires and strands with rusted and indented surfaces require a smaller transfer length because of improved bond properties. The strength of concrete seems to have less influence on the required transfer length, although with higher concrete strength there is a slight decrease in required transfer length. On the average, the transfer length varies from 50 diameters for strands to 100 diameters for wires. An expression that seems to give a reasonable value for the transfer length of strand is

$$L_t = \tfrac{1}{3} f_{se} D \tag{6.35}$$

where f_{se} is the effective prestress, in ksi, D is the diameter of strand, in in., and L_t is the transfer length, in in.

It should be emphasized that within the transfer length, the prestress is less effective and, therefore, the flexure, shear, and cracking strengths of the beam should be carefully investigated within the transfer zone using the reduced value of prestress.

vibrated only once during initial compaction. Revibration must be performed on plastic concrete before it reaches its vibration limit.

The so-called "cold joints" in concrete construction are formed when a concrete surface becomes too stiff before the next batch of concrete is placed against it. The concrete is considered completely hardened when it reaches its final set. It should be pointed out that the setting time of cement, discussed earlier in this chapter, does not adequately define the setting time of concrete which is greatly influenced by mix proportions. However, the setting times of concretes will vary considerably with different cements.

The rate at which concrete stiffens is greatly affected by its temperature as shown in Fig. 1.4. At low temperatures the setting may be excessively delayed for purposes of construction, and at high temperatures it may be excessively accelerated. This may be corrected for by the use of an accelerator or of a retarder, respectively. According to the specifications for chemical admixtures (ASTM C494) an accelerating admixture should reduce the time of initial set by 1 to 3 1/2 h, whereas a retarding admixture should increase this time by 1 to 3 1/2 h. It is the general practice to use accelerators during cold weather construction and retarders in hot weather. Frequently retarders are employed when a large mass of concrete is placed in layers to avoid the formation of cold joints.

1.10.7 Proportioning Concrete Mixtures

The *proportioning*[4,23] of concrete mixtures, sometimes called *mix design*, is the determination of the most economical and practical combination of ingredients for concrete that has the desired workability, strength, durability, and volume stability. There is no simple way to design a concrete mix to satisfy all of the desired properties. The required characteristics are governed by the use to which the concrete will be put and by conditions expected to be encountered during placement. If suitable materials are used, the desired properties of hardened concrete such as strength, durability, and watertightness, are dependent on the selection of a suitable paste, i.e., having an appropriate water–cement ratio and for some properties an adequate amount of entrained air. Since the quality of concrete depends upon its water–cement ratio, the water requirement should be minimized to reduce the cement content and thus produce an economical mix. The water and cement requirement can be minimized by using within practical limits (1) a low slump, (2) a large maximum size of aggregate, and (3) an optimum ratio of fine to coarse aggregates. The selection of the required *slump* of the concrete will depend on type of construction. Recommended values of slump, as given in ACI 211 Report,[23] are shown in Table 1.9.

The *maximum size aggregate* that can be used depends on the size and shape of the structural member and the distribution of reinforcement. Generally,

TABLE 1.9. Recommended Slumps for Various Types of Construction.[23]

Types of Construction	Slump, in.	
	Maximum[a]	Minimum
Reinforced foundation walls and footings	3	1
Plain footings, caissons, and substructure walls	3	1
Beams and reinforced walls	4	1
Building columns	4	1
Pavements and slabs	3	1
Heavy mass concrete	3	1

[a] May be increased 1 in. for methods of consolidation other than vibration.

the maximum size should not exceed one-fifth the minimum dimension of the member, one third the depth of unreinforced slab on grade, nor three-fourths the clear space between the reinforcing bars or between the steel bars and the forms. Since the amount of mixing water required decreases with increase in aggregate size, it is advisable to always use the largest practicable maximum size of coarse aggregate.

The recommended total *air content* for air-entrained concretes is given in Table 1.8. Note that the amount of air decreases with increase in maximum size of aggregate. As discussed earlier, entrained air is contained in the mortar fraction of the concrete, and in properly proportioned mixes, the mortar content decreases as maximum aggregate size increases.

The required *water–cement ratio* of a concrete mix is determined not only by strength requirements but also by durability requirements. Since different aggregates and cements generally produce different strengths at the same water–cement ratio, it is highly desirable to have or develop the relationship between strength and water–cement ratio for the materials actually to be used. In the absence of such data, the approximate and relatively conservative values given in the ACI 211 report[23] and shown in Table 1.11 may be used.

Other tables and charts are available in literature for prediction of strengths for given water-cement ratios and different ages. An example of such approximate relationships for air-entrained and non-air-entrained concrete mixes as given by the Portland Cement Association[4] is shown in Fig. 1.5.

The durability requirements for concretes in severe exposures, such as freezing and thawing or exposure to sea water or sulfates, may require that the water–cement ratio be below the value indicated by the strength requirement.

6.5.6 Flexural Bond

At intermediate points of pretensioned and post-tensioned bonded beams, bond stresses are developed between concrete and steel when the beam is subject to flexural shear. The bond stress is equal to the change in steel force between two adjacent points along the length of the tendon. Prior to cracking of concrete, the change of steel force in the tendon due to bending of beam is very small; therefore, the flexural bond stress is almost insignificant. After the cracking of concrete, the bond stress changes suddenly at the cracks due to the abrupt transfer of tension from concrete to steel at such points. The varying bond stress near the cracks cannot be easily determined. However, if it is assumed that the bond stress is uniform along the length, then the usual bond stress formula for reinforced concrete beams can be applied.

As load increases, the steel stress at a crack such as C in Fig. 6.14 is greatly increased. Likewise, the bond stress and the flexural bond length adjacent to the crack are also increased. When the stress in the tendon reaches the maximum stress f_{su}, the flexural bond length can be computed by the formula

$$L_b = \frac{(f_{su} - f_{se})D}{4u} \tag{6.36}$$

in which u is the average bond stress along the length L_b. It is to be noted that the bond stress along the length L_b is lower than that along the transfer length. Within the transfer length, the strand tends to expand and anchor to the concrete, while when the strand is stressed above f_{se} it tends to contract and pull away from the concrete. Assuming a conservative value $u = 250$ psi, and letting $f_{su} = 250{,}000$ psi and $f_{se} = 150{,}000$ psi, we have, as a reasonable value,

$$L_b = \frac{(250{,}000 - 150{,}000)D}{4 \times 250} = 100D$$

It can be seen clearly from Fig. 6.14 that if a major flexure crack such as C occurs very near the transfer zone, there is a real danger for the tendon to slip progressively from C toward the end of the beam. Obviously, to prevent such a general bond failure, it is necessary to provide sufficient embedment length of the tendon so that the flexure bond length L_b and the transfer length L_t will not overlap. Therefore, the minimum embedment length for strands should be

$$L = L_t + L_b = 50D + 100D = 150D$$

That is to say that within roughly 150 times the strand diameter from the end of a pretensioned beam, the steel stress should not reach its ultimate stress f_{su} when the ultimate load is applied.

An empirical formula for the minimum embedment (or development) length of prestressing strand specified by the 1971 ACI Code is

$$L = (f_{su} - 2/3 f_{se})D. \tag{6.37}$$

This requirement is exactly 150 times strand diameter for $f_{su} = 250$ ksi and $f_{se} = 150$ ksi.

6.5.7 Bearing at Anchorage

For tendons with end anchorages, where the prestress is transferred to the concrete by direct bearing, various designs may be used for transmitting the prestress: steel plates, steel blocks, or reinforced concrete ones.

The design of an anchorage consists of two parts: determining the bearing area required for concrete, and designing for the strength and detail of the anchorage itself. Stress analysis for any anchorage is a very complicated problem, because not only the elasticity but also the plasticity of concrete enters into the picture. As a result, anchorages are often designed by experience, tests, and usage, rather than by analysis.

The allowable bearing stress depends on several factors, such as the amount of reinforcement at the anchorage, the ratio of bearing to total area, and the method of stress computation. A value commonly allowed is $0.60 f'_c$, assuming uniform bearing over the entire contact area. Many building codes and bridge-design criteria also specify the allowable bearing stress as

$$f_{cp} = 0.6 f'_{ci} \sqrt{\frac{A'_b}{A_b}} < f'_{ci} \tag{6.38}$$

where f'_{ci} is the compressive strength of concrete at time of initial prestress, A_b is the bearing area of anchor plate of posttensioning steel, and A'_b is the maximum area of the portion of the anchorage surface that is geometrically similar to and concentric with the area of the anchor plate of the post-tensioning steel.

6.5.8 End Blocks

The portion of a prestressed member surrounding the anchorages of the tendons is often termed the end block. Throughout the length of the end block, prestress is transferred from more or less concentrated areas and distributed through the entire beam section. It is known that this length is not more than the height of the beam and often is much smaller except for pretensioned beams with long transfer length.

For beams with posttensioning tendons, end blocks are used to distribute the concentrated prestressing forces at the anchorage. A closely spaced grid

of both vertical and horizontal bars shall be placed near the face of the end block to resist bursting, and closely spaced reinforcement shall also be placed both vertically and horizontally throughout the length of the block.

Where all tendons are pretensioned wires or 7-wire strands, the use of an end block is not usually required. However, vertical stirrups acting at a unit stress of 20,000 psi to resist at least 4% of the total prestressing force is usually placed within the distance of $d/4$ of the end of the beam, the end stirrup to be as close to the end of the beam as practicable.

Studies made at the Portland Cement Association indicated an empirical equation for the design of stirrups to control horizontal cracking in the ends of pretensioned I-girders,

$$A_t = 0.021 \frac{T}{f_s} \frac{h}{L_t} \tag{6.39}$$

where A_t is the required total cross-sectional area of stirrups at the end of girder, to be uniformly distributed over a length equal to one-fifth of the girder depth, T is the total effective prestress force, in lb, f_s is the allowable stress for the stirrups, in psi, h is the depth of girder, in in., and L_t is the transfer length taken as 50 times the strand diameter, in in.

6.6 DESIGN FOR FLEXURE

6.6.1 Preliminary Design

Preliminary design of sections for flexure can be easily performed by using the internal couple concept, presented in Section 6.1. Under the working load, the lever arm a could vary between $0.30h$ and $0.85h$ with an average of about $0.60h$, where h is the total depth of the section. Hence the required effective prestress F can be estimated from the equation,

$$F = T = \frac{M_t}{0.60h}$$

where M_t is the total external moment produced by the design load. The depth h for a prestressed section varies between 50% and 80% of the depth of an equivalent reinforced concrete section, and may be taken at 70% for a first trial.

Having estimated the force F, the area of steel is computed by,

$$A_s = \frac{F}{f_s}$$

where f_s depends on the type of steel used but usually equals about 150 ksi. The area of concrete required is estimated by,

$$A_c = \frac{C}{f_{av}} = \frac{F}{f_{av}}$$

where f_{av}, the average precompression in the concrete, varies from 700 to 1300 psi for I and T beams and from 250 to 500 psi for solid slabs.

Preliminary design can also be made using the load balancing method, as will be explained later in this section.

6.6.2 Elastic Design

Design for working loads by the elastic theory can be accomplished by using formulas given in Section 6.4. But it is often more convenient to use the internal couple concept. In the following discussion, two cases will be considered.

CASE 1. The dead load moment M_G is small so that the c.g.s. cannot be located at the lowest possible position [Fig. 6.15(a)]. Allowing no tension in the concrete, the c.g.s. must then be located at distance $d_1 = M_G/F_0$ below the bottom kern point, where F_0 is the prestress at transfer. After losses of prestress have taken place, the permissible total external moment will be

$$M_T = F(k_t + k_b + d_1)$$

If a tension f'_t is allowed in the top fibers and f'_b in the bottom fibers, then the placement of the c.g.s. would be at a distance

$$d_1 = \frac{M_G + f'_t I/c_t}{F_0}$$

and the total permissible external moment after loss of prestress will be

$$M_T = F(k_t + k_b + d_1) + \frac{f'_b I}{c_b}$$

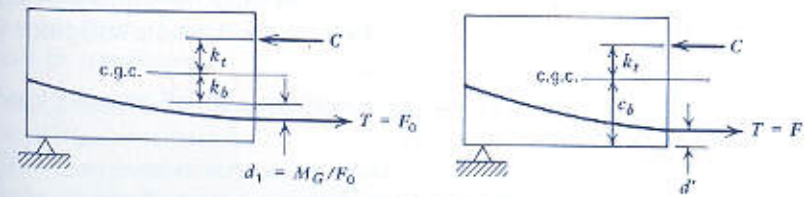

FIGURE 6.15. Elastic design by internal couple concept.

CASE 2. The dead load moment M_G is large so that the c.g.s. can be located at the lowest possible position as determined by the required concrete protection d' [Fig. 6.15(b)]. In this case, the stresses will be critical at prestress transfer and the total allowable external moment, not allowing tension in the concrete, will be

$$M_T = F(k_t + c_b - d')$$

If tensile stress f'_b is allowed for the bottom fibers, we have

$$M_T = F(k_t + c_b - d') + \frac{f'_b I}{c_b}$$

After the prestress F has been determined and located using the above formulas, the area of steel can be computed by

$$A_s = \frac{F}{f_s}$$

Then the extreme fiber stresses in concrete shall be computed under M_G and under M_T, using formulas given in Section 6.4. If the stresses are not satisfactory, the section shall be revised accordingly. This trial and error method of design is easy to learn although direct design formulas and computer programs are available elsewhere.

When using the elastic theory for design, allowable stresses should in fact differ for different structures and elements. However, most codes do specify definite values. Some of the typical ones as extracted from the 1971 ACI Code are listed below:

18.4—Permissible stresses in concrete—Flexural members

18.4.1—Flexural stresses immediately after transfer, before losses, shall not exceed the following:

(a) Compression ..... $0.60f'_{ci}$

(b) Tension stresses in members without bonded auxiliary reinforcement (unprestressed or prestressed) in the tension zone ..... $3\sqrt{f'_{ci}}$

Where the calculated tension stress exceeds this value, reinforcement shall be provided to resist the total tension force in the concrete computed on the assumption of an uncracked section.

18.4.2—Stresses at service loads, after allowance for all prestress losses, shall not exceed the following:

(a) Compression ..... $0.45f'_c$

(b) Tension in precompressed tensile zone ..... $6\sqrt{f'_c}$

(c) Tension in precompressed tensile zone in members where computations based on the transformed cracked section and

on bilinear moment deflection relationships show that immediate and long-term deflections comply with requirements of Section 9.5 ..... $12\sqrt{f'_c}$

18.4.3—The permissible stresses in Sections 18.4.1 and 18.4.2 may be exceeded when it is shown experimentally or analytically that performance will not be impaired.

18.5—Permissible stresses in steel

18.5.1—Due to jacking force ..... $0.80f_{pu}$ but not greater than the maximum value recommended by the manufacturer of the steel or of the anchorages

18.5.2—Pretensioning tendons immediately after transfer, or post-tensioning tendons immediately after anchoring ..... $0.70f_{pu}$

where f'_{ci} is the compressive strength of concrete at time of initial prestress, and f'_c is the specified compressive strength of concrete, both in psi, and f_{pu} is the ultimate strength of prestressing steel, in psi.

6.6.3 Ultimate Strength Design

In the ultimate strength design, the ultimate moment capacity of the section is to be no less than the design load moment multiplied by a factor of safety m, usually above 1.8. For under-reinforced sections, the ultimate lever arm will be around $0.9d$, where d is the effective depth from the c.g.s. to the extreme compressive fiber. Then the area of steel required is,

$$A_s = \frac{mM_T}{0.9\, df'_s}$$

Assuming that the concrete on the compressive side is stressed to $0.85f'_c$, then the required concrete area under compression is,

$$A_c = \frac{mM_T}{0.9d \times 0.85f'_c}$$

When designed by the above formulas, the section should be checked by the ultimate strength equations in Section 6.4. In addition, the following factors must be considered:

1. Load factors must be chosen considering the possible overloads for the particular structure.
2. Compressive stresses at transfer must be investigated for the tensile flange, generally by the elastic theory. In addition, the tensile flange should be capable of housing the steel properly.
3. Design of the web will depend on shear and other considerations.

4. Checks for excessive camber, deflection, and cracking should be performed.

6.6.4 Balanced-Load Design

The load balancing method explained in Section 6.1 can be conveniently used for design. To understand the relation between this method and the elastic and ultimate design method, one should examine the life history of a prestressed member under flexure as described in Fig. 6.16. Several critical points along with the various loading conditions are indicated on the load-deflection curve:

1. At the point of no deflection, the beam is subjected to a rectangular stress block across the section.
2. At the point of no tension, a triangular stress block acts across the section with zero stress at the bottom fiber of a simple beam.
3. At the point of cracking, the extreme fiber is stressed to the modulus of rupture.
4. At the point of yielding, the steel is stressed beyond its yield point so that complete recovery will not be obtained.
5. The ultimate load represents the maximum load carried by the member at failure.

It is noted that a factor of safety m_1 is applied to the working load $(DL + LL)$ to obtain the minimum yield point load and another factor of safety m_2 is applied to $(DL + LL)$ to the minimum ultimate load.

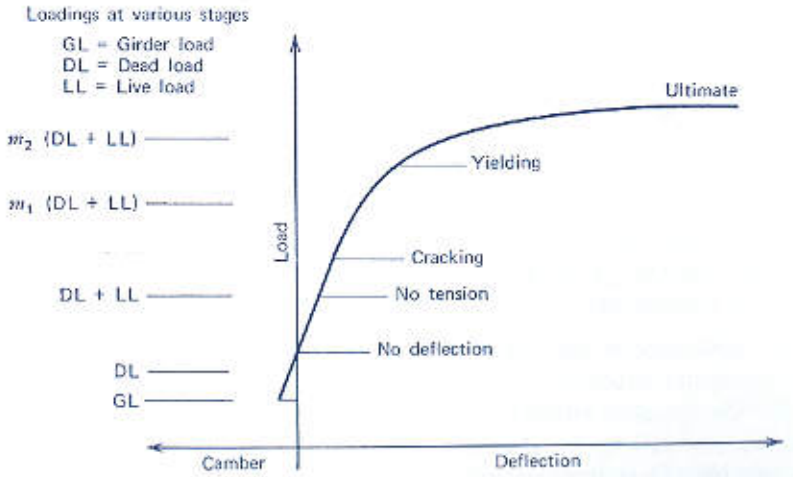

FIGURE 6.16. Life history of prestressed member under flexure.

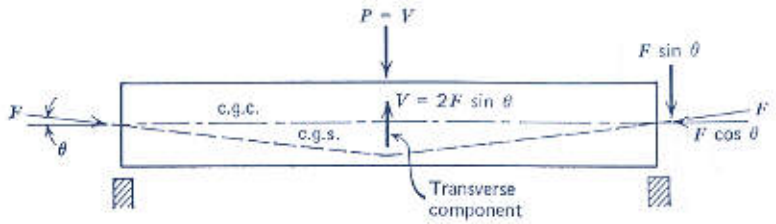

FIGURE 6.17. Balancing of a concentrated load.

Elastic design actually consists of matching the $(DL + LL)$ with the point of "no tension" (or some allowable tension) on the beam and ultimate design consists of matching the $m_2\ (DL + LL)$ with the "ultimate strength" of the beam. On the other hand, balanced-load design consists of matching the $DL + m_3 LL$ (where m_3 can be negative, zero, or some value much less than 1) with the point of no deflection. It is clear that, depending on the relative values of these loadings as compared to the relative values of the three stages of the beam behavior, designs based on the three approaches could yield the same proportions or widely varying ones. It should be pointed out that, regardless of what method is followed in the design, it is sometimes necessary to check for the behavior of the beam by one or both of the other methods.

Figure 6.17 illustrates how to balance a concentrated load by sharply bending the c.g.s. at midspan, creating an upward component,

$$V = 2F \sin \theta$$

If this V exactly balances a concentrated load P applied also at midspan, then the fiber stress in the beam at any section (except for local stress concentrations) is simply given by

$$f = \frac{F \cos \theta}{A_c} = \frac{F}{A_c}$$

for small values of θ. Any loading in addition to P will now cause bending in an elastic homogeneous beam (up to point of cracking), and the additional stresses can be computed by

$$f = \frac{Mc}{I}$$

where M is the moment produced by load other than P.

Similarly, Fig. 6.18 illustrates the balancing of a uniformly distributed load by means of a parabolic tendon whose upward component v (lb/ft) is given by

$$v = \frac{8Fh}{L^2}$$

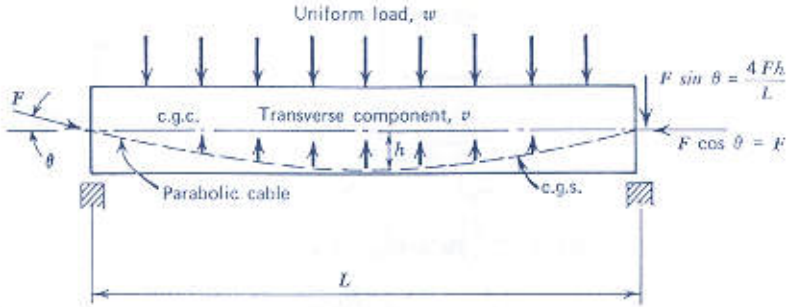

FIGURE 6.18. Balancing of a uniform load.

If the externally applied load w (including the weight of the beam) is exactly balanced by the component v, there will be no bending in the beam. The beam is again under a uniform compression with stress,

$$f = \frac{F}{A_c}$$

Should the external load be different from w, it is only necessary to analyze the moment M produced by the load differential and compute the corresponding stresses by the formula,

$$f = \frac{Mc}{I}$$

This procedure has already been illustrated in Example 6.1 of Section 6.1.

Now consider a cantilever beam (Fig. 6.19). The conditions for load balancing become slightly more complicated, because any vertical component at the cantilever end C will upset the balance, unless there is an externally applied load at that tip. To balance a uniformly distributed load w, the tangent to the c.g.s. at C will have to be horizontal. Then the parabola for

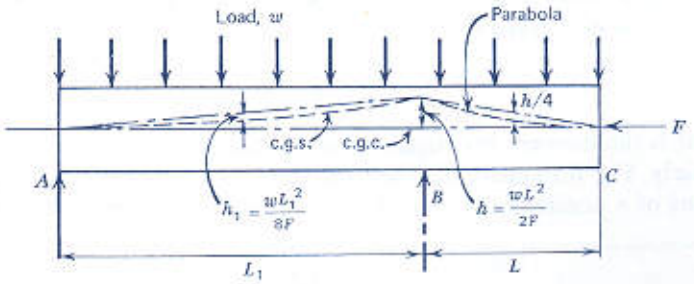

FIGURE 6.19. Load balancing for a cantilever beam.

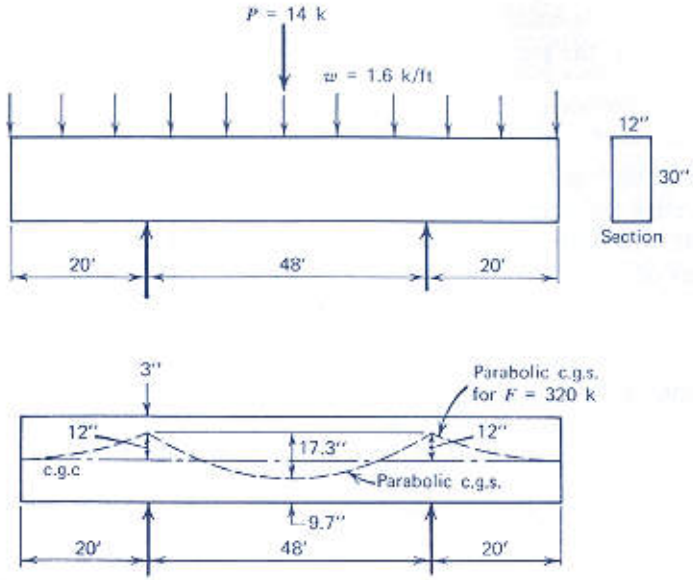

FIGURE 6.20. Example 6.2 and its solution.

the cantilever portion can best be located by computing

$$h = \frac{wL^2}{2F}$$

and the parabola for the anchor arm by computing

$$h_1 = \frac{wL_1^2}{8F}$$

EXAMPLE 6.2. A double cantilever beam is to be designed so that its prestress will exactly balance a total uniform load of 1.6 k/ft on the beam (Fig. 6.20). Design the beam using the least amount of prestress, assuming that the c.g.s. must have a concrete protection of at least 3 in. If a concentrated load of $P = 14$ k is added at midspan, compute the maximum top and bottom fiber stresses.

Solution: In order to balance the load in the cantilever, the c.g.s. at the tip must be located at the c.g.c. with a horizontal tangent. To use the least amount of prestress, the eccentricity over the support should be a maximum, that is, $h = 12$ in. or 1 ft. The prestress required is

$$F = \frac{wL^2}{2h} = \frac{1.6 \times 20^2}{2 \times 1} = 320 \text{ k}$$

In order to balance the load on the center span, using the same prestress, $F = 320$ k, the sag for the parabola must be

$$h_1 = \frac{wL_1^2}{8F} = \frac{1.6 \times 48^2}{8 \times 320} = 1.44 \text{ ft or } 17.3 \text{ in.}$$

Hence, the c.g.s. is located as shown in Fig. 6.20.

Under the combined action of the uniform load and the prestress, the beam will have no deflection anywhere and is under uniform compressive stress of

$$f = \frac{F}{A_c} = \frac{320{,}000}{360} = -889 \text{ psi}$$

Owing to the $P = 14$ k, the moment M at midspan is

$$M = \frac{PL}{4} = \frac{14 \times 48}{4} = 168 \text{ k-ft}$$

and the extreme fiber stresses are

$$f = \frac{Mc}{I} = \frac{6M}{bd^2} = \frac{6 \times 168 \times 12{,}000}{12 \times 30^2}$$
$$= \pm 1120 \text{ psi}$$

The resulting stresses at midspan are

$$f_{top} = -889 - 1120 = -2009 \text{ psi (compression)}$$
$$f_{bot} = -889 + 1120 = +231 \text{ psi (tension)}$$

Note that the actual tendon placement may not possess the sharp bend shown over the supports, and the effect of any deviation from the theoretical position must be investigated accordingly. Also note that $F = 320$ k is the effective prestress, so that under the initial prestress there will be a slight camber at midspan and either a camber or a deflection at the tips which can be computed.

For better stress conditions under the load P, it would be desirable to relocate the c.g.s. so that it would have more sag at midspan. Then a balanced condition would not exist under the uniform load w.

6.6.5 Choice of Beam Sections

The following shapes are frequently used for prestressed concrete sections under flexure:

1. Rectangular sections
2. T and channel sections
3. Symmetrical I and box sections
4. Inverted T and inverted channel sections

The suitability of these shapes will depend on the particular requirements: the simplicity, availability, and reusability of the formwork; easiness in placing concrete; functional, esthetic, as well as theoretical considerations. The rectangular shape is easiest for forming, but most uneconomical in material. The T-section is suitable for high ratios of M_G/M_T, where there is little danger of overstressing at transfer and where the concrete is effectively concentrated at the compressive flange. The inverted T-shape is good for low ratios of M_G/M_T, to avoid overstressing at transfer, but does not supply a high ultimate moment. The I and box shapes have more concrete near the extreme fibers and are efficient both at transfer and under ultimate loads, but have weaker webs and require more complicated forming.

For purposes of comparison, the various sections listed above can be categorized into four groups, and their relative structural efficiency and applications in terms of composite and noncomposite constructions are indicated in Table 6.10. Some typical sections commonly used in the U.S.A. are shown in Figs. 6.21–6.24.

6.6.6 Tendon Layouts and Limiting Zone for Tendons

Once the beam section is selected, the amount and location of the prestressing force can be determined by the methods presented in previous sections. In simple beams, the tendon layout is generally controlled by the maximum moment and end sections. After these two sections are designed, other sections can often be determined by inspection. However, it happens sometimes that intermediate points along the beam also may be critical, and in many instances, it would be desirable to determine the permissible and desirable profile for the tendons. To do this, a limiting zone for the location of the c.g.s. is obtained so that the tendons can be arranged to have their centroid fall within the limiting zone.

Although the method for establishing the limiting zone will be described with reference to simple beams, it is also applicable to the solution of more complicated tendon layouts involving cantilever and continuous spans where tendon location cannot be easily determined by inspection.

Referring to Fig. 6.25, having determined the layout of concrete sections, we proceed to compute their kern points, thus yielding two kern lines, one top and one bottom [part (c) of the figure]. Note that for variable sections these kern lines would be curved.

For a beam loaded as shown in part (a), the minimum and maximum moment diagrams for the girder load and for the total working load respectively are marked as M_G and M_T in part (b). If no tension is allowed in the concrete, then the center of pressure, the C-line, must not fall above the top kern line under the working load and prestress F nor below the bottom kern line under

TABLE 6.10. Types of Prestressed Concrete Section.

Group					
Variation			[a] [b]	[c] [c]	
Fabrication		Easy	Easy	Expensive in form	Difficult
Steel Placement		Adequate	Less Adequate	Good	Good
Noncomposite	Efficiency	Poor	Good	Very Good	Very inefficient, small ultimate moment capacity
	Application	Light load and short span	Especially good for long span roof when M_G/M_T large	Good for long span and heavy load	Short span and heavy load
Composite	Efficiency	Very good, particularly when shoring is used	Increase load capacity only slightly	Very good, particularly when shoring is used	Very good, particularly when shoring is used
	Application	Building members	Topping serves to tie all sections together. No forms required for composite pour	Long span building and bridge members	Bridge members

[a] More room for steel in lower flange.
[b] Better stability during erection.
[c] Torsionally stiff and strong.

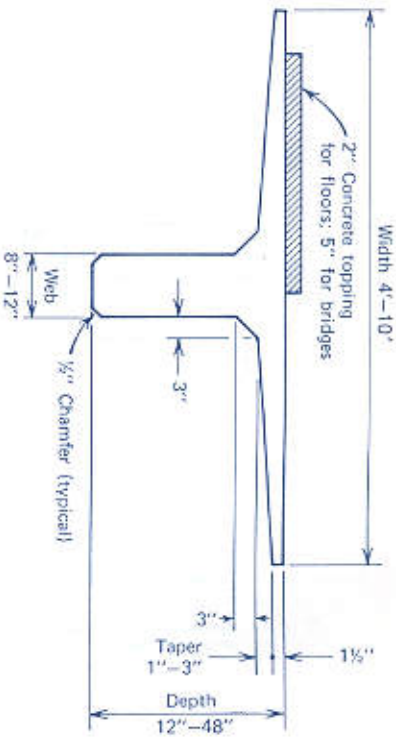

Table of Properties
(Width = 6'; web = 8"; taper = 2"; no topping)

Depth, in.	Area, in.^{2}	I, in.^{4}	c_b, in.
12	265	2360	9.2
16	297	6170	11.8
20	329	11,730	14.5
24	361	19,700	17.0
28	393	30,400	19.5
32	425	44,060	21.9
36	457	61,000	24.2

FIGURE 6.21. Typical single tee section.

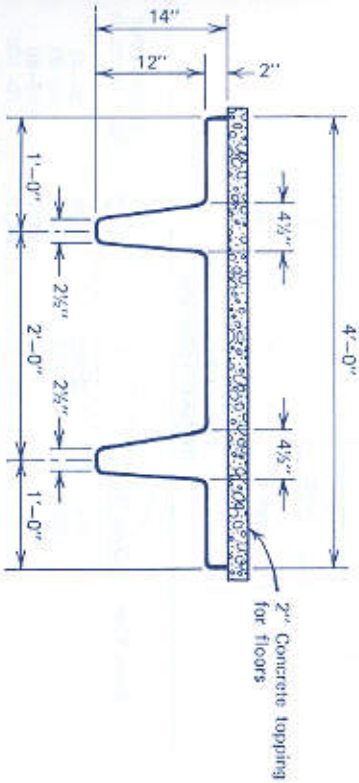

Table of Properties

Topping	Area, in.^{2}	I, in.^{4}	c_b, in.
With 2" topping	276	4456	11.74
Without topping	180	2862	10.00

FIGURE 6.22. Typical double tee section.

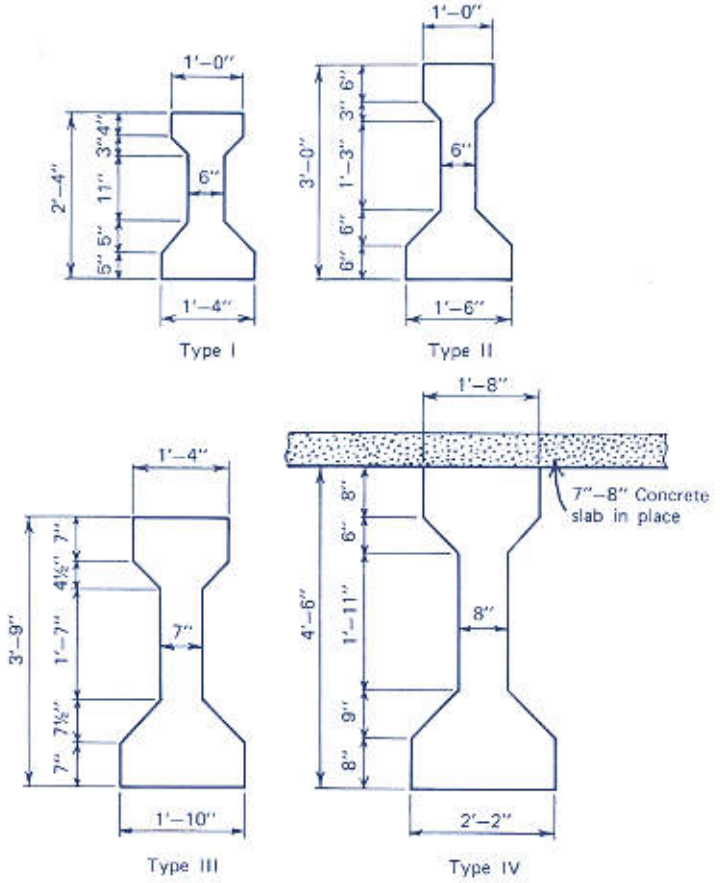

Table of Properties
(Without in-place slab)

Beam Type	Area, in.²	I, in.⁴	c_b, in.	Recommended Span Limits, ft
I	276	22,750	12.59	30–45
II	369	50,980	15.83	40–60
III	560	125,390	20.27	55–80
IV	789	260,730	24.73	70–100

FIGURE 6.23. Standard AASHO–PCI prestressed concrete I beams for highway bridges.

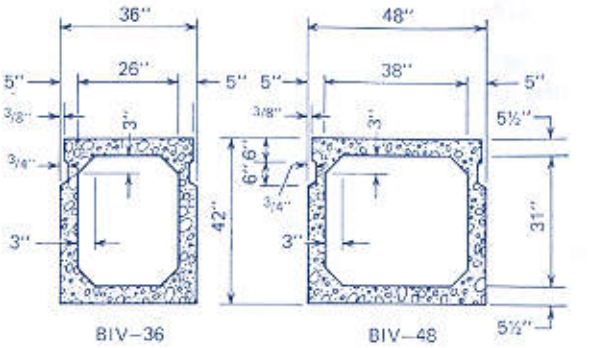

Table of Properties

Beam Type	Area, in.²	I, in.⁴	c_b, in.	Recommended Span Limits, ft: Draped Strand	Recommended Span Limits, ft: Straight Strand
BIV–36	710.5	158,644	20.73	103	87
BIV–48	842.5	203,088	20.78	103	88

FIGURE 6.24. Standard AASHO–PCI prestressed concrete box beams for highway bridges.

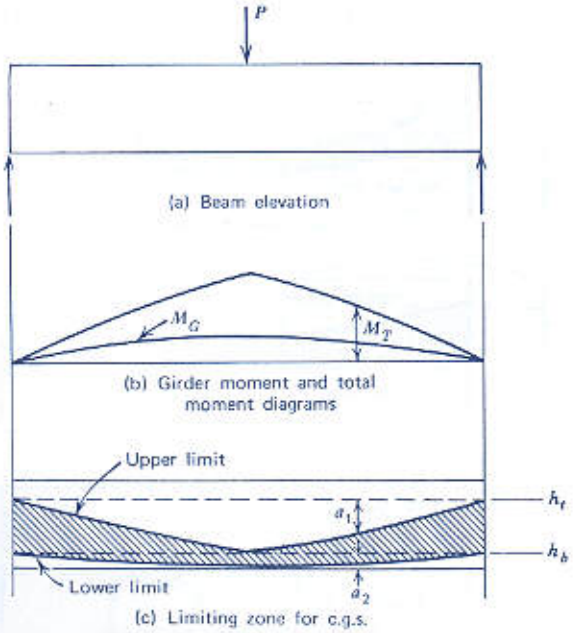

FIGURE 6.25. Location of limiting zone for c.g.s.

the girder load and initial prestress F_0. It is evident that to meet the first requirement, the c.g.s. must be located below the top kern at least a distance

$$a_1 = \frac{M_T}{F}$$

Likewise, to meet the second requirement, the c.g.s. must not be located below the bottom kern by a distance greater than

$$a_2 = \frac{M_G}{F_0}$$

Thus, it becomes clear that the limiting zone for the c.g.s. is given by the shaded area in Fig. 6.25(c), in order that no tension will exist either under the girder load or under the working load. The individual tendons, however, may be placed in any position so long as the c.g.s. of all the cables remains within the limiting zone.

The position and width of the limiting zone are often an indication of the adequacy and economy of design (Fig. 6.26). If some portion of the upper limit falls outside or too near the bottom fiber, as in part (a), either the prestress F or the depth of beam at that portion should be increased. On the other hand, if it falls too far above the bottom fiber, as in part (b), either the prestress or the beam depth can be reduced. If the lower limit crosses the upper limit, as in part (c), it means that no zone is available for the location

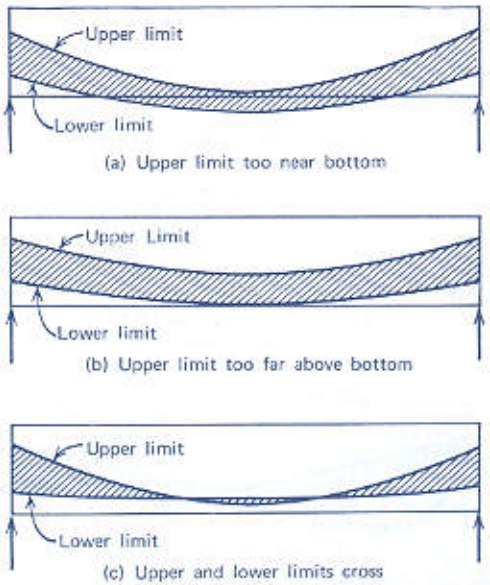

FIGURE 6.26. Undesirable positions for c.g.s. zone limits.

of c.g.s., and either the prestress F or the beam depth must be increased or the girder moment must be increased to depress the lower limit if that can be done.

It should be noted that if some tension f_t' is allowed in the concrete, it is possible to place the c.g.s. line slightly outside the limiting zone as shown in Fig. 6.25. The upper limit can be moved upward by an amount

$$e_t = \frac{f_t' I}{F c_b}$$

and the lower limit can be moved downward by an amount

$$e_b = \frac{f_t' I}{F_0 c_t}$$

The method described above does not consider the limitations of compressive stresses in concrete. These are usually satisfied when the beam section is selected.

Having determined the limiting zone for the tendons, one may choose many types of tendon layout. Some typical tendon layouts for pretensioned and posttensioned simple spans, and for single and double cantilevers are shown in Figs. 6.27–6.30. Depending upon the type of loading and the moment diagram, the tendon location must be determined for each beam so that all sections of the beam will satisfy stress and other requirements. It is noted that in pretensioned beams, the tendons must be straight or a series of straight segments, and curved tendons are generally used in posttensioned beams.

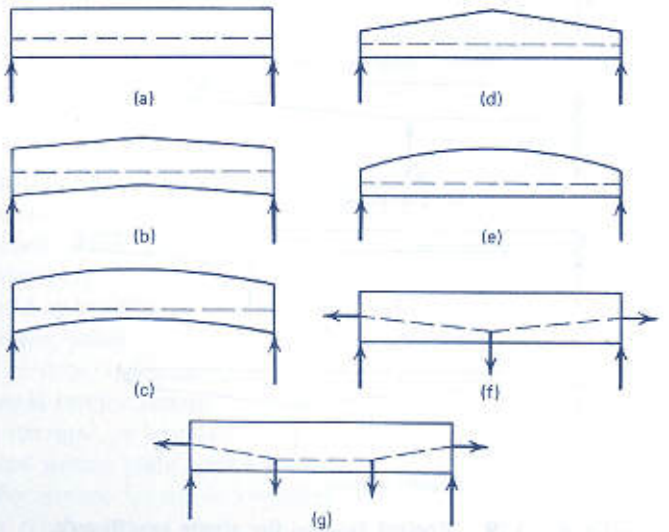

FIGURE 6.27. Layouts for pretensioned beams.

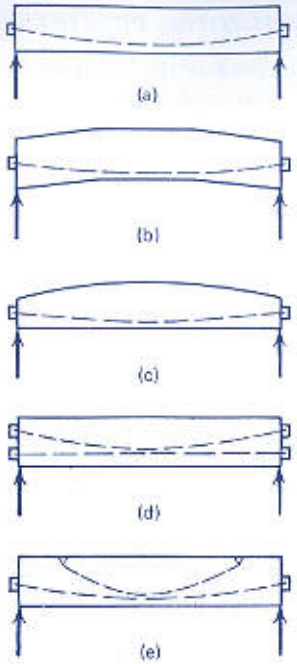

FIGURE 6.28. Layouts for posttensioned beams.

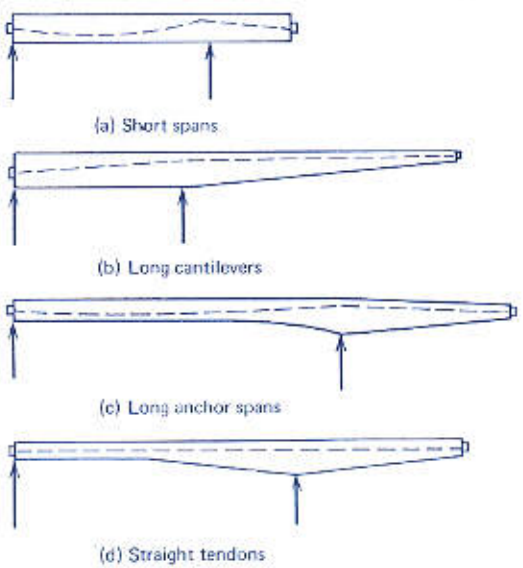

FIGURE 6.29. Typical layouts for single cantilevers.

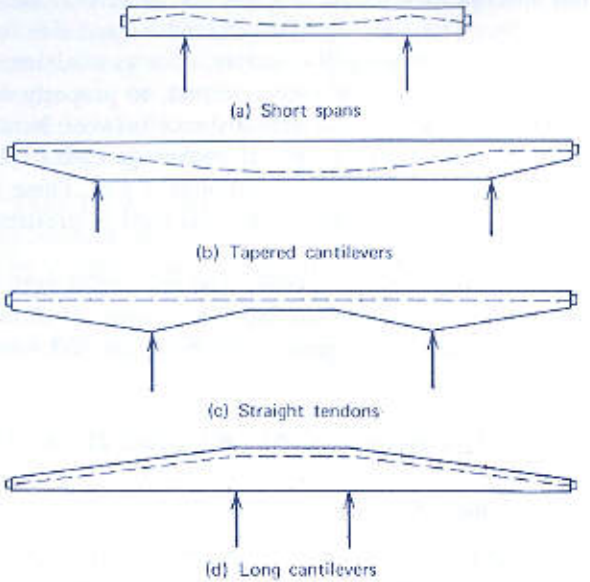

FIGURE 6.30. Typical layouts for double cantilevers.

6.6.7 Tendon Protection and Spacing

The minimum concrete protection for tendons is governed by requirements for fire resistance and for corrosion protection. The 1971 ACI Code specifies the following minimum thickness of concrete cover for prestressing steel, ducts and nonprestressed steel:

	Minimum Cover, in.
Cast against and permanently exposed to earth	3
Exposed to earth or weather:	
Wall panels, slabs, and joists	1
Other members	1 1/2
Not exposed to weather or in contact with the ground	
Slabs, walls, joists	3/4
Beams, girders, columns:	
Principal reinforcement	1 1/2
Ties, stirrups, or spirals	1
Shells and folded plate members:	
Reinforcement 5/8 in. and smaller	3/8
Other reinforcement	D but not less than 3/4

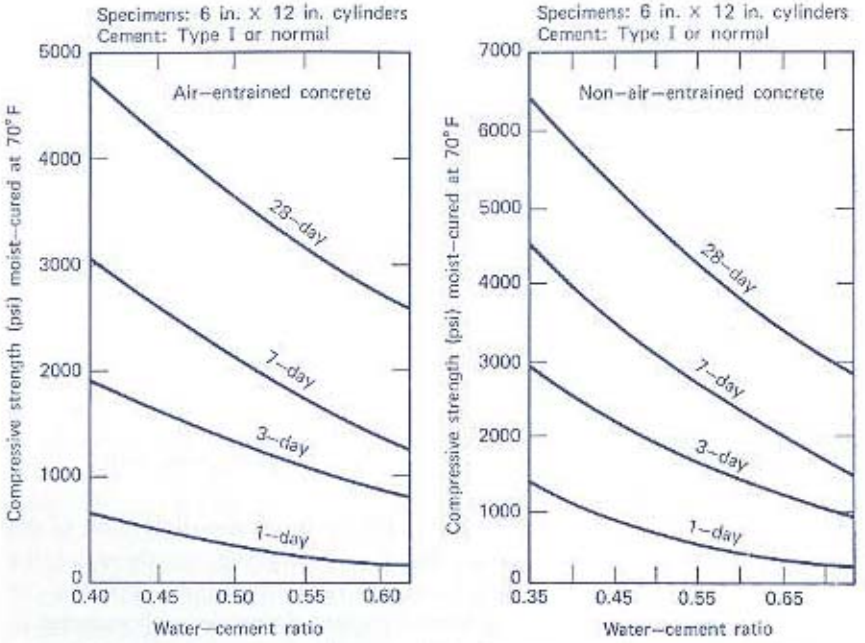

FIGURE 1.5. Typical relationship between water–cement ratio and compressive strength of concrete.[4]

ACI Committee 211[23] recommends that the water–cement ratio be kept below 0.40 or 0.45 for concrete exposed to sea water or sulfates, and below 0.45 or 0.50 for concrete exposed to cycles of freezing and thawing. The lower limits being for thin concrete sections such as railing, curbs, sills and ledges, and the higher limit for all other types of concrete structures.

For the selection of the *mix proportions* or batch weights a number of procedures have been developed. The most commonly used procedure is the ACI Committee 211[23] method of selecting proportions for concrete made with aggregates of normal density as distinguished from lightweight[24] and special high density aggregates. This method provides a first approximation of the mix proportions which must be checked by trial batches in the laboratory or field and adjusted, as necessary, to produce the desired characteristics of the fresh and hardened concrete.

In the *ACI method*[23] of mix proportioning for a normal weight concrete of specified strength the suitable slump (Table 1.9) and maximum size aggregate should first be selected. Once the slump and aggregate size are fixed, the procedure of computing the required batch weights for one cubic yard of concrete consist essentially of the following five steps:

1. Use Table 1.10 to determine the weight of water in pounds per cubic yard of concrete, required to produce a given slump for a given maximum size of aggregate, with or without air-entrainment.

2. Use Table 1.11 to determine the water–cement ratio to meet the strength requirement. The required weight of cement per cubic yard of concrete can now be computed by dividing the water content obtained in (1) by the water–cement ratio selected in (2). If the concrete is to be exposed to severe

TABLE 1.10. Approximate Mixing Water and Air Content Requirements for Different Slumps and Maximum Sizes of Aggregates.[23]

	Water, lb per cu yd of Concrete for Indicated Maximum Size of Aggregate						
Slump, in.	3/8 in.	1/2 in.	3/4 in.	1 in.	1 1/2 in.	2 in.	3 in.
Non-air-entrained concrete							
1 to 2	350	335	315	300	275	260	240
3 to 4	385	365	340	325	300	285	265
6 to 7	410	385	360	340	315	300	285
Air content (%)[a]	3	2.5	2	1.5	1	0.5	0.3
Air-entrained concrete							
1 to 2	305	295	280	270	250	240	225
3 to 4	340	325	305	295	275	265	250
6 to 7	365	345	325	310	290	280	270
Air content (%)[b]	8	7	6	5	4.5	4	3.5

[a] Approximate amount of entrapped air.
[b] Recommended total air content.

TABLE 1.11. Approximate Relationships Between Water–Cement Ratio and Compressive Strength of Concrete.[23]

	Water–cement Ratio, by Weight	
Compressive Strength at 28 Days, psi	Non-air-entrained Concrete	Air-entrained Concrete
6000	0.41	—
5000	0.48	0.40
4000	0.57	0.48
3000	0.68	0.59
2000	0.82	0.74

The minimum spacing of tendons is governed by several factors. First, the clear spacing between tendons, or between tendons and side forms, must be sufficient to permit easy passage of concrete, such as a minimum of 1 1/3 times the size of the maximum aggregates. Second, to properly develop the bond between steel and concrete, the clear distance between bars should be at least the diameter of the bars for special anchorage and 1 1/2 times the diameter for ordinary anchorage, with a minimum of 1 in. These limitations may not be necessary for small wires and strands used in prestressed work, and they are often bundled together.

The 1971 ACI Code calls for a minimum clear spacing at each end of the member of four times the diameter of individual wires or three times the diameter of strands, in order to properly develop the transfer bond.

6.7 CAMBER, DEFLECTIONS, AND SPAN-DEPTH RATIOS

6.7.1 Camber and Deflections

Deflections of prestressed beams differ from those of ordinary reinforced beams in the effect of prestress. While controlled deflections due to prestress can be advantageously utilized to produce desired cambers and to offset deflections due to loadings, excessive cambers due to prestress can cause serious troubles. Cambers or deflections due to prestress can be computed by taking the concrete as a free body separated from the tendons, which are replaced by a system of forces acting on the concrete. This approach will be illustrated by the following example.

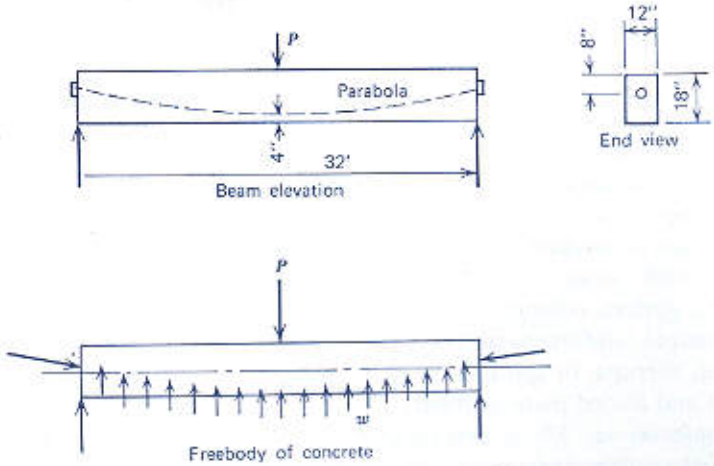

FIGURE 6.31. Example 6.3.

EXAMPLE 6.3. A concrete beam of 32 ft simple span (Fig. 6.31) is post-tensioned with 1.2 sq. in. of high-strength steel to an initial prestress of 140 ksi immediately after prestressing. Compute the initial deflection at midspan due to prestress and the weight of the beam, assuming $E_c = 4{,}000{,}000$ psi. Estimate the deflection after 3 months, assuming a creep coefficient of $C_c = 0.8$ and an effective prestress of 120 ksi at that time.

Solution: Take the concrete as a freebody and replace the tendon with forces acting on the concrete. The parabolic tendon with 6-in. sag at midspan is replaced by a uniform load acting along the beam with intensity.

$$w = \frac{8F6}{L^2} = \frac{8 \times 140{,}000 \times 1.2 \times 6}{32^2 \times 12} = 655 \text{ plf}$$

In addition, there will be two eccentric loads acting at the ends of the beam, each producing a moment of $140{,}000 \times 1.2 \times 1/12 = 14{,}000$ ft-lb.

Since the weight of the beam is 225 plf, the net uniform load on concrete is $655 - 225 = 430$ plf, which produces an upward deflection at midspan given by the usual deflection formula

$$\Delta_1 = \frac{5wL^4}{384E_cI} = \frac{5 \times 430 \times 32^4 \times 12^3}{384 \times 4{,}000{,}000 \times (12 \times 18^3)/12} = 0.434 \text{ in.}$$

The end moments produce a downward deflection given by the formula

$$\Delta_2 = \frac{ML^2}{8E_cI} = \frac{140 \times 1.2 \times 1 \times 32^2 \times 12^2}{8 \times 4{,}000{,}000 \times (12 \times 18^3)/12} = 0.133 \text{ in.}$$

Thus the net deflection due to prestress and beam weight is

$$\Delta = \Delta_1 - \Delta_2 = 0.434 - 0.133 = 0.301 \text{ in. upward}$$

The long-time deflection should be modified by two factors: first, the loss of prestress, which tends to decrease the deflection; and second, the creep effect, which tends to increase the deflection. Since the prestress is reduced from 140 to 120 ksi, the deflection due to prestress can be modified by the factor 120/140. Then, for the creep effect, the net deflection should be increased by a factor $(1 + C_c) = 1.8$. Thus, if the beam is not subject to external loads the eventual deflection after 3 months can be estimated as follows:

Camber due to initial prestress	$= 0.434 \times 655/430 - 0.133$
	$= 0.528$ in.
Initial deflection due to beam weight	$= 0.434 \times 225/430 = 0.227$ in.
Deflection after 3 months	$= (0.528 \times 120/140 - 0.227)$
	$\times 1.8 = 0.407$ upward

It is seen that, without external loads, the beam has a growth in camber of approximately 0.1 in. With some sustained external loads, it is conceivable that the beam would have some long-time downward deflection.

The above approach is a simple and practical method for estimating long-time deflections. More rigorous methods[5] are available, but such methods are extremely laborious and their use is justified only if the basic data for creep, shrinkage and relaxation are reliable.

The calculation for deflections due to external loads is similar to that for nonprestressed beams. So long as the concrete has not cracked, the beam can be treated as a homogeneous body and the usual elastic theory applied to it for deflection computations. When cracks begin to occur in the beam, the moment of inertia of the section will become smaller and the modulus of concrete and of steel will decrease so that the curvature and deflection will increase much faster.

Some simple formulas are listed in Fig. 6.32 to help the computation of camber due to prestress. They are derived from the well-known moment–area principles. In these formulas, the moment M at each section is computed by the prestress F (or more accurately the horizontal component of F) multiplied by the corresponding ordinate y as marked. Thus $M_1 = Fy_1$ and $M_2 = Fy_2$.

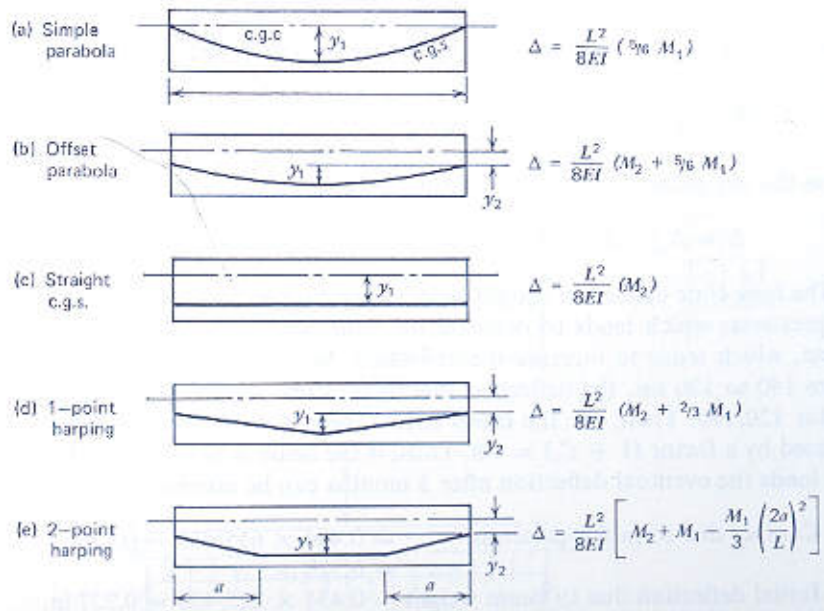

FIGURE 6.32. Formulas for computing midspan camber due to prestress (simple beams).

6.7.2 Span–Depth Ratios

For reasons of economy and esthetics, higher span–depth ratios are almost always used for prestressed concrete rather than for reinforced concrete. Higher ratios are possible because deflection can be much better controlled in prestressed design. On the other hand, if these ratios are too high, camber and deflection become quite sensitive to variations in loadings, in properties of materials, in magnitude and location of prestress, and in temperature. Furthermore, the effects of vibration become more pronounced.

Span–depth ratio limitations should vary with the nature and magnitude of the live load, the damping characteristics, the boundary conditions, the shape and variations of the section, the modulus of elasticity, and the length of span itself. However, as a result of accumulated experience, the following values may be taken as a preliminary guide for building designs.

For cantilever solid slabs, a span–depth ratio of 18 for floors and 20 for roofs has been found to be satisfactory. But cantilevers are sensitive to deflections and vibrations, and greater care should be taken. For example, a camber in the anchor span would usually produce a dip in the cantilever. Approximate limits for span–depth ratios commonly used in building design are listed in Table 6.11.

Generally speaking, when span–depth ratios are some 10% below the tabulated values, problems of camber, deflection, and vibration should not occur unless the loadings are extremely heavy and vibratory in nature. Occasionally, these ratios can be exceeded by 10% or more, if careful study would justify and ensure proper behavior.

TABLE 6.11. Approximate Limits for Span–Depth Ratios.

	Continuous Spans		Simple Spans	
	Roof	Floor	Roof	Floor
One-way solid slabs	52	48	48	44
Two-way solid slabs (supported on columns only)	48	44	44	40
Two-way waffle slabs (3 ft waffles)	40	36	36	32
Two-way waffle slabs (12 ft waffles)	36	32	32	28
One-way slabs with small cores	50	46	46	42
One-way slabs with large cores	48	44	44	40
Double tees and single tees (side by side)	40	36	36	32
Single tees (spaced 20-ft centers)	36	32	32	28

The above values are intended for both hard-rock concrete and lightweight concrete, but should be reduced by about 5% for lightweight concrete having E_c less than 3,000,000 psi. For long spans (say, in excess of about 70 ft) and for heavy loads (say, live loads over 100 psf) the above values should be reduced by from 5 to 10%. For in-place concrete in composite action with the precast elements, the total depth may be considered in computing the above span–depth ratios.

Little experience has been obtained for railway bridges of prestressed concrete to justify any limitation on their span–depth ratios; the usual ratios have been in the range of 10 to 14 for box sections up to 100 ft or more. For simple-span highway bridges of the I-beam type, up to about 200 ft, a span–depth of 20 is considered conservative, 22 to 24 is normal, while 26 to 28 would be the critical limit. Box sections can have ratios about 5 to 10% higher than I-beams, while T-sections spaced far apart should have ratios about 5 to 10% lower than I-beams. Again, there is no reason to believe that a fixed span–depth ratio will apply to all cases.

6.8 PARTIAL PRESTRESS AND NONPRESTRESSED REINFORCEMENTS

6.8.1 Partial Prestress

In the early stages of its development, prestressed concrete was generally designed according to the criterion that under working loads no tension would be allowed in the concrete. It was soon realized that structures designed with this criterion known as "full prestressing" often possess extra strength and that tensile stress in concrete need not be the sole design criterion. In many instances, controlled camber or deflection under a given loading condition or ultimate strength may be a more suitable design criterion. Designs based on these requirements often allow some tension in the concrete under working loads and thus are referred to as "partial prestressing."

There is no basic difference between these two types of design, because, although a structure may be designed for no tension under working loads, it will be subjected to tension under overloads. Therefore, the difference is rather a matter of degree; tensile stresses will be higher and occur more frequently for the same structure if designed for partial prestressing rather than full prestressing. A "fully prestressed" member will have higher cracking load than a "partially prestressed" member. Since cracking will generally affect the fatigue strength of a member, the degree of prestressing is then an important consideration in the design of structures subjected to repeated loads.

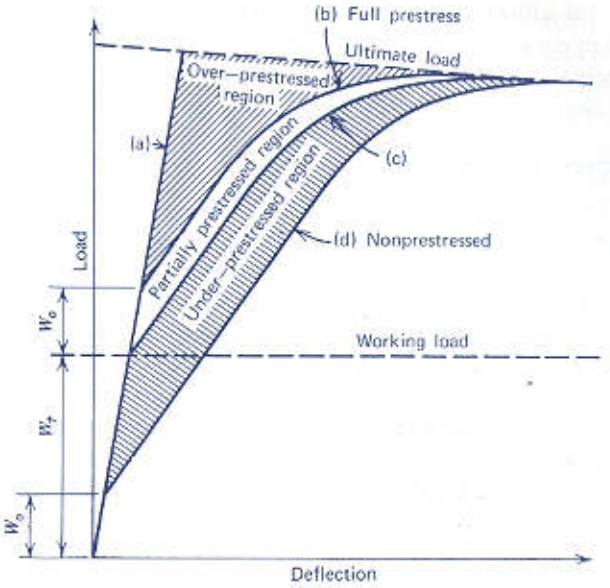

FIGURE 6.33. Load–deflection curves for varying degrees of prestress.

Figure 6.33 shows load–deflection curves for a bonded beam with its concrete subjected to varying degrees of prestress in which W_0 is the cracking load for a nonprestressed beam. The case of full prestress permitting no tension under working load is represented by curve (b). Partial prestressing permitting tension up to the modulus of rupture is shown by curve (c). A totally nonprestressed concrete beam is shown as curve (d). Then an overprestressed region is indicated between curves (a) and (b).

Partial prestress may be obtained by several different methods: (1) by using less steel for prestressing—this will save steel, but will also decrease the ultimate strength, which is almost directly proportional to the amount of steel; (2) by using the same amount of high-tensile steel, but leaving some nonprestressed—this will save some tensioning and anchorage, and may increase resilience at the sacrifice of earlier cracking and slightly smaller ultimate strength; (3) by using the same amount of steel, but tensioning them to a lower level—the effects of this are similar to those of method (2), but no end anchorages are saved; and (4) by using less prestressed steel and adding some mild steel for reinforcing—this will give the desired ultimate strength and will result in greater resilience at the expense of earlier cracking.

In comparison with full prestress, the advantages of partial prestress are: (1) better control of camber, (2) saving in the amount of prestressing steel and end anchorages, (3) possible greater resilience in the structure, and

(4) economical utilization of mild steel. Likewise, there are disadvantages: (1) earlier appearance of cracks, (2) greater deflection under overloads, (3) higher principal tensile stress under working loads, and (4) slight decrease in ultimate flexural strength for the same amount of steel.

6.8.2 Nonprestressed Reinforcements

Nonprestressed reinforcements can be placed at various positions of a prestressed beam to improve its behavior and strength at different stages. Frequently, one set of these reinforcements can serve to strengthen the beam in several ways: (1) to provide strength immediately after transfer of prestress along the compressive flange which may be under tension at transfer, or along the tension flange which may be subjected to high compressive stress at transfer; (2) to reinforce certain portions of the beam for special or unexpected loads during handling, transportation, and erection; (3) to distribute cracks under working loads and to increase ultimate capacity of the beams; and (4) to reinforce the concrete along directions which are not prestressed—web, end blocks, and flange slab reinforcements.

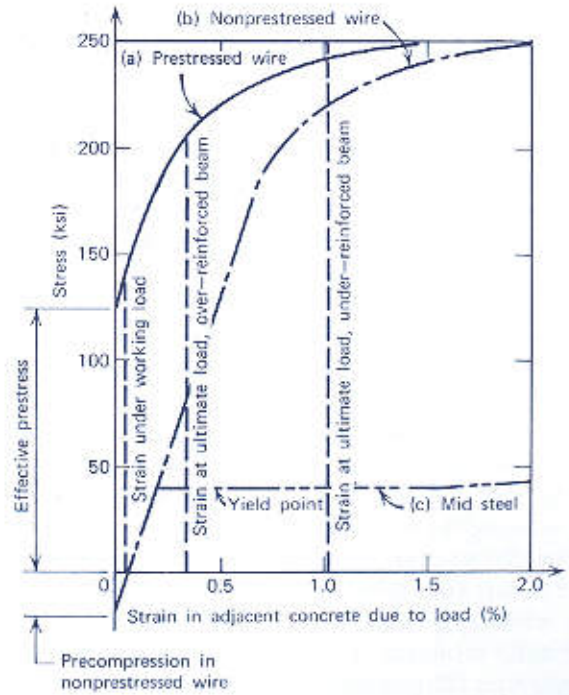

FIGURE 6.34. Stress-strain diagrams of prestressed and nonprestressed steel.

When nonprestressed reinforcements are used to carry compression, the compressive stress in the steel is generally quite high, because of shrinkage and creep in concrete. When used to carry tension, the reinforcements cannot function effectively until the concrete has cracked, because the shortening of concrete due to prestress prevents the steel from taking any tension until the concrete cracks. However, the design of these reinforcements is usually made on the assumption that they will be stressed to the usual allowable values (such as 20,000 psi for intermediate grade steel) and that their total tension will replace the tension in the portion of concrete which might be lost as a result of cracking.

Figure 6.34 shows the stresses and strains produced in various reinforcements under different stages of loading. It is noted that nonprestressed reinforcements will hardly be stressed at all under working loads, but will be effectively stressed at ultimate load, especially for under-reinforced beams.

6.8.3 Combination of Prestressed and Reinforced Concrete

While a combination of prestressed and reinforced concrete is evidenced in the use of nonprestressed reinforcement, the flexural strength is essentially supplied by the tendons, with the nonprestressed steel playing only a minor role. For certain types of construction, a full combination of prestressed and reinforced concrete could be the best design, making use of the advantages of both. Reinforced concrete has the advantage of simplicity in construction, being monolithic in behavior, and having no camber, less creep, and reasonably high ultimate strength. Prestressed concrete utilizes high-strength steel economically, produces a favorable distribution of stress under certain conditions of loading, and controls deflection and cracking.

Certain structural elements and systems would favor pure reinforced concrete; others would favor pure prestressed concrete; still others, partially prestressed concrete. But some will be best designed with a combination of reinforced and prestressed concrete having the nonprestressed steel carrying perhaps 50% or more of the total ultimate load.

One occasion for the economical use of this combination would be the case of high live load to dead load ratio, when prestressing alone would produce excessive camber. Another case would be high superimposed dead load requiring prestressing in stages which may be cumbersome. A third case would be the requirement of high ultimate strength or resilience to resist dynamic loadings. A fourth case would be limited areas requiring additional short reinforcements. There is also reason to believe that a heavy amount of nonprestressed steel used in conjunction with unbonded tendons will result in economy and in developing a high ultimate stress in the tendons.

For precast columns, prestressing will help control cracking during transportation and erection, and it will also contribute to the bending strength.

Nonprestressed steel will increase both the axial load and the flexural capacity. Hence a combination may be the best solution for certain cases. The use of nonprestressed reinforcement for joineries and continuity is, of course, frequently a simple and economical solution.

The nonprestressed steel does not act until the concrete cracks, and does not contribute toward the precracking strength. Hence if cracking could result in a primary or secondary failure, nonprestressed steel may not be of any help. The possibility of corrosion of the prestressing steel if the member cracks too early or too often should also be investigated.

6.9 CONTINUOUS BEAMS

Continuous beams may be totally cast in place with the tendons continuous from one end to the other as shown in Fig. 6.35. Alternatively, smaller precast elements may be made into continuous beams by special posttensioning arrangements or by composite construction with nonprestressed steel as shown in Fig. 6.36. In these beams, continuity is established to resist only the live load and/or a portion of the dead load.

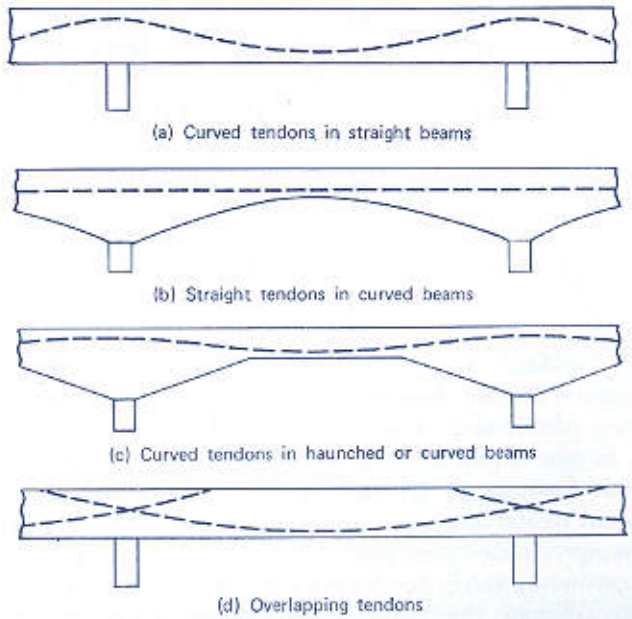

FIGURE 6.35. Layouts for full continuous beams.

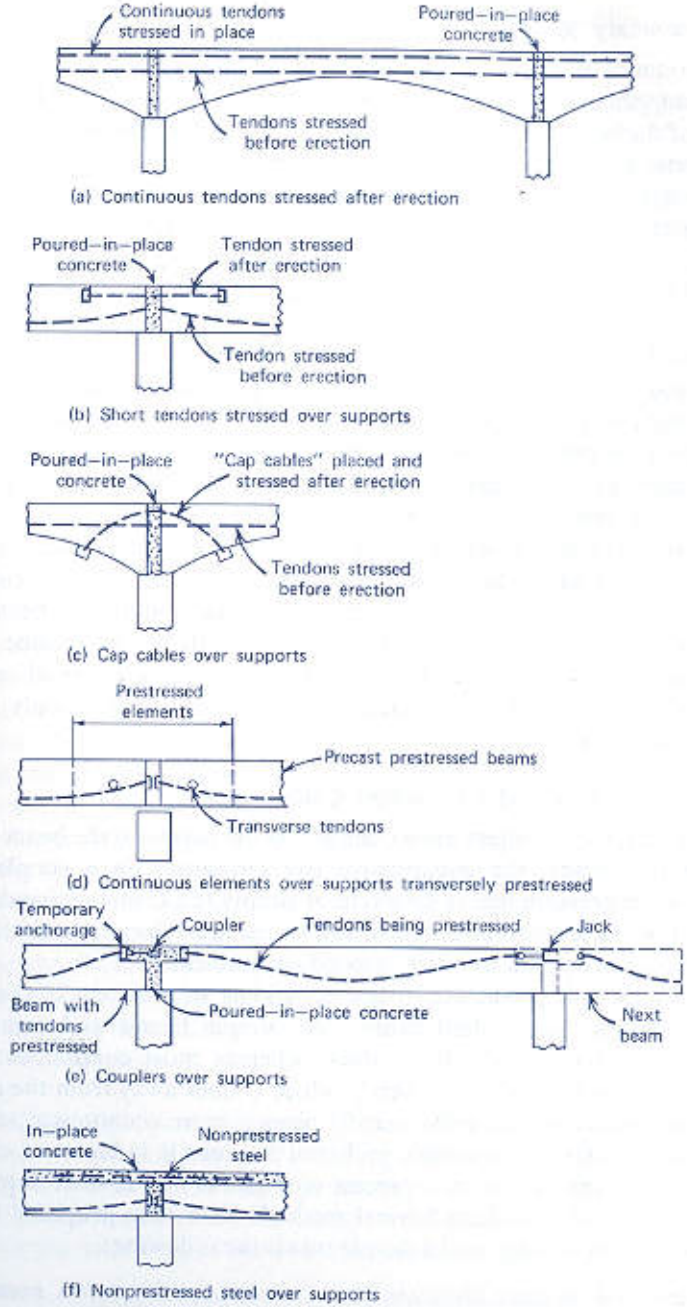

FIGURE 6.36. Layouts for partially continuous beams.

6.9.1 Secondary Moment

In a continuous beam or any statically indeterminate system, support reactions are generally induced by the application of prestress, because the bending of the beam due to prestress may tend to deflect the beam away from its supports. Since the beam is constrained from deflecting at the supports, reactions are induced. These reactions in turn produced "secondary moment" in the beam as distinguished from the "primary moment" due to eccentricity of the prestressing force. The overall effect of the prestressing force is, therefore, to produce a final moment which is equal to the primary moment plus the secondary moment.

The word "secondary" implies that the reactions and the moments are induced and, in no way, suggests that their magnitudes are small or insignificant. In fact, it is quite possible that the secondary moment could even be greater than the primary moment. The resulting stress due to the secondary moment must be accounted for along with the stresses caused by the prestressing force and other design loads.

Since the secondary moment is related to the secondary reactions which are concentrated forces acting on the beam, the secondary moment must vary linearly between consecutive supports of the continuous beam. The secondary moment and reactions vary directly with the magnitude of the prestressing force F. They are independent of EI. Thus, creep of concrete affects the magnitude of the secondary moment and reactions only insofar as E is reduced by creep.

6.9.2 Pressure Line and Concordant Cable

Under the action of prestress alone, neglecting the weight of the beam and all other external loads, the compressive stress resultant in a simple beam (known as the pressure line in concrete or simply the C-line) coincides with the c.g.s. line. In a continuous beam, the C-line must deviate from the c.g.s. line in amounts required to resist "secondary moment."

When a c.g.s. line produces a C-line coinciding with the c.g.s., that c.g.s. line is termed a "concordant cable." All simple beams and some continuous beams have concordant cables, whereas most continuous beams have "nonconcordant cables" which produce C-lines away from the c.g.s.

While a nonconcordant cable usually gives a more economical solution, a concordant cable is sometimes preferred because it induces no external reactions and works better in a precast continuous beam, since supporting points do not tend to deflect. Several methods have been proposed for obtaining concordant cables, and a simple rule is the following:

> "Every real moment diagram for a continuous beam on nonsettling supports, produced by any combination of external loadings, whether transverse loads or moments, plotted to any scale, is one location for a concordant cable in that beam."

The above theorem can be easily proved. Since any moment diagram due to the loads on a continuous beam is computed on the basis of no deflection over the supports, and since any c.g.s. line following that diagram will produce a similar moment diagram, that c.g.s. line will also produce no deflection over the supports; hence it will induce no reactions and is a concordant cable.

6.9.3 Linear Transformation

The C-line can be located from the c.g.s. line by linearly transforming it. Linear transformation is defined as the location of the C-line from the c.g.s. line by movements only over the interior supports of the continuous beam, without changing the intrinsic shape (i.e., the curvature and bends) of the c.g.s. line within each individual span. Since the C-line deviates from the c.g.s. line on account of the moments produced by the induced reactions, and since such moments vary linearly within each span, it follows naturally that the C-line can be linearly transformed from the c.g.s. line.

A simple method to determine the C-line from the c.g.s. line is to take the concrete as a free body and replace the tendons with a set of forces acting on the concrete. The moments over the supports due to these forces can then be computed and the C-line located by linear transformation.

When external loads are applied on the beam, additional moments will be produced, and the C-line will again be shifted. Moments in a continuous beam due to the external loads (including the weight of the beam) are computed by the usual elastic theory, using methods such as moment distribution. These moments are added to the prestressing moments previously calculated, thus yielding the final moments in the beam. This can also be performed by shifting the C-line from that obtained for prestressing only. The amount of shifting equals the moments due to external loads divided by the prestress. For simplicity, the effective prestress and the gross concrete area can be used for all computations.

EXAMPLE 6.4. A continuous, prestressed concrete beam with bonded tendons is shown in Fig. 6.37. The c.g.s. has an eccentricity at A, is bent sharply at D and B, and has a parabolic curve for the span BC. Locate the line of pressure (the C-line) in the concrete due to prestress alone, not considering the dead load of the beam. Consider an effective prestress of 250 k.

Solution: The primary moment diagram for the concrete is shown in part (b) of the figure. The corresponding shear diagram is computed and shown in

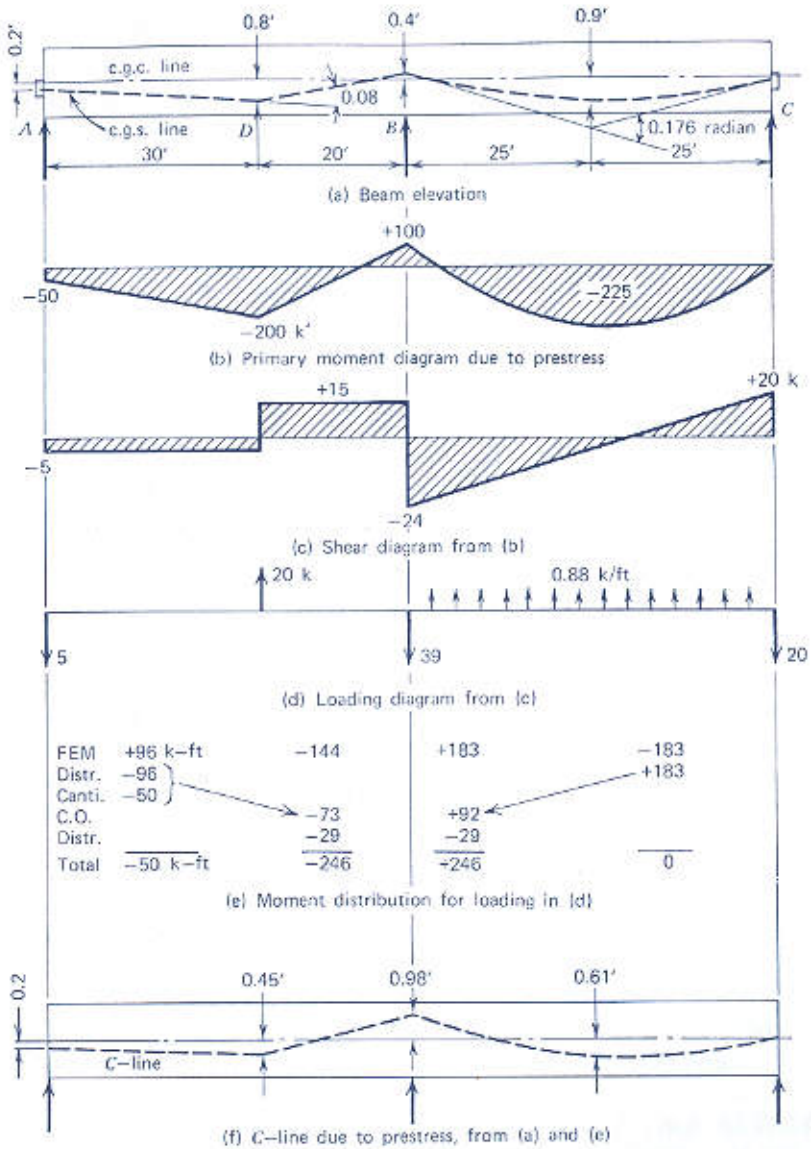

FIGURE 6.37. Example 6.4.

part (c), from which the loading diagram is drawn in part (d). For the loading in part (d) acting on the continuous beam, the fixed-end moments are:

$$M_{AB}{}^{F} = \frac{20 \times 20^2 \times 30}{50^2} = +96 \text{ k-ft}$$

$$M_{BA}{}^{F} = \frac{20 \times 30^2 \times 20}{50^2} = -144 \text{ k-ft}$$

$$M_{BC}{}^{F} = -M_{CB}{}^{F} = \frac{0.88 \times 50^2}{12} = +183 \text{ k-ft}$$

Moment distribution is performed in part (e). The resulting moment is 246 k-ft at B. The eccentricity of the line of pressure at B is, then, 246/250 = 0.98 ft.

The line of pressure for the entire beam can be computed by plotting its moment diagram and dividing the ordinates by the value of the prestress. But this is not necessary; since the line of prestress deviates linearly from the c.g.s. line, it is only necessary to move the c.g.s. line linearly so that it will pass through the points located over the supports, as in part (f). Thus the line of pressure at D will be translated upward by the amount of (0.98 − 0.4) 30/50 = 0.35 ft and is now located at 0.80 − 0.35 = 0.45 ft below the c.g.c. line. At midspan of BC, the line of pressure will be translated upward by the amount of (0.98 − 0.4) 25/50 = 0.29 ft and is now located at 0.61 ft below the c.g.c. line.

If desired, the secondary moment over the center support can be computed as 246 − 100 = 146 k-ft.

EXAMPLE 6.5. For the prestressed beam in Example 6.4, a uniform load of 1.2 k/ft is applied to the entire length of the two spans (including the weight of the beam itself). Locate the line of pressure in the concrete due to the combined action of the prestress and the external loads. Compute the stresses in concrete at section B, if the concrete section is as shown in Fig. 6.38 with I = 39,700 in.^{4} and A_c = 288 sq. in.

Solution: Since the moments and line of pressure due to prestress have been obtained in Example 6.4, we shall now obtain only the effect of external loads. By a simple moment distribution—see part (b) of the figure—the moment diagram can be plotted as in part (c). Dividing this moment by the prestress of 250 k, the shifting of C-line due to this external loading is given in part (d). Adding part (d) to Fig. 3.37(f) of the last example, the final location of the line of pressure for both prestress and external load is given in part (e).

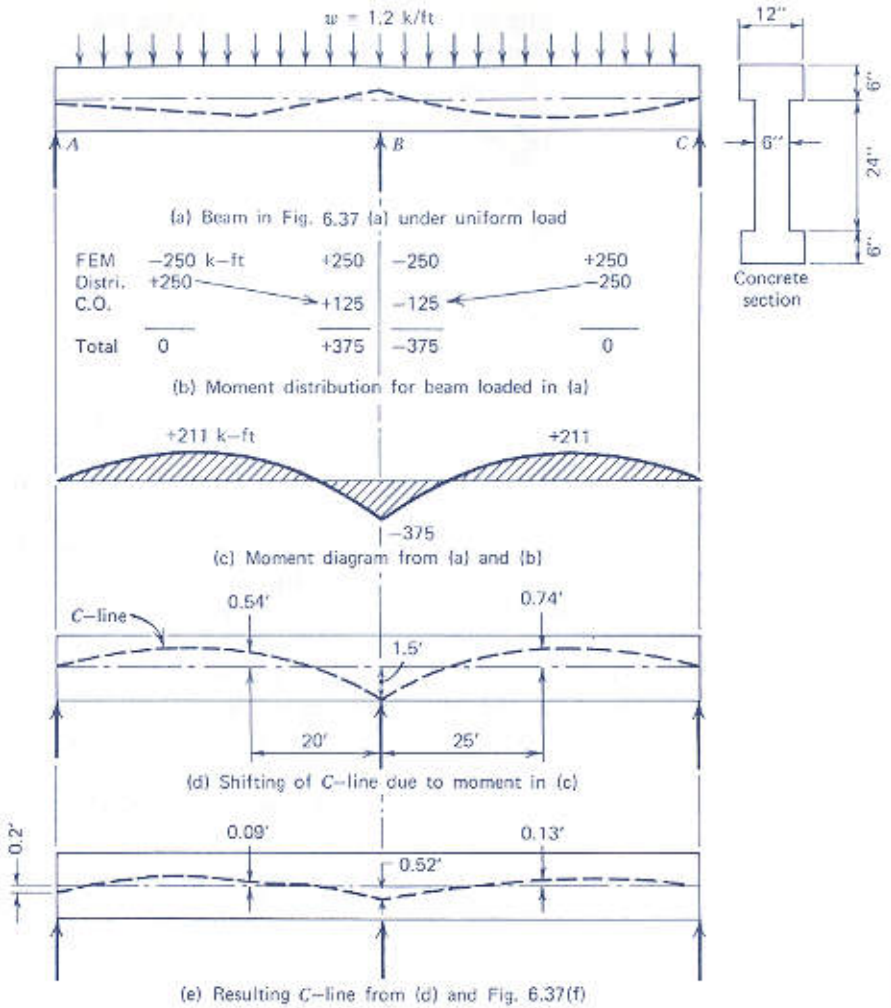

FIGURE 6.38. Example 6.5.

The resulting moment in the concrete at section B is $250 \times 0.52 = -130$ k-ft, and the stresses are

$$-\frac{250}{288} + \frac{130 \times 12 \times 18}{39{,}700} = -0.867 + 0.707$$

$$= -0.160 \text{ ksi for top fiber}$$

and

$$-0.867 - 0.707 = -1.574 \text{ ksi for bottom fiber}$$

6.9.4 Load-Balancing Method

This method is convenient for both the analysis and the design of prestressed concrete beams. When the external load is exactly balanced by the transverse component of the prestress, the beam is under a uniform stress f across any section,

$$f = \frac{F}{A_c}$$

For any change in load from that balanced condition, only the effects of change need to be computed. For example, if the additional moment is M, then the additional stresses are given by,

$$f = \frac{My}{I}$$

Thus, after load balancing, the analysis of prestressed continuous beams is reduced to the analysis of nonprestressed continuous beams. Since such analysis will be applied to only the unbalanced portion of the load, any inaccuracies in the method of analysis become relatively insignificant, and approximate methods may often prove sufficient.

In applying this method, it is often assumed that the dead load of the structure be balanced by the effective prestress. This would mean that a slight amount of camber may exist under the initial prestress. Sometimes, it is not necessary to balance all the dead load, since such balancing may require too much prestress and a limited amount of deflection may not be objectionable. On the other hand, when the live load to be carried by the structure is high compared to its dead load, it may be necessary to balance some of the live load in addition to the dead load.

Design by the load-balancing method gives a different visualization of the problem. It becomes a simple matter to lay out the cables in an economical manner, and to compute the required prestress as well as the corresponding fiber stresses in concrete. This method is illustrated in the following example.

EXAMPLE 6.6. For the continuous beam in Fig. 6.39, determine the prestress F required to balance a uniform load of 1.03 k/ft, using the most economical location of cable. Assume a concrete protection of at least 3 in. for the c.g.s. Compute the midspan section stresses and the reactions for the the effect of prestress and an external load of 1.6 k/ft.

Solution: The most economical cable location is one with the maximum sag so that the least amount of prestress will be required to balance the load. As shown in Fig. 6.39, a 3 in. protection is given to the c.g.s. over the center support and at midspan (a theoretical parabola based on these clearances

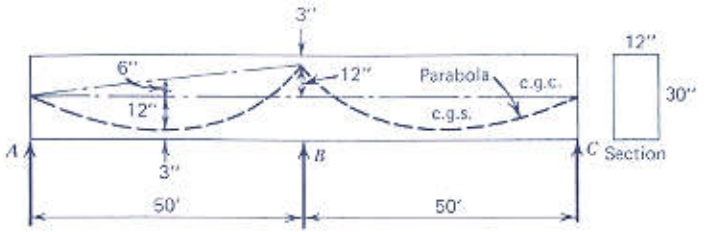

FIGURE 6.39. Example 6.6.

will have slightly less than 3 in. at a point about 20 ft from the exterior support). The c.g.s. at the beam ends should coincide with the c.g.c. and cannot be raised, not only because such raising will destroy the load balancing, but it will not help to increase the efficiency of the cable, since unfavorable end moments will be introduced.

The cable now has a sag of 18 in. and the prestress F required to balance the load of 1.03 k/ft is

$$F = \frac{wL^2}{8h} = \frac{1.03 \times 50^2}{8 \times 1.5} = 214 \text{ k}$$

The fiber stress under this balanced load condition is now

$$f = \frac{F}{A_c} = \frac{214{,}000}{360} = -593 \text{ psi}$$

Owing to the additional load of 0.57 k/ft, the moment at the center support is 178 k-ft and the corresponding stresses are

$$f = \pm 1190 \text{ psi}$$

So the resulting stresses over center supports are

$f = -593 + 1190 = +597$ psi tension in top fiber

$f = -593 - 1190 = -1783$ psi compression in bottom fiber

The reactions due to 1.03 k/ft can be computed from the vertical components of the cable and are, very closely,

exterior support: $R_A = 1.03 \times 25 - 1/50(214) = 25.8 - 4.3 = 21.5$ k

interior support: $R_B = 51.6 + 2 \times 4.3 = 60.2$ k

Under the action of 0.57 k/ft load, the reactions are, by the elastic theory,

exterior support: $R_A = 10.6$ k

interior support: $R_B = 35.6$ k

Hence the total reactions due to 1.6 k/ft load and the effect of $F = 214$ k are

exterior support: $R_A = 21.5 + 10.6 = 32.1$ k

interior support: $R_B = 60.2 + 35.6 = 95.8$ k

6.9.5 Cracking and Ultimate Strength

The behavior of prestressed concrete continuous beams is essentially elastic before cracking. Therefore, the cracking strength of the beam can be computed by the usual elastic theory. Generally, cracks start when the maximum tensile stress in the extreme fiber of the beam reaches the modulus of rupture of concrete.

As cracks develop, the stiffness of the beam is progressively reduced. The curvatures of the beam at the cracked sections also increase rapidly as can be seen from Fig. 6.10. This nonlinear deformation characteristic becomes important at loads approaching failure, and often leads to a redistribution of moment, resulting in a higher ultimate load than would otherwise be indicated by the elastic theory.

The ultimate strength of prestressed concrete continuous beams can be estimated by the theory of limit analysis based on three fundamental criteria: (1) equilibrium, (2) compatibility of deformation, and (3) moment–curvature relationship at each individual cross section. A general analysis which takes into account the nonlinear distribution of curvature along the beam, was presented by Guyon.[6] This method involves a trial-and-error approach by first assuming a bending moment distribution and then satisfying the equations of compatibility of deformation. The method may be applied for any load stage up to failure of the structure. Depending on the moment–curvature relationship, failure may be said to occur either when one or more cross sections rupture, or when the structure or a part of it becomes kinematically unstable.

An alternate approach[7] is to consider the effect of inelastic deformation as rotations concentrated at or near critical sections. Hence, the analysis is based on the moment–rotation relationship and the concept of "plastic hinge" theory. It should be emphasized that the properties of a plastic hinge are not the properties of the individual critical sections and the moment–rotation relationship for any critical section is dependent on much more than just the properties of the cross section involved. Whether there is full redistribution of moment depends upon the rotation capacities of the various critical sections. In general, for beams with sufficiently under-reinforced sections, full plastic hinges are formed at critical points of maximum moment. For over-reinforced sections or sections subject to shear failure, full plastic hinges may not develop and failure could occur before complete redistribution of moment.

A simplified method of calculation suggested by Bennett, et al.[8] neglects the effect of flexure between the hinges and considers only the compatibility of the rotation angles of the hinges at the critical sections. For a structure n times statically indeterminate, there are normally $n + 1$ hinges at failure. If a moment–rotation relationship is assumed for each hinge and the hinge at which ultimate moment and rotation occur is located, then the smaller rotations and the moments at the remaining hinges are easily derived. Bennett, et al. assumed that the ultimate rotation capacity θ_u is the same for all the critical sections and, that the moments and rotations are related as follows:

$$\frac{M}{M_u} = 0.5 + 1.4\frac{\theta}{\theta_u} \qquad \text{for } \frac{\theta}{\theta_u} \leq 0.25 \tag{6.40}$$

$$\frac{M}{M_u} = 0.8 + 0.2\frac{\theta}{\theta_u} \qquad \text{for } \frac{\theta}{\theta_u} \geq 0.25 \tag{6.41}$$

Having determined the angles of rotation at the critical sections, the ultimate load capacity of the beam can be calculated by the virtual work method.

EXAMPLE 6.7. Determine the ultimate load W_u of the two span continuous prestressed concrete beam shown in Fig. 6.40. The ultimate moment capacity of the beam section is $M_{uC} = 166.1$ in.-kips at C and $M_{uB} = 154.0$ in.-kips at B.

Solution: At ultimate load, plastic hinges are formed at B and C. By virtue of symmetry, a plastic hinge is also formed at B'. The ultimate moment and rotation will obviously occur at C, and for compatible rotation angles of the hinges,

$$\theta_B = \frac{\theta_C}{2\alpha} = \frac{\theta_C}{2(0.625)} = 0.8\theta_C = 0.8\theta_u$$

From Eq. (6.41)

$$\frac{M}{M_u} = 0.8 + 0.16 = 0.96$$

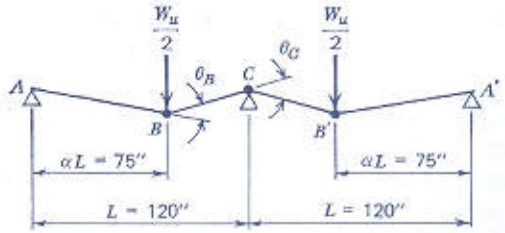

FIGURE 6.40. Example 6.7.

So the section at B is estimated to develop 96% of its ultimate moment capacity while the section C develops its full ultimate moment capacity. By the virtual work method,

$$2\left(\frac{W_u}{2}\right)(1) = M_{uC}\theta_C + 2(0.96M_{uB})\theta_B$$

Substituting $\theta_C = 2/(1 - \alpha)L$, $\theta_B = \theta_C/2\alpha$, and simplifying,

$$\frac{W_u}{2}\alpha(1 - \alpha)L = \alpha M_{uC} + 0.96M_{uB}$$

Now $\alpha = 0.625$, $L = 120$ in., $M_{uC} = 166.1$ in.-kips, $M_{uB} = 154.0$ in.-kips. Hence,

$$W_u = 17.9 \text{ kips}$$

This value compares closely to the experimental result of 18.6 kips obtained by Bennett et al.

The effect of moment redistribution in a continuous beam as its load capacity is approached is recognized by the 1971 ACI Code. The Code permits an adjustment of the negative moments due to design dead and live loads calculated by elastic theory for any assumed loading arrangement, provided that these modified negative moments are also used for final calculations of the moments at other sections in the span corresponding to the same loading condition. The adjustment may be either an increase or a decrease by not more than 20 $[1 - (q + q^* - q')/0.30]$ percent where q, q^*, and q' are reinforcement indices for nonprestressed tension steel, prestressed steel, and nonprestressed compression steel, respectively. Such an adjustment is permitted only when the section at which the moment is reduced is so designed that the net reinforcement index $q + q^* - q'$ (or $q_w + q_w^* - q_w'$ for flanged section) does not exceed 0.20. This limitation is to ensure the ability of the critical sections to deform inelastically by a sufficient amount.

It should be noted that if a continuous beam is prestressed with a nonconcordant tendon, the effect of a secondary moment induced by the prestressing force should be combined with the ultimate design moment due to dead and live loads, after allowing for the moment redistribution.

For beams with unbonded tendons, sufficient bonded steel should be provided to assure the rotation capacity required at the hinging sections and for control of cracking. In the case of continuous beams or slabs over two or more spans with one way prestressing, an adverse loading condition causing failure of the member or the unbonded tendons in one span may lead to loss of prestress and load carrying capacity in the other spans. Consideration should be given to the consequence of such failure if it could be expected to take place. One method of prevention would be to restrict the difference between the

weathering, the water–cement ratio should not exceed the values recommended by ACI Committee 211, which were stated earlier in this section.

3. Use Table 1.12 to determine the volume (in cubic yards) of coarse aggregate per cubic yard of concrete. Note that the amount of coarse aggregate varies with fineness modulus of the sand and maximum size of aggregate. Knowing the dry-rodded unit weight of coarse aggregate (pcf), its total weight in pounds can be computed by multiplying the volume selected in Table 1.12 by 27 (1 $yd^3 = 27\ ft^3$) and by the unit weight of the aggregate.

4. From (1), (2), and (3) the weight of sand required can be determined as follows: from the bulk specific gravity of the materials, the absolute volumes (in cubic feet) of water, cement, coarse aggregate, and air is subtracted from the volume of the concrete (27 ft^3) to get the absolute volume of the sand, which is subsequently converted to weight units (pounds).

5. The tables used and computations made in this method give batch weights for a saturated-surface-dry condition of the sand and coarse aggregate. Since the job aggregates may contain free moisture or be dry, the weights of aggregates and of water to be added to the mixer must be adjusted accordingly. For this purpose the free moisture or the absorption capacity data of the aggregates should be available.

TABLE 1.12. Volume of Coarse Aggregate per Unit of Volume of Concrete.[23]

Maximum Size of Aggregate, in.	Volume of Dry-rodded Coarse Aggregate[a] per Unit Volume of Concrete for Different Fineness Moduli of Sand			
	2.40	2.60	2.80	3.00
3/8	0.50	0.48	0.46	0.44
1/2	0.59	0.57	0.55	0.53
3/4	0.66	0.64	0.62	0.60
1	0.71	0.69	0.67	0.65
1 1/2	0.75	0.73	0.71	0.69
2	0.78	0.76	0.74	0.72
3	0.82	0.80	0.78	0.76

[a] Volumes are based on aggregates in dry-rodded condition as determined in accordance with ASTM C29.

These volumes are selected from empirical relationships to produce concrete with a degree of workability suitable for usual reinforced construction. For less workable concrete such as required for concrete pavement construction they may be increased about 10%. When placement is to be by pump, they may be reduced up to 10%.

Sample computations using this method are given in the ACI Committee 211 report.[23] It should be noted here that this method provides only an approximation of batch quantities. Depending on aggregate texture and shape, mixing-water requirements may be above or below the tabulated values. The resulting strength of the concrete may differ from that used in the mix design. For this reason the computed batch quantities must be checked by trial batches and necessary adjustments made. The trial batch test procedures are described in the ACI Committee 211 report.[23]

The principles used for proportioning normal-weight concrete mixtures apply directly to *lightweight concretes* containing lightweight aggregates characterized by rounded particle shape, coated or sealed surfaces, and relatively low values of absorption.[4] Another method specifically designed for proportioning structural lightweight concrete is given in a special report of ACI Committee 211.[24] Because of the variation in absorption of most lightweight aggregates, the water–cement ratio cannot be established accurately enough to be used as a basis for mix proportioning. For this reason, lightweight mixes are established by a series of trial mixes proportioned on a cement content basis. The strength results obtained for the several cement contents are plotted, and the cement content producing the required strength is determined from this graph. The maximum size of lightweight aggregate used in structural concrete is usually limited to 3/4 in. or smaller in order to obtain the desired strength at a minimum cement content. The larger the particle size of a lightweight aggregate, the lower its density and the weaker it is. The quantity of water required per cubic yard of lightweight air-entrained concrete averages about 415 lb, which is higher than that required by a normal-weight concrete.

1.10.8 Temperature of Concrete

The temperature of fresh concrete is affected by the temperature of its component materials. The initial temperature of freshly mixed concrete can be computed from the expression[4]:

$$T = \frac{0.22(T_a W_a + T_c W_c) + T_f W_f + T_m W_m}{0.22(W_a + W_c) + W_f + W_m}$$

where T is the temperature in °F, W the weight in pounds of ingredient per unit volume of concrete; suffixes a, c, f, and m refer to aggregate, cement, free moisture in aggregates, and mixing water, respectively (usually $T_a = T_f$). The 0.22 value is the approximate specific heat in Btu/lb/°F of the solid ingredients (cement and aggregate). The specific heat of water is 1.0.

Water is the easiest to cool and can be effectively used to lower the initial temperature of a concrete. Frequently *crushed ice* is used as part of

anchorages of all or some of the unbonded tendons. Another would be the addition of some bonded reinforcement.

6.10 FLAT SLABS

6.10.1 Method of Analysis

Flat slabs may be constructed with or without drop panels around the columns. The latter is often referred to as flat plate. In application, it is more frequent that flat slabs are continuous over two or more spans in each direction.

Prior to the cracking of concrete, the behavior of a prestressed slab is essentially elastic. Therefore, the analysis can be based on the classical elastic slab theory, using finite element or finite difference methods. However, the application of these methods can be quite tedious. For purposes of design, beam method using the concept of load balancing offers a practical approach. Utilizing this concept, Rozvany and Hampson developed procedures for optimum design in terms of minimum tendon area or slab thickness. In a similar manner, Brotchie and Russell made use of the moment balancing concept and developed design procedures for maximum material economy and optimum behavior in terms of ultimate strength and deflection. Also using the load balancing concept, a rigorous elastic analysis of the distribution of moments and direct forces induced by prestressing in flat plates was presented by Parme.[10–13]

For slabs with square or rectangular panels, where columns are quite flexible or are not rigidly connected to the slab, the beam method offers the simplest solution, especially when combined with the concept of the load balancing. In the beam method, the slab is treated as continuous beams in each of the two directions, assuming continuous nonyielding supports along column lines in one direction when analysis is being made for moment in the other direction. The effect of prestressing such a slab is analyzed just as is done for a continuous beam, including the computation of secondary moments.

When columns are relatively stiff and rigidly connected to the slab, the frame method is then used in which the stiffness of the column is taken into consideration. The frame is assumed to consist of a row of columns and strip of supported slabs, each strip being bounded laterally by the center line of the panel on either side of the column line.

By analyzing a continuous slab as a continuous beam or frame, the total moment across any section due to loading and the average position of the *C*-line under prestressing can be easily obtained. However, the distribution of the total moment and the variation of the position of the *C*-line along the width of the slab still remain to be determined. Approximations have been

used, for example, assuming 45% of the total moment to be carried by the middle strip and 55% by the column strip for a simple flat slab of uniform thickness supported by four corner columns. For the interior span of a slab continuous in both directions, a better approximation seems to be 25% by the middle strip and 75% by the column strip, although 40% and 60% respectively, are often used. It should be pointed out that with these approximate distributions of moment between column and middle strips, it will not produce a balanced load design for uniform loads, although slabs so designed have been found to be fairly level from a practical point of view.

EXAMPLE 6.8. A two-way prestressed lift slab has a plan as shown (Fig. 6.41). The 7 1/2 in. concrete slab weighs 94 psf and carries a live load of 75 psf; $f'_c = 4000$ psi; 1/4 in. wires grouped in six wires per unit are to be used

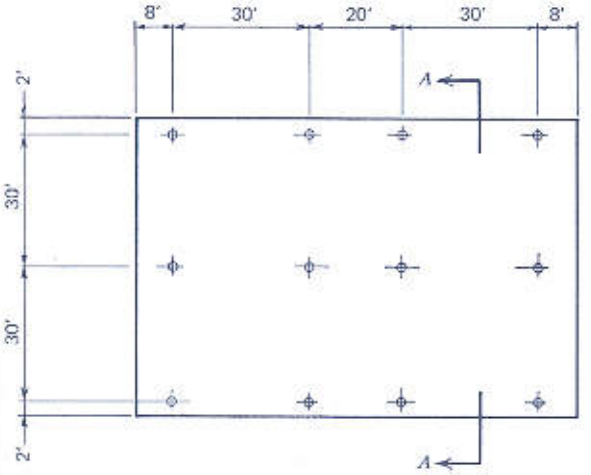

(a) Plan of slab

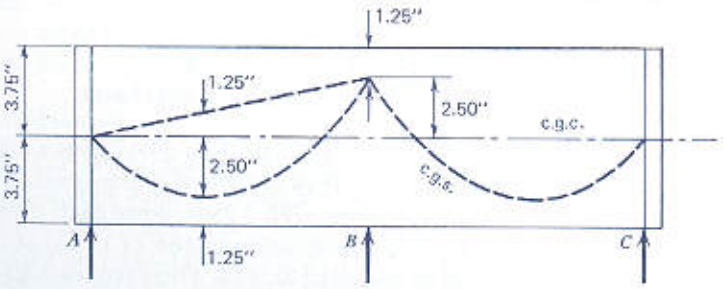

(b) Load balancing method

FIGURE 6.41. Example 6.8.

for prestressing with ultimate strength of 250 ksi; $f_0 = 150$ ksi; $f_e = 125$ ksi. Minimum coverage for the cables is 1 1/4 in. measured to the center line. Allowing no tension in the concrete, choose the location for the cables and compute the number of 64 ft long cables required for the slab. Use the beam method for analysis.

Solution: Using the load balancing approach, we can start off by assuming that for optimum behavior it will be desirable to balance the 94 psf of dead load plus 15 psf of the live load, or a total of 109 psf. Referring to Fig. 6.41(b), the cable sag h is very nearly 3.75 in. Hence, the effective prestress required is

$$F = \frac{wL^2}{8h} = \frac{109 \times 30^2 \times 12}{8 \times 3.75} = 39.4 \text{ k/ft}$$

and the slab is under uniform prestress of

$$f_{av} = \frac{39{,}400}{12 \times 7.5} = -437 \text{ psi}$$

for its dead load plus 15 psf live load.

To check the stresses under full live load, we compute the effect of 75 − 15 = 60 psf additional live load, which will produce a maximum moment over the center support of

$$-M = \frac{wL^2}{8} = \frac{60 \times 30^2}{8} = 6750 \text{ lb-ft}$$

And the maximum bending stresses are given by

$$f = \frac{Mc}{I} = \frac{6M}{bd^2} = \frac{6 \times 6750 \times 12}{12 \times 7.5^2}$$

The resultant maximum fiber stresses are

$$f_{top} = -437 + 720 = +283 \text{ psi tension}$$

$$f_{bot} = -437 - 720 = -1157 \text{ psi compression}$$

These stresses are not considered excessive, and $F = 39.4$ k/ft is satisfactory.

For the total length of the slab, the required effective prestressing force in the short direction will be $39.4 \times 96 = 3782.4$ kips. Since each prestressing unit of six 1/4-in. wires can provide an effective prestress of 37.5 kips, it would be sufficient to use 100 units of prestressing tendon. These tendon units should be placed in the column and middle strips according to a distribution of perhaps 60% and 40%, respectively.

6.10.2 Cracking and Ultimate Strength

Since the beam method or the frame method does not yield real stresses, it cannot be used to predict the cracking strength of flat slabs. Instead, the classical elastic plate theory should be used if a more accurate assessment of cracking strength is required. Fortunately, to ensure serviceability, allowable working stresses may be used as a guide for service load conditions. Furthermore, experiences have shown that if a minimum average compressive prestress of 200 psi is maintained in the concrete, the slab can be generally made crack free and watertight. Thus, in practice, an average of 200 to 350 psi is considered to be ideal for most practical situations.

It is important that the design by the beam method be checked to make sure it satisfies ultimate strength requirements. Using appropriate load factors, the ultimate moment should be computed as discussed in Section 6.4. When the live load is fairly high, say much over 50 psf, the ultimate moment furnished by the prestressing tendons is often inadequate. Rather than increasing the number of prestressing tendons, a general practice is to provide nonprestressed reinforcements at the critical sections. These reinforcements will not only help to increase the ultimate strength but also to distribute the cracks. Nonprestressed reinforcement should be provided over the columns in all cases. A suggested minimum amount is that required by Eq. (6.26) for the column strip each way for one-quarter the span. Where possible, some of the tendons should also pass through the columns or at least around their edges. It should be noted that the ultimate strength of each slab panel is primarily controlled by the total amount of tendons and nonprestressed reinforcements rather than their distribution.

The analysis of ultimate moment for one critical section as described above does not give a true indication of the load carrying capacity of the slab. Since the percentage of steel in the slab is relatively low, it permits the formation of plastic hinges. Thus, the yield-line theory applied to prestressed slabs, using the ultimate strength of the prestressed sections, will give reliable results. A practical design approach using load balancing in conjunction with yield-line theory has been developed by Power.[14]

6.10.3 Deflection

The deflection of flat slabs can be obtained by the theory of elasticity, but the time consumed in such an analysis could be enormous. When only approximate results are desired, it is possible to treat strips of the slab as beams and compute the accumulated deflection. For example, the center deflection of a slab is the sum of two deflections, one due to a continuous beam along the columns, another due to a perpendicular continuous beam along the middle (Fig. 6.42).

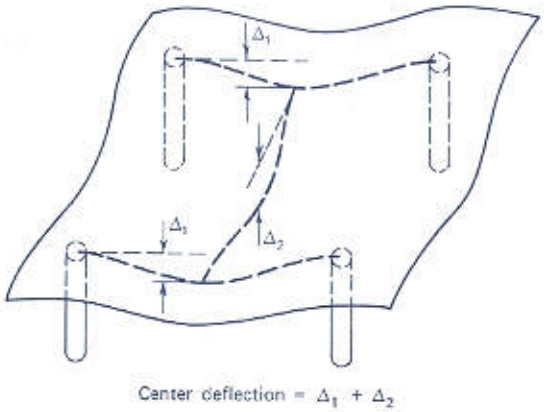

FIGURE 6.42. Estimating slab deflections.

6.10.4 Other Design Considerations

It has been found that prestressed flat slabs without drop panels are practical up to a span length of about 35 ft for the usual live loads. For spans ranging between 35 and 45 ft, drop panels around columns are provided to withstand the high bending and shear stresses in that region. Where spans exceed 45 ft, a beam–girder system or waffle system becomes more economical.

In order to ensure adequate stiffness and serviceability of the slab, the 1971 ACI Code Commentary[15] suggests that "for flat slabs continuous over two or more spans in each direction, the span–thickness ratio should generally not exceed 42 for floors and 48 for roofs. These limits may be increased to 48 and 52, respectively, if calculations verify that both short- and long-term deflection, camber, and vibration frequency and amplitude are not objectionable." It should be cautioned, however, that if the maximum span–thickness ratio is used to achieve minimum slab thickness, the required prestress may be relatively high. When the average compressive prestress in concrete is in excess of 500 psi, there is danger of excessive elastic shortening, shrinkage, and creep occurring in the slabs.

Punching shear in the flat slab around the columns should be checked. The critical section for computation is often taken as one-half the slab thickness away from the face of the column or of the drop panel. Very limited information is available on the ultimate punching shear strength of prestressed slabs. Scordelis, et al.,[16] developed the following relationship for normal weight prestressed slabs:

$$V_u = \left(0.175 - 24.2 \times 10^{-6} f'_c + 20 \times 10^{-6} \frac{F_e}{s}\right) bdf'_c$$

where F_e is the effective prestressing force per cable, in lb, s is the cable spacing, in in., b is the perimeter of columns, in in., and d is the effective depth of slab, in in. A similar relationship has been developed by Grow and Vanderbilt[17] for lightweight concrete prestressed slabs:

$$V_u = (360 + 0.30 f_{ce}) bd$$

where f_{ce} is the average effective prestress in concrete, in psi.

An approximate method is to compute nominal shear stress by formula (11–25) of the ACI Code Section 11.10.3, limiting it to $4\sqrt{f'_c}$ for average prestress up to 200 psi. It may be increased linearly from $4\sqrt{f'_c}$ for 200 psi average prestress up to $6\sqrt{f'_c}$ for 500 psi average prestress. Higher values may be permitted when justified by test data. For slabs over 10 in. thick, shear reinforcement as specified in the ACI Code Section 11.11.1 may be considered effective.

When considering transfer of bending from slab to column, the effective width of the slab may be taken as one-third to one-half the panel width.

For very long slabs, it is advisable to limit the maximum length of the slab between construction joints to 100 or 150 ft in order to minimize the effect of slab shortening and to avoid excessive friction loss of prestress.

6.11 TENSION AND COMPRESSION MEMBERS

6.11.1 Tension Members

A prestressed concrete tension member can be considered as a combined steel and concrete member whose strains and stresses before cracking can be evaluated, assuming elastic behavior and taking into account the effect of creep. If F_0 is the total initial prestress and F the total effective prestress, then the stresses in the concrete will be, for the initial prestress,

$$f_c = \frac{F_0}{A_c}$$

and, for the effective stress,

$$f_c = \frac{F}{A_c}$$

When a load P is applied externally (Fig. 6.43), both the steel and the concrete will elongate the same amount. Hence, the usual transformed-section method as applied to reinforced concrete can also be applied here. The stresses produced by P will be,

$$f_c = \frac{P}{A_t}$$

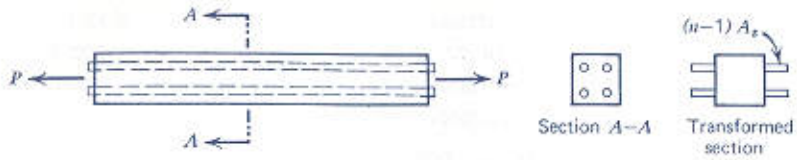

FIGURE 6.43. Prestressed-concrete tension member.

and, for steel,

$$f_s = \frac{nP}{A_t}$$

where

$$A_t = nA_s + A_c = nA_s + A_g - A_s = A_g + (n-1)A_s$$

and A_c is the net area of concrete, A_g is the gross area of concrete. In order to be exact, the value of $n = E_s/E_c$ should be chosen for the proper stress and duration of loading, taking into account the effect of creep if necessary.

Thus the resultant stresses due to the effective prestress plus the external load are, for concrete,

$$f_c = \frac{F}{A_c} - \frac{P}{A_t}$$

and for steel,

$$f_s = \frac{F}{A_s} + \frac{nP}{A_t}$$

It is important to investigate the strains in a prestressed concrete tension member, both those due to prestressing and those due to external loads. Under the initial prestress F_0, the stress in the concrete being F_0/A_c, the corresponding instantaneous unit strain will be

$$\varepsilon = \frac{F_0}{EA_c}$$

which will reduce to F/EA_c after the losses have taken place.

Under the action of external load P, the instantaneous strain is given by

$$\varepsilon = \frac{P}{EA_t}$$

In all cases, the value of E must be chosen with regard to the level of stress and the age of concrete. The effect of creep must be considered if required.

Generally speaking, prestressed concrete tension members have a very low reserve strength above the point of zero stress. If the member is not cast

as one piece (for example, if it is made up of blocks), cracking may coincide with zero stress. Beyond cracking, the load on the member will have to be carried by the steel alone. If the member is cast as one piece, and if shrinkage and other cracks have not occurred, the concrete will be able to take some tension before cracking. But, once the concrete has cracked, the tension lost as a result of cracking must be carried by the steel.

When heavy overloads are possible, prestressed tension members should not be designed on the basis of allowable stresses, but rather on the basis of the cracking or ultimate strength, with proper load factors. Load factors should vary with the type of structure. For example, in most buildings and long-span bridges, the load factor required will be smaller than in a short bridge subject to possible heavy overloadings. For liquid storage tanks, both the possibility and the magnitude of overloading are small, and a low load factor is employed.

An interesting concept is the use of prestressed concrete tension elements as a substitute for the reinforcement in the conventional reinforced concrete sections. Tests have shown that in such a composite beam, the prestressed element provides a restraining effect on its surrounding nonprestressed concrete so that a better control of cracking is achieved.[18] Furthermore, flexural cracking does not reduce the beam stiffness significantly until crack also develops in the prestressed element. The beam also has adequate fatigue strength against repeated loads up to about 70% of the load that would cause cracking in the prestressed tension element.

6.11.2 Columns under Axial Load

The strength of a concrete column may be controlled either by material failure or by buckling, depending on the slenderness of the column. For short columns, the material strength is the governing factor and there would appear to be little justification for prestressing. However, there are several constructional advantages of prestressing the column, such as the economy of precasting and mass production and the resistance to handling stresses. In the case of long columns, buckling often becomes an important design consideration. Since long columns are more susceptible to bending, it can be expected that the buckling strength of the column may be improved by prestressing.

A prestressed member is not subject to buckling due to its own prestress, but it is so under an external compressive load just like a column of any other material. On the other hand, prestressing with unbonded tendons not in contact with the concrete does produce buckling just as does the externally applied compressive load.

Within the working load range, the stresses in a short prestressed concrete column due to both prestress and external loads can be analyzed by the usual

elastic theory. If f_{ce} and f_{se} are the effective prestress in concrete and steel, respectively, and the column is subject to an external load P, then the resulting concrete and steel stresses will be

$$f_c = f_{ce} + \frac{P}{A_t} = f_{ce} + \frac{P}{A_g + (n-1)A_s}$$

$$f_s = f_{se} - \frac{nP}{A_t} = f_{se} - \frac{nP}{A_g + (n-1)A_s}$$

where A_t is the transformed area of the column section and $n = E_s/E_c$. It should be emphasized again that the stresses so calculated are only valid for short-time loadings just as in the case of reinforced concrete columns. For sustained loadings, the effects of shrinkage and creep of concrete must be taken into consideration.

The ultimate strength of short prestressed concrete columns containing closely spaced spirals is composed of the load carried by the concrete as well as the nonprestressed vertical reinforcement, if any, minus the residual tension in the prestressing steel. Hence, the ultimate load capacity of the column is

$$P_u = 0.85f'_cA_c + A'_sf_y - A_sE_s[\varepsilon_{se} - (\varepsilon_{cu} - \varepsilon_{ce})]$$

where A_c is the net cross sectional area of concrete, A'_s is the area of nonprestressed reinforcement, A_s is the area of prestressing steel, E_s is the modulus of elasticity of prestressing steel, f_y is the yield strength of nonprestressed reinforcement, ε_{se} is the strain in prestressing steel corresponding to effective prestressing force, ε_{ce} is the concrete strain under effective prestressing force, and ε_{cu} is the maximum strain in concrete at failure.

Tests have shown that when a small amount of spiral is used (approximately 22% less than that required by the ACI Code) its yield strength will be developed, thus contributing greatly to the ductility though not the strength of the column.[19] It also prevented the longitudinal splitting failure that generally occurred in columns without spirals.

In the case of slender columns, the ultimate strength is often governed by instability. Since the stress–strain relationship of concrete is nonlinear, the buckling load of a slender column can be determined by the inelastic column theory as

$$P_{cr} = \frac{\pi^2 E_t I_t}{l_{cr}^2}$$

where E_t is the tangent modulus of elasticity of concrete corresponding to the buckling stress, I_t is the moment of inertia of the transformed section of the column on the basis of E_t, and l_{cr} is the effective critical length which depends on the end condition of the column. Here E_t depends on the buckling

stress which in turn is a function of P_{cr}. Therefore, to obtain a solution from the above equation, one must also consider the functional relationship of the stress–strain curve of concrete as well as the equilibrium equation

$$P_{cr} = \sigma_{cr}A_t$$

where σ_{cr} is the buckling stress and A_t is the transformed area of column based on E_t.

6.11.3 Columns under Axial Load and Moment

Many columns, besides carrying direct compressive loads, are often required to resist bending moments which may be induced by transverse loads such as wind and earthquake, by eccentric loads or by frame action. In such instances, prestressing may be of considerable value in providing greater strength and stiffness to the column.

Before cracking, the stresses and deflections can be calculated by assuming the column to behave elastically. The stress at any section is the sum of the stresses due to effective prestress, the axial load P and the external moment M. Hence,

$$f_c = f_{ce} \pm \frac{P}{A_t} \pm \frac{Mc}{I_t}$$

For slender columns, the deflections of the column due to both eccentric prestressing and the applied moment could be quite significant and their effects on the stresses must be taken into account. Thus the critical stresses occurring at the midheight of the column are

$$f_c = f_{ce} \pm \frac{P}{A_t} \pm \frac{Mc}{I_t} \pm \frac{P\Delta_1 c}{I_t} \pm \frac{P\Delta_2 c}{I_t}$$

where Δ_1 is the deflection due to eccentric prestressing, which is calculated by the method given in Section 6.7, and Δ_2 is the deflection due to the applied load P and moment M, which is given by the well-known secant formula

$$\Delta_2 = \frac{M}{P}\left(\sec\sqrt{\frac{PL^2}{4E_cI_t}} - 1\right)$$

The ultimate strength of a column section under combined axial load and moment or under an eccentric load can be determined by considering the basic conditions of static equilibrium and strain compatibility (Fig. 6.44).

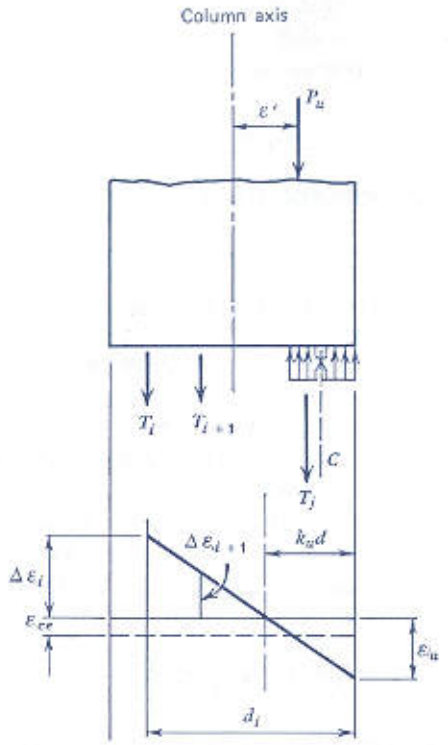

FIGURE 6.44. Stress and strain distributions on a column section.

These conditions lead to the following governing equations:

$$\Delta\varepsilon_i = \varepsilon_u\left(\frac{d_i - k_u d}{k_u d}\right)$$

$$T_i = A_i E_s(\varepsilon_{se} + \varepsilon_{ce} + \Delta\varepsilon_i)$$

$$P_u = C - \sum T_i$$

$$M_u = P_u e' = M_c + \sum M_{Ti}$$

where ε_{se} is the steel strain under effective prestress, ε_{ce} is the concrete strain under effective prestress, A_i is the area of the ith steel, M_c is the moment of C about the column center line, and M_{Ti} is the moment of T_i about the column center line. The solution of these equations can be expeditiously obtained by first selecting a value of $k_u d$ and then calculating P_u and M_u from the last two equations.

For a given column section, the results of the ultimate strength analysis can be conveniently expressed in the form of an interaction curve. Such

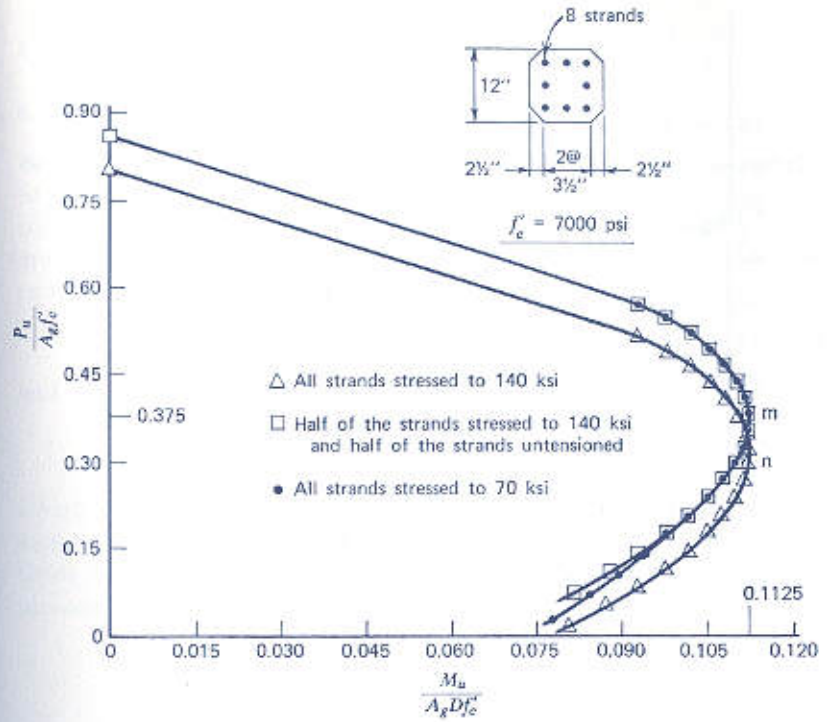

FIGURE 6.45. Interaction curves for symmetrical sections.

analyses have been performed on a number of symmetrical column sections, either fully or partially prestressed.[20] Typical interaction curves are shown in Fig. 6.45. Similar analysis has also been applied to an octagonal column with unsymmetrically placed holes.[21] The resulting interaction curves are shown in Fig. 6.46. These studies along with others have resulted in the tentative recommendations for the design of prestressed concrete columns.[22]

Characteristically, the interaction curve consists of two branches. The upper branch shows a reduction in axial load capacity as moment increases until the latter reaches a maximum value (points m and n in Fig. 6.45). The lower branch shows an increase in axial load capacity as moment increases. These characteristics are not unlike those of ordinary reinforced concrete columns. However, the mode of failure for prestressed concrete columns could be quite different.[20] If the maximum concrete strain is taken as 0.003, the entire range of the interaction curve generally represents the mode of compression failure. On the other hand, in the case of ordinary reinforced concrete columns, the upper branch of the interaction curve represents compression failure while the lower branch represents tension failure.

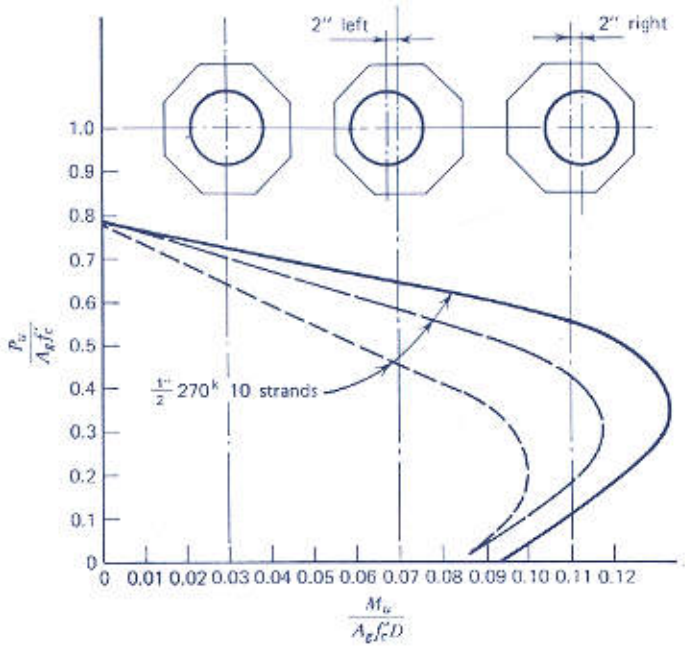

FIGURE 6.46. Interaction curves for unsymmetrical sections.[21]

A reduction in prestressing increases the axial load capacity of the column under a given bending moment. On the other hand, a reduction in prestressing may cause either an increase or a decrease in moment capacity of the column depending on whether the column is subject to a relatively high or low axial load.

The ultimate strength of slender prestressed concrete columns under combined axial load and bending is governed by instability. The analysis must take into account the deflection of the column. The governing equations are usually expressed in the form of the force equilibrium equation, the moment equilibrium equation and the strain–curvature equation.[23] Where the effects of creep and shrinkage are considered, these three equations can be modified according to the assumed creep and shrinkage properties of concrete.[24] To obtain a solution, one must solve these three equations with due regard to boundary conditions, and must often resort to numerical procedures usually involving extensive computational work.

6.12 TORSION

6.12.1 Pure Torsion

Before cracking, the behavior of a prestressed concrete member under pure torsion can be closely predicted by the elastic theory just as that of a plain or reinforced concrete member. According to St. Venant's theory, the maximum torsional shear stress v_t occurring at the middle of the longer sides of a rectangular section is

$$v_t = \frac{T}{\alpha b^2 h}$$

and

$$\theta = \frac{T}{\beta G b^3 h}$$

where T is the torque, b is the width of the rectangle, h is the depth of the rectangle, G is the shear modulus of concrete, which may be taken as 0.4 times the modulus of elasticity, θ is the angle of twist in radians, and α and β are constants depending on the proportion of the rectangle as given below:

h/b	α	β
1.0	0.208	0.141
1.2	0.219	0.166
1.4	0.227	0.187
1.6	0.234	0.204
1.8	0.240	0.217
2.0	0.246	0.229
2.5	0.258	0.249
3.0	0.267	0.264
5.0	0.292	0.291
10.0	0.312	0.312
110.0	0.331	0.331
∞	0.333	0.333

For flanged sections such as T, L, and I, although a solution can be obtained by numerical procedure, the common practice is to use an approximate analysis by assuming the torsion constant

$$K = \frac{T}{G\theta}$$

as the sum of the torsion constants of the component rectangles. Thus

$$K = \sum \tfrac{1}{3} b_i^3 h_i$$

where b_i and h_i are the width and depth, respectively, of the component rectangles. The maximum torsional shear stress in each component rectangle is then given by

$$v_{ti} = \frac{3Tb_i}{\sum b_i^3 h_i}$$

The torsional shear as calculated above and the compressive stress due to prestressing force represent a state of biaxial stress. Cracking occurs when the combined stress exceeds the concrete strength as defined by a failure criterion. Several failure theories have been compared with test results and it has been found that the effect of prestress is to increase substantially the cracking torque up to about 2.8 times that of a corresponding plain concrete member for values of prestress up to 0.7 of f'_c.[25] If the failure criterion is based on the maximum tensile stress theory, then the ratio of the cracking torque of a prestressed member T_{cr} to that of a corresponding plain concrete member T_{up} can be expressed as

$$\gamma = \frac{T_{cr}}{T_{up}} = \sqrt{1 + m\frac{f_p}{f'_c}}$$

where f_p is the compressive stress in concrete due to prestress and m is the ratio of the compressive strength to the tensile strength of concrete. The value of m has been chosen as 10 by Hsu[27] and as 12 by Bishara and Peir.[26]

Based on the skew bending mechanism, Hsu also presented an analysis of the cracking torque of prestressed members and obtained the same expression for γ as given above. A comparison of the theory with test data is shown in Fig. 6.47.

When cracking occurs, prestressed concrete members with no web reinforcement may fail immediately without much warning, often accompanied by considerable noise and flying debris. The directions of the cracks depend on the magnitude and the eccentricity of the prestressing force. The larger the prestressing force, the smaller is the angle of inclination of the crack. This type of sudden and destructive failure can be avoided by the addition of only a small amount of web reinforcement. As shown in Fig. 6.48, a prestressed member containing web steel of about 1.5% of the volume of the core enclosed within the closed stirrup is significantly more ductile than a comparable prestressed member but without web steel. When compared with a reinforced member containing the same amount of web steel, a significant increase in torsional strength due to prestress is indicated. When the

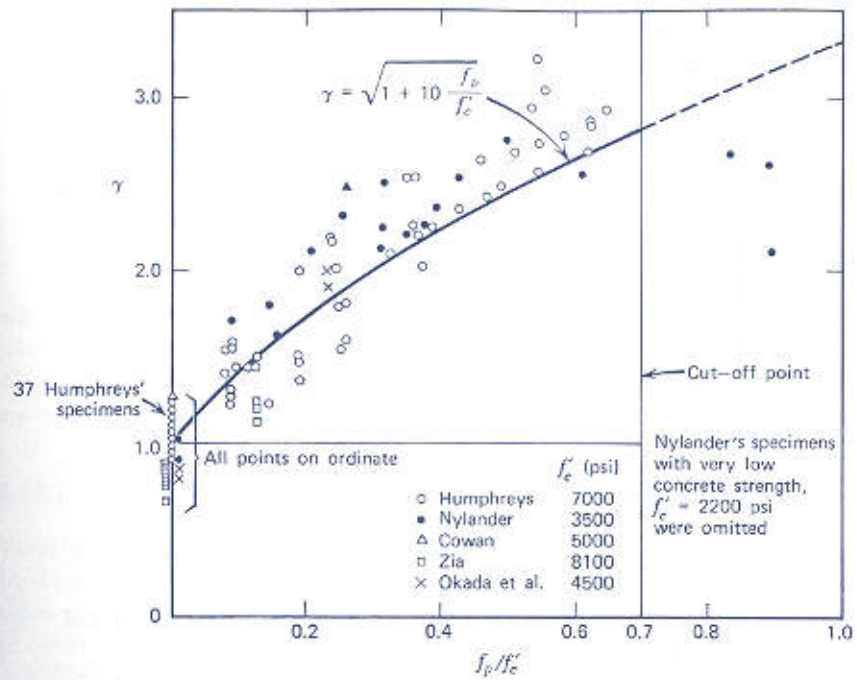

FIGURE 6.47. Comparison of theoretical value of γ with test data.[27]

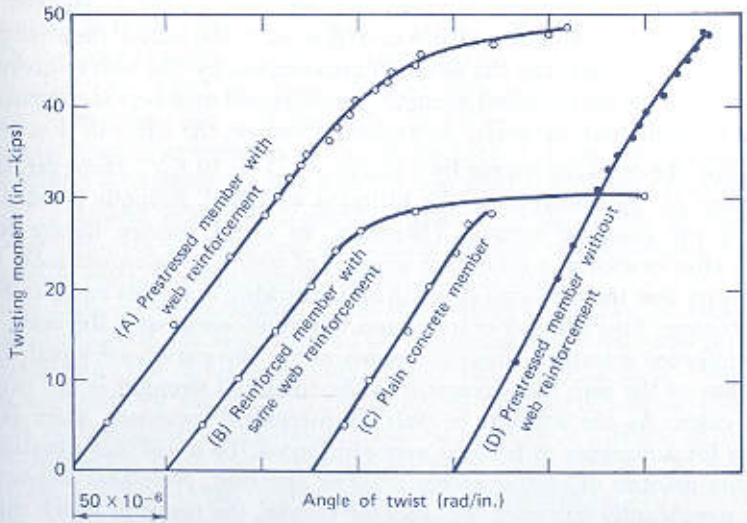

FIGURE 6.48. Typical torque–twist curves.

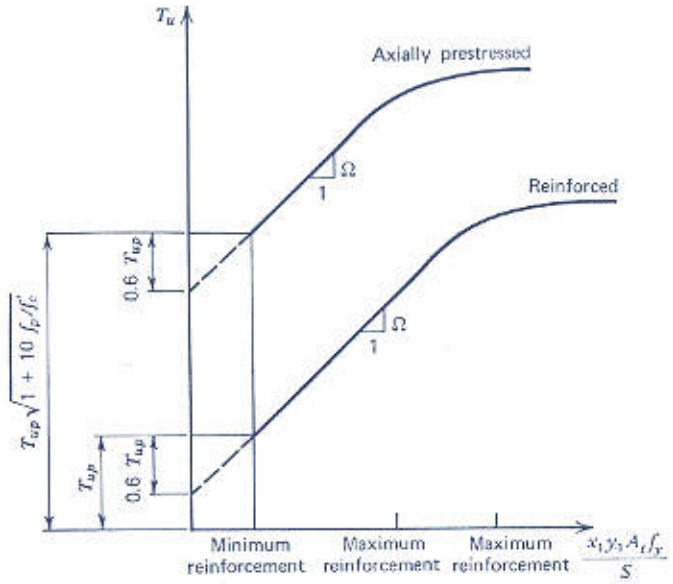

FIGURE 6.49. Torsional strength of prestressed and reinforced members with web reinforcement.

reinforced member is compared with a corresponding plain concrete member, the ductility provided by the web steel is also very obvious.

As in the case of reinforced concrete members, the torsional strength of prestressed members with web steel can be expressed as the sum of the strength contributed by concrete and the strength contributed by the web reinforcement.[28] In Fig. 6.49, the torsional strength of prestressed members is compared with that of reinforced members. As explained before, the effect of prestress is to increase the cracking torque by a factor of $\sqrt{1 + 10 f_p/f'_c}$. However, the contribution of the concrete to the ultimate torsional strength is only a portion of the cracking torque. Therefore, to avoid sudden failure immediately after cracking, a minimum amount of web reinforcement must be used to insure that the torsional strength after cracking is at least equal to the cracking torque. This amount of minimum web reinforcement is the same as that of reinforced members. Since the slopes of the two curves are equal, the contribution of the web reinforcement to the torsional strength is the same for both cases. As the amount of web reinforcement increases, there is a possibility for a member to become over-reinforced. To avoid this situation, a maximum amount of reinforcement must be specified. Note that although prestress significantly increases the cracking torque, the range in which mild steel reinforcement is effective is considerably reduced when compared with

corresponding reinforced concrete members. In other words, the maximum reinforcement for prestressed members is considerably less than that for reinforced members.

According to Fig. 6.49, the torsional strength of prestressed members is therefore given by

$$T_n = T_{up}\left(\sqrt{1 + 10\frac{f_p}{f'_c}} - 0.6\right) + \frac{\alpha_T x_1 y_1 A_t f_y}{s}$$

where A_t is the area of one leg of a closed stirrup, f_y is the yield strength of stirrup, s is the spacing of stirrup, x_1 is the small dimension of a rectangular closed stirrup, y_1 is the larger dimension of a rectangular closed stirrup, and α_T is the slope of the curve in Figure 6.49, and is equal to $0.66 + 0.33 y_1/x_1$.

6.12.2 Torsion Combined with Bending

Tests of prestressed concrete members subject to combined bending and torsion have been carried out by a number of investigators, involving specimens of rectangular, I, hollow box, and T sections. In spite of the difference in cross section, the general behavior is common to all.

Before cracking, prestressed concrete members under high ratios of torsion to bending behave almost elastically as evidenced by the linear torque–twist curve. As the ratio of torsion to bending decreases, the torque–twist curve increasingly loses its linearity well before cracks become visible, indicating the effect of minute flexure cracks induced by the higher bending moment.

In the post cracking stage, the range between the cracking and ultimate capacities of a beam increases with an increase in the bending-to-torque ratio. When the ratio is of the order of 8.0 or more, the ultimate moment capacity may be as much as twice the cracking moment. On the other hand, if the ratio is in the range of 2.0 to 3.0, the ultimate moment may be only 20 to 25% higher than the cracking moment. With increasing bending-to-torque ratio, the total amount of rotation and that of deflection are also substantially increased, showing considerable ductility.

The failure of prestressed concrete members because of bending and torsion occurs in the same form of skew bending as described in Section 5.4. A beam may fail in torsion mode for low ratio of bending to torque, or in bending mode for moderate to high ratios of bending to torque. The bending mode of failure may be governed either by yielding of stirrups or by yielding of prestressing steel and other longitudinal reinforcement. A comparison between a series of test results obtained by GangaRao and Zia and their theory[29] on skew bending mechanism is shown in Fig. 6.50. At high ratios of torque/moment, the torsional strength is increased by the addition of

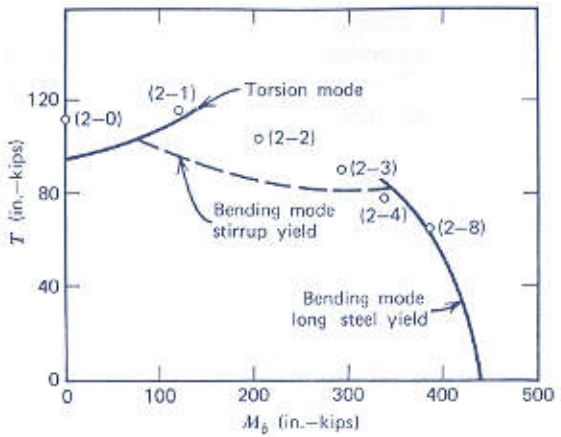

FIGURE 6.50. Comparison of test results with skew bending theory for rectangular prestressed concrete members containing web reinforcement.[29]

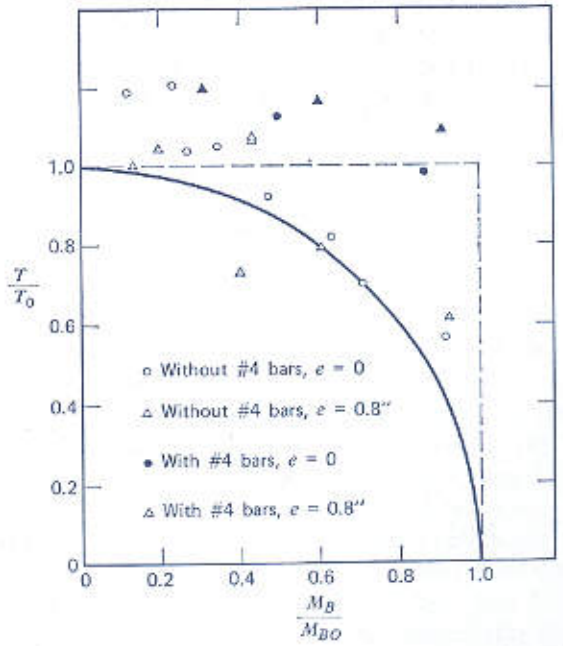

FIGURE 6.51. Interaction diagram based on GangaRao and Zia's test results.[29]

bending up to a certain limit. This is especially true for eccentrically prestressed members and for members containing unequal top and bottom reinforcement. Clearly, the application of external bending moment up to a certain amount simply modifies the axial compression to a more uniform distribution and thus increases the torsional shear resistance of the concrete. At low ratios of torque/moment, the effect of torsion is to reduce slightly the bending capacity of the beam.

Expressed as nondimensional interaction curves, GangaRao and Zia's test results are shown in Fig. 6.51. The data indicate a square interaction curve for beams augmented with longitudinal reinforcing bars. For beams with no additional longitudinal reinforcement, a circular interaction curve is indicated. These interaction curves are also in agreement with the test results obtained by other investigators.

6.12.3 Torsion Combined with Bending and Shear

In practice, torsion rarely occurs alone in a structure. It is usually accompanied by bending and shear. Owing to the complexity of the problem, only a few investigations[30–33] have been reported in the literature. In these investigations, tests have been conducted on members of rectangular, T, and I sections with uniform or eccentric prestressing. The effects of web reinforcement have also received some attention.

The general behavior of the members under combined loadings including shear is quite similar to that under combined torsion and bending. It is virtually elastic up to about 90% of the load producing initial cracking. Beyond cracking, members subjected to higher bending generally exhibit more ductility and greater strength.

Failure takes place also in the form of skew bending, either in torsion mode or in bending mode depending on the torque/moment ratio. When the ratio is in the order of 0.25 or less, bending mode of failure is most likely to occur; otherwise, torsion mode of failure develops.

For a given shear span, the torsional capacity can be increased up to about 30% in the presence of a small amount of bending and shear. The amount of increase will be smaller if the shear span becomes shorter. In comparison with beams under torsion and bending, the presence of shear in combined loading generally reduces the ultimate torsional capacity of a beam by about 10 to 20%. On the other hand, the bending capacity of a beam is not reduced under combined loads until the torque is equal to about 50% of the capacity of the beam under pure torsion.

Figure 6.52 shows a circular interaction curve as compared with the test results of several investigators. The test results encompass a wide range of the shear span–depth ratio. The interaction curve also compares closely with the test results of I beams as obtained by Gausel.[32]

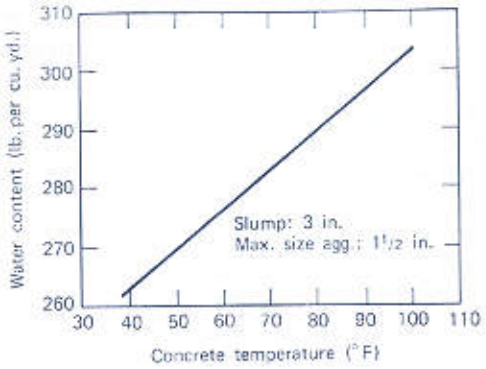

FIGURE 1.6. The water requirement of a concrete mix increases with an increase in temperature.[4]

the mixing water, since it is more effective than water in reducing the concrete temperature. One pound of ice in melting absorbs 144 Btu, whereas one pound of water heated 1°F absorbs only 1 Btu. When ice is used, the above expression for temperature of fresh concrete is modified as follows:

$$T = \frac{0.22(T_a W_a + T_c W_c) + T_f W_f + T_m W_m - 112 W_i}{0.22(W_a + W_c) + W_f + W_m + W_i}$$

where W_i is the weight in pounds of ice per unit volume of concrete.

The temperature of fresh concrete has a significant effect on its water requirement for a given slump. The higher the temperature of the concrete the higher is the water requirement as illustrated in Fig. 1.6. In practice any significant increase in water content cannot be permitted without increasing the cement content in order to maintain the required strength of the concrete. Also the higher temperature will accelerate the rate of setting as was shown in Fig. 1.4. Many specifications require that concrete, as placed, should have a temperature of less than 85° or 90°F. Ninety degrees is a reasonable and practical upper limit. During winter construction it is usually necessary to heat the concrete materials prior to batching and mixing. At temperatures above freezing it usually is sufficient to only heat the mixing water. At temperatures below freezing the aggregate needs also to be heated.

REFERENCES

1. Troxell, G. E., Davis, H. E., and Kelly, J. W., *Composition and Properties of Concrete*, McGraw-Hill Book Co., Inc., 1968.
2. Bogue, R. H., *The Chemistry of Portland Cement*, Reinhold Publishing Corp., 1955,

3. Taylor, H. F. W., *The Chemistry of Cements*, Academic Press, Vol. I, 1964.
4. *Design and Control of Concrete Mixtures*, Portland Cement Association, 1968.
5. Blanks, R. D. and Kennedy, H. L., *The Technology of Cement and Concrete*, John Wiley & Sons, Inc., 1963.
6. Price, W. H., "Grading and Surface Area," *ASTM STP* 169A, pp. 404–414, 1966.
7. Davis, H. S., "Effects of High-Temperature Exposure on Concrete," *ASTM Materials Research and Standards*, Vol. 7, No. 10, pp. 452–459, October 1967.
8. Lewis, D. H., "Lightweight Concrete and Aggregates," *ASTM STP* 169A, pp. 359–375, 1966.
9. "Guide for Structural Lightweight Aggregate Concrete," Report of ACI Committee 213, *ACI Journal*, Proceedings Vol. 64, No. 7, pp. 433–469, August 1967.
10. Polivka, Milos, "Radiation Effects and Shielding," *ASTM STP* 169A, pp. 298–308, 1966.
11. McCoy, W. J., "Mixing and Curing Water for Concrete," *ASTM STP* 169A, pp. 515–521, 1966.
12. Collins, W. D., "Typical Water Analysis for Classification with Reference to Industrial Use," *Proceedings ASTM*, Vol. 44, pp. 1057–1060, 1944.
13. "Requirement of Mixing Water for Concrete," *Indian Concrete Journal*, pp. 95–113, 1963.
14. Steinour, H. H., "Concrete Mix Water—How Impure Can It Be?," *Portland Cement Association Journal*, Vol. 2, No. 3, pp. 32–50, September 1960.
15. Halstead, W. J. and Chaiken, B., "Chemical Analysis and Sources of Air-Entrained Admixtures for Concrete," *Public Roads*, Vol. 27, No. 12, pp. 268–278, 1954.
16. Klieger, P., "Air-Entraining Admixtures," *ASTM STP* 169A, pp. 530–542, 1966.
17. Higginson, E. C., "Mineral Admixtures," *ASTM STP* 169A, pp. 543–555, 1966.
18. "Admixtures for Concrete," ACI Committee 212, *ACI Journal*, Proceedings Vol. 60, No. 11, pp. 1481–1524, November 1963.
19. Powers, T. C., *Properties of Fresh Concrete*, John Wiley & Sons, Inc., 1968.
20. Vollick, C. A., "Uniformity and Workability," *ASTM STP* 169A, pp. 73–89, 1966.
21. Kelly, T. M., "Setting Time," *ASTM STP* 169A, pp. 102–115, 1966.
22. Vollick, C. A., "Effects of Revibrating Concrete," *ACI Journal*, Proceedings Vol. 54, No. 9, pp. 721–732, March 1958.
23. "Recommended Practice for Selecting Proportions for Normal Weight Concrete," ACI Committee 211, *ACI Journal*, Proceedings Vol. 66, No. 8, pp. 612–628, August 1969.
24. "Recommended Practice for Selecting Proportions for Structural Lightweight Concrete," ACI Committee 211, *ACI Journal*, Proceedings Vol. 65, No. 1, pp. 1–19, January 1968.

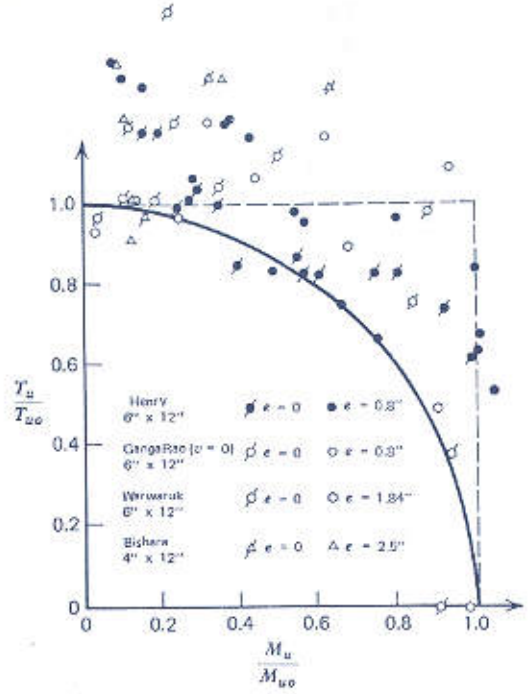

FIGURE 6.52. Interaction diagram for rectangular prestressed concrete members with and without eccentricity.

6.12.4 Design Criteria

The 1971 ACI Code provides, for the first time, the design procedures for reinforced concrete members subject to torsion. These procedures are not applicable to prestressed concrete members.

Although the general behavior of prestressed concrete members subject to torsion is now understood, not enough quantified information is available.[34] Active research in many areas is in progress at various laboratories and the development of appropriate design criteria by the ACI Committee 438, Torsion, is expected in the near future.

REFERENCES

1. Magura, D. D., Sozen, M. A., and Siess, C. P., "A Study of Stress Relaxation in Prestressing Reinforcement," PCI Journal, Vol. 9, No. 2, April 1964.

2. Yamazaki, J., Kattula, B. T., and Mattock, A. H., "A Comparison of the Behavior of Post-Tensioned Prestressed Concrete Beams with and without Bond," Structures & Mechanics Report SM69–3, Department of Civil Engineering, University of Washington, Seattle, Washington, December 1969.
3. "Tentative Recommendations for Concrete Members Prestressed with Unbonded Tendons," *ACI Journal*, Vol. 66, No. 2. February 1969. pp. 81–86.
4. MacGregor, J. G., Sozen, M. A. and Seiss, C. P., "Strength and Behavior of Prestressed Concrete Beams with Web Reinforcement," *Structural Research Series No. 201*, University of Illinois, August 1960.
5. Corley, W. G., Sozen, M. A., Siess, C. P., "Time-Dependent Deflections of Prestressed Concrete Beams," Highway Research Board Bulletin 307, 1961.
6. Guyon, Y., "The Strength of Statically Indeterminate Prestressed Concrete Structures," *Proceedings* of Symposium on the Strength of Concrete Structures, London, England, May 1956.
7. Baker, A. L. L., "Design of Reinforced and Prestressed Concrete Frames," Concrete Publications, London, England, 1956. Also, "Ultimate Load Design of Concrete Structures," Research Committee Report, *Proceedings* of Institute of Civil Engineers, February 1962, pp. 399–442.
8. Bennett, E. W., Cooke, N., and Nanghton, L. P., "Deformation of Continuous Prestressed Concrete Beams and its Effect on the Ultimate Load," *Proceedings* of Institution of Civil Engineers, London, May 1967, pp. 57–74.
9. Lin, T. Y., and Thornton, Keith, "Secondary Moment and Moment Redistribution in Continuous Prestressed Concrete Beams," *PCI Journal*, Vol. 17, No. 1, Jan.–Feb. 1972, pp. 1–20.
10. Lin, T. Y., "Load Balancing Method for Design and Analysis of Prestressed Concrete Structures," *ACI Journal*, Vol. 60, No. 6, June 1963, pp. 719–742.
11. Rozvany, G. I. N., and Hampson, A. J. K., "Optimum Design of Prestressed Flat Plates," *ACI Journal*, Vol. 66, No. 8, August 1963, pp. 1065–1082.
12. Brotchie, J. F., and Russell, J. J., "Flat Plate Structures," *ACI Journal*, Vol. 61, No. 8, August 1964, pp. 959–996.
13. Parme, A. L., "Prestressing Flat Plates," *PCI Journal*, Vol. 13, No. 6, December 1968, pp. 14–32.
14. Power, C. A., "Prestressed Flat Slabs," N.Z. *Engineering* (Wellington), Vol. 21, No. 8, August, 15, 1966, pp. 321–327.
15. Commentary on Building Code Requirements for Reinforced Concrete (ACI 318–71), American Concrete Institute, 1971.
16. Scordelis, A., Lin, T. Y., and May, H. R., "Shearing Strength of Prestressed Lift Slabs," *ACI Journal*, Vol. 55, No. 4, Oct. 1958, pp. 485–506.
17. Grow, J. B., and Vanderbilt, M. D., "Shear Strength of Prestressed Lightweight Aggregates Concrete Flat Plates," *PCI Journal*, Vol. 12, No. 4, August 1967, pp. 18–28.
18. Mirza, J. F., Zia, P., and Bhargava, J. R., "Static and Fatigue Strengths of Beams Containing Prestressed Concrete Tension Elements," Final Report, Project ERD-110-69-2, Highway Research Program, North Carolina State University, Raleigh, N.C.
19. Zia, P., Andrew, J. R., and Chawla, M. S., "Prestressed Concrete Columns under Concentric and Eccentric Loadings," Final Report, Project ERD-110-68-3, Highway Research Program, North Carolina State University, Raleigh, N.C., July 1969.
20. Zia, P., and Guillermo, E. C., "Combined Bending and Axial Load in Prestressed Concrete Columns," *PCI Journal*, Vol. 12, No. 3, June 1967, pp. 52–59.

21. Laszlo, G., Discussion on "Combined Bending and Axial Load in Prestressed Concrete Columns," by P. Zia and E. C. Guillermo, *PCI Journal*, Vol. 12, No. 6, December 1967, pp. 77–84.
22. Tentative Recommendations for the Design of Prestressed Concrete Columns," *PCI Journal*, Vol. 13, No. 5, October 1968, pp. 1–11.
23. Zia, P., and Moreadith, F. L., Ultimate Load Capacity of Prestressed Concrete Columns," *ACI Journal*, Vol. 63, No. 7, July 1966, pp. 767–788.
24. Wilhelm, W. J., and Zia, P., "Effects of Creep and Shrinkage on Prestressed Concrete Columns," *Journal of the Structural Division*, ASCE, Vol. 96, No. ST10, October 1970, pp. 2103–2123.
25. Zia, P., "Torsional Strength of Prestressed Concrete Members," *ACI Journal*, Vol. 32, No. 10, April 1961, pp. 1337–1359.
26. Bishara, A., and Peir, J. C., "Reinforced Concrete Rectangular Columns in Torsion," *Journal of Structural Division*, ASCE, Vol. 94, No. ST12, December 1968, pp. 2913–2933.
27. Hsu, Thomas T. C., "Torsion of Structural Concrete—Uniformly Prestressed Rectangular Members without Web Reinforcement," *PCI Journal*, Vol. 13, No. 2, April 1968, pp. 34–44.
28. Hsu, Thomas T. C., and Kemp, E. L., "Background and Practical Application of Tentative Design Criteria for Torsion," *ACI Journal*, Vol. 66, No. 1, January 1969, pp. 12–23.
29. GangaRao, H. V. S., and Zia, P., "Rectangular Prestressed Concrete Beams in Torsion and Bending," *Journal of Structural Division*, ASCE, Vol. 9., No. ST1, January 1973, pp. 183–198.
30. Gersch, B. C., and Moore, W. H., "Flexure, Shear and Torsion Tests on Prestressed Concrete I-Beams," *Bulletin* 339, Highway Research Board, 1962, pp. 43–66.
31. Bishara, A., "Prestressed Concrete Beams under Combined Torsion, Bending and Shear," *ACI Journal*, Vol. 66, No. 7, July 1969, pp. 525–538.
32. Gausel, E., "Ultimate Strength of Prestressed I-Beams under Combined Torsion, Bending and Shear," *ACI Journal*, Vol. 67, No. 9, pp. 675–678.
33. Henry, R. L., "Behavior of Rectangular Prestressed Concrete Beams under Combined Torsion, Bending and Shear," PhD Dissertation, North Carolina State University, Raleigh, N.C., January 1971.
34. Zia, P., "What Do We Know About Torsion in Concrete Members?," *Journal of the Structural Division*, ASCE, Vol. 96, No. ST6, June 1970, pp. 1185–1199.

7

Safety and Structural Design

E. ROSENBLUETH

7.1 SCOPE OF THIS CHAPTER

The first six chapters have provided bases for computing the strength of structural members and structures and predicting their deformability and the likelihood of their cracking. In this chapter the reader will find criteria for choosing load factors and factors of safety and a guide to adequate detailing. Of necessity the chapter delves into the loads and other actions* that may affect structures and into criteria of survival and serviceability. The subject matter of the chapter differs from that found in codes. Design charts are not presented so as not to tie the book to a particular legal document.

After stating the purpose of structural design, we discuss the place of the theory of probabilities in this branch of civil engineering. It is shown that a rational approach to design must rest on a quantitative evaluation of costs and of the consequences of failure as well as on the probability distributions of the parameters that govern structural behavior and safety. Since knowledge of the frequency distribution of a variable, coupled with the postulation of a stochastic model of the process that gives rise to that variable, forms the basis for calculating its probability distribution, these questions are treated with some detail for the variables that act on structures (loads, imposed deformations, wear, etc.) and for those which govern the responses of reinforced concrete structures (strength of concrete, yield-point stress of reinforcement, capacity in diagonal tension, etc.). Next we summarize a formal

* The term *action* is used here as a synonym of disturbance and of the French *sollicitation*.

theory of optimization and present some approximations to it, such as that of design for a fixed probability of failure. Emphasis is laid then on such matters as structural details and the ductility of various types of structural members under various conditions of stressing; their influence on design as an optimization process is discussed qualitatively. The chapter also touches upon the main considerations in strengthening damaged structures.

Here more questions are asked than are answered, but the reader will find a bibliography leading him to better approaches to design than those which have become conventional. In particular, he will benefit by acquiring or increasing his proficiency with mathematical tools in probabilities, statistics, and decision theory through the study of a work such as Reference 1.

Except where explicit reference is made to prestressed, lightweight, or other special types of concrete, specific values quoted apply directly to normal-weight, ordinary reinforced concrete. Remarks of a general nature apply to all types of concrete and methods of construction.

7.2 PURPOSE OF STRUCTURAL DESIGN

The purpose of structural design is to produce optimum structures. This tautology has far reaching implications.

Strength and disturbances that enter design are random variables and it is impossible to set a lower positive limit to strength and an upper limit to most disturbances. As a consequence the probability that any structure will fail during a given period of time is larger than some finite quantity. It follows that every structure will surely fail unless it is purposely demolished, so the purpose of structural design is not to prevent failures. A look at existing structures and ruins indicates that the mean natural lifespan of structures of most types is of the order of centuries and hence sufficiently short that the certainty of failure must color design.

Optimization should include consideration of initial cost; of the benefits to be derived from the structure while it survives; of the present values of maintenance, damage, and failure costs; and of the probabilities that the structure suffer damage or failure as a function of time. In turn the consequences of damage and failure involve such intangibles as loss of human lives and loss of prestige, while the benefits include other intangibles, such as esthetic values, and probabilities of damage or failure depend on the probability distributions of strength and of disturbances, both of them as functions of time.

There is a widespread opposition to explicit treatments of the possibility and consequences of failure. Many civil engineers are reluctant to admit that this possibility exists. They are also reluctant to place money values on matters that have traditionally been regarded as intangibles. Also, the adoption of

new methods meets with resistance because it demands a special effort. Yet we have seen that structural failure is not only a possibility but, in a sense, a certainty. Assigning money values to potential consequences of failure is actually done implicitly by every structural engineer whenever he makes a decision. If, say, the value of a human life were considered infinitely large, it would be impossible to build sufficiently safe structures.

The difficulties involved in the adoption of new methods are a more valid reason for postponing that adoption. Sufficiently practical methods have not been developed to deal, within the frame of explicit optimization, with every question arising in structural design. Now, a completely rational approach to decision making must take into account the costs of acquiring information and of carrying out the analysis, and if the stage of optimization methods is such that at times they exact too high a price from the designer's time or budget, he should resort to other, more traditional methods. There is no doubt that the time is ripe for applying explicit optimization to choose load factors and the like for building codes—it may be, too, for the design of outstanding structures and large groups of nominally identical structural elements or buildings, and eventually smaller jobs may merit this approach. Meanwhile an informal optimization should provide useful insight in the design of all structures.

7.3 RELIABILITY

A rational approach to design requires computing the probabilities that a structure undergo given degrees of damage and the probability that it suffer failure. Generically these quantities are referred to as *probabilities of failure*. Their complements, or probabilities of survival, are called *reliabilities*. For the sake of brevity, suppose that a structure has only two possibilities: survival or failure. Its reliability is $R = 1 - F$, where F is the probability of failure.

For most structures it is important to recognize that R varies with time. $R(t)$ is known as the *reliability function* and it is equal to the probability that the structure has survived up to time t. $F(t)$ is the *failure probability function* or probability distribution function of the time to failure. And $f(t) = dF/dt$ is the corresponding *probability density function*.

Usually, survival of a structure depends on that of its components. In a sense this is true even when "failure" is defined as excessive settlement or tilt, for example, for then the structure is treated as though it had a single component. The simplest criterion of component survival or acceptance is $X_i > S_i$, where X_i is a *resistance function* of the ith component and S_i is the corresponding effect of the disturbance (load, settlement, etc.). X_i may be a resisting moment or shear, an acceptable tilt or crack width, etc. S_i is often

known as *forcing function*. According to this criterion, if we drop subscript i, the reliability of the ith component is

$$R = \int_0^\infty [1 - P_X(u)]p_S(u)\,du \tag{7.1}$$

$$= \int_0^\infty P_S(u)p_X(u)\,du \tag{7.2}$$

where P_S and P_X are the probability distribution functions of S and X, respectively, and p_S and p_X are the corresponding probability density functions. Clearly, we must first evaluate these probability distributions. Equations (7.1) and (7.2) hold when S cannot be negative. They have been generalized to situations in which S can be either positive or negative.[2]

The stochastic models of many loading and failure processes lead to relatively simple and common probability distributions of the loading and resistance functions. Failure probabilities are available in the form of charts for cases in which S and X are independent variables with normal, truncated normal, and extreme distributions (see Reference 7.3, for example). Such distributions, however, are directly applicable only when they have deterministic parameters. As we shall see, this is not always a valid approximation. Under more general conditions Eqs. (7.1) and (7.2) must be evaluated numerically.

Calculation of R is particularly simple when both X and S are independent variables and they are assigned normal or lognormal distributions. Let

$$X \overset{d}{=} \mathcal{N}(\bar{X}, \sigma_X)$$

signify "The distribution of X is normal with expectation $\bar{X}$ and standard deviation σ_X," and let

$$S \overset{d}{=} \mathcal{N}(\bar{S}, \sigma_S)$$

Now, Eq. (7.1) can be written as

$$R = P(X - S > 0)$$

and

$$P_{X-S} \overset{d}{=} \mathcal{N}(\bar{X} - \bar{S}, \sqrt{\sigma_S^2 + \sigma_X^2})$$

It follows that

$$R = \Phi\left(\frac{\bar{X} - \bar{S}}{\sqrt{\sigma_S^2 + \sigma_X^2}}\right) \tag{7.3}$$

where Φ is the standardized normal distribution (with zero mean and unit standard deviation):

$$\Phi \overset{d}{=} \mathcal{N}(0, 1)$$

It has been profusely tabulated (see Reference 7.1 for brief tables of the standardized normal, t, and gamma distributions, and for a comprehensive list of tables of common probability distributions).

For example, if a beam having an expected resisting moment of 17 ton m with a standard deviation of 2 ton m is subjected to a load causing a bending moment whose expectation is 7 ton m and whose standard deviation is 1.5 ton m, its reliability is

$$\Phi\left(\frac{17 - 7}{\sqrt{1.5^2 + 2^2}}\right) = \Phi(4.0) = 1 - 3.17 \times 10^{-5}$$

from tables of the normal distribution, and so its probability of failure is 3.17×10^{-5}.

Now let X and S have lognormal distributions:

$$\ln X \overset{d}{=} \mathcal{N}(\ln \tilde{X}, \sigma_{\ln X})$$

$$\ln S \overset{d}{=} \mathcal{N}(\ln \tilde{S}, \sigma_{\ln S})$$

where ln is the natural logarithm, and $\tilde{X}$ and $\tilde{S}$ are the medians of X and S. It is convenient to write

$$R = P\left(\frac{X}{S} > 1\right) = P\left(\ln \frac{X}{S} > 0\right)$$

and to notice that

$$P_{\ln X/S} \overset{d}{=} \mathcal{N}\left(\frac{\ln \tilde{X}}{\tilde{S}}, \sqrt{\sigma_{\ln S}^2 + \sigma_{\ln X}^2}\right)$$

so that

$$R = \Phi\left(\frac{\ln \tilde{X}/\tilde{S}}{\sqrt{\sigma_{\ln S}^2 + \sigma_{\ln X}^2}}\right) \tag{7.4}$$

In order to set up an example comparable to the one for normal distributions, we notice that, when X has lognormal distribution,[1]

$$\sigma_{\ln X}^2 = \ln(1 + c_X^2) \tag{7.5}$$

where $c_X = \sigma_X/\bar{X}$ is the coefficient of variation of X. Accordingly, assume that $\tilde{X} = 17$ ton m, $\tilde{S} = 10$ ton m,

$$\sigma_{\ln X}^2 = \ln(1 + 2^2/17^2) = 0.0137$$

and

$$\sigma_{\ln S}^2 = \ln(1 + 1.5^2/7^2) = 0.0449$$

Substituting in Eq. (7.3), we find

$$R = \Phi(3.664) = 1 - 1.25 \times 10^{-4}$$

from tables of Φ.

As is usual we find that the probability of failure is quite sensitive to the types of the probability distributions of S and X. This is particularly true for very small probabilities of failure.[8]

Equations (7.1) and (7.2) are directly applicable to the calculation of the reliability of structural components that can fail either upon completion of the structure or not at all. Consider now a component having a constant resistance function and subjected to a stochastic loading function.* If the foregoing criterion of failure applies we can write

$$R(t) = \int_0^\infty P(\max_t S \leq u) p_X(u)\, du \tag{7.6}$$

If we know that there will be N independent load applications we may use the variable N instead of t. Equation (7.6) becomes

$$R(N) = \int_0^\infty P_S{}^N(u) p_X(u)\, du \tag{7.7}$$

This expression follows immediately from Eq. (7.6) because the probability distribution function of the largest of N specimens, all having the same probability distribution function P_S, is the Nth power of P_S.[1] Equation (7.7) has been derived using a different approach[4] and extended to the case when S may be either positive or negative.[2]

The probability that failure occurs at or before the Nth load application is $F(N) = 1 - R(N)$. The probability of failure at precisely the Nth application is $F(N) - F(N-1)$. And the probability of failure at the Nth application, given that the structure has not failed earlier, is

$$\mu(N) = \frac{F(N) - F(N-1)}{R(N-1)} \tag{7.8}$$

μ is known as the *risk*, or *hazard function*, or the *failure rate*. It has been shown that, under the foregoing assumptions, μ is a nonincreasing function of N, and $\mu(N)$ has been plotted for a number of specific distributions of S and X.[2]

When S is a continuous function of time, the absolute probability that failure occur in the interval between t and $t + dt$ is $f(t)\, dt$. The probability that it occur in this interval, given that it has not taken place earlier, is $\mu(t)\, dt$, and

$$\mu(t) = \frac{f(t)}{R(t)} \tag{7.9}$$

$$= -\frac{d}{dt} \ln R \tag{7.10}$$

* We reserve the term *stochastic* for random functions of time.

The reciprocal of μ is the (mean) *return period* of failure. When X is a deterministic constant and S is a generalized Poisson process, μ is constant. (This idealization is useful in earthquake and windresistant design.) This case and those in which μ is a monotone function of time have received the most attention in the theory of reliability.[5]

Typically, a risk function that decreases with time is associated with a situation in which the most probable cause of failure is due to faulty design; a constant risk function, with occasional overloading; and a risk function that increases with time is associated with cumulative damage. Later in this chapter we shall consider more elaborate criteria of failure as well as the problem of calculating the reliability of a structure from those of its components.

7.4 PROBABILITY DISTRIBUTIONS OF DESIGN PARAMETERS

It is clear that rational design of structures demands a probabilistic treatment of the actions that operate on structures and of the structural characteristics that determine response to those actions. To calculate the corresponding distributions we have two sources of information: those which do not depend on observations of the variable in question, and statistical information on that variable.

Prior information is derived from a stochastic model, in a wide sense of the word; that is, we form a conceptual model of the process that gives rise to the variable of interest and say that the model is stochastic when it involves one or more time-dependent random variables. The model may be quite simple and consist merely of a comparison with other phenomena about which experience provides an idea of the distributions in question, or it may be quite involved.

The adoption of a single model to explain a phenomenon is not always satisfactory. Two or more qualitatively different models may have to be considered, each with a different prior probability of being applicable. The distributions of the pertinent variables are then obtained by combining these probabilities with those derived from each model.

It is essential that the prior distribution—the initial guess—be already an educated one, based on the most reasonable models possible for the phenomenon in question.[6] Stochastic models have been proposed for a variety of problems in structural behavior, such as stresses in bridges, creep, and structural response to earthquakes, as well as for other phenomena of interest in civil engineering.[1,6]

When the amount of information is exceedingly meager, there is little advantage in attempting an explicit probabilistic treatment of design. A direct application of load or safety factors judged appropriate is just as

satisfactory.[7] Yet, the probabilistic approach tending toward optimization should be reflected in every stage of rational design, however qualitative may be this reflection.

Incorporation of the statistical data is achieved through *Bayes' theorem*, or formula, of the probabilities of hypotheses.[1,4,8] Indeed, the education of engineering judgment can be done in the quantitative framework of Bayes' theorem through an iterative process of successive incorporation of statistical data.[4] Let $P(A \mid H_i)$ denote the probability of event A if hypothesis H_i were true. We obtain the probability that the ith hypothesis be true, given that event A has occurred, using Bayes' formula:

$$P(H_i \mid A) = \frac{P(A \mid H_i)P(H_i)}{P(A)} \tag{7.11}$$

$P(H_i)$ is the prior probability, A the statistical information, $P(A)$ the probability that A occur independently of which hypothesis were true, and $P(H_i \mid A)$ the posterior probability that H_i be true.

We are interested in finding posterior distributions with uncertain parameters. Hypothesis H_i is the belief that one of the parameters of interest falls in the ith interval of its possible values. Incorporation of statistical data sharpens the distributions of the parameters.

It is important that the prior distributions cover all the possible values of the distribution parameters in an adequate manner, that is, that the priors be sufficiently *diffuse*.[1] It is also important that all conceivable conceptual models be adequately covered in the priors. Other than this, any subjective choice of the prior distribution of the parameters is theoretically acceptable. However, there are computational and theoretical reasons favoring the choice of *conjugate* distributions.[1,8] Given the form of the probability distribution of the variate in question, its parameters are said to have the corresponding conjugate distributions when they are defined by the sufficient statistics (expectations, modes, standard deviations, etc.) and the forms of the parameter distributions and of the posterior distribution of the variate do not change by the incorporation of additional data in Bayes' theorem. This in itself produces the computational advantages. The theoretical reason is of the type of Occam's razor; the incorporation of data should not change the form of the distributions, as it does not change the nature of the phenomenon under study; it could be argued that this would be true for any type of priors if they and the resulting posterior distributions were regarded as belonging to sufficiently rich forms of distributions, but the point is that the conjugates do this with the smallest number of statistics possible.

To give an example, suppose X has a normal distribution with unknown mean $\bar{X}$ but known standard deviation, σ_X. The conjugate distribution of $\bar{X}$

is normal. Its sufficient statistics are two of the following three quantities: $m' = E'(\bar{X})$, $s' = \sigma'(\bar{X})$, and n', where the prime is used to refer to the prior and n' is the size of a fictitious prior sample; n' plays the role of defining the weight we assign to the prior. The last two parameters are related through

$$s'^2 = \frac{\sigma_X^2}{n'} \tag{7.12}$$

Now let n observations of X have a mean m. The posterior expected value of $\bar{X}$ is[8]

$$m'' = \frac{m'n' + mn}{n' + n} \tag{7.13}$$

with variance

$$s''^2 = \frac{\sigma_X^2}{n' + n} \tag{7.14}$$

These expressions have been obtained by applying Eq. (7.11). The (Bayesian) posterior distribution of X is normal with expectation m'' and variance (square of the standard deviation) $s''^2 + \sigma_X^2$. In this case the "underlying" or "first-order" probability distribution, with known variance σ_X^2 and unknown mean $\bar{X}$, has the same form as the Bayesian distribution. The distribution of $\bar{X}$ and, under more general conditions, those of other parameters of the underlying distribution, are sometimes called "second-order" probabilities.

Some authors object to the use of second-order probabilities[3] and prefer to adopt modified parameters for the underlying distribution to describe the posterior distribution. This position cannot be defended on rational grounds. In general, the posterior (Bayesian) distribution of the variate has a different form from that of the underlying distribution. For example, when the distribution of X is normal with unknown mean and precision (reciprocal of the variance), the conjugate joint distribution of these parameters is the normal-gamma, and the marginal distribution of the mean is the t or Student distribution. This and other common distributions are treated in Reference 8.

As an example, suppose that the strength of standard cylinders of the concrete supplied by a premix company is assigned a lognormal distribution with known coefficient of variation of 15%, that the prior estimate of the expected strength is 250 kg/cm², and that $n' = 3$. According to Eq. (7.5), the variance of the logarithm of the strength is $\ln(1 + 0.15^2) = 0.02225$. We can find the prior expected logarithm of the strength from

$$E(Y) = \ln E(X) - \frac{\sigma_Y^2}{2} \tag{7.15}$$

where $Y = \ln X$ is normally distributed. This gives $\ln 250 - 0.02225/2 = 5.510$. Suppose now that ten specimens are tested, giving an average logarithm of the strength of 5.800. Applying Eqs. (7.13) and (7.14) we find $m'' = 5.733$ and $s''^2 = 0.00171$. Hence, the posterior (Bayesian) distribution of the logarithm of strength is normal with expectation 5.733 and variance $0.02225 + 0.00171 = 0.02396$. The posterior expected strength is found from Eq. (7.15):

$$\exp(5.733 + 0.02396/2) = 316 \text{ kg/cm}^2$$

Although the coefficient of variation of the underlying distribution of the cylinder strength is still 15.0%, we find from Eq. (7.5) that the coefficient of variation of the posterior distribution is 15.6%.

7.5 DEAD LOADS

There is a widespread belief that dead loads are ordinarily computed with a high degree of accuracy in civil engineering structures. The idea is unrealistic. The following examples substantiate this contention.

CASE 1. After its collapse it was found that the Quebec bridge had dead loads that exceeded the design values by 20 to 30%.[9]

CASE 2. Study of eight columns of a 48-story building gave actual dead loads of between 1.20 and 1.31 times their computed values.[10]

CASE 3. Actual weighing of representative samples of the floor and partitions in a 16-story apartment building having a reinforced concrete structure led to a recomputation of the average net contact pressure on the soil due to dead loads. It was found to be 1.7 ton/m² (0.35 ksf) greater than the computed value despite conscious errors on the safe side introduced in the original computations, such as counting twice the dead weight at intersections of structural members.[11]

CASE 4. Pressure cells were placed under three nominally identical apartment buildings done by a single contractor.[11] Average cell readings seemed trustworthy and measured dead loads 0.85 to 1.16 times the average computed values. The criteria of computation were the same as for Case 3.

CASE 5. Careful recomputation of dead loads in one office building led to the conclusion that all columns were overloaded and one had three times the design dead load.

The most common reasons for excess of actual dead load over its computed values are

1. Actual thicknesses almost systematically exceed their nominal values.

This is so because it is simpler to add than to remove material when compensating for inaccuracies. A series of measurements in reinforced concrete slabs in Sweden[12] showed that the difference between actual and nominal total depths had a mean value of 0.6 cm (0.24 in.) and a standard deviation of 0.9 cm (0.35 in.). The layer of grout that is often used before placing tile floors is intended to compensate for irregularities due to surface finish, deflections, and tilting; these factors normally lead to increased thicknesses. A five-fold increase with respect to the specified thickness has been observed in one instance, and, even with good workmanship, 1 to 2 cm (0.4 to 0.8 in.) increases in average thicknesses over a specified 4 cm (1.6 in.) are not uncommon. Similar remarks apply to plaster.

2. The designer is almost sure to neglect minor portions of structural and of nonstructural elements. A typical example is the mortar that falls into the holes of hollow tiles and blocks while erecting a wall. In some cases this factor has contributed about 40 kg/m² (8 psf) in walls and partitions having nominal thicknesses of 12 cm (4.7 in.).

3. As an asset to their products, some manufacturers claim smaller unit weights than the actual averages, or unit weights that are only attained in oven-dry samples.

4. Major discrepancies are usually due to architectural changes. (This was the chief contributing cause in Case 5.)

Dead loads smaller than computed values also occur, although less frequently.

The distribution functions of the unit weights of a large variety of natural and artificial construction materials have been found to be nearly normal.[13] Their coefficients of variation range from less than 1%, for concrete manufactured with aggregates from a common source, to 16% for volcanic tuffs. The unit weights of wood and other porous materials are very sensitive to moisture content.

If thicknesses and unit weights are taken to be independent of each other and to have normal distributions, the weight of any given element will not be normally distributed. Still, the distribution of the discrepancy between the computed and actual sum of the weights of many elements will approach normality. Its expectation will depend on the criteria used for dead load computation; values between 10%[14] and 25%[15] of the nominal dead load have been suggested.

There are cases when a deficiency in dead load may endanger the serviceability or the stability of a structure. Then, if we design for a fixed probability of failure (this criterion is discussed below), a double revision is in order, one with a dead load greater than expected and one with a smaller dead load. But rather than fixed percentage increases and decreases, it is advisable to analyze for *characteristic* values, that is, values that depend on

the distribution function of dead load, such as the 95% confidence limits. The coefficient of variation of dead loads can be estimated from published data on linear dimensions and unit weights.

It would be impractical to consider alternately high and low dead loads in continuous beams and in similar portions of structures; such refinements are hardly justified since relatively small variations are to be expected when the materials proceed from the same sources and construction practices are essentially uniform. Such variations can be conveniently dealt with by treating part of the dead load as an additional live load.

In the foregoing paragraphs we have given no attention to possible large deviations in dead load due to changes in architectural project or to errors in computations or in construction. Possibility of these severe and unpredictable modifications in dead load calls for provisions that will lead to ample warning of impending failure rather than for increased structural capacity. The comment reflects consideration that a structural design leading to negligible probabilities of failure under extreme deviations from the expected values of the variables is clearly too conservative, but that complete disregard of those possibilities, although often legally acceptable, is unrealistically unsafe. Providing for very ductile types of failure, coupled, if practicable, with other signs of danger, does not normally increase the cost of a structure in a marked degree; yet it invites safety measures to be taken in case of extreme overload.

7.6 LIVE LOADS IN OFFICE AND APARTMENT BUILDINGS

Live loads in office floors and in living quarters (dwellings, apartment buildings, hospitals, and jails) have received some attention. From available data[12,15–17] the following two design rules have been derived,[18,19] consistent with the criterion of design for a fixed probability of failure.

1. Where the possibility of social gatherings involving dancing is disregarded,

$$w_{dl} = w_0(1 + cfA^{-1/2}) \tag{7.16}$$

where w_{dl} is the design live load per unit area, w_0 is a live load per unit area that depends on the type of occupancy, c is a coefficient that depends on the shape of the influence surface (if we use a dash to denote mean value and let z stand for the ordinates of the influence surface, we may write $c^2 = \bar{z}^2/\overline{z^2}$), f is a coefficient having units of length, that depends on the type of occupancy and on the allowable probability of failure, and A is the area of surface where the influence ordinates are of appreciable magnitude.

2. Where the possibility of dancing is taken into consideration, w_{dl} should not be less than the value given by Eq. (7.16) nor less than some live load per unit area, say w_2, independent of A.

The influence surface on whose shape c depends is the one which corresponds to the generalized force (bending moment, shear, etc.) being computed and which serves as criterion for deciding on the safety of the structure. If A is taken as the tributary area in the usual sense, c is found to lie between 1.0 and 1.2 for most cases of practical interest; it is therefore proper to assume $c = 1.2$. This conclusion is not limited to structures having influence surfaces—hence structures of linear behavior—but applies equally to ductile structures that admit analysis through limit design.[19]

When computing the load on structural members that support more than one floor, A is the sum of the tributary areas of all the floors that gravitate on the member in question. Thus Eq. (7.16) replaces the arbitrary percentage reductions that abound in building codes, for the computation of axial forces due to live load in columns.

Whenever a less favorable condition of loading is associated with the absence of live load over part of the area, design should be checked against that condition, since the probability of zero live load during any period of time over practically any area is much higher than the probability that a large load be exceeded in that area at least once during the same period. This condition arises, for example, when carrying out an elastic analysis if the ordinates of the influence surface for the generalized stress in question are positive over some area A_1 and negative over A_2. In this case A should be replaced first with A_1 in Eq. (7.16), and the design revised for a generalized stress of opposite sign after replacing A with A_2. Similar criteria apply to limit design and to cases where $w_{dl} = w_l$ is to be assumed uniform.

The following two examples will illustrate some consequences of the design rules that we have set forth.[19] Consider first a cantilever beam carrying live load over a strip of width b at the section that lies a distance x from the free end [Fig. 7.1(a)]. From the definition of x and the shape of the influence surface [Fig. 7.1(b)] we find for this parameter the value $c = 2/\sqrt{3}$. Consequently, the bending moment due to live load is given by the conventional term, $w_0bx^2/2$, plus a term proportional to f: $w_0fx^2/2\sqrt{b/3}$. Both are shown in Fig. 7.1(c) at a scale such that the maximum bending moments from both terms are equal for purposes of comparison.

For the shear at any section we have the influence surface in Fig. 7.1(d), whence $c = 1$, and the shear again contains two terms:

$$V = w_0bx + w_0f\sqrt{bx}$$

[Fig. 7.1(e)]. We see that the choice of an equivalent uniform live load that would be adequate at the fixed end would underestimate bending moments

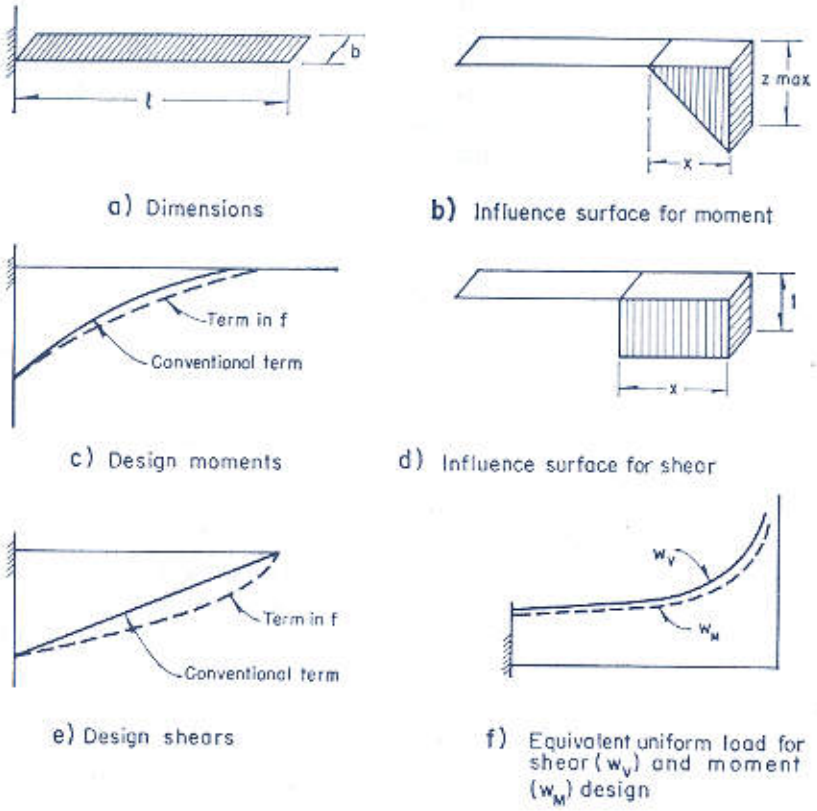

FIGURE 7.1. Cantilever beam.

and shears at all other sections [Fig. 7.1(f)]. (Rather than the exact values 1.0 and $2/\sqrt{3}$ for c in these examples, we could have used the suggested approximation $c = 1.2$ without introducing excessive errors.)

Figure 7.2 displays the corresponding results for a simply supported beam carrying a strip on which live load may act. Shear envelopes of opposite signs are obtained by considering alternately only positive and only negative values of the ordinates in the corresponding influence surfaces. Choice of a single equivalent uniform load for bending moment is possible in this instance in such a way that moments at all sections are correctly predicted. This same uniform load would give the correct maximum shears but would underestimate the shear at all interior sections.

The foregoing theory of live load is based on three simplifying assumptions: that live load is the only random variable; that design is based on a constant "allowable" probability of failure; and that this probability may be taken

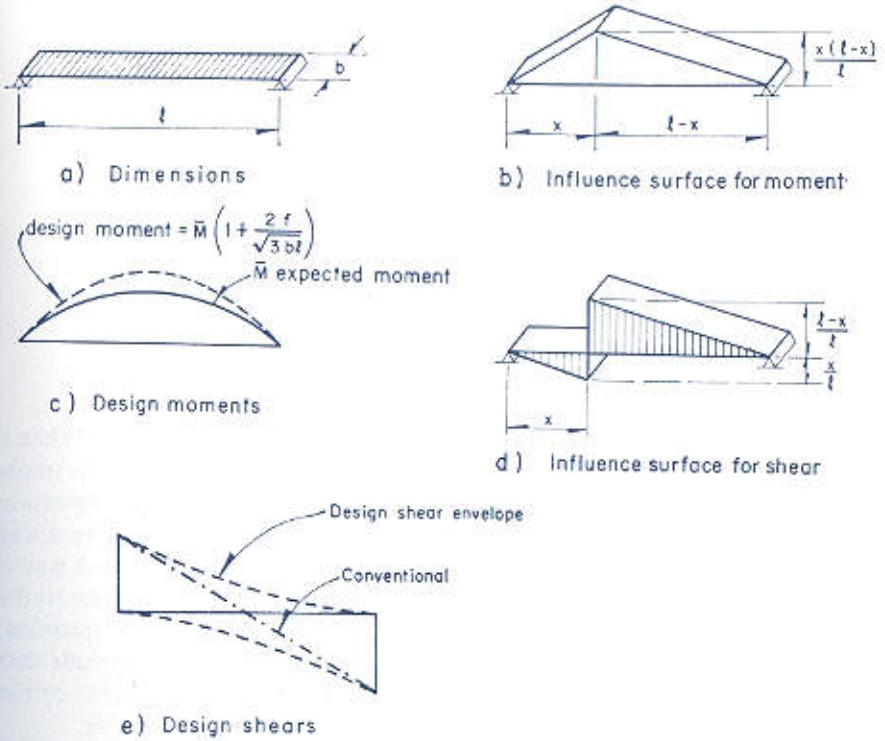

FIGURE 7.2. Simply supported beam.

equal to the lowest among those associated with all possible modes of failure (each mode involves either that a generalized force or deformation exceeds some critical value or that collapse occurs through the formation of some plastic-hinge mechanism). Despite these approximations, the theory improves considerably over the conventional approach while giving rise to manageable computations.

The matter of load distribution along beams that carry two-way slabs is closely related to the dependence of the design live load on tributary area. The distribution of dead load acting on a beam depends on the design of the slab panels carried by the beam. For the sake of simplicity let us suppose that a rectangular slab panel has been designed following Hillerborg's method. According to it the load at every point is split in any reasonable manner in the two directions parallel to the reinforcement. Suppose that the panel is divided as is customary for computing the total load carried by the beams (Fig. 7.3) and that all the load that acts on the triangles thus defined is assumed to be carried in the direction parallel to the panel's longer sides, while the load on

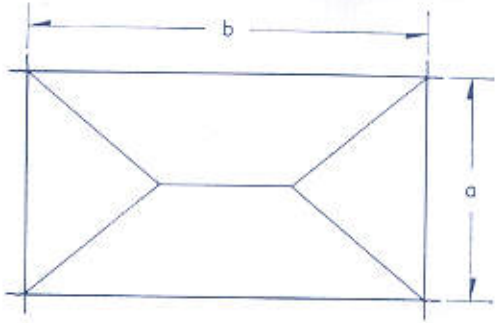

FIGURE 7.3. Division of a rectangular slab panel.

the trapezoids is carried in the direction parallel to the shorter sides. When a uniform load acts on the entire panel, the vertical load per unit length transferred from the slab to the supporting beams will vary precisely in proportion to the ordinates of the triangles and trapezoids in the figure. The resulting shear and moment diagrams are compared in Fig. 7.4 with those which would be produced by uniformly distributed loads per unit length giving rise to the same maximum shears and moments as the nonuniform loads in question. Comparing with the effects of uniformly distributed loads, we conclude that the shapes of the bending moment diagrams are not seriously affected by the distribution of loads but the shear diagram is made more unfavorable.

As we saw in connection with a uniform beam carrying live load over a rectangular strip, away from the supports the shear envelopes have ordinates that may greatly exceed those for the same total but uniformly distributed load. Combining both factors we conclude that, if conventional design adequately covers shear capacity near the supports, it leaves the beams underdesigned against shear away from these sections, especially when the ratio of live to dead load is high. It is advisable, then, to adopt a pair of shear envelopes that are more conservative than those in Fig. 7.2 and more than the diagram in Fig. 7.4. Those in Fig. 7.5 almost surely cover the worst conditions, whether the beams are statically determinate or continuous. To draw the envelope for positive shearing force, assume that the value at the left-hand support is constant over a length equal to one-sixth of the short span, after which section it varies linearly to the highest point at the right-hand support. The envelope for negative shearing force is obtained in a similar manner. Whether the envelopes we adopt for design in any specific case lie closer to those in Fig. 7.5 or to the shear diagram for dead load may be made to depend on the ratio of live to dead load, with w_{al} computed for the tributary area of the beam in question.

Another matter requiring attention in design of two-way slabs when the

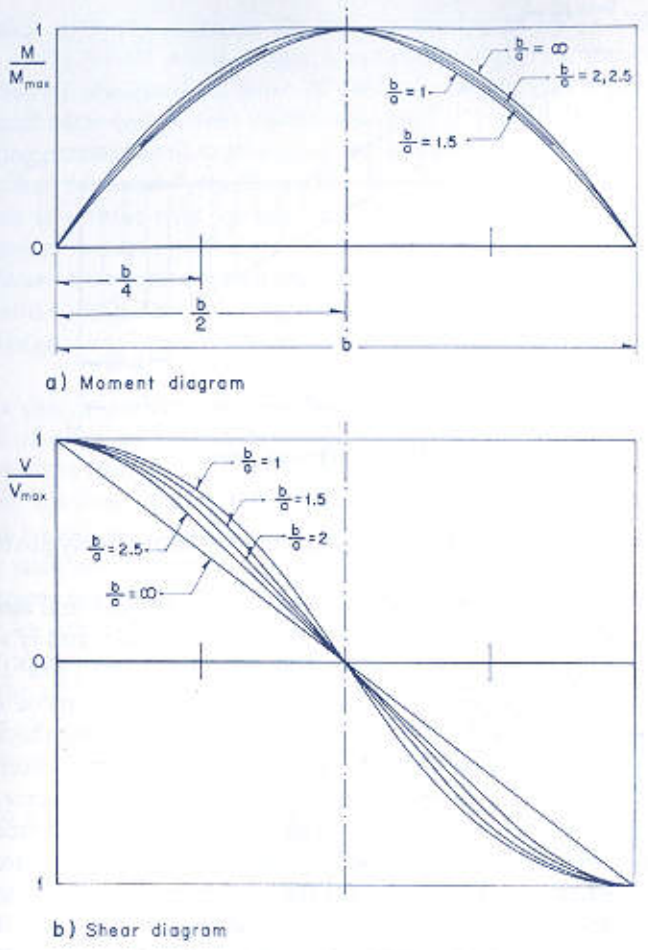

FIGURE 7.4. Shear and moment diagrams for the beam along the long span of a slab panel.

ratio of live to dead load is high concerns the possibility of negative bending moments near the center of a panel. The question arises in elongated panels having a large ratio of w_{al} (evaluated for an area of the order of the panel's short side squared) to dead load per unit area.

Some reduction in live load is justified when designing to resist earthquake, since there is a negligible probability that a strong earthquake will occur simultaneously with an exceptionally high live load. The same applies to wind resistant design. A reduction is also in order when computing pressures

2

Reinforcing Steel

John F. McDermott

2.1 INTRODUCTION

In a structural capacity, steel reinforcing bars and wire are utilized in concrete either as prestressed steel or as steel that is not purposely prestressed before service loadings are applied. The present chapter is confined to a discussion of nonprestressed steel, which is generally called "reinforcing steel." American Society of Testing Materials (ASTM) specifications cover the following seven types of American-produced reinforcing steel.[1]* ASTM designations A-82 and A-496 specify cold-drawn steel wire (smooth wire) and deformed steel wire, respectively, and A-185 and A-497 specify the corresponding welded fabric produced with these wires. American reinforcing bars are all hot-rolled; A-615 specifies deformed reinforcing bars produced from new billet steel (the major tonnage of reinforcing bars), and A-616 and A-617 specify deformed reinforcing bars produced from rerolled rail steel and axle steel, respectively.

2.2 ASTM DEFINED PROPERTIES

Reinforcing steel is the tensile component of reinforced concrete. Therefore, the tensile properties of reinforcing steel as specified by ASTM are of prime importance, and are summarized in Table 2.1. The steel modulus of elasticity, not shown in the table, can be assumed to be 29,000 ksi for design purposes. In the 1960's there was a general trend to the proportionately greater use of higher strength ($f_y \geq 60$ ksi) reinforcing bars, because of its superior

* See References.

TABLE 2.1. Basic Tensile Requirements for Reinforcing Steels.

Characteristic	ASTM Designation							
	A-82 Cold-Drawn Steel Wire	A-185 Welded Smooth Steel-Wire Fabric	A-496 Deformed Steel Wire	A-497 Welded Deformed-Steel-Wire Fabric	A-615 Deformed Billet Steel Bars	A-616 Rail-Steel Deformed Bars	A-617 Axle-Steel Deformed Bars
Tensile Strength, (min), ksi	80	75 (Size W1.2 and larger) 70 (Smaller than size W1.2)	85	80	70 (Grade 40) 90 (Grade 60) 100 (Grade 75)	80 (Grade 50) 90 (Grade 60)	70 (Grade 40) 90 (Grade 60)
Yield strength, (min), ksi	70	65 (Size W1.2 and larger 56 (Smaller than size W1.2)	75	70	40 (Grade 40) 60 (Grade 60) 75 (Grade 75)	50 (Grade 50) 60 (Grade 60)	40 (Grade 40) 60 (Grade 60)
Strain at which yield strength is measured, %	0.5	0.5	0.5	0.5	0.5 (Grade 40)[b] 0.5 (Grade 60)[b] 0.6 (Grade 75)	0.5[b]	0.5[b]
Elongation in 8 in., (min), %					7 to 12[a] (Grade 40) 7 to 9[a] (Grade 60) 5 (Grade 75)	5 to 7[a] (Grade 50) 4.5 to 6[a] (Grade 60)	7 to 12[a] (Grade 40) 7 to 8[a] (Grade 60)
Elongation in 2 in., (min), %					9 (Grade 60) 6 (Grade 75)[c]		
Min. pin diameter for bend tests	d or $2d$[a]	d or $2d$[a]	$2d$ or $4d$[a]	$2d$ or $4d$[a]	$4d$ or $5d$[a] (Grade 40) $4d$ to $8d$[a] (Grade 60)[a] $8d$[b] (Grade 75)[c]	$6d$ or $8d$[a]	$4d$ or $5d$[a] (Grade 40) $4d$ to $8d$[a] (Grade 60)
Reduction of area, (min), %	30	30					

[a] Depending on bar size; d is the nominal diameter of the reinforcing steel.
[b] Yield strength may be determined by the drop of the beam or halt in the gage of the testing machine.
[c] Only certain of the available sizes.

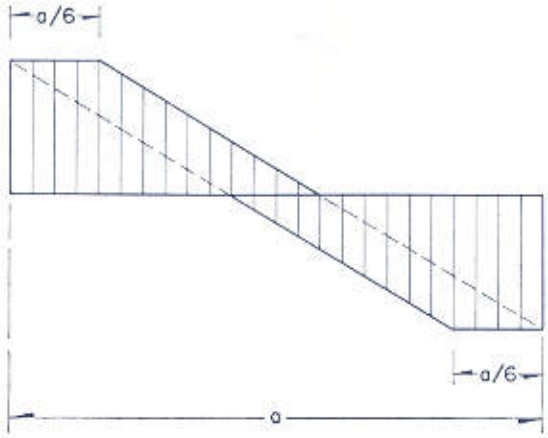

FIGURE 7.5. Design shears.

on a slowly consolidating soil, since settlements are more closely governed by the time average of loads than by their maxima.

One building code[13] specifies the following values for office and apartment buildings: $w_0 = 80$ kg/m² (16 psf), $w_1 = 250$ kg/m² (51 psf), and $cf = 7.5$ m (25 ft). For earthquake and wind resistant designs $w_{a1} = 100$ kg/m² (23 psf). And for computation of contact pressures on clay, for the purpose of computing settlements, $w_{at} = 40$ kg/m² (8 psf). Under static loading these design live loads are associated with a load factor of 1.4 and stress reduction factors of 0.8 to 0.9 for the reinforcement and $0.9(1 - c_v)$ for the concrete, where c_v is the expected coefficient of variation of concrete strengths. Under combined gravity and earthquake or wind loading the load factor is 1.1 and the stress reduction factors are 0.9 to 1.0 for the reinforcement and $1 - c_v$ in the concrete. In settlement computations in clay there is no load magnification nor stress reduction. Safety against shear failure in the ground is to be checked with the same live loads and load factors as used in structural design. Settlements in noncohesive subsoil are to be computed assuming those same live loads but a unit load factor.

The values quoted are not intended to cover positions of structures expressly destined to carry exceptionally high loads, such as those due to libraries and safety boxes, which admit a treatment similar to the one given below for warehouses. There is always the possibility that the type of occupancy may change for the worse. This situation has arisen most often in the mezzanines or second floors of office or apartment buildings whose ground floor houses stores; the first slab overlying the store is sometimes a candidate for storage of merchandise from ground-floor occupants.

Another relatively common situation is illustrated by an office building erected in 1957–1958 within a busy commercial section of Mexico City. Not long after its inauguration most of the floor beams had developed severe cracks and some had plainly visible deflections. It was found that the offices were being partially used as storage space for garments and fabrics. The design live load had been a uniform 200 kg/m² (41 psf); the applied live load exceeded ten times this value over an appreciable percentage of the floor area. The building was vacated; its cracked beams were strengthened; and in reopening it new leases were signed which included a limiting clause on live load. Some roof beams had also been damaged due to an advertising sign not considered in the design. Local strengthening allowed the structure safely to support the sign.

In the case of sudden collapse due to excessively high live loads that are atypical of office or apartment floors, there may be no convincing defense from the legal standpoint. And there are, of course, stronger reasons to be especially cautious against this possibility. It seems advisible, therefore, to design in such a way, always, that failure will be extremely unlikely to occur without adequate warning.

The upper tail of the distribution of the live load acting over a given floor area at an arbitrary instant is approximately normal.[21] Accordingly, the distribution of the maximum live load to be sustained over an extended period should be expected to be of the extreme type I, and there is some evidence favoring this assumption for loads due to persons while the lognormal distribution seems to be a better approximation for loads due to furniture.[12]

7.7 LIVE LOADS ON ROOFS

In regions of the world where the likelihood of snow can be discarded, the design of roofs is governed by considerations of earthquake and wind, people and occasional storage of materials, and rain and hail. Live loads in one building code[13] on flat roofs are not to be taken smaller than those given by Eq. (7.16) with $w_0 = 40$ kg/m² (8 psf) and $cf = 7.5$ m (25 ft), nor smaller than a uniform load that expresses the possibility of clogging of the roof drainage when certain construction practices are followed, or than a smaller uniform load when that possibility does not exist. Both uniform loads should clearly be functions of the climatic conditions.

In regions where snow may be abundant, snow loads govern design. There is apparently need for extensive surveys of snow loads on roofs of various shapes in different parts of the world, as extrapolation from statistical data of the depths of snow falls on the ground may lead to serious fallacies[4] and the stresses in shell roofs are quite sensitive to the distribution of snow as conditioned by the presence of valleys in the shells.[22] This last remark applies also, to some extent, to loads caused by hail.

7.8 LIVE LOADS ON CANOPIES

Horizontal and nearly horizontal canopies can collect large quantities of snow. Their main structural function, however, is often that of collecting debris from the facade, especially during earthquakes. They should be designed for these conditions. In some countries, canopies occasionally also hold large crowds to watch parades. One code requires a design live load of 400 kg/m² (82 psf) to account for this condition.[13]

It is difficult to establish a design criterion to produce canopies that resist falling debris. The mass that may fall is one of the most uncertain quantities that one meets in structural design of buildings. Whatever criterion is chosen, one should recognize that the energy absorption capacity of the canopy is far more important than its strength, and should design accordingly.

7.9 LIVE LOADS IN AUDITORIUMS, STAIRWAYS, AND CORRIDORS

Live loads specified for theaters, auditoriums, and other places where large groups of people may gather are based on less extensive information. The building code referred to[13] marks $w_0 = 200$ kg/m² (41 psf) and $cf = 3.0$ m (10 ft) under gravity loads, $w_{a1} = 250$ kg/m² (51 psf) under combined gravity and earthquake or wind, and $w_{a2} = 100$ kg/m² (20 psf) for settlement computations in clay. On these floors high live loads occur only seldom, and most of the time the live load is either zero or very small. When this is forgotten and the high loads specified for structural design are used to compute settlements or to design the foundation the result may be unsatisfactory. The writer knows of two motion picture theaters that have developed large differential settlements, with the center remaining at a higher elevation than the periphery, giving place to serious structural damage.

7.10 STORAGE LOADS

Observations in warehouses[23] indicate that there is a tendency to store the heavier loads in the lower stories. Most authors agree that live loads in warehouses are limited by an upper bound that can be established with almost deterministic accuracy and which is so likely to be closely approached during the expected lifespan of the structure that it should be taken as the design live load, without allowance for the observed systematic reduction with elevation above ground level nor for the size of the tributary area in question, and that one should proceed as though a change in the unit weight of the materials stored were virtually impossible. The same reasoning applies to the design of storage tanks.

Building codes reflect these ideas, calling for designs that consider from 80 to 100% of the maximum live load possible in terms of the nominal unit weight of the materials to be stored and of the nominal storage volume. Although this practice is probably wise in most instances, one should not lose sight of the following situations: (1) there are storage spaces without roof or with the roof so high that it is unlikely that they will ever be full; (2) a different material may be stored than the one assumed in design; (3) heavier liquids may be stored in tanks than was assumed in their design.

The designer may be legally protected in some of these cases of overload, especially if his drawings show the design loads and if, to the same effect, signs are posted in the storage rooms. But the aim of the designer should not be limited to legal protection. Aside, then, from designing so that there be adequate warning before failure, it is advisable in some instances to provide for higher live loads than those derived from a traditional analysis.

Many of the foregoing remarks apply with little change to the design of loading platforms, wharves, and the like. Live loads in excess of four times the design value are not altogether uncommon.

7.11 LIVE LOADS IN PARKING BUILDINGS

In accordance with most building codes, floors in parking garages for automobiles are often designed for unrealistically high uniform live loads. It is easy to verify that the average load over a large area in these structures cannot much exceed 150 kg/m² (31 psf). Locally, a fully loaded car may apply nearly concentrated loads amounting to, perhaps, 3 ton among the four wheels including impact. The concentrations produce, in proportion, higher positive and lower negative bending moments than a uniform load. In order that a uniform load cause the correct positive moments, it must be relatively high—probably not less than 350 kg/m² (72 psf). A better balanced result obtains by designing for a small uniform load—say 100 kg/m² (20 psf)—plus a concentrated force (say 1 metric ton) placed at the least favorable point.[13]

7.12 LIVE LOADS ON BRIDGES

Live loads on bridges have received a large share of attention. It is possible, for example, to predict almost deterministically the load imposed by a locomotive of given type, save for dynamic effects.[24] Simplified theoretical studies of loads on highway bridges,[25–27] which assume that vehicles of various weights have independent Poisson distributions, are adequate when traffic is freely flowing and not dense,[1] even though they are not entirely satisfactory under other conditions because of the tendency of the heavier trucks to line up one directly behind the other.[28] A prediction of loads on long-span

bridges must lay considerable weight on statistical studies of observed traffic. Such studies of loads on medium-span highway bridges lead to the conclusion that the design live loads for bending moment or for shear have nearly log-normal distributions.[29] Over short spans the maximum allowed truck load may govern design, even if the maximum actual load is not accurately predictable and so this load must be dealt with as a random variable. The combination of loads on two or more lanes lends itself to this type of treatment. But the greatest uncertainty comes from probable trends to increase the weight of vehicles in the near future, both on railroad and on highway bridges. Rational design live loads on bridges must be based on appropriately predicted weights of future vehicles.

For medium and long spans the effect of individual load concentration is small compared with the total weight of traffic. For highway bridges the total load depends on the type of vehicles, their distributions, density, and speed, the loaded length, and number of traffic lanes. Codes specify a distributed plus a concentrated load, which depend on the type of traffic and on the generalized force being computed—whether shear or bending moment. Efforts have been made to base bridge design loads on probabilistic reasoning.[30,31] To some extent, the AASHO loads H and H–S[32] can be justified on considerations of this character. There is an extensive literature on the subject (see, for example, References 33 and 34).

7.13 LIVE LOADS DURING CONSTRUCTION

Over no other type of live load does the engineer have so much control as over those applied in the construction stage. Yet no other type of live load causes so much damage. One frequently finds cracked and sagging slabs and beams whose state must be ascribed to overloading or premature loading during construction and where damage could have been prevented through adequate shoring.

Aside from the weight of concrete that has just been placed we must take into account the live load due to construction crews and that of buggies and other construction equipment. We can probably account well for live load due to people with the same criteria as live loads in apartment buildings. Buggies call for a criterion similar to the one deemed appropriate for parking floors, or at least for reckoning a nearly concentrated load that may act practically anywhere. And other equipment may require local provisions.

When designing for construction loads one not only has the usual choice of sections of structural members and their reinforcement but also chooses the distribution of shoring and the strength, modulus elasticity, and creep characteristics of concrete as determined by age at the time of loading. It is important to make realistic estimates of the evolution of the corresponding

parameters. This may require testing control specimens cured under essentially the same conditions of temperature and humidity as the concrete in the structural elements in question. Thereby construction need not be unduly delayed.

The distribution of live load among two or more consecutive floor systems, through connecting temporary struts, is amenable to accurate analysis.[35] On this basis one may decide to prestress the struts and compute the amount of prestressing required to compensate or overcompensate for the shortening of the struts and the floor deflections.

7.14 IMPACT

Buildings have collapsed under the action of impacts unforeseen in design. Yet severe impacts in most buildings occur so seldom that it is hardly worth doing much about them, other than tending toward great ductility and, especially in factories where the impact of lift trucks against columns is a very real possibility, protecting the columns against collision by surrounding them with rails.

Occasionally we do find very localized zones in buildings where impact is consciously and systematically going to occur. A frequent example is the floor for certain types of laundry equipment. The problem is, however, so localized and infrequent that the cost of overdesign is normally offset even by savings in the training of personnel in the design office, since such personnel is rarely in a position of thinking quantitatively of loads other than static forces.

Outside the realm of building design one meets with impact problems in a scale and with a frequency that demand attention. There are structures, such as forge-hammer foundations, whose main function is to resist impact. This is often the case in harbor works. In them the traditional methods of design, which lay weight on strength alone, do not apply. The traditionalist structural engineer must lighten himself of this burden and turn his attention to the ability of the structure to absorb energy, especially under repeated loading. Apparently insignificant details then become all important and design must proceed along the lines that produce a satisfactory earthquake-resistant structure. The next article will devote some attention to these questions.

7.15 EARTHQUAKES

7.15.1 Characteristics of Earthquakes

Strong motion earthquakes may originate in a number of ways: through volcanic action, collapse of cave and mine roofs, explosions, or tectonic

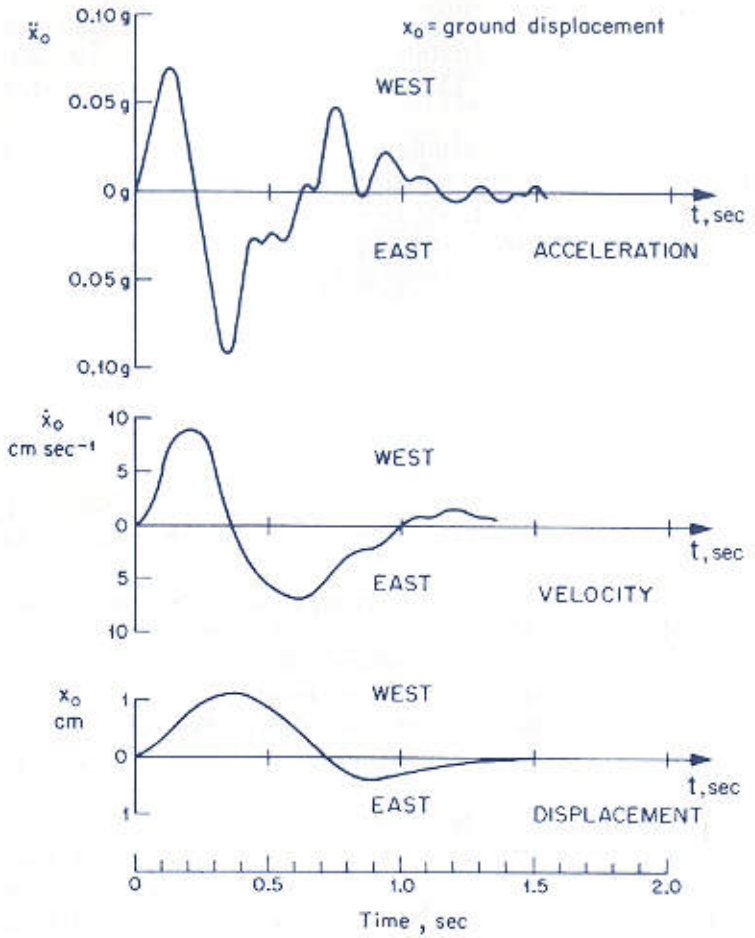

FIGURE 7.6. Record of a shallow, nearby earthquake of small magnitude on hard ground. (After G. W. Housner and D. E. Hudson, "The Port Hueneme Earthquake of March 18, 1957," Bulletin of Seismological Society of America, vol. 48, 162–168, 1958.)

activity. Those of the latter type are most interesting to the structural engineer because of the enormous amounts of energy that they can release and the extensive areas they may shake severely.

The following simplified classification of earthquakes has been proposed.[36]

1. Very shallow, nearby earthquakes of small amplitude, felt on hard ground. They consist essentially of a single sharp shock. The total duration

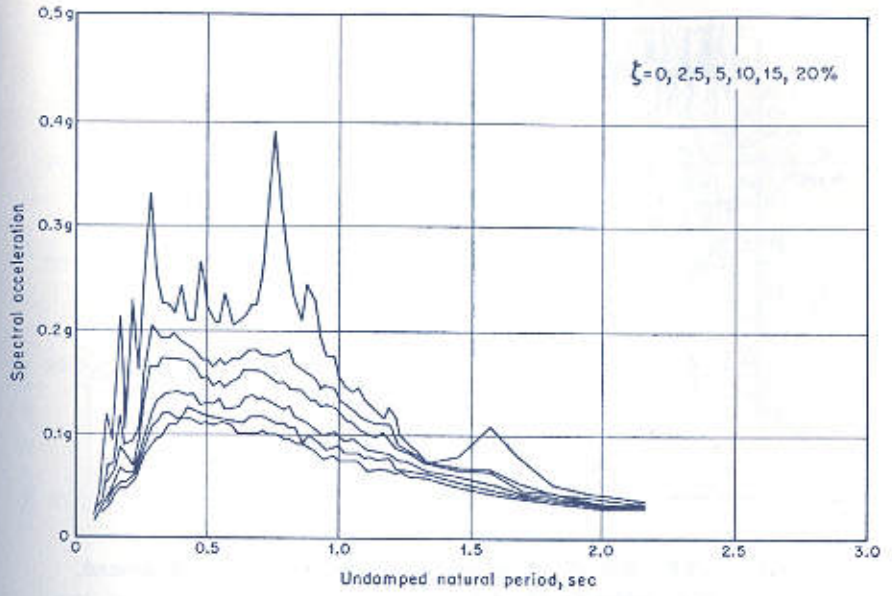

FIGURE 7.7. Response spectrum for accelerogram in Fig. 7.6. (After G. W. Housner.)

of perceptible motion does not exceed a few seconds. The magnitudes* of destructive motions of this type have ranged between 5.3 and 6.5. Examples are found in the earthquakes of Agadir, 1960,[37] Skopje, 1963,[38] Lybia, 1964,[39] San Salvador, 1964,[40] and Parkfield, 1967.[41] A typical record of nondestructive motion of this type is shown in Fig. 7.6, and its response spectrum† in Fig. 7.7.

2. Shallow earthquakes originating at moderate distances, felt on hard ground. These are irregular ground motions with mildly prevailing periods

* *Magnitude* is a measure of the energy released by the earthquake. The 1906 San Francisco earthquake had a magnitude of 8.4; that of Alaska in 1964 had 8.6. One unit increase in magnitude signifies a 32-fold increase in the energy released. On the other hand, *intensity* is a measure of the local destructive potential of an earthquake. A single temblor has one magnitude but its intensity varies with the station of interest.

† *Response spectrum* of a ground motion is a graph showing the maximum numerical values of certain responses of a linear, single-degree-of-freedom system (say, a viscously damped mathematical pendulum) as a function of the system's natural period of vibration. Responses chosen for the purpose are usually the system's absolute acceleration, or velocity or displacement relative to the ground. Ordinarily one curve is drawn for every percentage of critical damping that is of interest. Entering the spectrum with the natural period and percentage of damping of a structure idealized as a linear, single-degree system one obtains pertinent information for design, since forces and stresses can be computed from the maximum acceleration.

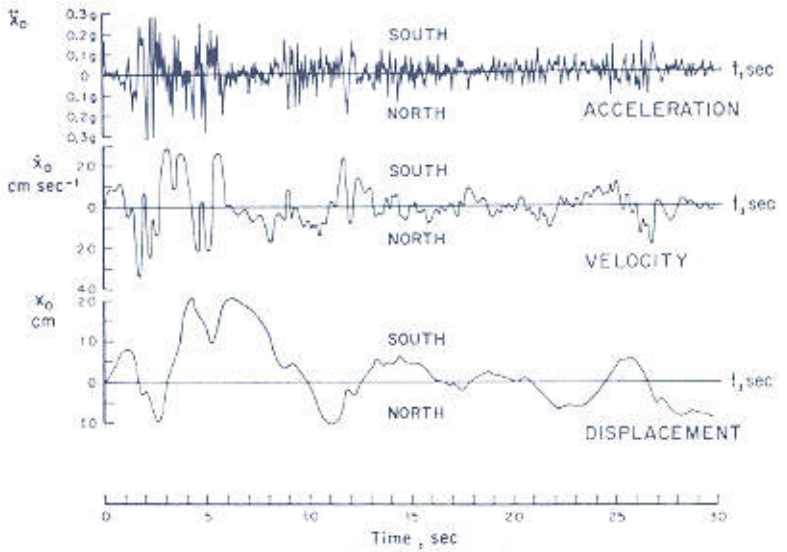

FIGURE 7.8. Record of a shallow earthquake on hard ground, originating at moderate distance.[50]

in the range of 0.05 to 0.5 sec. The motions last a few dozen seconds. Most of the strong earthquakes that have affected the western coast of the United States fall in this group when registered on firm ground. The most often quoted example of motions of this type is that of the NS component of the 1940 El Centro, California earthquake (Figs. 7.8 and 7.9).

3. Strong, distant earthquakes felt on soft ground within the range of linear behavior of the soil. Earthquakes of this type have pronounced, relatively long, prevailing periods and they last longer than those of the preceding type. They can be regarded as earthquakes of type 2 after going through a linear filter. In this group belong the Alaskan 1964 earthquake[42] wherever the soil did not undergo large permanent deformations, and several earthquakes in Mexico City.[43] The record and spectrum of one of the latter motions are shown in Figs. 7.10 and 7.11.

4. The same as type 3 but with appreciable inelastic deformations in the soil. Examples of this type of ground motion occurred in Coatzacoalcos during the 1959 Jáltipan earthquake,[44] in southern Chile during the quakes of May 1960,[45] and in the Alaskan and Niigata earthquakes of 1964.[46,47]

7.15.2 Structural Responses

Earthquakes of type 1 have received little attention. This is justified since they are similar to deal with as those of other types, they are relatively rare, and they affect comparatively small areas.

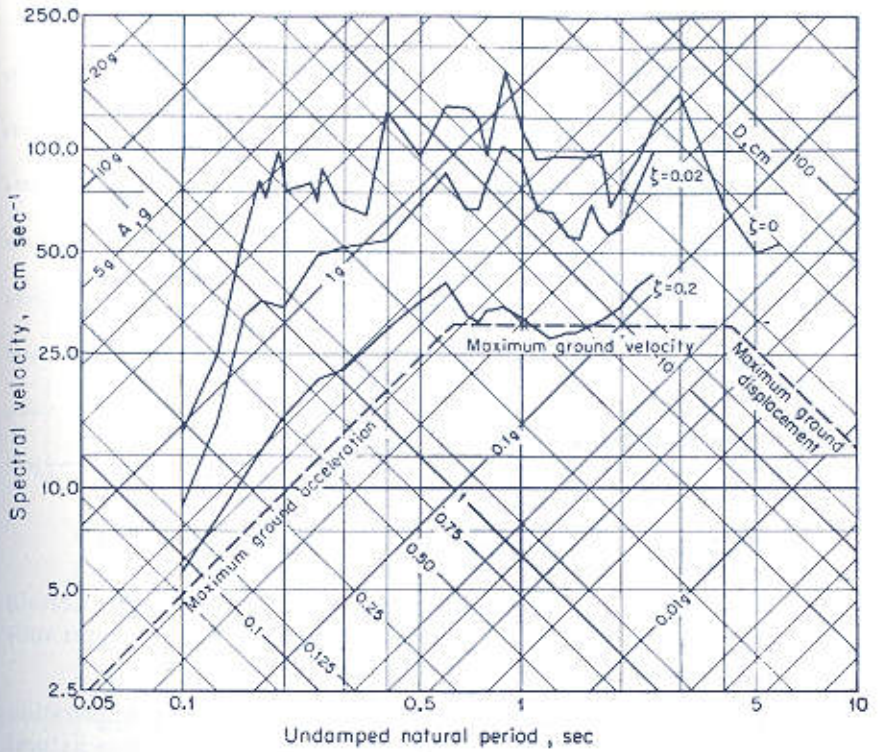

FIGURE 7.9. Response spectrum for accelerogram in Fig. 7.8.[50]

The distribution functions of the maximum responses of simple linear structures to ground motions of types 2 and 3 have been studied analytically and approximate solutions have been found.[48,49] Analytical solutions for the distributions of maximum responses of nonlinear structures and of complicated linear systems meet with difficulties, but a Monte Carlo approach is conveniently applied with the aid of digital or analog computers; important

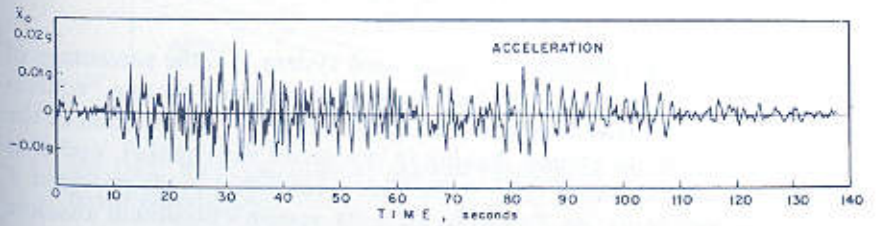

FIGURE 7.10. Record of strong, distant earthquake on soft ground within the range of linear behavior of the soil.

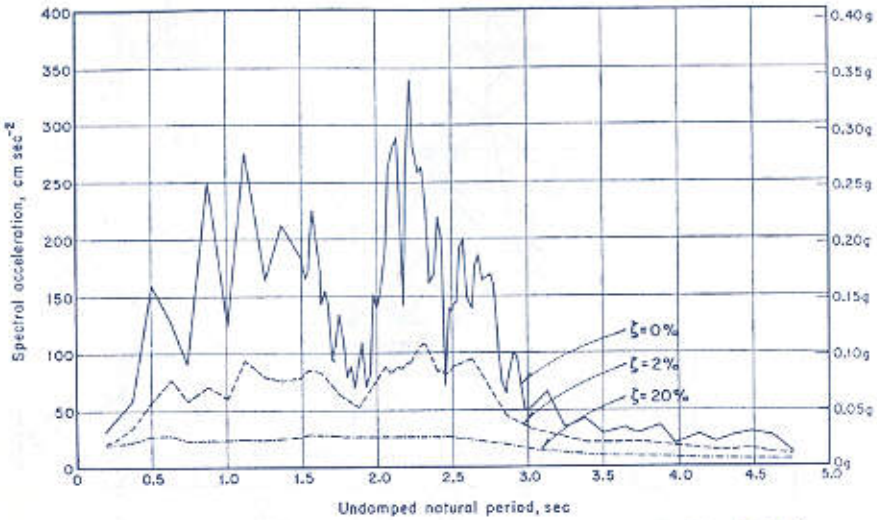

FIGURE 7.11. Response spectrum for accelerogram in Fig. 7.10.[48]

results can be expected to be produced thereby in the near future. Certain conclusions from the use of this technique are available for structures subjected to earthquakes of type 2. For example:[36]

1. The expected maximum numerical value of the absolute acceleration of a linear, single-degree structure resting on firm ground and whose natural period of vibration T, is neither very short (say $T \geq 0.1$ to $T \geq 0.5$ sec) nor very long (say, $T \leq 2.5$ to 5.0 sec) is almost inversely proportional to T and inversely proportional to the 0.4 power of the percentage of critical damping. A more accurate relation between expected maximum numerical values of the absolute acceleration, a is

$$\frac{a}{a_0} \simeq \left(1 + 3.77\zeta \frac{s}{T}\right)^{-0.45}$$
$$\simeq \left(1 + \pi\zeta \frac{s}{T}\right)^{-1/2}$$

where the subscript 0 identifies the undamped system, ζ is the percentage of damping, s is the duration of an ideal, white-noise ground motion "equivalent" to the earthquake considered (s is roughly equal to the duration of the phase of most intense ground shaking in the actual earthquake), and T is the system's natural period (Fig. 7.12). This relationship holds provided T is not excessively short. As T tends to zero, the system's maximum absolute acceleration approaches that of the ground, independently of the percentage of damping in the system (Fig. 7.13).

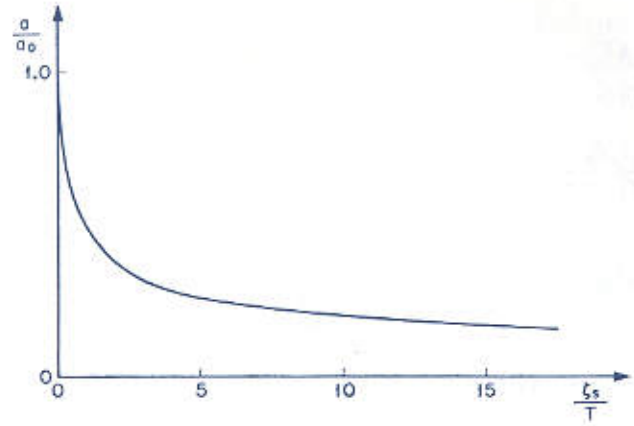

FIGURE 7.12. Reduction factor to account for damping.

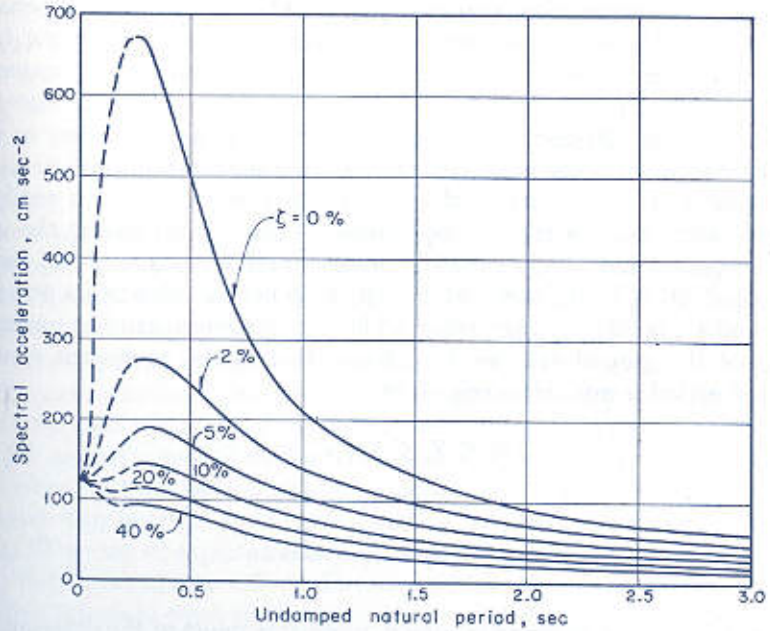

FIGURE 7.13. Normalized average acceleration spectra for California earthquakes.

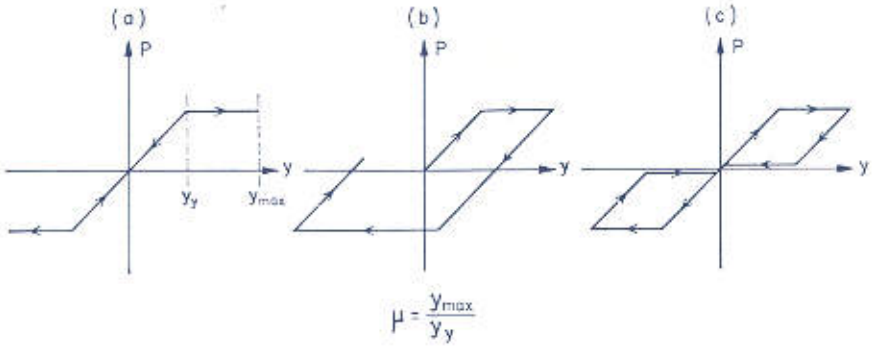

FIGURE 7.14. Three nonlinear systems.

2. Consider three bilinear systems, all having the same force–deformation curve on first loading but different unloading and reloading curves, as shown in Figs. 7.14(a), (b), and (c). They correspond respectively to an elastic system, a hysteretic elastoplastic system, and a system whose behavior approaches that of an anchored stack. Save for a small hysteretic loop, system *a* is representative of prestressed concrete frames whose major departure from linearity comes from the opening of flexural cracks that close upon unloading. System *b* idealizes the behavior of ordinary steel or reinforced concrete frames. And system *c* is a good idealization of structures X-braced with slender bars which only yield in tension and take a negligible compression. Now define an "equivalent" linear system having the same natural period and damping ratio as the nonlinear systems for small oscillations and let Y_0 be the expected maximum numerical value of its deformation under a family of earthquakes, all having the same maximum numerical value of the ground velocity. It is found that, if the equivalent system's natural period is not excessively short,

$$Y_0 \leq Y_a \leq Y_0\sqrt{\mu}$$

$$Y_b \simeq Y_0$$

$$Y_c \simeq Y_0 \frac{\mu}{\sqrt{2\mu - 1}}$$

where $Y_{a,b,c}$ are the expected maximum numerical values of the deformations of the systems in Figs. 7.14(a), (b), and (c), respectively, and μ is the *ductility factor*, that is, the ratio of maximum to yield-point deformations. The expression for Y_c is such that it equates the strain energies (areas under the force–deformation curves) of the nonlinear and equivalent linear systems.

3. The relationship expressed for structures of type *b* is approximately valid for a wide range of hysteretic systems that do not deteriorate appreciably in successive cycles and whose force–deformation curve is monotonic on first loading.

4. Equating the strain energies as for structure *c* furnishes a criterion that is conservative, when the natural period is not too short, for most hysteretic systems, even those whose first-loading force–deformation curve has a descending branch.

5. For very short natural periods the expected maximum accelerations of single-degree systems approach that of the ground, almost independently of the shape of the system's force–deformation curve.

6. For very long natural periods the expected maximum displacements tend to that of the ground.

7. Rough upper limits to the expected maximum deformation of a single-degree system that does not deteriorate in successive cycles of deformation are as follows.

(a) The maximum deformation of all linear single-degree systems having the same percentage of damping as the nonlinear structure in question.

(b) The deformation required to equate the strain energy developed by the nonlinear system to the maximum developed in this family of single-degree systems.

(c) The deformation required to equate the acceleration in the nonlinear system to the maximum developed in the family of single-degree systems.

This criterion usually errs appreciably on the safe side and, under very exceptional conditions (in certain elastic, undamped, nonlinear systems whose period increases with amplitude, for example) it may err slightly on the unsafe side. Yet it is adequate for many practical applications.

8. The expected maximum numerical values of the responses of multi-degree systems having linear behavior is approximately equal to the square root of the sum of squares of the corresponding expected maxima associated with the system's natural modes of vibration. This statement is limited to cases when no two natural modes—among those which affect the design responses significantly—have corresponding frequencies that are close together. (The sum of expected maximum numerical values is always an upper limit, but is sometimes too conservative.) More accurate expressions are available for cases when these conditions are not met. These criteria apply only within the range of intermediate natural periods of vibration; when the fundamental period is extremely short, the maximum absolute acceleration at every point in the structure comes close to the maximum ground acceleration, and when all the natural modes that contribute significantly to the deformations of the system are extremely long, the maximum responses approach

the sum of maximum numerical values of the ones associated with those modes.

9. The criterion of equating deformations of hysteretic structures with those of equivalent linear systems, as stated for the case of a single degree of freedom, carries over in a roughly approximate manner to structures having several degrees of freedom. However, even in well-designed structures local deformations often exceed by 100% those derived from an elastic analysis. In a multistory building, relative displacements between floors may be only slightly greater than obtained from elastic analysis, but maximum curvatures in the structural members are often as much as twice what the assumption of elastic behavior would indicate. And in a structure that is partially overdesigned or partially underdesigned to resist lateral loads, most of the energy absorbed in inelastic deformation will be dissipated in the weaker portions; hence, there will be much larger deformations in these portions (and smaller elsewhere) than indicated by elastic analysis.

7.15.3 Design Implications

The last remark in the foregoing paragraph has direct bearing on the care required in detailing reinforced concrete. Certain details of design and construction that are mildly objectionable under static loads become critical under the action of earthquakes. Such is the case with the cutting of tension steel in tension zones, insufficient lapping or anchorage, cold joints in which cleanliness is short of excellent, and so on.

In earthquake resistant design it is generally good practice to overdesign those portions of structural members that are inherently weaker or subjected to higher stresses, so a major portion of the member may be brought to participate in strain energy dissipation. Typical portions calling for these measures include the ends of most structural members because of the high local bending moments,[50,51] where it is normally advisable to reduce the spacing of ties, particularly at the top of vertically cast columns so as to compensate for the reduction of concrete strength; regions near points of cutoff of tensile steel, where the capacity in diagonal tension is thereby reduced[52,53] and there is need for more conservative practices than under static load;[54] regions near the ends of tensile bars in lapped splices, owing to the same reason; the vicinity of holes such as those called for in hydraulic or electrical pipes or fixtures, where over-reinforcement is advisable; etc.

Other matters of good practice are dictated by the nature of earthquake motions. The advisability of adopting certain other details is largely a function of the characteristics of the earthquakes to be expected. Thus, it is advantageous to verify that the vertical steel in columns be able to carry, in axial tension, some percentage of the load that the column carries under static

conditions (say 25% thereof) where earthquakes with important vertical accelerations are likely. (The maximum vertical ground acceleration need not exceed some fraction of gravity for a net upward acceleration to act in the floor systems, because of dynamic magnification.) But the practice would unnecessarily increase costs where important vertical accelerations are not expected.

The likelihood of some types of failure is especially sensitive to the number of loading cycles, but the same is not true of other manners of failure. For example, repeated alternating loading of beams that develop diagonal cracks tends to produce incremental failure through progressive growth of the cracks when the beams have little or no transverse reinforcement.[55] Consequently, other conditions being the same, one should be more conservative in evaluating the diagonal-tension capacity of concrete when earthquakes of long duration are expected than when designing against those of a more sudden type. Some structural engineers increase the allowable shear in the concrete by the usual 33% on hard ground but do not increase it when designing on soft soil where the possibility of distant-focus earthquakes controls design.

Examples described in the foregoing paragraphs merely illustrate some design considerations that are peculiar to earthquake engineering. Other matters are covered in References 51 and 56, although some specific numerical values in the latter document are open to question.

The majority of contemporary building codes that contain earthquake resistant provisions specify criteria for computing the base shear coefficient (ratio of seismic design shear at the base of the building to the building's weight) as a function of the building's fundamental period. This period is intended to be correct for small oscillations. It is either to be computed analytically or estimated on such crude bases as the building's external geometry or its number of stories. Damping and energy feedback into the ground are not taken explicitly into account. They are supposed to be incorporated into the base shear coefficients. Inelastic behavior, too, is implicit in these coefficients. Use of such criteria assumes that design is to be carried out with sufficient attention to details and to other concepts to which ductile behavior is especially sensitive, so that the ductility factors implied by the design coefficients can truly be developed.

Most contemporary codes recognize differences in ductility factors or in energy absorption capacity that are inherent to different structural solutions. This recognition affects the base shear coefficients used in design. For example, space frames are assigned considerably lower base shear coefficients than box-type structures.[57]

Questions of rigidities, and especially relative rigidities, are all important in earthquake resistant design. Rigidities are difficult to compute with

accuracy in reinforced concrete structures; they are sensitive to the level of stress and to stress history. For example, over a number of years and under the action of several minor quakes, many buildings have appreciably increased their fundamental periods of vibrations.[58] Even for small oscillations of undamaged structures, serious errors are often made in computing their fundamental period, chiefly through neglect of the contribution of "nonstructural" elements to stiffness.[59,60] Minor structural damage in some buildings has been known to lengthen their fundamental periods by about 50%, while minor structural repairs and replastering has brought their periods back almost to the original values under small-amplitude oscillations.[61]

Errors in the calculation of the fundamental period are usually not of serious consequences when the design acceleration decreases monotonically with period. If stiffness is overestimated, design will err on the safe side; and if it is overestimated because of neglect of secondary contributing elements, cracking of these elements will bring the period close to its computed value. Protection is achieved through the use of design accelerations that take them into account. For instance, one may adopt a design acceleration independent of natural period in the range of very short periods of vibration when in this range the accelerations would increase with period.

Miscalculation of the center of torsion is to be expected in almost all real structures. Protection is achieved by specifying an "accidental" torsion, to be added to the computed value at each story.[62] This aims at incorporating other sources of torsion not normally computed, such as asymmetric distribution of nominally symmetric live and dead loads, dynamic magnification,[63] rotational components of ground motion,[64] etc. (We speak here of *additional*, not *minimum* accidental torsion as specified in some building codes.)

A realistic appraisal of the state of earthquake resistant design places greater uncertainty on the occurrence and characteristics of future earthquakes than on any other variable,[65] but it recognizes that the dynamic properties and behavior of real structures cannot by far be predicted deterministically.

7.16 WAVE AND SHIP FORCES ON HARBOR STRUCTURES

7.16.1 General

In reinforced concrete engineering of harbor works we are chiefly concerned with four types of wave action: direct abrasion, often combined with corrosion and weathering; hydrodynamic pressures; mooring forces; and berthing impact.

In the absence of chemical and electrical actions of cavitation forces, and of weathering due to cycles of freezing and thawing, abrasion proper of dense

concrete subjected to the action of high-velocity water currents is such a slow process that it is hardly worth considering in design (see Reference 66 for numerical data on rate of wear in various types of concrete). The rate of wearing depends considerably on surface irregularities.[67] Charts showing critical pressure and velocity conditions for various kinds of irregularities are available.[68]

Hydrodynamic forces set up by wave action against rigid, vertical walls can be computed with high accuracy, using the simplified Sainflou formulas, when the train of waves is a steady-state harmonic process.[69,70] The standing wave under these conditions is known as *clapotis*. Pressure due to breaking waves, however, can be much greater, and is often computed using the Minikin formulas.[70]

7.16.2 Characteristics of the Disturbance

A much better idealization of wind-generated waves is, rather than a harmonic motion, a long-duration nearly stationary, narrow-band Gaussian process.[71,72] It is customary to describe the process either in the form of power spectral density, of Fourier spectra, of the average of the largest third of wave lengths, or of some other quantity as a function of period. From the spectrum description it is possible to derive the distribution functions of pressures against geometrically simple structures, such as piles,[73] under the assumption that the amplitudes of motion are sufficiently small to keep the process in the linear range.

If the criterion of failure is directly related to the mean square pressure, this manner of presenting data is quite useful. But when the criterion of failure is based on maximum force or maximum response, this type of description is inadequate, since the probability is 1 that any given amplitude of the disturbance, or amplitude of the response of a linear system, will be exceeded at least once in a stationary Gaussian process of infinite duration. When using such criteria of failure it is important to recognize that nonlinear behavior of waves at large amplitudes prevents the components of wave action from building up indefinitely large amplitudes. This precludes at present the application of simple probabilistic approaches to the effects of wave action on structures unless supplemented with an exercise of judgment.

The classical theory of wave pressures on vertical walls, when the wave breaks at the wall or a short distance therefrom has undergone important changes, owing mostly to the formation of an air cushion between the wave and the wall.[69] In shallow water and under the action of very steep waves it is important to recognize these phenomena, which invalidate a probabilistic approach based on the assumption of linear behavior. It is practical to estimate the parameters, such as wave height and period, of a set of design conditions relying essentially on judgment.

Similar remarks apply to mooring forces. The state of knowledge is such that, given a wave disturbance, the characteristics of the vessel, those of the mooring cables, and their initial tension, a reasonably accurate estimate can be made of the forces developed at any later instant.[74] But the differential equations involved are strongly nonlinear, and further study is necessary before a satisfactory probabilistic method of design can be established.

Berthing forces can be computed from the energy in the vessel and in the corresponding virtual mass of water an instant before impact. The total energy of impact is closely given by the mass of the vessel times the square of its berthing speed. This approximation is derived from the assumption that the virtual mass of water moving with the ship equals the mass of displaced water.

The speed of approach to a quay wall or dolphin can be estimated from the same data and computations that serve to find the mooring forces. The force-deformation relation for commercially available fenders and camels can be estimated from data supplied by the manufacturers. The relation for fenders made *ad hoc* can be computed. An estimate can also be made of the pertinent relations for the vessel. We arrive thus at a force–energy curve in which we englobe all energies which we take for granted will be absorbed. In other words, we englobe all energies excluding the one that will have to be resisted by the reinforced concrete structure that we are designing, be it a pier, a dolphin, or a quay wall, as though this structure were rigid. If we can also estimate the structure's force-deformation curve, we immediately arrive at the total energy demand imposed on it and the maximum force for which we must provide. When justified, the inertia forces in the structure itself can also be taken into account.

7.16.3 Design Implications

As in earthquake resistant design and even to a higher degree, in design against mooring and berthing forces, the energy absorbing capacity of the structure is of paramount importance, and details must be designed with due recognition of the probability that the structure will be subjected to many dozen cycles of amplitudes close to the maximum.

7.16.4 Tsunamis

The design of many harbor structures is dictated by the possibility of *tsunamis*, or "tidal waves." These phenomena are mostly caused by submarine landslides due to earthquakes.[75] In some cases fault displacements and other seismic events may also cause tsunamis. The ratio of the energy associated with a tsunami to that liberated by an earthquake can vary in order of magnitude from one earthquake to another. Hence, data on recurrence times of

tsunamis are best estimated directly from statistical information on their occurrence and magnitude. The assumption that they occur in accordance with a Poisson process allows calculating their probabilities for any given time interval.[36] This statistical information is available for some sites, and analyses and model studies can be used, albeit with some reservations, to predict the local amplitude and speed of the waves.[76]

From judicious consideration of the effect of past tsunamis[76] and from a study of the measures that are taken in tsunami-stricken coasts,[77] the empirical criteria of design that are currently used to provide against excessively frequent damage from this cause can be supplemented and improved. Use of the finite element technique has proved valuable for the calculation of tsunami induced forces.[78]

7.17 WIND

7.17.1 General

Wind action on structures has static and oscillatory components. The aerodynamic effects are due to the following phenomena.[79]

1. Vortex shedding. The vortices shed alternately from opposite sides of the body usually cause cross-wind oscillations often observed in tall stacks and towers and in some suspension bridges.[80]
2. Galloping. The phenomenon occurs mostly in ice-covered wires and in stranded cables. It may be regarded as caused by negative damping induced by unfavorable lift forces.
3. Stalling flutter. This occurs mostly on bowl-shaped structures such as microwave reflectors.
4. Forced vibrations induced by periodic components of turbulent flow.
5. Classical flutter, which consists in instability due to coupling between separate degrees of freedom. It has been observed in bowl-shaped structures and suspension bridges.

Exceptionally, some structures such as cylindrical steel tanks have presented nonoscillatory divergent instability.[79]

Ordinarily, forced vibrations are of relatively little concern in the design of structures subjected to wind action in the open field. This is because, in free flow, the power spectrum of wind has maxima around 0.01 cycles per hour and between 6×10^{-3} and 2×10^{-2} cps.[81] In the neighborhood of 1 to 2 cycles per hour the energy content is quite small and beyond 0.3 cps it is negligible. However, the proximity of other structures induces buffeting and interference which cause the appearance of appreciable components in the wind spectrum with frequencies of up to 0.5 cps. Hence, it is only in relatively

flexible structures that forced vibrations due to wind acquire importance for design purposes. The major components of wind-induced oscillations are usually self excited:

Sensitivity to short-lasted gusts is much a function of the structure's outer dimensions. In order that a gust act effectively on a structure it must traverse at least eight times the structure's dimension in the wind direction. For example, structures measuring 20 m (65 ft) or more in the wind direction should be designed for maximum wind speeds averaged over intervals of not less than about 10 sec. Slender structures should be designed for higher gust factors.

7.17.2 Classification of Structures for Wind Resistant Design

In accordance with the characteristics of wind action the following classification has been devised for design purposes.[82]

Type 1. Structures relatively insensitive to gusts and to aerodynamic effects, such as office and apartment buildings up to 60 m (200 ft) tall; theaters; industrial, and other buildings, having relatively rigid roofs; and bridges consisting of slabs, beams, trusses, or arches.

Type 2. Slender or thin structures especially sensitive to short-duration gusts but whose fundamental period does not exceed 2 sec and which do not belong to type 3. Type 2 includes most elevated tanks, signs, parapets, transmission towers, antennas, etc.

Type 3. Same as type 2 but the shape of these structures favors vortex shedding. This type covers stacks and short suspension bridges.

Type 4. These structures have special aerodynamic problems. They may be inherently unstable (as in the case of wires in areas of frost, and parabolic dish antennas); they may have two or more natural periods of vibration close to each other (as some flexible roofs and suspension bridges); or their fundamental period may exceed 2 sec.

7.17.3 Wind Speed

The speed of wind at a given point in space is a random variable having very nearly a Weibull distribution (nearly a Raighley distribution, which is Weibull's with a shape factor of 2). As a consequence, the maximum speed over a given time interval—say, the yearly maximum—practically has an extreme type I distribution.[81] However, much statistical work has been done for wind speeds in the United States[82] and in the USSR under the assumption that the distribution of the maxima is extreme type II. The latter assumption is consistent with, among others, an underlying lognormal distribution of speeds.[83] Available data seem to favor the former approximation while the extreme type II gives excessively conservative results for very long recurrence periods.[81]

The parameters for the distributions of maxima in tropical storms are markedly different from those in other winds. When winds of both types of origin can affect a given site, it is proper to use a linear combination of two extreme distributions. Tornadoes also merit a separate statistical treatment.[84]

The variation of speed with altitude can be approximated closely by

$$\frac{v}{v_g} = \left(\frac{z}{z_g}\right)^{\alpha} \quad \text{when } z \le z_g$$
$$= 1 \quad \text{when } z \ge z_g \tag{7.17}$$

where v denotes speed, z is elevation above ground level, subscript g refers to the gradient speed elevation, and α is a parameter characteristic of the topography at the site (Fig. 7.15). The elevation z_g is also a function of the local topography. Table 7.1 contains typical values of α and z_g for various topographies. It is based on data in References 81–83 and 85. The gradient velocity, v_g, depends little on local topography and can be obtained from maps

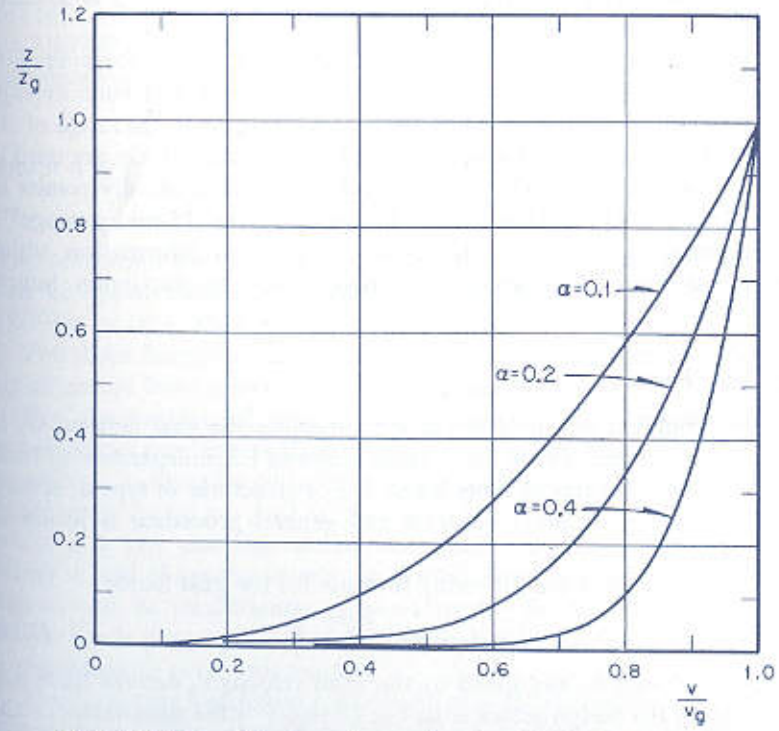

FIGURE 7.15. Wind speed as a function of height above ground.

strength-to-cost ratio, especially for $f_y = 60$ ksi, and deformed wire fabric, because of its improved bond strength and crack-control properties.

The available sizes and basic dimension details specified by ASTM are presented in Tables 2.2 and 2.3 for reinforcing bars and fabric wire, respectively. Grade 75 ($f_y \geq 75$ ksi) reinforcing bars are generally produced only to special order, but the remainder of the reinforcing steels are generally available in most of the sizes listed.

The ASTM deformation requirements for reinforcing bars and deformed steel wire are listed in Tables 2.4 and 2.5. For deformed bars, the deformations are protrusions (Fig. 2.1a) and, consequently, the capacity of a bar for transferring shear between the bar and the surrounding concrete is governed largely by the bearing area[2] of the transverse lugs. To ensure proper bearing, ASTM further specifies that the angle between a transverse deformation and the axis of a bar shall not be less than 45°. For deformed wire, the deformations are generally indentations (Fig. 2.1b) and the bond of the concrete to the steel is governed by both the bearing area and the critical shearing area of concrete shear keys[3] at the outer diameter of the wire, i.e., the concrete protrusions mating the steel indentations. Consequently, ASTM specifies that a minimum of 25% of the total surface area of a deformed wire shall be deformed by measurable deformations.

For identification, American reinforcing bars are given a raised-pattern mark, as indicated in Fig. 2.2.[4] Grade 40 steel bars include the initial identification of the producing mill, the number corresponding to the bar size, and a letter or symbol corresponding to the type of steel ("N" for new billet steel, a rail symbol for rail steel, or "A" for axle steel). Grades 60 and 75 have this identification and, in addition, either the number or the additional longitudinal ribs to identify the grade.

2.3 AS-PRODUCED PROPERTIES

Variation of Properties. Some variation occurs in the mechanical properties of reinforcing steels, although the variation is generally conservative with respect to the ASTM specifications. For example, an industry-wide sampling and subsequent testing of Grade 60 steel bars resulted in the yield-stress distribution shown in Fig. 2.3.[5] Although steel producers generally aim for strength levels about 5 to 10 ksi above the minimum specified, such factors as (1) the variations in chemical composition from bottom to top of each ingot and from ingot to ingot throughout a heat, and (2) the variation in cooling rates of bars in a hot bundle invariably result in some variation of the strengths and ductilities of reinforcing bars in any given heat. Indirectly, this has been reflected in the safety factors employed in reinforced-concrete design.

TABLE 2.2. Sizes of Reinforcing Bars Specified by ASTM.

Available Bar Designation Numbers									Nominal Dimensions			
Deformed Billet Steel Bars, A-615			Rail Steel Deformed Bars, A-616			Axle-Steel Deformed Bars, A-617			Unit Weight lb/ft	Diameter, in.	Area, sq. in.	Parameter in.
Grade 40	Grade 60	Grade 75	Grade 50	Grade 60		Grade 40	Grade 60					
3	3		3	3		3	3		0.376	0.375	0.11	1.178
4	4		4	4		4	4		0.668	0.500	0.20	1.571
5	5		5	5		5	5		1.043	0.625	0.31	1.963
6	6		6	6		6	6		1.502	0.750	0.44	2.356
7	7		7	7		7	7		2.044	0.875	0.60	2.749
8	8		8	8		8	8		2.670	1.000	0.79	3.142
9	9		9	9		9	9		3.400	1.128	1.00	3.544
10	10		10	10		10	10		4.303	1.270	1.27	3.990
11	11	11	11	11		11	11		5.313	1.410	1.56	4.430
	14	14							7.65	1.693	2.25	5.32
	18	18							13.60	2.257	4.00	7.09

TABLE 7.1. Parameters Related to Wind Speed.

Topography	k_1 for Structures Type 1	z_g, m (ft)	α
Heavily built-up urban centers	0.7	430–550 (1400–1800)	0.34–0.50
Wooded or hilly country, industrial and suburban zones	0.8	350–400 (1150–1300)	0.22–0.30
Flat open country	1.0	275–300 (900–1000)	0.14–0.17
Promontories, sea coasts	1.2	210–250 (700–800)	0.09–0.12

corresponding to given recurrence periods, such as the one in Reference 85, in which, however, wind velocities have been reduced to a height of 30 ft above the ground; gradient velocities for other return periods can be derived from the distributions of maximum speeds. (In tropical storms, α is so small that v may be taken independent of z.[86])

Various established practices exist concerning the criterion for averaging wind speeds in time. There are reasons for preferring the maximum average speed in a period in the range of 5 to 30 min, particularly in the range of 10 to 15 min. However, a 1 hr averaging period is common; 10 min are used in Japan and 5 min in the USA.[81] The fastest mile, which usually results in appreciably higher speed (about 30% higher than the 15-min average[81]), is also common in the USA.[86] Reference 85 contains information which permits transforming data about the fastest mile into maximum hourly speeds.

7.17.4 Gust Factors

In a much simplified scheme Reference 82 specifies the gust factors, G, in Table 7.1 for structures of type 1 and a gust factor of 1.2, independent of local topography, for structures of types 2 and 3. For structures of type 4, special studies are required. A more accurate and general procedure is found in Reference 85.

Davenport[87] advances the following formula for the gust factor

$$G = 1 + \Gamma r \sqrt{B + R} \tag{7.18}$$

In all cases G should be multiplied by the wind velocity v, derived from Eq. (7.17) to obtain the design velocity. In Eq. (7.18), Γ is the peak factor, r the roughness factor, B the excitation by background turbulence, and R the

excitation turbulence resonant with the structure,

$$R = \frac{Fs}{\beta}$$

where F is the gust energy ratio, s the size reduction factor, and β the damping ratio. β is of the order of 1 to 2% for reinforced concrete structures. Graphs are provided in Reference 87 for the calculation of the rest of these quantities.

7.17.5 Static Effects

The design velocity affected by the gust factor, Gv, is used for calculating drag and lift pressures, q, according to the expression

$$q = \frac{1}{2} C\rho(Gv)^2 \tag{7.19}$$

where C is a dimensionless coefficient, or shape factor (drag: from about 0.4 for smooth cylinders to about 0.9 on the windward side of flat surfaces, considerably more for lattice structures, and negative for the leeward side; lift: usually $-2.1 < C < 2.1$), and ρ is the density of air (0.125 kg sec^2/m^4 (0.00237 lb sec^2/ft^4) at sea level and temperature of 15 deg centigrade). If v is expressed in km/hr, Eq. (7.19) becomes

$$q = 0.00486\, C(Gv)^2 \tag{7.20a}$$

and if it is expressed in miles/hr,

$$q = 0.00256\, C(Gv)^2 \tag{7.20b}$$

The correction for air density as a function of altitude above sea level, Z, can be approximated by multiplying q, as obtained from Eqs. (7.20a) or (7.20b), by $(8 + Z)/(8 + 2Z)$, where Z is in km.[82]

The shape factors to use in most cases of practical interest can be obtained or estimated from information in References 82, 88–95.

The fluctuations of pressure in turbulent flow produce "accidental" eccentricities even in strictly symmetric surfaces. In relatively rigid structures exposing a rectangular surface it is adequate to take the horizontal accidental eccentricity equal to $\pm(0.3L^2/8H + 0.05L)$ when $L \leq 2H$, and to $\pm L/8$ when $L \geq 2H$, and the vertical accidental eccentricity equal to $\pm 0.05H$, where L and H are the length and height of the exposed surface.[82] The provision may be insufficiently conservative for flexible structures, say those whose fundamental period of vibration exceeds 2 sec; Reference 81 describes a procedure to cover this matter.

The foregoing horizontal eccentricity should be combined with accidental eccentricities due to inaccurate predictions of stiffnesses, and with the computed eccentricity.

7.17.6 Dynamic Effects

Aerodynamics is a specialized subject. The reader will find guidance in several works on the subject, such as References 82, 87, 96–101. In the last two of these references he will also find information on the similitude and turbulence requirements that must be satisfied when testing models in wind tunnels, as this approach must be adopted when studying any unusual structure.

7.17.7 Design Implications

Certain portions of buildings, such as lightweight roofs, windows, and cladding, may fail under wind forces that are essentially static. Because of the frequency with which these forces are applied and particularly because of wind turbulence, we must design these portions under conditions of low-cycle fatigue, that is, recognizing that there will be dozens of loading cycles. The same remark applies to structures type 1. Consequently, many of the criteria that we expounded in connection with earthquakes carry over to wind resistant design. However, during a single wind storm the forces applied do not ordinarily change signs and, owing to the prevalence of wind from some directions, inelastic effects are in large measure cumulative. Hence, we should not stress ductility as much as we did when considering seismic action.

In structures subject to large oscillations the number of force applications may be at least an order of magnitude higher. Therefore we should be concerned with fatigue proper as well as with low-cycle fatigue. The comfort of the occupants and damage to nonstructural members, as governed by large oscillations, are also matters to consider in wind resistant design, particularly in that of tall buildings. In all cases we must recognize in design the possibility that the loads on the structure be smaller than their nominal values, as this situation increases the probability of roof lifting and of overturning and may bring about unfavorable changes in natural frequencies. The possibility of architectural changes deserves special attention.

7.18 SHRINKAGE

7.18.1 Nature of Shrinkage

One special type of imposed deformation is shrinkage. We classify it thus because a convenient way of including it in computations lies in replacing it with deformations of opposite sign, such as to satisfy boundary conditions.

Shrinkage is inherently nonuniform. It proceeds from the surfaces exposed to the atmosphere toward the interior. Only when it occurs at extremely slow rates, and thanks to creep of concrete, does shrinkage induce stresses sufficiently small as not to cause cracking. Even then concrete is almost sure to crack if restraints prevent or sharply reduce its possibility to decrease in length. Reinforcing steel, rather than preventing cracking due to shrinkage, practically insures cracking. But, when used in sufficient amounts and spaced closely enough, reinforcement leads to cracks that are so small and closely spaced that they become acceptable.

7.18.2 Effects of Shrinkage

Usually, differential shrinkage must be guarded against to a greater degree than uniform shrinkage. This is often the case in pavement slabs whose tendency to curve because of differential shrinkage may dictate the spacing of joints and the amount of reinforcement to a greater extent than the loads that the slab is intended to support.

Shrinkage is also a phenomenon to consider when designing on the basis of allowable deflections. Restrictions imposed by steel in asymmetrically reinforced members are such that shrinkage nearly always adds to the deflections due to load. Differential shrinkage is usually responsible for even greater deflections, since the concrete in horizontally cast members has a higher water content near the top.

Shrinkage is capable of appreciably modifying the stresses in statically indeterminate structures. Indeed, shrinkage together with temperature variations govern the spacing between construction joints.

As with all stresses due to imposed deformations, those caused by shrinkage do not greatly decrease the capacity of a structure if the criterion of failure is collapse, provided these deformations are accompanied by a sufficiently extensive redistribution of bending moments and other generalized forces. In other words, in designing against collapse we may practically ignore imposed deformations if the structure is sufficiently ductile; if ductility is insufficient we cannot proceed in this manner without serious consequences. For example, the capacity of beams to resist shear, when their transverse reinforcement consists only of vertical stirrups, is very sensitive to longitudinal tension. The collapse of a warehouse in 1955, which led to revision of the ACI code provisions on diagonal tension and the ensuing 1955 code, must be attributed in part to longitudinal tension caused by shrinkage.[102,103] This was possible because an end plate, which was supposed to provide longitudinal freedom through sliding at the support, developed excessive restraint.

Even when enough ductility is provided to prevent collapse due to shrinkage, other forms of damage due to this phenomenon may turn a structure unacceptable. Effects of shrinkage may rarely be ignored, even if they are only recognized informally by supplying a minimum percentage of reinforcement.

Concrete made with portland cement of high C_3A content is susceptible to sulfate attack. In normally retarded cements, C_3A, in the presence of gypsum, is converted to the monosulfate hydrate, $C_3A{\cdot}C\bar{S}{\cdot}H_{18}$, which upon exposure to sulfate waters, is further converted to the trisulfate hydrate, $C_3A{\cdot}3C\bar{S}{\cdot}H_{32}$. Under certain conditions, the formation of the trisulfate hydrate, also called ettringite, is accompanied by large expansion. Since hardened concrete is not free to expand, high tensile stresses are produced by the formation of the trisulfate hydrate. The tensile stresses often reach the tensile strength of concrete, and thus lead to cracking. It is obvious, therefore, that limitations must be placed on the C_3A content of a portland cement whenever either low rate of heat evolution or sulfate resistance are among the properties desired in concrete.

Regarding *ferrite phase*, generally in commercial portland cements its compound composition corresponds to C_4AF, but this can vary from C_2F to C_6A_2F. The nature of the reactions with water and the products of hydration of the ferrite phase are analogous to the aluminate phase. As compared to C_3A, however, the rate of reactivity of the ferrite phase slows down as the iron to alumina ratio increases in the composition. One way to reduce the deleterious effects of a high proportion of C_3A in a portland cement is, therefore, to increase the iron oxide content of the cement raw-mix so that more alumina gets tied up as ferrite phase, and less of it is thus available to form C_3A.

Depending upon the impurities in the raw materials, and the operating conditions during cement manufacturing process, some *deleterious compounds* can be present in the final product. Such substances include alkalis, uncombined or free lime, and free magnesia (periclase). Free lime and magnesia become hard-burnt due to exposure to the high clinkering temperatures and therefore exhibit delayed hydration reactions which may lead to unsoundness or cracking of hardened concrete. Alkalis, in the presence of reactive siliceous aggregates, become responsible for disruptive alkali–aggregate reactions in concrete.

In the presence of water, the hydration reactions of both alite and belite produce calcium hydroxide and a calcium silicate hydrate of an approximate composition $C_3S_2H_3$. The calcium silicate hydrate, because of its mineralogical similarity to the natural mineral tobermorite, and because of its gel-like properties, is often referred to as *tobermorite gel*. The setting, hardening (strength development), shrinkage, and creep characteristics of a portland cement paste are greatly influenced by tobermorite gel.

Alite and belite, however, differ from each other in their rates of hydration. There is a good correlation between rate of hydration and *heat of hydration*. The data in Table 1.1 shows that C_3S hydrates more rapidly than C_2S. This is also corroborated by comparative rates of strength development in two cements having different percentages of C_3S and C_2S as shown in Fig. 1.1.

Rapid hydration, resulting in high heat evolution, is not always desirable. In mass concrete, high temperature rise has frequently led to thermal strain and cracking. For such applications it is essential to limit the C_3A and C_3S content of portland cement.

TABLE 1.1. Heats of Hydration of Compounds in Portland Cements.[3]

Compound	Heat of hydration, cal/g compound,[a] at 0.4 water/cement ratio, 21°C, and age indicated.		
	3 days	90 days	13 yr
C_3S	58	104	122
C_2S	12	42	59
C_3A	212	311	324
C_4AF	69	98	102

[a] These values have been obtained by least square analysis of test data.

1.4 DIFFERENT TYPES OF PORTLAND CEMENT

As mentioned above, by modifying the compound composition, it is possible to manufacture *different types of portland cement* having variable characteristics with regard to rate of hardening, rate of heat evolution, and resistance to attack by sulfate waters. Five types of portland cement are defined in

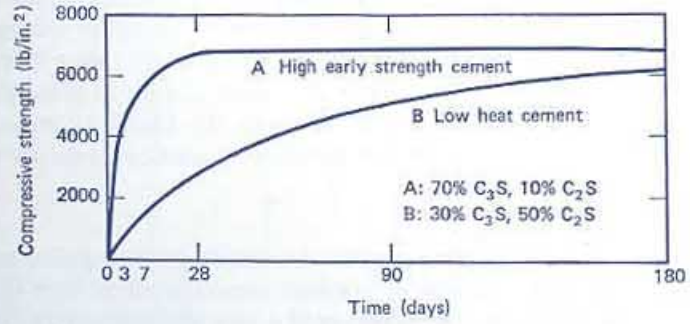

FIGURE 1.1. Variation of compressive strength with curing time for 1:3 mortars made from two different Portland cements (constant W/C ratio).[3]

7.18.3 Design Provisions

The ACI code[104] now requires

$$\rho \geq 200/f_y \tag{7.21}$$

where ρ is the minimum ratio of steel required for this purpose and f_y is the minimal yield stress of this steel. It is specified that this reinforcement be spaced not more than 46 cm (18 in.) on centers.

Equation (7.21) ignores most of the significant variables. A more ambitious code requirement is[105]

$$a_s \geq \frac{450x}{(x + 100)f_y} \tag{7.22}$$

for structural elements not directly exposed to atmospheric weathering and twice this much for elements directly exposed thereto. Here a_s is the required area of steel per unit width, in cm²/cm, f_y is in kg/cm², and x is the structural element's smallest dimension in a direction perpendicular to the steel in question. No reinforcement is required in directions in which the structural element measures less than 150 cm (5 ft). Equation (7.22) can also be put in the form

$$\rho = \frac{450}{(100 + x)f_y} \qquad \text{where } x \text{ is in cm and } f_y \text{ is in kg/cm}^2$$

$$\simeq \frac{6.4}{(40 + x)f_y} \qquad \text{where } x \text{ is in in. and } f_y \text{ is in ksi}$$

where ρ is the required ratio of steel. This provision does not take into account the characteristics of the concrete mix that is to be used, save that it calls for greater ratio of reinforcement in special concretes that tend to shrink more than mixes made with aggregates of normal weight. Even so, it is already too complicated for most practical applications. It may be preferable to compute the maximum ratios required, which correspond to, say, $x = 10$ cm (4 in.), if this is the thinnest slab or shell in the project under consideration. Then Eq. (7.22) can be put in the form of Eq. (7.21), to give $\rho = 128/f_y$, with f_y in psi, for unexposed structural elements, and twice this much for elements that are exposed. In thicker elements, the required ratio decreases while a_s increases but does not exceed the equivalent of No. 4 bars of A34 steel 27 cm (10.5 in.) on centers or No. 6 bars 30 cm (12 in.) on centers, depending on whether the concrete surface is or is not exposed.

Vertical cracks having a maximum width at midheight of deep beams are classical in members whose lateral faces are insufficiently reinforced with longitudinal bars (Fig. 7.16).[106] Criteria such as Eqs. (7.21) or (7.22) coupled with a limitation on the maximum spacing of steel for volumetric changes lead to designs that are usually satisfactory from this point of view.

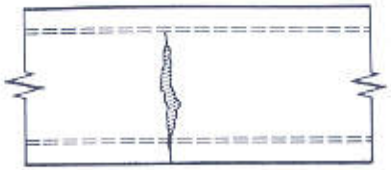

FIGURE 7.16. Cracks in deep member without longitudinal reinforcement along the lateral faces.

Although no reinforcement of this sort is needed in the direction of x when $x \leq 150$ cm (5 ft), common experience speaks of inclined cracks near the supports of beams having little or no web reinforcement even when computations indicate the presence of shearing stresses far below those which the unaided concrete in the web should be able to take. These cracks can be recognized because their widths increase with shrinkage. The cracks develop chiefly through a combination of shrinkage and diagonal tension; consequently, longitudinal reinforcement at intermediate elevations of the beam is only mildly effective in controlling the cracks. It may be advisable to supply vertical stirrups as well, designed in accordance with Eqs. (7.21) or (7.22) after letting x tend to infinity. The same applies to the design of ties in columns that may be subjected to appreciable shearing forces.[107]

Trustworthy correlations exist between the cement and water contents of concrete and its shrinkage strains under given atmospheric conditions and for given aggregates (see Chapter 3). The fact that relative humidity and the exact composition of the aggregates are unknown at the design stage makes this a random variable in structural design and it should be treated accordingly.

In principle, a more rational approach would be desirable to compute the optimum amount of reinforcement as a function of predicted shrinkage and other imposed deformations, rather than adopting a specified minimum percentage. But the initial investment at stake is very small and the change in total utility is negligible in most cases. Hence, it is hardly worth going through such an analysis except in the design of special structures for which cracking would be especially objectionable and its control especially costly. In most practical instances it suffices to follow code requirements and use the minimum slump compatible with ease in casting, resorting to revibration or the use of special cements or admixtures where a more drastic reduction in cracking is desired.

7.19 TEMPERATURE CHANGES

7.19.1 General

Effects of temperature changes, as those of shrinkage, can be included in calculations as imposed deformations. In the same manner as shrinkage,

temperature changes are random variables, mostly because of the difficulties involved in predicting the changes in temperature that the concrete itself will undergo. The situation is reflected in the difficulties involved in specifying the required spacing between contraction or expansion joints.

7.19.2 Examples

The following cases illustrate the problems encountered. They refer to buildings in Mexico City, where the daily change in temperature is 15°C (27°F) on the average; the relative humidity is lowest in winter (an average of 55%) and highest during the rainy season (an average of 70% in summer).

The first example concerns sloping roofs over which often no protection, or at most a layer of bituminous material, is placed so the concrete slab and beams are almost directly exposed to the sun and atmosphere. In servants' rooms built atop roofs on apartment buildings, cracked beams and walls are commonplace. A room 4 m (13 ft) long is likely to have cracks about 0.4 mm (0.16 in.) wide in its unreinforced masonry walls.

Contrasting with this, two medium-cost apartment buildings are 40 m (130 ft) long without construction joints and have developed no more than hair cracks over a period of several years. Their roof slabs are covered with a fill of cinder to give drainage slopes, with an average thickness of 15 cm (6 in.), plus impervious material and a layer of brick. Clearly the roof slab and beams are adequately isolated from temperature changes.

The last example concerns the roof shell of an industrial building (Fig. 7.17). The right-hand end columns were conservatively reinforced to take the thrust due to the static load on the cylindrical shells plus lateral force due to earthquake. Yet they developed severe diagonal cracks that can only be attributed to differential temperature changes and differential shrinkage in the shell. The structure was covered with asphalt; the black color made it absorb a considerable amount of heat.

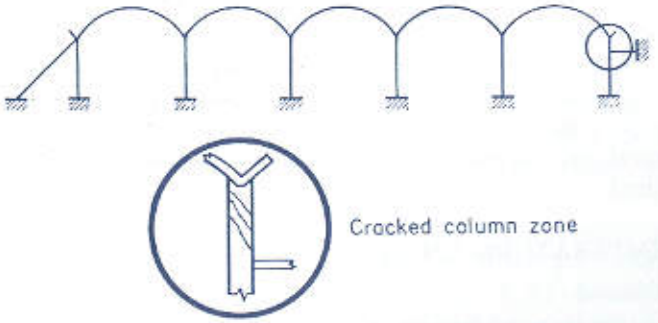

FIGURE 7.17. Roof shell of an industrial building.

Evidently temperature effects should not be taken into account in design by simple rules of thumb, which may err by orders of magnitude. The degree of exposure and the geometry of structures are variables that must be incorporated explicitly.

7.19.3 Quantitative Treatment

Theoretical studies are available on the evolution of temperatures inside structural members of various shapes when subjected to a specified history of external temperatures, such as a steady-state variation.[108] The step from the results of such studies to practical conclusions on the amount of steel required is still not easy.

7.20 SETTLEMENTS AND DESIGN OF FOUNDATIONS

7.20.1 Types of Settlement

The largest imposed deformations that we meet in practice are due to settlements. Three types of settlement will be distinguished (Fig. 7.18): maximum settlement, average tilt, and angular distortion. It is impossible to set absolute limits below which the various types will be acceptable. The "allowable" values contained in Table 7.2 are intended to serve as rough guides.

7.20.2 Maximum Settlement

The maximum settlement around the periphery needs to be limited because of possible damage to public installations and to adjoining structures. Depending on their state, an insignificant settlement may actually suffice to

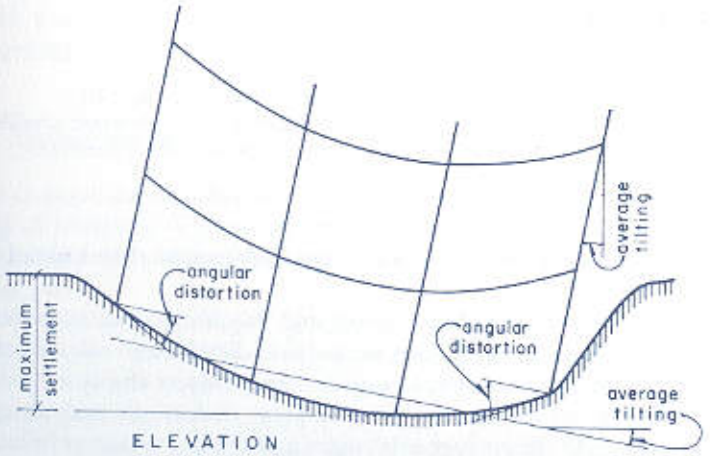

FIGURE 7.18. Types of settlement.

TABLE 7.2. Allowable Settlements.

Type of Settlement	Limit: Monthly Increment	Limit: Annual Increment	Limit: Total
Maximum settlement			
Damage to public utilities, cm	3.0	10	30
Damage to public utilities, in.	(1.2)	(4.0)	(12)
Damage to adjoining buildings, cm	1.2	4	10
Damage to adjoining buildings, in.	(0.5)	(1.6)	(4)
Average tilt, %			
Visible tilt	—	—	*
Transverse component of gravity	—	—	0.2α
Effects on machinery and equipment	—	—	0.1
Difficulties in crane girder operation	—	—	0.3
Angular distortion			
Cracking of plaster	0.2	0.25	0.3
Cracking of walls of light-weight concrete blocks	0.2	0.25	0.3
Cracking of walls of normal-weight concrete blocks	0.3	0.4	0.5
Cracking of walls of burned clay bricks	0.5	0.7	1.0
Serious damage to reinforced concrete frames	1.0	1.5	2.0

* $\frac{100}{100 + 3h} \cong \frac{100}{100 + h'}$

h = height of building in meters

h' = height of building in feet

if h tends to zero, the allowable tilt tends to 1%

if $h = 50$ m ($h' \cong 150$ ft), the allowable tilt = 0.4%

if h tends to ∞, the allowable out-of-plumbness tends to 33 cm (1 ft)

α = ratio of maximum story shear to weight of building above elevation considered; it is usually smallest at ground level where it equals the base shear coefficient.

damage them seriously, while a much larger settlement than quoted in the table may be innocuous.

Even in the absence of public utilities and adjoining structures there are reasons for limiting the maximum settlement. Settlement calculations are normally made treating the subsoil as of uniform compressibility in horizontal strata, which is not realistic. There are angular distortions and tilting that increase directly with the average settlement and are not apparent in ordinary computations. The ratio of differential to maximum settlement of spread

footings on sand is normally about 0.75.[109] A design method has been developed[110] to optimize the foundation depth of partially compensated foundations on clay taking into account the probability distribution of the tilt. It is assumed that the foundation is infinitely rigid and that losses due to average settlement and to tilt are proportional to the squares of these quantities. The method has also been put in deterministic format, in terms of "allowable" average settlement and tilt.

7.20.3 Tilting

Visibility of tilts to the naked eye depends on the existence of reference lines. At a contraction joint, small tilts in opposite senses are plainly visible, while an isolated building, 50 m tall, may tilt imperceptibly, perhaps by as much as 0.7% out of plumb as against 0.4% given by Table 7.2. Also, at a contraction joint, the danger of pounding may dictate the limiting tilt.

Even severe angles of tilt are usually small compared with the lateral accelerations, expressed as a fraction of gravity, that structures can withstand in seismic regions. However, if design takes advantage of moderate or large ductility factors, as it does to lower the required seismic coefficients, appreciable tilting will result in a nonlinear structure having asymmetrical yield points. For these systems the deformations are no longer, on the average, of the same order as those of equivalent linear systems but tend to grow systematically in the direction of lower yield strength. This is the reason for limiting the tilt in Table 7.2 as a function of the seismic coefficient that the structure would withstand if it were plumb.

Damage to delicate machinery, such as turbogenerators, may take place with such small angles of tilt as 0.02% while other pieces of equipment may escape unhurt through a rotation of 180°.

7.20.4 Angle Changes

Angular changes due to differential settlement are responsible for much major cracking of buildings. Yet we are far from having a quantitative means for predicting the extent of cracking and of other damage that differential settlement will cause.

In designing against collapse, ductility and the velocity of deformation are all important. A minor differential settlement is capable of exhausting the capacity of a beam to deform if it was on the verge of diagonal-tension failure, especially when the movement occurs rapidly. But a major angular change will not cause more than unsightly cracks in a very ductile structure; and the cracking will be less severe if settlement occurs slowly.

7.20.5 Orders of Magnitude

Despite all the uncertainties involved, orders of magnitude derived from experience deserve respect. No experienced designer would anticipate serious difficulties in an ordinary building where maximum settlement would not exceed 5 cm (2 in.), and he would be extremely cautious with one that was expected to settle more than 25 cm (10 in.).

7.20.6 Role of Foundations

Clear understanding of the consequences of differential settlements is essential in order to design a foundation sensibly. A foundation has two main functions to fulfill. Expressed in deterministic language: (1) distributing the load to the ground to prevent shear failures and excessive settlement, and (2) limiting displacements (especially differential settlements) to prevent damage in the superstructure and in nonstructural elements. Damage in the foundation, originating in its high rigidity and hence sensitivity to differential settlements, is normally of no consequence; damage to the superstructure, originating in excessive flexibility of the foundation, may be quite serious. A foundation is properly designed when it saves the building, be it at its own expense.

7.20.7 Design of Foundations

Many different methods are being used for the design of foundations. Some of them take into account bending moments of the order of millions of pound–inches while the rest neglect these moments, as aptly put by A. L. L. Baker.[15] The second category includes those methods which regard a foundation "as an inverted floor system" and assume that column bases are fixed in space. Such methods may lead to a satisfactory design if the foundation soil is sufficiently rigid; otherwise they produce unacceptably weak and flexible infrastructures.

The following approach may be used for surface and compensated foundations with or without friction piles.

1. Compute loads and bending moments transmitted by the superstructure to the foundation assuming that the latter is infinitely rigid. Computations may have to be carried out for more than one condition of loading.
2. Decide on an economical set of bending moment diagrams in the foundation girders. The diagrams should satisfy statical requirements consistent with the loads and moments of the first step and with a contact pressure distribution that nowhere gives contact stresses on the ground in excess of allowable values. It is often satisfactory to take for this step a uniform contact pressure and assume that the column bases do not move vertically.
3. Establish bounds on the settlements that the pressure distribution of Step 2 will produce on the ground. Due to uncertainties about soil properties and about the consequences of the excavation and construction procedures, more than one assumption must often be made about the compressibility of the soil at different points under the foundation in order to establish these bounds. ("Bounds" in the sense that the probability that they be exceeded is deemed adequately low.)
4. Decide whether these settlements and associated angle changes are sufficiently small not to cause excessive harm, as discussed above. Also verify that the required plastic-hinge rotations are not too large. If these conditions are fulfilled, design the foundation for the bending moment diagrams of Step 2 and for the corresponding shears and contact pressures, using the same load factors as are considered appropriate in design of the superstructure and providing adequate details to develop the ductility required in accordance with the calculated plastic-hinge rotation. If the differential settlements computed in Step 3 are too large, proceed with the following steps.
5. If the computed bounds on the differential settlements are orders of magnitude greater than allowable values, it may be concluded that contact pressure redistribution due to deformation of the foundation will not greatly affect the design. A rather rigid foundation will therefore be required. Under the assumption that the foundation is infinitely rigid, estimate the contact pressure distribution. Often it will be advisable to choose two extreme distributions in order to cover uncertainties in this respect; one distribution may arise, say, from preconsolidation of part of the site due to a former construction. For a partially compensated foundation on soft clay the two extremes may be a uniform distribution and the one shown in Fig. 7.19(a), while for a foundation on noncohesive material they may be again a uniform distribution and the one illustrated in Fig. 7.19(b), but entirely different distributions may be indicated in each particular case. If the computed differential settlements are not much greater than the allowable values, it is necessary to use a trial-and-error approach, anticipating at this step the results of Steps 6 and 7 and repeating Steps 5 to 7 if required.
6. Compute shears and bending moments in the foundation to satisfy statical requirements for the forces and moments of Step 1 and the contact pressures of Step 5. Incorporate the contribution of the superstructure to resist the ensuing deformations; rapid approximate methods are available for typical cases.[113] Compliance with statical requirements in the foundation may be accomplished in a number of ways; in any case an attempt should be made at this stage to approach the elastic solution. At every intersection of a column and two foundation girders running in different directions, one may allot part of the column load to one girder and the rest to the other; and where two girders intersect in the absence of a column, one may estimate the reaction between both girders, taking into account, in a rough manner, the

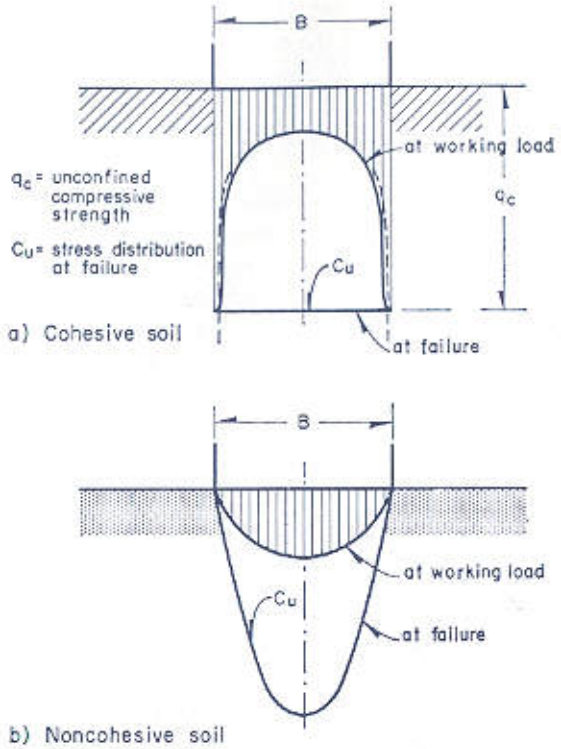

FIGURE 7.19. Extreme soil pressure distributions.

relative rigidities and the deformations imposed by other forces. Alternatively one may verify conditions of equilibrium at a number of sections through the foundation.

7. Check that the stresses, differential settlements, and plastic-hinge rotations associated with the computed moments and shears be acceptable; adjust areas of reinforcement accordingly, modify cross sections if necessary, and recompute shear and bending moments if the changes are sufficiently drastic to merit this. In this step one may assume that some girders (say, all those running in one direction and the end girders in the opposite direction) remain elastic and all the others develop plastic hinges; this may overestimate the required rotations; if the rotations exceed allowable values, attempt a second trial in which certain plastic hinges are introduced in the girders that had been assumed to remain elastic.

8. Complete the design for the conditions established in the last two steps. For this purpose use higher stresses and lower load factors than for design of the superstructure under static loads. Design details for the amount of

ductility required. Check also that the foundation be capable of taking one statically consistent set of shears and moments under statically applied loads, with the ordinary stress-reduction and load magnification factors; this condition may coincide with the solution found in Step 2, for example. If required, modify the design of the superstructure to make it capable of withstanding the imposed differential settlements without harm.

Some analytical difficulties may arise in Step 6 due to over-all torsion of the foundation. If the infrastructure consists of an orthogonal set of girders and has open sections, its torsional stiffness may be many times smaller than that in flexure. Over-all torsion will have to be resisted mostly by the superstructure, with the columns straining diagonally, especially those at and near the structures' corners; the floor systems are also strained diagonally.

The torsional stiffness of a closed box may compare with the girder's stiffness in flexure. The closed box may be furnished by the slabs and retaining walls of basements or by foundation cells. Since the torsional stiffness of individual members will be much smaller than that of the box it will ordinarily be acceptable under these conditions to assume in Steps 6 and 7 that the corners of the building remain fixed, design for the shears associated with the computed torsion, and verify that the torsional deformations are not excessive. In cases when the torque varies markedly along the foundation it may be justified to embark into an analysis involving combined torsion and flexure.[112]

Rather than resorting to a closed box it is sometimes advisable to introduce one or two diagonal girders in addition to the orthogonal system.

Rigid foundation elements, such as spread footings, on groups of point-bearing piles require attention to compatibility of the piles' deformations. Efficient methods are available[113] for computing the loads on the piles under these conditions. Foundation members between groups of point-bearing piles, on the other hand, are usually sufficiently flexible that the pile caps may be assumed not to suffer vertical displacement.

7.21 COMPRESSIVE STRENGTH OF CONCRETE

The most common index of the quality of concrete is its compressive strength as determined from standard tests on 6 in. × 12 in. cylinders. The corresponding coefficient of variation is sensitive to the degree of control and manner of mixing concrete. Typical values are given in Table 7.3.[114] These have been computed without reference to the specified strength. On the basis of the specifications for a given job, the contractor aims at a mean strength (higher than the one assumed in design), but the mean strength attained may differ substantially therefrom. If the coefficients of variation were computed

TABLE 7.3. Standards of Concrete Control.

Class of Operation	Coefficients of Variation for Different Control Standards, %			
	Excellent	Good	Fair	Poor
Over-all variations:				
General construction	below 10	10 to 15	15 to 20	above 20
Laboratory control	below 5	5 to 7	7 to 10	above 10
Within-test variations:				
Field control	below 4	4 to 5	5 to 6	above 6
Laboratory control	below 3	3 to 4	4 to 5	above 5

with respect to the mean strength assumed before the concrete was mixed, considerably higher values would be found.

From the frequency distribution of strengths in a particular job, Johnson[12] finds that high strengths are adequately represented by a normal distribution, but that the tail for low values, which is the most significant portion, departs from the Gauss curve and approaches an extreme distribution of type II with zero as minimum value. Freudenthal[23] concludes that the distribution is nearly lognormal under conditions of good control and that it is nearly extreme of type II, also with zero as minimum strength, under those of deficient control.

Differences between expected and actual mean strengths lead to larger dispersions in strength than ordinarily recognized. A formal Bayesian treatment of the probability distribution of strength with, say, an underlying extreme type II distribution having unknown mean and variance can, of course, be carried out, and the possible applicability of several distributions can be dealt with simultaneously. This is worth doing in large jobs and in the drafting of a building code. But the lack of analytical aids makes the general approach impractical for most jobs at present. Matters are greatly simplified if we take the logarithm of the strength to have a normal distribution with unknown mean but known variance, which is equivalent to specifying the coefficient of variation of strength. This, as we illustrated in Section 7.4, is sufficiently simple for practical purposes.

The ACI standards[114] use Student's distribution for concrete strength. The distribution is arrived at by the method of maximum likelihood assuming that the underlying population is Gaussian. As recommended in the Standards and applied in the Code[104] the resulting formulas are to be used only in conjunction with a large sample of test results. Assuming that the underlying

distribution is normal, the use of Bayes' theorem is not worthwhile under these conditions since it leads practically to the same results as the method of maximum likelihood. However, Bayes' theorem should be used when the sample is of limited size whatever the form of the underlying distribution.

Differences between core and cylinder strengths can be significant. On the basis of test results, Petersons[115] has proposed the relation

$$\begin{aligned} f_{co} &= f_{cy} && \text{when} \quad f_{cy} < 140 \text{ kg/cm}^2 \text{ (2 ksi)} \\ f_{co} &= 0.7 f_{cy} + 42 \text{ kg/cm}^2 \text{ (+0.6 ksi)} && \text{when} \quad f_{cy} \geq 140 \text{ kg/cm}^2 \end{aligned} \tag{7.24}$$

Here f_{co} is core strength and f_{cy} is the standard cylinder strength. Besides, for a given f_{cy}, f_{co} varies with position within a structural member; even in a beam it increases appreciably with distance from the top, and it is considerably more variable than f_{cy}.[115] Thus, if f_{cy} is practically uniform, Petersons finds that f_{co} exhibits a coefficient of variation of about 0.10. The coefficient of variation of strength in place can be estimated from

$$c_{co} \cong \sqrt{c_{cy}^2 + 0.10^2} \tag{7.25}$$

where c_{co} and c_{cy} are the coefficients of variation of core and cylinder strengths.[116] This expression is based on the assumption that f_{co}/f_{cy} and f_{cy} are independent variables and that $0.10\, c_{cy} \ll c_{cy}$. Other test results[117–19] do not confirm the numerical values in Eq. (7.25). There is need for considerably more research in this area.

Workmanship affects the dispersion of strengths as well as the quality of curing. The first matter can be recognized by choosing an appropriate c_{cy}, in accordance with Table 7.3, to enter Eq. (7.25). The effects of the quality of curing must be taken into account together with considerations on the duration of the aging process before the structure undergoes its first major loading. If, as is usual, this takes place long after the 28-day standard for cylinder tests, the effective strength may be associated with somewhat greater cylinder strengths than those derived from control tests. The net result is that the value of f_{cy} to use in Eq. (7.24) to obtain the expected f_{co} ranges from about 0.9 to about 1.0 times the control-cylinder strength. The latter value can be estimated from code[104] requirements and from the ACI recommended practice for evaluation of standard tests.[114]

The in-place strength must be further modified as a function of the rate of loading. Based on the expression[120]

$$f_c = f_{c1}(1 + 0.08 \log r) \qquad 0.1 \leq r \leq 10{,}000$$

where f_c is the strength at a rate of loading r (psi/sec) and f_{c1} is the strength for $r = 1$, Allen[116] has calculated the parameter of the probability distributions of the in-place strength for a variety of loading conditions and two qualities of workmanship.

Additional factors to consider in connection with in-place strength are the effects of the volume of material under stress and the stress distribution in the structural member in question. The classical statistical theories of strength of materials[3,112] are not strictly applicable to concrete, as its behavior is intermediate between those of perfectly brittle and plastic materials. Nevertheless, the statistical theory of brittle solids gives the correct form for estimating the influence of volume in geometrically similar specimens,

$$\frac{E(X)}{E(X_0)} = \alpha + (1 - \alpha)\left(\frac{V_0}{V}\right)^{\beta} \tag{7.26}$$

where X denotes the strength of a specimen, V is its volume, α and β are positive constants, and subscript 0 refers to a standard specimen.[121] We see that the expected strength of a specimen whose volume tends to infinity tends to $\alpha E(X_0)$. This is also the strength of the weakest constituent element of the material. Using V_0 as the volume of a cube 10 cm (4 in.) in side, it has been found empirically that $\alpha = 0.58$ and $\beta = 1/3$.[121] All the data plotted in the range $V > V_0$ fall above the line defined by Eq. (7.26). The same theory permits estimating the coefficient of variation of X as a function of V/V_0 given values of α and β. The probability distribution of X is extreme type II.

The influence of stress distribution, however, is not adequately predicted by the foregoing theory. A more promising approach lies in a conceptual model that idealizes concrete as a cubic lattice in which concentrated masses are connected to each other by linearly elastic rods along the edges and diagonals of the cubes.[122] The rod strengths are independent random variables. The model correctly predicts stress-strain curves under various states of stress as well as the probability distributions of strength. It is also useful for predicting the effects of transverse reinforcement on ductility.

The effects of repeated loading will be taken up subsequently.

7.22 TENSILE STRENGTH AND MODULUS OF ELASTICITY OF CONCRETE

7.22.1 Tensile Strength

For a given set of aggregates the tensile strength of concrete, as determined from split-cylinder tests, is nearly proportional to the square root of the compressive strength (Chapter 3). The relationship might lead to the conclusion that the coefficient of variation of split-cylinder test results should be about half that of compressive strength. However, a comparison of coefficients of variation of published test results[123] indicates that there is not much difference between those of tension and of compression; in fact, the former may be somewhat larger.[121]

Equation (7.26) applies at least as well to tensile strengths as to compressive strengths. Results of one series of experiments give $\alpha = 0.43$ and again $\beta = 1/3$ for V_0 the volume of a 10-cm (4-in.) cube.[121]

When tensile strengths are not directly controlled but assumed on the basis of compressive strengths, considerably larger dispersions can be anticipated relative to the expected strength.

7.22.2 Modulus of Elasticity

Essentially the same remarks apply to the modulus of elasticity as to tensile strengths. From the viewpoint of ultimate strength the precise modulus of elasticity of concrete is of little importance. But this variable affects to a large extent the deflections of reinforced concrete structural members and, even more, those of prestressed members. It is true that the consequences of excessive deflections usually involve economic losses several orders of magnitude lower than those due to collapse. But this does not justify replacing the modulus of elasticity of concrete with a deterministic value.

7.23 ULTIMATE STRAIN OF CONCRETE

The ultimate strain of concrete, ε_u, enters into calculation of the capacity of structural members under bending or combined bending and axial force as well as in the calculation of the amount of redistribution that can take place in statically indeterminate structures. However, these variables are not very sensitive to ε_u, so that a crude description of its probability distribution is adequate for most practical purposes.

Ultimate strain is chiefly a function of concrete strength, force eccentricity, moment gradient, amount of compressive reinforcement, rate of loading, and degree of transverse confinement. Taking into account only the concrete cylinder strength, the following expression has been proposed for the expected ε_u in unconfined concrete,[124]

$$E(\varepsilon_u) = 0.004 - 2.1 \times 10^{-6} f_{cy} \tag{7.27}$$

where f_{cy} is in kg/cm^2. (The coefficient of f_{cy} becomes 0.00015 when f_{cy} is in ksi.) The corresponding coefficient of variation is 0.12. These results were derived from tests on beams and columns lasting approximately from 15 min to 2 hr. Allen[116] assigns ε_u a normal distribution with expectation given by Eq. (7.27) and coefficient of variation 0.10, which is conservative for tests lasting around 15 min.

A comparable statistical study is not available for confined concrete.

7.24 YIELD POINT OF REINFORCEMENT

Based on available test results, the static yield stress of reinforcing bars can be assigned a normal distribution with expectation equal to 1.072 times the nominal yield strength and a coefficient of variation of 0.099.[118] Consequently the probability of not meeting the nominal yield stress is 24.9%.

Other data on structural steel[12,29] favor a skewed probability distribution, such as the lognormal, for the yield stress. The normal distribution proposed gives a good fit in the range of low experimental values, which is the most significant in design. However, even when samples from individual mills taken over a short time span have approximately normal distributions, the variations in the distribution parameters from one mill to another and from one time interval to another in a single mill, combined with a tendency toward truncation at very small yield stresses, introduce positive skewness in the over-all distribution.[125]

When the same metallurgical composition and rolling process are used for bars of different diameters, there is a marked tendency for the mean yield stress to decrease with bar diameter.[125] This is usually counteracted by using a different composition or process for different ranges of diameters.

The rate of loading affects the yield stress of ASTM A36 steel in accordance with the expression[116]

$$\begin{aligned} E(f_y - f_{y0}) &= 61(10^6\dot{\varepsilon})^{0.24} \qquad f_y \text{ and } f_{y0} \text{ in kg/cm}^2 \\ &= 0.87(10^6\dot{\varepsilon})^{0.24} \qquad f_y \text{ and } f_{y0} \text{ in ksi} \end{aligned} \tag{7.28}$$

where f_y is the yield stress at a strain rate $\dot{\varepsilon}$ in sec^{-1} and f_{y0} is the static yield stress. It seems reasonable to take the same coefficient of variation for f_y as for f_{y0}. Equation (7.28) indicates that in A36 steel, load durations of 4 to 10 sec, which are associated with wind gusts, give a load-rate increase of about 210 kg/cm² (3 ksi) over $E(f_{y0})$ while for earthquakes, which may be associated with load durations of the order of 1 sec in moderately tall buildings, the increase may be of the order of 300 kg/cm² (4.2 ksi).[116] The effect of strain rate on the yield stress of other grades of steel may be somewhat less pronounced.[126]

7.25 MODULUS OF ELASTICITY OF REINFORCEMENT

Based on test results, Allen[116] proposes a normal distribution for the modulus of elasticity of steel, with an expectation of 2.06×10^6 kg/cm² (29.2×10^3 ksi) and a coefficient of variation of 0.03. This variable is insensitive to strain rate within the range of interest in structural design. A more precise description of its probability distribution is not justified in view of the minor effects

it has on the behavior of reinforced concrete. However, a systematic overestimate is introduced in the moduli of elasticity of deformed bars when the cross-sectional areas are based on weight per unit length, and it is worth correcting for this factor. Accordingly, an expected modulus of 2×10^6 kg/cm² (28.3×10^3 ksi) may be realistic.

The modulus of prestressing steel is often 5 to 10% lower than that of reinforcing bars. Wire strands behave with even smaller effective moduli. Creep of prestressing steel must be taken into account in design. Available data[127,128] provide guides to estimate the expected modulus and the creep or relaxation parameters but comprehensive statistical studies are apparently wanting.

7.26 GEOMETRY

There are random discrepancies between actual and nominal cross-sectional dimensions of structural members, areas of reinforcing bars, position of reinforcement, and alignment of the members. The differences, expressed as percentages of the nominal dimensions, are generally not independent of these dimensions. Johnson[12] found that the differences between nominal and actual effective depths of slabs had practically normal probability distributions that were practically independent of the nominal depth. For bottom reinforcement this distribution had expectation zero. For top reinforcement the mean effective depth was about 0.9 cm (0.4 in.) smaller than nominal. For both types of reinforcement the standard deviation was about 1.0 cm (0.4 in.).

Based on these and other observations, on building tolerances, and on judgement, Allen assigns the actual effective depth of bottom reinforcement a normal distribution with expectation equal to d' and standard deviation of $0.025\,d' + 0.5$ cm ($0.025\,d' + 0.2$ in.), where d' is the nominal depth. To the width of beams he assigns a normal distribution with expectation equal to the nominal value and standard deviation 0.32 cm (0.125 in.).

It is reasonable to assign the effective depth of top steel a normal distribution with expectation $d' - 0.9$ cm and the same standard deviation as for the bottom steel. These distributions give an appreciable probability that code tolerances[104] not be met but they seem representative of standard practice. When special measures are taken to comply with structural drawings, the probability of an important discrepancy can be made to approach zero, as when especially rigid forms and reinforcement supports are used.

Discrepancies between actual and nominal cross-sectional dimensions of columns can be assigned the same probability distribution as beam widths. Vertical alignment of columns and bearing walls is also subject to discrepancy. It is reasonable to assign the difference between actual and nominal eccentricity of load the same distribution as to the discrepancies in beam widths.

TABLE 2.3. Sizes of Steel Wire Specified by ASTM.

A82[a]	A496[b]	Size No.	Nominal Diameter, in.	Nominal Area, in.^{2}	Unit Weight lb/ft
W0.5	—	0.5	0.080	0.005	—
W1	D1	1	0.113	0.010	0.034
W1.2	—	1.2	0.124	0.012	—
W1.5	—	1.5	0.138	0.015	—
W2	D2	2	0.159	0.020	0.068
W2.5	—	2.5	0.178	0.025	—
W3	D3	3	0.195	0.030	0.102
W3.5	—	3.5	0.211	0.035	—
W4	D4	4	0.225	0.040	0.136
W4.5	—	4.5	0.240	0.045	—
W5	D5	5	0.252	0.050	0.170
W5.5	—	5.5	0.264	0.055	—
W6	D6	6	0.276	0.060	0.204
W7	D7	7	0.298	0.070	0.238
W8	D8	8	0.319	0.080	0.272
—	D9	9	0.338	0.09	0.306
W10	D10	10	0.356	0.10	0.340
—	D11	11	0.374	0.11	0.374
W12	D12	12	0.390	0.12	0.408
—	D13	13	0.406	0.13	0.442
W14	D14	14	0.422	0.14	0.476
—	D15	15	0.437	0.15	0.510
W16	D16	16	0.451	0.16	0.544
—	D17	17	0.465	0.17	0.578
W18	D18	18	0.478	0.18	0.612
—	D19	19	0.491	0.19	0.646
W20	D20	20	0.504	0.20	0.680
—	D21	21	0.517	0.21	0.714
W22	D22	22	0.529	0.22	0.748
—	D23	23	0.541	0.23	0.782
W24	D24	24	0.553	0.24	0.816
—	D25	25	0.564	0.25	0.850
W26	D26	26	0.575	0.26	0.884
—	D27	27	0.586	0.27	0.918
W28	D28	28	0.597	0.28	0.952
—	D29	29	0.608	0,29	0.986
W30	D30	30	0.618	0.30	1.020
W31	D31	31	0.628	0.31	1.054

[a] Cold drawn smooth wire, used for welded steel wire fabric A185.
[b] Deformed wire, used for welded deformed-steel wire fabric A497.

TABLE 2.4. ASTM Requirements for Reinforcing-Bar Deformations.

Bar Designation No.	Maximum Average Spacing	Minimum Average Height	Maximum Gap (Chord of 12 1/2 % of Nominal Perimeter)
3	0.262	0.015	0.143
4	0.350	0.020	0.191
5	0.437	0.028	0.239
6	0.525	0.038	0.286
7	0.612	0.044	0.334
8	0.700	0.050	0.383
9	0.790	0.056	0.431
10	0.889	0.064	0.487
11	0.987	0.071	0.540
14	1.185	0.085	0.648
18	1.58	0.102	0.864

Shape of Stress-Strain Curve. Within the region of yielding, typical stress–strain curves for reinforcing steels can be generally classified either as "flat-top" (Fig. 2.4) or as "round-house" (Fig. 2.5) referring, respectively, to an abruptly yielding steel or a steel that strain-hardens as it yields. Most Grade 40 through Grade 60 reinforcing bars are basically carbon–manganese steels with a stress–strain curve that during yielding is either flat or only very gradually strain hardening during yielding. However, Grade 75 reinforcing bars generally achieve their superior strength through the addition of other alloying elements, which usually results in more of a round-house stress–strain curve. Generally wires also have a round-house stress–strain curve because their superior strength is mostly achieved through cold work.

Yield Strain. The desirability of having either a flat-top or a round-house stress–strain curve depends on the application of the steel. A round-house behavior could possibly result in more even concrete cracking during steel yielding,[6] which could conceivably be an advantage where some steel yielding cannot be avoided during the life of a reinforced concrete structure. However, a consistent proportional elastic limit, yield stress, and concomitant yield strain are easier to define for a flat-top steel than for a round-house steel. Also, the assumption of the elastic-pure plastic behavior, in which the proportional elastic limit and the yield point are the same and no strain hardening is assumed, leads to simpler design theories.

Consequently, most reinforced-concrete theories assume an idealized elastic-pure plastic stress–strain curve, and the validity of the ACI Code[7] ultimate-strength-design formulas for beams and columns depends on the

Bar specifications[129] allow a tolerance of 6% below nominal for the area of an individual bar and 3.5% the mean area in a lot of bars. Usually these limitations are amply met in practice; indeed, careless fabrication tends to produce oversized cross sections. We may assign this variable a normal distribution with mean equal to the nominal area and coefficient of variation of about 3% for an individual bar. We shall assume that the within-lot coefficient of variation is 2%. It follows that the coefficient variation of the lot means is approximately $(3^2 - 2^2)^{1/2} = 2.24\%$. Relative to the lot mean, the mean area of a bar has a coefficient of variation of $0.02/n^{1/2}$, where n is the number of bars in the lot, and relative to the nominal area the coefficient of variation is approximately $(5 + 4/n)^{1/2}\%$. Allen[116] assumes that the sum of the areas of tensile reinforcement at a beam cross section has a coefficient of variation of 1.5% independent of n.

7.27 STRENGTH OF REINFORCED CONCRETE MEMBERS

One approach to the calculation of the probability distribution of the capacity of reinforced concrete members consists in assuming that it is proportional to the product of powers of several random variables which are taken as independent of each other. Dimensional analysis sets certain restrictions on the variables and on their exponents. The logarithm of strength is then a linear combination of several independent random variables (the logarithms of the pertinent parameters). The situation lends itself to straightforward regression analysis.

Using this approach Zsutty[130] takes the ultimate moment, M_u, of a beam equal to a constant times the product of powers of the concrete cylinder strength, the steel yield stress, the area of reinforcement, and the width, b, and depth, d, of the beam. The expression for M_u can be put in the form

$$\frac{M_u}{bd^2 f_{cy}} = k\left(\frac{f_y}{f_{cy}}\right)^{\alpha_1} \rho^{\alpha_2} \tag{7.29}$$

where ρ is the ratio of steel and k and $\alpha_{1,2}$ are constants to be derived from the regression analysis. No discrepancy is assumed between nominal and actual dimensions because the analysis is done for laboratory specimens.

Shah[131] takes

$$\frac{P_u(1 + e'/d)}{bdf_{cy}} = k\left(\frac{f_y}{f_{cy}}\right)^{\alpha_1} (\rho + \rho')^{\alpha_2}\left(1 + \frac{e'}{d}\right)^{\alpha_3} \tag{7.30}$$

for tied columns, where e' is the eccentricity, P_u is the ultimate load, and $\rho + \rho'$ is the total ratio of steel. Tensile and compressive failures are treated separately.

This approach can be much improved by using formulas that reflect the nature of the phenomenon under study. One advantage then is that results can be extrapolated considerably outside the range covered by the test results analyzed, which is not the case for expressions of the form of Eqs. (7.29) or (7.30). Thus, for any positive α_2, Eq. (7.30) predicts that P_u tends to zero as $\rho + \rho'$ decreases indefinitely, which is obviously incorrect.

In order to apply the better approach, Allen[116] uses the expression

$$M_u = A_s f_s d\left(1 - \frac{\rho f_s}{2\alpha_t f_c}\right) \tag{7.31}$$

for tensile failures and

$$M_u = 2k_2 k(1 - k_2 k)\alpha_c b d^2 \tag{7.32}$$

for compressive failures, where α_c and α_t are empirical coefficients, f_c is the core strength of concrete, kd is the depth to the neutral axis, and k_2, the depth to the compression resultant divided by d, is given by

$$k_2 = 0.49 - 0.013 f_c$$

$\alpha_t f_c$ and $\alpha_c f_c$ are the mean stresses in the compressive stress block at failure. Accordingly, k is a function of $\alpha_c f_c$ as well as of ρ, of k_2, of the steel modulus, and of ε_u. The test results analyzed by Allen include only those of beams reinforced with steel having a well-defined yield plateau and in which the reinforcement did not develop strain hardening before failure of the beam. They exclude members having very small ratios of reinforcement, which often exhibit the phenomenon of "hyperstrength."[106] (The phenomenon can be explained on the basis of the statistical theory of plastic materials. In a region of constant bending moment the steel stress is a maximum at sections where the concrete has cracked. For ordinary laboratory beams the total length of cracks is much shorter than a standard specimen used for determining the steel yield stress. Hence, the expected yield stress in the beams exceeds the one found directly on the bars. Since the rate of variation of the reinforcement stress is highest in beams having very small steel ratios, and since the resisting moment arm, $k_2 k$ is close to d in these beams, test results interpreted in terms of the usual yield stress indicate a value of k_2 in excess of one for these members.)

The virtues of Allen's analysis stand out in the light of the dispersions that he obtains for the ratio of test to calculated ultimate moment. For tensile failures the coefficient of variation is 3.1% and for compressive failures it is 5.7%. These compare favorably with Zsutty's,[130] 6.4% and 11.2%, respectively. The difference is essentially due to the use of prediction formulas that reflect the nature of the phenomenon in question. Shah's[131] results for columns would surely be much improved by applying a similar analysis.

The purpose of calibrating prediction formulas against test results is to apply the formulas to the prediction of the behavior of prototypes. They are also useful for gaging the adequacy of expressions commonly used in design. Allen[135] uses a Monte Carlo technique to arrive at histograms of the ratio of "actual" to code ultimate moment assuming different rates of loading and qualities of workmanship. The code ultimate moment is computed from

$$M_u = A_s f_y d\left(1 - 0.59\frac{\rho f_y}{f'_c}\right) \tag{7.33}$$

where all quantities are assigned their nominal values. The ratios of reinforcement chosen do not exceed 0.75 ρ_b, where ρ_b is the balanced value, complying with the ACI Code.[104] A normal probability distribution is fitted to each histogram through the point of 1% and 10% probabilities of failure. For static loading and minimum workmanship it is found that the mean ultimate moments of the normal distributions exceed the code values by about 5 to 7% and that the coefficient of variation lies between 10% and 21%. Within these ranges, conditions are more favorable for the deeper beams and for those having the smaller percentages of reinforcement. With good workmanship the mean ultimate moment is 7 to 10% higher than the code value and the coefficient of variation lies between 9% and 14%. For higher rates of loading the ratio of ultimate to code moment increases, particularly for the shallower beams, for which it becomes approximately equal to 1.3. Surprisingly, with 0.75 ρ_b as ratio of reinforcement, and even with 0.54 ρ_b, there is a high percentage of compression failures particularly in conjunction with minimum workmanship. This is due to the randomness of the variables involved.

The conclusion that the expected ultimate moment systematically exceeds the code value seems to stand in contradiction with the Monte Carlo study by Borges and Butler,[132] who find that the expected strength of a beam is appreciably smaller than that of a fictitious beam having the mean mechanical properties throughout. However, we should recognize that nominal values used in the code formula are conservatively biased and that the empirical coefficients α_1 and α_2 already take care of randomness along the beam while Borges and Butler analyze members made up of randomly independent segments.

The prediction formulas used by Zsutty and Shah, despite their shortcomings, provide good approximations to the test results considered in their studies. In both cases the strength is given by the product of several independent variables having well-behaved distributions. Hence, the strength can be expected to have practically a lognormal distribution. This is indeed the case for beams as well as for columns. Accordingly, the interpretation of

histograms resulting from Monte Carlo studies would be more properly achieved by fitting lognormal rather than normal distributions.

Allen's analysis could also be improved and extended by taking into account size and stress-gradient effects through the use of advanced statistical theories of the strength of materials; by incorporating the effects of design round-offs to whole numbers of bars, commercially available bar sizes, and rounded-off cross-sectional dimensions, as has been done in Monte Carlo studies on the reliability of timber structures;[133] by recognizing the exercise of job inspection and control, which do away with a large fraction of the exceptionally low values; and by dealing explicitly with the effects of repeated loads.

Comparable analyses are not available for other modes of failure nor for other types of structural members. Often, design formulas, such as that in the ACI Code[104] for shear in beams and other formulas contained in the earlier chapters of this book, are simple algebraic approximations to a "lower envelope" of test results. They come close to a curve marking the expected value of strength minus some factor times the standard deviation. If the third and higher moments of the probability distribution of strength, normalized with respect to its expectation, do not vary greatly with the design parameters, these formulas furnish approximations to strengths associated with a constant, relatively small probability of failure. The relationship of this practice with the use of local factors and with structural reliability will be taken up later. The assumption concerning the higher moments of the distribution of strength is probably met in practice, since strength in general can be expected to approach a lognormal distribution for the reasons given in connection with ultimate moment.

Before moving to other questions it is worth pointing out the advisability of specifying strict tolerances on steel yield *forces* and adopting a lenient practice for yield stress and cross-sectional area. Thus one can obviate unnecessary rejection of some bar lots. The effects of having a smaller area with the correct yield force are small on the shear, torsional, and anchorage capacities of structural members as well as on their deflections, and they are negligible on the ultimate moment and axial load. Such specifications should be supplemented with a limitation on the maximum yield force, so as to decrease the probability of brittle failures in modes other than tensile failures in flexure. When the steel is supplied by weight the contract should also include a clause limiting the maximum allowable cross-sectional areas of bars.

7.28 DEFLECTIONS

Code formulas for calculating deflections[101] are based on many simplifying assumptions. Nevertheless they can be expected to provide estimates of

expected deflections which are only slightly biased to overestimate them for the bare structure under the conditions most often met in practice, since the formulas have been adjusted to do so.

In special cases it is important to take into account deflections not due to flexure, such as those produced by shear in very short spans and in I beams or deflections due to shrinkage in beams whose reinforcement is grossly asymmetric. The shearing deformations of beam–column intersections can also be significant in buildings subjected to lateral loads. In actual buildings, though, these calculations of deflections often overestimate them appreciably because they ignore the contribution of floor finish and other "nonstructural" elements. The latter remark is borne out by the results of natural period measurements in buildings (Section 7.14).

For loads not producing yielding of the reinforcement one would expect the deflections of bare structural members to be approximately lognormally distributed, with a coefficient of variation somewhat greater than for ultimate moment (say, 20 to 30%). A much wider spread can be expected at higher loads.

The desire to limit deflections under static loading is based mostly on considerations of appearance, damage to nonstructural elements, vibrations under live load, and the danger of instability by ponding. Since the magnitude of deflections visible to the naked eye is an increasing function of the span but sufficiently small deflections cannot be detected, independently of the span length, some codes specify allowable deflections which are a constant plus a fraction of the span between supports[134] or of the span between points of inflection[105] while the ACI Code[104] fixes them as a fraction of span between supports. The phenomenon of arching in plastered partitions would also favor the specification of a constant plus a fraction of the span between inflection points. The possibility of damage to a partition standing under the beam or slab would lead to specifying an absolute limit rather than a function of the span. And several of the consequences of excessive deflections can be obviated by using adequate cambers.

Criteria are available, based on experimental data, for establishing limits of perception and of tolerance to vertical steady state vibrations and to those caused by traffic[135] as well as to wind induced oscillations.[136] Drift limitations in earthquake resistant design, however, are fixed arbitrarily by many building codes and by current practice.

7.29 DUCTILITY

For beams failing in flexure the ductility ratio can be defined as the ratio of the curvature at ultimate moment to the curvature at yield. The following expression has been derived[50] for calculating the ductility ratio, in this sense, in under-reinforced beams,

$$\mu = \frac{\varepsilon_u}{\varepsilon_y}\frac{1 - k_c}{q_u} \tag{7.34}$$

where μ is the ductility ratio, ε_u is the ultimate concrete strain, equal to 0.004 under short-term loading, ε_y is the yield strain of steel, n is the modular ratio, ρ, ρ' are the tensile and compressive ratios of reinforcement, and f_u is the average compressive stress in concrete, equal to $0.7 f_{cy}$ if $f_{cy} \leq 350$ kg/cm² (5 ksi), and equal to 70 kg/cm² (1.5 ksi) + $0.4 f_{cy}$ if $f_{cy} \geq 350$ kg/cm² (see Fig. 7.20). The formula is in good agreement with test results. A threefold increase in ε_u is attained by confining the concrete, for example through the use of helical reinforcement or closely spaced ties.[137]

$$k_c = \sqrt{\rho n^2 + 2\rho n} - \rho n$$

$$q_u = \frac{(\rho - \rho')f_y}{0.7 f_u}$$

Allen[116] has performed a Monte Carlo analysis for ductility ratio as given by Eq. (7.34) with $\rho' = 0$, parallel to that for ultimate moment. He finds a much wider spread than for ultimate moment (coefficients of variation of 20 to 40%); small sensitivity to loading rate; a direct dependence of μ on the quality of workmanship; and an appreciable number of very low values [40 to 60% of that predicted by Eq. (7.34)] due to compressive failures even when ρ does not exceed 0.75 ρ_b. The probability distributions of μ are positively skewed and sometimes bimodal. He also finds that Eq. (7.34) is a better predictor than the formula in the ACI Code,[104] which errs on the unsafe side. Still, this analysis disregards the spreading of plastic hinges and the effects of strain hardening, of transverse reinforcement, and of details.

The ductility ratio cannot be expected to give more than a rough measure of ductility. It is true that Eq. (7.34) is conservative when compared with the results of a few cycles of loading provided the anchorage and splice details are exceptionally well designed,[50] but it does not give information about the effects of a moderate number of cycles nor about the shape of the descending branch in moment–rotation curves. The latter allows greater redistribution of moments, and hence a greater capacity of statically indeterminate members, than can be predicted by theories that assume failure takes place as soon as one section reaches its ultimate moment.[138]

Several code formulas are based exclusively on strength. By disregarding the effects of design parameters on ductility they lead to designs with uneven degree of safety or variable expected consequences of failure. This is the case with the ACI Code[104] requirements for the design of slender beams which may undergo nonlinear lateral buckling. The ductility of slender beams can be

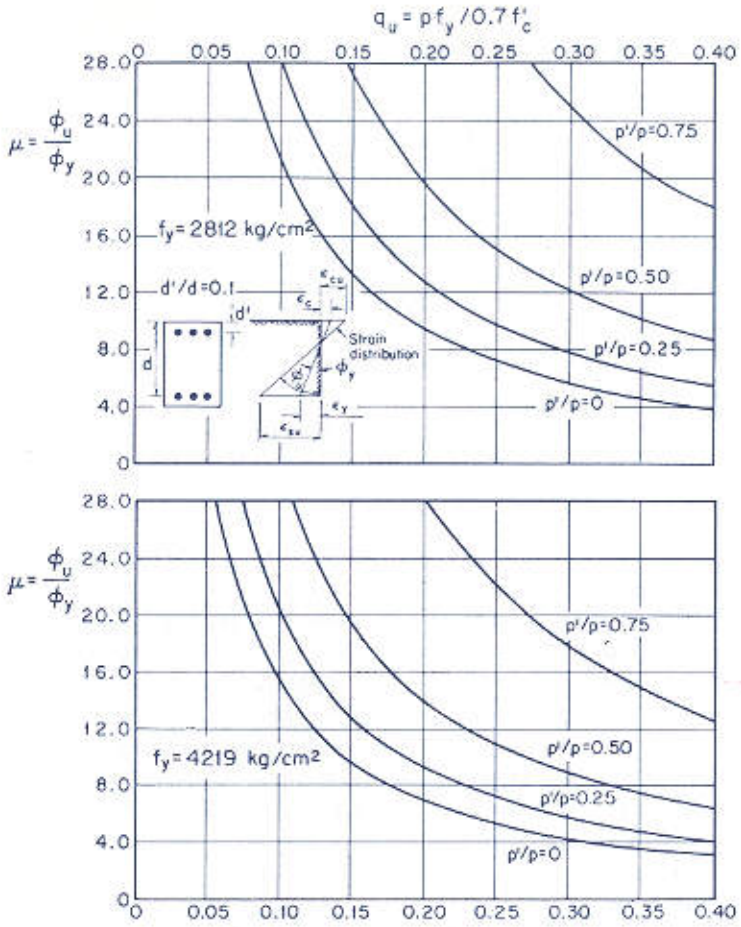

FIGURE 7.20. Variation of the ductility factor for beams of unconfined concrete with respect to q_u.[50]

much lower than that of beams of ordinary dimensions, but this fact is not reflected in the code requirements.

7.30 CRACKING OF STRUCTURAL MEMBERS

The width of cracks in reinforced concrete members depends on a great many variables and is characterized by a large dispersion in nominally identical specimens. The phenomenon is complicated and there are, apparently, no satisfactory theories to predict it. One simplified theory that explains the effects of the most important variables is found in Reference 139.

Empirical and semiempirical studies have led to a wide variety of formulas for predicting mean crack width. It is found that mean and maximum widths in a member are practically proportional to the steel strain at sufficiently high strains.[139–143] They increase either with the fourth root of the area of concrete surrounding the steel[139,143] or with the cube root of the product of these quantities.[142] The frequency distribution of crack widths in nominally identical specimens subjected to the same loading is very nearly Gaussian with a coefficient of variation of 0.42, so that the width of one crack in a hundred exceeds twice the mean width.[143] These studies neglect the influence of shrinkage on cracking, which may be important at low computed steel stresses.

There is considerable discrepancy concerning "allowable" crack widths. American practice[104] implicitly tends to limit the *average* width at the tensile face to 0.32 mm (0.013 in.) in exterior and 0.41 mm (0.016 in.) in interior members while the European Concrete Committee[142] recommends a *maximum* width, at the level of reinforcement, of 0.1 mm (0.004 in.) in aggressive corrosive atmospheres, 0.2 mm (0.008 in.) in exterior members, and 0.3 mm (0.012 in.) in interior protected members. Since these widths are at the faces of structural members, they are related with appearance rather than with the possibility of corrosion. The dependence on exposure leads to limits on a quantity that is only remotely related to the danger of corrosion.

A few available data[145] indicate that crack widths of as much as 0.25 mm (0.010 in.) at the faces of exterior members do not favor corrosion provided the concrete is dense and the cover is not less than 1.3 cm (0.5 in.). Results of a research project[146] indicate that corrosion is as adequately obviated by dense uncracked concrete 1.1 cm (7/16 in.) thick as by a thicker cover and it is inadequately prevented by porous or severely cracked concrete whatever its thickness. It follows that concrete covers in excess of about 1.3 cm (0.5 in.) are useless for the prevention of corrosion.

7.31 FATIGUE

Depending on the magnitude of the disturbance applied we speak of *low-cycle fatigue* when the disturbances are so high that the number of load cycles required to cause failure is not more than a few dozen, or of *fatigue proper* when that number is of the order of hundreds or more.

There is some information on low-cycle fatigue[36,50,147] but not enough to derive frequency distributions of the number of cycles to failure. When repeated loading is not associated with large-scale stress reversal, the mechanisms of failure are usually the same as under static loading, and the reductions in structural capacity and in ductility factor do not exceed a few percent. Under large-scale stress reversals there may be qualitative changes in the failure mechanisms, and the reduction in capacity or in ductility factor may be

significant. For example, when a reinforcing bar that has yielded in tension is subjected to compression, the cracks that made the yielding possible tend to close, and the spacing of ties that would have been adequate under monotonic loading may prove insufficient to prevent bar buckling. In general, the possibility of these changes in failure mechanisms is recognized by changes in detailing rather than by modifications in load factors or in the amount of reinforcement. Some considerations of this nature will be made when we deal with design details.

Failure in fatigue proper takes place by the progressive spreading of cracks in the concrete or in the steel. Most studies on the reliability of specimens and structural members subjected to repeated loads refer to the condition in which the applied load varies periodically between two fixed levels. Except for the gain of strength of concrete with time, the corresponding hazard function should be monotonically increasing. Hence, such failure probability density functions as the lognormal, which lead to hazard functions that increase and then decrease with time, are not acceptable for large values of t despite their popularity in the literature, which hinges on their providing good fits to short-range experimental data.

A satisfactory stochastic model[148] assumes that the expected increment of crack penetration during an application of load is proportional to the depth already penetrated by a crack. Assuming further that the maximum expected increment is much smaller than the crack depth which produces failure, a failure probability function is obtained which agrees closely with many available data on plain concrete prisms, prestressed concrete beams, and aluminum specimens. The corresponding hazard function increases monotonically with time.

Data on fatigue are usually obtained in the laboratory for periodic loading between two fixed limits. It is desirable to be able to compute, from these data, the reliability of a structural member subjected to a complicated program of loading or to a stochastic one. The most widely used deterministic model for this purpose is the Palmgren–Miner assumption, according to which a specimen fails when

$$\sum_i \frac{n_i}{N_i} = 1 \tag{7.35}$$

where n_i is the number of load cycles applied of the ith type and N_i is the number of those cycles that would cause failure under a periodic loading program. Experimental data indicate that the approximation is roughly correct for most materials of interest under a very irregular loading sequence in the range of low-cycle fatigue but gives large systematic errors for programs in which high loads prevail in the first stages and small loads in the rest or viceversa. Accordingly, modified versions of Eq. (7.35) have been proposed, some of which take into account the order in which loading cycles are applied.[147,149,150]

Still assuming that the specimen properties are deterministic, expressions have been found for the expected life and variance making the Palmgren–Miner assumption under random loading.[151]

7.32 OPTIMIZATION

7.32.1 General

We have given a cursory view of the actions to which structures are subjected and of structural properties, with emphasis on the probability distributions of the pertinent variables. It is time to look again at the purpose of all this. We wish to compute reliabilities in order to arrive at the expected losses due to damage and failure and the expected benefits to be derived from the existence of the structure under consideration. Combining these with the expected initial cost of the structure we have a basis for choosing the best—the optimum—alternative.

Our choice should be the best, among the available alternatives, in the light of all the objectives that we may have. But a general approach to the task of comparing—of ordering—requires that we measure all the alternatives in terms of our preferences, by means of a scalar. We shall call this measure of preference *utility*.

7.32.2 Utility

In order to measure utility we shall introduce the following relations; xPy means "alternative x is preferred to y;" $x\bar{P}y$ means "x is not preferred to y;" and xIy means "the subject is indifferent between alternatives x and y." The simultaneous propositions $x\bar{P}y$ and $y\bar{P}x$ imply xIy. We shall require that these relations operate according to certain rules: given any two alternatives x and y, either xPy or $x\bar{P}y$ is true, and at least one of the propositions $x\bar{P}y$, $y\bar{P}x$ is true; and the simultaneous propositions xPy and yPz imply xPz, and similarly for the relations $\bar{P}$ and I.

Given a set of alternatives we shall assign to each a *utility* u_i, such that $u_i > u_j$ if iPj, and $u_i = u_j$ if iIj. Then $i\bar{P}j$ implies $u_i \leq u_j$. Let there be n alternatives ordered so that $1\bar{P}2\bar{P}\cdots\bar{P}n$. We choose u_1 and u_n arbitrarily subject only to the condition $u_1 < u_n$ if $nP1$, and $u_1 = u_n$ if $nI1$. Following Von Neumann and Morgernstern[152] we devise a lottery such that the probability of alternative 1 is α while that of alternative n is $1 - \alpha$ and find that value of α for which the subject is indifferent between alternative i and the lottery. Then,

$$u_i = \alpha u_1 + (1 - \alpha)u_n \tag{7.36}$$

In this manner we assign utilities to all the alternatives. This method has been proposed in connection with structural design.[4] [There are some practical difficulties associated with the application of Eq. (7.36). Though having its own shortcomings, Churchman–Ackoff's method[153] circumvents these difficulties.]

According to Eq. (7.36), the utility associated to a decision that may have one of several possible outcomes is the expected value of the corresponding utilities. Once a set of utilities $\{u_i\}$ has been assigned it can be transformed into $\{au_i + b\}$, where a and b are constants and $b > 0$, without changing the ensuing decisions.

For most commodities, including money, the utility increases more slowly than does the amount of the commodity (Fig. 7.21). However, over a small range of variation relative to the maximum loss that the subject can suffer, the relation is almost linear. Thus, for an individual whose maximum possible loss barely exceeds \$100,000, a probability of 10^{-3} of losing \$100,000 is much worse than the loss, with certainty, of \$100. But he is practically indifferent between a probability of 10^{-3} of losing \$100 and the certainty of losing \$1.

Before assigning utilities we must decide for whom we wish to optimize: who the subject is, whether the owner, the user, or society. Usually the answer is that the utility should be a weighted factor of the utilities of these subjects. Once the point has been settled it is an easy task to assign utilities to material benefits and losses. "Intangibles" present a difficult problem, though. A guide in solving it is found in answers to the question, how much is the subject willing to pay to obtain this benefit or to avoid this loss. Thus,

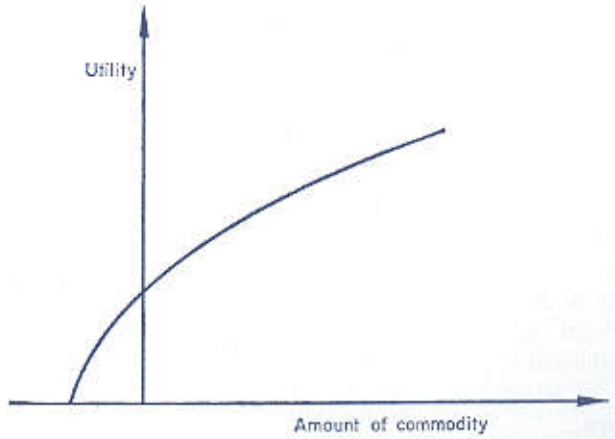

FIGURE 7.21. Utility as a function of the amount of a commodity.

rather than asking what the value of a human life may be, we do well to ask how much society is willing to pay to save a human life. Studies of behavior indicate that society is willing to pay, approximately, the expected present value of an average individual's contribution to gross national product.[154] Loss of prestige accompanying a structural failure involves a utility loss at most equal to that associated with the loss of a human life. And so on.

7.32.3 Objective Function

An objective function is any monotonic function of utility. Maximizing utility is equivalent either to maximizing or to minimizing an objective function. These functions are chosen so that they offer computational advantages over the direct consideration of utility.

One convenient objective function in structural design is

$$Z = B - C - D \tag{7.37}$$

where B is the benefits derived from the existence of the structure, C the initial cost, and D the cost of damage or failure.[155] All quantities are expected present values and, usually without undue error, B and C can be expressed directly in monetary units while, if the losses caused by failure, in case failure occurs, are appreciable compared to the subject's maximum possible loss, a correction must be applied to this term to account for the curvature in the relation between utility and money. Often, the expected benefits derived from the existence of the structure while the structure survives undamaged are practically independent of the design parameters. The objective function can then be taken advantageously as $C + D$ and it is to be minimized.

In the rest of this article the word *failure* will denote any form of failure or damage.

In Eq. (7.37), if we assume that there can be only one mode of failure and that the structure ceases to be of service after it fails, we can write

$$B = \int_0^\infty bRg\, dt \tag{7.38}$$

and

$$D = \int_0^\infty Hfg\, dt \tag{7.39}$$

where b denotes the expected benefits per unit time (say, the rent produced by a building for the owner, after deducing maintenance and operating costs), R is the reliability, g a discount function, H the loss due to failure in case of failure, and f the failure probability density function. An expression similar to Eq. (7.38) can be written for C but is not worth considering when the

construction takes a relatively short time. We shall take the discount function to be of the form

$$g(t) = e^{-\gamma t} \tag{7.40}$$

where γ is a constant. This corresponds to operating at a constant rate γ of continuous compound interest and hence is of fairly general applicability. Under special circumstances other discount functions are more in order.

7.32.4 Structural Reliability Optimization

Consider the problem of choosing the structural parameters so that the resulting utility is a maximum. Suppose first that the structure can either fail upon completion or not at all. This is often a reasonable idealization of structures subjected essentially to permanent loads provided the effects of sustained loads do not lower the structural capacity too rapidly. If the structure is built in a relatively short time the discount function can be taken equal to 1. Then we may write Eq. (7.37) in the form

$$Z = B^*R - C - HF \tag{7.41}$$

$$= B^* - C - (B^* + H)F \tag{7.42}$$

where B^* is the expected benefits that the structure would produce if it never failed.

Let X and S denote the strength and forcing functions at $t = 0$ and let x and s denote nominal values of these variables (they may be the corresponding expectations, or the "guaranteed minimum" strength and "maximum probable" load, etc.). It is desired to find x for which Z is a maximum, so that $dZ/dx = 0$ with $d^2Z/dx^2 < 0$.

This solution assumes that the structure is destroyed or abandoned after failure. Alternatively we may consider the policy of reconstructing or repairing the structure systematically whenever it fails. If we compute the prior probability of failure, F, from such strong beliefs that the occurrence of failure does not modify its value as obtained from Bayes' theorem, Eq. (7.41) must be replaced with

$$Z = B^* - C - (C + H)\sum_{i=1}^{\infty} iF^iR$$

$$= B^* - C - \frac{(C + HF)}{1 - F} \tag{7.43}$$

By comparing the optimal values of Z for the two policies we find that it is always advisable to rebuild the structure. This conclusion implies that the structure should be rebuilt without change in its design, which seems absurd. The paradox stems from the unrealistic assumption that the designer's

estimate of F is not modified by the structure's failure. Actually F is obtained from the probability distributions of S and X, and the parameters of these distributions are uncertain. In practice, the information gained from the occurrence of failure does change the estimate of F. A solution is available in which this information is formally incorporated.[155] A more realistic treatment would recognize that structural failure ordinarily prompts a study to revise the probability distribution of S and X.

From the viewpoint of design these considerations are usually unimportant. The optimum failure probability is in most cases so small that the denominator $1 - F$ in Eq. (7.43) can be replaced with 1.

Using formulations that differ slightly from the one presented here, the optimum x has been computed for a number of cases[3,12] in which X and S have normal, extreme, and lognormal distributions. Usually results are given in the form of charts for the optimal load factor, $v_0 = x_0/s$, where subscript 0 identifies optimal values. Often the nominal values are *central*, that is, expectations, modes, or medians of the variates, and it is assumed that C is a linear function of v:

$$C = a + cv \tag{7.44}$$

Here a and c are constants. This expression is usually sufficiently accurate in the range of v having practical interest.

It is often reasonable to approximate the lower tail of the failure probability distribution by the expression

$$F = \alpha e^{-\beta v} \tag{7.45}$$

where α and β are constants. It has been shown that Eq. (7.45) furnishes a close approximation under a wide variety of practical conditions.[156]

Assuming that B^* and H are not affected by v, Eq. 7.42 gives

$$\left.\frac{dC}{dF}\right|_{F_0} = B^* + H \tag{7.46}$$

Substituting Eqs. (7.44) and (7.45) into (7.46) supplies the optimum factor of safety and probability of failure:

$$v_0 = \frac{1}{\beta}\ln\frac{\alpha}{F_0} \tag{7.47}$$

$$F_0 = \frac{c}{\beta(B^* + H)} \tag{7.48}$$

In the case of systematic reconstruction, sufficiently accurate results are obtained by replacing $F_0/(1 - F_0)$ with F_0, which leads to

$$F_0 = \frac{c}{\beta(C_0 + H - c/\beta)} \tag{7.49}$$

in place of Eq. (7.48). This expression combined with Eq. (7.47) can be solved by iteration.

For a typical office building having a reinforced concrete frame it was found that $\alpha \cong 2$, $\beta \cong 2.5$, and $(B^* + H)/c \cong 1000$. Consequently, from Eqs. 7.47 and 48, $\nu_0 \cong 3.4$ and $F_0 \cong 4 \times 10^{-4}$. (This is the optimum probability of structural failure for the example chosen. Smaller values are optimum for individual members.) Very little difference was found when using Eqs. (7.47) and (7.49).

When the policy of systematic rebuilding is adopted we find

$$Z = B^* - C - (C + H)F^* \tag{7.50}$$

and

$$F^* = \sum_{i=1}^{\infty} \int_0^{\infty} f_i g \, dt \tag{7.51}$$

where, in turn, f_i is the probability density function of the time to the ith failure. Equation (7.50) is of the same form as Eq. (7.42) if $B^* + H$ is replaced with $C + H$ and F with F^*. Thus, optimization in design when R is a time function can be treated in the same manner as when it is time independent.

Consider now the case in which the disturbance is a generalized Poisson process with rate of occurrence $\lambda(S)$ while the distribution of X is time independent. Here $\lambda(S)$ is the *rate*, or expected number of times that S will be exceeded per unit time, and $1/\lambda(S)$ is the mean *recurrence period*. Then, from Eq. (7.6),

$$\begin{aligned} R(t) &= \int_0^{\infty} e^{-\lambda(u)t} p_X(u)\, du \\ &= E_X(e^{-\lambda t}) \end{aligned} \tag{7.52}$$

where $E_X(\cdot)$ denotes expectation with X as the random variable. Similarly,

$$f(t) = E_X(\lambda e^{-\lambda t}) \tag{7.53}$$

In this case the risk function [Eq. (7.9)] is time independent and equal to λ if X is deterministic, and it is a decreasing function of time when X is random. It can also be shown that $u(t)$ is nonincreasing when the probability distribution of X and S are time independent and the disturbances are stochastically independent.[155]

Suppose that the system is not to be rebuilt after failure. Let g be $\exp(-\gamma t)$ and let b and H be time independent. Then Eq. (7.37) gives

$$Z = E_X\left(\frac{b - H\lambda}{\gamma + \lambda}\right) - C \tag{7.54}$$

When the structure is to be systematically rebuilt, we find from Eqs. (7.50) and (7.51) that[155]

$$Z = \frac{b - (C + H)E_X(\lambda)}{\gamma} \tag{7.55}$$

The foregoing results have also been derived using the theory of Markov processes.[157]

In Eqs. (7.54) and (7.55) it is convenient to write $E_\xi(\cdot)$ for $E_X(\cdot)$ and to put $\lambda(X)$ in the form $\lambda(\xi x)$, in which $\xi = X/x$. In some problems, such as the earthquake resistant design of office and apartment buildings, $\lambda(\xi x)$ may be approximated by $A\xi^{-r}x^{-r}$, where A and r are constants, r lies between 2 and 3, and x is a quantity such as the design spectral pseudovelocity or the design base shear coefficient.[158] Assume that $\lambda \ll \gamma$ and that H is independent of x. If $\phi = E(\xi^{-r})$ and if Eq. (7.44) applies, Eq. (7.54) can be written in the form

$$Z = \frac{b - A\phi H x^{-r}}{\gamma} - a - cx$$

so that $dZ/dx = 0$ leads to

$$x_0 = \left(\frac{A\phi H r}{c\gamma}\right)^{1/(r+1)} \tag{7.56}$$

Assuming that $cx_0 \ll H$, Eq. (7.55) gives rise to Eq. (7.56) with H replaced by $a + H$. The latter assumption can be waived using an iteration procedure.

The optimal x_0 is associated with

$$\lambda_0 = \lambda(\phi x_0) = (A\phi)^{1/(r+1)}\left(\frac{c\gamma}{Hr}\right)^{r/(r+1)} \tag{7.57}$$

When $\ln \xi$ is normally distributed with expectation $\ln \tilde{\xi}$ ($\tilde{\xi}$ is the median of ξ) and standard deviation σ, we find

$$\phi = \tilde{\xi}^{-r} e^{-r^2\sigma^2/2} \tag{7.58}$$

The assumption concerning the distribution of ξ is often justified in earthquake resistant design. In general, we can write

$$\xi = \prod_i \xi_i(y_i/\tilde{y}_i) \tag{7.59}$$

where the y_i's are design parameters (strength, damping, natural period, ductility factor, etc.) and $\tilde{y}_i = \exp[E(\ln y_i)]$. If the number of such parameters is large, if they have reasonably well behaved distributions, and if most of them are relatively independent of each other we may assume $\ln \xi$ to be

normally distributed, with median $\tilde{\xi} = \exp\left(\sum_i \ln \tilde{\xi}_i\right)$ and variance

$$\sigma^2 = \sum_i \eta_i^2 \operatorname{var}\left(\ln \frac{y_i}{\tilde{y}_i}\right)$$

where $\tilde{\xi}_i = \xi_i(1)$ and $\eta_i = d\,(\ln \tilde{\xi}_i)/d[\ln (y_i/\tilde{y}_i)]$ at $y_i = \tilde{y}_i$. In moderately damped structures, $\eta_i = 1$ when y_i represents strength; for mass and stiffness, respectively, $\eta_i = \pm 1/2$ times the value corresponding to natural period; and for the damping ratio, $\eta_i = -0.4$, provided the natural period is not too short.

As an example, suppose that x stands for design base shear coefficient, $A = 3 \times 10^{-3}$ yr^{-1}, $r = 2.5$, $H = \$200{,}000$, $\gamma = 0.06$ yr^{-1}, $a = \$20{,}000$, $c = \$50{,}000$, $\tilde{\xi} = 1$, and $\sigma = 0.2$. We find $\phi = 1.133$. In first approximation, according to Eq. (7.56) when the structure is not to be rebuilt, $x_0 = 0.850$, while if it is to be rebuilt systematically, $x_0 = 0.873$. The iteration procedure gives $x_0 = 0.922$ in the latter case and is associated with $\lambda_0^{-1} = 81.3$ yr as optimum return period.

We can also waive the assumption $\lambda \ll \gamma$ if we specify b, evaluate Eq. (7.54) numerically, and find x_0 by trial and error. In this manner, when $b = \$3000$ yr^{-1}, the policy of no reconstruction yields $x_0 = 0.900$.

As is common in optimization problems, Z_0 is almost insensitive to x within the range of interest.

An extension of this approach can be used to decide when we should provide different lines of defense ("defense plateaus") such as the use of weak, almost dispensable partitions.[155]

7.32.5 Optimum Reliabilities of Structural Members

Consider a statically determinate structure subjected to a set of forces, which are stochastic functions but remain proportional to each other. The corresponding actions on the members, S_i, also remain proportional to each other and to some stochastic forcing function, S. The structure fails when the smallest of the quantities $X_i - S_i$ becomes negative, where X_i is the resistance function of the ith structural member. Hence, the reliability of the structure under a single load application is

$$R = \int_0^\infty \prod_{i=1}^m [1 - P_{X_i}(S_i)] p_S(S)\, dS$$
$$= \int_0^\infty \prod_{i=1}^m \left[1 - P_{\xi_i}\left(\frac{u}{\nu_i}\right)\right] p_\theta(u)\, du \qquad (7.60)$$

where m is the number of members, $\xi_i = X_i/x_i$, $\theta = S_i/s_i = S/s$, and $\nu_i = x_i/s_i$.

In general we should not assume that the ξ_i's are independent. Environmental factors and common biases of manufacturing tend to make these variables appreciably correlated. Let us assume, therefore, that $\xi_i = \kappa_i \xi$, where the κ_i's and ξ are independent stochastic variables. For given dispersions of the ξ_i's, complete correlation of member resistance functions corresponds to zero dispersion of the κ_i's, while the absence of correlation is associated with zero dispersion of ξ. Then Eq. (7.60) must be replaced with

$$R = \int_0^\infty \prod_{i=1}^m \left[1 - P_{\kappa_i}\left(\frac{u}{\nu_i}\right)\right] p_{\theta/\xi}(u)\, du \qquad (7.61)$$

Under the assumption that $B^* + H$ is insensitive to the ν_i's, the optimization process consists in solving the system of equations

$$\left.\frac{\partial C}{\partial \nu_i}\right|_{\nu_{i0}} = (B^* + H) \left.\frac{\partial R}{\partial \nu_i}\right|_{\nu_{i0}}$$

where ν_{i0} is the optimal ν_i. The solution may be obtained by methods of mathematical programming. When $F_0 = 1 - R_0$ is sufficiently small an iteration procedure is also available. In a specific structure having 20 nominally identical members it was found that the optimal load factor varied between 1.75 for complete correlation and 2.02 for uncorrelated member strengths.[155] Indeed, it has been shown that, for sufficiently low probabilities of failure, the actual probability always lies between those for complete and for zero correlation and that the former is always the smaller of the two.[2] This conclusion can be extended to the optimum load factors.

In the foregoing paragraphs we have dealt with the optimization of structural member reliabilities from the viewpoint of a global objective function. Considerable work has been done on a two-step approach, in which, for a given structural reliability, member reliabilities are found which minimize the total cost, and the optimum overall reliability is separately computed.[159] In part this is justified because over a wide range of conditions the relative values of the optimum failure probabilities of the members are practically independent of the overall reliability. In many cases the same is true of the relative values of the optimum load factors. Hence, a change in structural reliability calls for a simple type of redesign.

A statically indeterminate structure can usually fail in one of several modes (plastic mechanisms). Hence, each mode can be treated as a member of a statically determinate structure. In plastic structures, the resistance function associated with a mode of failure is the sum of the contributions of the sections or members involved. Since a critical member or section is usually involved in more than one mode of failure there may be a strong correlation among the modal resistance functions aside from that due to the correlation among the members or sections themselves. Individual problems have been

solved by mathematical programming,[159] and reinforced concrete frames have been studied assuming independence of the section resistance functions,[160] but a simple general solution is not available. The bounds on structural reliability associated with complete and nil correlation are, nevertheless, found quite readily[161] and there are indications that the solution lies close to the former bound.

Some work has been done on the reliability of structures subjected to loads that are functions of more than one independent variable.[162]

7.32.6 Other Criteria of Failure and Damage

Thus far we have treated reliability optimization in structures for which the criterion of failure is that a forcing function exceed a resistance function. Little work has been done on more complicated criteria of failure, such as those involving cumulative damage. The material we mentioned earlier in this Section permits calculating the reliability of structural members subjected to repeated loading. The reliability of structures subjected to earthquake loading, applying Munse–Yao's criterion of failure,[150] has been studied using a Monte Carlo approach.[163] Efforts in this direction are not more than exploratory.

Often a structure may successively undergo various stages of damage or failure. For example, excessive drift under lateral loads may first inconvenience the occupants; larger deformations may cause nonstructural damage. Next would come structural damage, and finally, collapse. Reliability optimization can be studied for these structures by extending the approach we outlined above for structures that can only suffer one type of failure.[158] A more efficient approach uses Markovian dynamic programming and treats the various stages of failure as discrete states.[157]

Some types of damage are better dealt with as continuous states. This is true of settlements, tilting (within a range of tilts), cracking, deflections, etc. Reliability then is not a useful concept. Rather, we may use as objective functions the sum of the expected present value of the initial cost and a loss function. The latter can often be approximated as a constant times the square of a structural response such as tilt or crack width, the probability distribution of which is in turn a function of the design parameters. Only the expectation and variance of the response enter in the calculation of the expected loss. Finally, the design parameters that make the objective function a minimum can be obtained (see Reference 110, for example).

7.33 CODE FORMATS

There are many ways in which building code requirements can be formulated. The most popular format is deterministic and uses characteristic values of

load and strength, and split or partial factors (load factors and stress reduction factors) together with a set of design restrictions such as minimum allowable dimensions and percentages of reinforcement and standard details. We shall devote some attention to these presentations.

Traditionally the *factor of safety* is defined as the minimum ratio of resisting to acting stress; the minimum is taken for the entire structure, structural member, or section, and often a different factor of safety is quoted for each conceivable type of failure. In heterogeneous structures, such as those of reinforced concrete, a different set of factors of safety is given for each constituent material.

Stress reduction factors (ϕ factors as used in the ACI Code[164]) are the reciprocals of the corresponding factors of safety. Since the quantities involved in the definitions are random variables, the traditional definition must be replaced with

$$\nu_X = \min \frac{\text{nominal resisting stress}}{\text{nominal acting stress}}$$

where ν_X is the factor of safety and the nominal values are chosen in a systematic way as functionals of the distribution functions of resisting and acting stress. The stresses in this expression are often replaced with generalized forces (such as bending moment or shearing force) depending on the criterion of failure.

On similar grounds the *load factor* may be defined as

$$\nu_S = \frac{\text{nominal load required to cause failure}}{\text{nominal acting load}}$$

Various arguments are invoked to justify the use of either load factors, stress reduction factors, or both. Introduction of these factors is no more than a matter of convenience so long as we shy away from explicit optimization as a method of design. Consciousness of the aim of structural design should serve to establish these factors in a more consistent manner than is customary.

Consider two alternate designs of a structure. In the first design, all nominal loads are multiplied by a load factor ν_S and stress–strain curves are assigned their nominal shapes. In the second design, all loads are given their nominal values while the ordinates (stresses) in the stress–strain curves are affected by the stress reduction factor $1/\nu_S$; in other words, nominal strengths, yield stresses, and moduli of elasticity are divided by a factor of safety, taken equal to ν_S. The two designs will be identical. If the load factor and the safety factor are to affect, respectively, all the loads or all the stresses alike, they will be interchangeable. If both types of factor are to be used in the design of a structure, their individual values will be immaterial; only the product of $\nu_S \nu_X$ will be significant.

Normally the yield and maximum ("ultimate") stresses are affected by

TABLE 2.5. ASTM Deformation Requirements for Deformed Steel Wire.

Deformed Wire Size Number	Deformation Requirements: Spacing, Maximum in.	Deformation Requirements: Spacing, Minimum in.	Deformation Requirements: Minimum Average Height of Deformation, in.
D-1	0.285	0.182	0.0045
D-2	0.285	0.182	0.0063
D-3	0.285	0.182	0.0078
D-4	0.285	0.182	0.0101
D-5	0.285	0.182	0.0113
D-6	0.285	0.182	0.0124
D-7	0.285	0.182	0.0134
D-8	0.285	0.182	0.0143
D-9	0.285	0.182	0.0152
D-10	0.285	0.182	0.0160
D-11	0.285	0.182	0.0187
D-12	0.285	0.182	0.0195
D-13	0.285	0.182	0.0203
D-14	0.285	0.182	0.0211
D-15	0.285	0.182	0.0218
D-16	0.285	0.182	0.0225
D-17	0.285	0.182	0.0232
D-18	0.285	0.182	0.0239
D-19	0.285	0.182	0.0245
D-20	0.283	0.182	0.0252
D-21	0.285	0.182	0.0259
D-22	0.285	0.182	0.0265
D-23	0.285	0.182	0.0271
D-24	0.285	0.182	0.0277
D-25	0.285	0.182	0.0282
D-26	0.285	0.182	0.0288
D-27	0.285	0.182	0.0293
D-28	0.285	0.182	0.0299
D-29	0.285	0.182	0.0304
D-30	0.285	0.182	0.0309
D-31	0.285	0.182	0.0314

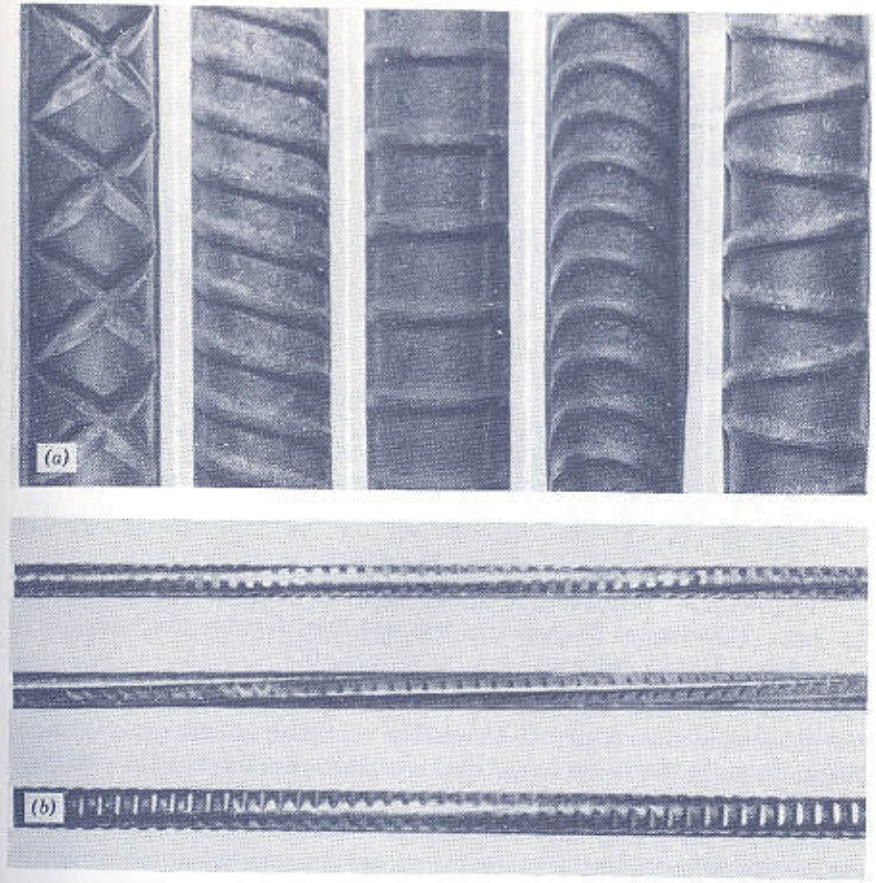

FIGURE 2.1. Reinforcing steel. (a) Typical reinforcing steel bars. (b) Typical deformed wires. (Courtesy of University of Illinois.)

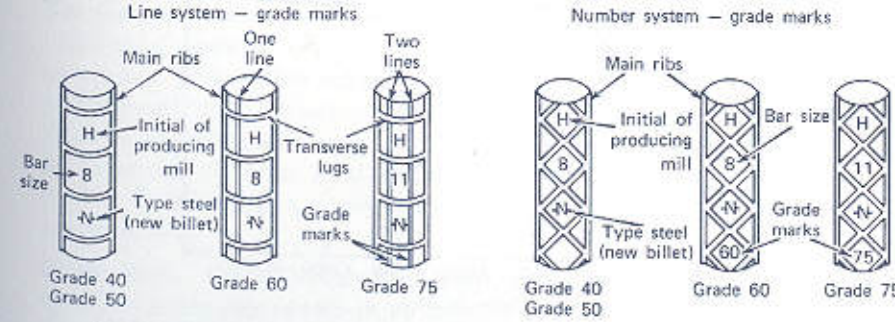

FIGURE 2.2. Reinforcing-bar identifications. (Courtesy of the Concrete Reinforcing Steel Institute.)

stress reduction coefficients while moduli of elasticity are taken equal to their nominal values. When following this practice the v_S and v_X remain equivalent for systems in which stresses are independent of the moduli of elasticity, such as those behaving linearly and all statically determinate structures; the equivalence becomes an approximation in other cases.

Advantage in the use of load factors arises when the forces that act in different directions or in opposite senses are multiplied by different numbers. Consider the probability of overturning of a prism that rests on rock when both the material of the prism and the rock have high compressive strengths ("high" as referred to the average contact stress under gravity load) and static lateral forces act on the prism. Practically, overturning will occur when the resultant of forces acting on the prism passes through an edge of its base. Probability of this event will be unaffected by changes in stress reduction coefficients, or in the load factor if both vertical and lateral forces are multiplied by the same number. A simple way to provide protection against overturning is to use a higher factor for the lateral than for the vertical forces. It is awkward to supplant this scheme with the requirement that the resultant of the nominal forces pass inside a kernel. In other examples it is equally objectionable to modify stress reduction factors as a function of the direction in which forces act. There is thus good reason to use load factors, provided these depend on the direction and sense of the loads.

Load factors need not appear explicitly in the computation but may be incorporated in the specified forces themselves. A building code may call for wind pressures that are greater than their expected magnitudes over some time span while, at the same time, it preserves the acceleration of gravity equal to its actual value.

Types of failure associated with insensitivity to stress reduction coefficients usually occur without warning. Signs of impending failure depend essentially on material behavior. Hence, it is expedient to use stress reduction coefficients in order to reflect the availability of warning, and leave load factors untouched on this account. Even if material properties could be specified or predicted deterministically, it would be justified to introduce stress reduction coefficients. These should depend on the nature and extent of phenomena that precede failure, such as large deformations and cracking. Actually, though, these coefficients are conditioned to a greater extent by the uncertainty in structural capacity that stems from uncertainty in material properties.

With the use of stress reduction factors to reflect notice of impending failure we may have to introduce factors greater than unity. We may avoid this situation by a proper choice of nominal forces and strengths. The stress reduction factor should depend on the number of critical sections involved in failure, since the coefficient of variation of their combined strength is a decreasing function of that number. On the other hand the stress reduction factor should be a decreasing function of the volume of highly stressed material at failure, because of statistical and stress-gradient effects, unless the criterion of failure includes these effects explicitly.

Use of reduced load factors or increased stress reduction factors for the combination of earthquake and gravity loads is justified in part by the small probability that a very high live load be present at the time of a strong earthquake. Also by the fact that the coefficient of variation of the combined effects of seismic and gravity loads is smaller than the greater of the corresponding coefficients of variation. By adjusting either factor we can make the failure probabilities depend on the severity of failure, thus being more conservative for columns than for beams. Design formulas and moment coefficients can also be adjusted for the same purpose.

Some building codes require that not more than some percentage of the control tests give values smaller than the nominal strengths to use in conjunction with the foregoing factors. For concrete strengths there is a tendency to relate the nominal value with the expected strength and the corresponding standard deviation under the assumption that the actual strengths have a Student distribution.[101] This does not apply to yield stress and cross-sectional areas of reinforcement, the tolerances for which were discussed earlier. In the same code the nominal dead loads are taken approximately equal to their expectations, while the document has no control over live, earthquake, wind, and other loads to be assumed for design.

Other codes prefer what the European Concrete Committee (CEB) calls a semiprobabilistic format with split factors.[141,166] In it the nominal strengths and loads are taken as the expected values minus or plus a coefficient times the corresponding strandard deviation. When strengths and loads are both normally distributed, their nominal values are associated with a fixed probability that a more unfavorable value is met in practice. The approach is similar to those proposed in Reference 165, where it is shown that the probability of failure for a given load factor is not very sensitive to the coefficients of variation of strength and load nor to the types of probability distribution, provided the factor that multiplies the standard deviations lies within a certain range and the probability distributions are normal, lognormal, or extreme. However, this advantage is only apparent, since the central load factors should not be appreciably affected by the choice of nominal values, and the amount of information required to attain a given accuracy in the probability of failure is also independent thereof. The virtue of using this sort of nominal values is a legal one granted that the nominal strength is sufficiently low so that a lower value makes negligence a likely cause of failure, but not so low that it cannot be fixed accurately without too extensive an amount of testing, and that the corresponding limitations are also met for the nominal

loads. Nominal values such that they are met in, say, 95% of the cases seem appropriate from this point of view.

Other building codes and similar documents[82,105] specify nominal values that result from combining the foregoing criteria. Still others[166] introduce an *importance factor*, which separately takes care of adjusting the probability of failure as a function of the severity of the consequences of failure. In the case of two-way slabs there is an additional reason for this factor, since the usual methods of analysis (yield-line and Hilleborg's) underestimate the structural capacity.

Consistently with these approaches, for design purposes we should assume load eccentricities and cross-sectional dimensions that differ from those in the structural drawings, so that there be a fixed small probability that the actual values are more unfavorable than the ones assumed. Since geometric discrepancies between drawings and the structure have practically normal distributions (Section 7.25), it is reasonable to take for the design eccentricities the expected values plus a number of times the standard deviation and for effective depths and widths of cross sections the expected values minus the same number of times the standard deviation of these variables. Thus, one code[105] calls for design widths and effective depths of structural members 2 cm (0.8 in.) smaller than those in the structural drawings (save that there is no reduction for the effective depth of bottom reinforcement in horizontal members) and an "accidental" eccentricity of 2 cm (0.4 in.) to be added to the computed eccentricities in columns and other compression members. Reductions in cross-sectional dimensions may be waived when special provisions are to be adopted in casting.

It has been shown that errors in design formulas can be treated as random variables, usually with well-behaved probability distributions.[167] We can take care of these variations by combining them with randomness of loads or of strengths and increasing the load factors accordingly, or in a number of other ways. When we consciously introduce biases such as errors on the safe side in design formulas, as was mentioned in connection with the shear strength of beams, we affect the overall safety factor. This gives us an additional degree of freedom through which we can take into account uncertainties in methods of analysis or the questions of the severity of damage and of warning of impending failure.

Cornell has presented a method whereby a building code can be devised so that it practically furnishes any set of specified probabilities of failure.[168] It has been shown that a number of "equivalent" code formats can be adopted which lead essentially to the same failure probabilities.[169,170] The ACI and CEB split factor formats have received the most attention in this respect.[171,172]

Cornell's approach can be fitted to any combination of probability distributions of strength and forcing function. Suppose first that both variables

are normally distributed. According to Eq. (7.3) the reliability is equal to the standardized distribution function of the variable

$$\beta = \frac{\bar{X} - \bar{S}}{\sqrt{\sigma_X^2 + \sigma_S^2}} \tag{7.62}$$

which may be called the *safety index*. Equation (7.62) can be put in the form

$$\beta = (\nu - 1)(\nu^2 c_X^2 + c_S^2)^{-1/2} \tag{7.63}$$

in which ν is the central load factor and c_X and c_S are the coefficients or variation of X and S, respectively.

An approximate linearization of the square root is now introduced by noticing that, whenever x and y are nonnegative variables,

$$(x^2 + y^2)^{1/2} = (x + y)\alpha$$

where α is a function of x/y and always lies between 0.707 and 1. If x and y are roughly of the same magnitude, α is practically constant. Thus, assuming $\alpha = 0.75$ introduces errors smaller than 10% when $0.25 \leq x/y \leq 4$.

Accordingly, we write Eq. (7.63) as

$$\beta = \frac{\nu - 1}{(\nu c_X + c_S)\alpha}$$

whence

$$\nu = \nu_X \nu_S$$

where

$$\nu_X = \frac{1}{1 - \alpha\beta c_X} \tag{7.64}$$

(so that $\phi = 1 - \alpha\beta c_X$) and

$$\nu_S = 1 + \alpha\beta c_S \tag{7.65}$$

ν_X and ν_S are split safety factors, one for resistance and the other for load and they depend essentially only on c_X and on c_S, respectively, while the probability of failure is reflected on β alone. In turn we can write

$$\nu_X = \prod_i \nu_i \qquad \nu_S = \prod_j \nu_j$$

where

$$\nu_i = \frac{1}{1 - K_i \beta c_i} \qquad \nu_j = 1 + K_j \beta c_j$$

where ν_i are partial safety factors, each associated with material strength, fabrication, or errors involved in calcuations of resistance while the ν_j's are associated with total load or with load calculations; c_i and c_j are the

corresponding coefficients of variation; and each of the factors K_i and K_j is almost constant over the range of greatest practical interest. This manner of dealing with partial factors can be calibrated against an existing code to determine the magnitude of the uncertainties it implies; variations in the quality of control and in the accuracy of calculations can then be explicitly recognized and incorporated into the corresponding safety factor.

Rather than using central factors as in the foregoing presentation, we may work with nominal safety factors, which relate nominal values of the variables. Thus, if

$$X^* = \frac{\bar{X}}{1 - k_X c_X}$$

and

$$S^* = \bar{S}(1 + k_S c_S)$$

are the nominal resistance and loading functions and k_X and k_S are constants, the nominal safety factor $\nu^* = X^*/S^*$ is given by

$$\nu^* = \frac{1 - k_X c_X}{1 + k_S c_S}\,\nu \tag{7.66}$$

The use of split nominal factors or of safety margins in other formats can also be expressed in terms of the coefficients of variation.

It is found that the central safety factor is quite sensitive to the coefficients of variation of strength and load. This is particularly true of ν_X relative to c_X [Eq. (7.64)], since ν_X tends to infinity as c_X approaches $1/\alpha\beta$ (notice that $\alpha \cong 0.75$ and $\beta \cong 2.6$ to 4 for many practical conditions, so that extreme sensitivity arises as c_X approaches 1/3). This situation is due mostly to our having assigned X a normal distribution, which gives a finite probability of X being negative. Use of nominal safety factors appreciably reduces the sensitivity to c_X and c_S in their usual ranges of values but does not do away with the objectionable situation for large c_X.

As we have seen, X can usually be assigned a lognormal distribution, since it can be expressed as the product of several relatively well-behaved, nearly independent, random variables. The same is true of some disturbances, such as earthquake loads (although gravity loads are more nearly normally distributed). Let us assume that both X and S have lognormal distributions. Then, according to Eq. (7.4) we may take as safety index the quantity

$$\beta = \frac{\ln \tilde{X}/\tilde{S}}{\sqrt{\sigma^2_{\ln S} + \sigma^2_{\ln X}}} = \frac{\ln \tilde{X}/\tilde{S}}{\sqrt{\ln (1 + c_S^2) + \ln (1 + c_X^2)}}$$

where $\tilde{S}$ and $\tilde{X}$ are the medians of S and X. Hence,

$$\nu = \exp\left[\beta\sqrt{\ln (1 + c_S^2) + \ln (1 + c_X^2)}\right] \tag{7.67}$$

$$\simeq e^{(c_S + c_X)\alpha\beta} \tag{7.68}$$

[see Eq. (7.5)].

The split-factor format is again feasible, with $\nu_S = \exp(\alpha\beta c_S)$ and $\nu_X = \exp(\alpha\beta c_X)$. The error introduced by the linearization in Eq. (7.68) taking α as a constant is of the same order of magnitude as with the normal distributions, provided $c_S + c_X$ does not exceed about 0.7. For larger coefficients of variation the error is kept reasonable by writing $\sqrt{\ln (1 + c^2_{S,X})}$ for $c_{S,X}$ in the expressions for the split factors. Notice that the safety factors in this treatment refer to the modes of the variables rather than to their expectations. The two functionals are related through the expression

$$\bar{X} = \tilde{X} e^{\sigma^2/2} \tag{7.69}$$

where $\sigma = \sigma_{\ln X}$.

An interesting alternative is based on the treatment of safety presented in Reference 172. Let ν_S be the central load factor that would be required to produce a given probability of failure if only loads were random while strength was deterministic, and let ν_X be the central factor required if only strength were random. Then when both S and X are random, the combined central safety factor required to produce the same failure probability is given approximately by

$$\nu - 1 = \nu_S - 1 + \nu_X - 1$$

or

$$\nu = \nu_S + \nu_X - 1 \tag{7.70}$$

The error introduced by this assumption is less than about 10% over the entire range of possible safety factors when both S and X are normally distributed. It is usually smaller when they are lognormally distributed, if the safety factors are referred to the medians of the variables.

ν_S as well as ν_X can in turn be put in a form similar to Eq. (7.70) in terms of the partial safety factors required to produce the given probability of failure when all the uncertainty lies in the total load, load calculations, material strength, etc. Consequently we may write

$$\nu - 1 = \sum_i (\nu_i - 1) \tag{7.71}$$

where the ν_i's are these partial safety factors. Despite the foregoing presentation and aside from a minor computational simplification and a concession to current code formats, there is no advantage in the use of split factors.

When we are willing to admit that the ratio X/S is lognormally distributed, it is simple to allow explicitly for variations in the probability of failure and

for uncertainty in the main variables that enter design by proceeding as we did in connection with earthquake resistant design. The straightforward approach is particularly useful when the dependence of load or strength on these variables is nonlinear. Suppose that the following expression is valid with sufficient accuracy,

$$\frac{X}{S} = A \prod_i Y_i^{\alpha_i} \tag{7.72}$$

where A is a constant, the Y_i's are independent random variables, and the α_i's are constants. Then,

$$v = \frac{\bar{X}}{\bar{S}} = A \prod_i \bar{Y}_i^{\alpha_i} \tag{7.73}$$

and, using Eq. (7.5),

$$\sigma^2_{\ln v} = \sum_i \alpha_i^2 \ln (1 + c_{Y_i}^2) \tag{7.74}$$

The reliability is then the standardized normal distribution function of $\beta = (\ln v)/\sigma_{\ln v}$. The dependence of X/S on the Y_i's can usually be given the form of Eq. (7.72) by adjusting straight lines on log paper.

An unorthodox but practical code format would specify values of β and require that Eqs. (7.73) and (7.74) be used in its calculation. It would also specify means for computing or estimating the medians and coefficients of variation. In particular, many of the pertinent variables have probability density functions that are almost symmetric about their expectations; the medians of these variables are practically equal to their expected values. For lognormally distributed variables one would apply Eq. (7.69).

Information presented in previous articles leads to the conclusion that dead loads are approximately normally distributed, with mean between 1.05 and 1.25 times the values computed in conventional ways (depending on the type of structure and on the criterion used for computing the loads) and a coefficient of variation of the order of 0.05. The distributions of the maximum live loads per unit area in buildings over a relatively long time span is approximately extreme type I, with coefficient of variation inversely proportional to the square root of the tributary area and with expectation dependent only on the type of occupancy of that area. The distribution of the total load has a median approximately equal to its expectation, which is the sum of the expected dead and live loads and a variance equal to the sum of the two variances. These distributions do not take into account gross changes in dead loads, due to architectural decisions, nor changes in occupancy. Other than increasing the coefficients of variation slightly, these eventualities are better taken care of by affecting the modes of failure so that they be associated with adequate warning.

The information presented also permits assigning probability distributions to material strengths and to the discrepancies between nominal and actual cross-sectional dimensions. Nevertheless, if wear and the possibility of damage from impact are not explicitly recognized in design, it is appropriate to assume cross-sectional dimensions somewhat smaller than the expected values, much as is done in codes that specify characteristic values of these dimensions.

Adjustments to commercial sizes of reinforcing bars, to whole numbers of bars, and to multiples of 5 cm (2 in.), or to whole numbers of inches of the outer dimensions of cross sections introduce discrepancies between computed and specified properties of cross sections. The distributions of these discrepancies, given a computed dimension or an area of reinforcement, are practically uniform between steel areas associated with successive whole numbers of bars or with successive round numbers or successive commercial sizes.

This format as well as some of the preceding ones produces a code in which the failure probabilities can be made approximately equal to some prescribed values, to which will be associated a value of β. Optimization can be achieved as indicated in this chapter, both when we consider the possibility of failure only upon completion and when failure may be caused by a disturbance such as earthquake or wind, which may be idealized as a Poisson process.

Established practice in codes and specifications is to stipulate tolerances on concrete slump, strength, and unit weight, on steel yield point, tensile strength, and elongation, and on dimensions. This has some drawbacks: If the tolerances are not met, either nothing is done, in which case the owner gets a poorer product than he paid for (higher probabilities of failure, larger deflections, wider cracks, etc.), or the structure is strengthened, or it is partially torn down and rebuilt—and in these two latter cases there are losses for both builder and owner. If the tolerances are met but the structure is of a quality inferior to that specified, the owner suffers a loss. And if the contractor produces a structure of better quality than specified, so as to raise the probability of meeting specifications, he gets no reward therefor.

A more convenient approach fixes penalties for failing to meet the specifications and bonuses for a superior quality job. The approach is explicitly worked out in Reference 173 regarding concrete strength as the only variable as a function of which penalties and bonuses can be established. Of course, if the penalty exceeds some value it is preferable for everyone concerned to strengthen the structure or to tear it down and rebuild it.

This situation is akin to the one surrounding code treatment of serviceability, although most codes do contain limitations on the depth of structural members and on the percentage and spacing of reinforcement so as indirectly to control the probabilities of large deflections, vibrations, and cracks. On the

other hand, there is consensus to the effect that the main realm of codes is safety, and many claim that serviceability should not even be covered by a code. An attractive alternative would consist in dropping these limitations from codes and to specify penalties and bonuses as functions of structural behavior.

7.34 DETAILING REQUIREMENTS AND RESTRICTIONS IN CODES

7.34.1 General

These requirements and limitations seem arbitrary at first sight. Some are indeed remnants of previous editions of the code and are not justified at present. Most, however, fulfill a function. Usually not much harm ensues from respecting them, other than a nearly systematic loss of economy, since most requirements of this type reflect overgeneralizations. We shall consider some of the most important restrictions and detailing requirements in the following paragraphs.

7.34.2 Slab Thickness

Many building codes require that a slab be at least so many inches deep, independently of panel dimensions and of continuity conditions. The limitation is not related to deflections. There are two conceivable reasons for establishing this absolute limit. The first concerns the fact that inaccuracies in dimensions and effects of abrasion are not covered by stress reduction factors unless we set a lower limit to cross-sectional dimensions. The second is the desire to protect the slab against the effects of concentrated loads, especially impact. However, it seems preferable to combine the load and stress factors with a geometric correction to be taken into account in design, supplemented with a clause that the slab be able to resist a concentrated load of so many pounds [say, 1 ton (2.2 kip)[105]] concentrated at any point. The load can be made a function of the construction procedure and intended occupancy.

Thermal and acoustic insulation and protection against burglars often impose limitations in thickness that exceed the one required by a structural code.

Limitation of slab thickness as a function of panel dimensions is intended to limit deflections and vertical vibrations. Formulas of this sort are crude when they do not explicitly include other pertinent variables. In uncommon projects it is justified to compute the deflections and amplitude of oscillation, compare with results of similar computations for slabs of known performance, and take a better founded decision.

7.34.3 Cross-Sectional Dimensions of Columns

For the reasons expounded in Section 7.33, rather than limiting the cross-sectional dimensions or area of columns as done in most codes, there is advantage in using geometric corrections coupled with an accidental eccentricity of longitudinal forces.

In some thin members there is danger, when following primitive construction practices, that concrete be lost during installation of door and window frames and replaced with low-strength mortar. To offset this possibility one firm designs the vertical steel so that it be able to carry the entire axial load if the column cross-sectional area does not exceed 225 cm² (35 in.²); it interpolates linearly between 100% and 0% of the axial load for areas between 225 and 475 cm² (74 in.²).

7.34.4 Cover

A thick cover is not needed to insure adequate penetration of concrete nor to protect reinforcement against corrosion. Thick covers actually serve to develop high bond stresses, especially in deformed bars.[174] A requirement such as "the net cover shall not be less than 1 cm (3/8 in.) nor less than one bar diameter (or one equivalent bar diameter for bundled reinforcement)"[105] seems adequate. Yet in some cases it may prove too stringent and it may lead to large cracks. The cover can then be made even smaller if the bond stresses to be developed are smaller than those which a one-bar-diameter cover can sustain or if sufficient and closely spaced transverse reinforcement is provided so as to protect against split failures.

These remarks must be modified when wear or certain types of surface finish are anticipated or when it is desired to furnish fire protection.

7.34.5 Construction Joints

Construction joints should be designed. They should ordinarily act always in compression. Otherwise they may lead to undesirably large cracks. Thus the joint in Fig. 7.22(a) is preferable to that in Fig. 7.22(b).

There are various ways for achieving a good bonding surface. They all require extreme cleanliness. Moreover, at sections that may be critical for earthquake or impact loading it is important that the probability of producing a relatively weak surface be minimized. It is often justified at those sections to furnish additional reinforcement: in any structural member a small portion having excessive strength is acceptable; the converse may imply serious local damage; and the cost involved in the extra protection is insignificant.

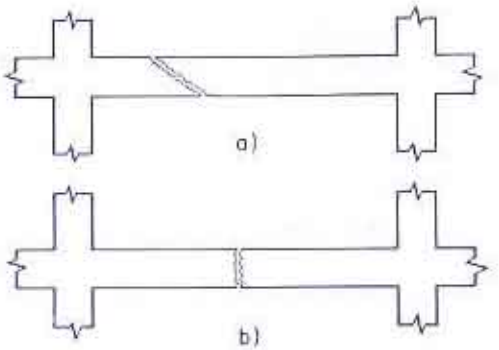

FIGURE 7.22. Construction joints.

7.34.6 Minimum and Maximum Reinforcement

The lower bound should be proportional to $\sqrt{f'_c}$, for it tends to insure that, once the member has cracked, the reinforcement will be able to carry a bending moment greater than the one which the concrete resists before cracking. This affords protection against quite brittle tensile fracture of the concrete under accidental overload.

The lower bound can be waived if the maximum expected bending moment lies considerably below the one which the member resists before cracking. In fixing this escape clause the dispersions of loads and strengths should be recognized.

There is a wide disparity in specifications that limit the spacing of flexural reinforcement in slabs and shells. Since there seem to be no bases to justify bar spacings in excess of three or four times the slab or shell thickness and experience is limited, it seems wise to limit the spacing to distances of the order of 3.5 times the thickness.

Clearly, flexural reinforcement should also satisfy whatever limitations are deemed appropriate for temperature and shrinkage reinforcement.

Ductility is much a function of the steel percentage. Hence limitation in the ACI code[101] that the net percentage of reinforcement not exceed 75 percent of the computed balanced value. (As we saw in Section 7.26, however, this does not insure the absence of compression failures.) As with other limitations that tend to insure adequate ductility, there is the possibility of waiving this one if the maximum forces to be expected are much below those which would cause failure. Considering the possibility of earthquakes, evaluation of these forces should recognize their dependence on the ductility factor. Suppose that it is decided to use such a large percentage of net tensile reinforcement that the ductility factor will be reduced to half of what can be achieved with normal care in design and construction. Most structures in this situation

should be required to withstand lateral forces equal to at least twice what would be normally regarded as adequate.

7.34.7 Minimum and Maximum Vertical Reinforcement in Columns

All the reinforcement in columns should satisfy the limitations adopted for temperature and shrinkage reinforcement and for flexural reinforcement. Additional requirements are described in connection with cross-sectional dimensions of columns. In regions of the world where important vertical accelerations are commonplace, a further limitation in terms of the vertical force is also in order (see Section 7.14).

The net percentage of tensile reinforcement in columns is normally nil. The ductility in this case increases rapidly with the percentage of hoop reinforcement if failure is in compression.[80]

Other than this there is little reason for setting a lower limit to the vertical reinforcement in columns. Of course, the limits for flexural, temperature, and shrinkage steel should be respected.

There is little justification for an upper limit to the percentage of vertical reinforcement, such as 8%. If the congestion of steel does not hamper casting, the only reason for using the smallest possible amount of reinforcement is an economical one, and it is easily overrun by architectural considerations.

7.34.8 Transverse Reinforcement

Code requirements on helical reinforcement in columns are based on extensive laboratory experience with members that fulfill them, and practically no experience with other specimens. Hence it would be dangerous to adopt original criteria in detailing helical reinforcement.

Effects of helical reinforcement on load carrying capacity become significant only at such high compressive strains that the shell is in the process of spalling. This explains code formulas that call for a percentage of helical reinforcement slightly larger than that required to compensate for loss of the shell. These codes allow a reduction in the load factor or an increase in the working stresses of columns containing at least that amount of helical reinforcement; or the code may produce comparable results by specifying a smaller minimum eccentricity in helically reinforced than in tied columns.

The criteria that either full or no credit be given to helical reinforcement, depending on its quantity, can be debated for highly redundant structures and for those whose behavior is governed by their capacity to absorb energy. It is probably adequate as a code requirement, but it merits revision when evaluating the safety of existing structures.

The superior ductility of helically reinforced over tied columns is spectacular. Scanning the literature on earthquake damage, no case is found of

damage to the former type of columns, as against the countless failures of tied columns.

Ties in columns and stirrups in beams serve to keep the reinforcement in place during casting, resist diagonal tension and torsion, restrain the concrete in compression, and prevent or delay buckling of longitudinal bars and splitting of concrete in regions of anchorage or lap splicing.

To keep the longitudinal reinforcement in place, the diameter and spacing of transverse reinforcement should bear relationships with the transverse dimensions of the member and with the diameter of the main reinforcement. Some engineers specify transverse reinforcement with area not smaller than 1/10 that of a single longitudinal bar or bundle. Its spacing does not normally exceed a distance on the order of 30 cm (12 in.) because of shrinkage and temperature requirements; there are also the traditional requirements that tie spacing should not exceed 48 times the tie diameter nor 12 to 16 bar diameters; presumably these specifications incorporate in a satisfactory way the other parameters that should govern the size and spacing of ties in columns for purposes of proper casting.

In horizontally cast members, the ties or stirrups should be able to carry, without buckling, the weight of the top reinforcement plus that of the concrete being cast, and a small live load. Stirrup spacing should be such that the top steel does not bend excessively under these loads.[107]

Experimental evidence concerning the effectiveness of rectangular lateral reinforcement to restrain concrete in compression indicates that such reinforcement raises the ductility but does not affect the capacity of the concrete it confines; some tests have indicated that the effect of square ties on capacity is negligible.[175] An analytical study[122] having limited experimental confirmation, led to an expression for computing tie effectiveness. Putting that expression in terms applicable to design and aiming at the increase in ductility that even rectangular ties furnish, it is suggested that their effectiveness be evaluated from the formula

$$\rho'_{eq} = \frac{\rho''}{x_1/x_2 + x_2/x_1}$$

where ρ'_{eq} is the equivalent volumetric ratio of circular helical reinforcement, ρ'' is the volumetric ratio of rectangular ties, and x_1, x_2 are the depth and width of the enclosed section. The effectiveness of this reinforcement may be somewhat greater in regions of high bending moments. Its function is especially important in regions of plastic compressive deformation of beams.

The main effects of repeated alternating loading of ordinary frames of reinforced concrete are spalling of the concrete, bond degradation, widening of cracks, the Bauschinger effect in the steel, and a decrease in the concrete modulus of elasticity.[176] Accordingly, their energy absorbing capacity may

be reduced drastically even if their strength and ductility factor remain essentially constant. The use of closed ties ("tie-stirrups") in zones of plastic hinging is most effective in obviating or retarding these deleterious effects.

Neglect of the restraint offered by the cover and by the curvature of a member under bending permits computing the spacing of ties required to prevent buckling of the main reinforcement when strained up to yielding. According to a study of this nature,[177] the maximum spacing should be proportional to the square root of the yield stress. If we admit that a spacing of 12 bar diameters is satisfactory when the vertical steel has a yield point f_y of 4200 kg/cm² (60 ksi), for a different f_y it should be $12\sqrt{60/f_y}$ where f_y is in ksi, giving 16 bar diameters in columns with structural grade vertical reinforcement.

One other function is met by transverse reinforcement: in precast piles it helps prevent damage during driving, especially near the ends of the pile. Criteria for its design in these conditions are still empirical.[178,179]

7.34.9 Other Reinforcement Serving during Construction

We have seen ties and stirrups fulfilling a function during the process of casting and during pile driving. There are other examples of reinforcement that may be indispensable at some stage of construction but which ceases to be useful afterwards. This is particularly true of bridges when special methods of construction are resorted to, and it is true of precast members.

Many situations merit special attention. Examples are found when considering the possibility of wind or earthquake action on walls and partitions at intermediate stages of construction. Another classical instance arises in foundation beams that are monolithic with a floor slab. A casting joint is often chosen at the underside of the slab [Fig. 7.23(a)], so that if the top reinforcement in the beam is placed as might seem most efficient [Fig. 7.23(b)] this member will be unprotected against negative bending moments at one stage of construction, due to soil movements, and huge cracks are likely to develop. A suitable arrangement of the top reinforcement is shown in Fig. 7.23(c).

7.34.10 Splices

For the sake of expediencey in construction, sleeve splices are often used for larger-diameter bars in columns. Some available devices are capable of developing the full compressive capacity of the bar but are weak in tension. It is claimed that this is not objectionable when the designer knows that the bar will not be called upon to act in tension. There is a place for this practice when the possibility of appreciable tensions is extremely small. But there is room for caution in deciding on this matter, since the structural engineer

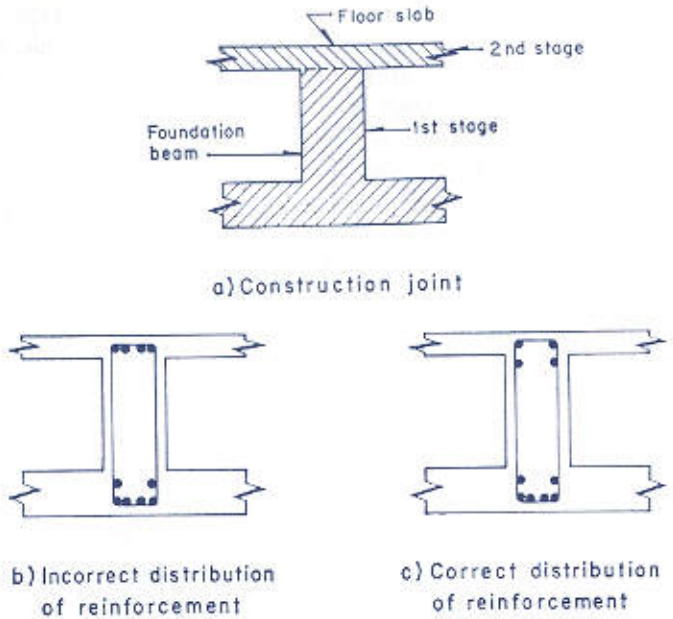

FIGURE 7.23. Casting joint in foundation beams.

should be conscious of the likelihood of loading conditions not considered explicitly in design.

Lapped splices required to develop the yield stress of large-diameter bars are so long that they are impractical. For reasons of economy, such bars are spliced by welding or through use of devices. Design of welded connections must also pay due attention to the development of ductility to whatever extent this is needed in the face of very unfavorable loads or resistances.

Whatever solution is adopted for splicing, it is advisable to heed the universal code prohibition that concerns the splicing of a large fraction of the longitudinal steel in a structural member at any given section and obviating splices at sections of highest stress.

7.34.11 Corner Reinforcement and Beam–Column Intersections

Consider a small piece of concrete reinforced alike in two perpendicular directions and subjected to pure shear parallel to those directions (Fig. 7.24). The piece may be regarded as half the depth of a two-way slab near one of its corners, or as a portion of a shell or a wall under membrane stresses, or as an approximation to a beam–column intersection. More generally, we are concerned with portions of structural members in which the reinforcement is not parallel to the principal stresses. There are general criteria to evaluate the

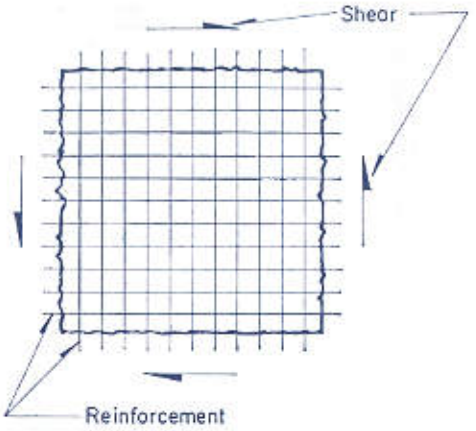

FIGURE 7.24. Piece of concrete equally reinforced in two perpendicular directions.

amount of reinforcement required in each direction to prevent yielding or to insure structural capacity.[180] It is clear from the initial symmetry of the stress–strain curve of concrete about the origin that the reinforcement will not be appreciably stressed until the concrete cracks diagonally. The situation is similar to the one met with vertical stirrups in beams: the stirrups are subjected even to a small compressive stress until appearance of the first diagonal crack.[181] The need to place diagonal reinforcement under these and similar conditions, if it is desired to limit the size of these cracks without using too high a percentage of steel parallel to the maximum shearing stress, can be decided along criteria similar to the one used for requiring inclined stirrups in beams.

According to this criterion, there will be need to use inclined reinforcement if the average shear in the intersection triangle (with dimensions reduced as has been discussed) exceeds approximately $\sqrt{f'_c}$ (in kg/cm²; $4\sqrt{f'_c}$ in psi). Here the acting forces should be multiplied by the load factors and $\sqrt{f'_c}$ should be affected by a stress reduction factor. This criterion would apply to the beam–column intersections in Fig. 7.25 for example. Since the state of stress is not one of pure shear, the "average shear" to use for this comparison may be defined, with reference to the figure, as $(F_1/d_2 + F_2/d_1)/2$. The amount of inclined reinforcement required may be taken equal to that which would resist the excess of this average stress over $\sqrt{f'_c}$ (in kg/cm²). Equivalent criteria may be set up for corner reinforcement in slabs, computing the average shear as a function of the torsional moment.

Beam–column connections of the type depicted in Fig. 7.26(a) behave

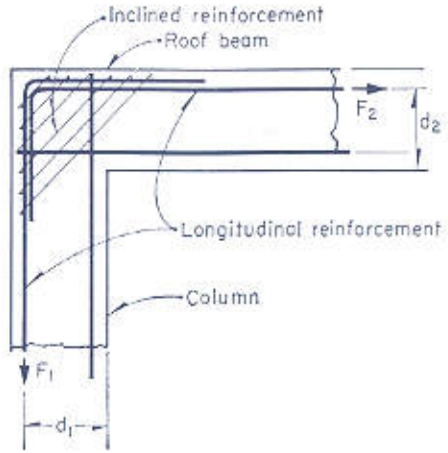

FIGURE 7.25. Inclined reinforcement at column–roof beam intersection.

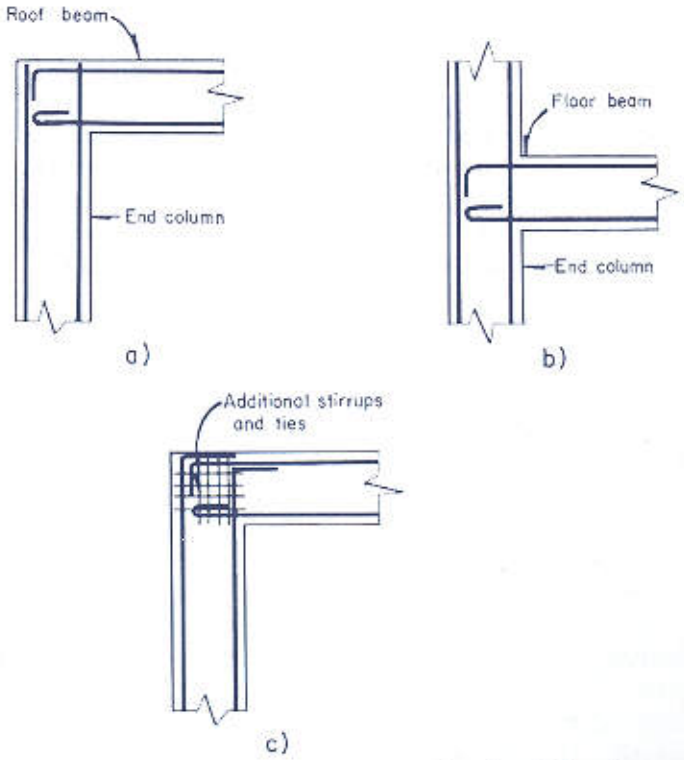

FIGURE 7.26. Some beam–column connections in reinforced concrete structures.

poorly. One frame that complied with code requirements is known to have failed due to a detail of this sort.[182] Connections of the type in Fig. 7.26(b) behave poorly under earthquake-like loading because of lack of lateral restraint.[183,184]

These objections are surmounted by using ties or stirrups [Fig. 7.26(c)]. Some criteria for design of this reinforcement take the shear at the intersection as the only relevant variable.[183,184] The ultimate shear considerably exceeds the one that can be developed in beams, perhaps by around 60%.

7.35 STRENGTHENING EXISTING STRUCTURES

The decision to strengthen a structure may follow from the fact that the structure has been damaged, or from a desire to change the demands imposed on it, or because it is discovered that the structure was improperly designed or built. The first case usually involves a difficult evaluation of structural capacity. In all cases there normally are difficult problems associated with construction procedures

A project to strengthen an existing structure will often forcefully bring to the foreground matters that can only be dealt with in explicit terms of probabilities of failure. This is so because the relation between cost and safety may differ so widely from standard problems that it may preclude simple extrapolation from established practice. In a structure designed to be built there is a nearly continuous variation of initial cost with load factor. In an existing one there is often a pronounced discontinuity between no strengthening at all and the slightest strengthening, since the latter alternative may require removal of a large share of veneer and other nonstructural elements.

There is always need for an evaluation of the actions that are going to operate on the structure and of structural capacity. In attempting to evaluate the capacity of existing structures the designer is confronted with a unique experience; in no other situation are the naive conventions of ordinary designs so dramatically exposed. Even in carefully built structures the designer finds enormous differences between what the structural drawings show and the actual geometry. If he tests cores he usually finds substantially greater dispersions in strength than he anticipated. And if he tries to be realistic about the contribution of "nonstructural" elements, normally disregarded in design, he often finds this contribution is of the same order as that of the elements taken into consideration. Only after facing problems of this nature can the structural engineer claim experience, and only then does he boast his humility as does the earnest soil mechanicist.

In view of such uncertainties, load tests are often resorted to. Interpretation of a test is almost straightforward when the anticipated type of load will act in the same direction as the applied load during the test and will be

of the same nature—acting only once and essentially as a static load. If the load test is to yield significant results and yet not be excessively severe, the total load acting on the structure during the test (including dead load already in place) should slightly exceed the load factor for live load times the design live load plus as a similar term for dead load.

Interpretation of load-test results cannot be deterministic even under these simple conditions. For one thing the structure does not have exactly the same capacity after the test as it did before. For another, the loads and other actions that will operate on the structure are not deterministically known. Also, it is usually impractical to test a complete structure; either representative or suspect portions of it are selected for this purpose.

Load testing can be coupled with application of Bayes' theorem [Eq. (7.11)]. Under the simplifying assumption that only one distribution of loads is of interest and that the resistance does not vary with time, the posterior failure probability density is equal to the prior density truncated at the test load and normalized.[4] Hence,

$$R'(W) = \frac{R(W)}{R(W_1)} \qquad \text{if } W \geq W_1$$
$$= 1 \qquad \text{if } W \leq W_1$$

where W is any load, W_1 is the test load, and R and R' are the prior and posterior reliabilities.

For example, the prior reliability of a given structure may have been 75% at 1.5 the design load, and 25% at twice the design load. Suppose that the structure passes a load test at 1.5 the design load. Its probability of surviving twice the design value will now be $0.25/0.75 = 0.33$.

When the design loads will act in a direction different from that of the test load or when they will be of different nature, interpretation of load test results becomes complicated and requires a major dose of judgment. For example, it is a common occurrence that badly damaged structures pass a standard load test and yet are poorly suited to resist earthquakes.

The contributions of so-called nonstructural elements (walls, partitions, stairways, floor finishes, etc.) to strength and stiffness are difficult to evaluate. In what is normally called "the structure itself," departures from code practice require unorthodox methods of analysis and often constitute sources of uncertainty. Typical situations of this sort arise in columns having much less or much more helical reinforcement than codes specify, at joints where anchorage is apparently insufficient in the light of available test results, and where poor details exist or defective materials have been used.

Evaluating the capacity of a structure seems impossible when drawings are not available. Still, there is an obvious lower limit: the structure has a load

factor of 1 for the loads it is carrying before strengthening. However, even this criterion may turn out not to be conservative when designing against lateral forces, as strengthening on this basis may introduce dangerous torques because of unforeseen differences in stiffness; this source of uncertainty may be dispelled by resorting to vibration tests. Under dynamic loads, ignorance of actual strengths may lead to unavoidable overdesign.

Many solutions used in strengthening existing structures are adequate for special cases and we shall not discuss them. One group of solutions deserves attention though: external prestressing. It finds an effective application in beams whose damage consists of nearly vertical cracks at or near points of cutoff of the main steel. In an ordinary beam, external longitudinal prestressing of the type shown in Fig. 7.27 raises the shear capacity between 4% and 8% of the longitudinal force applied,[185] or an amount given approximately by Eq. 5.22. In a beam weakened or damaged because of main-steel cutoffs the increase is about 100% until the capacity catches up with that of a beam having no cutoffs (Fig. 7.28).[185] The same type of prestressing is useful for resisting the flexural capacity of beams and other structural members when governed by tension.

The shear capacity of diagonally cracked beams is effectively raised through the use of external, prestressed stirrups (as in Fig. 7.29, for example) or prestressed straps (Fig. 7.30). Their contribution can be assumed equal to that of ordinary stirrups.[102,185]

Longitudinal prestressing brings about a decrease in ductility while the use

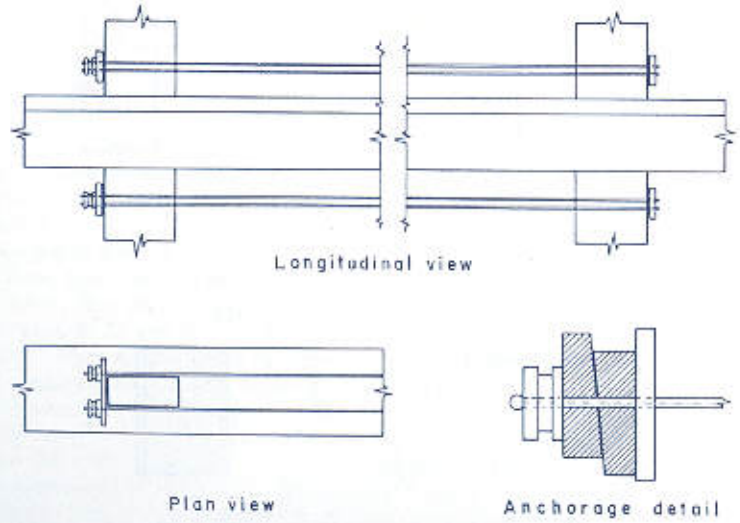

FIGURE 7.27. External longitudinal prestressing.

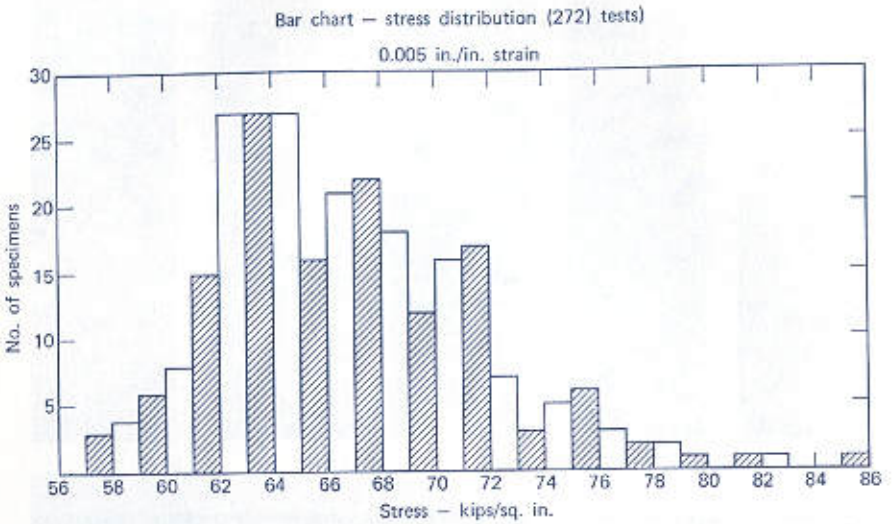

FIGURE 2.3. Distribution of stress at 0.005 in./in. strain in grade 60 bars. (Courtesy of the American Iron and Steel Institute and Wiss, Janney, Elstner, and Associates, Northbrook, Ill.)

yield strain of the steel not exceeding the strain (about 0.35%) at which concrete in compression begins to unload in a reinforced-concrete member. Column formulas are based on the steel compression yield strain not exceeding the concrete unloading strain. Beam formulas defining balanced design are based on the tensile steel behaving as an idealized elastic-pure plastic material acting compositely with concrete having a maximum compressive strain of 0.3%, so that any significant rounding of the steel tensile stress–strain curve at yielding (that is, steel yield strain greater than about 0.35%)

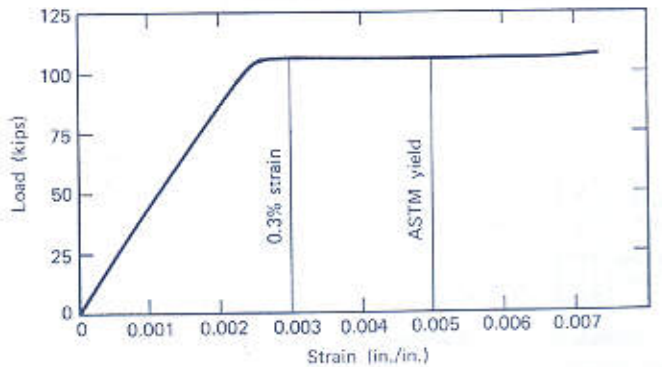

FIGURE 2.4. Load–strain curve for No. 11 A615 Grade 60 steel bar—typical "flat-top" curve.

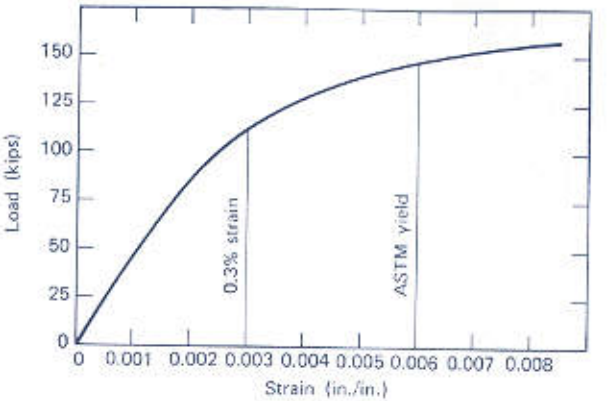

FIGURE 2.5. Load–strain curve for No. 11 A615 grade 75 steel bar—typical "round-house" curve.

tends to cause an unconservative prediction of steel percentage resulting in a balanced design.

There is an apparent discrepancy between the steel yield strains as specified by ASTM (Table 2.1) and those assumed (0.3 to 0.35%) by ACI.[7] However, an industry-wide study[5] of the stress–strain curves for Grade 60 steel revealed that both the ASTM definition and the ACI assumption of yield strain resulted in about the same yield stress for the flat-top Grade 60 steels. Therefore, the need for changing the ASTM definition of yield strain for the flat-top Grade 60 steel is not critical, especially since such a change would require more expensive product testing (that is, autographic stress–strain curves would probably be needed for all acceptance tests).

2.4 REINFORCING-BAR PROPERTIES RELATED TO INELASTIC BEHAVIOR

The discussion in the previous section related mainly to the yield behavior of reinforcing steels as it affects the conventional ultimate-strength design of structures. This section relates to the aspects of inelastic behavior beyond yielding and to the aspects of repeated loading which are beyond the scope of conventional ultimate-strength design, but are of importance in the design of structures to resist earth-quakes or blast loads. These considerations involve evaluation of a number of steel properties not covered by the ASTM specifications.

Strain Rate. For all dynamic loadings, the general tendency is that an increase in strain rate results in an increase in yield strength, particularly for flat-top steels, and in a proportionately lesser increase in tensile strength, (Table 2.6).[8] Ductility is not significantly affected by strain rate. Under blast

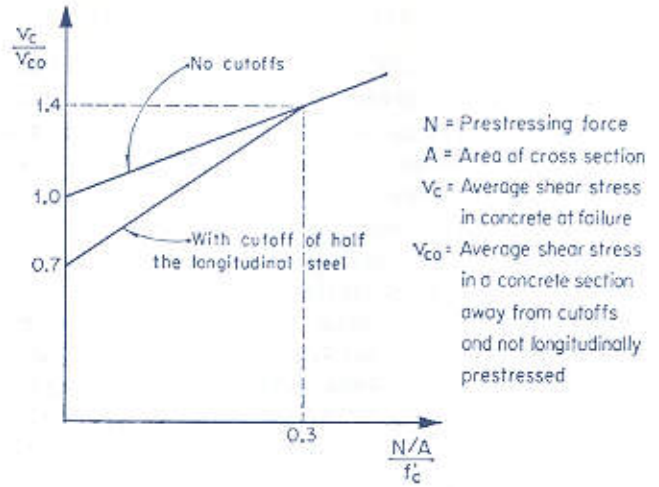

FIGURE 7.28. Shearing strength of a member due to external prestressing.[185]

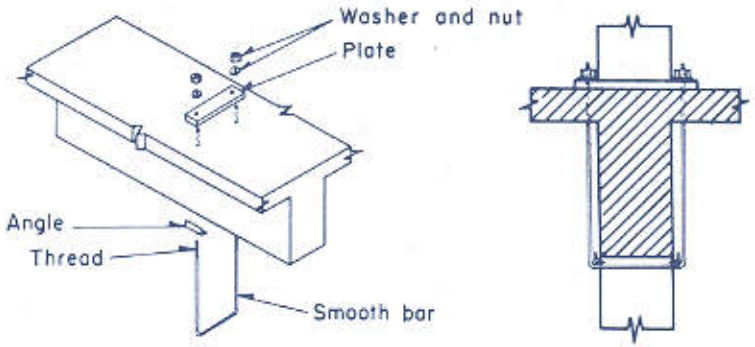

FIGURE 7.29. External stirrups.

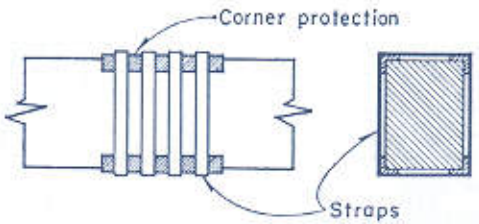

FIGURE 7.30. External prestressed straps.

of prestressed stirrups increases it. Their combination is useful in the fortification of structures to resist earthquakes when the weakening effect of main-steel cutoffs is present, since it results in a simultaneous gain in strength and ductility.

ACKNOWLEDGMENTS

The manuscript for this chapter has been completed in November 1970. The writer is indebted to Luis Esteva, Octavio Rascón, and Enrique Mendoza, of the National University of Mexico, for their numerous contributions to this chapter. Valuable suggestions were received from Roger Díaz de Cossío, of the same institution, and from C. Allin Cornell, of the Massachusetts Institute of Technology.

REFERENCES

1. Benjamin, J. R., and Cornell, C. A., *Probability, Statistics, and Decision for Civil Engineers*, McGraw-Hill Book Company, Inc., 1970.
2. Ang, A. H.-S., and Amin, M., "Reliability of Structures and Structual Systems," *Proc. Am. Soc. of Civ. Engrs.*, Vol. 94, EM2, pp. 671–691, April 1968.
3. Borges, J. F., and Castanheta, M., *Structural Safety*, Laboratório Nacional de Engenharia Civil, Lisbon, 1968.
4. Turkstra, C. J., *Theory of Structural Design Decisions*, SM Study No. 2, Solid Mechanics Division, University of Waterloo, Waterloo, Ontario, Canada, 1970.
5. Barlow, R. E., and Proschan, F., with contributions by Hunter, L. C., *Mathematical Theory of Reliability*, John Wiley & Sons, Inc., 1965.
6. Cornell, C. A., "Stochastic Process Models in Structural Engineering," *Department of Civil Engineering, Stanford University, Technical Report* No. 34, May, 1964.
7. Julian, O. G., "Synopsis of First Progress Report of Committee on Factors of Safety," *Proc. Am. Soc. Civ. Engrs.*, Vol. 83, ST4, pp. 1316.1–22, July 1957.
8. Raiffa, H., and Schlaifer, R., *Applied Statistical Decision Theory*, Graduate School of Business Administration, Harvard University, 1961, Student Ed., The MIT Press, 1968.
9. Swain, G. F., *Structural Engineering*, McGraw-Hill Book Company, Inc., 1927 (quoted in Ref. 14).
10. "Dead Load Stresses in the Columns of Tall Buildings," *Engineering Experimental Station, Ohio State University, Bull.* No. 40 (quoted in Ref. 14).
11. Marsal, R. J., and Mazari, M., *The Subsoil of Mexico City*, Facultad de Ingeniería, Univ. Nacl. Autónoma de México, First Panam. Conference on Soil Mechanics and Foundation Engineering, September 1959.
12. Johnson, A. I., "Strength, Safety and Economical Dimensions of Structures," *Bull. Div. of Bldng. Statics and Structl. Engrg. of the Royal Inst. of Techn.*, Stockholm No. 12, 1953.
13. Rosenblueth, E., *Folleto Complementario: Disposiciones Generales, Cargas Muertas, Cargas Vivas y Viento, Proyecto de Reglamento de las Construcciones en el Distrito Federal*, Ediciones Ingeniería, 1962.

14. Freudenthal, A. M., in Closing Discussion of "The Safety of Structures," *Proc. Am. Soc. Civ. Engrs.*, Vol. 73, pp. 208–218, 1947.
15. Baker, A. L. L., *Raft Foundations, The Soil-Line Method of Design*, Concrete Publications Limited, 1948.
16. Horne, M. R., "The Variation of Mean Floor Loads with Area," *Engineering*, Vol. 171, pp. 179–182, February 1951.
17. Jauffred, F. J., "Carga Viva Debida a Muebles en Unidades de Habitación y Oficina en el Distrito Federal," Master's Thesis, Univ. Nacl. Autónoma de México, 1959. Also, *Ingeniería*, Vol. 30, No. 4, pp. 60–75, October 1960.
18. Baker, J. F., Horne, M. R., and Heyman, J., *The Steel Skeleton*, Vols. 1 and 2, Cambridge University Press, 1956.
19. Rosenblueth, E., "Teoría de la Carga Viva en Edificios," *Ingeniería*, Vol. 29, No. 4, pp. 51–72, October 1959.
20. Areán, F., "Estudio de la Carga Viva en Edificios: Aplicación al Diseño Plástico de Losas," Civil Engrg. Thesis, Univ. Nacl. Autónoma de México, 1956.
21. Corotis, R. B., "Statistical Measurement and Prediction of Building Design Loads," M.Sc. thesis, Massachusetts Institute of Technology, 1968.
22. Lundgren, H., *Cylindrical Shells*, Vols. 1 and 2, The Danish Technical Press, and The Institution of Civil Engineers, 1951.
23. Dunham, J. W., "Design Live Loads in Buildings," *Proc. Am. Soc. Civ. Engrs.*, Vol. 72, pp. 429–443, 1946.
24. *Specifications for Steel Railway Bridges for Fixed Spans not Exceeding 400 Feet in Length*, American Railway Engineering Association, 1947.
25. Stephenson, H. K., "Highway Bridge Live Loads Based on Laws of Chance," *Proc. Am. Soc. Civ. Engrs.*, Vol. 83, pp. 1314.1–23, 1957 (quoted in Ref. 4).
26. Greenshields, B. D., and Weida, F. M., *Statistics with Application to Highway Traffic Analysis*, The Eno Foundation for Highway Control, 1952 (quoted in Ref. 1).
27. Haight, F. A., *Mathematical Theories of Traffic Flow*, Academic Press, Inc., 1963.
28. Stephenson, H. K., and Cloninger, K., "Methods of Converting Heavy Motor Vehicle Loads into Equivalent Design Loads," *Texas Engineering Experimental Station, Bull.* No. 127 (1952).
29. Freudenthal, A. M., "Safety and the Probability of Structural Failure," *Trans. Am. Soc. Civ. Engrs.*, Vol. 121, pp. 1337–1372, 1956.
30. Freudenthal, A. M., "Reflections on Standard Specifications for Structural Design," *Trans. Am. Soc. Civ. Engrs.*, Vol. 113, pp. 265–287, 1948. Discussions, pp. 288–292.
31. Ivy, R. J., Lin, T. Y., Mitchel, S., Roab, N. C., Richey, V. J., and Shefey, C. F., "Live Loading for Long-Span Highway Bridges," *Trans. Am. Soc. Civ. Engrs.*, Vol. 119, pp. 981–994, 1954. Discussions, pp. 995–1004.
32. *Standard Specifications for Highway Bridges*, 9th Ed., The American Association of State Highway Officials, Washington, D.C., 1965.
33. "Final Report," *Proceedings of the Fourth International Congress on Bridge and Structural Engineering, Cambridge, England*, 1952.
34. Freudenthal, A. M., "Methods of Safety Analysis of Highway Bridges," *Proceedings of the Sixth International Congress on Bridge and Structural Engineering, Stockholm*, pp. 655–664, 1960.
35. Grundy, P. and Kabaila, A., "Construction Loads on Slabs with Shored Formwork in Multistory Buildings," *Proc. Am. Concrete Inst.*, Vol. 60, pp. 1729–1738, December 1963.
36. Rosenblueth, E., and Newmark, N. M., *Fundamentals of Earthquake Engineering*, Prentice-Hall, Inc., 1971.

37. Despeyroux, J., "The Agadir Earthquake of February 29th 1960. Behavior of Modern Buildings during the Earthquake," *Proceedings of the Second World Conference on Earthquake Engineering, Japan*, pp. 521–542, 1960.
38. Ambraseys, N., "The Skopje Earthquake of July 26, 1963," *Skopje International Seminar on Earthquake Engineering*, 1964.
39. Minami, J. K., "Relocation and Reconstruction of the Town of Barce, Cyrenaica, Libya, Damaged by the Earthquake of 21 February, 1963," *Proceedings Third World Conference on Earthquake Engineering, New Zealand*, pp. V96–V108, 1965.
40. Rosenblueth, E., and Prince, J., "El Temblor de San Salvador, 3 de Mayo de 1965; Ingeniería Sísmica," *Revista Sociedad Mexicana de Ingeniería Sísmica*, Vol. 3, No. 2, pp. 33–60, December 1965.
41. Housner, G. W., and Trifunac, M. D., "Analysis of Accelerograms—Parkfield Earthquake," *Bull. Seism. Soc. of Am.*, Vol. 57, No. 6, pp. 1193–1220, December 1967.
42. Shannon and Wilson, Inc., *Anchorage Area Soil Studies, Alaska, Report to U.S. Army Engineer District, Anchorage, Alaska*, 1964.
43. Herrera, I., Rosenblueth, E., and Rascón, O. A., "Earthquake Spectrum Prediction for the Valley of Mexico," *Proceedings of the Third World Conference on Earthquake Engineering, New Zealand*, Vol. 1, pp. 61–74, 1965.
44. Díaz de Cossío, R., "Foundation Failures during the Coatzacoalcos (México) Earthquake of 26 August 1959," *Proceedings of the Second World Conference on Earthquake Engineering, Japan*, pp. 473–486, 1960.
45. Rosenblueth, E., "Temblores Chilenos de Mayo 1960; Sus Efectos en Estructuras Civiles," *Ingeniería*, Vol. 31, No. 1, pp. 1–31, January 1961.
46. Steinbrugge, K. V., "Structural Engineering Aspects of the Alaskan Earthquake of March 27, 1964," *Proceedings of the Third World Conference on Earthquake Engineering, New Zealand*, Vol. 3, pp. S50–75, 1965.
47. Falconer, B. H., "Niigata Earthquake, Japan 1.02 p.m., 16 June, 1964," *Internatl. Inst. of Seismology and Earthq. Engrg., Tokyo*, 1964.
48. Rosenblueth, E., and Bustamante, J. I., "Distribution of Structural Response to Earthquakes," *Proc. Am. Soc. Civ. Engrgs.*, Vol. 88, EM3, pp. 75–106, June 1962.
49. Herrera, I., and Rosenblueth, E., "Response Spectra on Stratified Soil," *Proceedings of the Third World Conference on Earthquake Engineering, New Zealand*, Vol. 1, pp. 44–60, 1965.
50. Blume, J. A., Newmark, N. M., and Corning, L. H., *Design of Multistory Reinforced Concrete Buildings for Earthquake Motions*, Portland Cement Association, 1961.
51. "Seismic Details for Special Ductile Frames," *Proc. Am. Concrete Inst.*, Vol. 67, No. 5, pp. 374–379, May 1970.
52. Ferguson, P. M., and Matlob, F. N., "Effect of Bar Cutoff on Bond and Shear Strength of Reinforced Concrete Beams," *Proc. Am. Concrete Inst.*, Vol. 56, No. 7, pp. 5–25, July 1959.
53. Baron, M. J., "Shear Strength of Reinforced Concrete Beams at Points of Bar Cutoff," *Proc. Am. Concrete Inst.*, Vol. 63, No. 1, pp. 127–134, January 1966.
54. Díaz de Cossío, R., and Rosenblueth, E., "Reinforced Concrete Failures during Earthquakes," *Proc. Am. Concrete Inst.*, Vol. 58, No. 5, pp. 571–590, November 1961.
55. Meli, R., and Díaz de Cossío, R., "Evaluación de Daños en un Miembro de Conceto Reforzado," *Revista IMCYC*, Vol. 2, No. 11, pp. 38–67, November 1964.
56. *Uniform Building Code*, 1967 Edition, International Conference of Building Officials, 1967.

57. *Earthquake Resistant Regulations. A World List*, compiled by the International Association for Earthquake Engineering, Tokyo, 1966.
58. *Earthquake Investigations in California, 1934–35*, U.S. Coast and Geodetic Survey, Special Publication No. 201.
59. Blume, J. A., and Binder, R. W., "Periods of a Modern Multistory Office Building during Construction," *Proceedings of the Second World Conference on Earthquake Engineering, Japan*, pp. 1195–1205, 1960.
60. Blume, J. A., "Period Determination and Other Earthquake Studies of a Fifteen-Story Building," *Proceedings of the First World Conference on Earthquake Engineering, Berkeley*, pp. 11.1–27, 1956.
61. Del Valle, E., and Prince, J., "Analytical and Experimental Studies of Vibration in Two Buildings," *Proceedings of the Third World Conference on Earthquake Engineering, New Zealand*, Vol. 2, pp. II. 648–662, 1965.
62. Rosenblueth, E., and Esteva, L., *Folleto Complementario: Diseño Sísmico de Edificios*, Proyecto de Reglamento de las Construcciones en el Distrito Federal, Ediciones Ingeniería, 1962.
63. Rosenblueth, E., and Elorduy, J., "Responses of Linear Systems to Certain Transient Disturbances," *Proceedings of the Fourth World Conference on Earthquake Engineering, Santiago*, Vol. 1, pp. A185–196, 1969.
64. Newmark, N. M., "Torsion in Symmetrical Buildings," *Proceedings of the Fourth World Conference on Earthquake Engineering, Santiago*, Vol. 2 pp. A3.19–32, 1969.
65. Borges, J. F., and Castanheta, M., "General Recommendations Derived from Basic Studies on Structural Safety," *Final Report, IABSE Symposium on Concepts of Safety of Structures and Methods of Design, London*, pp. 293–305, 1969.
66. Inozemtsev, Yu. P., Pashkov, N. N., Pshenitsyn, P. A., Rosanov, N. P., Sacharov, V. I., and Shalnev, K. K., "Cavitational-Erosion Resistance of Hydrotechnical Concretes on Cement and Polymer Binders," *Proceedings of the Eleventh International Congress of the Association for Hydraulic Research, Leningrad*, Vol. 1, Paper 1.48, 1965.
67. Echávez, G., "Erosión en Concreto Causada por Flujo de Alta Velocidad," *Instituto de Ingeniería*, 226, August 1969.
68. Ball, J. W., "Construction Finishes and High-Velocity Flow," *Proc. Am. Soc. Civ. Engrgs.*, Vol. 89, CO2, pp. 91–110, September 1963.
69. Wiegel, R. L., *Oceanographical Engineering*, Chapter 2, Prentice-Hall, Inc., 1964.
70. Chow, V. T., "Oceanography," in V. T. Chow, ed., *Handbook of Applied Hydrology, A Compendium of Water-Resources Technology*, Section 2, McGraw-Hill Book Company, Inc., 1964.
71. Longuet-Higgins, M. S., "On the Statistical Distribution of the Heights of Sea Waves," *J. Marine Research*, Vol. 11, pp. 245–266, 1952.
72. Kinsman, B., *Wind Waves, Their Generation and Propagation on the Ocean Surface*, Prentice-Hall, Inc., 1965.
73. Borgman, L. E., *The Statistical Distribution of Ocean Wave Forces on Vertical Piling*, Hydraulic Engineering Laboratory, University of California, May 1964.
74. Wiegel, R. L., *Oceanographical Engineering*, Chapter 19, Prentice-Hall, Inc., 1964.
75. Gutenberg, B., "Tsunamis and Earthquakes," *Bull. Seism. Soc. Am.*, Vol. 29, No. 4, pp. 517–526, October 1939.
76. Wiegel, R. L., *Oceanographical Engineering*, Chapter 5, Prentice-Hall, Inc., 1964.
77. Horikawa, K., "Evaluation of Tsunami Protection Measures," *Proceedings of the Tsunami Meetings Associated with the Tenth Pacific Science Congress, Monograph* No. 24, 1U66, pp. 250–262, July 1963.

78. Heitner, K. L., *A Mathematical Model for Calculation of the Run-Up of Tsunamis*, Earthquake Engineering Research Laboratory, California Institute of Technology, 1969.
79. Scruton, C., "Aerodynamics of Structures," *Proceedings of the International Research Seminar: Wind Effects on Buildings and Structures, Ottawa*, Vol. 1, pp. 115–161, September 1967.
80. Farquharson, F. B., *Model Investigations which Influenced the Design of the New Tacoma Narrows Bridge*, University of Washington, Engineering Experimental Station, April 1954.
81. Davenport, A. G., "The Dependence of Wind Loads on Meterological Parameters," *Proceedings of the International Research Seminar: Wind Effects on Buildings and Structures, Ottawa*, Vol. 1, pp. 19–82, 1968.
82. *Manual de Diseño de Obras Civiles*, Instituto de Investigaciones de la Industria Eléctrica, Comisión Federal de Electricidad, Vol. 1, Sect. B, "Solicitaciones," pp. 185–389, 1969.
83. Thom, H. C. S., "New Distributions of Extreme Winds in the United States," *Proc. Am. Soc. Civ. Engrgs.*, Vol. 94, ST7, pp. 1787–1801, July 1968.
84. Thom, H. C. S., "Tornado Probabilities," *Monthly Weather Rev.*, pp. 730–736, 1963 (quoted in Ref. 81).
85. Velozzi, J., and Cohen, E., "Gust Response Factors," *Proc. Am. Soc. Civ. Engrs.*, Vol. 94, ST6, pp. 1295–1313, June 1968.
86. Sherlock, R. H., "Wind Forces on Structures: Nature of the Wind," *Proc. Am. Soc. Civ. Engrs.*, Vol. 84, ST4, pp. 1708.1–16, July 1958.
87. Davenport, A. G., "Gust Loading Factors," *Proc. Am. Soc. Civ. Engrs.*, Vol. 93, ST3, pp. 11–34, June 1967.
88. Woodruff, G. B., and Kozak, J. J., "Wind Forces on Structures: Fundamental Considerations," *Proc. Am. Soc. Civ. Engrs.*, Vol. 84, ST4, pp. 1709.1–13, July 1958.
89. Singell, T. W., "Wind Forces on Structures: Forces on Enclosed Structures," *Proc. Am. Soc. Civ. Engrs.*, Vol. 84, ST4, pp. 1710.1–24, July 1958.
90. Pagon, W. W., "Wind Forces on Structures: Plate Girders and Trusses," *Proc. Am. Soc. Civ. Engrs.*, Vol. 84, ST4, pp. 1711.1–29, July 1958.
91. *Handbook of Pressure Coefficients for Wind Loads*, Associate Committee of the National Building Code, Ottawa, Canada, 1961.
92. Baines, W. D., "Effects of Velocity Distribution on Wind Loads and Flow Patterns on Buildings," *Wind Effects on Buildings and Structures, Proceedings of the Conference at the National Physical Laboratory*, HMSO, Vol. 1, pp. 197–223, 1965.
93. Esquillan, N., "Les Règles Françaises 1963 Définissant les Effets du Vent sur les Constructions," *Wind Effects on Buildings and Structures, Proceedings of the Conference at the National Physical Laboratory*, HMSO, Vol. 1, pp. 309–331, 1965.
94. Jensen, M., and Franck, N., "Proposed Code Practice for Wind Loads for Denmark," *Wind Effects on Buildings and Structures, Proceedings of the Conference at the National Physical Laboratory*, HMSO, Vol. 1, pp. 333–351, 1965.
95. Maher, F. J., "Wind Loads on Basic Dome Shapes," *Proc. Am. Soc. Civ. Engrs.*, Vol. 91, ST3, pp. 219–245, June 1965.
96. Dickey, W., and Woodruff, G. B., "The Vibrations of Steel Stacks," *Trans. Am. Soc. Civ. Engrs.*, Vol. 121, pp. 1054–1087, 1956.
97. Dockstanter, E. A., Swiger, W. F., and Ireland, E., "Resonant Vibrations of Steel Stacks," *Trans. Am. Soc. Civ. Engrs.*, Vol. 121, pp. 1088–1112, 1956.

98. Penzien, J. M., "Wind Induced Vibrations of Cylindrical Structures," *Proc. Am. Soc. Civ. Engrs.*, Vol. 83, EM1, pp. 1141.1–25, January 1957.
99. Farquharson, F. B., "Wind Forces on Structures: Structures Subject to Oscillation," *Proc. Am. Soc. Civ. Engrs.*, Vol. 84, ST4, pp. 1712.1–13, July 1958.
100. *Wind Effects on Buildings and Structures, Proceedings of the Conference at the National Physical Laboratory, Teddington, Middlesex*, 1963, HMSO, 1965, in two volumes.
101. *Proceedings of the International Research Seminar: Wind Effects on Buildings and Structures*, Ottawa, 1967, University of Toronto Press, 1968, in two volumes.
102. Anderson, B. G., "Rigid Frame Failures," *Proc. Am. Concrete Inst.*, Vol. 53, No. 7, pp. 625–636, January 1957.
103. Hognestad, E., and Elstner, R. C., "Laboratory Investigation of Rigid Frame Failure," *Proc. Am. Concrete Inst.*, Vol. 53, No. 1, pp. 637–668, January 1957.
104. American Concrete Institute, *Building Code Requirements for Reinforced Concrete* (ACI 318–71), 1971.
105. "Reglamento de Construcciones del Distrito Federal," Chapter 28, *Diario Oficial, México, D.F.*, Vol. 32, 9 February 1966, pp. 44–80.
106. Soretz, S., "Contribución a la Investigación sobre los Aceros de Refuerzo para Concreto y sobre Concreto Armado," *Publicaciones Técnicas, Ecatepec*, Vol. 5, 1963.
107. Mendoza, E., "Estribos para Armar," Submitted for publication in *Ingeniería*, 1974.
108. Fintel, M., and Khan, F. R., "Effects of Column Exposure in Tall Structures—Temperature Variations and Their Effects," *Proc. Am. Concrete Inst.*, Vol. 62, No. 12, pp. 1533–1566, December 1965.
109. Terzaghi, K., and Peck, R. B., *Soil Mechanics in Engineering Practice*, John Wiley & Sons, Inc., 1960.
110. Reséndiz, D., and Herrera, I., "A Probabilistic Formulation of Settlement-Controlled Design," *Proceedings of the Seventh International Conference on Soil Mechanics, México, D.F.*, Vol. 2, pp. 239–245, 1969.
111. González P., J. A., "Influencia de la Superestructura en Hundimientos Diferenciales de Edificios," *Ingeniería*, Vol. 33, No. 3, pp. 209–211, July 1963.
112. Malcolm, D. J., and Redwood, R. G., "Shear Lag in Stiffened Box Girders," *Proc. Am. Soc. Civ. Engrs.*, Vol. 96, ST7 pp. 1403–1419, July 1970.
113. Teng, W. C., *Foundation Design*, Prentice-Hall, Inc., 1962.
114. ACI Committee 214, *Recommended Practice for Evaluation of Compression Test Results of Field Concrete*, American Concrete Institute, 1965.
115. Petersons, N., "Strength of Concrete in Finished Structures," *Trans. Royal Inst. Techn., Stockholm*, No. 232, 1963.
116. Allen, D. E., "Probabilistic Study of Reinforced Concrete in Bending," *Division of Building Research, National Research Council of Canada, Technical Paper* No. 311, *Ottawa* 1970.
117. Bloem, D. L., "Concrete Strength Measurement—Cores versus Cylinders," *Proc. Am. Soc. Testing Matls.*, Vol. 65, pp. 668–696, 1965.
118. Campbell, R. H., and Tobin, R. E., "Core and Cylinder Strengths of Natural and Light-Weight Concrete," *Proc. Am. Concrete Inst.*, Vol. 64, No. 4, pp. 190–195, April 1967.
119. Bloem, D. L., "Concrete Strength in Structures," *Proc. Am. Concrete Inst.*, Vol. 65, No. 3, pp. 176–187, March 1968.

120. Troxell, G. E., and Davis, H. E., *Composition and Properties of Concrete*, McGraw-Hill Book Company, Inc., 1956.
121. Bolotin, V. V., *Statistical Methods in Structural Mechanics*, Holden-Day, Inc., 1969.
122. Roy, H. E. H., and Sozen, M. A., "A Model to Simulate the Response of Concrete to Multi-Axial Loading," *University of Illinois Structural Research Series*, No. 268, 1963.
123. Rüsch, H., and Vigerust, G., Discussion of "Tensile Splitting Test and High Strength Concrete Test Cylinders" by S. Thalow, *Proc. Am. Concrete Inst.*, Vol. 53, No. 12, Pt. 2, pp. 1318–1324, December 1957.
124. Mattock, A. H., Kriz, L. B., and Hognestad, E., "Rectangular Concrete Stress Distribution in Ultimate Strength Design," *Proc. Am. Concrete Inst.*, Vol. 57, No. 2, pp. 875–928, February 1961.
125. Baker, M. J., "Variations in the Mechanical Properties of Structural Steels," *Final Report, IABSE Symposium on the Concepts of Structures and Methods of Design, London*, pp. 165–174, 1969.
126. Nagaraja Rao, N. R., Lohrman, M., and Tall, L., "Effect of Strain Rate on the Yield Stress of Structural Steels," *Am. Soc. Testing Matls. J. Matls.*, Vol. 1, No. 1, pp. 241–262, March 1966.
127. Podolny, W. Jr., "Understanding the Steel in Prestressing," *J. Prestressed Concrete Inst.*, Vol. 12, No. 5, pp. 54–66, October 1967.
128. *Symposium International sur les Aciers de Précontrainte, Contribution Française, FIP, Madrid, Cahiers de la Recherche* No. 26, Association Française de Recherches et d'Essais sur les Matériaux et les Construction, Paris.
129. *Standard Specifications for Billet-Steel Bars for Concrete Reinforcement*, Designation A15–65, American Society for Testing Materials, 1966.
130. Zsutty, T., "Error Studies for Reinforced Concrete Beams," *Proc. Am. Soc. Civ. Engrs.*, Vol. 89, ST6, pp. 235–270, December 1963.
131. Shah, H. C., "Regression Analysis of Reinforced Concrete Columns," *Proc. Am. Soc. Civ. Engrs.*, Vol. 90, ST1, pp. 37–59, January 1964.
132. Borges, J. F., and Butler, D. J., "Computer Experiments Concerning Random Nonlinear Structural Behavior," *Final Report, IABSE Symposium on Concepts of Safety of Structures and Methods of Design, London*, pp. 201–209, 1969.
133. Wood, L., "The Factor of Safety in Design of Timber Structures," *Proc. Am. Soc. Civ. Engrs.*, Vol. 84, ST7, pp. 1838.1–18, November 1958.
134. *Standards and Codes for Buildings in Seismic Regions* (CH-8-57), Moscow, 1957.
135. Wright, D. T., and Green, R., "Human Sensitivity to Vibration," *Department of Civil Engineering, Queen's University, Report* No. 7, *Kingston, Ontario*, February 1959.
136. Chang, F.-K., "Movement in Tall Buildings," *Civil Engineering*, Vol. 37, No. 8, pp. 70–72, August 1967.
137. Casillas, J., "Características Carga-Deformación de Columnas Zunchadas de Concreto," *Ingeniería*, Vol. 33, No. 4, pp. 373–386, October 1963.
138. Rosenblueth, E., and Díaz de Cossio, R., "Instability Considerations in Limit Design of Concrete Frames," *Proceedings of the International Symposium on Flexural Mechanics of Reinforced Concrete, Miami, Am. Soc. of Civ. Engrs.—Am. Concrete Inst.*, pp. 439–463, 1964.
139. Broms, B. B., "Crack Width and Crack Spacing in Reinforced Concrete Members," *Proc. Am. Concrete Inst.*, Vol. 62, No. 10, pp. 1237–1256, October 1965.
140. Kaar, P. H., and Mattock, A. H., "High Strength Bars as Concrete Reinforcement, Part 4—Control of Cracking," *Journal, PCA Research and Development Labs.*,

Vol. 5, No. 1, pp. 15–38, January 1963. Also *PCA Development Department Bulletin* D59.
141. Kaar, P. H., "An Approach to the Control of Cracking in Reinforced Concrete," Paper 8, *Causes, Mechanism, and Control of Cracking of Concrete*, American Concrete Institute, Publication SP-20, pp. 141–157, 1968.
142. Gergely, P., and Lutz, L. A., "Maximum Crack Width in Reinforced Concrete Flexural Members," Paper 6, *Causes, Mechanism, and Control of Cracking of Concrete*, American Concrete Institute, Publication SP-20, pp. 87–117, 1968.
143. Base, G.D., Read, J. B., Beeby, A.W., and Taylor, H. P. J., "An Investigation of the Crack Control Characteristics of Various Types of Bar in Reinforced Concrete Beams," *Cement and Concrete Association, Research Report* 18, Pt. 1, December 1966.
144. Comité Européen du Béton—Fédération Internationale de la Précontrainte, *International Recommendations for the Design and Construction of Concrete Structures*, Principles and Recommendations, English Edition, Cement and Concrete Association, London, 1970.
145. Abeles, P. W., "Studies of Crack Widths and Deformation under Sustained and Fatigue Loading," *Proc. Prestressed Concrete Inst.*, Vol. 10, No. 6, pp. 43–52, December 1965.
146. Bailey, T., "The Corrosion of Reinforcing Steel in Cracked Concrete," *J. Am. Concrete Inst.*, Vol. 18, No. 10, pp. 1137–1144, June 1947.
147. *Proceedings of the International Symposium on the Effects of Repeated Loading of Materials and Structures*, RILEM-Instituto de Ingenieria, 1966.
148. Rascón, O. A., "Stochastic Model to Fatigue," *Proc. Am. Soc. Civ. Engrs.*, Vol. 93, EM3, pp. 147–155, 1967.
149. Hilsdorf, H. K., and Kesler, C. E., "Fatigue Strength of Concrete Under Varying Flexural Stresses," *Proc. Am. Concrete Inst.*, Vol. 63, No. 10, pp. 1059–1079, October 1966.
150. Yao, J. T. P., and Munse, W. H., "Low-Cycle Axial Fatigue Behavior of Mild Steel," *Am. Soc. Testing Matls. Spec. Publ.*, No. 338, pp. 5–24, 1962.
151. Crandall, S. H., Mark, W. D., and Khabbaz, G. R., "The Variance in Palmgren–Miner Damage due to Random Vibration," *Proceedings of the Fourth U.S. National Congress on Applied Mechanics, Berkeley*, Vol. 1, pp. 119–126, 1962.
152. Von Neumann, J., and Morgenstern, A., *Theory of Games and Economical Behavior*, Princeton University Press, 1943.
153. Churchman, C. W., Ackoff, R. L., and Arnoff, E. L., *Introduction to Operations Research*, John Wiley & Sons, Inc., 1961.
154. Ackoff, R. L., personal communication.
155. Rosenblueth, E., and Mendoza, E., "Reliability Optimization in Isostatic Structures," *Proc. Am. Soc. Civ. Engrs.*, Vol. 97, EM6, pp. 1625–1642, December 1971.
156. Chow, V. T., "Statistical and Probability Analysis of Hydrologic Data," in V. T. Chow, ed., *Handbook of Applied Hydrology, A Compendium of Water-Resources Technology*, Section 8. McGraw-Hill Book Company, Inc., 1964.
157. Vanmarcke, E. H., *First Passage and Other Failure Criteria in Narrow-Band Random Vibration: A Discrete State Approach*, MIT Department of Civil Engineering, R69–68, October 1969.
158. Esteva, L., "Seismicity Prediction: A Bayesian Approach," *Proceedings of the Fourth World Conference on Earthquake Engineering, Chile*, Vol. 1, pp. A1:172–184, 1969.
159. Moses, F., "Approaches to Structural Reliability and Optimization," in M. Z. Cohn, ed., *An Introduction to Structural Optimization*, SM Study No. 1, Solid Mechanics Division, University of Waterloo, Waterloo, Ontario, Canada, pp. 81–120, 1968.
160. Tichý, M., and Vorlíček, M., "Safety of Reinforced Concrete Framed Structures," *Flexural Mechanics of Reinforced Concrete, Proceedings of the International Symposium, Miami, Am. Soc. of Civ. Engrs.—Am. Concrete Inst.*, pp. 1.1–1.47, November 1964.
161. Cornell, C. A., "Bounds on the Reliability of Structural Systems," *Proc. Am. Soc. Civ. Engrs.*, Vol. 93, ST1, pp. 171–200, February 1967.
162. Paloheimo, E., "The Probability of Failure and Safety of Structural Section Loaded with a Multidimensional Force-Combination," *Final Report, IABSE Symposium on Concepts of Safety of Structures and Methods of Design, London*, pp. 59–69, 1969.
163. Kasiraj, I., and Yao, J. T. P., "Fatigue Damage in Seismic Structures," *Proc. Am. Soc. Civ. Engrs.*, Vol. 95, ST8, pp. 1673–1692, August 1969.
164. Comité Européen du Béton–Fédération International de Précontraint, *Proposed International Recommendations for the Design and Construction of Concrete Structures*, May 1970.
165. Ang, A. H. S., and Amin, M., "Safety Factors and Probability in Structural Design," *Proc. Am. Soc. Civ. Engrs.*, Vol. 95, ST7, pp. 1389–1405, July 1969.
166. *Standards and Regulations for Design of Concrete and Reinforced Concrete Structures* NyTU, 123–155, Construction Committee of the Council of Ministers of the USSR, Moscow, 1955.
167. Tichý, M., "Artificial Equation Errors," *Final Report, IABSE Symposium on Concepts of Safety of Structures and Methods of Design, London*, pp. 259–271, 1969.
168. Cornell, C. A., "A Probability-Based Structural Code," *Proc. Am. Concrete Inst.*, Vol. 66, No. 12, pp. 974–985, December 1969.
169. Lind, N. C., "Deterministic Formats for the Probabilistic Design of Structures," in M. Z. Cohn, ed., *An Introduction to Structural Optimization*, SM Study No. 1, Solid Mechanics Division, University of Waterloo, Waterloo, Ontario, Canada, pp. 121–142, 1969.
170. Cornell, C. A., "Structural Safety Specifications Based on Second-Moment Reliability Analysis," *Final Report, IABSE Symposium on Concepts of Safety of Structures and Methods of Design, London*, pp. 236–245, 1969.
171. Ravindra, M. K., Heany, A. C., and Lind, N. C., "Probabilistic Evaluation of Safety Factors," *Final Report, IABSE Symposium on Concepts of Safety of Structures and Methods of Design, London*, pp. 35–46, 1969.
172. Baker, A. L. L., *The Ultimate-Load Theory Applied to the Design of Reinforced and Prestressed Concrete Frames*, London Concrete Publications, 1956.
173. Esteva, L., Rosenblueth, E., and Damy, J. E., "Bonus and Penalty in Acceptance Criteria for Concrete," Submitted for publication in *Proc. Am. Concrete Inst.*, 1973.
174. Ferguson, P. M., and Thompson, J. M., "Development Length of High Strength Reinforcing Bars in Bond," *Proc. Am. Concrete Inst.*, Vol. 59, No. 7, pp. 887–922, July 1962.
175. Roy, H. E. H., and Sozen, M. A., "A Note on the Ductility of Concrete," *International Symposium on the Flexure Mechanics of Reinforced Concrete, Am. Soc. of Civ. Engrs.–Am. Concrete Inst.*, Vol. 1, pp. 7.1–20, 1964.
176. Bertero, V. V., and Bresler, B., "Seismic Behavior of Reinforced Concrete Framed Structures," *Proceedings of the Fourth World Conference on Earthquake Engineering, Chile*, Vol. 2, pp. B2.109–124, 1969.
177. Bresler, B., and Gilbert, P. H., "Tie Requirements for Reinforced Concrete Columns," *Proc. Am. Concrete Inst.*, Vol. 58, No. 5, pp. 555–570, November 1961.

178. Lee, D. H., *Sheet Piling, Cofferdams, and Caissons*, London Concrete Publications Limited, 1945.
179. Chellis, R. D., *Pile Foundations*, McGraw-Hill Book Company, Inc., 1961.
180. Rosenblueth, E., "Shell Reinforcement not Parallel to Principal Stresses," *Proc. Am. Concrete Inst.*, Vol. 52, No. 1, pp. 61–71, September 1955.
181. Richart, F. E., "An Investigation of Web Stresses in Reinforced Concrete Beams," *University of Illinois Engineering Experimental Station, Bull.* 166, 1927.
182. McKaig, T. H., *Building Failures*, McGraw-Hill Book Company, Inc., 1962.
183. Hanson, N. W., and Connor, H. W., "Seismic Resistance of Reinforced Concrete Beam-Column Joints," *Proc. Am. Soc. Civ. Engrs.*, Vol. 93, ST5, pp. 533–560, October 1967.
184. Corley, W. G., and Hanson, N. W., "Design of Beam-Column Joints for Seismic Resistant Reinforced Concrete Frames," *Fourth World Conference on Earthquake Engineering, Chile*, Vol. 2, pp. B3. 69–82, 1969.
185. Díaz de Cossío, R., and Martínez, E., "Estudio de Marcos Sujetos a Carga Lateral," *Ingeniería*, Vol. 31, No. 4, pp. 9–24, December 1961.

APPENDIX

Table of Conversion Factors: British to S.I. Units*

Multiply	*by*	*To Obtain*
	Length	
inches	2.5400	centimeters
feet	0.3048	meters
yards	0.9144	meters
	Area	
square inches	6.4516	square centimeters
square feet	0.0929	square meters
square yards	0.8361	square meters
	Volume	
cubic inches[a]	16.3871	cubic centimeters
cubic feet	0.0283	cubic meters
cubic feet	28.3169	liters
cubic yards	0.7646	cubic meters
quarts (liquid)	0.9464	liters
gallons (liquid)	3.7854	liters
[a] Also, first moment of area, or section modulus		
	Moment of Inertia	
$(\text{inches})^4$	41.6231	$(\text{centimeters})^4$
	Mass	
ounces (mass)	28.3495	grams (mass)
pounds (mass)	0.4536	kilograms (mass)
tons (2000 pounds)	907.1847	kilograms
	Velocity	
feet/second	30.4800	centimeters/second
miles/hour (U.S.)	1.6093	kilometers/hour
	Acceleration	
g(gravity 32.174 feet/second^2)	9.8067	meters/second^2
g(gravity 32.174 feet/second^2)	980.67	galileo (gal)

* Selected conversion factors from ASTM Metric Practice Guide, ASTM, 1972.

Table of Conversion Factors: British to S.I. Units (*Contd.*)

Multiply	*by*	*To obtain*
	Force	
pounds (force)	4.4482	newtons
pounds (force)	0.4536	kilograms
	Force/Length	
pounds/inch	1.7513	newtons/centimeter
pounds/foot	14.5939	newtons/meter
	Stress (Pressure)	
pounds/inch^2 (psi)	0.6895	newtons/centimeter^2
pounds/foot^2 (psf)	47.8803	newtons/meter^2
pounds/inch^2 (psi)	0.0703	kilograms/centimeter^2
pounds/foot^2 (psf)	4.8824	kilograms/centimeter^2
	Density (Mass/Volume)	
pounds/inch^3	27.6799	grams/centimeter^3
pounds/foot^3	16.0185	kilograms/meter^3
pounds/yard^3	0.5933	kilograms/meter^3
	Bending Moment (Torque)	
inch-pounds	0.0115	kilogram-meter
inch-pounds	11.2985	newton-centimeter
foot-pounds	0.1383	kilogram-meter
foot-pounds	1.3558	newton-meter
	Temperature*	
degrees Fahrenheit	$t_C = (t_F - 32) / 1.8$	degrees Celsius
degrees Fahrenheit	$t_K = (t_F + 459.67) / 1.8$	degrees Kelvin
degrees Celsius	$t_K = t_C + 273.15$	degrees Kelvin
	Energy (Work)	
British thermal units (Btu)	251.996	calories
British thermal units (Btu)	1055.056	joules
foot-pounds	1.3558	joules
calories	4.1868	joules
Btu/pound	2.326	joules/gram
	Power	
Btu/hour	0.2931	watts
foot-pounds/second	1.3558	watts
horsepower	7.457	watts

* Conversion equations, not multiplication factors.

Table of Conversion Factors: British to S.I. Units (*Contd.*)

Multiply	*by*	*To obtain*
	Heat Transfer	
	Thermal Conductivity	
Btu-inches/hour foot^2 °F	0.1240	kilogram calories/hour meters °K
Btu-inches/hour foot^2 °F	0.1441	watts/meter °K
	Heat Capacity	
Btu/pound °F	4.1868	joules/gram °K
	Thermal Conductance	
Btu-hour foot^2 °F	0.0568	watt/meter °K
Btu/hour foot^2 °F	4.882	kilogram calories/hour meter^2 °K
	Thermal Diffusivity	
Foot^2/hour	0.2581	cm^2/sec

Index

Abram's law, 69
Abrasion, 440, 495
ACI Code, 213–217, 237, 271, 283, 287, 348, 404
Admixtures (*see also* Cement; Concrete; Cracking; Shrinkage)
  accelerating, 24, 25, 71
  air-entraining, 8–9, 25
  calcium chloride, 25, 112
  chemical, 24
  definition, 23
  fly ash, 26
  mineral, 26
  retarding, 24, 25, 135
  types, 24
  water-reducing, 24
Adsorption (*see* Cement; Gel)
Aggregate (*see also* Concrete; Cracking; Creep; Durability; Pozzolan; Shrinkage; Water content)
  absorption, 15, 18, 111
  alkali reaction, 8, 14, 15, 27
  cement ratio, 91, 126
  coarse, 13, 69, 91, 92, 101, 103, 106
  crushed, 80, 81
  deleterious substances, 18
  durability, 15
  effect on concrete deformation, 99, 101 106, 108, 124–125
  effect on drying shrinkage, 109–112
  effect on strength of concrete, 19, 69, 71, 92, 101
  effect on thermal properties of concrete, 19, 29, 136–139, 140–141
  fine, 13
  fineness modulus, 16, 17
  grading requirements, 16, 17, 18
  gravel, 80–81, 101–102, 111–113, 115, 124, 141, 144
Aggregate (*continued*)
  heavyweight, 20, 21
  lightweight, 20, 101, 102, 103, 105, 111, 125, 137, 139
  porosity of, 124
  saturated surface-dry, 18
  shape, 15, 16
  sieve analysis, 16, 18
  size, 16, 69, 71
  size effects, 34, 37, 69, 71, 91, 92, 101, 103, 106, 111, 124, 136
  sources, 13
  specific gravity, 15
  strength, 66
  surface moisture, 18
  surface texture, 16
  thermal properties, 19–20
  unit weight, 20
Air-entrainment (*see also* Cement; Concrete; Durability; Water content)
  air content, 31–32, 35
  effect on durability, 31
  effect on shrinkage, 112
  effect on strength of concrete, 81, 95
  effect on thermal properties, 136
  effect on water content, 37
  factors affecting, 25–26
  purpose of, 30–31
Alite, 3, 4
Anchorage (*see also* Bond; Tendons)
  in mass concrete, 188, 189
Axial compression (*see* Columns; Concrete)
Axial compression and bending (*see* Columns)
Axial tension (*see* Concrete; Cracking; Tension members)

Ball penetration test, 29
Barite, 20–21, 136, 137

Bauschinger effect (*see* Reinforcing steel)
Bayes' theorem (*see also* Reliability), 414, 460, 478, 504
Basalt, 111, 124, 136, 138
Beams, prestressed (*see also* Bond; Columns; Design; Prestressing; Shear; Tendons; Torsion)
  AASHO-PCI sections, 358–359
  bearing at anchorage, 345
  bonded, 303, 327, 331
  cables, concordant and non-concordant, 374
  camber, 364
  choice of sections, 354–356
  composite sections, 336–337, 342, 373
  continuous, 372–384
  cracking moment, 328–329, 334, 381
  curvature, 333–336
  deflections, 346, 366, 369
  design, allowable stresses, 348–349
    balanced load, 350
    basic concepts, 303–309
    elastic, 347–348
    end blocks, 345
    linear transformation, 375
    preliminary, 346
    ultimate strength, 349
    web reinforcement, 341
  long time deflections, 365–366
  moments, primary and secondary, 374
  over-reinforced, 329, 332
  sections, properties of, 357, 358, 359
  span-depth ratios, 367
  strength, 329–333, 349, 382–383
  stresses in concrete, 326
  stresses in steel, 327
  tendon, protection and spacing, 363–364
  tendon layouts, 355–363
  transfer bond, 342–345
  unbonded, 303, 327, 331
Beams, reinforced (*see also* Bond; Columns; Design; Reinforcing steel; Shear; Torsion)
  balanced amount of reinforcement, 201, 216
  bending, biaxial, 217
  bending, modes of failure, 200–201
  bending strength, 201, 212, 214–217
  bending with axial load, 203, 205, 209, 214
  continuous, 229, 283
  corbels, 273
Beams, reinforced (*continued*)
  cracking, 171–173, 201, 203, 249, 273–275, 279
  curvature, 206, 279–280
  cyclic loading, 55, 436
  deep, 272, 276
  deflections, 200, 277–294
  design, 211–219
  doubly reinforced sections, 202
  ductility, 201–202, 289–290, 470–472, 496–499, 500–505
  holes, 276
  long time deflections, 277–278, 283–288
  over-reinforced, 201, 206
  plastic hinges, 234–235, 290–293, 457, 471, 483
  reinforcement limitations, 201, 202, 203, 216
  stiffness, 173–176, 201, 277, 281
  strain distribution, 203
  stress blocks, equivalent, 212, 292, 293
  transformed section, 208
  under-reinforced, 201, 216
Belite, 3, 4
Bleeding, 29–30, 73, 77, 85, 88
Bond (*see also* Anchorage; Beams; Cracking; Design; Prestressing; Reinforcing steel; Splices; Tendons)
  adhesion, 160
  anchorage, 152, 166, 179
  deformed, 151, 160
  degradation of, 176, 498
  development length, 179–182, 184, 185, 316, 318, 320, 344, 345
  flexural, 152, 166
  friction, 160
  galvanized steel, 59
  in lightweight aggregate concrete, 178
  lap splices, 61, 178, 182
  of compressive reinforcement, 177, 178
  plain, 160
  prestress, flexural, 344
    transfer of, 342, 343
  pullout, 152, 166–167
  slip, 151, 157–158, 162, 320
  strength, 160, 162–163, 166
  stress, distribution of, 155, 157–158, 165–166
    flexural, 152–153
  structural steel, 187
  tests, 152, 162, 166–170
  top bars, 177

Bond (*continued*)
  wedging, 161, 165
Bonds, microcracking, 67, 103
  particle, 66, 69, 92, 141
Braced frames (*see* Design)
Brackets (*see* Beams; Corbels)
Bridges (*see* Design)
Buckling (*see* Design)

Capillaries, 70, 109, 126, 141
Carbonation shrinkage (*see also* Shrinkage), 108, 112, 116
Cement, air-entraining, 8
  calcium silicate, 2–5
  content in concrete, 32, 69, 135
  deleterious components, 4
  false set, 2
  final set, 6
  fineness, 71, 112, 125, 142
  gel, 4, 66, 71, 104, 109, 112, 115, 141
  gel-space ratio, 70
  hydration, 4–5, 70, 123, 127, 136
  initial set, 6
  paste, 109, 134, 137, 140
  Portland, 1, 2–9, 11
  quick set, 3
  setting time, 6
  soundness, 6, 8
  special cements, 8–13
  strength requirements, 8
Chimney stacks, 436, 444
Code formats (*see also* Reliability; Safety)
  calibration of, 490
  Cornell's, 488
  deterministic, 484
  first-order, 488
  probabilistic, 488–494
  second-moment, 488
  semi-probabilistic, 487
Coefficient of variation (*see also* Probability distributions; Safety)
  definition of, 411
  use in calculation of reliability, 411, 489
Cold joints, 34
Columns, prestressed (*see also* Beams)
  axially loaded, 389, 391
  eccentrically loaded, 393
  interaction diagram, 395–396
  partially prestressed, 395
  slender columns, 393
Columns, reinforced (*see also* Beams)
  axially loaded, 197–199
Columns, reinforced (*continued*)
  biaxial bending, 217
  compression and bending, 195, 203, 206, 212, 214
  ductility, 197–199
  eccentricity, accidental, 440, 447, 488, 495
  interaction diagram, 196, 210, 213
  lateral reinforcement, 197, 199, 203
  longitudinal reinforcement, 197
  shortening, 294
  slender columns, 197
  spiral reinforcement, 197, 199
  strength 209, 212
  ties, 197, 203
Compliance (*see* Creep)
Compression (*see* Columns; Concrete; Splices)
Concrete, fresh, ball penetration test, 29
  compaction, 69, 77, 90, 94, 108, 126
  consistency, 29
  consolidation (*see* compaction)
  final set, 33
  initial set, 33
  mix proportioning, 39
  remolding test, 28
  revibration, 33, 451
  seawater, 22
  segregation, 8, 29, 69, 85
  slump, 29, 35–37
  structure, 27, 28
  temperature, 33–34, 39–40
  vibration, 69
  water gain, 30
  water requirement, 40
  workability, 8, 28, 31, 71
Concrete, hardened (*see also* Deformations)
  aging, 70–71, 105, 123, 142
  curing, 81, 85, 87, 109, 113, 134, 142
  durability, 4, 8, 19, 31, 141
  heavyweight, 20, 21
  lightweight, 101, 102, 103, 105, 111, 125, 137, 139
  maturity, 70, 133
  quality, 90–91
  strength (*see* Concrete, strength)
  stress-strain (*see* Deformation)
  sulfate attack, 4, 8
  thermal properties, 136–144
  unit weight, 32, 94, 108
  voids, 70, 91

Concrete, strength, accelerated curing test, 85–87
acceptance test, 86, 88
coefficient of variation, 459, 462
combined stress, 67, 82–85
compression, 65, 66, 68–79, 85–92, 199, 459–462
test, 75
confinement effect, 199, 471, 498, 503
cores, 87–88
cracking, 159
curing, 81, 87, 113, 134, 461
effect of aggregate, 69, 71, 92, 101
effect of aging, 70–71
effect of air-entrainment, 81, 95
effect of cement, 4, 7, 69
effect of creep, 119
effect of size, 73–77
effect of temperature, 143
effect of water-cement ratio, 68–70
equation of strength, 82–85
failure criteria, 82–83
fatigue, 93–96
flaws, 67
flexural, 79–80
gel-space ratio, 70
impact, 92–93
loading rate, 77–79, 98, 99, 101, 106
microcracking, 67, 98, 103, 122
modulus of rupture, 80
mortar, 67, 69
nature of, 66
non-destructive tests, 88–92
rebound hammer, test, 88–89
repeated loads, 471, 473
shear, 83
splitting test, 80
tensile, 65–68, 79–82, 224, 280, 462
tension test, 80
triaxial, 82
ultrasonic pulse test, 90–92
Construction joints (*see* Joints)
Corbels (*see* Beams)
Corrosion, 22, 58, 135, 174, 363, 473, 495
Cracking (*see also* Beams; Shear; Shrinkage; Slabs; Torsion)
control of, 67, 170–173
detection of, 91
effect of admixtures, 135, 451
effect of aggregates, 112
effect of loading, 155
effect of shrinkage, 133–136
Cracking (*continued*)
in aggressive environment, 135, 174
influence on stiffness, 174–176
mechanism, 155–160, 162, 164, 165
microcracking, 67, 98, 103
strains in cracked elements, 175
stresses in cracked elements, 155, 165–166
Cracks, spacing, 159
width, 65, 135, 159–160, 170–174, 473
Creep (*see also* Beams; Columns; Concrete; Mortar; Relaxation)
basic, 121, 127
compliance, 123
drying, 121
free, 124
influence of age, 123
influence of aggregate, 124–125
influence of cement, 125
influence of humidity, 127
influence of size, 127
influence of strength, 125
influence of stress, 122, 129
influence of temperature, 127, 133
nature of, 119–122
Poisson's ratio, 108, 129
prediction of, 129–133
rate of, 123
recovery, 121
relation to shrinkage, 120
specific, 122, 131
stochastic model for, 413
superposition, 121, 129
tension, 129
torsional, 129
ultimate, 130

Deflections (*see also* Beams; Columns; Slabs)
human response to, 277, 470
Deformations (*see* Beams; Columns; Creep; Design; Shear; Shrinkage; Strain; Torsion)
Densification, 94, 108
Design (*see also* Beams; Columns; Earthquake design; Shear; Slabs; Torsion)
aids, 211
balanced design, 201, 216, 471
braced frames, 436
bridges, 413, 443, 444
buckling, of beams, 471
of reinforcement, 474, 499
codes, purpose of, 494

Design (*continued*)
collapse, 288, 291
concrete cover, 163, 495, 497, 498
corner reinforcement, 500
cut-off, reinforcement, 438, 505, 507
damage, 484
defense plateaus, 482
deflection criterion, 277, 278, 451, 469–470, 484, 493
details, 59, 60, 61, 62, 185, 438, 471, 494, 504
dimensions, variation, 465
ductility, 197–199, 201–202, 289–290, 470–472, 496–499, 500–505
environmental conditions, 448–453
errors in computation, 418, 488, 489
fatigue, 448, 471, 473, 484
lifespan, 408
overturning, 448, 486
preliminary design, 346
reinforcement, maximum, 450, 496
minimum, 450, 495
repairs, 440, 503
serviceability criterion, 277–278, 493
shear envelope, beams, 422
spalling, 497, 498
strength, variations, 467–468
tolerances, 465, 469, 493
unit weight, construction materials, 417, 493
Development length (*see* Bond; Tendons)
Diagonal tension (*see* Shear, in reinforced concrete, failure modes)
Diffusion (*see also* Shrinkage), 108, 115, 117, 141
Diffusivity, thermal, 138
Dolerite, 138, 141
Dolomite, 136, 137
Dolphins (*see* Harbor structures)
Ductility (*see* Beams; Columns; Design; Earthquake design; Reinforcing steel)
Durability (*see also* Corrosion; Freezing and thawing; Sulfate attack)
aggregate, 15
concrete, 19, 31, 35–36

Earthquake design (*see also* Beams; Columns; Design; Reinforcing steel)
base shear coefficient, 439
bilinear systems, 436
Earthquake design (*continued*)
cumulative damage, 484
drift limitations in, 455, 470, 484
ductility, 470–472
during construction stage, 499
effects on construction joints, 495
energy absorption, 54, 55, 442, 498
energy feedback to ground, 439
fundamental period, 439–440
modes of vibration, 437
optimum design to resist, 481, 493
pounding due to, 455
stiffness degradation, 55, 176
Earthquakes, characteristics, 429
intensity of, 431
magnitude of, 431
spectra of, 431
stochastic model, 413
structural response to, 413, 432, 455
vertical acceleration, 438, 497
Endurance limit (*see also* Fatigue), 94
Ettringite, 4, 9
Extensibility, 134, 135

Failure (*see also* Beams; Bond; Columns; Concrete; Design; Safety; Shear; Slabs; Tension)
criterion, concrete, 67, 82, 83
probability, 407, 409, 477, 479, 483–484
recurrence period, 413, 480
warning of, 418, 425, 427, 486, 488, 492
Falsework, 89
Fatigue (*see also* Concrete; Design; Endurance limit; Reinforcing steel; Strain; Strength)
design for, 448, 471, 473, 484
reinforcing steel, 57, 58
Fire protection, 89, 495
Flat slabs (*see* Slabs)
Foundation design, angular distortion due to settlement, 453, 455
footings, 236, 454, 459
methods of, 456
settlement, 453, 456, 499
tilting, 455
Freezing and thawing, 19, 31, 440

Galvanized reinforcement (*see also* Bond; Corrosion; Reinforcing steel), 59
Gel (*see* Cement; Concrete)
Gillmore test, 6
Granite, 111, 112, 113, 124, 138, 141

TABLE 2.6. Effect of Strain Rate Yield Stress of Steel Reinforcing Bars.[8]

Average Strain Rate, in./in./sec	f_{yd}/f_y Values											
	f_y^a = 56 ksi, Upper Yield Point	51 ksi, Lower Yield Point	f_y^a = 59 ksi, Upper Yield Point	57 ksi, Lower Yield Point	f_y^a = 87 ksi, Upper Yield Strength	81 ksi, Lower Yield Strength	f_y^a = 93 ksi, at 0.006 Yield Strain	f_y^b = 45 ksi,	f_y^c = 47 ksi	f_y^d = 40 ksi	f_y^d = 70 ksi
0.001	1.23	1.07	1.09	1.02	1.05	1.03	—	1.05			
0.01	1.32	1.14	1.17	1.07	1.08	1.05	1.01	1.11			
0.1	1.42	1.21	1.27	1.16	1.11	1.08	1.03	1.19			
Between 0.1 and 1.0									1.33		
1.0	1.51	1.28	1.40	1.25	1.18	1.10	1.08	1.28			
225										2.18	1.78

f_y is the steel yield stress, based on a static (or nearly static) strain rate.
f_{yd} is the steel dynamic yield stress, based on a dynamic strain rate (typical of structures subjected to blasts or earthquakes.
[a] W. L. Cowell, "Dynamic Tests of Concrete Reinforcing Steels," U.S. Naval Civil Engineering Laboratory, Port Hueneme, California, AD 622554, September 1965.
[b] "Design of Structures to Resist the Effects of Atomic Weapons—Strength of Materials and Structural Elements," *Manual* EM 1110-345-414, U.S. Army Corps of Engineers, March, 1957.
[c] C. P. Siess, "Behavior of High Strength Deformed Reinforcing Bars Under Rapid Loading," Department of Civil Engineering, University of Illinois, Urbana, Illinois, February 1962 (unnumbered).
[d] R. G. Crum, "Tensile Impact Tests for Concrete Reinforcing Steels," *ACI Journal, Proceedings* Vol. 56, No. 1, p. 59, July 1959.

TABLE 2.7. Range of Reinforcing Steel Ratio to Insure Ductile Failure.[8]

ASTM A615 Reinforcing Steel	f_y, ksi	f_{yd}, ksi[a]	ACI Code Minimum ρ^b	$\rho' = 0$		$\rho' = 0.5\rho$ (Assuming that the Compression Steel Yields)	
				ρ_1	$\rho_2{}^c$	ρ_2	$\rho_2{}^c$
Grade 40	40		0.0050	0.0030	0.034	0.0059	0.068
		60		0.0020	0.023	0.0040	0.046
Grade 60	60		0.0033	0.0020	0.018	0.0040	0.037
		84		0.0014	0.013	0.0028	0.026
Grade 75	75		0.0027	0.0022	0.013	0.0044	0.025
		90		0.0018	0.011	0.0037	0.021

[a] f_{yd}/f_y for each steel corresponds to about 1.0 in. per in. per sec strain rate (Table 2.6).
[b] $200/f_y$, ACI Committee 318, *ACI Standard Building Code Requirements for Reinforced Concrete* (ACI 318-71) Detroit, 1971, Section 10.5.1 (f_y in psi).
[c] Values of ρ_2 for Grade 40 steel are based on an assumed 0.2% offset at yielding, values of ρ_2 for Grade 60 and Grade 75 steel are based on the EUL yield strain specified by ASTM for those steels.

loadings, strain rates can be high, typically as high as 1.0 in. per in. per sec[9] and their generally beneficial effect is worth considering in design. However, earthquake loadings produce strain rates which are less than those produced by blast, and consequently their effect is usually neglected.

Ductile Failure. Steel yielding followed eventually by concrete crushing without steel rupture or premature bond or shear failure (that is, ductile failure) is considered mandatory in earthquake- and blast-resistant design and is desirable in all designs. The reinforcing index $\rho f_y/f_c$—or just ρf_y relative to the reinforcing steel—is the basic parameter for establishing the theoretical limits or ductile failure of a flexural member, as based on compatibility analyses at the steel yield strain and at the steel ultimate strain. From such analyses, Table 2.7[8] gives lower, ρ_1, and upper, ρ_2, limits on the percentage, ρ, of the tensile reinforcing bars in 4000-psi concrete beams that would theoretically result in a ductile failure. For any given grade of reinforcing bar in a concrete of a given strength, ρ_1 and ρ_2 can thus be considered important properties for achieving ductile structures.

The ACI *Code*[7] does not permit a percentage greater than 0.75 times the balanced-design percentage. As discussed in Reference 10, this ensures a ductile failure in flexural members when the yield strain is somewhat greater than f_y/E, illustrated in Table 2.8.

Griffith's criterion, 67
Gypsum, 3, 125

Harbor structures, 427, 429, 440–443
Hazard function, 412, 474, 480
Holes (*see* Beams; Slabs)
Hot-weather concreting, 135
Humidity, effect on creep, 113, 127
  effect on shrinkage, 113
  effect on thermal expansion, 142
Hydration, 3, 4, 70, 123, 127, 136

Igneous rocks, 13, 14, 15
Impact (*see* Concrete; Loads; Rebound hammer)

Joints, beam-column, 243
  construction, 495
  design considerations, 438, 449, 452, 499–503

Laitance, 30
Limestone, 111, 136, 138, 141
Load factors, 412, 424, 458, 459, 485, 487, 489, 494, 504
Load tests, 503
Loads, dead, 416–418, 492, 504
  during construction, 428
  earthquake (*see* Earthquake design)
  effect of architectural changes, 417, 418, 492
  hail, 425
  impact, 429, 442
  live, bridges, 427–428
    buildings, 418–427
  ponding, 277, 470
  rain, 425
  repeated, 55, 56, 412, 448, 471, 473, 474, 484, 498
  snow, 425, 426
  tornadoes, 445
  wave forces, 440–443
  wind, 443–448

Mortar, creep, 123
  in hollow-tile and hollow-block walls, 417
  shrinkage, 109
  strength, 67, 69
  strength test, 8

Non-destructive tests, 88

Optimization, objective function, 477
  of load factors, 483
  reliability, 478–484
  utility, 475
Overturning, 448, 486

Partial safety factors, 485, 488, 489, 491
Piers (*see* Harbor structures)
Plastic hinges (*see* Beams)
Poisson process, 413, 480
Poisson's ratio, 73, 106, 129
Pores, 70, 104, 141
Pozzolan, influence on alkali-aggregate reaction, 14, 27
  influence on properties of concrete, 10–11, 26
  types, 10, 26
Prestressing (*see also* Beams; Columns; Design; Shear; Slabs; Tendons; Tension)
  chemical, 309
  creep and shrinkage effects, 315, 317
  effective prestress, 325
  elastic design, 347–349
  elastic shortening, 314
  end blocks, reinforcement, 346
  flat slabs, 367, 384, 387
  internal couple concept, 303–304, 307, 346–347
  kern point, 306
  load balancing concept, 303, 306, 308, 350–352, 379, 384
  losses, 310, 322–324, 325
  methods, 309–310
  partial prestressing, 331, 368–372, 387, 392, 395
  pressure line, 374
  relaxation, in steel, 95, 121, 317–318, 320, 323
  strands, 322
  systems, 302, 309, 310–312, 315
  tension members, 389
  thermal, 309
  transfer length, 342–345
Probabilities (*see also* Failure; Probability distributions; Reliability; Risk; Safety)
  of hypotheses, 414
  posterior, 413
  prior, 413

Probability distributions, 410, 413–415, 444, 460
Proportioning of concrete mixes, 34, 36–39

Quartz, 78, 111, 112, 124, 136, 138, 141
Quay walls (*see* Harbor structures)

Rate of loading, 77, 98, 99, 101
Rebound hammer, 88, 89
Reinforcing steel (*see also* Beams; Bond; Columns; Corrosion; Design; Shear; Slabs; Splices; Strain; Torsion)
  ASTM specifications, 42–48, 62
  axle steel, 43
  balanced design ratio, 53
  Bauschinger effect, 55
  bending, 59, 60, 62
  bend-test, 43
  bent bars, 219, 220
  cold-drawn wire, A-82, 43
  confinement, 292, 293
  corrosion of, 58
  cut-off, 179, 180
  deformation requirements, 44, 47, 48
  deformed (*see* Bond)
  dimensions of bars, 44, 45
  dimensions of wires, 44, 46
  ductility, 43, 51, 53–57
  fabrication of, 59
  fatigue strength of bars, 57, 58
  fatigue strength of wire fabric, 58
  galvanized, 59
  hooked bars, 59, 60, 185
  identifying marks on bars, 44, 49
  in columns, 198
  index, 203
  inelastic behavior, 51–57
  lapped splices, 61
  mechanical splices, 62
  plain (*see* Bond)
  properties of, as produced, 42–51
  protective coatings, 58, 59
  reduction of area, 43
  rusting, 58
  sizes (*see* dimensions)
  strain energy capacity, 54–55
  strain hardening, 289
  strain rate, 51, 52
  stress-strain curves, 47, 199, 205, 209, 215
  tensile strain, 51, 52
Reinforcing steel (*continued*)
  tensile strength, 43, 51–52
  top (*see* Bond)
  transverse, 197, 219, 220, 229
  welded wire fabric, deformed, A-497, 43
  welding, 57, 59, 60, 61, 62
  yield strain, 43, 47, 50, 51
  yield strength, 43, 51, 52, 464
  yield stress, 199, 464, 469, 493
Relaxation, concrete, 121
Reliability (*see also* Code formats)
  fixed, 417, 418
  forcing function, 410
  of structural members, 474, 482, 483
  of structural systems, 482, 483
  optimization, 478, 482
  reliability function, 409, 477
  resistance function, 409
Rhyolite, 138
Risk (*see* Hazard function)
Risk function (*see* Hazard function)
Rotational capacity, 103, 105

Safety (*see also* Code formats; Design; Fixture; Load factors; Reliability; Risk; Utility)
  factors, 413, 479, 485, 490, 491
  hazard function, 412
  index, 489
  margin, 490
  probability distributions, 413–416
  probability of failure, 409
  reliability, 409–413
  risk, 412
  statistical approach, 407–475
  stochastic model, 413
Sandstone, 111, 112, 115, 124, 141
Sedimentary rocks, 13, 14, 15
Shear, in prestressed concrete, combined with bending, 338
  combined with torsion, 403
  composite section, 342
  principal tensile stress, 337
  punching in flat slab, 388
  strength, 338–341
  web reinforcement, 341–342
Shear, in reinforced concrete, alternating loads, 229
  axial load effect, 226, 449
  beam-column joints, 243, 244, 500, 501
  brackets, 245, 246, 263

Shear, in reinforced concrete (*continued*)
critical section, 238
cut-off, effect of, 225
dowel effect, 225, 227, 231
effect on deflection, 470
failure modes, 220–236
failure, premature, 53
flat slabs, 236–238
footings, 236–238
holes, influence of, 238
in strengthened structures, 505
inclined cracking load, 222, 231, 234, 237
orthogonal reinforcement, 500
member size effect, 226
span, 224
strength, 227, 237
stresses, 219, 223, 229, 238
transverse reinforcement, 197, 219, 220, 229, 438, 439, 451, 471, 495, 497, 498, 501
walls, 275–276
web reinforcement, 228–230
Shrinkage, carbonation, 108, 116–117
column shortening, 294
cracking due to, 133–136, 448–449
differential, 114
diffusion, 108, 115, 117, 141
drying, 108, 114, 127
effect of shape on, 115
effect on deflections, 283, 449
effect on strength, 449
effective thickness, 119, 133
free, 108, 114
in prestressed concrete, 315–317
influence of admixtures, 112
influence of aggregates, 19, 76, 109–112, 124
influence of cement, 112
influence of curing, 113
influence of humidity, 113
influence of size, 114
influence of water content, 112
irreversible, 108
moisture movement, 108
non-uniform, 114
plastic, 30, 135
prediction of, 115, 118
relation to creep, 120
restrained, 124, 134
reversible, 108
ultimate, 115, 118–119
volume to surface ratio, 115
Slabs, prestressed, cracking strength, 387
deflection, 387
flat slabs, analysis, 384–387
punching shear, 388
serviceability, 388
span-depth ratio, 388
stiffness, 388
ultimate capacity, 387
Slabs, reinforced, ductility, 238
holes, 238
moment transfer to columns, 241
shear reinforcement, 238
Splices, compression, 178
design, 438, 498, 499
lap, 182, 183
mechanical, 182, 183
tension, 182, 183
welded, 182
Storage loads (*see* Loads)
Strain, concrete (*see also* Creep; Shrinkage; Temperature effects)
capacity, 105
compressive, 96–103
effect of cyclic load, 94, 106
energy, 82, 93, 436
failure, 68, 101
flexural, 106
rate, 77, 99
stress-strain characteristics, 97–103
tensile, 106
ultimate, 463, 471
volumetric, 108
Strain, steel, energy, 54
rate, 51–53
tensile, 47–51
under cyclic load, 55–57
Strength (*see* Beams; Bond; Columns; Concrete; Cracking; Reinforcing steel; Shear; Torsion)
Stress (*see* Beams; Bond; Columns; Concrete; Cracking; Reinforcing steel; Shear; Torsion)
Sulfate attack, 4, 8
Swelling, 108, 115–116, 141

Temperature effects (*see also* Concrete)
creep in concrete, 127, 133
fresh concrete, 33–34, 39–40
shrinkage, 119
strength of concrete, 143
structural design, 451, 496

Temperature effects (*continued*)
thermal expansion, 19, 140
Tendons (*see also* Beams; Prestressing; Slabs)
anchorage, 316, 318, 320, 345
elongation of, 324
friction, 322
layouts, 355, 361, 362, 363
limiting zone for, 355, 359, 360
linear transformation, 375
protection for, 363
slippage, 320
spacing, 363
Tension members, prestressed, 389–391
Ties (*see* Transverse reinforcement)
Torsion, in prestressed concrete, combined with bending, 401–403
combined with bending and shear, 403–404
cracking torque, 398
pure, 397
strength, 398, 400–401
stress, 397–398
Torsion, in reinforced concrete, combined with axial load, 267–269
combined with flexure, 256–261
combined with flexure and shear, 266
combined with shear, 261–266
design, 269–272
failure modes, 249
membrane analogy, 251
pure, 249–250
sand heap analogy, 251
strength, 251–255
transverse reinforcement, 253, 257, 261, 262, 265, 267, 268
Trachyte, 136
Transfer length (*see* Beams, Prestressing)
Transformed section (*see* Beams, reinforced)
Transverse reinforcement (*see* Columns; Shear)
Triaxial stresses (*see* Concrete; Strength)
Tsunamis (*see* Waves)

Ultimate strain (*see* Strain, concrete)
Ultimate strength (*see* Beams; Columns; Shear; Torsion)
Ultrasonic pulse test (*see* Concrete; Strength)
Unbonded beam (*see* Beams, prestressed)
Utility, discount function, 477
discount rate, 478
objective function, 475, 477, 484

Van der Waals' forces, 66

Walls (*see* Shear, walls)
Warning of failure, 418, 425, 427, 486 488, 492
Water-cement ratio, effect on creep, 126
limits for durability, 35–36
strength relationship, 35, 36, 37, 68–70
Water content, 135, 137
effect on shrinkage, 112
Water content of mixes, effect of air-entrainment, 37
effect of maximum aggregate, 37
effect on slump, 37
Water gain (*see* Concrete, fresh)
Waves, tidal, 442
Tsunamis, 442
wind-generated, 440, 441, 442
Wear (*see* Abrasion)
Wharves (*see* Harbor structures)
Wind, during construction stage, 499
dynamic effects, 448
flutter, 443
forced vibrations, 443
galloping, 443
gradient velocity, 445
gust factor, 446
optimum design to resist, 493
speed, 444
static effects, 447
tornadoes, 445
tropical storms, 445–446
vortex shedding, 443
Workability (*see* Concrete, fresh)
Workmanship, 461, 468, 471

TABLE 2.8. Yield Strain Limitations for Ductile Failure in Flexural Members.[10]

Grade	f_y/E	Upper Limit, for Ductile Failure, for the Strain at the Yield Strength when $0.75\rho_b$ Tensile Steel Only is Used,[a] $0.001 + 4f_y/3E$
40	0.00138	0.00284
60	0.00207	0.00376
75	0.00259	0.00445

[a] ρ_b is the balanced design steel percentage for tensile steel only (neglecting any compression steel).

Energy Capacity. Maximization of strain-energy-absorption capacity will generally result in a structure with superior resistance to either blast or earthquake loadings. Again, ρf_y is the main parameter affecting the strain energy in a flexural member of a given concrete strength. As shown for 4000-psi concrete beams in Figs. 2.6 and 2.7,[8] strain energy is maximized by a smaller ρf_y, but not so small as to result in steel rupture. The steel ductility merely

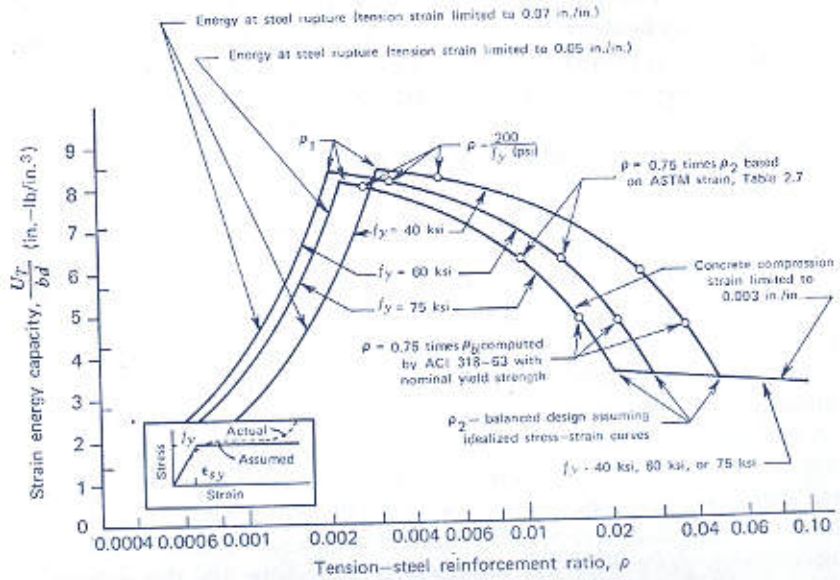

FIGURE 2.6. Strain energy capacity of rectangular concrete beam with only tension reinforcing steel.[8]

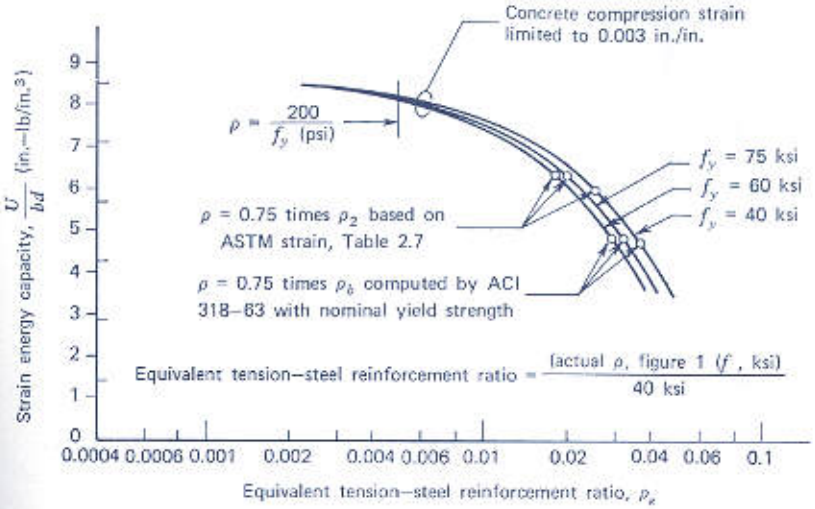

FIGURE 2.7. Strain energy capacity of ductile beams of equal static strength.[8]

determines the minimum ρf_y that can be used without the steel rupturing rather than the concrete crushing, which would usually correspond to ρ less than about 0.5%.

Bauschinger Effect. As for other steels of comparable strength and composition, reinforcing bars subjected to inelastic reversed loadings exhibit the Bauschinger effect, that is, an appreciable lowering of the proportional elastic limit in both tension and compression (but attainment of a stress at least equal to the original yield strength) and eventual stabilization of this behavior after several cycles of a given pattern of inelastic loading (Fig. 2.8).[11] This affects the behavior of reinforced-concrete structures (Fig. 2.9).[12] (Under earthquake loadings there is stiffness degradation but no appreciable strength degradation during subsequent cycles, until the concrete crushes.) In one comparison,[13] the behavior of joints with about the same ρf_y and the same constraint was about the same for Grade 40 and Grade 60 steel reinforcement, as would be expected, since the Bauschinger effect is about the same for both steels. Because the Bauschinger effect thus governs earthquake response to some extent, the difference between a flat-top and a round-house stress–strain curve is mostly eliminated during the early inelastic cycling; consequently, an ideal elastic-pure plastic stress–strain curve is not specifically needed for a seismic design, although it may be desirable for the conventional static-load design of the same structure.

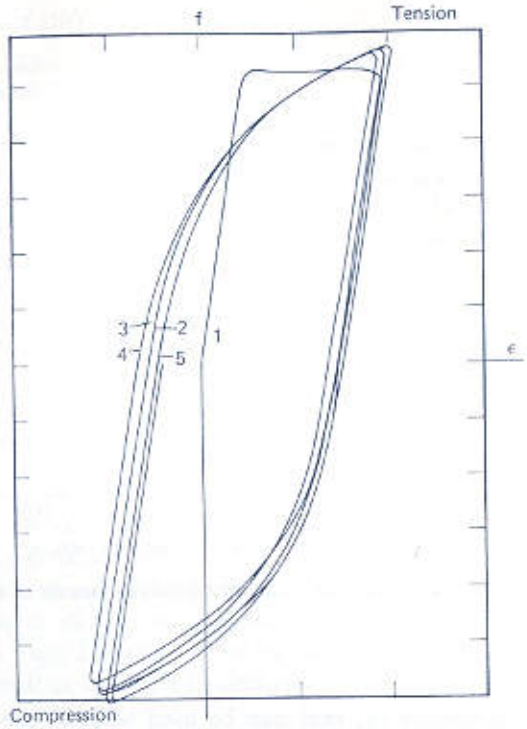

FIGURE 2.8. Repeated reversed loading of a reinforcing steel bar.[11] (Reprinted by permission of the American Society for Testing and Materials, Copyright ASTM.)

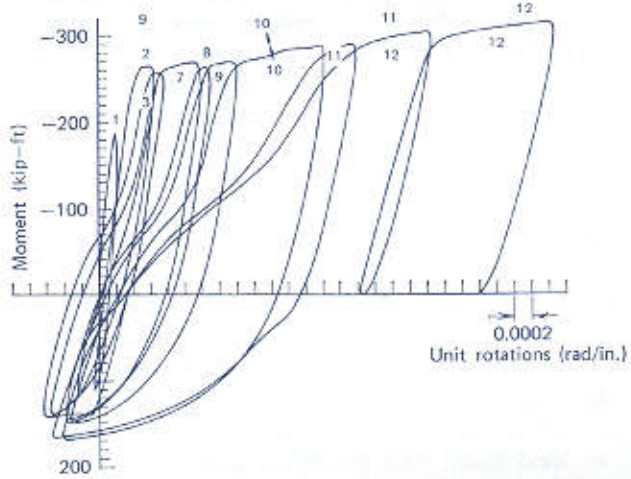

FIGURE 2.9. Repeated reversed loading of a frame subassemblage in an earthquake-simulation test.[12]

Seismic Requirements. The special requirements for earthquake-resistance designs suggest various desirable, but in certain cases impractical, inelastic properties for reinforcing bars, which are as follows:

1. Sufficient ductility in the bar, ensured if $\rho > \rho_1$ (Table 2.7).
2. Sufficient ductility in a welded splice, which is difficult to obtain; therefore, avoid splices in inelastic regions.
3. Sufficient tensile-strength to yield-strength ratio, to afford the development of the moment gradient over the plastic region (adequately provided by steels conforming to the ASTM specifications, but the yield strengths should not greatly exceed the specified values).
4. Upper limit on yield strength, to preclude within a plastic hinge the development of high bending moments and concomitant unanticipated high shearing stresses, with subsequent premature shear failures (very difficult to maintain an upper limit in production because of high tensile–yield ratios currently specified).

2.4.1 Fatigue Strength

Reinforcing Bars. Fatigue of reinforcing steels has not been a problem, inasmuch as there has been no evidence of failures of structures in public use in the United States attributed directly to reinforcing-bar fatigue. However, the trend to increase the yield strength, and hence the allowable stresses, of reinforcing steel suggests that fatigue strength could become a limitation in the design of structures, such as bridge-deck slabs, which are subjected to a great number of loading cycles with a relatively large range of stresses occurring within each cycle. Although the fatigue strengths of smooth bars generally increase approximately in proportion to tensile strength, it has been observed that the notch effects inherent in the surface geometry of deformed bars cause the fatigue strengths of deformed bars to be less than for smooth bars and to be relatively unaffected by the material strength (Fig. 2.10).[14] Each plotted point in Fig. 2.10 is an extrapolation from one of the S–N curves in References 14, 15, 16, 17, and 18. Other data, not included in Fig. 2.10 but similar to the data shown, are given in References 19 and 20. Consequently, there has been a recommendation that the design stress range for deformed reinforcing bars be limited to 20 ksi in structures subjected to a large number (10^6 or more) of loading cycles.[21] The fatigue strength of a properly made butt-welded joint between reinforcing bars has been found to be almost as high as the bar fatigue strength,[22] but tack welds greatly lower the fatigue strength.[23] Thus, tack welding should always be avoided. Also bar bends are detrimental to fatigue strength,[15] and should be avoided in the highly stressed portions of bars in bridges and other structures subjected to repeated loading.

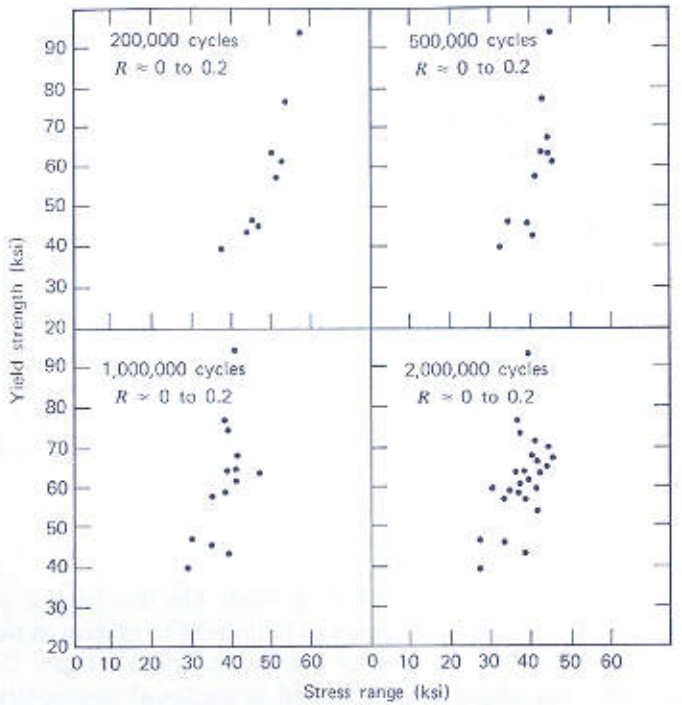

FIGURE 2.10. Data from reinforcing steel bar fatigue tests reported in five references.[14–18] (Note: R = Minimum Stress/Maximum Stress.)

Wire Fabric. Fatigue of wire fabric has, likewise, not been a problem, and the welded connections at the wire crossings have not presented a fatigue problem. Limited research suggests that the fatigue limit of welded wire fabric is not less than about 20 ksi.[24,25,26]

2.4.2 Preparation for Construction

Coatings. The need for protecting reinforcing steel from rusting in concrete constructions has been controversial, mainly since concrete is a rust inhibitor because it is alkaline. The expense of protection against rust in good-quality concrete generally is not warranted except for structures in corrosive environments, such as structures exposed to special chemical attack or saline attack from the ocean. There has been some consideration that chemical attack on bridge decks and parking garage floors by deicing salts could warrant special corrosive protection. Light rust (other than loose rust scale) that unprotected reinforcing steel may develop in storage at a job site generally is not detrimental for bond of deformed bars[27] and welded wire fabric,[28] as determined in laboratory tests. The effect of initial rusting on subsequent

long-time performance, particularly in structures exposed to a corrosive environment, has not been investigated adequately, and loose flaky rust is detrimental to bond.

Galvanizing. Occasionally, reinforcing steel is protected by galvanizing, in which the reinforcement is coated with zinc by hot dipping. Advantages cited to warrant the extra cost of galvanizing are (1) the prevention of rust on reinforcing steel before it is placed in concrete, (2) a reduced tendency for spalling of concrete as a result of the formation of corrosion products if concrete cracking affords a way for a corrosive environment to reach and attack the steel, and (3) prevention of rust staining on very thin reinforced-concrete wall panels (where stainless steel reinforcement has occasionally been used) and on certain precast structures with projecting steel elements. Some tests[29] have indicated that galvanizing is not detrimental to bond strength, but it appears from the results of other tests[30] that the bond strength of galvanized plain (undeformed) reinforcing steel bars is sensitive to the chromate content of the concrete, the strength being less with a lower chromate content. Sharp bends in reinforcing steel prior to galvanizing should be avoided because of possible loss of ductility in severely cold-bent steel due either to strain aging during galvanizing or to hydrogen absorption during improper pickling before galvanizing.[31] Bending after galvanizing may cause the zinc coating to flake off locally.

Fabrication and Detailing. In preparation for construction, the shop fabrication of reinforcing steel may include cutting the steel to required lengths, cold bending the steel, welding intersecting layers of the steel in mat subassemblies, and/or coiling the mat subassemblies or cutting them to length. Most welded wire fabric and deformed welded wire fabric are fabricated into sheets or coils by the manufacturer, but subsequent fabrications of the fabric into special configurations, such as stirrup cages or cages for column fire-protection encasement, are generally made by contractors. Some of the reinforcing-bar producers fabricate most of the reinforcing bars they produce, but most reinforcing bars are fabricated by independent fabricators.

The standard ACI hooks for proper anchorage of bars in concrete are given in Fig. 2.11.[4] References 32 and 33 give a comprehensive review of standard practices for detailing reinforcing steel.

Proper shop fabrication provides reliable reinforcing steel products for all types of construction. However, the designer should realize that the process of fabrication unavoidably alters certain mechanical properties of the reinforcing steel where the reinforcing steel is either bent or welded. In general, both bending and welding significantly reduce the ductility and the fatigue strength[23,24] of the steel at the bend or weld, except that the fatigue strength of butt welds is reduced only slightly.[22] Under well-controlled shop conditions,

ACI STANDARD HOOKS

All specific sizes recommended by CRSI below meet requirements of ACI 318-63

RECOMMENDED END HOOKS

All Grades*

D = 6d for #3 through #8
D = 8d for #9, #10, and #11
D = 10d for #14 and #18

Bar Size#	180° HOOKS		90° HOOKS
	A or G	J	A or G
#3	5	3	6
#4	6	4	8
#5	7	5	10
#6	8	6	1-0
#7	10	7	1-2
#8	11	8	1-4
#9	1-3	11½	1-7
#10	1-5	1-0½	1-10
#11	1-7	1-2½	2-0
#14*	2-2	1-8½	2-7
#18*	2-11	2-3	3-5

With Grade 40 only, where available depth is limited, bars may be bent with D = 5d for #3 through #11.

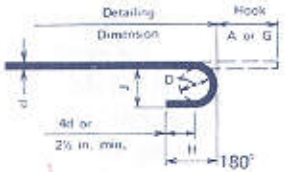

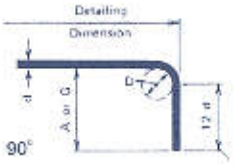

(a)

STIRRUP AND TIE HOOKS

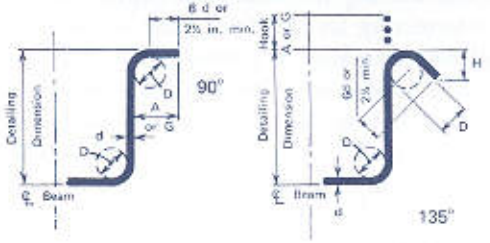

STIRRUPS
(Ties Similar)

Stirrup and Tie Hook Dimensions
Grades 40-50-60 ksi

Bar Size	D Min.†	90° Hook	135° Hook	
		Hook A or G	Hook A or G	H Approx
#3	1½	4	4	2½
#4	2	4½	4½	3
#5	2½	6	5½	3½

(b)

FIGURE 2.11. ACI Standard Hooks.[4]

bending and welding (but not bending after welding at the same spot) are generally satisfactory, but a designer should detail the location of bends and welds to occur where superior ductility or fatigue strength is not required, and he should be sure that the steel specified is readily weldable under the conditions specified. Thus, bends or welds should be avoided at the locations of maximum bending moments within the plastic-hinge regions of earthquake-resistant rigid frames, and at locations of maximum stress in bridges.

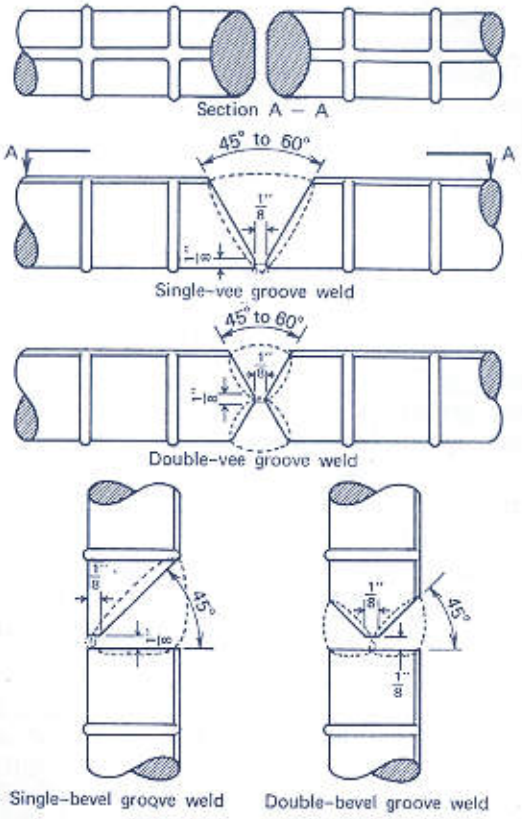

FIGURE 2.12. Welded splices.[34]

Splices. Reinforcing bars and wire fabric can generally be spliced by lapping, and the ACI *Code*[7] and other codes specify the required laps, which are based on the results of many bond tests of currently available deformed bars, smooth and deformed wires, and smooth and deformed fabric. However, for the large-diameter reinforcing bars, such as Nos. 11, 14, and 18, the lengths of such laps can become excessive, and either mechanical or welded splices are advisable. If the splice will always be in compression, simple devices used mainly just to align the abutting reinforcing bars are satisfactory. However, the splice must frequently take both tension and compression. The design of such splices—using the ACI *Code*—is governed by the requirement that the splice be able to resist without unloading a tensile thrust equal to 125% of the reinforcing-bar design yield thrust. For certain structures, another requirement, not specified in the *Code*, is that the strains in the splice must not be so great that, in effect, the steel at the splice behaves as if it had a pronounced round-house stress–strain curve.

Mechanical splices that can resist both tension and compression are generally exothermic splices formed either by a molten filler metal inside a jacket or by the thermit process. Steel welded splices generally can resist either tension or compression, and butt-welded joints are preferable; however, for smaller size bars other types of welded splices involving the use of back-up angles or plates can be used. Some suggested details for butt-welded splices appear in Fig. 2.12.[34]

2.4.3 Performance Expectations

Reinforcing steels are inexpensive constructional steels and, consequently, effect the economy of reinforced-concrete construction. However, economy is achieved by producing the steels to meet, with consistent reliability, specific ASTM mechanical properties.[1] In addition, some proprietary new billet steels are produced to a specified chemistry for superior weldability and bendability.[10]

Where the designer needs and expects certain composition-dependent properties, such as weldability or exceptional ductility, special arrangements must be made to achieve the composition limitations necessary for the performance expectations. The manufacturer of a reinforcing steel can best advise whether a given steel can be welded and what precautions must be taken to ensure weldability.

REFERENCES

1. *1973 Annual Book of ASTM Standards*, Part 3, American Society for Testing and Materials, 1973.
2. C. A. Menzel, "A Proposed Standard Deformed Bar for Reinforcing Concrete," *Proceedings of the Seventeenth Semi-Annual Meeting of the Concrete Reinforcing Steel Institute*, Colorado Springs, Colorado, September 1941.
3. L. M. Sur, H. G. Kohler, R. Jensen, and C. E. Kesler, "Optimum Properties for Deformed Wire," *T. & A. M. Report No. 654*, Department of Theoretical and Applied Mechanics, University of Illinois, Urbana, Illinois, May 1965.
4. *Manual of Standard Practice*, 21st ed., Concrete Reinforcing Steel Institute, 1973.
5. "Final Report on Bar Tests for the Committee of Concrete Reinforcing Bar Producers, American Iron and Steel Institute," Wiss, Janney, Elstner, and Associates, Northbrook, Illinois, April 30, 1970.
6. J. E. Funnell and D. K. Curtice, "Study of Continuously Reinforced Concrete Pavements," *Final Report Sw-RI Project No. 07-1864*, Southwest Research Institute, San Antonio, Texas, October 1966.
7. *Building Code Requirements for Reinforced Concrete*, American Concrete Institute, 1971.
8. "Effect of Steel Strength and of Reinforcement Ratio on the Mode of Failure and Strain Energy Capacity of Reinforced Concrete Beams," Reported by ACI Committee 439, *ACI Journal*, March 1969.

9. "Design of Structures to Resist the Effects of Atomic Weapons" *U.S. Army Corps of Engineers, Manual* EM 1110-345-414, March 1957.
10. "Uses and Limitations of High Strength Steel Reinforcement," Reported by ACI Committee 439, *ACI Journal*, February 1973.
11. A. Singh, K. H. Gerstle, and L. G. Tulin, "The Behavior of Reinforcing Steel Under Reversed Loading," *Materials Research and Standards*, January 1965.
12. N. W. Hanson and H. W. Connor, "Seismic Resistance of Reinforced Concrete Beam-Column Joints," Paper No. 5537, *Journal of the Structural Division, Proceedings ASCE*, October 1967.
13. N. W. Hanson, "Seismic Resistance of Concrete Frames with Grade 60 Reinforcement," *Journal of the Structural Division, Proceedings ASCE*, Paper No. 8180, June 1971.
14. M. M. Kobrin and A. G. Sverchkov, "Effect of Component Elements of Deformation Patterns on the Fatigue Strength of Bar Reinforcement," *Experimental and Theoretical Investigations of Reinforced Concrete Structures*, Scientific Research Institute for Plain and Reinforced Concrete, GOSSTROIIZDAT, Moscow, 1963, translated from the Russian by the Portland Cement Association.
15. J. F. Pfister and E. Hognestad, "High Strength Bars as Concrete Reinforcement, Part 6, Fatigue Tests," *Journal of the PCA Research and Development Laboratories*, January 1964.
16. H. Wascheidt, "On the Problem of Fatigue Strength of Steel Bars Embedded in Concrete," *Foreign Literature Study* No. 521, Portland Cement Association, 1965.
17. M. Kokubu and H. Okamura, "Fundamental Study on Fatigue Behavior of Reinforced Concrete Beams Using High Strength Deformed Bars," (English summaries), *Transactions of the Japan Society of Civil Engineers*, No. 122, October 1965.
18. J. M. Hanson, K. T. Burton, and E. Hognestad, "Fatigue Tests of Reinforcing Bars—Effect of Deformation Pattern," *Portland Cement Association R\|D Ser.* 1311, July 1967.
19. J. M. Hanson, N. F. Somes, I. Helgason, W. G. Corley, and E. Hognestad, "Fatigue Strength of High Yield Reinforcing Bars," *Interim Report*, Project No. 4–7 of the NCHRP, PCA, February 1970.
20. J. C. MacGregor, I. C. Jhamb, and N. Nuttall, "Fatigue Strength of Hot Rolled Deformed Reinforcing Bars," *ACI Journal*, March 1971.
21. *Strength and Serviceability Criteria, Reinforced Concrete Bridge Members, Ultimate Design*, Bureau of Public Roads, U.S. Department of Commerce, August 1966.
22. W. W. Sanders, P. G. Hoodley, and W. H. Munse, "Fatigue Behavior of Welded Joints in Reinforcing Bars for Concrete," *Welding Journal*, December 1961.
23. K. T. Burton and E. Hognestad, "Fatigue Tests of Reinforcing Bars—Tack Welding of Stirrups," *ACI Journal*, May 1967.
24. P. Mohan, "An Investigation of the Fatigue Strength of Concrete Slabs Reinforced with Welded Wire Fabrics," Master-of-Science Thesis, Oklahoma State University, Stillwater, Oklahoma, August 1963.
25. N. M. Hawkins and L. W. Heaton, "The Fatigue Properties of Welded Wire Fabric," *Report* No. SM 71-3, Department of Civil Engineering, University of Washington, Seattle, September 1971.
26. T. Melville, "Fatigue Tests of Welded Deformed Wire Fabric," *Bull. Appl. Res. Lab., U.S. Steel Corp.*, Pittsburgh, July 1971.
27. E. L. Kemp, F. S. Brezny, and J. A. Unterspan, "Effect of Rust and Scale on the Bond Characteristics of Deformed Reinforcing Bars," *ACI Journal*, September 1968.
28. H. M. Rejali and C. E. Kesler, "Effect of Rust on Bond of Welded Wire Fabric," *American Road Builders' Association, Technical Bulletin* No. 265, 1968.

29. B. Bresler and I. Cornet, "Galvanized Steel Reinforcement in Concrete," *Final Report of the Seventh Congress of the International Association for Bridge and Structural Engineering*, Rio de Janeiro, Brazil, 1964.
30. A. Hofsoy and I. Gukild, "Bond Studies on Hot Dipped Galvanized Reinforcement in Concrete," *ACI Journal*, March 1969.
31. I. Cornet and B. Bresler, "Some Recent Developments in the Use of Galvanized Steel Reinforcement in Concrete," *Proceedings of the Ninth International Conference on Hot Dip Galvanizing*, Dusseldorf, 1970.
32. *Manual of Standard Practice for Detailing Reinforced Concrete Structures* (ACI 315–73), American Concrete Institute, 1973.
33. *Reinforcing Bar Detailing*, Concrete Reinforcing Steel Institute, 1970.
34. *CRSI Handbook*, Concrete Reinforcing Steel Institute, 1973.

3

Properties of Hardened Concrete

Adam M. Neville

3.1 INTRODUCTION

Concrete is in some respects elastic but to a large extent it is a nonelastic material. The nonelastic features of concrete have contributed greatly to its success and are largely responsible for its ubiquity and versatility. Above all, the construction of complex structures is possible as the nonelastic deformation of concrete which occurs in local zones of statically indeterminate structures results in a redistribution of stresses to a more equitable state. While concrete is not alone in being partly elastic and partly nonelastic, it is probably unique in that many of its structural properties depend on age or time and on the environmental conditions of temperature and humidity. For this reason, the mechanical and physical properties of concrete must be well understood by the designer and constructor: it is not possible to rely blindly on numerical values given in a handbook.

There is one additional feature of concrete which sets it apart from other structural materials: its combination of high compressive strength and low tensile strength. Once upon a time, cracking was viewed as a fault of design or workmanship; however, careful analysis has shown that under normal and reasonable stress conditions, reinforced concrete is cracked but, providing the individual cracks and deformations are not excessively large, it* performs satisfactorily with respect to its load-carrying capacity and durability. The qualifications on crack width and deformations mean that, in design,

* Refers only to reinforced concrete—not generally to cracked plain concrete.

we must be able to evaluate the strength and deformation of concrete at any time. This explains the importance in design and construction of the physical and mechanical properties of concrete to which this chapter is devoted: strength, fatigue, impact, deformation, shrinkage, creep, and thermal sensitivity.

3.2 NATURE OF STRENGTH OF CONCRETE

The complexity of this topic arises from the fact that concrete is heterogeneous at several levels of observation. At the "macro" level it consists of coarse aggregate particles surrounded by a mortar matrix; but mortar itself consists of sand grains and hydrated cement paste; the paste is virtually never fully hydrated so that the products of hydration are intermingled with remnants of unhydrated cement; the products of hydration themselves consist of particles of different orders of magnitude, notably gel and crystalline particles such as calcium hydroxide.

In all good quality structural concrete the strength of the aggregate particles themselves is greater than that of the other components of concrete so that the important elements in a consideration of the strength of concrete are the strength of the hydrated cement itself and the strength of the hydrated cement–aggregate interface.

As already mentioned, hydrated cement consists mainly of gel, which is an agglomeration of extremely small particles, intertwined and cross-linked so as to form a porous mass. The particles are mostly platy or fibrous and the important feature is the small size of the particles—surface–volume ratio equivalent to that of spheres with a diameter of the order of 90 Å—and this indeed is why the material is classified as a gel. The large surface–volume ratio means that surface forces are large compared with gravity and other body forces. The bonds between the particles are relatively weak and physical in nature, and are referred to as van der Waals forces. This partly explains why compressive strength is large and tensile strength is low.

On the other hand, the bonds within the particles are chemical in nature: ionic and covalent. Such bonds are stronger than the physical bonds but the very large surface area of gel (2 million cm^2 per g) means that the total physical bond force is large. This explains why hydrated cement paste cannot be dispersed on immersion in water: only limited swelling takes place.

Following the strength of the gel itself, we should now consider the bond between the cement paste and the aggregate. This is mainly physical in nature but with some aggregate types, e.g., limestone, some chemical bond may also exist. Mechanical effects also assist bond, mainly in the form of interlocking of the aggregate and the paste. The surface texture of aggregate affects bond strength and the size of the bond area, and this partly explains why the aggregate influences the strength of concrete.

3.2.1 Microcracking

An important feature of the coarse aggregate–matrix interface is that it contains very fine cracks even before any load has been applied to the concrete.[1] Compressive stress whose magnitude is not more than about 30% of the compressive strength (i.e., a stress–strength ratio of 0.3) does not appear to cause propagation of these bond cracks but at higher stresses they increase in length, width and number. Slow crack propagation continues up to a stress–strength ratio of 0.7 to 0.9, when the cracks open through the mortar so as to bridge the existing bond cracks, and a continuous crack pattern results. This is the fast crack propagation stage, which may lead to failure with time under a sustained load.

The development of cracking can probably be explained in terms of Griffith's criterion[2] modified for inelastic effects and various states of stress. Essentially, the presence of small initial flaws or cracks is postulated, and, from the requirements of minimum potential energy in equilibrium, crack propagation can be shown to occur when the rate of energy release due to external forces reaches the rate of energy requirement of surfaces formed by an infinitesimally small crack extension. Strictly speaking, the latter is the energy of the newly formed surfaces plus the energy required to produce plastic deformations (or a microcracking region) near the crack tip.[3]

The application of Griffith's criterion to concrete was suggested in 1959,[4] but the problem is somewhat more complicated than in a brittle material such as glass owing to the development of a microcracking region near the crack tip. Thus the total crack surface is greater than the surface of the main crack. The size of the microcracking region increases with the size of the main crack so that, as the main crack grows, the rate of the energy requirement increases at an increasing rate. This continues until the highly stressed zone in which the microcracks are developing reaches its maximum potential size (owing to the shape of the specimen or the stress distribution), and at that instant the main crack begins to grow spontaneously.[5] This means that the critical strain energy release rate has been reached: rapid crack propagation takes place until a total collapse of the concrete has occurred.

At this point it is reasonable to ask: what determines the path taken by the developing cracks? Apart from local inequalities in strength, the path is influenced by zones of higher rate of energy requirement, i.e., by what might be termed crack arresters in the form of aggregate particles and reinforcing bars. The crack therefore takes a detour; as a result, its length is greater so that a higher energy is required.

The presence of crack arresters thus prevents the development of a running crack under a given overall stress. As in mortar there are fewer crack arresters

ASTM C150. The typical physical–chemical characteristics of commercially available products are shown in Table 1.2.

1.4.1 Standard Specifications for Portland Cement

Although several Federal and State agencies may require portland cements to conform to special standards, the ASTM C150 standard is among the most widely used.

Chemical requirements included in ASTM C150 generally serve as a guideline to attain certain physical qualities, but some of the physical requirements such as time of setting, soundness, and compressive strength are of more practical significance.

1.4.2 Time of Setting

The stiffening characteristics of a cement paste are determined by time of setting tests. During the hydration process of cement compounds, the two stages which are used to describe the setting characteristics of cement paste are the *initial set* and the *final set*.

Setting-time tests of a cement could be performed by using either the Gillmore Apparatus (ASTM C266) or the Vicat Apparatus (ASTM C191). In the Gillmore method, which is commonly used in the United States, a cement paste pat about 3 in. in diameter and 1/2 in. in thickness is made on a glass plate and stored in a moist closet. The pat is periodically withdrawn from the moist closet and subjected to indentations by standard needles. The needle for the initial-setting-time test weighs 1/4 lb and has 1/12 in. diameter, while the needle for the final-setting-time test weighs 1 lb and has 1/24 in. diameter. The cement is considered to have acquired its initial set or final set when the pat will bear, without appreciable indentation, the appropriate Gillmore needle. All five types of standard ASTM portland cements, when tested by this method, are expected to conform to an initial setting time of not less than 60 min, and a final setting time of not more than 10 h.

The Vicat apparatus and test method is quite similar in principle to the Gillmore test. There are slight differences in the specifications of needle weights and diameters and in the dimensions of the cement paste test samples.

1.4.3 Soundness

Due to cracking caused by some expansive reactions occurring after hardening of cement, certain constituents of portland cement such as high C_3A, high SO_3, crystalline MgO, and free CaO could prove deleterious with regards to the durability of structural concrete. Accelerated tests have been developed to determine the soundness of cement. The ASTM C151 describes an autoclave test where a standard molded bar of cement is exposed to saturated

TABLE 1.2. Typical Calculated Compound Composition, Fineness, and Relative Rates of Strength Development of Commercial U.S. Cements.[4]

ASTM C 150		Compound Composition, %				Fineness, cm^2/g	Compressive Strength, % of Strength of Type I Cement			
Type	Description	C_3S	C_2S	C_3A	C_4AF	Wagner	1 day	7 days	28 days	3 months
I	General purpose	50	24	11	8	1800	100	100	100	100
II	Moderate heat of hydration and moderate sulfate resisting	42	33	5	13	1800	75	85	90	100
III	High early strength	60	13	9	8	2600	190	120	110	100
IV	Low heat	26	50	5	12	1900	55	55	75	100
V	Sulfate resisting	40	40	4	9	1900	65	75	85	100

present, this argument may explain why concrete is generally stronger than mortar of the same water–cement ratio.[6]

It is important to realize that the increase in the microcracking region with an increase in the crack size also prevents the formation of a running crack; otherwise, any local failure in concrete would lead to collapse, and the strength of concrete would be inadequate for many structural purposes. Thus, microcracking is a beneficial phenomenon.

This argument applies only to a tensile stress field; in compression, the rate of strain energy released is independent of the length of the main crack, so that stabilization of a crack occurs only when it meets an obstruction or a zone of higher energy demand. Other cracks then begin to grow but they in turn become stabilized, too. Thus, a progressive development of cracks takes place with an increase in the overall applied stress. As a consequence, the slope of the stress–strain curve decreases with an increase in stress (see Section 3.9.1) and eventually the state of gradual collapse is reached. The same argument can explain, at least in part, why concrete is stronger in compression than in tension.

It is relevant to note that in uniaxial compression, cracking occurs in the direction of the applied stress as in all other directions there is a normal compressive component of stress. The lateral tensile strain in uniaxial compression is of interest from the standpoint of failure considerations, and experimental results[7,8] have shown that, at the point of initial cracking, this strain is about the same as the failure strain in the extreme fibre in flexure, varying between 80 and 160 millionths.

Nevertheless, it is still uncertain whether the mechanism of failure of concrete can be expressed in terms of a limiting magnitude of extension strain alone. This criterion is not applicable for multiaxial compressive stress fields, and in fatigue a larger strain is developed than under static loading (see Section 3.9.3).

3.3 FACTORS INFLUENCING STRENGTH OF CONCRETE

This is an extensive topic whose full treatment can be found in specialized books on properties of concrete.* However, some of the fundamental influences on strength of concrete are of such direct importance in design and construction that they will be included in this chapter.

3.3.1 Water–Cement Ratio

The most important among the factors determining the strength of concrete is the water–cement ratio. Admittedly, the water–cement ratio versus strength

* e.g., A. M. Neville: Properties of Concrete, Sir I. Pitman and Wiley-Interscience, 2nd Ed., 1973, 686 pp.

relation has not the validity of a physical law, and is subject to limitations with respect to the degree of compaction, type and strength of aggregate, its quantity and maximum size, etc., but for practical purposes the strength of concrete at a given age can be reliably estimated as a function of the water–cement ratio. The water–cement ratio rule was first propounded by Abrams as far back as 1919 but at the present stage of concrete technology it is probably best to use the form stated by Gilkey[9]:

"For a given cement and acceptable aggregates, the strength that may be developed by a workable, properly placed mixture of cement, aggregate, and water (under the same mixing, curing, and testing conditions) is influenced by the:

1. ratio of cement to mixing water,
2. ratio of cement to aggregate,
3. grading, surface texture, shape, strength, and stiffness of aggregate particles,
4. maximum size of the aggregate."

When the maximum size of aggregate is 1 1/2 to 1 3/4 in., and with normal weight aggregates, factors 3 and 4 are of lesser importance; and when the aggregate–cement ratio is not less than 4 (as is usual in structural concrete), factor 2 is not very significant. However, mixes with a very high cement content (say, 800 lb per cu yd of concrete) exhibit a retrogression of strength, particularly when a large-size aggregate is used so that the use of a low water–cement ratio in such a mix does not lead to a high strength at later ages. This behavior may be due to high shrinkage in a very rich mix (see Section 3.10.1) coupled with cracking at the interface between the matrix and the large aggregate particles.

Thus, in a general case, all of the factors listed by Gilkey apply and, as observed by Walker and Bloem,[10] "the strength of concrete results from: (1) the strength of the mortar; (2) the bond between the mortar and the coarse aggregate; and (3) the strength of the coarse aggregate particles, i.e., its ability to resist the stresses applied to it."

A condition necessary for the application of the water–cement ratio rule is that full compaction of the concrete has been achieved: a mix may have a high strength "on paper" but this strength will not be reached in practice if full compaction cannot be achieved in the field with the means available. This is shown in Fig. 3.1, which illustrates the fact that with low water–cement ratios higher strength can be achieved when vibration is used to compact (consolidate) the concrete than with hand placing. The choice of a suitable vibrator and its proper use are important, as segregation can lead to even greater strength reduction than inadequate compaction.

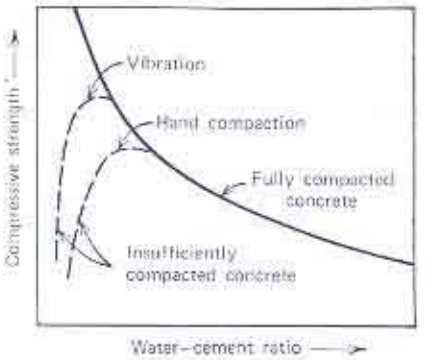

FIGURE 3.1. The general shape of the relation between strength and water–cement ratio of concrete.

The water–cement ratio rule, although a convenient practical parameter, is not a fundamental property of concrete as the real factor in strength is the presence of voids in the hardened state. The water–cement ratio is a way of expressing the presence of voids in that it defines the porosity of the hardened cement paste at a given stage of hydration (commonly expressed as age but more correctly as maturity, i.e., product of time and temperature).[11] Nevertheless, from a fundamental point of view, it is more correct to relate strength to the concentration of the solid products of hydration of cement in the space available for these products. Powers and Brownyard[12] have determined the relation between the strength development and the gel–space ratio. This ratio is defined as the ratio of the volume of the hydrated cement paste to the sum of the volumes of the hydrated cement and of the capillary pores. The calculation of the gel–space ratio from the knowledge of mix proportions and the elementary physics of hydration of cement is straightforward but is rarely of interest in structural engineering.

The above discussion of the water–cement ratio rule applies only to concrete made with the usual Portland cements. The pattern of strength of aluminous (high-alumina) cement concrete appears to be somewhat different; in any case, the structural use of this type of cement requires caution as strength may decrease very considerably under warm and moist storage conditions.[13,14]

3.3.2 Gain of Strength with Time

The increase in the strength of concrete with time is well known but is not often fully taken into consideration in design. It is almost an invariable custom to specify the 28-day strength and yet in practice 28 days after placing is far too late to determine whether the concrete in the structure is strong

enough on the one hand or uneconomically too strong on the other. For this reason strength at 7 days is often determined, and extrapolation from 7 to 28 days is of interest. From a wide range of tests on concretes made with a Type I cement it appears that the ratio of the 28-day to 7-day strengths lies generally between 1.3 and 1.7, with the majority of the results falling above 1.5. The exact value depends on the chemical composition and fineness of cement. Moreover, in a hot climate the early gain in strength is high, and therefore the ratio is lower than at moderate temperatures.

When cements other than Type I are used, a considerable variation in the rate of gain of strength is possible, and prediction of the late strength from early values should be based on experimental results. This is so also when the fineness of cement departs considerably from that usually encountered in commercial cements; particles larger than approximately 30 μ contribute very little to the strength at ages earlier than about 1 month.

Mixes with a low water–cement ratio gain strength relatively more rapidly than mixes with higher water–cement ratios. Thus, if the strength of real importance is that at the age of 1 year, but measurement of strength is made at, say, 7 days care in the interpretation of the results is necessary: the mix with a low water–cement ratio, although satisfactory at 7 days, may prove not strong enough at 1 year. The explanation of this behavior lies in the fact that with a low water–cement ratio, cement grains are closer to one another and a continuous system of gel is established more rapidly.

The gain in strength beyond the age of 28 days may be taken into account in those structures in which the design load is not applied until a later stage, as is often the case. This is done for instance, in the British code,[15] but of course no allowance for the late gain of strength can be made when accelerators are used. Therefore, the use of accelerators requires special approval unless clearly established in the specification.

3.3.3 Maximum Size of Aggregate

Use of large-size aggregate is sometimes considered advantageous as with such aggregate less water is required for a given workability so that a lower water–cement ratio can be used and a higher strength expected. However, the presence of large-size aggregate may lead to a reduction in strength, probably due to a lower total interface area; this means that the stresses between the aggregate and the paste are high. Also, the restraining effect of large aggregate on the shrinkage of the cement paste is locally high and hence large internal stresses are induced.

It seems therefore that there are two opposing effects on strength when large aggregate is used, and in practice the net result depends on the mix proportions. Generally, high strength of rich mixes is adversely affected by the use of large-size aggregate but in lean mixes, say with less cement than

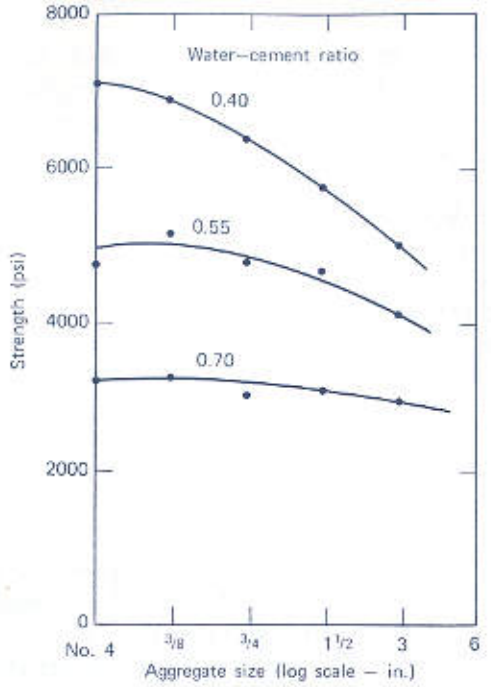

FIGURE 3.2. Influence of maximum size of aggregate on compressive strength of concrete (slump between 3.8 and 5.8 in.).[16]

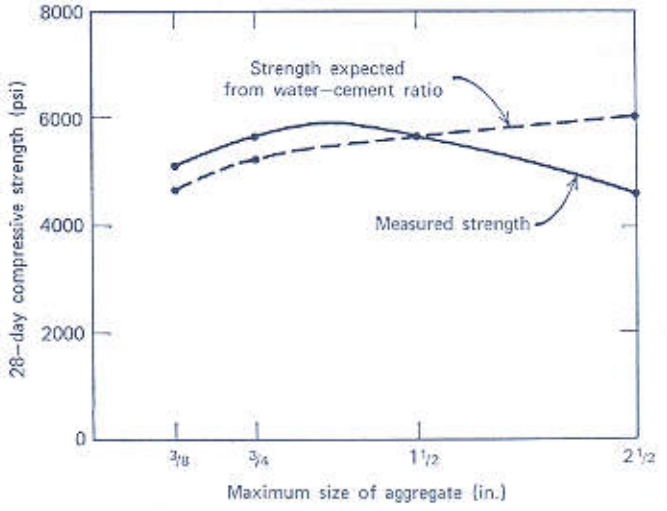

FIGURE 3.3. Strength of concretes made with aggregates of different maximum size—actual and expected from the water–cement ratio.[17]

470 lb per cu yd of concrete and a strength lower than 4000 psi, the detrimental effects of large aggregate are small.[16] This is illustrated in Fig. 3.2.

Aggregates of different sizes but of a given type can be evaluated also on the basis of strength of concrete per 1 lb of cement per cu yd of concrete: this is a reasonable approach as the cost of cement largely influences the price of concrete. It appears that in lean mixes, large aggregate gives the best value but in rich mixes it is the smaller aggregate that results in highest strength per pound of cement per cubic yard of concrete.[17] A typical relationship between aggregate size and compressive strength is shown in Fig. 3.3.

A further limitation on the general influence of aggregate size on strength of concrete lies in the role of shape and texture of the particles actually used. Generally, rounded particles result in a lower strength than crushed aggregate; the effect is greater with respect to tensile than compressive strength and is greater in high-strength concrete than at high water–cement ratios.

3.4 COMPRESSIVE STRENGTH TESTS

Because of the low tensile strength of concrete, structures have as a rule been designed so that the main structural action of concrete is in compression. Furthermore, the compressive strength of concrete is much easier to determine than its tensile strength. For these reasons, a great deal of information on the compressive strength of concrete test specimens is available.

3.4.1 Shape and Proportions of Test Specimens

In the U.S., the test specimens are in the shape of cylinders with a height–diameter ratio of 2 but in many European countries cubes are used. The strength obtained from these two types of specimens is generally not the same and there are, in fact, some fundamental differences between them.

The first one concerns the direction in which the load is applied relative to the direction of casting: in a cylinder, the two directions coincide, while in a cube the load is applied in a direction normal to the direction in which the specimen is cast. With a well-proportioned and well-compacted mix, which results in an isotropic specimen, this difference may not be significant[18] but in many cases, particularly when bleeding occurs, the deformation of the different layers of the specimen is not the same and this can be reflected in the recorded strength.

The second difference between cubes and cylinders of standard proportions arises from the stresses developed at the interface between the specimen and the platen of the testing machine. Because of the difference in the values of the modulus of elasticity and the Poisson's ratio of steel and concrete, the

lateral strain in the platen is smaller than in the concrete if it were free to move. Thus a shearing stress is induced. This end effect decreases in magnitude with an increase in the distance from the platen and becomes negligible at a distance of about $\sqrt{3}/2$ times the lateral dimension of the specimen.[19] The end effect can be readily seen in a standard cylinder tested to failure: at either end there is a nearly intact cone with a height of $\sqrt{3}/2$ times the diameter of the cylinder, but in between the cones lateral strain can freely develop and is evidenced by a bulging of the specimen. In a cube, two intact pyramids are present but their apices are within one another so that the zone of unrestrained lateral expansion is absent. As a result, uniaxial compression free from shear cannot exist in a cube.

For this reason, the strength of cubes is generally higher than the strength of cylinders made with the same mix. It follows also that to measure the strength of concrete free from the influence of the platen characteristics it is necessary to use cylinders longer than about 1.7 diameters. The standard cylinder has a height–diameter ratio of 2, and such cylinders have been found to yield uniform strength results.

If the actual specimen has a height–diameter ratio different from 2, a correction has to be applied to the measured strength in order to make it comparable with the strength of standard cylinders. (Specimens with different height–diameter ratios are encountered in the case of cores cut from concrete structures.) ASTM Standard C42–69 gives the following correction factors:

height–diameter ratio:	2.00	1.75	1.50	1.25	1.00
correction factor:	1.00	0.98	0.97	0.94	0.91
increase in strength, percent:	0.00	0.02	0.03	0.06	0.09

The actual behavior of concrete is somewhat more complex than would appear from the above fixed values as the correction factor depends not only on the height–diameter ratio but also on the level of strength of the concrete.[20] This is shown in Fig. 3.4, from which it is apparent that high-strength concrete is little affected by the height–diameter ratio. Since the strength of cylinders with a height–diameter ratio of unity is approximately the same as the strength of cubes,[11] it follows that in high-strength concrete the shape of the test specimen is of little importance.

Conversely, in low-strength concrete, the strength derived from the application of the ASTM correction factor to a core with a height–diameter ratio smaller than 2 would be higher than the strength of an actual standard cylinder. This observation is of importance as it is generally when the strength of concrete is lower than specified that cores are taken and their strength has to be related to the standard cylinder strength.

Specimens with a height–diameter ratio greater than 2 can obviously be

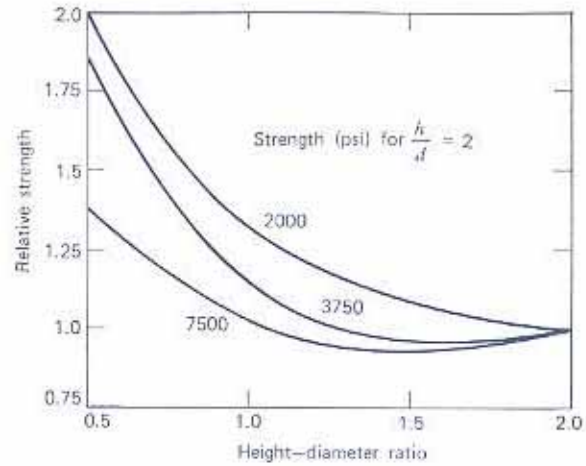

FIGURE 3.4. Influence of the height–diameter ratio on the measured strength of a cylinder for different strength levels.[20] (Reprinted by permission of the American Society for Testing and Materials, Copyright ASTM.)

trimmed with the aid of a diamond saw but the strength is little affected by the height–diameter ratio within the range of 1.5 to 2.[21]

All these data apply to concretes made with normal weight aggregate and to mixes of the usual proportions. The end effect is smaller the more homogeneous the material and is therefore less significant in mortar than in concrete. Lightweight aggregate concrete is also less influenced by the end effect and therefore by the height–diameter ratio, probably because the modulus of elasticity of lightweight aggregate is closer to the modulus of paste than is the case with normal-weight aggregate. It has been found[22] that with lightweight aggregate concrete the correction factor for a cylinder with the height–diameter ratio of unity is 0.95, compared with the ASTM value of 0.91. It would therefore be expected that cubes and cylinders of lightweight aggregate concrete differ little in the measured strength and this has indeed been confirmed by tests on concretes with a unit weight of between 40 and 60 lb per cu ft.[23]

There is one further feature of testing of compression specimens which should be borne in mind. The platen, which is supported by a spherical seat, is subject to bending and possibly distortion whose magnitudes depend on the thickness of the platen and on the diameter of the spherical seat. When the platen is too flexible (a soft platen) the compressive stress on the specimen is higher near its center than around the perimeter; the same occurs when the end surface of the specimen is slightly convex—a situation sometimes produced in capping of cylinders.

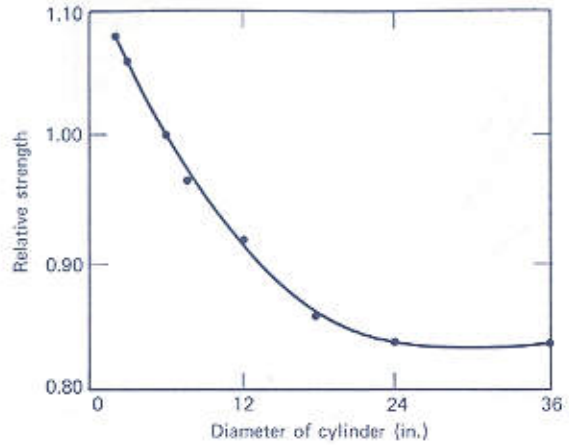

FIGURE 3.5. Compressive strength of cylinders of different sizes.[24]

3.4.2 Size Effect

There is one further property of the compression test specimens which affects the measured strength: their size. Figure 3.5 shows the relative strength of cylinders of various sizes, and it is apparent that the decrease in the measured strength with an increase in the size of the specimen does not continue indefinitely. This is reassuring as one could otherwise fear that the strength of massive members, e.g., piers, is greatly inferior to the strength of the test cylinders from the same mix. In fact, the size effect operates only up to a lateral dimension of the specimen of about 18 in., and all larger specimens or members record approximately the same strength.[25]

The size effect is more pronounced in rich mixes than in lean ones; for instance, the ratio of the strength of an 18-in. cylinder to the strength of a 6-in. cylinder (both with a height–diameter ratio of 2) is 0.85 when the cement content is 470 lb per cu yd of concrete but it is 0.93 when cement content is 282 lb per cu yd of concrete. As in the case of the effect of shape on strength, the size effect is much less pronounced in lightweight aggregate concrete than when normal-weight aggregate is used.

The size effect arises from the fact that the probability of the presence of a weak element* (i.e. an element of a certain level of strength) is greater the larger the volume of the concrete which is subjected to a given level of stress.[26] If it is the weakest element that governs the strength of a specimen, then the measured strength decreases with an increase in the size of the specimen.

* For treatment of statistical aspects of strength and testing see, for instance, A. M. Neville and J. B. Kennedy, *Basic Statistical Methods for Engineers and Scientists*, 2nd Ed., Intertext, New York, 1974, 368 pp.

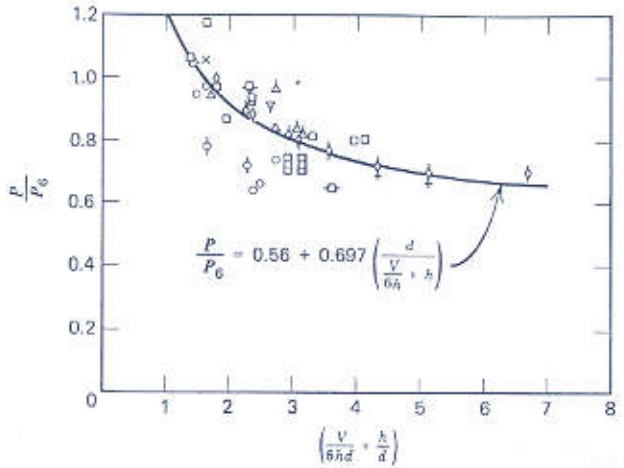

FIGURE 3.6. General relation between ratio of strength of concrete specimens P to strength of 6-in. cube P_6, and $V/6hd + h/d$, where V is volume of specimen, h its height, and d is its least lateral dimension.[27]

The assumption of the weakest-link behavior of concrete is not quite correct, as it is possible that, to some extent, the difference in the measured strength of specimens of different sizes arises from the fact that smaller specimens are indeed better compacted (because it is easier to do so) and exhibit also a smaller amount of bleeding (because the height involved is smaller). Thus, to a certain degree, the concrete in smaller specimens is of better quality and therefore stronger.

Recent work[27] has suggested a general relation between the strength of concrete and the shape and size of the specimen in terms of $(V/6hd) + (h/d)$, where V is the volume of specimen, h is its height, and d is its least lateral dimension. Figure 3.6 indicates the fit of experimental data to the relation postulated.

3.4.3 Rate of Application of Load

Standard compression tests require that the stress be applied at a controlled and specified rate, as this rate affects the measured strength. The reason for this is that the lower the rate at which the stress increases the lower the measured strength, as shown in Fig. 3.7, probably because a slow rate allows more creep to take place; as a result, strain increases more rapidly and it is likely that when a limiting strain has been reached failure takes place largely regardless of the magnitude of the applied stress. It has been found, for instance, that if the load is gradually increased up to failure over a period of 30 min, the measured ultimate strength is 88% of the strength recorded when the rate of application of stress is 30 psi/sec.[28] With an extremely slow rate of

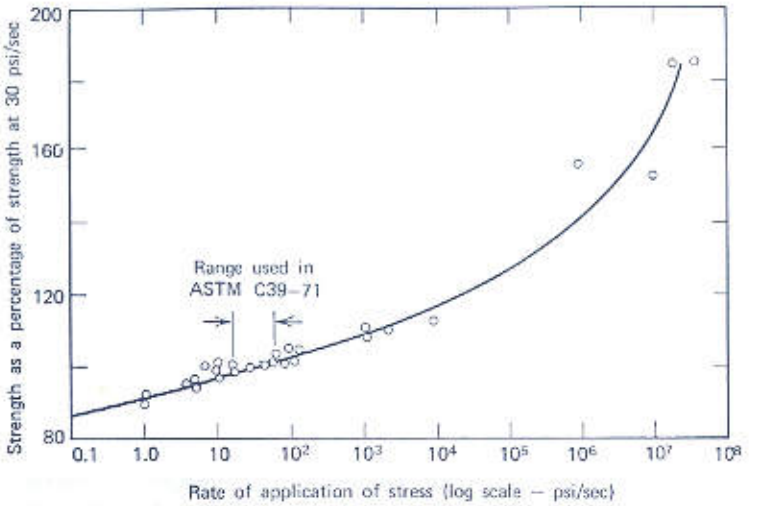

FIGURE 3.7. Influence of the rate of application of load on the compressive strength of concrete.[28] (Reprinted by permission of the American Society for Testing and Materials, Copyright ASTM.)

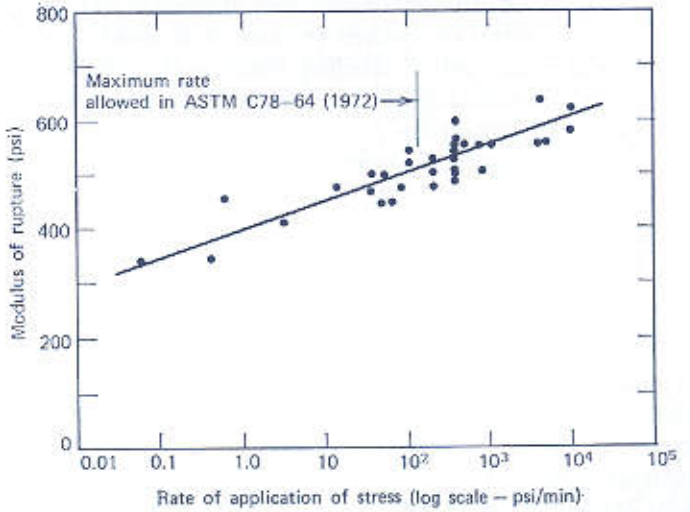

FIGURE 3.8. Influence of the rate of application of load on the modulus of rupture of concrete.[31]

application of load, the ultimate strength may be reduced to little over 70% of the strength under a stress applied at 30 psi/sec.[29] However, within the practical range of speeds of loading of ordinary testing machines (10 to 100 psi/sec for 6-in. cylinders) the effect of the rate of application of load is small: only about ±3% of the strength at the standard rate prescribed by the ASTM C39–71 (20 to 50 psi/sec). The rate of application of load is of importance only at stresses approaching the failing load and, in fact, the ASTM C39–71 permits the application of load at a higher rate up to one-half of the anticipated ultimate load. The reason for this is that it is only near the ultimate strength that the fast crack propagation stage is reached and it is then that the rate of loading has a large effect on the measured strength. In general, the effect of the rate of application of load is greater in lean mixes than in rich ones; for instance, in a 1:18 mix the effect is twice as large as in a 1:3 mix.[30]

Although this section is concerned with compressive testing, it may be relevant to note that flexure tests are also affected by the rate of application of load. For this reason, ASTM C78–64 (1972) prescribes a rate of not more than 150 psi/min. An experimental relation between the modulus of rupture and the rate of application of stress is shown in Fig. 3.8.

3.5 STRENGTH OF CONCRETE UNDER VARIOUS STATES OF STRESS

The preceding section dealt with the compressive strength of concrete as this is the state of stress most common in design. Nevertheless, strength under other states of stress is often of interest. For instance, tensile strength of concrete is of importance in prestressed concrete at transfer of prestress or in the web of a beam subjected to shear; vertical loads on top and bottom beam surfaces lead to a state of biaxial stress; and in prestressed pressure vessels the state of stress is even more complex.

3.5.1 Tensile Strength

While the compressive strength test is virtually standardized, there are several fundamentally different types of tensile tests. However, there exists no generally satisfactory means of determining the tensile strength of concrete, and developments in testing methods are still taking place.

Ideally, the tensile strength should be determined by direct tension, but application of axial tension is difficult and no standard direct tension test exists; however, some success has been obtained with epoxy bonded ends and lazy-tongs grips.

A common test is the flexure test, ASTM C78–64 (1972), in which a simple beam loaded at third-points is used with a span three times its depth.

The maximum tensile stress reached is referred to as the modulus of rupture. This stress overestimates the tensile strength of concrete for three reasons. First, the calculation of the modulus of rupture is based on a linear stress distribution while in fact the stress block is parabolic. Second, crack propagation from the extreme fibre is blocked by the less stressed adjacent fibres so that a higher stress may be reached prior to collapse of the test specimen than would occur in axial tension. Third, only the extreme fibre is subjected to the maximum stress so that weak elements located other than in this fibre do not lead to premature failure; thus a higher stress can be reached. For all these reasons—although they vary in their relative contribution—the modulus of rupture is on the average 50% higher than the direct tensile strength of concrete.

A more recent test of the tensile strength of concrete is the splitting test, ASTM C496–71, or the indirect tension test. Here, a cylinder, placed with its axis horizontal between the platens of a compression testing machine, is subjected to compression in a diametral plane with resultant tension at right angles. The horizontal tensile stress is $2P/(\pi LD)$, where P is the applied compression, D is the diameter of the cylinder, and L is its length. To avoid crushing failure in the vicinity of the platens, packing strips are inserted between the generatrix and the platen.

The splitting test is simple to perform and has the additional advantage of using specimens made in standard compression cylinder moulds. The measured strength is close to the true tensile strength of the given concrete, although the presence of a normal compressive stress may slightly reduce the failing load (by about 5%[32]), the actual stress system being biaxial compression-tension. The relation between the splitting strength and the modulus of rupture is shown in Fig. 3.9; this seems to be independent of the aggregate used.

Recently, the use of a ring test for the determination of the tensile strength of concrete was suggested[34] but this test has not yet been adopted by ASTM. Essentially, the specimen is cast in the shape of a thick ring, and hydrostatic pressure is applied against the inside surface of the ring. Failure takes place by radial cracking. The resulting strength is slightly higher than the direct tensile strength probably owing to the stress system existing in a thick cylinder.

We can see that the various tests yield different values of the strength of concrete. This, in itself, is not important and indeed neither the compressive nor the tensile strength of concrete determined in a test on a specimen describes the strength of the concrete in the actual structure (see Section 3.6). Thus any one of the tension tests can be used, providing the stresses in the structure being designed are related to the type of test used.

Broadly speaking, the tensile strength of concrete is related to its compressive strength but the two are not proportional to one another; the ratio of

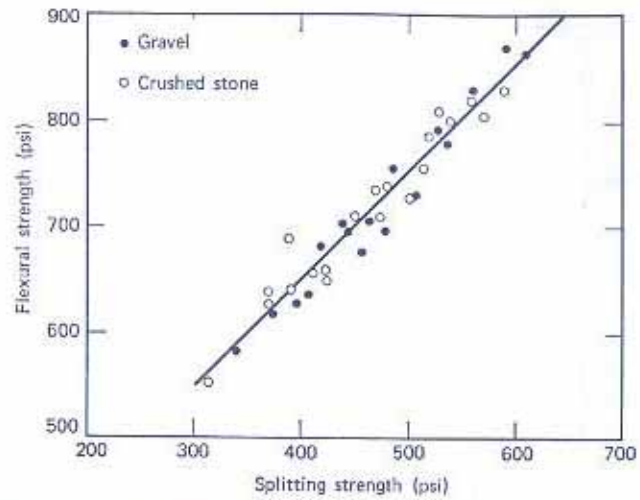

FIGURE 3.9. Relation between flexural and splitting strengths of concrete.[33] (The flexural strength was determined under third-point loading.)

the former to the latter decreases with an increase in the level of strength and is on the average 1/6 when the compressive strength is 2000 psi but only 1/11 at 10,000 psi (Fig. 3.10). The relation can be written in the form

$$f_t = k(f'_c)^n \tag{3.1}$$

where f'_c is the compressive strength, f_t is the tensile strength, and k and n are empirical coefficients. [The European Concrete Committee[35] recommends the use of values $k = 9.5$ and $n = 0.5$ when the tensile strength (in psi) is determined by a flexural test.]

The relation between tensile and compressive strengths depends not only on the level of strength but also on some other factors, notably on the type of aggregate used. Specifically, crushed coarse aggregate is much more beneficial with respect to the tensile strength than to the compressive strength, with the result that the strength ratio is higher when crushed aggregate is used than is the case with gravel. Conversely, air entrainment has a greater effect on the compressive strength than on tensile strength so that again, the coefficients in the expression given above have to be adjusted; this is particularly so for rich and strong mixes.[36]

There are some other, mostly minor, differences in the influence of various factors on the two strengths, compressive and tensile; one worth mentioning is that inadequate curing reduces the tensile strength relatively more than it reduces the compressive strength.[36]

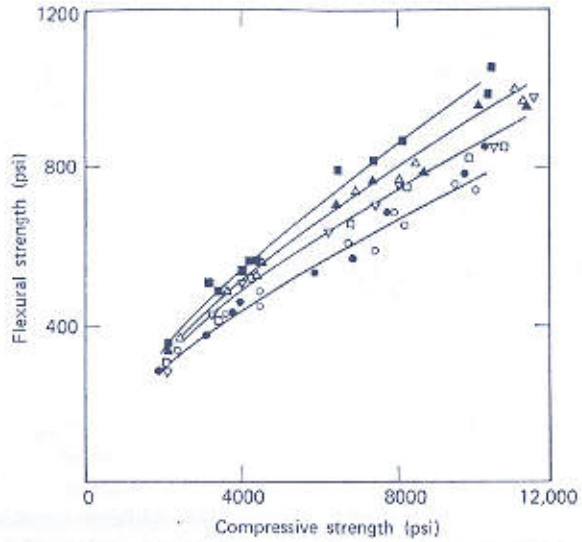

FIGURE 3.10. Relation between tensile (flexural) strength and compressive (cube) strength for concretes made with different aggregates[6] (British Crown copyright).

3.5.2 General Equation of Strength

In the preceding sections, the strength of concrete in uniaxial compression and tension was discussed, mention also being made of flexural strength. In practice, the state of stress is frequently more complex but of course experimental determination of the strength of concrete under bi- and triaxial stresses is very difficult. Tests have been carried out on cubes, cylinders, tubular specimens, and on plates. Variations in size, shape, loading conditions, and loading devices often make correlation of results difficult. Reviews of earlier studies[37,38,39] point out some of these difficulties.

Generally, in deriving equations of strength, failure is considered as a phenomenon obeying the laws of classical continuum mechanics. In this case a sufficiently large unit volume of concrete is considered so that the material is assumed homogeneous and isotropic. Theories of failure, such as maximum stress, maximum strain, internal friction, and strain energy fall into this category. Applicability of these theories to concrete has been suggested at various times, although no one of these has general validity for all states of stress in concrete. In general, these theories can be expressed in terms of principal stress components, so that

$$F(\sigma_1, \sigma_2, \sigma_3) = 0 \tag{3.2}$$

where σ_1, σ_2, and σ_3 are the three principal stresses. Equation (3.2) defines a "failure surface" in the stress–space coordinate system. The actual shape of the failure surface and thus the precise formulation of Eq. (3.2) have to be determined experimentally. Once the equations have been established from experimental data, they can be used as criteria in analyses or in design to define safe limits of stress under conditions for which these equations are valid.

Because concrete strength depends on a large number of factors, e.g., composition, age, moisture content, state of stress, and previous stress history, it is almost impossible to establish a general failure criterion valid for all conditions. Bresler and Pister[38] propose a failure criterion in terms of "mean" stresses. The mean normal and shearing stresses are defined with respect to a small spherical element of volume having a surface S. At any point on the surface of this element the normal and shearing stresses have values σ_S and τ_S respectively. Then the mean normal and shearing stresses, σ_a and τ_a respectively, are:

$$\sigma_a = \lim_{S \to 0} \left[\frac{1}{S} \int_S \sigma_S \, dS \right] = \tfrac{1}{3}(\sigma_1 + \sigma_2 + \sigma_3) \tag{3.3}$$

and

$$\tau_a = \lim_{S \to 0} \left[\frac{1}{S} \int_S \tau_S^2 \, dS \right]^{1/2}$$

$$= \frac{1}{\sqrt{15}} [(\sigma_1 - \sigma_2)^2 + (\sigma_2 - \sigma_3)^2 + (\sigma_3 - \sigma_1)^2]^{1/2} \tag{3.4}$$

The failure criterion can be conveniently defined in terms of the two mean stresses, with due account of the intermediate principal stress. The best fit for the test results obtained by Bresler and Pister is the following (Fig. 3.11):

$$(\tau_a/f'_c) = A + B(\sigma_a/f'_c) + C(\sigma_a/f'_c)^2 \tag{3.5}$$

where σ_a and f'_c are taken positive when compressive, and f'_c is the strength of a standard cylindrical specimen in uniaxial compression.

Evaluation of coefficients A, B, and C requires three points on the failure curve. The simplest tests to provide these data would be uniaxial compression, uniaxial tension, and biaxial compression.

For practical cases of biaxial stress, empirical curves can be used. Figure 3.12 shows such a curve for the case when there is no end restraint induced by the platens (cf. Section 3.4.1). If the restraint is not eliminated, the apparent strength in biaxial compression is much higher, but this is misleading as far as the majority of actual stress situations in structures is concerned. In reality thus, when $\sigma_1 = \sigma_2$, and $\sigma_3 = 0$, the strength is only 16% higher than in uniaxial compression. Biaxial tensile strength has been found to be no

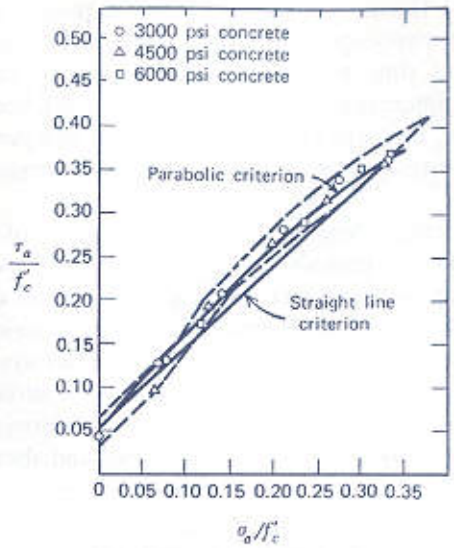

FIGURE 3.11. Relation between normal and shearing mean stresses at failure (based on 6 × 12 in. cylinders).[38]

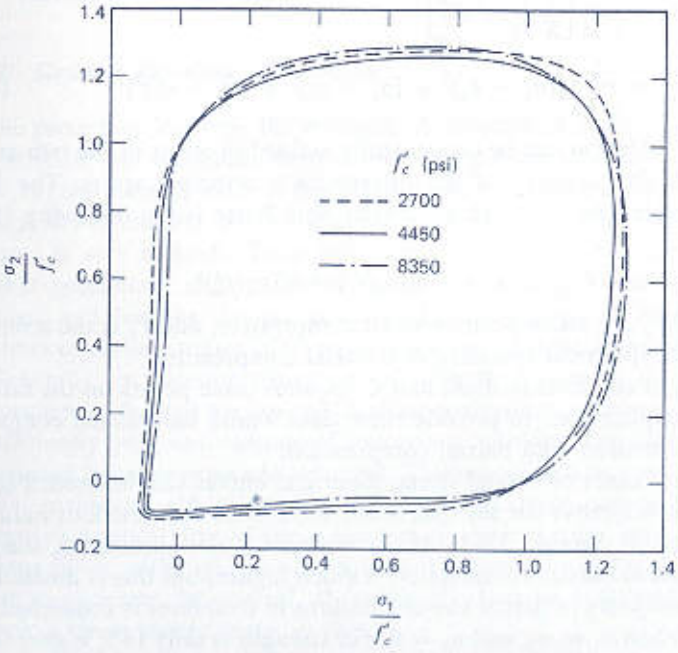

FIGURE 3.12. Interaction curve for biaxial stress σ_1 and σ_2 when the end restraint is effectively eliminated.[39]

different from uniaxial tensile strength.[39] These findings were confirmed by Nelissen.[40]

In biaxial compression-tension, the relative strength at any particular biaxial stress combination decreases as the level of uniaxial compressive strength increases.[39] This agrees with the observed data on the variation in the ratio of tensile to compressive strengths with the level of strength (see Section 3.5.1).

In formulating a general equation of strength the concept of failure must be clearly defined: the use of the ultimate load-carrying capacity is preferable to the state of extensive cracking. Whichever definition is used the general form of Eq. (3.5) seems to be applicable, but the values of coefficients in the equation must be determined for the "failure" state appropriate for the design condition.

3.6 ACTUAL AND MEASURED STRENGTH

The discussion in Section 3.5 has made it clear that the strength measured by a test specimen does not represent an inherent property of the concrete but is affected by the characteristics of the specimen used. Thus, test specimens do not tell us the real strength of the concrete in the structure, and in fact the main purpose of using them is to assess, rather than to measure, the strength of the concrete in the structure. The word "assess" has a qualitative connotation about it because all that we can say is that, if of two sets of similar specimens made from two concretes one set is significantly stronger, it is reasonable to expect that the structure made of this concrete contains concrete that is stronger, too. But even this statement is subject to the qualification that the concrete in the structure has been properly compacted and cured.

Thus, test specimens, treated and cured in a standard manner, give an indication of the potential quality of the concrete in the structure but not of the actual strength, which is affected by the temperature history, occurrence or absence of frost, as well as by inadequacy of compaction, presence of segregation and bleeding, and the like.

3.6.1 Accelerated Curing Test

As a corollary, it can be argued that it does not matter what numerical value the specimen yields. For instance, the specimen could be tested at an age considerably earlier than 28 days. Such an early test would be advantageous as the quality of any part of the structure would be known before it has become overlaid by other concrete, at which time it is too late to remove the concrete if it is too weak or to economize on cement if it is too strong. Unfortunately, the 24-hour strength is subject to vagaries and is extremely

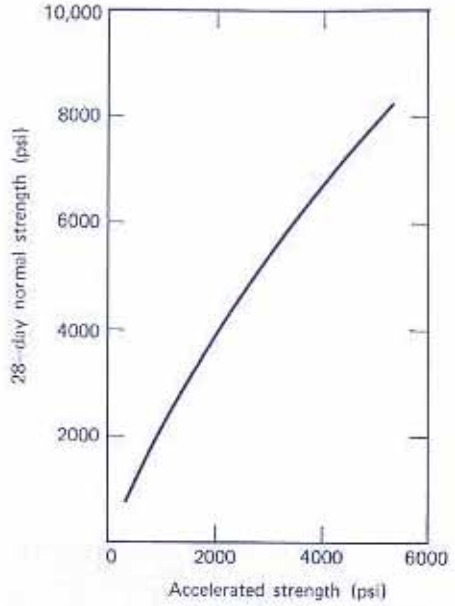

FIGURE 3.13. Relation between strength determined by the accelerated curing test and the 28-day strength of concrete moist-cured at 68°F.[42] (Reprinted by permission of the American Society for Testing and Materials, Copyright ASTM.)

sensitive to the early temperature history, which is not reflected in the later strength.

It is therefore necessary for the concrete to have achieved a greater proportion of its potential strength before testing, and to satisfy this requirement accelerated curing tests have been developed.[41,42] Originally, this test was intended to correlate with the 28-day strength under normal curing, so that the 28-day strength could be predicted from the accelerated curing strength. Figure 3.13 shows such a typical correlation.

The use of accelerated curing is still controversial but where such curing is adopted it is generally for the purpose of prediction of the 28-day strength. It seems that such an objective is restricted and not entirely sound. We suggest therefore that correlation between the accelerated curing strength and the 28-day normal curing strength be established at the preliminary mix design stage; it is then possible to decide that a certain accelerated curing strength is adequate. Further testing for the purpose of control and acceptance of concrete on site should be in the form of accelerated curing strength only. It is hoped that this proposal will gradually be accepted.

The details of accelerated curing vary between different investigations. In

King's original proposal,[41] standard concrete cylinders are made but the moulds are immediately covered by top plates, sealed with grease on the metal surfaces of contact in order to prevent drying. Within 30 min of adding the mixing water, the cylinders, in their covered moulds, are placed in an airtight electric oven, which is then switched on. The oven temperature should reach 200°F in about an hour and the cylinders are kept at this temperature for a further 5 hr, making a total of 6 hr in the oven. At the end of this period the cylinders are removed from the oven, stripped, allowed to cool, and tested in compression in the standard manner, the time allowed for these operations being 30 min. Thus the strength of the concrete is determined within 7 hr of casting.

In Smith and Chojnacki's procedure,[42] the cylinders are placed complete with moulds and cover plates in boiling water 20 min after the concrete has reached a needle penetration resistance of 3500 psi. The cylinders are maintained in the water bath for 16 hr, then are demoulded, allowed to cool, and capped. They are tested one hour after removal from the boiling water. It is desirable that the concrete has set to a sufficient degree before boiling as otherwise a lower strength is obtained. To measure the set, ASTM Standard C403–70 may be used, and the boiling commences at a fixed time after the given degree of set has been achieved. Since such a procedure takes into account the setting time of concrete, variations due to different cements and admixtures are allowed for.

The various procedures do not yield the same accelerated curing strength but, as already stated, the actual numerical value obtained is of no importance, except that habit makes us feel uncomfortable when the "strength" is described by a low "value."

3.6.2 Cores Cut from a Structure

If the test specimens, accelerated or normal, indicate that the strength of concrete is inadequate it is generally wise to check the strength of the concrete in the actual structure. Three principal methods are available.

The most obvious one is to cut cores from the structure but this is expensive and may result in damage which is difficult to repair. The main difficulty, however, arises in comparing the core strengths with the cylinder strengths which were specified. Generally, the cores have a lower strength than standard cylinders made from the same mix because curing of structures is almost invariably inferior to the curing prescribed for test specimens. The age of the core must of course be taken into account. The ratio of core strength to the standard cylinder strength is smaller the higher the strength level, being about 0.7 when the cylinder strength is 8500 psi but nearly unity when the cylinder strength is 2500 psi.[43] These values were obtained in tests

on cores cut from structures considered to be properly cured and would probably be lower when curing is patently inadequate.

The position in the structure from which the core is cut is also relevant. Generally, the core strength is lower the higher the position within a concrete lift,[43] probably owing to bleeding, but the effect ceases to be significant at depths greater than 1 to 2 ft.

3.6.3 Rebound Hammer Test

The difficulties, expense and damage of core cutting would be avoided if the strength of concrete could be tested in situ. Indeed, a great deal of the effort involved in the preparation of standard cylinders for acceptance purposes would be unnecessary if an in situ test could speedily and reliably give an estimate of strength. Such a test would, of course, have to be nondestructive.

Unfortunately, no satisfactory test has as yet been developed but there exist two tests which are of value within a limited scope, mainly for comparison purposes with other parts of the same structure. This limitation arises from the fact that neither test measures the strength directly, or even determines a property uniquely related to strength. However, for given materials and broadly the same mix proportions, the property measured is related to strength.

One of these tests is the rebound hammer or impact hammer test. Here, the rebound of an elastic mass from the surface of the concrete is measured and thus the hardness of the concrete surface layer is determined. For given mix proportions and hardness of aggregate, the hardness of the concrete and its strength are related. A typical relation is shown in Fig. 3.14.

Since the hardness is measured over a very small area, the test is sensitive to local variations in the concrete. For instance, the presence of a large piece of hard aggregate immediately underneath the plunger would result in an abnormally high rebound number; conversely, the presence of a void in a similar position would lead to a very low result. For this reason, it is desirable to take 10 to 12 readings spread over the area to be tested, and to assume their average value as representative of the concrete. The scatter of results is greater than in compression testing but the cost per test result in the case of the rebound hammer is very low.

The result of a rebound test is expressed as the ratio (in percent) of the distance travelled by a spring-loaded mass after rebound to the initial extension of the spring; this is called the rebound number. The actual number depends on the energy stored in the spring and on the size of the mass so that the rebound hammer has to be carefully standardized. Furthermore, the number recorded is affected by gravity with the result that the position of the hammer relative to the vertical affects the magnitude of the rebound number. Specifically, the rebound number of a floor is smaller than that of a soffit of

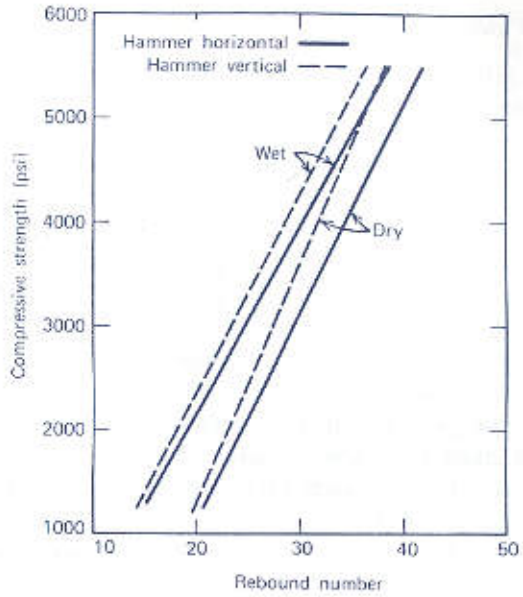

FIGURE 3.14. Relation between compressive strength of cylinders and rebound number.[44]

the same concrete, with vertical and inclined surfaces yielding intermediate values.

The main disadvantage of the rebound hammer test is that it determines the hardness of the concrete surface and is insensitive to the properties of the concrete in the center of its mass. Thus the rebound number recorded is affected by superficial changes which do not affect the concrete core, for instance, the degree of saturation and carbonation.

As already mentioned, the elastic properties of the aggregate greatly influence the rebound number so that the relation between the number and the compressive strength has to be established for any given aggregate and for the overall mix proportions used. The test is therefore primarily of value as a check on the uniformity of concrete in different parts of a structure or in a number of similar precast members, but the actual strength of the concrete with which the comparison is being made has to be determined by a compression cylinder test.

There is one further use of the rebound hammer: it can be employed to determine whether a given part of a structure has reached a strength adequate to remove the falsework or to be put into service. This check is of value when the temperature is unusually low. Likewise, the rebound hammer can be used to assess damage due to frost or fire.

steam for 3 h at 295 ± 10 psi. The maximum autoclave expansion permissible for all five types of portland cements (ASTM C150) is 0.80%.

Cements which have a high C_3A content are generally unsuitable for structures exposed to sulfates. ASTM C452 describes a standard procedure for determining the potential expansion of portland-cement mortars exposed to sulfate attack.

Deleterious expansion can also result from the relatively high alkali content of a cement when certain siliceous materials are used as concrete aggregates. ASTM C227 describes a mortar-bar method to determine alkali reactivity of cement-aggregate combination.

1.4.4 Compressive Strength

The strength characteristics of a cement are determined by a standard test method (ASTM C109), whereby determination of compressive strength of 2 in. mortar cubes is made at certain age intervals. The minimum compressive strengths required of Type I portland cement (ASTM C150) are: 1800 psi at 3 days, and 2800 psi at 7 days. Type III cement is required to gain strength at relatively rapid rates, whereas Types IV and V at relatively slower rates (Table 1.2), which are reflected in the ASTM specifications. The compressive strengths of all the five types of portland cement may be similar after 3 months of hydration, hence it is only the early hydration characteristics of portland cements which can be exploited in terms of their different engineering applications.

The ASTM Specification C150 also includes requirements with regard to the tensile strength, heat of hydration, and false set of portland cements, but these requirements apply only when specifically requested by a purchaser.

1.5 MODIFIED PORTLAND CEMENTS

In addition to the five types of portland cements standardized by ASTM, the following *modifications of portland cement* are also available commercially:

Air-Entraining Portland Cements. These produce concrete with improved resistance to freeze–thaw action. One way to make air-entrained concrete is to use an air-entraining cement which will incorporate well-distributed minute air bubbles in the hardened cement paste. Air-entrainment leads to some other advantages in properties of fresh concrete, such as better workability and resistance to segregation. Types I, II, and III portland-cement clinkers, when interground in the presence of small quantities of suitable admixtures, yield corresponding Types IA, IIA, and IIIA air-entraining portland cements, specified in ASTM C150. The acceptable air-entraining admixtures such as fatty acids and their soaps, wood resins and their soaps, and

lignosulfonates are specified in ASTM C226. On small jobs, where careful control is not envisaged, use of air-entraining cements obviously offers a convenient way to make air-entrained concrete. However, the most common method of producing the entrainment of air in concrete is by adding a suitable air-entraining agent during concrete mixing. These air-entraining admixtures for concrete are specified in ASTM C260.

Expansive Cements. These are now being used in the United States to produce shrinkage-compensating and chemically prestressed concretes. The type K shrinkage-compensating expansive cement, which at present, due to a large number of field applications, is the best known of all other types, consists generally of a portland cement clinker interground with suitable portions of gypsum and expansive component. The expansive component is a portland-like clinker, which in addition to C_3S and C_2S contains an anhydrous calcium sulfoaluminate ($C_4A_3\bar{S}$), calcium sulfate, and lime. The expansive component can either be produced separately by heat treatment of a raw-mix containing suitable proportions of limestone, bauxite and gypsum, or can be incorporated directly into portland-cement clinker by making the necessary modifications in the chemical composition of the raw-mix. The expansion accompanying the formation of ettringite, $C_3A{\cdot}3C\bar{S}{\cdot}H_{32}$, when taking place under conditions of restraint, produces compressive stresses which successfully counteract the adverse effects of tensile stresses caused by the drying shrinkage of the concrete.

Type K and Type M expansive cements, with greater potential expansions, are also reported to be available now for the purpose of chemically prestressing precast structural elements such as slabs, walls, pipes, and even large-size building units. Type M cement is either a mixture of portland cement, calcium aluminate cement, and calcium sulfate, or an interground product made with portland-cement clinker, calcium-aluminate clinker, and calcium sulfate. Type S cement is a portland cement containing a large C_3A content and an excess of calcium sulfate above the usual amount found in other portland cements.

Masonry Cements. These are preferred over other types of portland cement when a rapid rate of strength development is of no consequence but workability and water retention of cement are of main concern. Masonry brickwork and plastering jobs are among the important uses of masonry cements. Generally, these cements are an interground product of portland-cement clinker, gypsum, an air-entraining agent, a plasticizing agent such as hydrated lime, and a considerable proportion of an inert material such as ground limestone, chalk, talc, or clay. Some 40–50% inert material may be present. Masonry cements have to be ground to a very high fineness in order to meet the compressive strength requirements. The 28-day compressive strength of

3.6.4 Ultrasonic Pulse Test

Another test which gives an indirect determination of the strength of concrete in situ is the ultrasonic pulse test, in which the longitudinal wave velocity across a concrete thickness is determined. Here, the properties of the entire thickness of the concrete are involved so that the degree of compaction of the concrete in the structure is reflected in the results. Indeed, for a given aggregate and overall mix proportions, the ultrasonic pulse test measures the variation in the density of concrete and, since under such conditions density also affects strength, the ultrasonic pulse velocity and strength are related. Specifically, the lowering of density by inadequate compaction or by an increase in the water–cement ratio decreases both the compressive strength of concrete and the velocity of the pulse transmitted through it.

Strictly speaking, the pulse velocity is not determined directly but is calculated from the time taken by a pulse to travel a carefully measured distance. Concrete from 4 in. to 8 ft thick can normally be tested, but tests have been made on thicknesses up to 50 ft.

When access to two opposite faces of a concrete member is not possible, the pulse velocity can be measured along a path parallel to the surface of the concrete (with access to the surface only); the accuracy of readings is, however, reduced. Moreover, under such circumstances, the properties of the surface layer only are determined.

The ultrasonic pulse velocity technique can be used as a means of quality control of products which are supposed to be made of similar concrete but a direct determination of strength of concretes made of different materials in unknown proportions is not possible. Nevertheless, because there is a broad tendency for concrete of higher density to have a higher strength (provided the specific gravity of the aggregate is constant), a general classification of the quality of concrete on the basis of the pulse velocity is possible. Typical figures for concretes made with normal-weight aggregate are given in Table 3.1.

TABLE 3.1. Classification of the Quality of Concrete on the Basis of Pulse Velocity.[45]

Longitudinal Pulse Velocity 10^3 ft/s	Quality of Concrete
>15	Excellent
12–15	Good
10–12	Doubtful
7–10	Poor
<7	Very poor

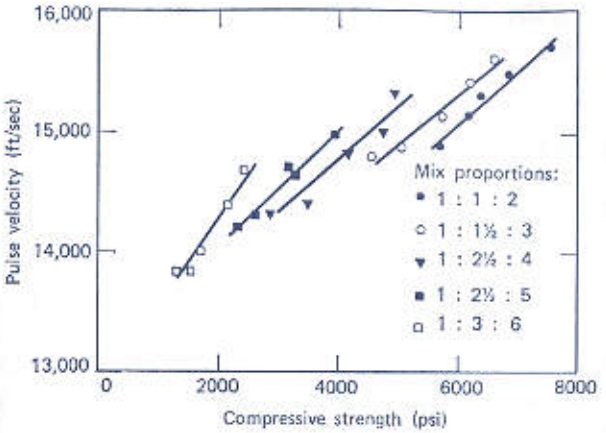

FIGURE 3.15. Relation between ultrasonic pulse velocity and compressive strength for concretes of different mix proportions[46] (British Crown copyright).

It is important to remember though that both the quantity and type of coarse aggregate affect the pulse velocity while, at a constant water-cement ratio, the influence of coarse aggregate on strength is small. Thus, for different mix proportions, there exists a different relation between the pulse velocity and strength; this is shown in Fig. 3.15. This is, however, not as inconvenient as might seem because for concretes of the same age, the effects of aggregate–cement ratio and water–cement ratio balance one another[47] so that at a constant workability (which is usually the case in practice) and age there is a unique relation between pulse velocity and strength.

Nevertheless, in practice it is highly desirable to establish experimentally the relation between pulse velocity and strength of test cylinders used on a given job. The moisture condition of the cylinders is of importance as, if the cylinders are wet and the concrete in the structure dry, the strength of the latter can be underestimated by 15%.[48]

In addition to the control of the quality of concrete, ultrasonic pulse measurements can be used to detect the development of cracks in structures and to check deterioration due to frost or chemical action. These are very important applications of the technique, which is suitable for the detection of any development of voids in concrete. Cracks with a component at right angles to the direction of propagation of the pulse cause the pulse to diffract around the crack: this increases the time of travel of the pulse and hence decreases the apparent velocity. It should be noted, however, that when the plane of the crack coincides with the direction of propagation of the pulse,

it can pass on either side of the crack so that the pulse velocity is not affected.[49] Thus determination of the pulse velocity in several directions is desirable.

3.7 IMPACT STRENGTH OF CONCRETE[50]

Impact strength is of importance primarily in connection with pile driving and with foundations for machines exerting impulsive loading, but accidental impact (e.g. during handling of precast members) is also of interest. Extensive tests on impact strength of concrete have been made by Green.[51] As principal criteria he considered the ability of a specimen to withstand repeated blows and to absorb energy. In particular, he studied the number of blows the concrete can withstand before reaching the no-rebound condition, this stage indicating a definite state of damage.

Impact tests, when conducted with a relatively small hammer (1-in. diameter face) lead to a greater scatter of results than tests on static compressive strength of the concrete.[51] This arises from the fact that in the standard compression test some relief of a highly stressed weak zone is possible owing to creep, while in the impact test no redistribution of stresses is possible during the very short period of deformation. Hence, local weaknesses have a greater influence on the recorded strength of a specimen.

In general, Green found that the higher the static compressive strength of the concrete the lower the energy absorbed per blow before cracking, but the impact strength of concrete increases with its compressive strength (and therefore age) at a progressively increasing rate (Fig. 3.16). The relation is different for each coarse aggregate and storage condition of the concrete. For the same compressive strength, the impact strength is greater for coarse aggregate of greater angularity and surface roughness. This supports the suggestion[52] that impact strength is more closely related to the tensile strength of concrete than to its compressive strength. Thus concrete made with a gravel coarse aggregate has a low impact strength, failure taking place owing to insufficient bond between mortar and coarse aggregate. On the other hand, when the surface of the aggregate is rough, the concrete is able to develop the full strength of much of the aggregate in the region of failure. The influence of fine aggregate is not well defined but the use of fine sand usually leads to a slightly lower impact strength.

Storage conditions influence the impact strength in a manner different from compressive strength. Specifically, the impact strength of water-stored concrete is lower than when the concrete is dry, although the former concrete can withstand more blows before cracking. Thus, as already stated, the compressive strength without reference to storage conditions does not give a satisfactory indication of the impact strength.[51]

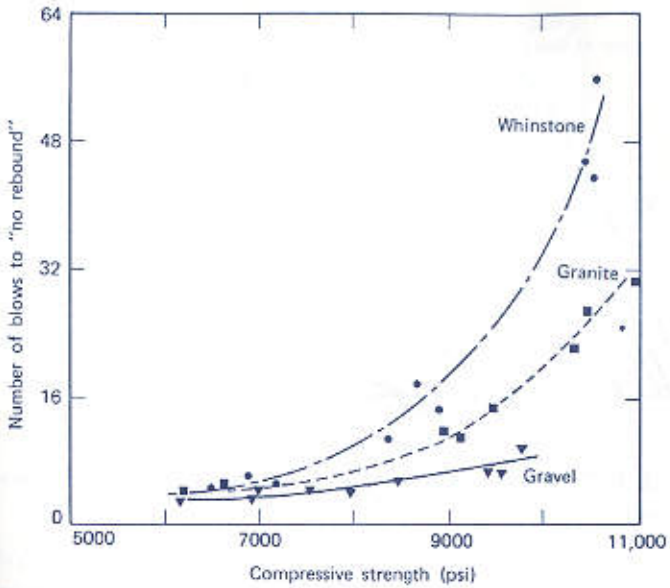

FIGURE 3.16. Relation between compressive strength and number of blows to 'no-rebound' for concretes made with different aggregates and Type I cement, stored in water.[51]

There is evidence that under uniformly applied impact loading (a condition difficult to achieve in practice) the impact strength of concrete is significantly greater than its static compressive strength; an increase of 30–80% has been suggested. This increase in strength would explain the greater ability of concrete to absorb strain energy.[53]

3.8 FATIGUE STRENGTH OF CONCRETE

A material is said to fail in fatigue if failure takes place after a number of repeated loads, each smaller than the static compressive strength. The changes in the stress–strain curve with the number of applied cycles are shown in Fig. 3.17 for compressive loading of concrete between the limits σ_l and σ_h such that $0 \leq \sigma_l < \sigma_h$. The stress–strain curve is first concave toward the strain axis (a hysteresis loop being formed on unloading), then becomes almost straight (the concrete being virtually elastic); the nearly straight line shifts at a decreasing rate as the cycling progresses (i.e., there is some irrecoverable set), and eventually becomes concave toward the stress axis. As this concavity increases, the concrete approaches fatigue failure.

This behavior takes place only when σ_h is above a limiting value known as

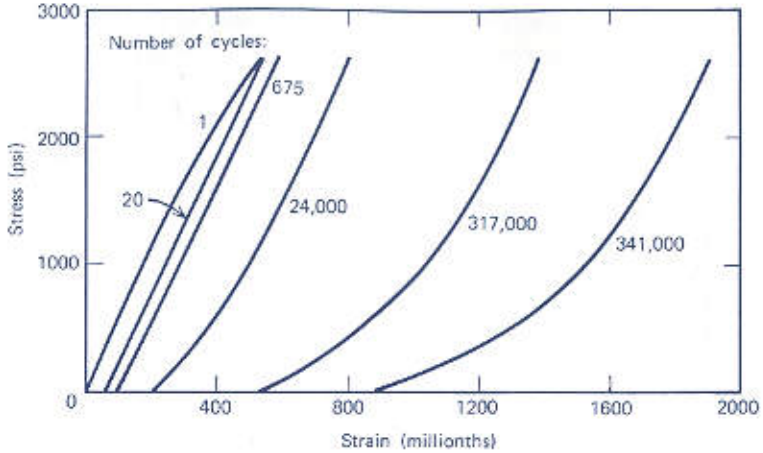

FIGURE 3.17. Stress–strain relation of concrete under cyclic compressive loading.[54]

fatigue limit or endurance limit; otherwise, changes beyond the straight stress–strain curve do not occur. Moreover, cyclic loading below the fatigue limit improves the subsequent fatigue strength of concrete, i.e., concrete loaded a number of times below its fatigue limit will, on subsequent loading above this limit, exhibit a higher fatigue strength than concrete never loaded before. The static strength is also improved by previous cycling below the fatigue limit; the increase in strength is up to 15%, and is probably due to densification of concrete. A similar effect is caused by a prolonged static compressive stress[55] below a limit value corresponding to failure under sustained load.

Fatigue loading is accompanied by extensive cracking and the strain at failure can be much greater than in a standard static test.[56] Generally, the concrete with a longer fatigue life has a higher nonelastic strain at failure.[68]

Strictly speaking, concrete does not appear to have a fatigue limit, i.e., a fatigue strength at an infinite number of cycles (except when stress reversal takes place). It is usual therefore to refer to fatigue strength at a very large number of cycles, such as 10 million.

The fatigue strength can be represented by means of a modified Goodman diagram (Fig. 3.18). The ordinate from a line at 45° through the origin shows the range of stress ($\sigma_h - \sigma_l$) for a given number of cycles; σ_l is generally greater than zero (arising from the dead load), while σ_h is due to the dead plus live (transient) load. Thus a range of stress that a given concrete can withstand a specified number of cycles can be read off the diagram. For a given σ_l the number of cycles is very sensitive to the range of stress. For

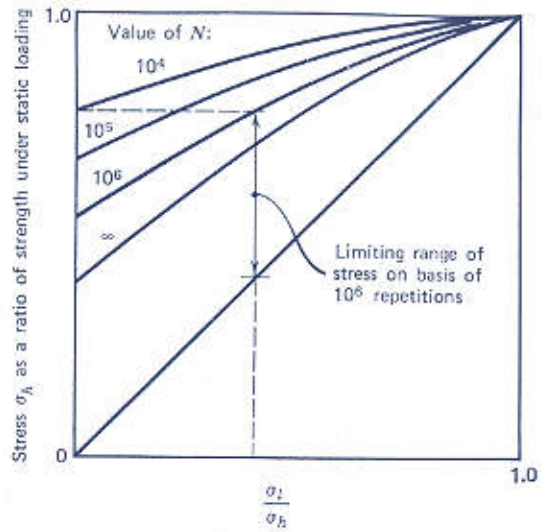

FIGURE 3.18. Modified Goodman diagram for concrete in compression fatigue.[50]

instance, an increase in range from 57.5 to 65% of the ultimate static strength has been found to decrease the number of cycles 40 times.[57]

The modified Goodman diagram (Fig. 3.18) shows that for a constant range of stress, the higher the value of the minimum stress the lower the number of cycles that a given concrete can withstand. This is of significance in relation to the dead load of a concrete member which is to carry a transient load of a certain magnitude.

From the fact that the lines of Fig. 3.18 rise to the right it can also be seen that the fatigue strength of concrete is lower the higher the ratio σ_h/σ_l. Figure 3.19 shows the decrease in the number of cycles to failure with the increase in the ratio of σ_h to the static ultimate strength.

An important characteristic of the fatigue behavior of concrete is that, at a given number of cycles, fatigue failure occurs at the same fraction of the ultimate strength, independently of the level of this strength, of the presence or absence of air entrainment,[59] and of the age of the concrete.[60] Thus, fatigue strength can be described by a single parameter.

If the cycling is not continuous but rest periods occur, the fatigue strength is improved; however, rest periods whose duration is more than 5 min lead to no further increase in fatigue strength. The explanation of this phenomenon is probably in terms of the relaxation of concrete, primary bonds, which have remained intact, restoring the internal structure to its original configuration.

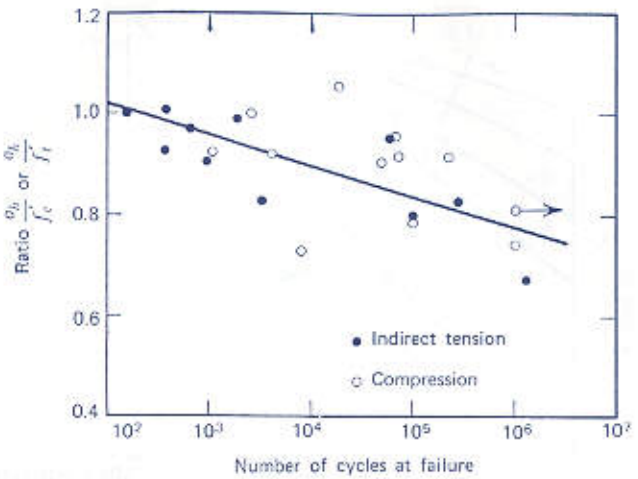

FIGURE 3.19. Influence of the ratio of the upper limit of cycling stress, σ_h, to the static strength on the fatigue life in compression and in tension.[58]

The mechanism of fatigue failure is outside the scope of this chapter but it may be relevant to mention that the behavior of concrete in fatigue is not closely related to its behavior under impact loading.[60] Indeed, the latter does not impair the static strength of concrete[61] while in fatigue failure occurs, by definition, at a load smaller than the static strength.

3.9 DEFORMATION OF CONCRETE UNDER COMPRESSIVE STRESS

The deformation of concrete is important because the stress distribution in concrete elements, both reinforced and prestressed, as well as internal force and moment distribution in structures composed of such elements, are related to strain in concrete. The present section is concerned with instantaneous deformation under axial compression, while the succeeding two sections deal with the nonelastic deformations: shrinkage and creep.

Concrete can be treated as an elastic material but in fact it is only partially so in that the deformation occurring under a load of any but very short duration never completely disappears. Nevertheless, for the purpose of many design calculations concrete is considered to have an elastic component of strain and its short-term stress–strain curve is taken to have a linear elastic portion and a nonlinear inelastic portion. If an increasing stress is applied at a

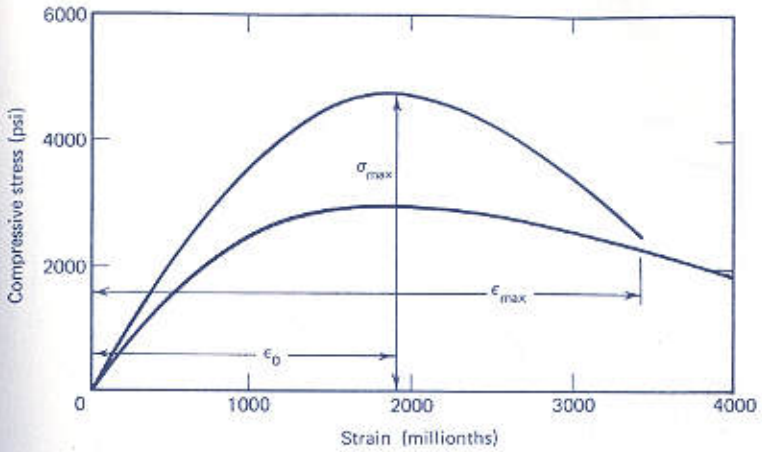

FIGURE 3.20. Typical stress–strain curves for concrete showing the descending part of the curve.

constant rate of strain, the stress-strain curve has the shape shown in Fig. 3.20, i.e., there is a descending as well as ascending part. While the constant-rate-of-stress method of testing compression specimens does not exhibit this behavior, the normal loading conditions in structures are better approximated by the shape of Fig. 3.20. This is the rationale of the parabolic stress block in ultimate load calculations.

3.9.1 Stress–Strain Curve

We define as the initial tangent modulus of elasticity the slope to the curve at the origin (Fig. 3.21) but it is, of course, possible also to determine a tangent modulus at any point on the curve. The latter, however, applies only to small load increments or decrements in the vicinity of the tangent point, and the distinction between the initial tangent modulus and a tangent modulus at a given stress should be carefully realized. The slope of the linear part is approximately the same in compression and in tension. The chord in Fig. 3.21 determines the secant modulus of elasticity. This clearly varies with the magnitude of the stress so that the stress at which the secant modulus is determined has to be stated.

Figure 3.21 shows also the strain development on immediate removal of the applied stress. The secant of the unloading curve is usually parallel to the initial tangent to the loading curve. As the secant on unloading is easy to establish, this indirect method of determination of the initial tangent modulus is frequently used.

It is interesting to note that both the cement paste and the aggregate,

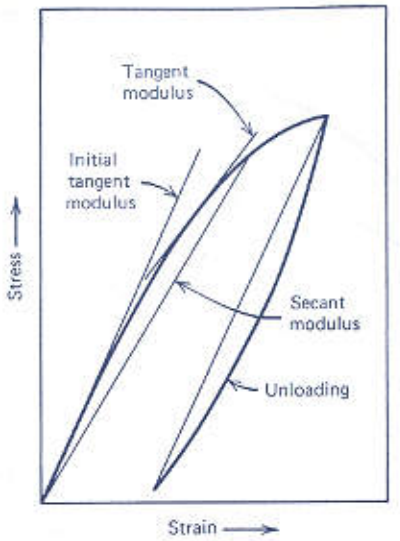

FIGURE 3.21. Typical stress–strain curve for concrete.

when individually subjected to stress, have a sensibly linear stress–strain relation. Why should a material consisting of two linear components depart from linearity? The explanation lies in the presence of interfaces between the aggregate and cement paste at which microcracks form. These microcracks, as mentioned in Section 3.2.1, develop progressively, making varying angles with the applied stress. Thus, there is a progressive increase in the local stress intensity and in the magnitude of strain, the strain increasing at a faster rate than the applied stress so that the stress–strain curve bends over with an apparent pseudo-plastic behavior.[62,63] The shape of the stress–strain curve is strongly affected by the rate of application of stress, as shown in Fig. 3.22 (cf. Section 3.4.3).

A further problem arises from the fact that eccentric loading, producing a stress gradient, leads to a higher maximum stress and a higher corresponding strain, ε_0, than axial loading, the reason for this being the difference in the time-rate of application in the two cases. Thus, there is some doubt about transferring the stress–strain curve obtained on an axially loaded cylinder (which is customarily tested in the laboratory) to the stress–strain relation in a beam.

Differences in the shapes of the stress–strain curves in flexure and in axial compression were found by Bresler,[65] but Hognestad et al.,[66] using a different technique, did not confirm this and believe the two curves to be closely similar. The structural behavior which would result from the use of a flexural stress–strain curve would differ only slightly from that predicted on the basis of a

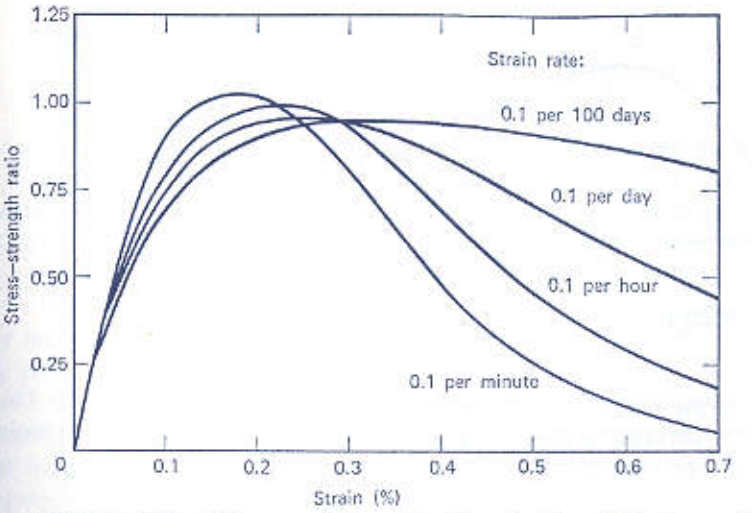

FIGURE 3.22. Influence of the rate of application of strain on the shape of the stress–strain curve.[64]

typical compression stress–strain curve. Therefore, from the practical point of view, at the present time, the curves derived from axial compression tests are commonly used.

A number of expressions for the stress–strain curve have been proposed by various investigators but none is completely satisfactory (and of course a factor for the rate of application of stress has to be included). One difficulty is that the curvature of the stress–strain curve is greater the greater the aggregate content (cf. Section 3.2.1) and yet standard expressions purport to apply to all concretes.

A commonly used expression is that proposed by Hognestad,[67] which consists of a parabola for the ascending part and a straight line for the descending part, Fig. 3.23(a). In equation form:

$$\text{for } 0 < \varepsilon < \varepsilon_0: \qquad \frac{\sigma}{\sigma_{\max}} = 2\frac{\varepsilon}{\varepsilon_0}\left(1 - \frac{1}{2}\frac{\varepsilon}{\varepsilon_0}\right) \tag{3.6}$$

$$\text{for } \varepsilon_0 < \varepsilon < \varepsilon_u: \qquad \frac{\sigma}{\sigma_{\max}} = 1 - 0.15\frac{\varepsilon - \varepsilon_0}{\varepsilon_u - \varepsilon_0} \tag{3.7}$$

where ε_0 = strain at maximum stress $\sigma_{\max}$, ε_u = ultimate strain, σ_u = stress at failure. Initial tangent modulus E is

$$E = \left.\frac{d\sigma}{d\varepsilon}\right|_{\varepsilon=0} = 2\frac{\sigma_{\max}}{\varepsilon_0} \tag{3.8}$$